THE GEOCHEMICAL EVOLUTION OF THREE ALKALINE COMPLEXES IN THE KUBOOS - BREMEN IGNEOUS PROVINCE, SOUTHERN NAMIBIA.

By

Robert Hugh Smithies

Submitted as requirement for the degree of
DOCTOR OF PHILOSOPHY
of RHODES UNIVERSITY,
Grahamstown,
South Africa.

November, 1991

All arguments and interpretations
presented in this thesis are my own,
except where referenced.

R.H. Smithies

LIST OF TABLES

LIST OF FIGURES

LIST OF PLATES

ACKNOWLEDGEMENTS

I would like first of all to thank Professors J. Marsh and F. Pirajno for their supervision and guidance throughout this study.

Without the willingness of GEMIN to support postgraduate work at univer sities, this project would not have been possible. The company's generosity in providing full financial assistance over the three years of study is most gratefully acknowledged. Particular thanks are extended to Mr C Johnston for the time he gave to organising various aspects of the study, and for his supervision in the field.

On a more general note, I would like to thank all of the staff of the Geology Department at Rhodes University. Without the assistance and, more particularly, the guidance of Professors H.V. Eales and R.E. Jacob my five years at Rhodes would not have been as rewarding as they were. Messrs R. Harris and C. Mallinson spent numerous hours instructing me in various computer applications, R. Skae aided me in the operation of the microprobe, J. Hepple assisted me in matters too numerous to detail here and Mrs L. Wadeson and C. Davis helped me with administrative matters. My study at Rhodes also benefitted greatly from discussion with my fellow students including Wolfgang Maier, Bernd Teigler, Billy De Klerk, Ian De Klerk and Johan Stephenhoffe.

Over the last three years I have utilised the facilities at numerous laboratories outside Grahamstown and benefitted much from instruction and supervision by, and discussions with, Dr D. Cornell (ICP laboratory - Stellenbosch University), Drs B. Eglington and R. Harmer (Radiogenic isotope laboratory - CSIR, Pretoria) and Dr C. Harris (Oxygen isotope laboratory - University of Cape Town). My visits to the University of Cape Town also allowed for numerous stimulating discussions with Professor D. Reid. To these people I am most grateful.

Field work in Namibia would not have been possible without the company and assistance of Wolfgang Maier, Bernd Teigler, Murray Beidler, Harold Mills, Lynne Smithies and Phoenix Hoyle.

Samples from a nepheline syenite intrusion within the Marinkas Kwela Carbonatite Complex (sample numbers RS 112 - 120) were kindly supplied by the Geological Survey of Namibia.

Last but not least, I would like to thank my family for their encouragement throughout my years studying. My stepmother, Chris, spent hours sorting out matters on the production side of this thesis. My father spent days scrawling abusive things (not always, I have to confess, without point) on some of my early manuscripts while muttering darkly about "wretched scientists" who "wantonly mangle" his beloved English language. My wife, Lynne, spent years simply putting up with me.

To all of the persons mentioned above, as well as to those who have had anything to do with my work over the last three years and who have inadvertently gone unacknowledged, I am highly grateful.

ABSTRACT

The Kuboos-Bremen Igneous Province comprises a linear zone of alkaline complexes that intrude Proterozoic and Pan-African rocks and trends in a northeast direction from the northwest of the Cape Province in South Africa into southern Namibia. Of the three most southerly complexes in Namibia, two comprise silicate rocks ranging from nepheline syenite to alkali-granite and are called the Grootpenseiland and Marinkas Kwela Complexes (GPC and MKC). The Marinkas Kwela Carbonatite Complex is the third and most northerly of the complexes. Isotopic age determinations on a number of rock types from both the silicate complexes yield ages around 520Ma and are consistent with published Pan-African ages for the Province.

Each silicate complex shows a migrating locus of intrusion from Si-undersaturated rocks in the southwest to Si-oversaturated rocks in the northeast. The complexes overlap in outcrop. The rocks are moderately to highly felsic and none reflects primary magma compositions. The Si-undersaturated rocks from both complexes include side-wall cumulates formed from magmas that fractionated alkali-feldspar, clinopyroxene and amphibole. Foyaites also occur in the MKC and have a compositional range reflecting alkali-feldspar fractionation and, probably, some interaction with dolomite country rocks.

Major and trace element data suggest that critically saturated alkali syenites occurring in both complexes evolved *via* protracted feldspar fractionation, and that critically saturated alkali-feldspar syenite occurring only in the GPC is a cumulate. The two rock types cannot be related genetically.

Of the Si-oversaturated rocks in both complexes, those in the compositional range monzonite to granite were intruded before alkali-granites. Compositional diversity amongst the former reflects fractionation of feldspar and of mafic phases, but that process cannot genetically link the rocks to the alkali-granites.

Isotopic compositions of Sr and Nd indicate that the silicate magmas were derived from an upper mantle source region characterised by low time-integrated Rb/Sr ratios and high time-integrated Sm/Nd ratios. However, the evidence of Sr and O isotopic data is that the Si-oversaturated melts possibly interacted with a crustal component, presumably the Proterozoic rocks of the Namaqua Metamorphic Province. This interaction may explain the occurrence of apparently co-genetic rock series that evolved on opposite sides of the feldspar join in Petrogeny's Residua System.

The Marinkas Kwela Carbonatite Complex was emplaced before the final intrusive phases of the MKC and exhibits unusually pronounced late-stage enrichment in manganese. The earliest intrusive rocks in the complex were nepheline syenites which were fenitised by later intrusions of sôvites. Although the commonly occurring magmatic sequence of sôvite-beforsite-ferrocarbonatite is observed at Marinkas Kwela, sôvites do not appear to have been parental to beforsites. Removal of apatite and early crystallisation of magnetite distinguish magnetite-rich beforsite from co-genetic apatite-rich beforsite. Two further magmatic sequences, the first from apatite-rich beforsite through ferrocarbonatite to Mn-rich ferrocarbonatite (high Fe/Mn) and the second from magnetite-rich beforsite to Mn-rich ferrocarbonatite (low Fe/Mn), reflect fractionation of dolomite and of dolomite+magnetite respectively.

TABLE OF CONTENTS

CHAPTER 1 INTRODUCTION

This chapter outlines the scope and purposes of the study that follows, and provides some observations on the regional geological setting. For convenience, some notes on nomenclature are also included here.

1.1 Scope And Purposes Of This Study

The alkaline igneous rocks that are the focus of this study form part of the Kuboos - Bremen Igneous Province, a linear zone of intrusions of Pan-African age which extends in a north-easterly direction for at least 270km from the western Richtersveld region of South Africa to the Great Karas Mountains in southern Namibia. First described by Söhnge and De Villiers (1948), the Province consists of a number of discrete intrusive complexes which are located with a remarkably high degree of linearity (Fig 1.1).

Some aspects of the geology of these complexes have been covered in regional studies by Söhnge and De Villiers (1948), Kröner (1975), Kröner and Blignault (1976), Martin and Porada (1977), Blignault (1977) and Allsopp *et al.* (1979). Only two of the complexes, however, have so far received detailed attention in the literature - the Younger Bremen Complex (Middlemost, 1967) towards the northeastern end of the Province, and the Kanabeam Complex (Reid, in press).

This study deals with three complexes in the central part of the Province. They lie to the southwest of the Kanabeam Complex between

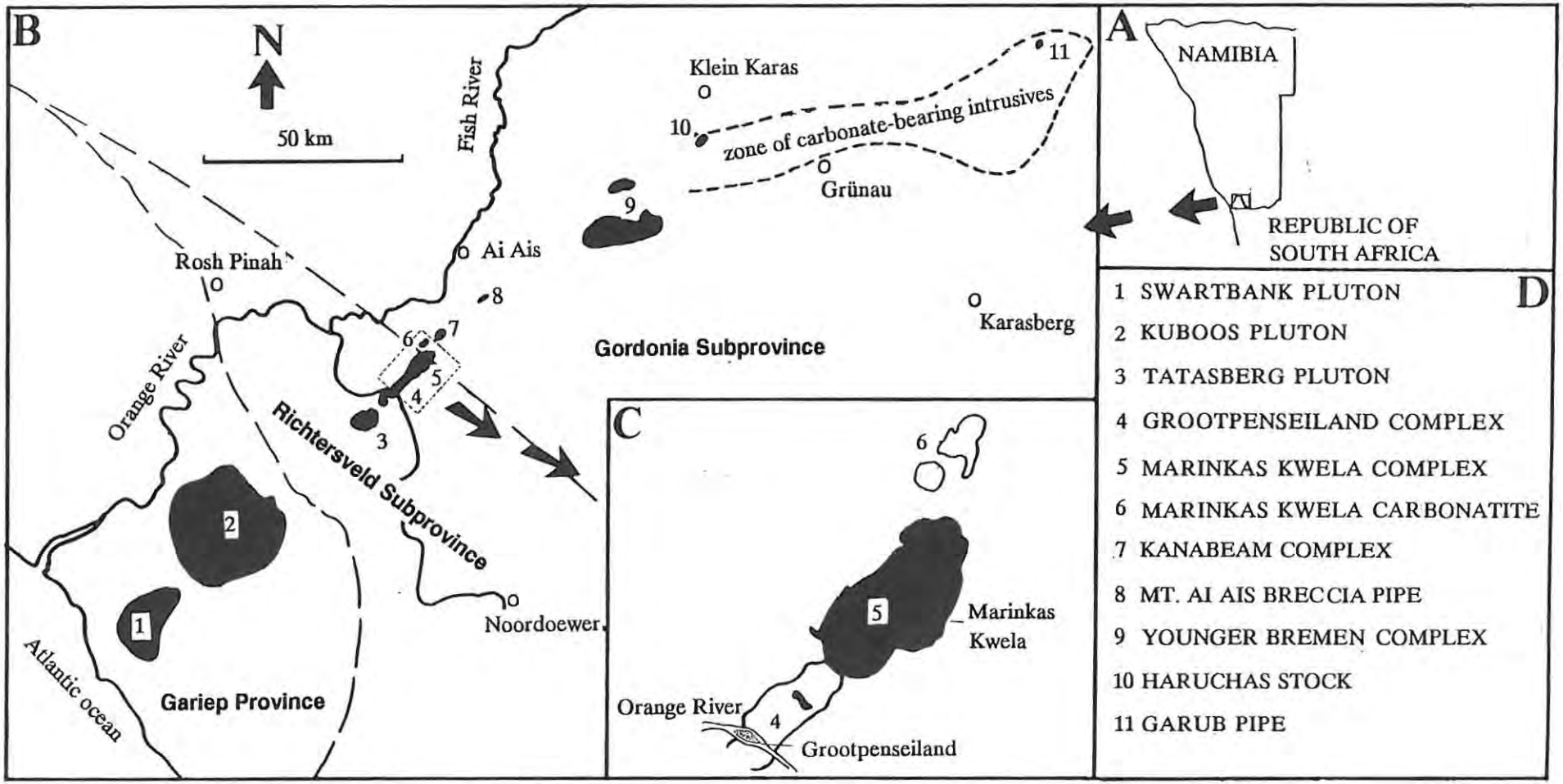

Figure 1.1 Regional locality map showing **A)** the locality of the area of study with respect to the international border between Namibia and the Republic of South Africa, **B)** the linear distribution of intrusive centres in the Kuboos - Bremen Igneous Province, and **C)** a more detailed view of the intrusive complexes that are the focus of this study. The names quoted in **D** correspond to numbered localities in **B** and **C**. Note that three complexes lie in **C** and that an outlier of complex '5' occurs within complex '4'. (Modified after Reid, in press).

the latter and the vicinity of Grootpenseiland in the Orange River (Fig 1.1). The most northerly of them is composed predominantly of carbonatite, and will be referred to as the **'Marinkas Kwela Carbonatite Complex'**.

The other two complexes, which are composed of silicate rocks, require a brief explanatory note. In some of the earlier literature - for example, Kröner and Blignault (1976) and Allsopp *et al.* (1979) - the outcrops occurring on both banks of the Orange River opposite Grootpenseiland (and extending on the Namibian side for some 15km beyond the river) were included in the Tatasberg Complex (Fig 1.1). For reasons elaborated later, they are dealt with in this thesis as two discrete albeit overlapping complexes.

The central purpose of this study is to unravel the geochemical and petrological evolution of the three complexes. Within that general context, two particular issues may be worthy of special mention here.

- First, the two silicate complexes offered the rare opportunity to study a wide range of Si-undersaturated and Si-oversaturated rocks that are closely related in space and time, and to examine whether there is possibly a genetic relationship between the two types of magma.

- Second, some of the accumulated isotopic data afford scope to elaborate on existing estimates of the age of the Province. Previous isotopic data (Allsopp *et al.*, 1979) have suggested that the intrusive ages of the complexes vary in the range 500Ma to 550Ma.

The carbonatite complex is also of special interest because of the rarity of known carbonatites and the known association with them of high concentrations of the Rare Earth elements and niobium. In this particular complex an additional feature of interest is the unusually pronounced late-stage enrichment in manganese.

1.2 The Regional Geological Setting.

The rocks into which the intrusive phases of the Kuboos - Bremen Province were emplaced preceded those phases by 200My to 1500My (Hartnady *et al.*, 1985; Tankard *et al.*, 1982; Allsopp *et al.*, 1982; Reid, 1979a and 1979b; Kröner and Blignault, 1976; Joubert, 1986). They are petrographically very diverse.

Rocks of the **Namaqua Metamorphic Province** of about 1000Ma to 2000Ma form the basement to the region depicted in Figure 1.1. Three subprovinces are represented:-

- the **Richtersveld Subprovince** (Reid, 1979a and b, 1982), which is the main host for the rocks under detailed study and which comprises a calc-alkaline volcanic-plutonic complex that has undergone metamorphism of low to medium grade;

- the **Gordonia Subprovince,** which includes high-grade gneisses that are in tectonic contact with the northern edge of the Richtersveld Subprovince; these gneisses host the remainder of the rocks under study;

- and the **Bushmanland Subprovince,** which also includes high-grade gneisses in tectonic contact with the Richtersveld Subprovince - in this case along the southern edge.

The **Gariep Group** comprises a deformed geosynclinal assemblage. It crops out in the south of the region where it obscures much of the contact between the Richtersveld and Bushmanland Subprovinces. Pegmatites that intrude the Bushmanland Subprovince indicate a maximum age of 950Ma to 1000Ma for the Group (Nicolaysen and Burger, 1965).

The **Nama Group** (Germs, 1972) crops out sporadically throughout the region and comprises a stable platform sequence that is complementary to the Gariep Group. It is dominated by clastic sediments and dolomites and lies unconformably on rocks of the Namaqua Metamorphic Province. Intrusion of these sedimentary rocks by magmas of the Kuboos - Bremen Igneous Province indicates a *minimum* age of 500Ma to 550Ma (Allsopp *et al.*, 1979). Ages of around 550Ma to 650Ma would be consistent with paleontological and paleomagnetic data (Tankard *et al.*, 1982).

The **Kuboos - Bremen Igneous Province** is not orientated parallel to any known tectonic feature of the foregoing crustal elements (Martin, 1965), although it intrudes all of them. Rocks in the Province demonstrate a wide compositional range from granite to nepheline syenite. Those of felsic composition predominate; although most of the complexes remain to be studied in detail it seems highly unlikely that mafic rock types will be found to be more than 5% of the total exposure of the Province. Granites and Si-oversaturated syenites dominate the Province to the southwest, forming the Swartbank, Kuboos and Tatasberg Plutons. Si-undersaturated rocks become proportionally more important to the northeast. The presence of the Marinkas Kwela Carbonatite Complex - the only carbonatite complex known in the Province - more or less rounds out the full compositional spectrum of rock types generally associated with intra-continental alkaline magmatism.

The Swartbank and Kuboos Plutons, which crop out over much larger areas than do the other complexes, appear to be the deepest-seated intrusions in the Province. Of the remainder, Middlemost (1967) and Blignault (1977) demonstrated intrusive contact between the Younger Bremen Complex and rocks of the Nama Group: and during the course of the present study, numerous xenoliths of Nama dolomite were observed in two of the complexes studied (Plate 1.1). Because deposition of the Nama Group and development of the Province appear to have been more or less synchronous within the range 500Ma to

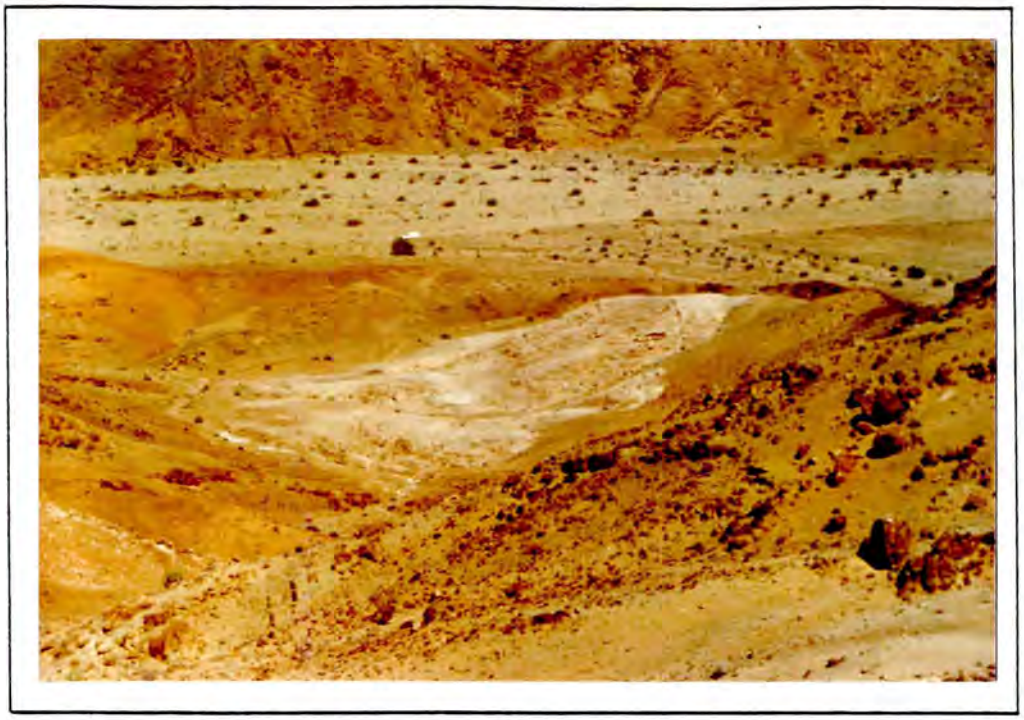

Plate 1.1 View looking west, approximately 1.5km northeast of the Orange River, within the most southerly of the two silicate complexes. The circular white outcrop central to the plate is a xenolith of Nama dolomite.

650Ma (see above), and because maximum thickness of the Nama Group in the general region is only 2500m (Tankard *et al.*, 1982), it follows that at least the Younger Bremen Complex and two of the complexes studied here intruded to within 2.5km of the paleosurface. Further work may establish that all or most of the other relatively small complexes north of the Kuboos Pluton are similarly epizonal.

1.3 Petrographic Nomenclature

Little to do with nomenclature of ***alkaline rocks*** seems consistent. The confusion that results extends even to the meaning of the term 'alkaline rock' itself which, in the words of Sørensen (1974), "has been used differently by different petrographers and sometimes in so vague a way that it is hard to know what is covered by the term". Sørensen (1974) advocates the definition put forward by Shand (1922) and describes alkaline rocks as those "characterised by the presence of

feldspathoids and/or alkali-pyroxenes or amphiboles" (Sørensen, 1974 p.71). It is in this petrogaphic sense that the term 'alkaline rock' will be used.

Other igneous rocks that are closely related in space and time to alkaline rocks, but contain no feldspathoids, alkali-pyroxene or alkali-amphibole, will be called ***'alkaline-related rocks'.*** Such rocks are a common and significant feature of alkaline magmatic provinces.

The rocks under study are broadly subdivided herein on a normative basis into those that are Si-undersaturated, Si-oversaturated and critically saturated. The latter contain no nepheline and very little or no quartz. More detailed subdivisions are made later where systematic variations in mineralogy and chemistry are observed among spatially related rocks. Such rocks are grouped into 'series'.

Nomenclature used for ***Si-saturated rocks*** is based on the classification scheme of Streckeisen (1976) that is reproduced in Figure 1.2. However, in order to conform with the definition of alkaline rock adopted above, a granitic or syenitic rock that contains alkali-pyroxene or alkali-amphibole, but that plots in the field of alkali-feldspar granite or alkali-feldspar syenite, will be termed 'alkali-granite' or 'alkali-syenite'. Where necessary for purposes of further distinction, the term 'alkali-granite' will be prefixed by the name of the characteristic mineral, for example, 'arfvedsonite alkali-granite'.

An attempt to clarify the nomenclature of ***Si-undersaturated rocks*** is offered in Figure 1.3. The classification scheme draws heavily on that of Streckeisen (1976), but modifications have been made to include much of the terminology which takes some account of the importance of mafic minerals in the classification of feldspathoid-bearing rocks, and has become common in the literature. Inadequacies still remain. An example which affects this study is that two types of foyaite are juxtaposed in the central part of the area under consideration, one of them showing intergranular textures and the other not. As a means of

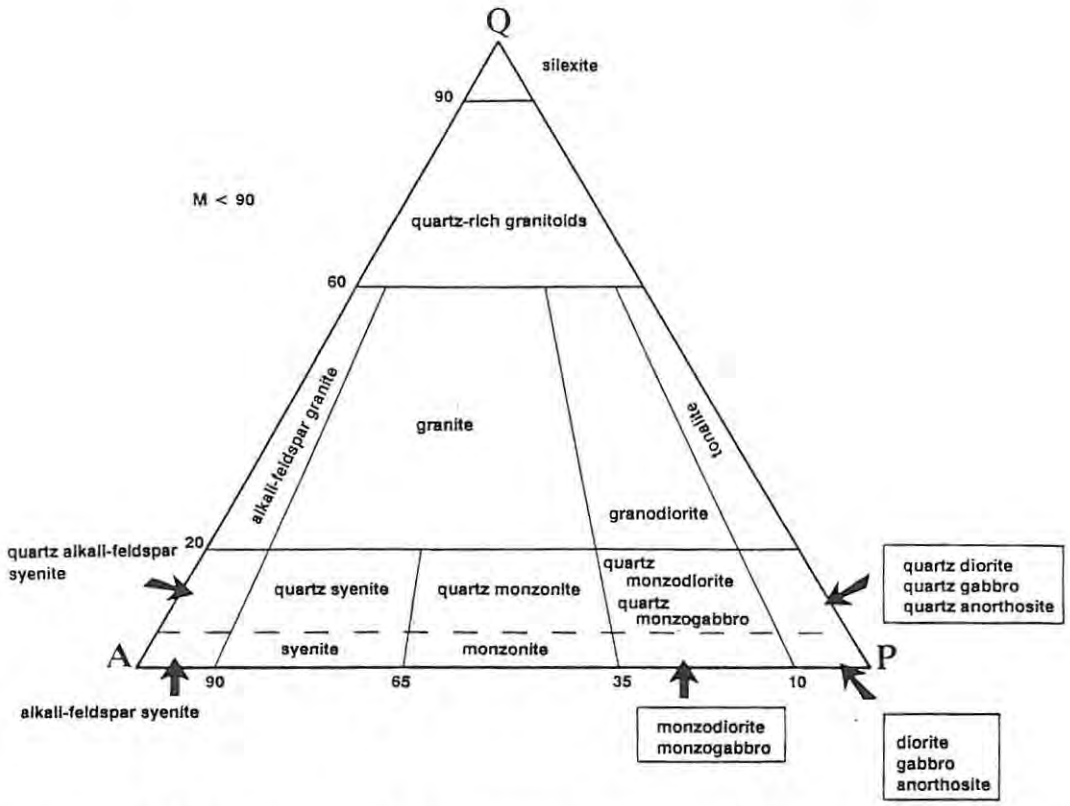

Figure 1.2 Nomenclature of Si-oversaturated igneous rocks. (After Streckeisen, 1976).

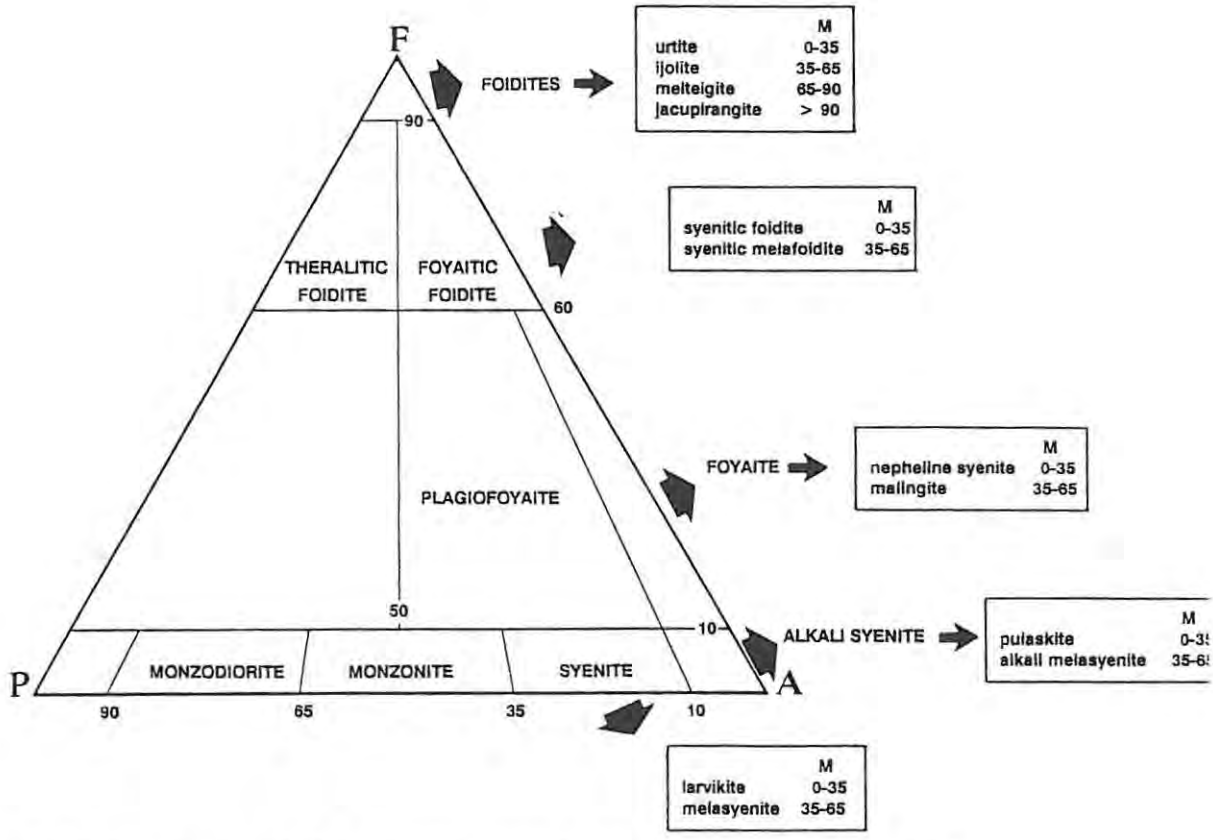

Figure 1.3 Nomenclature of Si-undersaturated igneous rocks. (Modified after Streckeisen, 1976).

distinguishing clearly between them, the former will be called 'foyaite' and the latter 'nepheline syenite'.

For the nomenclature of ***carbonatites,*** the classification scheme of Streckeisen, as advocated by Le Bas (1987), will be followed. Coarse-grained calcite-rich carbonatite will be termed 'sôvite', dolomite-rich carbonatite will be termed 'beforsite' and, where Fe-rich carbonates dominate the mineralogy, the rock will be termed 'ferrocarbonatite'.

CHAPTER 2 : GENERAL GEOLOGY AND FIELD RELATIONSHIPS

2.1 Introduction

In the Kuboos-Bremen Province as a whole, the proportion of Si-undersaturated rocks increases from southwest to northeast (Chap.1). The reverse, however, can be the case in individual complexes. Reid (in press) first demonstrated this in respect of the Kanabeam Complex. In addition, Reid (pers. comm.) recognised that, in the central portion of the Province, the intrusive sequence from Si-undersaturated in the southwest, to Si-oversaturated in the northeast, is repeated along *three* loci of intrusion, namely, Grootpenseiland and Marinkas Kwela as well as Kanabeam.

This broad observation by Reid is demonstrated in detail in Figure 2.1 which presents field data gathered during the course of this study. Northeast from the vicinity of Grootpenseiland, silicate rocks crop out continuously for a distance of about 15km. A sequence from Si-undersaturated to Si-oversaturated is evident over the first 5km and manifests itself again over the next 10km. This repetition is the basis for recognising the presence of two discrete intrusive complexes.

More specifically, in each complex the sequence of intrusion from southwest to northeast is as follows: (1) Si-undersaturated rocks crop out in the southwest; (2) outcrops of critically saturated rocks are more or less centrally located and have been intruded by dykes of Si-oversaturated rocks; and (3) a large stock of Si-oversaturated rocks crops out in the northeast. The names

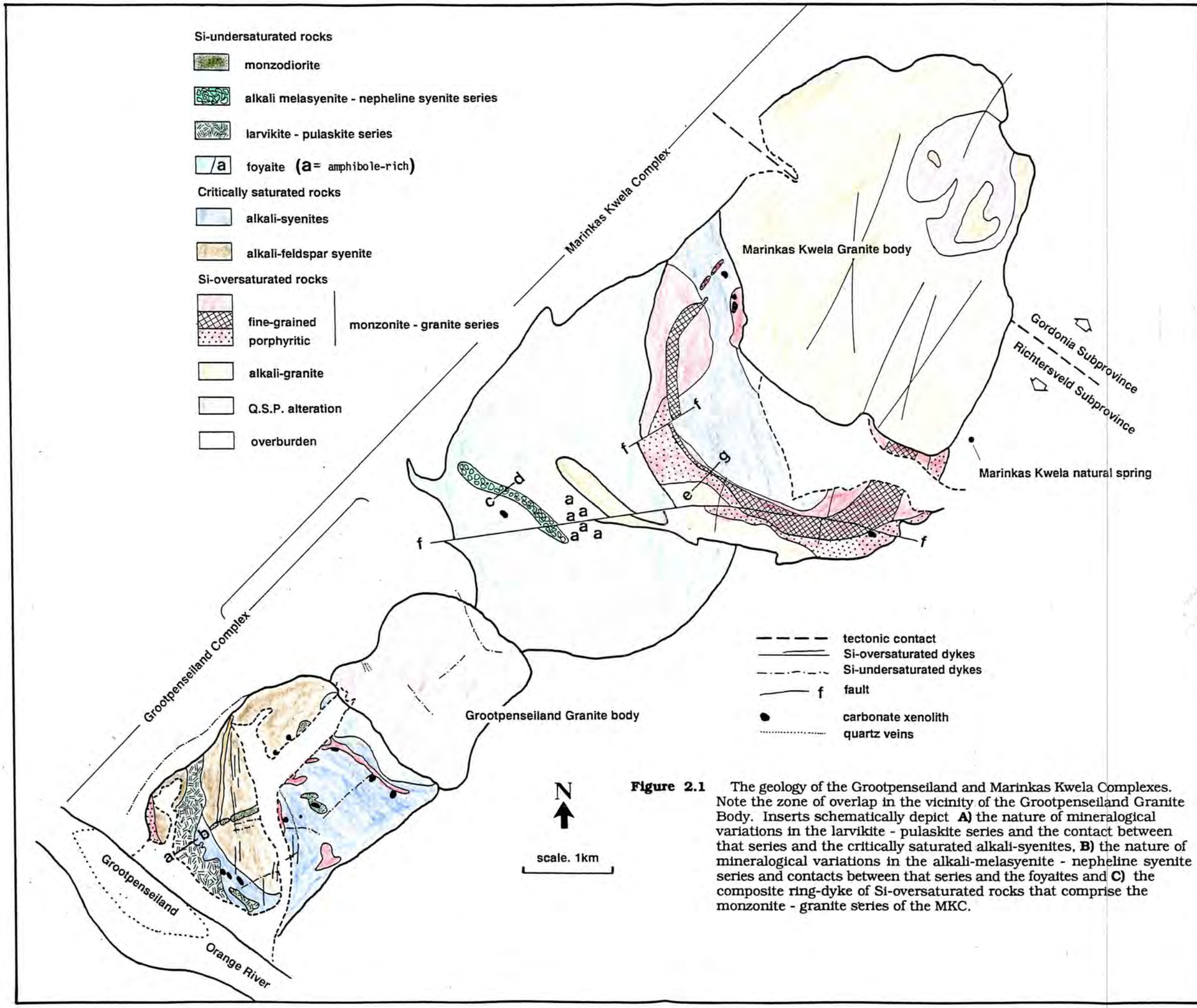

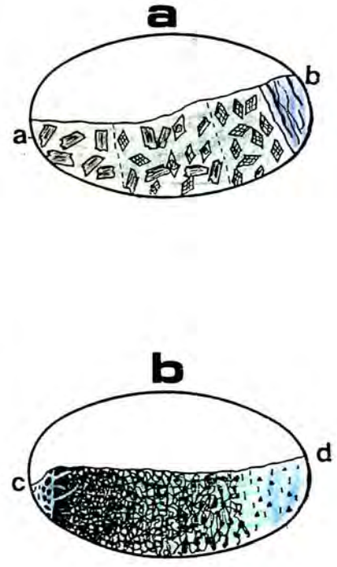

Figure 2.1 The geology of the Grootpenseiland and Marinkas Kwela Complexes. Note the zone of overlap in the vicinity of the Grootpenseiland Granite Body. Inserts schematically depict **A)** the nature of mineralogical variations in the larvikite - pulaskite series and the contact between that series and the critically saturated alkali-syenites, **B)** the nature of mineralogical variations in the alkali-melasyenite - nepheline syenite series and contacts between that series and the foyaites and **C)** the composite ring-dyke of Si-oversaturated rocks that comprise the monzonite - granite series of the MKC.

'Grootpenseiland Complex' (abbr. GPC) and *'Marinkas Kwela Complex'* (MKC) have been adopted from Reid (pers. comm. 1990); similarly, the two granite stocks will be called the ***Grootpenseiland Granite*** and the ***Marinkas Kwela Granite*** . Figure 2.1 indicates that at present outcrop level the two complexes impinge on one another with the Si-oversaturated Grootpenseiland Granite intruding Si-undersaturated rocks of the MKC.

The Marinkas Kwela Carbonatite Complex (Fig 2.2) forms a discrete intrusion to the northeast of the GPC-MKC outcrop. Its centre is about 1.5km from the northwestern edge of the MKC outcrop.

The carbonatite complex obviously lends itself to discussion as a discrete entity (Chap. 2.6). As regards the GPC and the MKC, it seems appropriate to present them together under the three headings 'Si-undersaturated Rocks', 'Critically Saturated Rocks' and 'Si-oversaturated Rocks' (Chaps. 2.3, 2.4 and 2.5 below). A principal reason for this approach is that some rock types and 'series' (see Nomenclature, Chapter 1) are common to both complexes, as Figure 2.1 illustrates. Taking them together avoids repetition and also acknowledges a possibility that some specific rock types which are common to both complexes may have been derived from common parental magmas.

Before discussing the complexes, it is necessary to refer to the general area in which they crop out, and to the country rocks. This is done in Chapter 2.2 below.

Table 2.1 (also available in loose-leaf form in an appended pocket) summarises the lithological subdivisions as well as the relative age, outcrop proportion, geographical disposition and mineralogy of the various rock types. Some data on which it draws anticipate chapters that follow, but it is useful to present the table here.

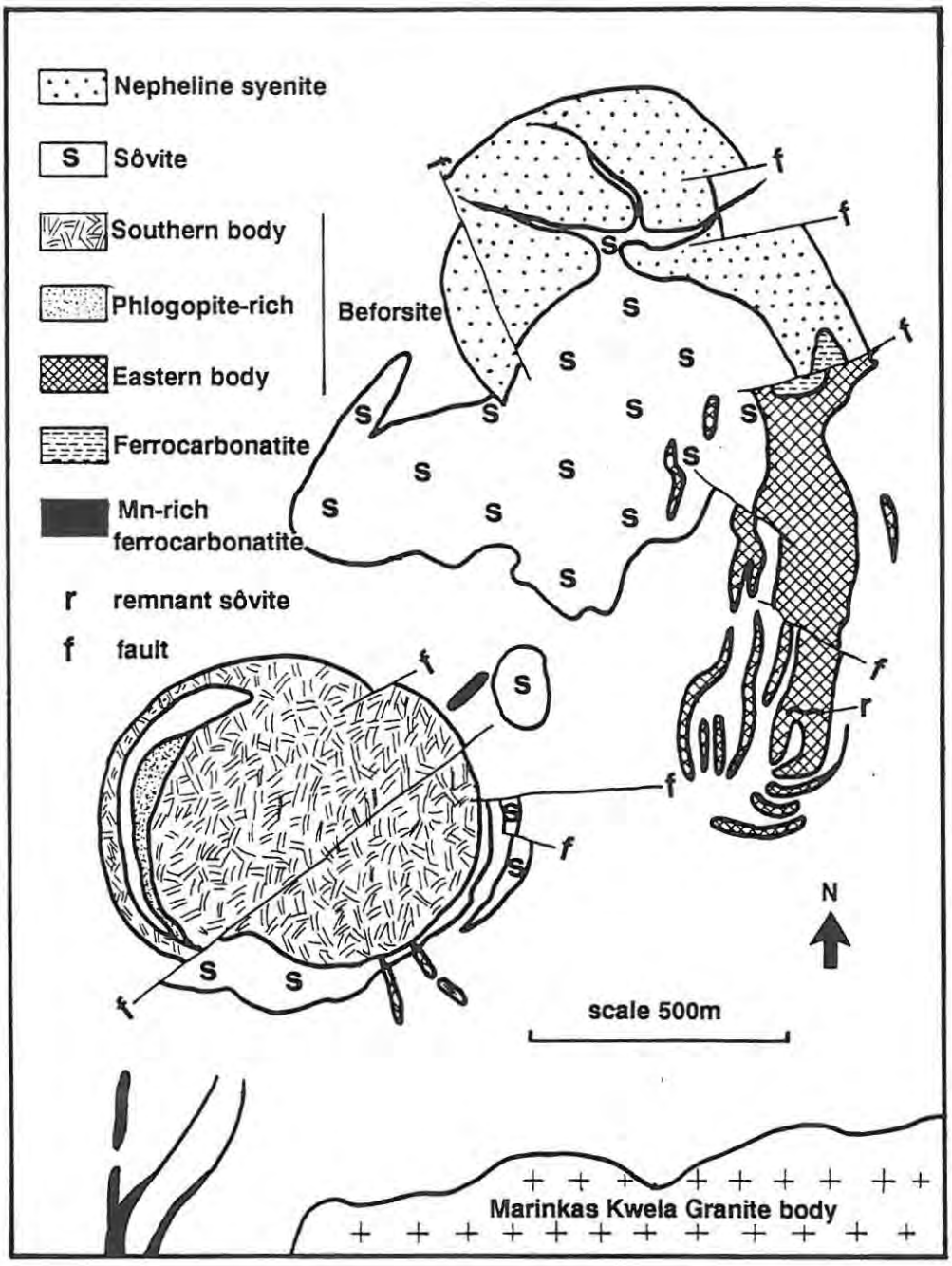

Figure 2.2 The geology of the Marinkas Kwela Carbonatite Complex. Note the locality of the 'remnant sôvite' in the southern portion of the Eastern Beforsite body. A series of E-W trending Mn-rich ferrocarbonatites also occur approximately 3-4km to the east of the Eastern Beforsite body but for reasons of scale are not depicted in this figure. (Simplified after Schommarz, 1988).

Table 2.1 Summary of field and petrographic data for the rocks of the GPC and the MKC

Rock series	Symbol used throughout this study	Relative proportion and intrusive age GPC	Relative proportion and intrusive age MKC	Relative mineral proportions	
		oldest youngest	oldest youngest	Primitive rocks	Evolved rocks
Silica undersaturated rocks					
Monzodiorites	○			plag > k-fsp > biot, amph > cpx	
Larvikite - pulaskite series	●			plag > k-fsp > biot > cpx	k-fsp > amph > cpx > ne
Alkali melasyenite - nepheline syenite series	⊠			k-fsp > plag > amph > ne > cpx, biot	k-fsp > ne > amph > cpx > so
Foyaite clinopyroxene-rich	□			k-fsp > ne > cpx, amph > so	
amphibole-rich	■				
Critically saturated rocks					
	GPC MKC				
Alkali-syenite series	◇ ◆			k-fsp >> cpx	
Alkali-feldspar syenite	☆			k-fsp	
Silica oversaturated rocks					
	GPC MKC				
Monzonite - granite series	✣ △			plag, k-fsp > biot > cpx	k-fsp > amph > cpx
(feldspar porphyries)	▲				
(Grootpenseiland Granite)	✚				
Alkali-granites (Marinkas Kwela Granite)	× × ✳			k-fsp > cpx > amph	

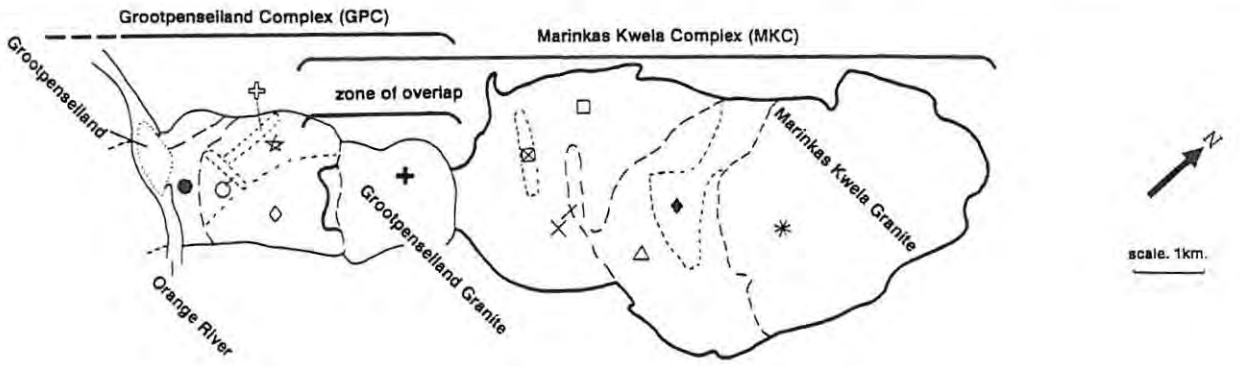

2.2 The General Area And The Country Rocks

The place-names adopted for the complexes - Grootpenseiland and Marinkas Kwela - relate respectively to an island in the deeply incised valley of the Orange River (Plate 2.1.), and to a natural spring that emerges at the base of an escarpment at a point approximately 9km northeast of the island (Plate 2.2). Both plates demonstrate the rugged terrain which is characteristic of the general area. For the most part, a very arid climate ensures moderately good outcrop exposures, although many of the steeper slopes are covered by scree.

All rocks of the GPC and most rocks of the MKC intrude leucocratic rocks belonging to the Vioolsdrif suite of the Richtersveld Subprovince. The far northern part of the MKC also intrudes across the tectonic transition zone separating the Richterveld Subprovince from the quartzofeldspathic gneisses of the Gordonia Subprovince. The latter is host to the Marinkas Kwela Carbonatite Complex, which is the only one of the three complexes with which extensive country-rock metasomatism is associated. Elsewhere, contacts are commonly sharp and no chilled margins are observed.

2.3 Silica-undersaturated Rocks Of The GPC And MKC

Under this heading fall two rock series and two further rock types which crop out as shown in Figure 2.1

(1) Medium-grained and melanocratic ***monzodiorite*** constitutes a discontinuous elongated body of about 700m by 20m in the southwest of the GPC, where it is hosted by critically saturated rocks.

(2) Leucocratic rocks form a series that evolves from medium-grained ***larvikite*** to medium- to coarse-grained

Plate 2.1 View looking eastwards up the Orange River valley showing Grootpenseiland in the foreground.

Plate 2.2 View looking northeast at the sharp escarpment that defines the southeastern edge of the Marinkas Kwela Granite. At the base of this escarpment, and to the south, rises a natural spring referred to as 'Marinkas Kwela'.

pulaskite. They occur in a thin, irregular outcrop in the far southwest of the GPC, mostly within 200m of the Orange River. These rocks are also hosted in critically saturated rocks. Numerous small contorted inclusions of monzodiorite with long axes up to 0.5m were found at several localities in the larvikite-pulaskite outcrop.

(3) A series grading from ***alkali-melasyenite*** to ***nepheline syenite*** crops out in a band which, located in the southwest of the MKC, measures about 2km by 200m and has a roughly east-west orientation. The rocks are generally coarse-grained and range from melanocratic to leucocratic. The body they form is surrounded by-

(4) ***foyaites***, which crop out extensively in the southwestern one-third of the MKC.

Three main lines of field evidence suggest that, with the exception of the foyaites, these Si-undersaturated rocks may be xenoliths or screens.

- The monzodiorite displays no chilled margins whether in contact with critically saturated rocks or forming inclusions in rocks of the larvikite - pulaskite series.

- The larvikite - pulaskite body is intruded by small dykes of the critically saturated alkali-syenite (Chap 2.4 below) that surrounds it. Furthermore, it grades from biotite-rich larvikite in the south to amphibole-rich pulaskite in the north, and the compositional planes exhibited in this gradation are more or less parallel to the steeply-dipping contacts between the larvikite - pulaskite body itself, and the alkali-syenite (Inset A of Fig 2.1).

- A similar phenomenon is evident with regard to the alkali-melasyenite - nepheline syenite body *vis-à-vis* the foyaites.

In this case, the southern margin of the body consists of fine-grained alkali- melasyenite. Gradation occurs northwards into coarse-grained nepheline syenite and the compositional planes are more or less parallel to a steeply-dipping southern contact (Inset B of Fig 2.1). Close to that contact, moreover, alkali-melasyenite xenoliths up to 1m in diameter lie in the foyaite (Plate 2.3). Further discussion of the relationship between the body of alkali-melasyenite - nepheline syenite and the foyaites, including the northern boundary where the nepheline syenite abuts foyaite, is best left until petrographic and chemical evidence has been considered (Chaps. 3 and 5).

The **foyaites** are predominantly coarse-grained and highly leucocratic. They can broadly be subdivided into clinopyroxene-rich and amphibole-rich varieties. The former are more common. They occur mainly to the northeast of the Grootpenseiland Granite,

Plate 2.3 Outcrop of foyaite (leucocratic phase in left of plate) and alkali-melasyenite of the alkali-melasyenite - nepheline syenite series (melanocratic rock in the right of plate). Note the rounded xenoliths formed by the latter within the foyaites.

but a small outlier surrounded by GPC rock types also occurs to the southwest of the Granite. The amphibole-rich variety is found only in the central part of the foyaite outcrop and in small, late-stage dykes which intrude that outcrop.

2.4 Critically Saturated Rocks Of The GPC And MKC

Two critically saturated rock types were found - alkali-feldspar syenite which is confined to the GPC, and alkali-syenite which is found in *both* complexes.

The ***alkali-feldspar syenite*** is medium- to coarse-grained and leucocratic. Most specimens have been highly altered, probably during later intrusions of granitic dykes. The rock weathers easily and outcrops are poor. Perthite is the dominant phase and the mafic mineral assemblage changes from biotite-rich near the southwestern edge of the GPC, to amphibole-rich in the central part. Pegmatitic pods and bands occur sporadically.

Alkali-syenites compose a large portion of the GPC; they also crop out in a small, centrally located area of the MKC (Fig 2.1). These highly leucocratic rocks are very inhomogeneous in texture, sometimes ranging from fine-grained to very coarse-grained across a single outcrop. Very coarse-grained granular varieties occur in topographically higher parts of the central and northeastern portions of the GPC. The rocks may demonstrate discontinuous and contorted layering on a scale of up to 30cm. The layers alternate from highly felsic and coarse-grained to less felsic and fine-grained. The fine-grained layers show a distinctive alignment of feldspar parallel to the banding.

The two critically saturated rock types were often difficult and sometimes impossible to distinguish from one another *in the field* but, as later chapters will show, some important differences exist between them, notably in their mafic mineral composition

(Chapter 4) and in their geochemistry (Chapter 5). The contact between the two types in the GPC proved elusive in the field. It probably lies under overburden in a river channel that, running north to south, bisects the GPC outcrop area (Fig. 2.1).

The contact between the alkali-syenites of the GPC and the foyaites of the MKC is sharp and near vertical. Foyaite appears to have intruded alkali-syenite, but the irregular nature of the contact leaves some uncertainty about the relationship.

2.5 Si-oversaturated Rocks Of The GPC And MKC

Si-oversaturated rocks compose nearly half the outcrop of the GPC. In the MKC, the proportion is even larger (Fig 2.1). There is a wide range of alkaline-related rock types, some of them common to both complexes. Alkali-granite also occurs in both complexes. It should be noted that, in terms of rock type, the two granite stocks are different: the Grootpenseiland Granite falls into the alkaline-related group whilst the Marinkas Kwela stock is alkaline

2.5.a Alkaline-Related Rocks: The Monzonite - Granite Series

The range of Si-oversaturated alkaline-related rocks in the MKC is wider than in the GPC. It extends from mesocratic monzonite through syenite and granite to highly leucocratic alkali-feldspar granite. The rocks occur in a sequence of circular dykes that overlap to form a wide ring-dyke in which the most evolved rock type - alkali-feldspar granite - forms a discontinuous outer envelope. The rocks are mostly hypidiodmorphic granular and of medium to coarse grain-size. Complicating the picture are both fine-grained and porphyritic varieties. Respectively these occur within and around the ring-dyke (see Inset C, Fig. 2.1) and represent subsequent circular dykes. The absence of chilled

margins along the contacts in the ring-dyke suggests that the intrusions followed one another fairly rapidly.

The most extensive exposure of alkaline-related rocks in the GPC is that of the Grootpenseiland Granite. The stock that it forms has an outcrop-area of about 4km^2. Sharp intrusive contacts with foyaite are evident to both the northeast and southwest. The stock is overwhelmingly of alkali-feldspar granite and is extensively altered. Also found in the GPC are rocks in the range granite to alkali-feldspar granite (and of both hypidiomorphic granular and porphyritic texture) which crop out in the form of numerous small plugs and northerly-trending dykes within critically-saturated rocks (Chap. 2.4).

All of the foregoing alkali-related rock types (*i.e.*, the full range monzonite to alkali-feldspar granite occurring in the MKC, and the limited part of that range that occurs in the GPC) are grouped in this study under the general heading of **'monzonite - granite series'**. As will be shown in subsequent chapters, this grouping is consistent with mineralogical and chemical similarities between rocks of the GPC and equivalent types in the MKC. But it must also be noted that the inclusion of the Grootpenseiland Granite in the 'series' hinges on only one fresh sample. No other fresh samples of this stock were found.

2.5.b Alkali-granites

Leucocratic and medium- to coarse-grained rocks in the compositional range of alkali-granite make up the remainder of both complexes and can be sub-divided into two varieties.

The **Marinkas Kwela Granite** forms a stock covering about 12km^2 in the far north of the complex and shows sharp contacts with all the rocks it intrudes. It is made up mostly of hypidiomorphic granular varieties containing aegirine-augite ±

arfvedsonite. Quartz-feldspar porphyries also occur; they are found in topographically higher parts of the granite body where they are virtually devoid of mafic minerals and associated with hypidiomorphic granular varieties that are similarly leucocratic. Additionally, in the north-east corner of the body an ovoid depression of about 2km^2 marks a zone of intense alteration characterised by a pervasive assemblage of quartz + sericite + pyrite (Plate 2.4).

Aegirine-augite alkali-granite occurs in both complexes. In the GPC it is found in plugs and northerly-trending dykes which cross-cut the more numerous plugs and dykes of alkali-feldspar granite (noted above) in the southwestern part of the complex. The rock represents the youngest intrusive phase observed in the GPC. It is leucocratic and medium- to coarse-grained. In the MKC, aegirine-augite alkali-granite crops out in the central part of the complex along the southern edge of the ring-dyke discussed above. It displays sharp intrusive contacts both with foyaite and with porphyries of the monzonite - granite series.

Plate 2.4 Highly fractured yellow rock typical of quartz-sericite-pyrite alteration of the Marinkas Kwela Granite.

2.6 The Marinkas Kwela Carbonatite Complex

The Marinkas Kwela Carbonatite Complex crops out over an area of about 2.5km^2 and trends in a northeastern direction (Fig 2.2). It consists of a series of intrusions that have fenitised the gneissic country rock to form an aureole up to 500m in width. The complex pre-dates the Marinkas Kwela Granite, since the latter crops out within the aureole but is unfenitised. A **porphyritic nepheline syenite** that is intruded, fenitised and brecciated by carbonatite (Schommarz, 1989), and which crops out in the north of the area (Plate 2.5), represents the first recognisable event in the evolution of the complex.

Four main types of **carbonatite** can be recognised in the complex.

(1) **Sövite** crops out over a large and topographically low area in the centre of the complex. It is clearly the earliest of the carbonatite intrusions. The sôvite body appears to have been built by numerous magma pulses as evidenced by sharp contacts between mineralogically distinct sôvites (Plate 2.6). Amphibole and/or clinopyroxene crystals are sometimes elongated perpendicular to these contacts. According to Nash (1972) and Barker (1989), such features indicate chilled margins. Both silicate-poor and silicate-rich sôvites are present but the complex nature of the body does not allow the sequence of intrusion to be identified. Le Bas (1977) has observed that early sôvites in the Homa Bay area of western Kenya appeared to have "soaked into the country rocks", and the same description seems applicable to the contact between the sövite and the gneissic country rock at Marinkas Kwela.

(2) **Beforsites** occur in the south of the complex as a circular intrusion and along the eastern margin as an elongated intrusion (Fig. 2.2 and Plate 2.5). Both bodies are

Plate 2.5 View looking south-southwest at the Marinkas Kwela Carbonatite Complex. Rubble outcrop in the foreground is of nepheline syenite, the two dark outcrops are of beforsite, while the light coloured and topographically low portion shown in the centre of the plate is sôvite.

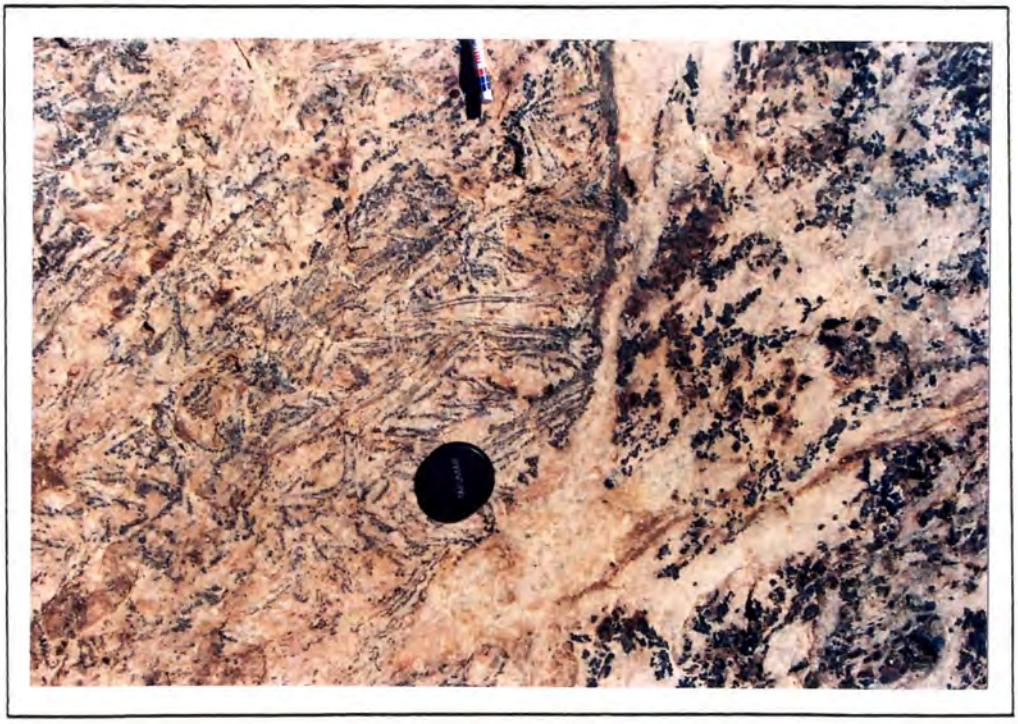

Plate 2.6 Outcrop of sôvite showing a contact between clinopyroxene-rich sôvite (left) and amphibole-rich sôvite (right).

topographically prominent and have dark brown weathering surfaces. Three features of the ***southern beforsite*** body that distinguish it from the eastern beforsite are: (i) its magnetite-rich character; (ii) the lack of flow textures; and (iii) the presence of abundant phlogopite adjacent to fenitised xenoliths of country-rock. The abundant magnetite occurs both as veins and as irregular blebs ranging from less than 1mm to many metres in diameter (Plate 2.7). In contrast, the ***eastern beforsite*** body is poor in magnetite; it exhibits contorted flow-banding defined by narrow layers that are rich in apatite; and the xenoliths it contains are of sôvite, some of which are apatite-rich and flow-banded. (In Chapter 11 these xenoliths will be called 'remnant sõvites'.) Flow-banding in the eastern beforsites roughly parallels the northerly trend of the body itself and commonly shows abrupt terminations, suggesting that the body is a multiple intrusion of numerous individual dykes.

Plate 2.7 Outcrop of southern beforsite showing abundant magnetite blebs (dark spots).

(3) **Ferrocarbonatite** occurs as rare, randomly orientated dykes in the northern portion of the eastern beforsite body. The rock is rich in magnetite. No flow-banding was observed in the field.

(4) **Mn-rich Ferrocarbonatite** forms dykes which are radial to both the beforsite bodies but do not intrude either. The dykes are up to 3m thick, discontinuous, highly brecciated and covered by a distinctive dark weathering surface.

Together, sövites and beforsites account for more than 90% of the outcrop, and ferrocarbonatite and Mn-rich ferrocarbonatite for less than 5% each. The presence of Mn in such a high concentration is highly unusual, but otherwise the proportions of the rock types in the complex are consistent with those described by Le Bas (1987) for carbonatite complexes in general.

2.7 Summary Conclusion

A *provisional* sequence may be summarised as follows:-

A. .In the GPC:-

- the earliest intrusive phase is represented by Si-undersaturated monzodiorite
- this was followed by intrusion of Si-undersaturated larvikite-pulaskite, which contains xenoliths of monzodiorite and is penetrated by dykes of critically saturated alkali-syenite
- unclear from the evidence so far presented is the relationship between the two critically saturated rock types,*viz,* the alkali-syenites and the alkali-feldspar syenite

- next to be emplaced were Si-oversaturated rocks in the range granite to alkali-feldspar granite, plugs and dykes of which intrude both the critically saturated rock types

- Si-oversaturated alkali-granites were the last to be emplaced. Dykes containing these rocks cross-cut those of granite to alkali-feldspar granite.

No *direct* evidence was found to place the Grootpenseiland Granite in this sequence but, because the rock falls in the range granite to alkali-feldspar granite, it might provisionally be allocated a place in or close to the penultimate stage.

B. In the MKC:-

- the earliest phase of which evidence remains is probably the Si-undersaturated series alkali-melasyenite - nepheline syenite, comprising a xenolith or screen within

- foyaites.

- The ring-dyke composed of rocks in the Si-oversaturated monzonite - granite series post-dates both the foyaites and the critically saturated alkali-syenites of the MKC.

- Finally, Si-oversaturated alkali-granites intruded, *inter alia,* the monzonite - granite series.

The chronological position of the alkali-syenites *vis-à-vis* the foyaites remains uncertain on the evidence so far presented.

C In the Marinkas Kwela Carbonatite Complex, the sequence is as follows: nepheline syenite, sövite, beforsite, and ferrocarbonatite/Mn-rich ferrocarbonatite.

D. .Relationships *between* the complexes

- The Marinkas Kwela Carbonatite Complex pre-dates the Marinkas Kwela granite of the MKC.

- The Si-oversaturated Grootpenseiland Granite of the GPC intrudes and post-dates the Si-undersaturated foyaites of the MKC. The latter *may* post-date the critically saturated alkali-syenites of the GPC; if they do, an implication *may* be that phases of the GPC are generally older than analogous phases of the MKC. Against that, the evidence in this chapter does not eliminate the possibility that some or all of the rock types common to both complexes (*viz*, alkali-syenite and alkali-granite together with those rock types falling in the range granite - alkali-feldspar granite in the monzonite - granite series) represent co-genetic magma series.

The next eight chapters deal with the silicate rocks. Detailed discussion of the carbonatites follows in Chapters 11 and 12.

CHAPTER 3: PETROLOGY OF THE SILICATE ROCKS

Three silicate rock series, and five further major silicate rock types, were defined in Chapter 2. Such diversity is not unknown elsewhere in the Kuboos - Bremen Province. Reid (in press) describes eleven major lithologies in the nearby Kanabeam Complex. This chapter is restricted to the petrological characteristics of the silicate rocks. A few brief references will be made to mineral compositions, but the main discussion of mineral chemistry is reserved for Chapter 4

Although epizonal intrusions commonly show a large degree of alteration, zones of intense alteration are not common in the GPC and MKC. The petrology of the few altered rocks that occur scarcely warrants separate treatment and will be discussed in the concluding section of this chapter.

3.1 Si-undersaturated Rocks

3.1.a Monzodiorite

No significant mineralogical differences were observed between samples of monzodiorite from xenoliths in the larvikite - pulaskite series, and samples from the larger body of monzodiorite which is surrounded by critically saturated rocks.

The rock consists essentially of subhedral to euhedral phenocrysts of calcic plagioclase (An_{80-58}) and diopside which are set in a groundmass of plagioclase (An_{20-5}), alkali-feldspar, diopside, biotite and ferroan pargasite. Plagioclase phenocrysts are up to 1.2cm across. Their cores are altered to sericite and prehnite. The

phenocrysts of diopside are up to 0.9cm across; some are rimmed by amphibole while others consist of a complex vermicular-like intergrowth of diopside and biotite. Rare phenocrysts of ferro-kaersutite and biotite also occur. Sphene is a common accessory phase and occurs as large wedge-shaped phenocrysts or as a medium- to coarse-grained interstitial phase which commonly rims magnetite and groundmass diopside. Apatite commonly forms stout prismatic grains up to 2mm in diameter which sometimes occur as inclusions in phenocrysts of other minerals.

3.1.b The Larvikite - Pulaskite Series

Rocks in this series exhibit hypidiomorphic granular textures. The dominant felsic constituent is braid-microperthite. Plagioclase (An_{56-10}) occurs only in larvikite (Fig 3.1), mostly as cores to microperthite. Nepheline occurs only in pulaskite where it is a minor component (up to 10%) lying interstitially between feldspar laths (Plate 3.1). The ratio of felsic to mafic constituents increases only slightly from larvikite to pulaskite.

The gradation from biotite-rich larvikite to amphibole-rich pulaskite has already been noted in Chapter 2. Amphibole (ferroan pargasite to hastingsite) can often be seen to rim biotite, particularly in the larvikite (Plate 3.2), although both minerals also occur as discrete subhedral to euhedral grains. Diopside is a common subhedral phase in both larvikite and pulaskite and is sometimes rimmed by amphibole.

Fine- to medium-grained magnetite occurs as subhedral grains which are often rimmed by sphene or biotite. Sphene is abundant (±2%) and forms inclusions within amphibole and biotite. Apatite is also abundant (± 2%); a coarse-grained prismatic variety is associated with the mafic phases, while a fine-grained acicular variety is commonly enclosed within feldspar. Accessory zircon and fluorite occur throughout, commonly in association with mafic minerals. A

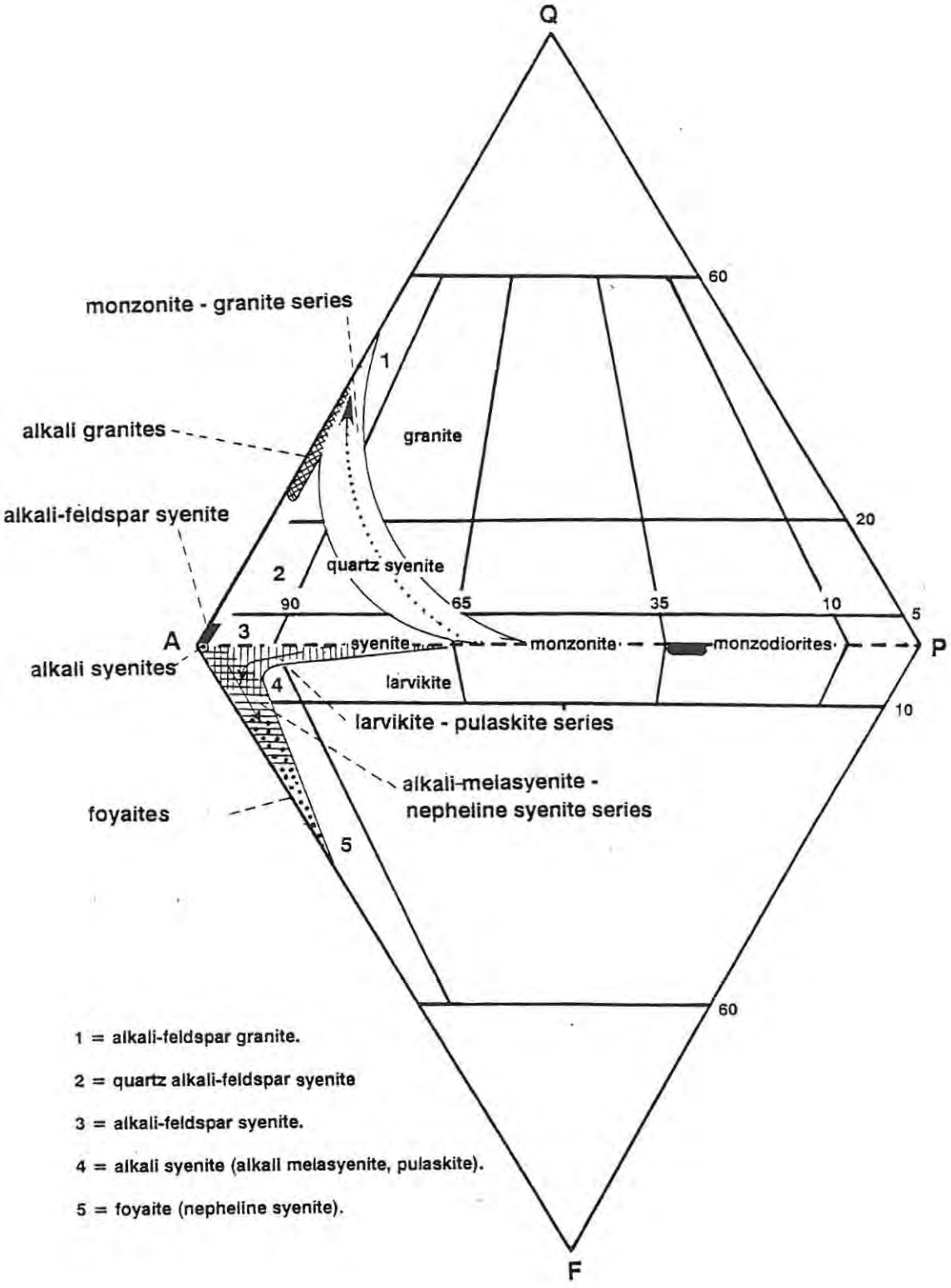

Figure 3.1 Classification scheme for Si-oversaturated and Si-undersaturated rocks (simplified after Streckeisen, 1976) schematically showing the compositional range of the various series and rock types found in the GPC and MKC.

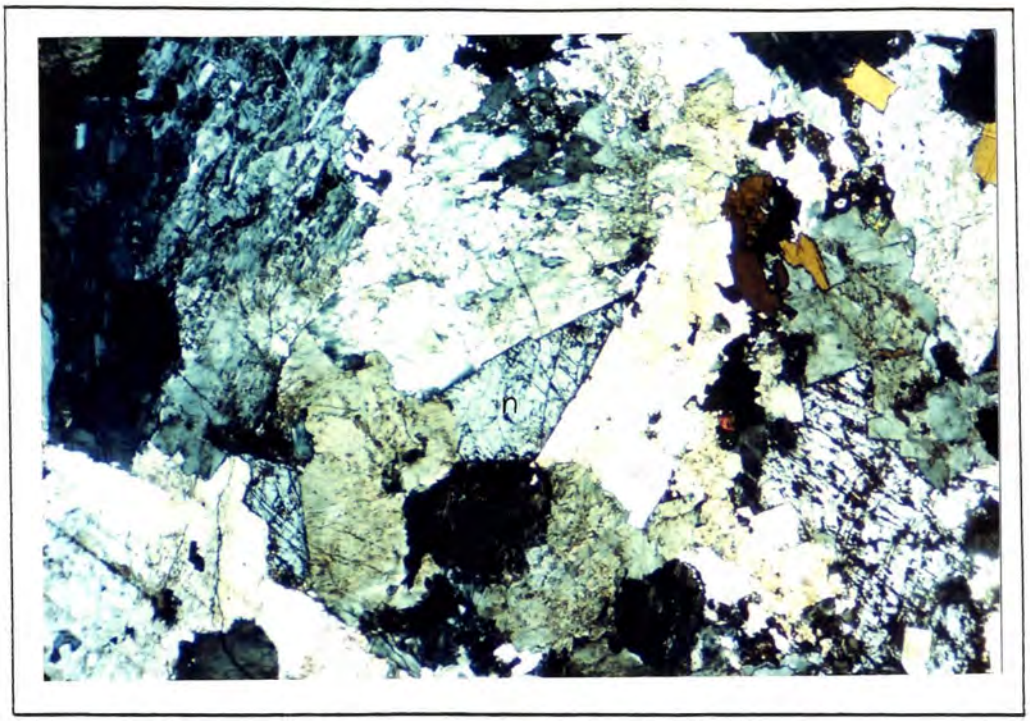

Plate 3.1 Photomicrograph showing the interstitial habit of nepheline (**n**) in pulaskites. (XP, x20).

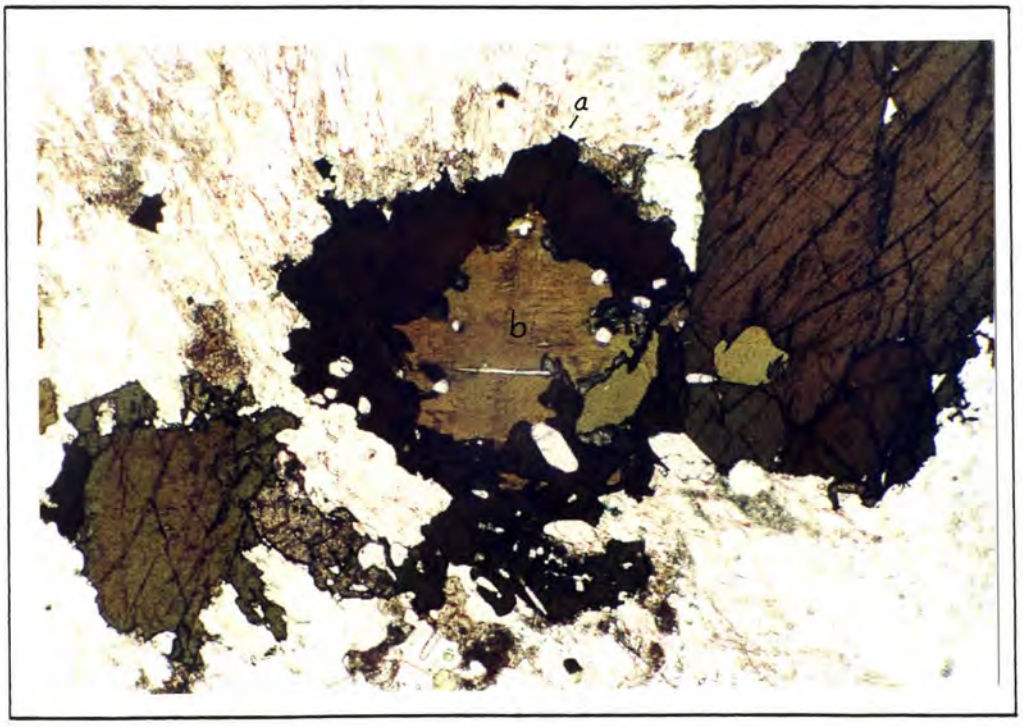

Plate 3.2 Photomicrograph of larvikite, showing a sequence of crystallisation from biotite (cores - '**b**') to amphibole (rims - '**a**'). (PPL, x20). The same crystallisation sequence from biotite to amphibole is observed within the series, from larvikite to pulaskite.

brown acicular mineral, tentatively identified later (Chap. 4.8.d) as bastnaesite, forms a rare accessory phase.which is usually enclosed within nepheline. The abundance of sphene and apatite decreases from larvikite to pulaskite, and that of the brown acicular mineral increases. (For the latter, the term '?bastnaesite' will be used in further references. Optically, its features are consistent with those of bastnaesite.)

3.1.c The Alkali-melasyenite - Nepheline Syenite Series

Rocks of this series are predominantly coarse-grained (although a fine-grained variety was noted in Chapter 2). The more mafic rocks have a mottled, intergranular appearance (Plate 3.3) produced by mafic aggregates lying within a framework of coarsely perthitic alkali-feldspar having a grain-size of 0.2 - 1.0cm. Plagioclase (An_{12-5}) is rare. Although ferroan pargasite is the dominant mafic phase, diopside and biotite (both rimmed by the amphibole) also occur, as do small grains of magnetite. The aggregate phases commonly show a granoblastic polygonal texture consisting of triple junctions, and are poikilitically enclosed by large grains of intergranular nepheline (Plate 3.4). Large (± 3mm) grains of prismatic apatite, large (± 2mm) anhedral grains of sphene, and accessory zircon are associated with the mafic phases, while ?bastnaesite forms inclusions in nepheline and feldspar.

The nepheline syenite has a hypidiomorphic granular texture. In the most evolved samples, sodian hedenbergite is abundant and shows reaction relationships with amphibole. The gradation noted in Chapter 2 from alkali-melasyenite to nepheline syenite (Fig. 3.1) is marked by the increase in the proportion of modal nepheline from ±5% to ±15%, and the rapid disappearance of plagioclase. A decrease also occurs in the modal proportion of mafic phases, from ±35% to ±10%, and these phases tend to occur as large discrete grains rather than as aggregates. Aegirine-augite is ubiquitous as a late

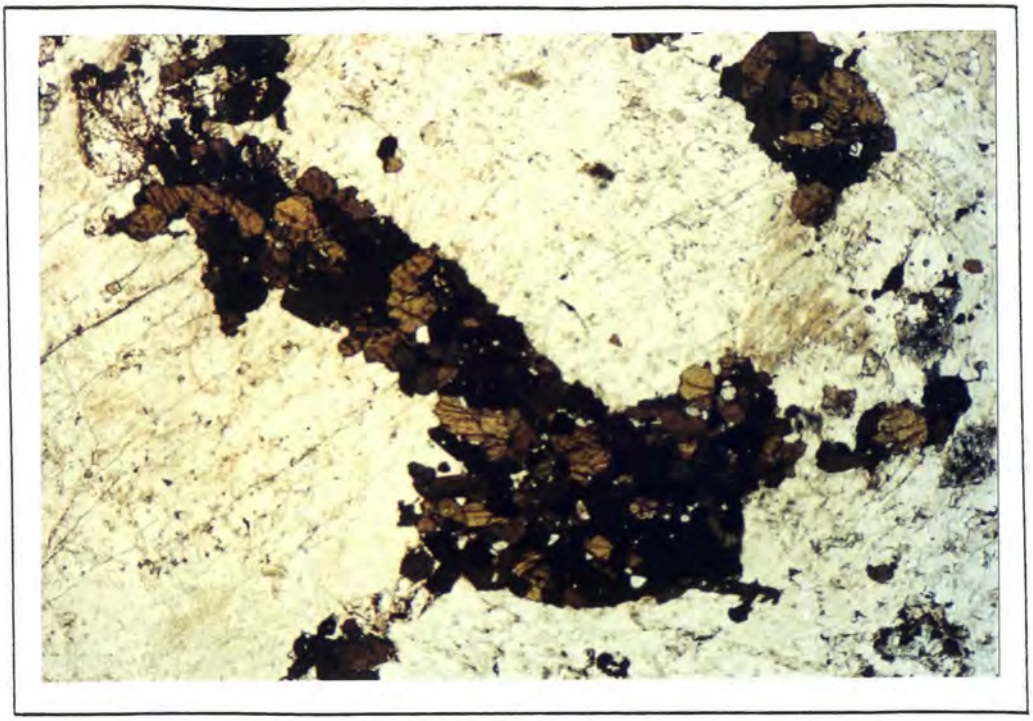

Plate 3.3 Photomicrograph showing the mottled appearance of the alkali-melasyenites, produced where aggregates of amphibole (dark phases) lie interstitially to perthite(light phases). (PPL, x20).

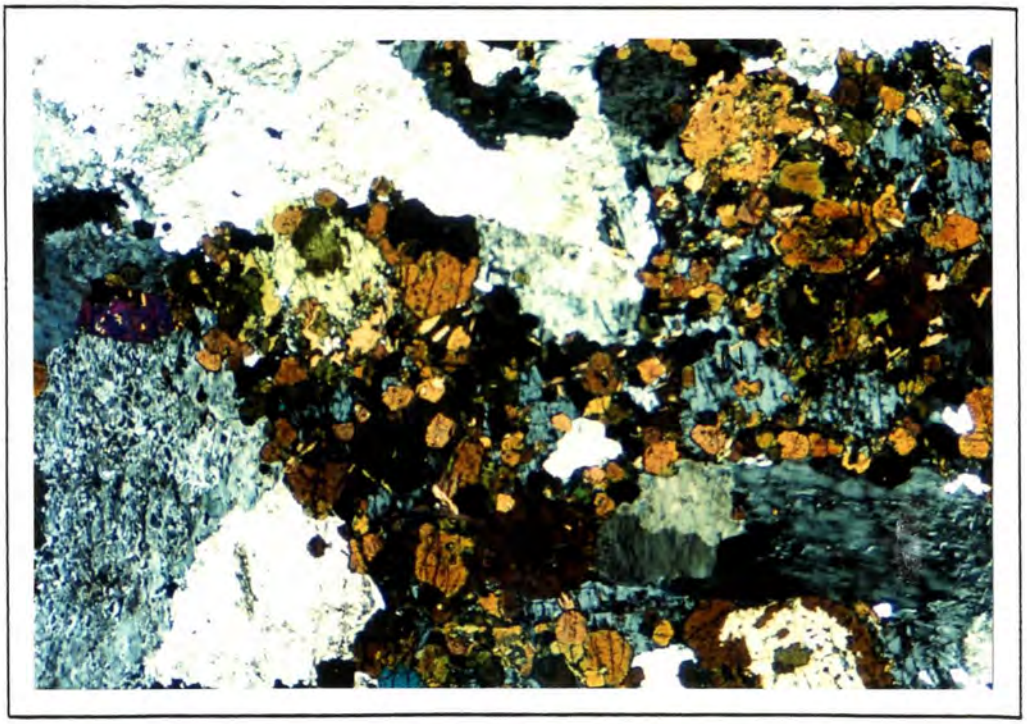

Plate 3.4 Photomicrograph of a rock from the alkali-melasyenite - nepheline syenite series, showing amphibole poikilitically enclosed within nepheline (**n**). (XP, x20).

crystallising phase, and often surrounds amphibole or, rarely, magnetite.

Partial recrystallisation of the rock is suggested by the presence of coarse exsolution features in alkali-feldspar and the granoblastic polygonal textures of the aggregates. The latter features could, alternatively, be the result of rapid nucleation of primary amphibole.

3.1.d The Foyaites

Textural features were cited in Chapter 1 (under 'Nomenclature') as the basis in this study for distinguishing 'nepheline syenite' from foyaite. As was noted in Chapter 2, these two rock types are in contact along the northern boundary of the alkali-melasyenite - nepheline syenite body. The foyaites all show intergranular textures characterised by a network of tabular perthite grains that are randomly orientated or show slight preferential alignment (Plate 3.5). As noted above, the nepheline syenite has a hypidiomorphic granular texture.

The foyaites were broadly subdivided in Chapter 2.3 into clinopyroxene- and amphibole-rich varieties. In the former, diopside to sodian hedenbergite is commonly the sole mafic phase, but it is sometimes extensively rimmed by amphibole. In the amphibole-rich variety, hastingsite to taramite is commonly the sole mafic phase; biotite may occur as very minor inclusions in the amphibole or as late-stage reaction rims around magnetite. Late-stage aegirine-augite commonly rims amphibole in the amphibole-rich foyaite but is rare in clinopyroxene-rich foyaite.

The two types of foyaite demonstrate a common felsic mineralogy in which braid-microperthite is the dominant constituent; the mineral may show additional exsolution in the form of thin albite rims. Inhomogeneous patch-microperthite is developed in foyaite that contains abundant sodalite. Nepheline ranges in abundance from

10% to 25% (Fig.3.1), and lies interstitially to feldspar except in some specimens of sodalite-bearing foyaite where subhedral to euhedral nepheline occurs. Where present, sodalite also lies interstitially to feldspar, and sometimes represents a reaction product of nepheline (Plate 3.6). Both nepheline and sodalite may show partial to complete alteration to natrolite.

Fine- to medium-grained magnetite occurs as subhedral grains which are often rimmed by sphene or biotite. Sphene and apatite are rare accessory phases. Accessory fluorite occurs in both kinds of foyaite, usually in association with mafic minerals, and ?bastnaesite is also found enclosed within feldspar and nepheline.

3.2 Critically Saturated Rocks

3.2.a The Alkali-feldspar Syenite

In this rock type, braid-microperthite may compose as much as 90% of total constituents. The braid-microperthite is commonly very turbid and often sericitised. Oligoclase-albite is a rare (<3%) exsolution product from alkali-feldspar. Biotite is the main mafic phase (<10%) in the least evolved samples, and may form clusters of large radiating plates (Plate 3.7), up to 4cm in diameter, that are partially rimmed by magnetite. In the more evolved rocks, amphibole is the main mafic phase. Diopside is rare but always present. Sphene, apatite, fluorite and zircon are accessory phases but all are extremely rare - there is an unusually low proportion of accessory minerals in these rocks. Also of significance is that interstitial quartz occurs in some samples, especially in the pegmatitic bands noted in Chapter 2.4; the implications of this will be discussed in Chapter 8.2.

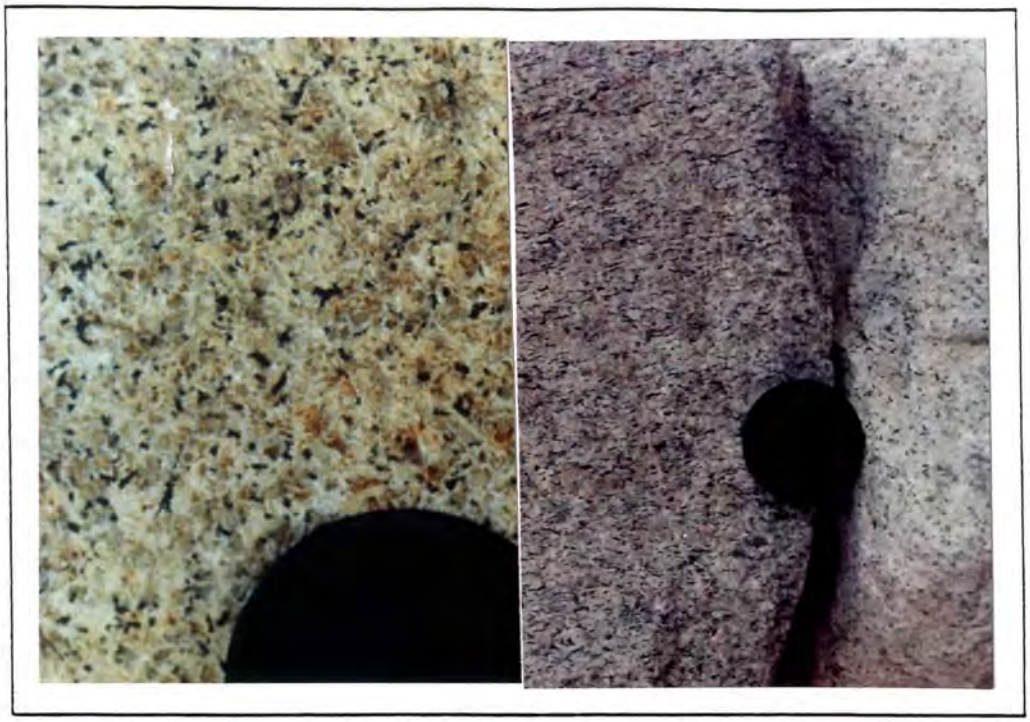

Plate 3.5 Textural variation of foyaite. The plate on the left shows the more common intergranular, or 'foyaitic', texture produced where nepheline (now partly altered and red-brown in colour) lies in a network of tabular perthite grains. The plate on the right shows a foyaite with a foliation produced by alignment of perthite (and hence also of interstitial amphibole).

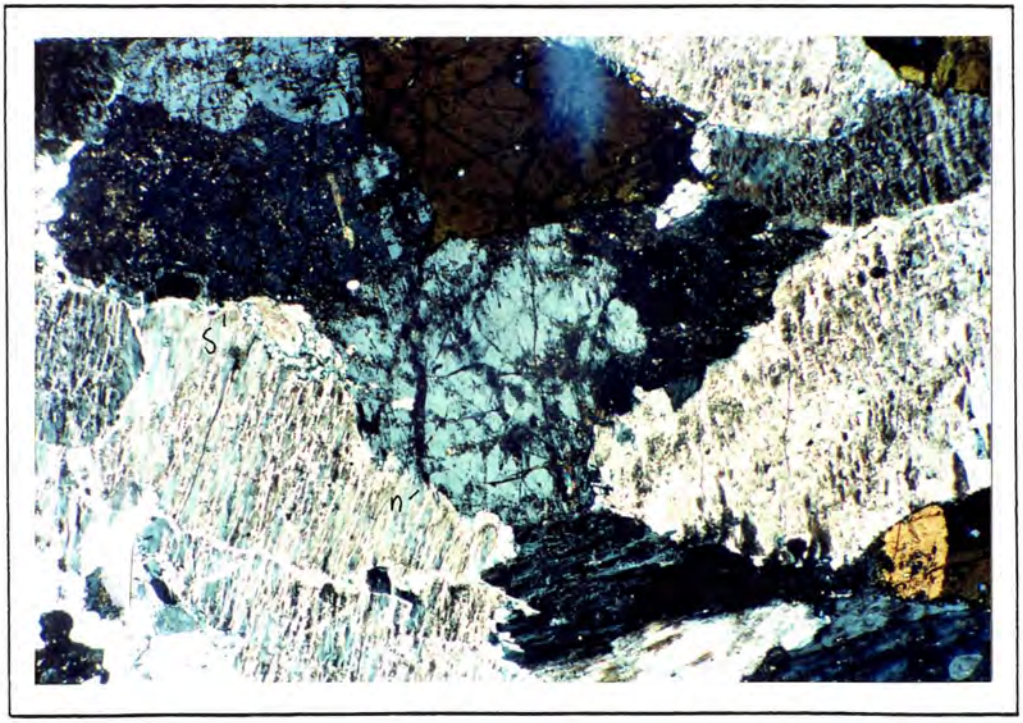

Plate 3.6 Photomicrograph showing alteration of nepheline (**n**) to sodalite (**s**) in a nepheline syenite. (XP, x20).

3.2 b The Alkali-syenites

These rocks contain up to 95% subhedral to euhedral microperthite, commonly of a very inhomogeneous patch variety. Amphibole (hastingsite to katophorite) is the dominant mafic constituent, followed by annite > aegirine-augite > magnetite, with accessory zircon, fluorite, allanite and an unidentified inclusion within amphibole. Subhedral to anhedral grains of amphibole lie interstitially to feldspar and, in extreme cases, may enclose it poikilitically. Biotite forms rims around magnetite and also occurs in amphibole as a patch-like intergrowth with aegirine-augite. The abundance of magnetite varies inversely to that of amphibole, and the magnetite may occur in any one of four modes: (1) as a late interstitial phase; (2) as a rim surrounding amphibole; (3) as intergrowths with other mafic minerals; or (4) as subhedral grains at feldspar grain boundaries. Zircon occurs as anhedral grains moulded interstitially around feldspar and, less commonly, as subhedral grains up to 3mm in size or (Plate 3.8).

Mineralogically, the layers that constitute the discontinuous and contorted banding noted in Chapter 2.4 differ only in the relative proportions of minerals.

Relationships between microperthite grain-boundaries suggest that the alkali-syenites underwent limited low-temperature re-equilibration. The albite exsolution lamellae in the microperthite commonly extend into, and replace, K-feldspar lamellae of neighbouring microperthite grains. Pollard (1983), studying rocks of granitic composition, termed similar textures 'swapped rims' and invoked sub-solidus albitisation as the cause. The same interpretation is suggested here.

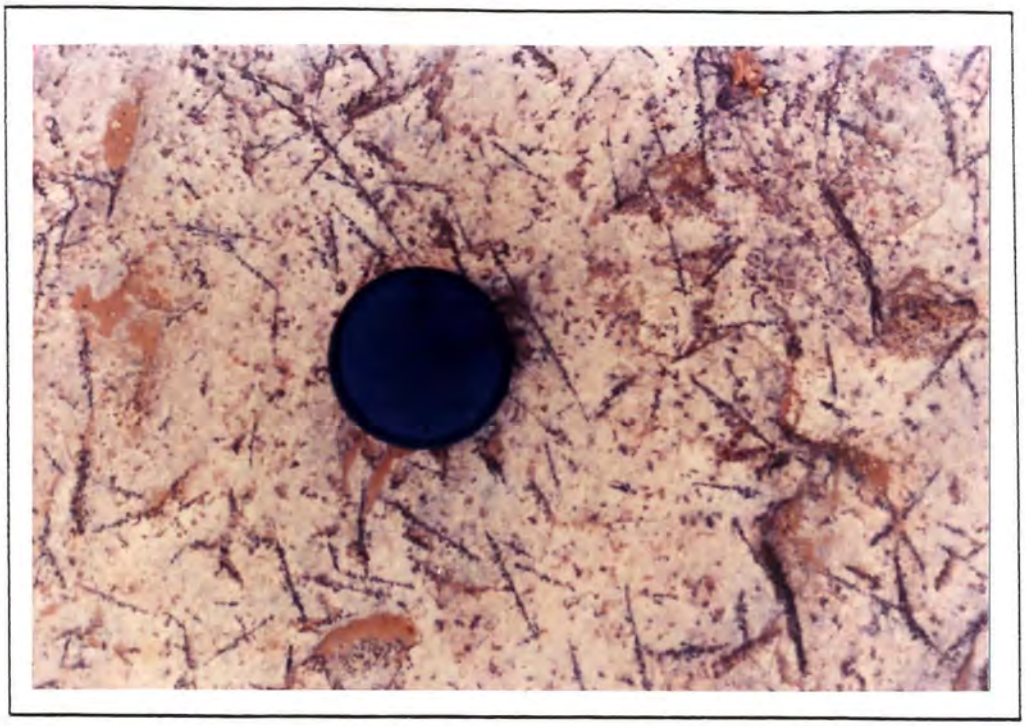

Plate 3.7 Alkali-feldspar syenite showing, in plan view, the large plates of biotite.

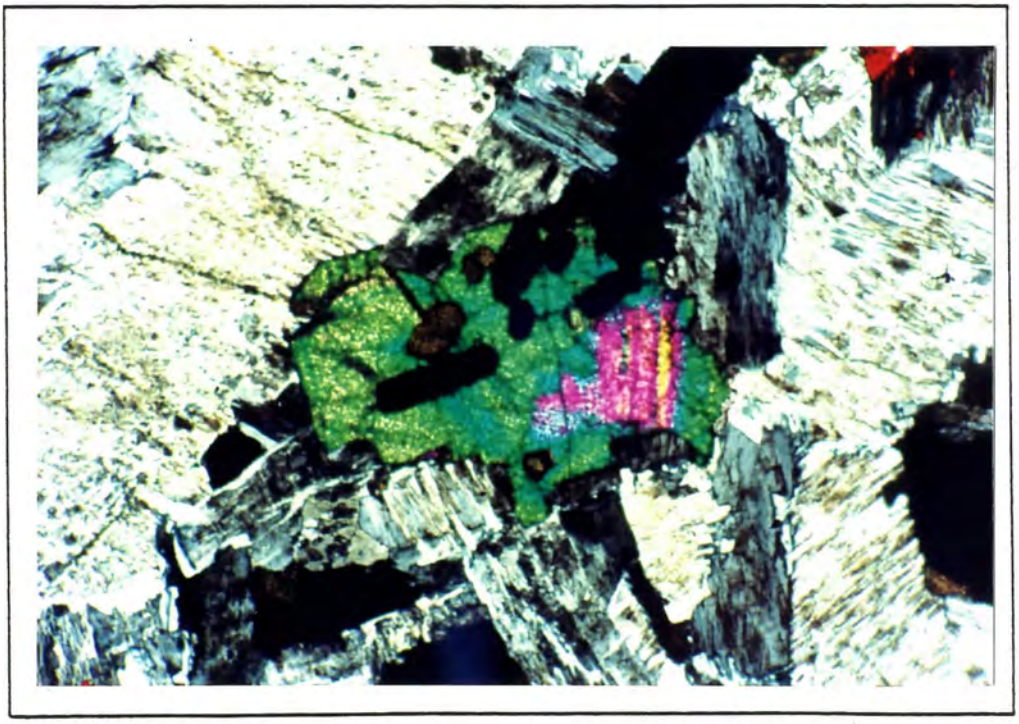

Plate 3.8 Photomicrograph of alkali-syenite showing a large grain of zircon enclosing euhedral grains of amphibole. (XP, x20).

3.3 Si-oversaturated Rocks

3.3.a The Monzonite - Granite Series

Under this heading are included all of the alkaline-related rocks of both complexes, *i.e.*, the full range monzonite to alkali-feldspar granite that occurs in the MKC, and the limited part of that range that occurs in the GPC. A reason for grouping them together in the one 'series' is that the relevant GPC rock types (granite to alkali-feldspar granite) prove, on thin section analysis, to be identical in mineralogy to corresponding types in the MKC.

Braid-microperthite is always the most abundant mineral. It occurs both as suhedral to euhedral grains, and as extensive rims around plagioclase. Numerous small but discrete blebs of albite also occur within microperthite, and 'swapped rims' are common between neighbouring microperthite grains. Plagioclase exhibits compositional zonations from calcic cores to sodic rims. The cores of plagioclase are commonly sericitised and may contain small inclusions of biotite. Quartz lies interstitially to feldspar and ranges in abundance from accessory proportions in monzonite to 30% in alkali-feldspar granite.

Amphibole (ferro-tschermakite to ferro-edenite) is usually the most abundant mafic phase. It is commonly subhedral and may contain cores of altered diopside. Biotite is common and occurs either as inclusions within the amphibole, or as discrete subhedral to euhedral grains which are sometimes partially rimmed by magnetite.

Sphene and apatite are abundant accessory phases only in the less evolved rocks whereas zircon and allanite are abundant accessory phases only in the more evolved rocks. Zircon occurs mostly as small euhedral grains along feldspar or quartz grain-boundaries, or as inclusions in amphibole, biotite or feldspar. Accompanied by apatite, zircon also occurs in fine fractures and may contain inclusions of

microperthite (Plate 3.9). Allanite is usually an anhedral interstitial phase up to 2mm in size. It may partially rim amphibole or biotite, or poikilitically enclose small grains of microperthite (Plate 3.10). Zoned euhedral allanite occurs only in the most evolved alkali-feldspar granite. Fluorite occurs in accessory proportions.

The porphyritic varieties in the series contain aggregates and phenocrysts of braid-microperthite and plagioclase, the latter commonly having sericitised cores and microperthite rims. The phenocrysts are anhedral (angular) to euhedral. Compositionally, these 'feldspar porphyries' are syenites and granites *sensu stricto*, and differ mineralogically from the hypidiomorphic granular types only in having slightly higher proportions of modal amphibole.

The fine-grained varieties in the series have been highly altered and consist of up to 80% quartz. Biotite and magnetite are the only mafic phases.

3.3.b The Si-oversaturated Alkaline Rocks

The alkali-granites have hypidiomorphic granular textures. Their mineralogy is dominated by subhedral to euhedral microperthite, and they contain up to 25% quartz which forms clusters of subhedral to anhedral grains. In the alkali-granite of the Marinkas Kwela Granite body, the microperthite is of a coarse patch variety (sometimes microcline microperthite) which is commonly rimmed by clear albite. This patch-microperthite distinguishes the Marinkas Kwela Granite from other alkali-granites in the two complexes. In these latter rocks - *i.e.*, those occurring as dykes in the south of the GPC and in the centre of the MKC - the microperthite is of a braid variety.

Mafic minerals crystallise interstitially to feldspar. Aegirine-augite is the most common phase. Once again there is a difference between the alkali-granite of the Marinkas Kwela Granite body, and alkali-

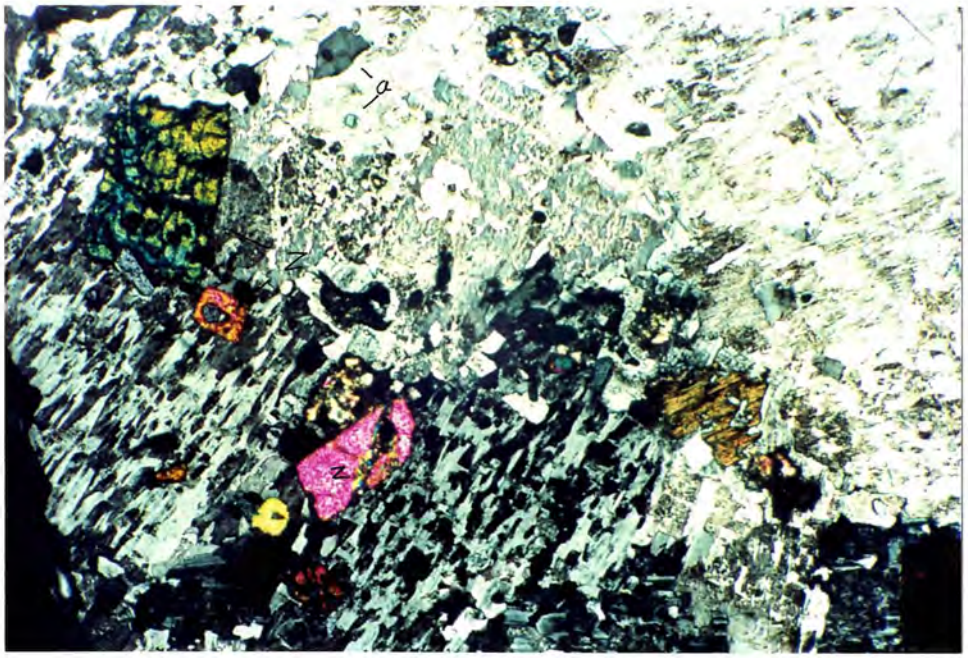

Plate 3.9 Photomicrograph of a granite from the monzonite - granite series of the MKC, showing numerous grains of zircon (**z**) and apatite (**a**). Although not obvious from the photomicrograph, the portion of the sample shown has been slightly fractured. Both zircon and apatite concentrate along those fractures. (XP, x20).

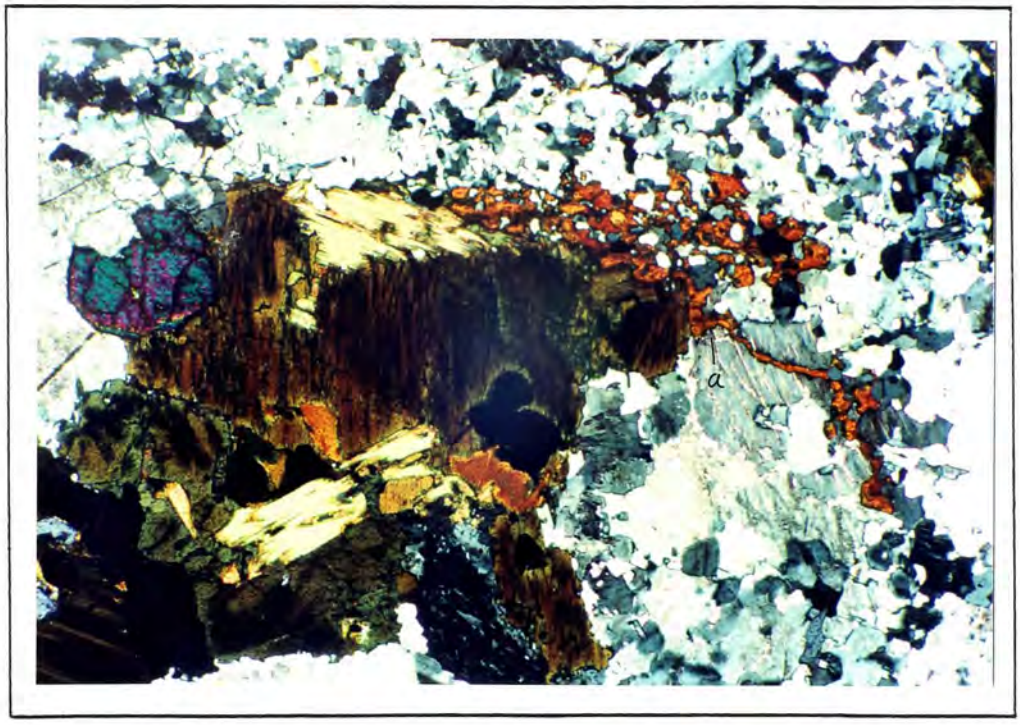

Plate 3.10 Photomicrograph of alkali-feldspar granite from the monzonite - granite series of the MKC, showing late-stage allanite (**a**) poikilitically enclosing grains of perthite and quartz. (XP, x20).

granites elsewhere in the two complexes. In the Marinkas Kwela Granite, aegirine-augite is commonly accompanied by arfvedsonite or, rarely, by ferro-winchite rimmed by riebeckite. In the other alkali-granites, ferro-winchite is the predominant amphibole.

Fluorite is the most common accessory phase, and is commonly associated with mafic phases, particularly arfvedsonite. Apatite, zircon and magnetite are extremely rare accessory phases (or are absent).

The quartz-feldspar porphyries that occur in the Marinkas Kwela Granite body (see Chap. 2.5) contain phenocrysts (up to 3mm) and aggregates of quartz and microperthite. The groundmass consists of a fine-grained mixture of quartz, braid-microperthite, minor albite, aegirine-augite and arfvedsonite as well as accessory magnetite, zircon, allanite and sphene. Aegirine-augite and arfvedsonite commonly form clots which may enclose groundmass phases.

3.4 Petrology Of Altered Silicate Rocks

3.4.a The Si-undersaturated And Critically Saturated Rocks

Alteration of these rocks is apparent up to 20 metres away from major intrusions of the Si-oversaturated rocks, but in most other cases the alteration aureoles are considerably narrower. In the Si-undersaturated rocks, nepheline and sodalite are transformed to natrolite. In both groups of rocks, microperthitic exsolution lamellae become more coarse, feldspars become turbid, and distinct grains of albite exsolve from microperthite. In some rocks, microveins filled with albite and aegirine-augite ± quartz are common, and brecciation may occur in extreme cases. The most intense alteration observed is in the clinopyroxene-rich foyaite where it is in contact with the Grootpenseiland Granite.

3.4.b The Si-oversaturated Rocks

The large quartz-sericite-pyrite zone in the Marinkas Kwela Granite body is the most conspicuous example of alteration in either complex. The zone shows evidence of two styles of alteration: carbonatisation and quartz-sericite-pyrite (Q.S.P.) alteration.

Carbonatisation resulted in the replacement of microperthite by calcite, and of mafic phases (aegirine-augite and arfvedsonite) by chlorite, sericite and goethite. During intense carbonatisation, quartz was recrystallised into acicular aggregates with abundant interstitial calcite. Pyrite does not appear to have been formed during carbonatisation

Q.S.P. alteration followed carbonatisation and began with sericitisation of feldspar and the formation of cubic grains of pyrite (now limonite), up to 2mm in size. Extreme cases of sericitisation have resulted in the total replacement of feldspar by a fine-grained aggregate of sericite. Sericitisation was followed by partial removal of calcite (deposited during carbonatisation) and partial dissolution of quartz. A characteristic of the latter process is the presence of ghost-like rims of minute sericite flakes that penetrate into (and parallel) the outer rims of quartz grains or follow fractures in quartz grains; they may even transgress across unfractured and optically continuous quartz grains. While minor fluorite occurs in all samples, it is more likely to be an original constituent of the alkali-granites than an alteration mineral. Killick and Odell (1980) report the presence of small grains of galena in the alteration assemblages, but none was found during the present study.

Both the Grootpenseiland Granite body and the Marinkas Kwela Granite body contain highly leucocratic rocks that have been altered through partial to total replacement of mafic constituents by magnetite, goethite, K-feldspar, albite (or microperthite), quartz and

chlorite. Anhedral grains of fluorite up to 3mm in size are often associated with the altered mafic phases. In most cases, primary microperthite has become very turbid due to the presence of minute inclusions of Fe oxides. Sericitisation of feldspar has also occurred. Additionally, but only in the rocks of the Grootpenseiland Granite, progressive alteration of the mafic phases has been accompanied by transformation of patch-microperthite into microcline-microperthite and albite.

The composite ring-dyke in the MKC consists of numerous intrusive phases of hypidiomorphic granular Si-oversaturated rocks (Chap. 2.5). In these rocks, feldspars are turbid and exsolution lamellae are very coarse. In some instances, fine quartz-filled fractures occur. It seems quite likely that the effects of alteration were cumulative, with early intrusions being affected by all subsequent ones. The finer-grained and younger rock types in the ring-dyke show alteration similar to but more intensive than that described in the preceding paragraph. The alteration has resulted in an assemblage containing up to 80% quartz which occurs as fine anhedral grains. Groundmass microperthite has been partially sericitised and biotite partially to completely altered to magnetite, goethite and chlorite.

The only striking example of alkali-metasomatism of the Si-oversaturated rocks occurs at certain contacts between feldspar porphyries and alkali-granites in the MKC. Here, the alkali-granites have been transformed into a dark fine-grained assemblage of aegirine-augite, microperthite and quartz.

CHAPTER 4: MINERAL CHEMISTRY OF THE SILICATE ROCKS

4.1 Procedure

The compositions of mineral phases were determined by electron microprobe (see appendix 3). Representative analyses are presented in Tables 4.1 to 4.5, and the complete set of analyses can be found in Appendix 2. The symbols used in this chapter are in Table 2.1 (see appended pocket).

For clinopyroxene, amphibole and opaque phases, the proportions of ferric and ferrous iron were estimated on the basis of stoichiometry according to the procedure of Droop (1987). Because of the extreme stoichiometric variability of biotite, no attempt was made to estimate Fe^{3+}/Fe^{2+} ratios in that mineral. Alkali-feldspar was invariably very coarsely perthitic; consequently, some 20 to 50 analyses were made of grains in each sample, using a defocussed (50μ m) beam, and the results then were averaged.

4.2 Clinopyroxene

Clinopyroxene occurs in all unaltered rock types except the alkali-feldspar granites of the monzonite - granite series. It is mostly calcic and ranges in composition from Mg-rich diopside to Fe-rich hedenbergite (terminology after Morimoto *et al.*,1988), but compositional trends to more sodic clinopyroxene can be seen in late crystallising clinopyroxene in more evolved rock types.

Table 4.1. Average clinopyroxene analyses.

	Monzodiorite series		Larvikite - pulaskite series		alkali melasyenite - nepheline syenite series		Clinopyroxene-rich foyaites		Amphibole-rich foyaites	
	avg.	s.d.	avg.	s.d.	avg.	s.d.	avg.	s.d.	avg.	s.d.
[wt%]	n = 48		n = 96		n = 34		n = 59		n = 20	
SiO2	51.43	1.60	51.64	0.81	50.58	1.85	50.32	1.17	49.53	0.66
TiO2	0.46	0.32	0.28	0.11	0.42	0.42	0.25	0.10	0.28	0.04
Al2O3	2.29	1.53	1.10	0.34	2.23	1.98	1.38	0.32	1.13	0.19
Cr2O3	0.02	0.03	0.01	0.02	0.03	0.09	0.00	0.00	0.00	0.00
Fe2O3	5.15	1.45	3.29	1.86	5.60	1.93	8.93	6.07	10.59	3.05
FeO	3.99	2.44	9.18	2.69	6.65	2.31	10.18	3.23	13.53	1.21
MnO	0.37	0.13	0.89	0.12	0.68	0.15	1.18	0.32	1.48	0.21
MgO	12.91	1.93	10.42	1.66	10.86	3.65	5.54	2.31	2.25	1.19
CaO	23.02	1.22	22.13	0.80	21.55	3.56	18.51	5.03	15.64	2.85
Na2O	1.09	0.39	1.08	0.46	1.41	0.40	3.33	2.87	4.40	1.61
Total	100.73	0.60	100.01	0.51	100.03	0.56	99.64	0.96	98.82	0.59
Cations based on 6 oxygens									Cations based on 6 oxygens	
Si	1.90	0.05	1.96	0.02	1.91	0.07	1.96	0.03	1.98	0.03
Al	0.00	0.00	0.00	0.00	0.00	0.00	0.00	0.00	0.00	0.00
Fe3+	0.00	0.00	0.00	0.00	0.00	0.00	0.00	0.00	0.00	0.00
Al	0.10	0.07	0.05	0.02	0.10	0.09	0.06	0.02	0.05	0.01
Fe3+	0.14	0.04	0.09	0.05	0.16	0.06	0.26	0.18	0.32	0.09
Ti	0.01	0.01	0.01	0.00	0.01	0.01	0.01	0.00	0.01	0.00
Cr	0.00	0.00	0.00	0.00	0.00	0.00	0.00	0.00	0.00	0.00
Mg	0.67	0.10	0.59	0.09	0.56	0.10	0.32	0.13	0.13	0.07
Fe2+	0.07	0.08	0.26	0.10	0.17	0.08	0.33	0.11	0.45	0.04
Mn	0.00	0.00	0.00	0.00	0.00	0.00	0.02	0.02	0.03	0.02
Mg	0.04	0.06	0.00	0.00	0.05	0.15	0.00	0.00	0.00	0.00
Fe2+	0.05	0.03	0.03	0.02	0.04	0.04	0.00	0.01	0.00	0.00
Mn	0.01	0.00	0.03	0.01	0.02	0.00	0.02	0.01	0.02	0.02
Ca	0.91	0.05	0.90	0.03	0.87	0.15	0.77	0.21	0.67	0.12
Na	0.08	0.03	0.08	0.03	0.10	0.03	0.25	0.21	0.34	0.12
Total	4.00	0.00	4.00	0.00	4.00	0.00	4.00	0.00	4.00	0.00

	Alkali-syenite series		Alkali-feldspar syenite series		Monzonite - granite series		Marinkas Kwela granite body		Alkali-granite (MKS)	
	avg.	s.d.	avg.	s.d.	avg.	s.d.	avg.	s.d.	avg.	s.d.
[wt%]	n = 12		n = 11		n = 24		n = 41		n = 11	
SiO2	50.81	1.22	52.30	0.36	50.43	0.57	52.38	0.62	49.48	0.34
TiO2	0.20	0.13	0.37	0.12	0.26	0.09	1.10	0.56	0.20	0.03
Al2O3	1.12	0.78	1.00	0.22	1.05	0.53	0.26	0.07	0.19	0.04
Cr2O3	0.00	0.00	0.01	0.01	0.03	0.08	0.02	0.03	0.00	0.00
Fe2O3	16.61	7.53	0.32	0.31	3.44	0.47	25.03	5.01	5.98	0.53
FeO	11.02	6.23	11.19	0.35	10.20	2.50	4.14	3.47	20.55	0.56
MnO	1.25	0.63	0.94	0.05	0.65	0.13	0.87	0.38	1.47	0.05
MgO	0.54	0.51	11.88	0.39	9.47	1.89	0.66	0.65	1.23	0.08
CaO	10.64	5.71	20.91	0.42	23.07	0.43	5.00	3.46	15.47	0.52
Na2O	7.34	3.49	0.56	0.07	0.70	0.15	11.07	2.12	3.29	0.24
Total	99.53	0.61	99.47	0.30	99.31	0.65	100.53	1.02	97.86	0.60
Cations based on 6 oxygens										
Si	2.00	0.01	1.99	0.01	1.94	0.02	2.01	0.02	2.03	0.01
Al	0.00	0.00	0.02	0.01	0.00	0.00	0.00	0.00	0.00	0.00
Fe3+	0.00	0.00	0.00	0.00	0.00	0.00	0.00	0.00	0.00	0.00
Al	0.05	0.03	0.03	0.01	0.05	0.02	0.01	0.00	0.01	0.00
Fe3+	0.49	0.21	0.01	0.01	0.10	0.01	0.73	0.15	0.18	0.02
Ti	0.01	0.00	0.01	0.00	0.01	0.00	0.03	0.02	0.01	0.00
Cr	0.00	0.00	0.00	0.00	0.00	0.00	0.00	0.00	0.00	0.00
Mg	0.03	0.03	0.67	0.02	0.54	0.10	0.04	0.04	0.08	0.00
Fe2+	0.37	0.21	0.28	0.02	0.30	0.11	0.13	0.11	0.70	0.02
Mn	0.04	0.02	0.00	0.00	0.00	0.00	0.03	0.01	0.02	0.01
Mg	0.00	0.00	0.00	0.00	0.00	0.00	0.00	0.01	0.00	0.00
Fe2+	0.00	0.00	0.08	0.02	0.03	0.03	0.00	0.00	0.00	0.00
Mn	0.00	0.01	0.03	0.00	0.02	0.01	0.00	0.01	0.03	0.01
Ca	0.45	0.25	0.85	0.02	0.95	0.01	0.21	0.14	0.68	0.02
Na	0.56	0.25	0.04	0.00	0.05	0.01	0.82	0.15	0.26	0.02
Total	4.00	0.00	4.00	0.00	4.00	0.00	4.01	0.03	4.00	0.00

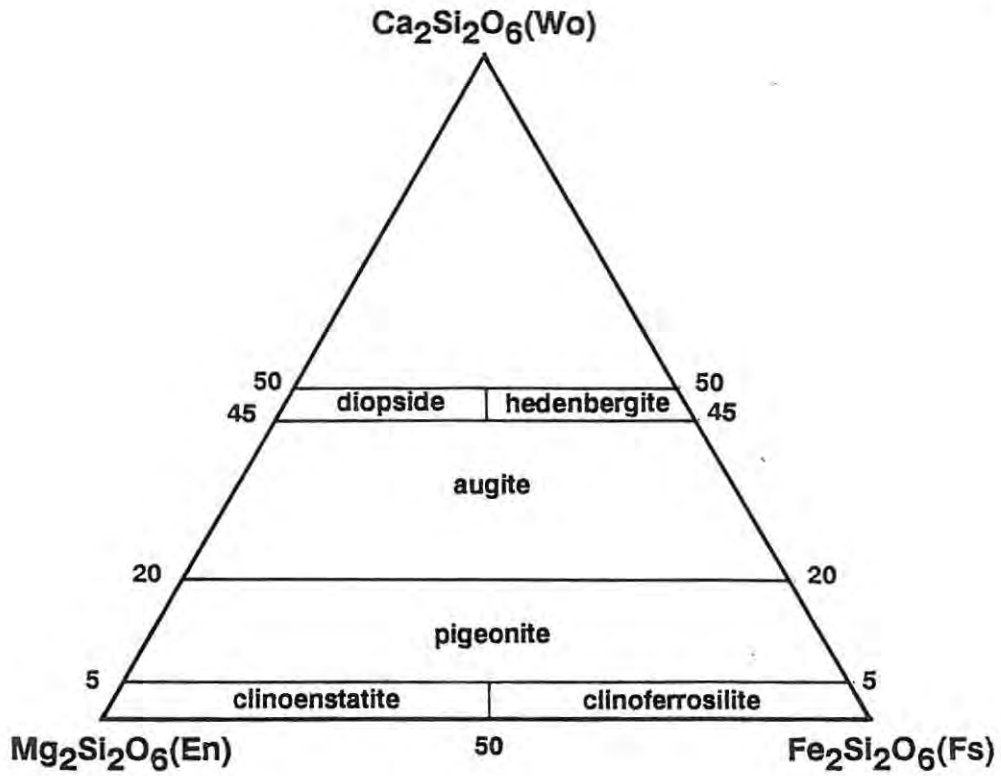

Figure 4.1 Nomenclature for clinopyroxenes (after Morimoto *et al.* 1988)

Representative analyses of clinopyroxene are presented in Table 4.1 and are reported following the nomenclature of Morimoto *et al.* (1988) (Fig.4.1).

Compositional fields of pyroxene in the Si-undersaturated rock types show extensive overlap (Fig.4.2) and become progressively more Fe-rich in the following order:-

monzodiorite	$(Ca_{42-52}Mg_{28-44}\Sigma Fe_{7-22})$
alkali-melasyenite - nepheline syenite series	$(Ca_{45-50}Mg_{25-37}\Sigma Fe_{13-30})$
larvikite - pulaskite series	$(Ca_{46-51}Mg_{16-39}\ \Sigma Fe_{13-35})$
foyaites	$(Ca_{45-47.8}Mg_{34-54}\Sigma Fe_{46-66})$.

The Mg# of clinopyroxene* in the alkali-melasyenite - nepheline syenite series and the larvikite - pulaskite series decreases in a systematic way that parallels mineralogical changes already noted in Chapters 2 and 3, *i.e.*, from alkali-melasyenite to nepheline syenite, and from larvikite to pulaskite. These trends strongly suggest that rocks in each series are internally related through some genetic process.

At compositions corresponding to $Ca_{45}Mg_{34}\Sigma Fe_{66}$, clinopyroxene in the clinopyroxene-rich foyaite shows a trend to Na-enrichment, with light green sodian hedenbergite ranging up to $\boldsymbol{Ac}_{35}$ (Figs. 4.2 and 4.3). Late-stage clinopyroxene, which mostly occurs in the amphibole-rich foyaites, is distinctly enriched in Na (up to $\boldsymbol{Ac}_{99}$). Such data are consistent with those presented by Nash and Wilkinson (1970), Stephenson (1972), Larsen (1976) and Ferguson (1978), which showed that a compositional gap occurs between Ca-rich and Na-rich clinopyroxene in rock series in which alkali-amphibole crystallises. According to Ferguson (1978), the Na-rich composition of late crystallising clinopyroxene is related to the development of a peralkaline residual melt.

While it was frequently difficult to distinguish between the two critically saturated rock types in hand specimen (Chap 2.4), they may be clearly distinguished in terms of clinopyroxene composition. In the alkali-syenites, clinopyroxene is unzoned and shows strong Na-enrichments (Fig. 4.3) from aegirine-augite ($\boldsymbol{Di_6Hd_{68}Ac_{25}}$) to aegirine ($\boldsymbol{Di_{0.3}Hd_{1.4}Ac_{98}}$). In the alkali-feldspar syenite, clinopyroxene is Na-poor, and lies within the range of augite ($Ca_{40\text{-}49}Mg_{52\text{-}58}\Sigma Fe_{40\text{-}44}$).

In terms of ***Di-Hd-Ac***, the trend defined by clinopyroxene in the Si-undersaturated rocks closely resembles trends in many other alkaline rock series (Fig. 4.3). Clinopyroxene in the Si-oversaturated rocks shows much greater ***Hd***-enrichment than does clinopyroxene of the Si-undersaturated rocks, and seems to follow the pantellerite

---

* Mg# = Mg/(Mg+ΣFe), with all Fe as Fe^{2+}.

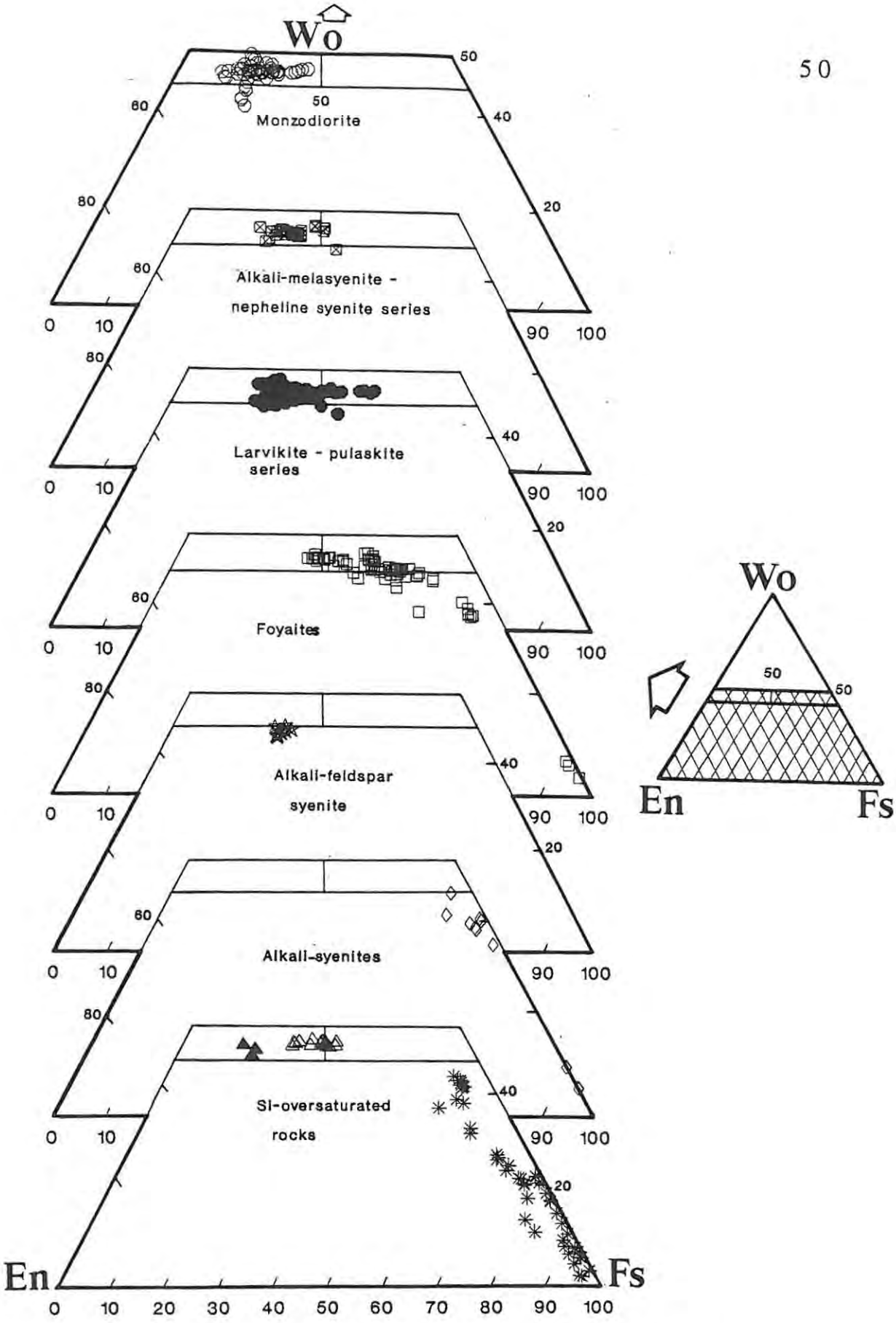

Figure 4.2 Plot of ***En-Fs-Wo*** (Mol%) showing the compositional range of clinopyroxene from the various rock series and types of the GPC and the MKC. All symbols given in Table 2.1 (see loose-leef appendix). Note that the trend to extreme ***Fs***-enrichment is accompanied by enrichment in the ***Ac*** component and is more correctly depicted in terms of the components ***Di-Hd-Ac*** (Fig. 4.3).

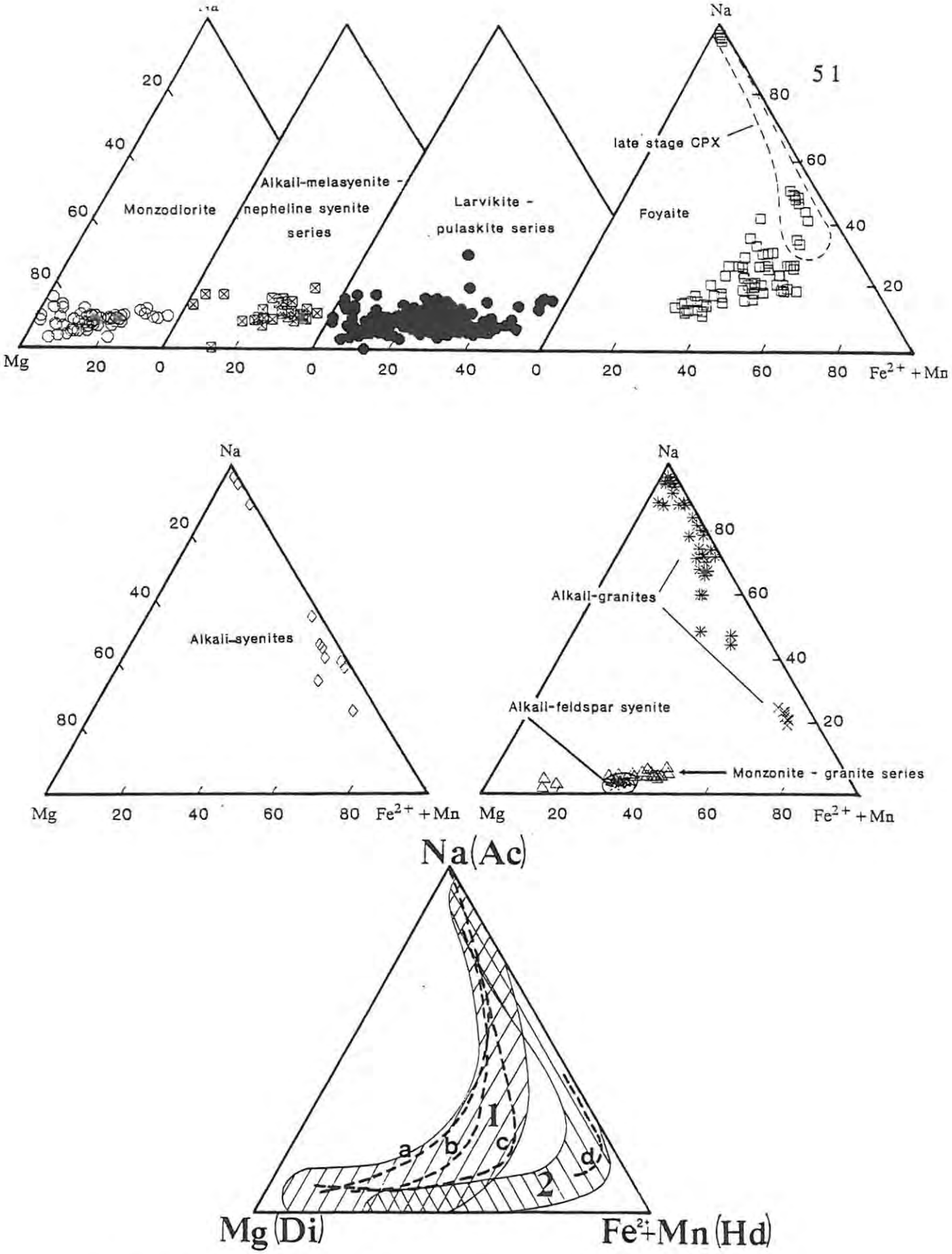

Figure 4.3 Plot of ***Di-Hd-Ac*** (Mol%) showing the compositional range of clinopyroxene from the various rock series and types of the GPC and the MKC. All symbols are given in Table 2.1. The bottom triangle compares the fields for clinopyroxene in the Si-undersaturated and Si-oversaturated rocks with other alkali-pyroxene trends: **a)** Uganda (Tyler and King, 1967), **b)** Velasco, Bolivia (Fletcher and Beddoe-Stephens, 1987), **c)** South Qôroq, Greenland (Stephenson, 1972) and **d)** Pantellerite trend (Nicholls and Carmichael, 1969).

trend of Nicholls and Carmichael (1969). This may be because stabilisation of Fe^{3+} in a melt is strongly dependent upon melt composition (Sack *et al.*, 1980; Dickenson and Hess, 1986) and, at constant fO_2, T and P, may increase with increasing activity of silica (Dickenson and Hess, 1986).

4.3 Amphibole

The most common and abundant mafic mineral in the GPC and MKC, amphibole exhibits a wide compositional range in both complexes. Texturally, little of the amphibole can be considered as a liquidus phase and, particularly in the more evolved rock types, it occurs interstitially between feldspar laths, indicating crystallisation at quite a late stage.

On a plot of Na *vs.* Ca (Fig. 4.4), most amphibole in the Si-undersaturated rocks, and all amphibole in the monzonite - granite series, falls into the calcic group (terminology after Leake, 1978). The range of amphibole compositions from the Si-undersaturated and critically saturated rocks extends into the field for sodic-calcic amphiboles, but only the alkali-granites contain alkali-amphibole.

The nomenclature scheme used for amphibole (Leake, 1978) is presented in Figure 4.5. Figure 4.6 shows the compositional range of amphibole in terms of Mg#, while representative analyses of amphibole are presented in Table 4.2. Much of the scatter seen in Figure 4.6 may be attributed (1) to compositional zoning according to substitutions other than $Mg \rightleftharpoons Fe$ substitution, (2) to stabilisation of Fe-oxides (which could significantly affect the Mg# of co-precipitating amphibole), and/or (3) to late-stage or subsolidus alterations.

The compositional fields for amphibole in the **Si-undersaturated** rocks show a large degree of overlap, but a trend towards Fe-enrichment (Fig. 4.6) occurs in the same sequence of rock types as

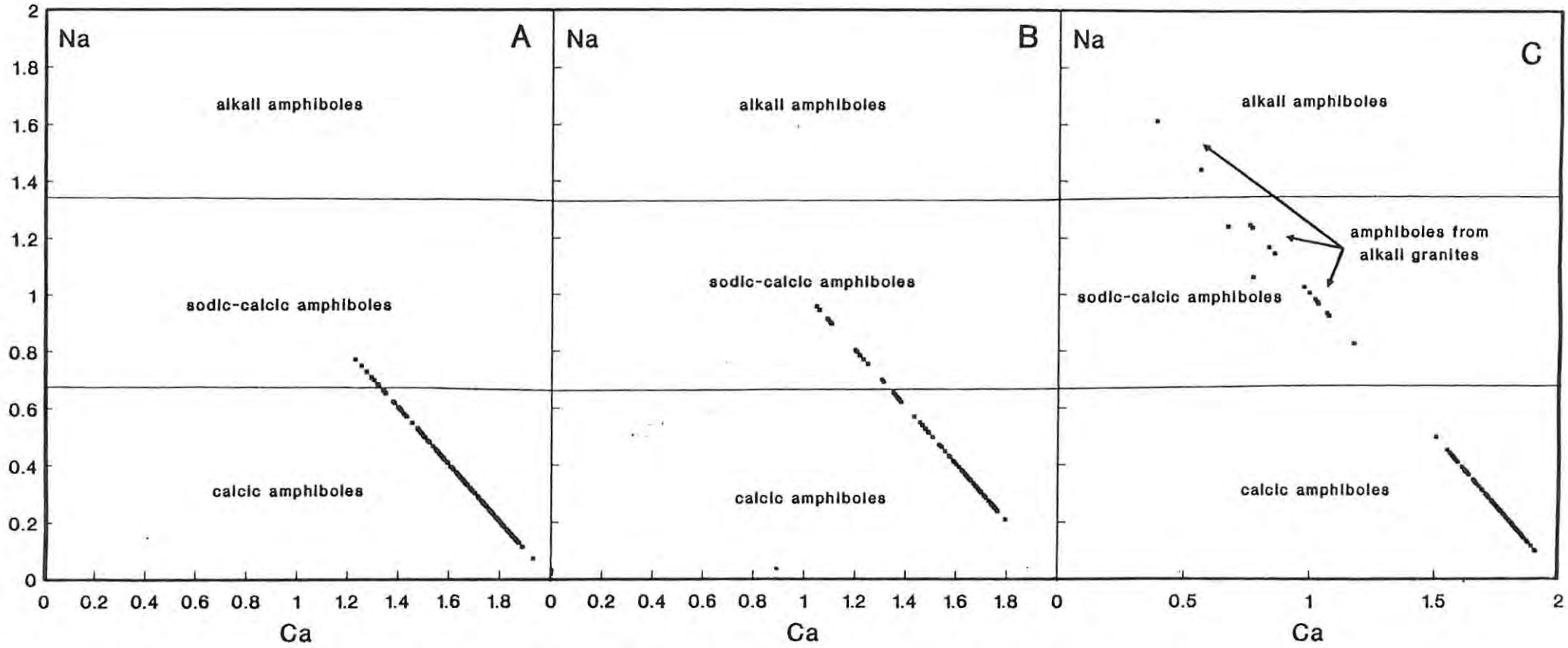

Figure 4.4 Plot of Na *vs.* Ca (cationic proportions) for amphibole from **A)** Si-undersaturated rocks, **B)** critically saturated rocks and **C)** Si-oversaturated rocks. Included are the fields for alkali-amphibole, sodic-calcic amphibole and calcic amphibole (terminology after Leake, 1978)

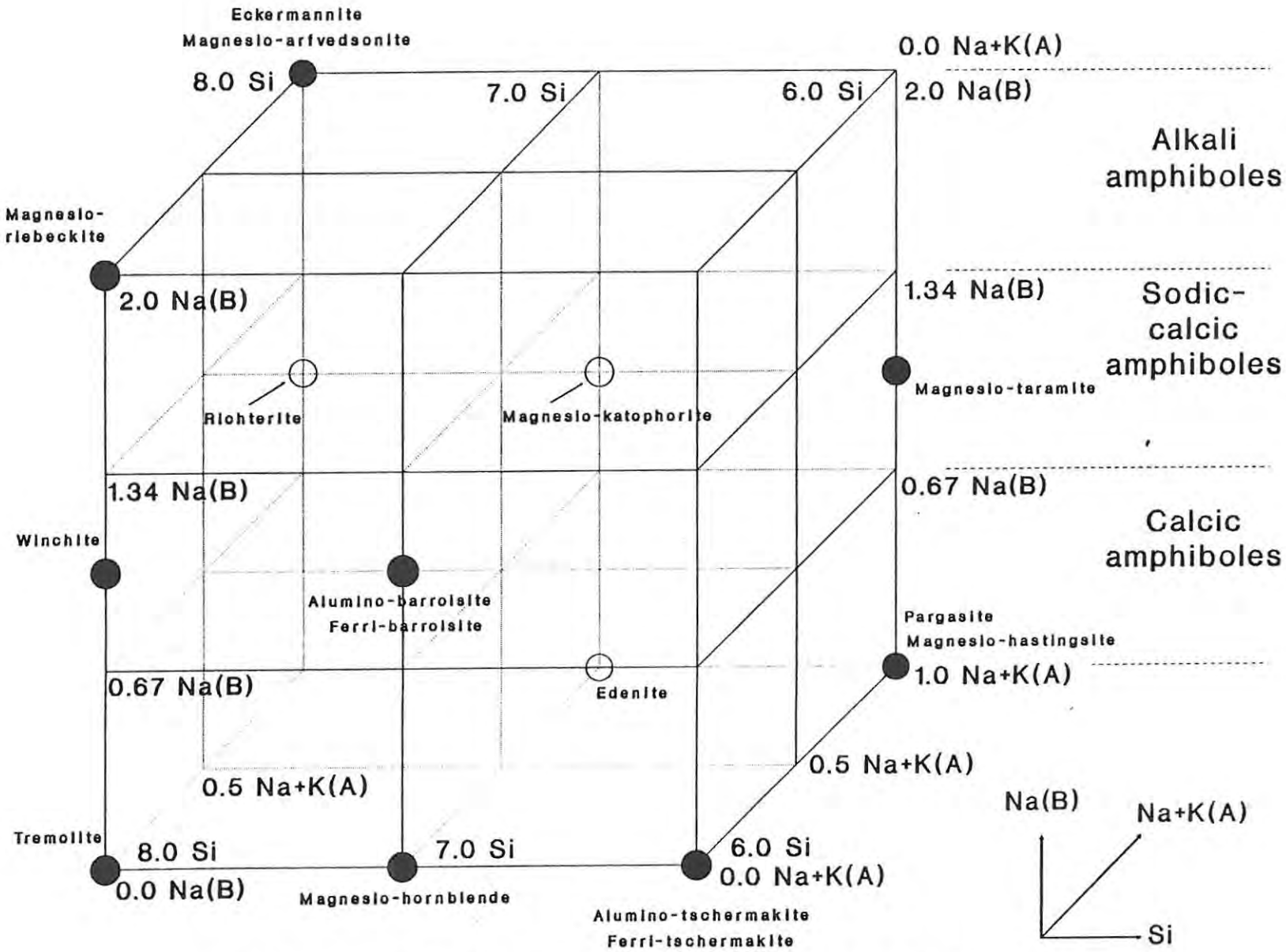

Figure 4.5 Nomenclature scheme for amphibole (redrawn after Leake, 1978), giving names for the Mg-rich end-members of amphibole types encountered in the rocks of the GPC and the MKC.

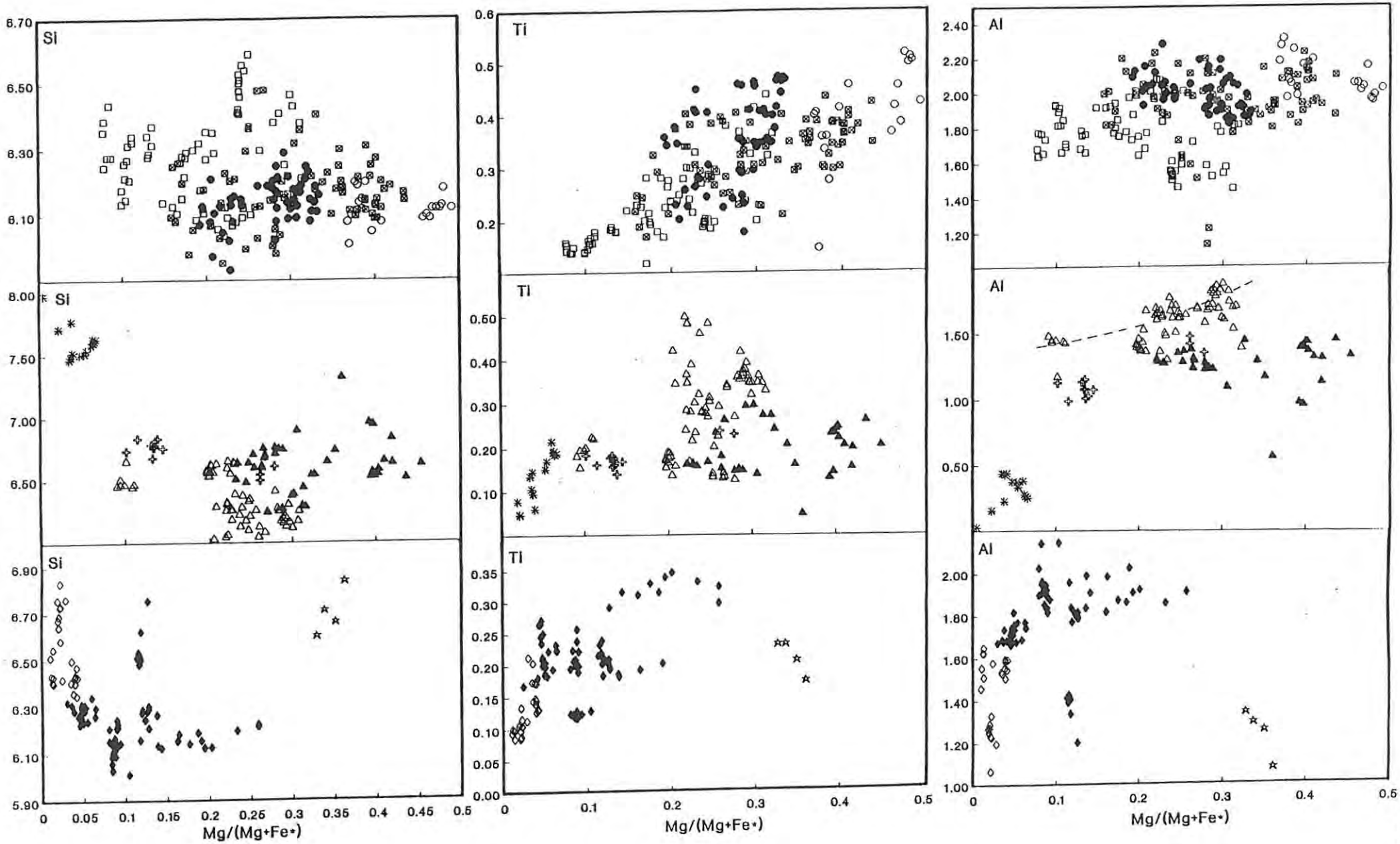

Figure 4.6 Plot of cationic proportions vs. Mg# for amphibole from the Si-undersaturated rocks **(Top plots)**, Si-oversaturated rocks **(Middle plots)** and critically saturated rocks **(Bottom plots)**. Symbols as in Table 2.1.

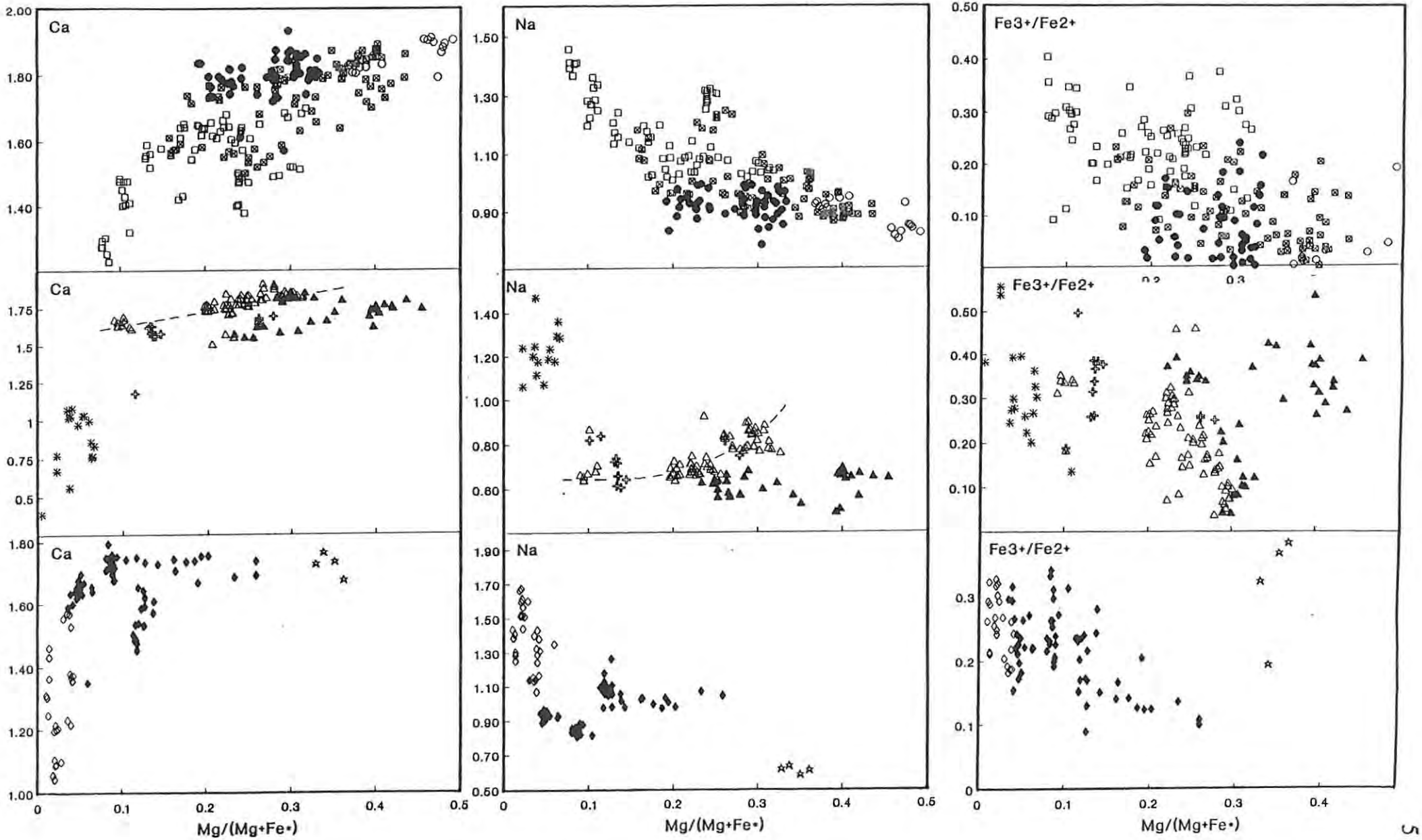

Figure 4.6 Continued.

Table 4.2. Average amphibole analyses.

	Monzodiorites		Larvikite - pulaskite series		Alkali melasyenite - nepheline syenite series		Foyaite series		Alkali-syenite series (GPC)		Alkali-syenite series (MKC)		Alkali-feldspar syenite series		Monzonite - granite series		Marinkas Kwela Granite body	
	avg.	s.d.	avg.	s.d.	avg.	s.d.	avg.	s.d.	avg.	s.d.	avg.	s.d.	avg.	s.d.	avg.	s.d.	avg.	s.d.
[wt%]	n = 28		n = 58		n = 83		n = 90		n = 30		n = 66		n = 4		n = 107		n = 19	
SiO2	39.42	1.27	38.98	0.57	38.78	0.81	39.09	0.87	39.60	1.13	38.17	1.57	43.39	0.81	40.91	1.75	48.36	1.97
TiO2	3.43	0.65	3.02	0.67	2.73	0.52	1.90	0.62	1.07	0.30	1.78	0.46	1.79	0.19	2.15	0.79	1.02	0.50
Al2O3	11.75	1.11	10.62	0.53	10.57	0.87	9.31	0.93	7.69	0.91	9.49	1.22	6.82	0.52	8.26	1.36	1.42	0.66
Fe2O3	2.20	6.53	1.81	1.45	2.56	1.71	5.87	1.94	7.48	1.21	6.80	5.79	6.34	1.25	5.41	2.40	7.48	3.89
FeO	18.18	5.22	22.65	1.01	20.85	1.41	21.91	1.45	26.42	0.86	24.17	4.42	18.33	0.87	20.98	2.40	25.34	2.18
MnO	0.35	0.05	0.86	0.08	0.85	0.23	1.27	0.24	1.43	0.21	1.15	0.16	0.88	0.03	0.72	0.16	2.07	0.73
MgO	7.96	1.16	5.12	0.79	5.64	1.49	3.76	1.32	0.53	0.23	2.01	0.98	7.09	0.39	5.35	1.56	1.00	0.68
CaO	10.41	2.90	10.62	0.31	10.16	0.77	8.83	0.83	7.52	0.97	9.27	1.70	10.42	0.12	10.38	0.51	4.20	1.95
Na2O	2.78	0.73	3.02	0.15	3.18	0.29	3.76	0.38	4.32	0.55	2.95	0.61	2.03	0.05	2.27	0.31	4.93	1.85
K2O	1.99	2.06	1.46	0.08	1.43	0.09	1.46	0.09	1.43	0.08	1.52	1.05	0.78	0.12	1.07	0.23	0.73	0.28
Total	98.47	0.52	98.16	0.61	96.75	1.01	97.16	0.94	97.49	0.71	97.31	0.89	97.87	0.71	97.50	0.97	96.55	1.21
Cations based on 23 oxygens																		
Si	6.04	0.28	6.15	0.07	6.16	0.11	6.28	0.13	6.50	0.15	6.20	0.26	6.70	0.09	6.45	0.24	7.78	0.35
ivAl	1.93	0.19	1.85	0.07	1.84	0.11	1.71	0.14	1.48	0.17	1.77	0.21	1.24	0.10	1.51	0.23	0.24	0.16
Fe3+	0.03	0.09	0.00	0.00	0.00	0.00	0.01	0.02	0.02	0.03	0.03	0.09	0.06	0.04	0.04	0.07	0.07	0.05
Ti4+	0.00	0.00	0.00	0.00	0.00	0.00	0.00	0.00	0.00	0.00	0.00	0.00	0.00	0.00	0.00	0.00	0.00	0.00
viAl	0.19	0.09	0.12	0.08	0.15	0.06	0.05	0.04	0.01	0.02	0.05	0.05	0.00	0.00	0.03	0.05	0.12	0.22
Ti	0.39	0.08	0.36	0.08	0.33	0.06	0.23	0.07	0.13	0.04	0.22	0.06	0.21	0.02	0.25	0.09	0.12	0.06
Fe3+	0.37	1.16	0.21	0.17	0.31	0.21	0.71	0.24	0.90	0.14	0.83	0.79	0.67	0.10	0.60	0.25	0.83	0.44
Fe2+	2.34	0.67	2.99	0.15	2.77	0.22	2.95	0.22	3.63	0.13	3.29	0.61	2.37	0.14	2.77	0.34	3.41	0.32
Mg	1.66	0.47	1.20	0.18	1.33	0.34	0.90	0.31	0.13	0.06	0.47	0.24	1.63	0.08	1.25	0.35	0.24	0.16
Mn	0.04	0.01	0.12	0.01	0.11	0.03	0.17	0.03	0.20	0.03	0.15	0.04	0.12	0.01	0.10	0.02	0.28	0.10
Mg	0.15	0.54	0.00	0.00	0.00	0.00	0.00	0.00	0.00	0.00	0.02	0.10	0.00	0.00	0.00	0.00	0.00	0.00
Fe2+	0.00	0.00	0.00	0.00	0.00	0.00	0.00	0.00	0.00	0.00	0.00	0.00	0.00	0.00	0.00	0.00	0.00	0.00
Mn	0.00	0.01	0.00	0.00	0.00	0.00	0.00	0.00	0.00	0.00	0.00	0.03	0.00	0.00	0.00	0.00	0.00	0.00
Ca	1.71	0.51	1.79	0.05	1.73	0.11	1.52	0.13	1.32	0.18	1.62	0.30	1.72	0.03	1.75	0.09	0.72	0.33
Na	0.14	0.05	0.21	0.05	0.27	0.11	0.48	0.13	0.68	0.18	0.32	0.10	0.28	0.03	0.25	0.09	1.26	0.34
Na	0.69	0.18	0.72	0.05	0.71	0.06	0.69	0.07	0.70	0.04	0.61	0.13	0.33	0.04	0.45	0.14	0.28	0.32
K	0.38	0.37	0.29	0.02	0.29	0.02	0.30	0.02	0.30	0.02	0.31	0.21	0.15	0.02	0.22	0.05	0.15	0.06
Total	15.68	0.23	15.72	0.05	15.71	0.07	15.70	0.04	15.70	0.03	15.58	0.09	15.33	0.06	15.45	0.18	15.35	0.55

obtained in the case of clinopyroxene. The molecular proportions of Si, Na and K increase in sympathy with Fe and, correspondingly, those of Mg, Al, Ti and Ca show a decrease (Fig. 4.6). Changes of the same nature can be seen in individual grains, although compositional zoning is only slight. Both the overall compositional range and the trends to more alkaline amphibole are very similar to those for amphibole from Si-undersaturated rock series of the Red Hill Alkali Complex of New Hampshire (Henderson *et al.*, 1989).

Such transitions to more alkaline amphibole are most pronounced in the foyaites where hastingsitic hornblende is replaced by taramite. They are least pronounced in the pulaskites. In the latter, amphibole is generally more Ca- and Al-rich and Na-, Mn- and Si-poor compared to amphibole of similar Mg# in the foyaites.

Differences between the **critically saturated** rocks have already been noted in respect of clinopyroxene compositions. The rocks differ also as regards their amphibole compositions. Amphibole in the alkali-feldspar syenite is less alkaline, and has much higher Mg#, than that in the alkali-syenites. The concentrations of Si, Ti and Al in amphibole also differ between the two rock types. Indeed, the amphibole of the alkali-feldspar syenite is compositionally closer to that of the monzonite - granite series (at similar Mg#) than to amphibole in any other rocks of either complex.

Alkali-syenite is one of the rock types that occurs in both complexes, and it is noted here that amphibole from alkali-syenite of the MKC is more primitive (*i.e.*, has higher Mg#) and less alkaline than amphibole from alkali-syenite in the GPC.

Amphibole in **Si-oversaturated rocks** is generally more silicic than that from the Si-undersaturated rocks (Fig. 4.6). Systematic major-element variations were detected only in amphibole of the monzonite - granite series in the MKC (*i.e.*, in hastingsite and ferro-edenite to ferro-tschemakite and ferro-hornblende); with decreasing Mg# the amphibole becomes richer in Si and Mn (and Fe^{3+}/Fe^{2+}

increases), and poorer in Na, K, Al and Ca. Amphibole from rocks of the monzonite - granite series in the GPC is virtually identical to amphibole in similarly evolved rocks of the same series in the MKC. Compositional zoning of amphibole is neither common nor extreme in the Si-oversaturated rocks.

4.3.a Coupled Substitutions In The Amphibole Structure

Compositional trends in all the foregoing groups of amphibole can be seen in terms of coupled cation substitutions. The coupled substitution $CaAl^{iv} \rightleftharpoons NaSi$, in conjunction with $Mg \rightleftharpoons Fe^{2+}(Mn)$ substitution, is known to be a prevalent evolutionary feature of amphibole in Si-undersaturated rocks (Giret *et al.*, 1980; Larsen, 1976; Henderson *et al.*,1989). In this study, of the amphibole that shows significant Na-enrichment both $CaAl^{iv} \rightleftharpoons NaSi$ and $Mg \rightleftharpoons Fe^{2+}(Mn)$ substitutions are approximately balanced in terms of cation numbers, and may be reasonable descriptions of compositional trends. The coupled substitution $Ti+O \rightleftharpoons Fe^{3+} + (OH^-,F^-)$ is also implicated by trends to less Ti-rich compositions and to higher Fe^{3+}/Fe^{2+} ratios (Fig. 4.6). In contrast, $Mg \rightleftharpoons Fe^{2+}(Mn)$ substitution alone seems to dominate the less Na-enriched amphibole, with $\square Ti \rightleftharpoons NaAl^{iv}$ substitution possibly accounting for the trend away from initial kaersutite compositions.

The substitution $CaAl^{iv} \rightleftharpoons NaSi$ alone adequately describes most compositional variations in amphibole of the alkali-syenites, but variable concentrations of Ti and increasing Fe^{3+}/Fe^{2+} ratios also point to $Ti+O \rightleftharpoons Fe^{3+}+(OH^-,F^-)$ exchange.

Compositional evolution of amphibole in rocks of the monzonite - granite series can best be explained in terms of the substitutions $NaAl^{iv} \rightleftharpoons \square Si$ and $Mg \rightleftharpoons Fe^{2+}(Mn)$. Giret *et al.* (1980) consider such substitutions to be typical of basic to intermediate Si-oversaturated rocks. These authors also suggest a progression to more Na-rich compositions, occurring through $CaAl \rightleftharpoons SiNa$ substitution at late

magmatic stages. While no such trends to alkali-enrichment were observed in amphibole of the monzonite - granite series, they were (as noted above) evident in amphibole of the Si-undersaturated rock types.

4.4 Biotite

Biotite is more abundant than amphibole only in the larvikite and in early alkali-feldspar syenite of the GPC. The only major compositional variations in biotite of the various rock types are between concentrations of Fe and Mg (Table 4.3 and Fig . 4.7), and this is a feature of biotite from other alkaline rock series (Henderson *et al.*,1989; Upton *et al.*,1985). The Mg# decreases in the same order of rock series/types as it does for clinopyroxene and amphibole. Biotite from the alkali-syenite of the GPC is close to the pure annite end-member composition, whilst that of the Grootpenseiland Granite shows a deficiency in Al^{iv} which is possibly indicative of sericitic alteration.

As with clinopyroxene and amphibole, biotite displays distinctive differences in terms of Mg# between the two critically saturated rocks. Biotite of the alkali-feldspar syenite is compositionally similar to biotite of the monzonite - granite series.

4.5 Relationships Between Coexisting Mafic Phases

Rock (1982), Wones and Gilbert (1982), Henderson and Gibb (1986) and Henderson *et al.* (1989) have shown that the distribution of Fe and Mg between coexisting amphibole and biotite should be such that $Mg\#_{biot} \approx Mg\#_{amph}$. In Figure 4.8, all clinopyroxene, amphibole and biotite analyses are plotted in terms of Mg -ΣFe(as Fe^{2+}) - Na. While $Mg\#_{biot} \approx Mg\#_{amph}$ for some of the rock series, it can be seen that the average $Mg\#_{biot}$ clearly exceeds $Mg\#_{amph}$ in the alkali-melasyenite - nepheline syenite and monzonite - granite series. In

Table 4.3. Average biotite analyses.

	Orange River Granite body		Monzonite - granite series		Alkali-syenite series		Larvikite - pulaskite series	
	avg.	s.d	avg.	s.d.	avg.	s.d.	avg.	s.d.
[wt%]	n = 5		n = 26		n = 7		n = 35	
SiO2	36.18	0.60	35.53	0.90	32.80	0.40	34.94	0.52
TiO2	3.06	0.10	3.68	0.40	2.71	0.55	4.53	0.80
Al2O3	9.68	0.50	12.15	0.73	11.00	0.13	13.15	0.27
FeO	33.42	0.33	26.57	2.59	37.15	1.03	25.94	2.67
MnO	0.45	0.18	0.34	0.09	1.23	0.27	0.62	0.11
MgO	1.59	0.24	7.62	1.70	0.54	0.41	7.60	1.71
CaO	0.08	0.04	0.12	0.56	0.08	0.03	0.01	0.03
Na2O	0.10	0.03	0.13	0.06	0.14	0.03	0.24	0.07
K2O	8.19	0.26	8.68	0.27	7.43	0.32	8.71	0.22
Total	92.76	0.89	94.82	0.90	93.07	0.60	95.73	0.70
Cations based on 22 oxygens								
Si	6.11	0.10	5.67	0.10	5.68	0.04	5.52	0.05
Ti	0.39	0.01	0.44	0.05	0.35	0.07	0.54	0.09
Al	1.93	0.09	2.29	0.13	2.25	0.04	2.45	0.06
Fe2+	4.72	0.05	3.55	0.39	5.38	0.17	3.43	0.39
Mn	0.06	0.03	0.05	0.01	0.18	0.04	0.08	0.02
Mg	0.40	0.06	1.81	0.39	0.14	0.11	1.79	0.39
Ca	0.01	0.01	0.02	0.10	0.01	0.01	0.00	0.00
Na	0.03	0.01	0.04	0.02	0.05	0.01	0.07	0.02
K	1.77	0.04	1.77	0.04	1.64	0.06	1.76	0.04
Total	15.43	0.07	15.64	0.04	15.69	0.07	15.63	0.06

	Foyaite series		Alkali melasyenite - nepheline syenite series		Monzodiorite series	
	avg.	s.d.	avg.	s.d.	avg.	s.d.
[wt%]	n = 8		n = 29		n = 11	
SiO2	34.14	0.62	33.59	0.60	35.13	0.55
TiO2	3.39	0.13	3.86	0.63	4.24	0.34
Al2O3	12.35	0.46	12.81	0.57	14.55	0.19
FeO	29.94	1.70	24.29	1.78	19.99	0.66
MnO	0.91	0.20	0.63	0.13	0.36	0.09
MgO	5.45	1.14	7.87	1.15	11.76	0.39
CaO	0.02	0.04	0.02	0.03	0.00	0.01
Na2O	0.28	0.04	0.26	0.05	0.22	0.06
K2O	8.54	0.49	8.45	0.24	8.85	0.39
Total	95.02	0.61	91.60	0.91	95.10	0.88
Cations based on 22 oxygens						
Si	5.57	0.07	5.32	0.09	5.41	0.04
Ti	0.42	0.01	0.46	0.07	0.49	0.04
Al	2.37	0.07	2.39	0.10	2.64	0.05
Fe2+	4.09	0.29	3.23	0.26	2.58	0.09
Mn	0.13	0.03	0.09	0.02	0.05	0.01
Mg	1.32	0.27	1.85	0.26	2.70	0.08
Ca	0.00	0.01	0.00	0.00	0.00	0.00
Na	0.09	0.01	0.08	0.01	0.07	0.02
K	1.78	0.10	1.71	0.04	1.74	0.06
Total	15.76	0.06	15.09	0.06	15.68	0.05

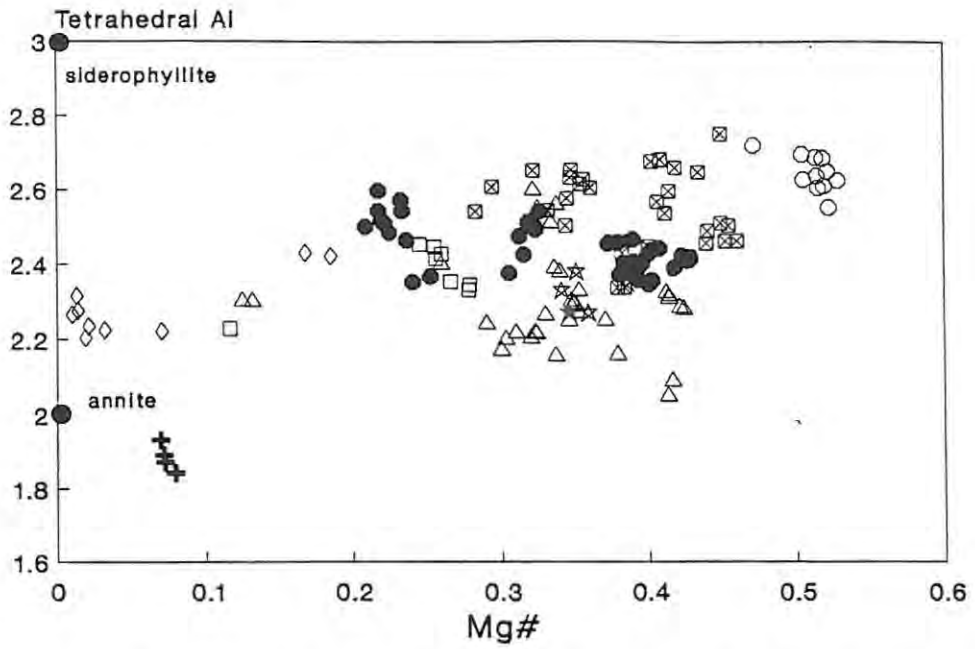

Figure 4.7 Tetrahedral Al *vs.* Mg# for biotite from the rocks of the GPC and the MKC. Symbols as in Table 2.1.

both of these series, textural relationships indicate that the crystallisation of biotite preceded that of amphibole, reversing part of Bowen's (1922) discontinuous reaction series. Under such circumstances it is possible that $Mg^{\#}_{biot} > Mg^{\#}_{amph}$

As noted in Chapters 2 and 3, rocks of the larvikite - pulaskite series vary systematically from biotite-rich to amphibole-rich. Biotite in the larvikite has a significantly higher Mg# than amphibole in the pulaskite, but in transitional rocks where the two minerals coexist , $Mg^{\#}_{biot} \approx Mg^{\#}_{amph}$ (Fig. 4.8). Crystallisation of biotite ahead of amphibole in other alkali-igneous complexes has been documented by, for example, Foland and Henderson (1976) and Upton and Thomas (1980). According to Wones and Gilbert (1982) the phenomenon may be a feature of magmas with low H_2O fugacities and moderately high K_2O concentrations. A gradual increase in the fugacity of H_2O will cause the mole fraction of $KAlSi_3O_8$ in a melt to decrease (Burnham 1979), causing gradual stabilisation of amphibole in preference to biotite.

Amphibole from the monzodiorite has higher Mg# than the most Mg-rich biotite from the larvikite. This would seem to rule out a direct genetic link between the two lithologies since the larvikite - pulaskite series evolved from biotite-rich to amphibole-rich.

Figure 4.8 also shows that, in all of the rock types/series except the alkali-syenites and alkali-granites, the trend to lower Mg# with increasing Na-enrichment is more or less continuous from clinopyroxene to amphibole. Furthermore, amphibole roughly fills the compositional gap between early- and late-forming clinopyroxene in the foyaites. Similar close relationships between clinopyroxene and amphibole have been noted in other alkaline igneous complexes (Larsen,1976; Ferguson, 1978; Henderson *et al.*,1989).

4.6 Feldspar

Because of the extremely coarse nature of exsolution lamellae, analyses of alkali-feldspar from all the rock types show a very wide range of compositions. In some cases, lamellae are inhomogeneously distributed within a single grain. Stephenson (1976) and Parsons and Brown (1988) attributed the presence of very coarsely perthitic alkali-feldspar in alkaline igneous complexes in Greenland to recrystallisation in the presence of aqueous alkali solutions and hence a high volatile pressure. A similar explanation may apply here.

4.7 Nepheline

While fresh nepheline is compositionally homogeneous, weathering and low temperature alteration commonly converts the mineral into a mass of gieseckite, natrolite and other zeolites which impart a pink colouration to the phase in hand specimen.

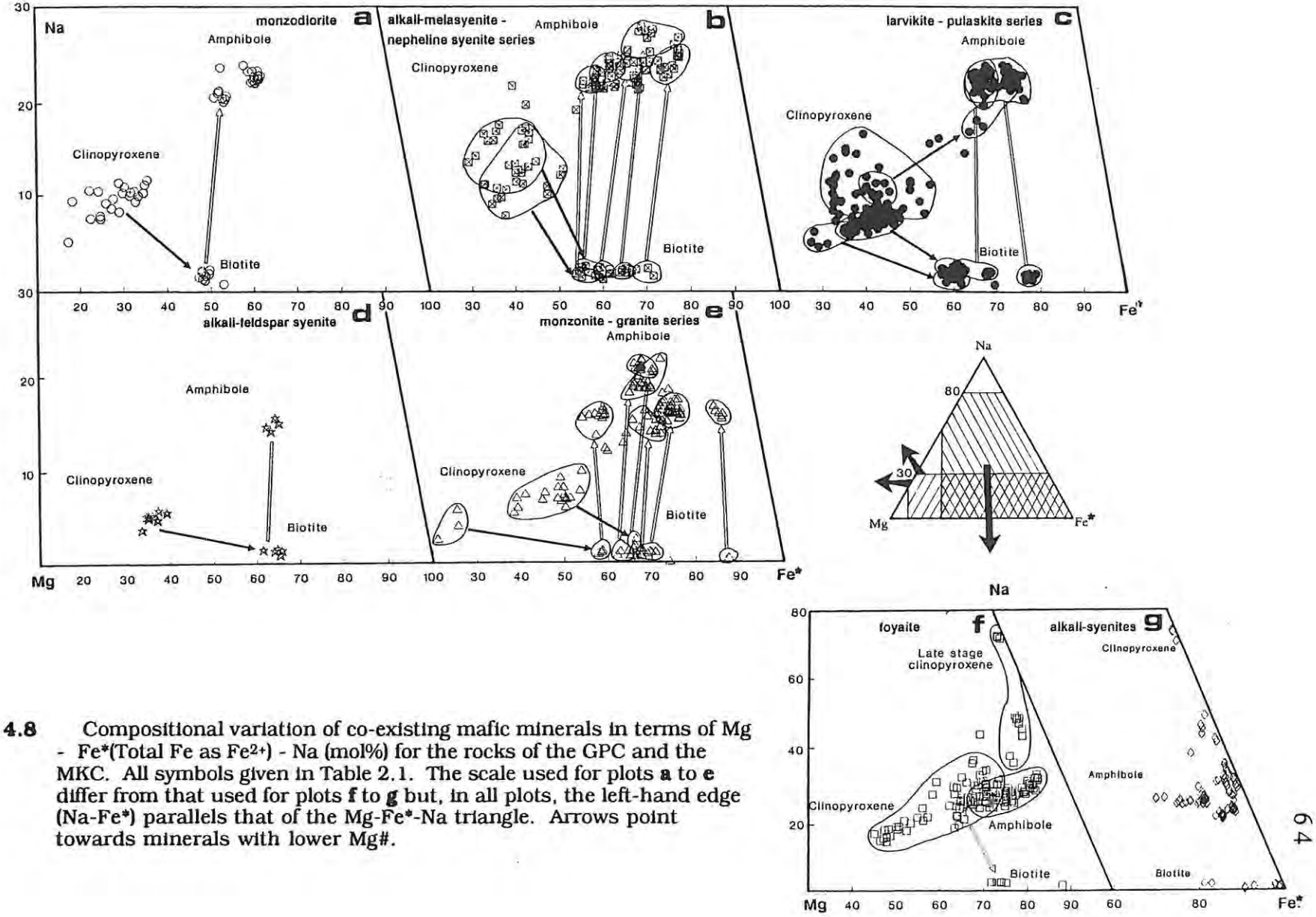

Figure 4.8 Compositional variation of co-existing mafic minerals in terms of Mg - Fe*(Total Fe as Fe^{2+}) - Na (mol%) for the rocks of the GPC and the MKC. All symbols given in Table 2.1. The scale used for plots **a** to **e** differ from that used for plots **f** to **g** but, in all plots, the left-hand edge (Na-Fe*) parallels that of the Mg-Fe*-Na triangle. Arrows point towards minerals with lower Mg#.

In Table 4.4 and Figure 4.9, the composition of nepheline is expressed in terms of molecular % $NaAlSiO_4$(ne) - $KAlSiO_4$(ks) - SiO_2(Q). Figure 4.9 shows that the highest range in 'excess Si' occurs in pulaskite (10 - 5%) followed by foyaites (8 - 4%) and by rocks of the alkali- melasyenite - nepheline syenite series (6 - 3%). There are no significant compositional differences between phenocrystic and interstitial nepheline in the foyaites.

Hamilton (1960) suggested that the degree of Si-oversaturation in nepheline is a function of temperature. A comparison with Hamilton's data (Fig 4.9) indicates that nepheline in the pulaskite crystallised within the range 850° to 750° C; in the foyaites, within the range 785° to 690° C; and in the alkali-melasyenite - nepheline syenite series, within the range 730° to 660° C. The relatively low figures in the latter case are particularly interesting in view of the evidence for recrystallisation presented in Chapter 3.1.c.

4.8 Accessory Phases

4.8.a Opaques

Nearly all the opaque phases belong to the magnetite-ulvôspinel solid solution series. In all rock series/types, magnetite is predominantly Ti-rich, although Ti-poor magnetite ($Ulv_{\pm 1.0}$) does commonly form small inclusions in feldspar. These may be the results of exsolution from feldspar under oxidising conditions. Ilmenite exsolution lamellae were noted only in magnetite from the larvikite - pulaskite series and the monzonite - granite series. In both cases, exsolution lamellae are rare, with the respective phases approaching end-member compositions (Ulv_{2-6}, Il_{83-87}). Within the observed range of Fe-Ti oxide compositions, the concentrations of Ti and Mn show a positive correlation, with the most Ti-rich magnetite and ilmenite containing up to 6.5 and 7.2 wt% Mn respectively. According to Haggerty (1976), Mn-rich ilmenite is a feature of

Table 4.4. Average nepheline and sodalite analyses

	Larvikite - pulaskite series		Alkali melasyenite - nepheline syenite series		Foyaite series	
	nepheline		nepheline		nepheline	
	avg.	s.d	avg.	s.d.	avg.	s.d.
[wt%]	n = 14		n = 19		n = 32	
SiO2	46.18	1.14	44.48	0.38	45.49	0.83
Al2O3	32.59	0.37	32.56	0.15	32.38	0.70
FeO	0.24	0.05	0.26	0.05	0.36	0.13
CaO	0.51	0.08	0.26	0.03	0.25	0.14
Na2O	16.00	0.78	16.66	0.17	16.72	0.40
K2O	5.03	0.35	5.45	0.28	5.23	0.34
Total	100.56	0.85	99.67	0.29	100.43	1.81
Q	8.87	2.90	5.22	0.80	6.37	1.08
ne	74.06	2.52	76.46	0.54	76.18	0.73
ks	17.06	1.07	18.32	0.88	17.45	1.04

	Alkali melasyenite - nepheline syenite series		Foyaite series	
	sodalite		sodalite	
	avg.	s.d.	avg.	s.d.
[wt%]	n = 8		n = 26	
SiO2	38.09	0.75	38.39	0.86
Al2O3	31.58	0.34	31.56	0.38
FeO	0.14	0.05	0.20	0.05
CaO	0.17	0.03	0.15	0.06
Na2O	26.07	0.58	26.01	0.93
K2O	0.02	0.01	0.07	0.24
Total	96.07	0.83	96.39	0.84

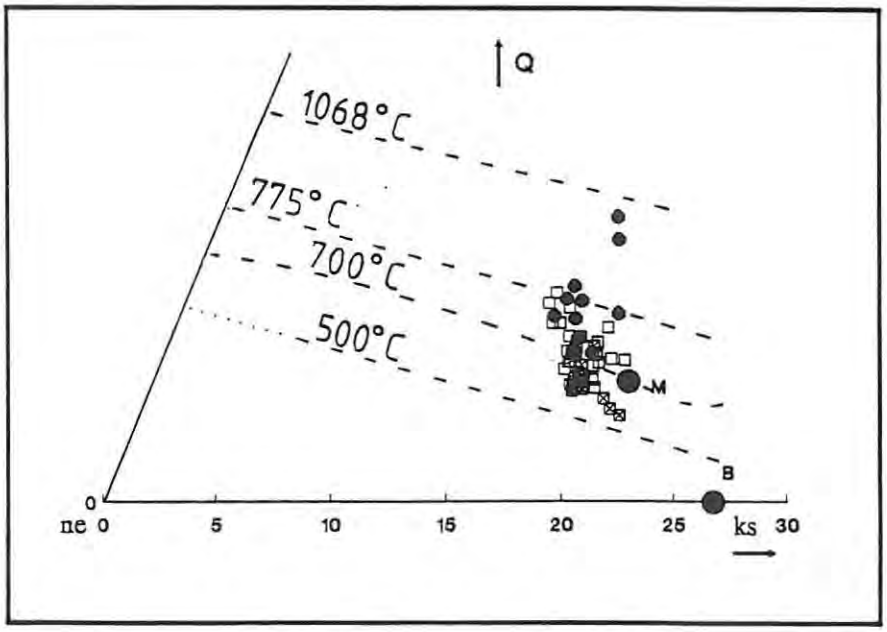

Figure 4.9 Plot of ***ne-ks-Q*** (mol%) showing the compositional range of nepheline from the Si-undersaturated rocks. Symbols as in Table 2.1. Superimposed are isotherms which relate the degree of 'excess silica' in the nepheline structure to the temperature of crystallisation (after Hamilton, 1960).

alkaline rocks. Mn-rich Fe-Ti oxides have been noted from the Laacher See tephra in Germany (Wörner and Schminke, 1984).

4.8.b Sphene

In Chapter 3 it was noted that sphene is a common accessory phase in monzodiorite, in the larvikite - pulaskite series, and in the less evolved rocks of the alkali-melasyenite - nepheline syenite series and monzonite - granite series. It is also a rare phase in the foyaites.

According to Deer *et al.* (1982), sphene commonly contains at least trace concentrations of the Rare Earth Elements (REE). Sphene analysed in the present study contains significant concentrations of REE, Zr and Nb, with ΣREE (= La+Ce+Pr+Nd+Y as wt% REE_2O_3) ranging between 0.97 and 2.58 wt% (Table 4.5). Ratios of La to Y are high (0.6 - 1.7) and according to Fleischer (1978) this is typical of sphene from alkali rocks, the more Y-rich sphene being confined to granitic pegmatites.

In rocks discussed here, no obvious relationships were found between rock type and ΣREE concentrations in sphene. However, compared to the cores of sphene crystals, the rims were invariably found to be depleted in ΣREE with no significant change in La/Y ratios (Y plotted in place of Ho on chondrite-normalised diagrams). Many sphene analyses exhibited negative La anomalies on chondrite-normalized plots (Fig.4.10). Henderson (1980) and Sawka *et al.* (1990) noted the same feature in sphene from other localities, and Sawka *et al.*(1990) ascribed it to crystallisation of allanite which tended to increase the concentration of Ce relative to La in the melt. In regard to the rocks discussed here, co-precipitation of allanite may be the cause of La anomalies in sphene from the Si-oversaturated rocks, but the absence of allanite from some Si-undersaturated rocks requires a different explanation (discussed below) for La anomalies in sphene.

Table 4.5 Representative analyses of accessory phases

	Larvikite - pulaskite series			Alkali melasyenite - nepheline syenite series		Monzonite - granite series	
	Apatite			Apatite		Apatite	
[wt%]	c	r	gm	c	r	c	r*
SiO2	0.26	0.32	0.26	0.44	0.77	0.73	5.24
CaO	55.20	55.13	55.12	54.95	54.36	54.65	46.72
P2O5	39.56	39.54	39.78	38.51	37.92	38.38	30.24
La2O3	n.d.	0.39	0.44	0.50	0.69	0.69	3.89
Ce2O3	0.73	0.72	0.79	0.87	1.20	1.24	6.34
Nd2O3	0.25	0.24	0.27	0.31	0.32	0.33	1.34
Y2O3	n.d.	0.08	0.08	0.08	0.09	0.15	1.00
F	6.22	6.47	6.96	7.10	7.26	6.25	5.88
Total	102.22	102.89	103.70	102.76	102.61	102.42	100.65
O=F	2.64	2.74	2.95	3.01	3.08	2.65	2.49
Total	99.58	100.15	100.75	99.75	99.53	99.77	98.16

	Larvikite - pulaskite series		Alkali melasyenite - nepheline syenite series		Monzonite - granite series	
	Sphene		Sphene		Sphene	
[wt%]	c	r	c	r	c	r
SiO2	29.93	29.91	30.40	30.45	30.41	30.41
TiO2	35.14	34.60	32.01	31.60	34.36	32.76
Al2O3	1.28	1.46	2.22	2.54	2.20	2.73
FeO	1.24	1.42	1.77	1.99	1.24	1.53
CaO	26.53	26.52	27.31	27.37	27.27	27.55
ZrO2	0.53	0.55	1.07	1.32	0.49	1.28
Nb2O5	1.08	0.88	2.96	2.26	1.09	0.88
La2O3	0.32	0.33	0.36	0.36	0.46	0.25
Ce2O3	1.07	1.28	0.87	0.82	1.04	0.67
Pr2O3	0.18	0.16	0.12	n.d.	n.d.	n.d.
Nd2O3	0.52	0.53	0.27	0.27	0.25	0.23
Y2O3	0.33	0.28	0.19	0.21	0.19	0.18
ThO2	n.d.	n.d.	n.d.	n.d.	n.d.	n.d.
F	n.d.	n.d.	0.75	0.97	0.68	1.03
Total	98.15	97.92	100.30	100.16	99.68	99.50
O=F			0.32	0.41	0.29	0.44
Total			99.98	99.75	99.39	99.06

	Larvikite - pulaskite series	Alkali-syenite series		Monzonite - granite series		Monzonite - granite series
[wt%]	Bastnaesite(?)	REE-sphene		Allanite		Zircon
SiO2	11.92	26.90	27.31	33.17	33.00	32.4
TiO2	0.08	20.39	20.62	1.78	2.04	-
Al2O3	0.66	-	-	12.06	11.14	-
FeO	0.97	5.72	5.80	14.50	13.93	-
MnO	-	1.13	1.13	-	-	-
CaO	3.03	4.28	4.68	11.08	10.53	-
ZrO2	0.13	0.98	1.04	0.00	0.13	64.77
Nb2O5	0.00	8.03	8.13	0.00	0.85	n.d.
La2O3	23.80	7.51	4.59	6.85	5.78	n.d.
Ce2O3	28.28	12.05	14.78	11.98	11.27	0.17
Pr2O3	1.98	2.17	1.46	1.00	1.10	-
Yb2O3	-	-	-	-	-	0.1
Nd2O3	6.96	3.61	4.07	2.78	3.01	-
Y2O3	0.80	0.53	0.55	0.20	0.46	0.49
HfO2	-	-	-	-	-	0.97
ThO2	7.97	3.05	3.02	0.79	1.05	0.11
F	5.60	-	-	0.52	0.49	-
Total	92.18	96.34	97.17	96.71	94.78	99.01
O=F	2.37			0.22	0.21	
Total	89.81			96.49	94.57	

c = phenocryst core; r = phenocryst rim
r* = REE-rich apatite rim
n.d. = not detected
- = not determined

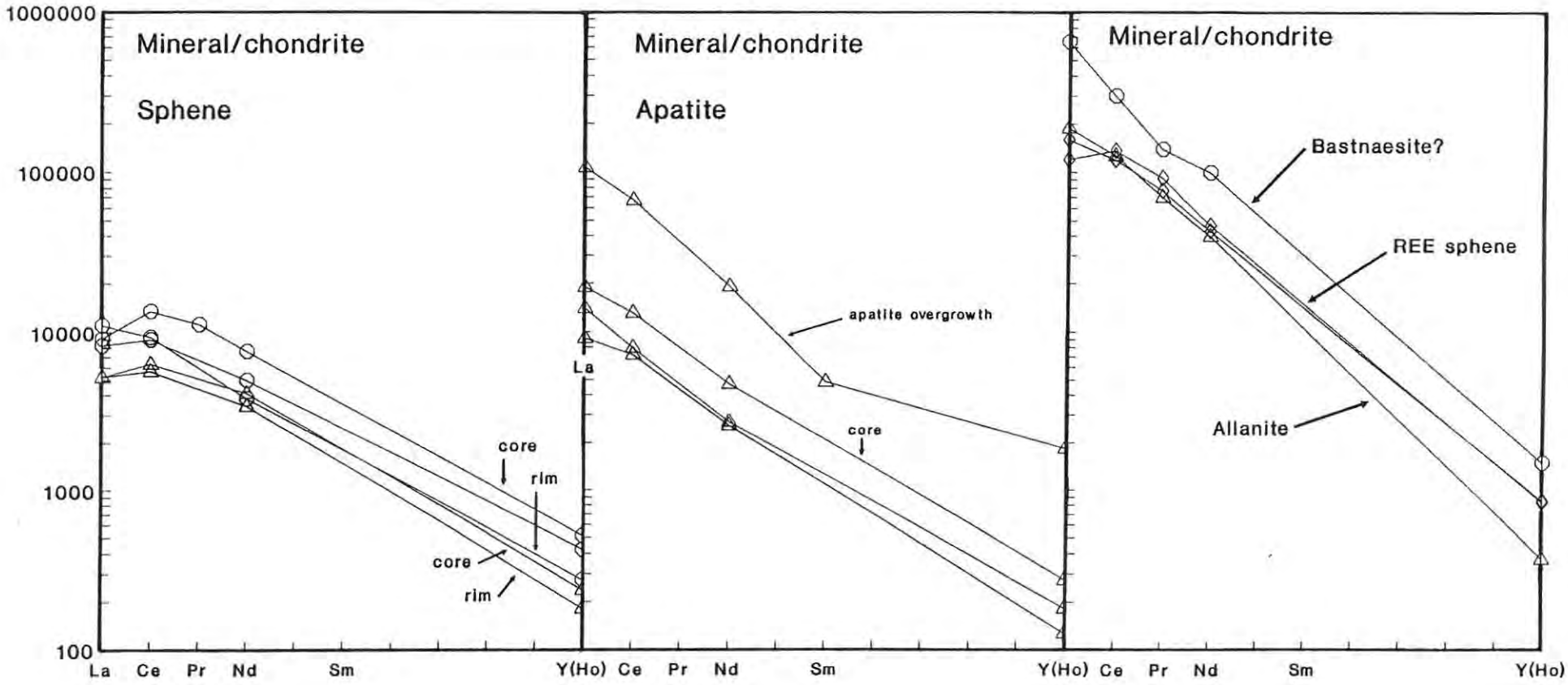

Figure 4.10 Chondrite-normalised REE patterns for sphene, apatite, allanite and two REE-rich accessory phases. Symbols as in Table 2.1.

4.8.c Apatite

As Chapter 3 indicated, apatite occurs as an accessory phase in all rocks except alkali-syenites and alkali-granites. At least two generations are usually present, manifested as (1) large stout prismatic grains (commonly with clouded cores), and (2) late fine-grained acicular grains in the groundmass. Semi-quantitative analyses for fluorine show both generations to be fluorapatite.

Like sphene, fluorapatite is strongly enriched in REE and particularly in light REE. In those samples in which Y was detected, La/Y ratios range up to 3.4 (Table 4.5.). Variations in ΣREE (= La+Ce+Nd+Sm+Y as wt%. REE_2O_3) are generally between 0.35 to 5.38 wt%, and show no obvious relationship to the composition of the host rock. The large prismatic grains commonly have inclusion-free rims which are richer in ΣREE compared to the cores; no systematic change in La/Y ratios from core to rim is observed. Furthermore, where groundmass fluorapatite was analysed (pulaskite and monzodiorite), it too had higher REE concentrations than co-existing prismatic grains. Such enrichments of REE in late-crystallising phases suggest that the REE have Bulk D of less than unity.

The apatite grains found in fine fractures in rocks of the monzonite - granite series (Chap. 3.3. a) are of particular interest. The grains consist of partially resorbed fluorapatite (La/Y= 3.5, ΣREE= 2.6 wt%) which is abruptly rimmed by a later generation of fluorapatite in which ΣREE concentrations reach 12.75 wt% REE_2O_3. The rims are also enriched in SiO_2 (up to 5.55 wt%.) and depleted in CaO and P_2O_5. They may relate to late-stage hydrothermal alteration, possibly during subsequent intrusion of more evolved members of the monzonite - granite series.

4.8.d Additional Accessory Phases

Less common accessory phases include zircon, allanite, the ?bastnaesite mentioned in Chapter 3.1.b. and a further and unidentified REE-rich phase. Table 4.5 gives representative analyses.

Zircon occurs in all rock types with the exception of nepheline syenite, the foyaites and the alkali-granites. It is usually a late interstitial phase but may also occur as small euhedral crystals along feldspar grain boundaries. In the monzonite - granite series, zircon also occurs in fine fractures and its occurrence there, like that of apatite, possibly relates to late-stage hydrothermal alteration. Analyses of zircon invariably indicate small concentrations (<1wt%) of REE, Hf and Th; Ce/Y ratios are low (± 2).

Allanite occurs in all rocks of the monzonite - granite series, and in some alkali-syenites. Analyses consistently show high concentrations of REE (up to 23 wt% La+Ce+Pr+Nd+Y as REE_2O_3), and extreme La/Y ratios around 60 (Fig 4.10).

The tentatively identified bastnaesite occurs as small brown lath-shaped grains included in the nepheline of all nepheline-bearing rocks, or as subhedral inclusions in amphibole from the alkali-syenite of the GPC. The mineral rapidly volatilises under the microprobe beam. If low totals obtained were attributed to the presence of CO_2, the composition of the mineral would approximate that of the REE carbonate bastnaesite [(Ce,La)(CO_3)F]. In any case, the mineral seems compositionally closer to bastnaesite than to any other relatively common REE phase.

It was shown in Chapter 4.8.b that the explanation by Sawka *et al* (1990) for La anomalies in sphene would fail to account for such anomalies in the allanite-free Si-undersaturated rocks. While the available data are insufficient for a firm conclusion to be drawn, the steeply-inclined chondrite-normalised profiles for the bastnaesite-like mineral suggest that its crystallisation could have the same

effect on the melt concentrations of light REE as does the crystallisation of allanite.

The unidentified REE-rich phase (Chap. 3.2.b) occurs in alkali-syenite as small, anhedral, dark to light brown grains included in amphibole or lying along fine fractures. Microprobe analyses indicate the phase to be a Ti-rich silicate containing up to 26wt% ΣREE_2O_3 (La+Ce+Pr+Nd+Y), 5wt% Nb_2O_5 and 3.5 wt% ThO_2. It may belong to the sphene group, for which dominant cationic substitutions include Ca⇋REE and Ti⇋Fe, Nb (Deer *et al.*, 1980). Sphene has previously been reported with even higher ΣREE. For example, Exley (1980) recorded up to 46.12 wt% REE_2O_3 in sphene from the Skye granite in Scotland.

CHAPTER 5: GEOCHEMISTRY OF THE SILICATE ROCKS

5.1 Introduction

Most of this chapter falls into two parts dealing with major elements (Chap. 5.3) and trace elements (Chap. 5.4). Under most major sub-headings in each part, rock series/types will be discussed in a sequence from Si-undersaturated to Si-oversaturated. Although some preliminary interpretations will be offered, a principal aim will be to point out salient features that have relevance to discussion in later Chapters.

Whole-rock major- and trace-element compositions were determined by X-Ray Fluorescence at Rocklabs (Closed Corporation) in Pretoria, while determinations of the Rare Earth elements were carried out by Inductively Coupled Plasma Spectrometry at Stellenbosch University and at the Royal Holloway and Bedford New College, England (see Appendix 3 for details). Representative analyses are presented in Table 5.1 and CIPW Norms in Table 5.2, while the complete data set can be found in appendix 4. All data are plotted on an anhydrous basis with total Fe as FeO. Relevant mineral-melt distribution coefficients are presented in Table 5.3, which is also available in loose leaf (appended pocket).

While the geochemistry of the GPC and the MKC is complicated by the large range of rock types present, all the rocks are feldspar-rich and most of them are highly evolved. From these general characteristics it is reasonable to suppose that processes involving feldspar - either fractionation or accumulation - were more important than any others in controlling overall compositional differentiation to more highly evolved rock types. To monitor fractionation or accumulation of

Table 5.1. Representative whole-rock analyses from the various rock-series of the GPC and the MKC

	ORS 133	ORS 102	ORS 108	ORS 99	ORS 112	ORS 92	ORS 62	ORS 130	ORG 11	ORS 14	ORF 30	ORF 46
[wt%]	1	2	3	4	5	6	7	8	9	10	11	12
SiO2	49.76	58.70	60.05	61.49	62.40	62.67	62.80	63.31	66.86	74.86	53.74	59.58
TiO2	1.80	1.20	0.59	0.20	0.10	0.88	0.97	0.54	0.25	0.04	1.46	0.41
Al2O3	16.77	18.47	18.79	17.12	17.86	18.71	18.53	17.44	14.99	12.72	17.39	19.24
FeO*	8.54	5.29	4.42	6.16	5.68	3.41	3.42	3.59	3.49	1.30	8.17	3.67
MnO	0.21	0.16	0.16	0.21	0.21	0.09	0.07	0.14	0.09	0.05	0.23	0.17
MgO	4.42	1.91	0.63	0.07	0.02	0.67	0.99	0.67	0.33	0.04	3.34	0.65
CaO	8.32	4.11	2.19	1.76	1.07	1.72	2.01	1.76	0.99	0.36	6.09	1.92
Na2O	4.03	4.99	6.30	5.76	6.34	5.46	6.13	5.37	5.48	5.75	5.16	7.79
K2O	2.84	4.19	4.96	5.31	5.33	5.30	5.28	5.23	5.10	4.41	3.25	4.86
P2O5	1.30	0.78	0.26	0.00	0.08	0.21	0.43	0.19	0.09	0.07	1.00	0.16
H2O-	0.15	0.11	0.14	0.12	0.13	0.10	0.18	0.10	0.12	0.10	0.23	0.23
LOI	1.31	0.71	0.73	0.31	0.46	0.61	0.45	0.86	0.68	0.32	0.84	1.17
Total	99.45	100.62	99.22	98.51	99.68	99.83	101.26	99.20	98.47	100.02	100.90	99.85
ppm												
Zn	97	79	86	96	91	52	46	55	87	55	108	65
Cu	37	22	11	3	2	9	9	7	0	0	24	8
Ni	31	18	5	6	9	1	3	7	7	2	23	4
Co	21	8	5	0	0	4	1	2	1	1	15	5
Mo	2	2	6	10	5	2	2	10	11	1	29	13
Nb	88	105	116	293	197	91	84	131	343	158	309	212
Zr	255	331	473	789	398	195	159	581	614	80	473	581
Y	38	42	33	84	72	25	19	49	70	27	62	45
Sr	1586	1152	654	43	27	559	525	411	144	18	1435	739
Rb	72	96	133	114	143	103	100	157	390	189	97	139
U	2	4	8	7	14	7	2	14	15	15	5	14
Th	9	9	21	64	64	16	16	25	79	20	11	28
Pb	9	12	23	17	11	9	14	9	31	10	24	38
Cr	38	43	13	11	<12	12	16	<11	23	19	28	<13
V	174	61	27	<11	32	<11	27	37	<17	<16	71	<25
Ba	2019	2000	1298	33	46	2062	2426	1627	286	<15	1823	1205
Sc	12	12	<10	<9	<8	<10	<10	<10	13	<9	8	<8
F	1311	1868	1308	1308	1003	1300	1214	1396	2605	2696	1290	1370
Cl	262	125	604	330	203	290	273	645	484	7	762	986
La	116.77	126.31	123.65	466.00	434.80	82.74	76.85		191.62	68.79	235.44	
Ce	200.00	241.22	223.86	775.00	662.13	159.25	132.58		303.91	146.67	450.55	
Pr	22.80	23.25	20.65	85.28	68.49	16.43	13.85		30.61	11.92	46.47	
Nd	85.34	80.63	66.74	276.62	209.29	53.50	50.70		94.28	38.51	148.30	
Sm	11.20	10.59	8.16	32.98	24.52	7.68	6.72		12.19	5.28	21.38	
Eu	3.60	3.34	2.30	1.13	0.87	3.37	4.02		1.24	0.25	4.34	
Gd	9.11	7.77	5.90	23.93	17.86	5.50	5.13		10.23	3.94	15.44	
Dy	7.26	6.82	5.49	19.38	15.41	4.71	4.26		10.33	3.86	13.01	
Ho	1.47	1.51	1.27	4.00	3.24	0.86	0.80		2.31	0.92	2.34	
Er	4.07	4.13	3.53	9.80	7.98	2.45	2.48		7.03	2.58	6.11	
Yb	3.08	3.18	3.03	7.35	5.58	2.46	2.05		6.81	2.77	5.97	
Lu						0.37	0.33				0.91	

FeO* = all Fe as FeO

1 Monzodiorite (GPC)
2 Larvikite (GPC)
3 Pulaskite (GPC)
4-5 Alkali-syenites (GPC)
6-7 Alkali-feldspar syenites (GPC)
8 Granite (GPC)
9 Granite - Grootpenseiland Granite body (GPC)
10 Alkali-granite (GPC)
11 Alkali melasyenite (MKC)
12 Nepheline syenite (MKC)

Table 5.1. Continued

	ORF 6	ORF 24	ORF 23	MKS 67	MKS 66	MKS 59	MKS 61	MKS 29	MKS 43	MKG 16	MKG38
[wt%]	13	14	15	16	17	18	19	20	21	22	23
SiO2	56.89	58.14	55.36	63.99	59.61	60.05	70.03	62.36	69.98	76.40	76.75
TiO2	0.20	0.27	0.34	0.17	0.85	0.90	0.26	0.72	0.02	0.01	0.04
Al2O3	20.35	21.01	19.64	18.30	18.51	17.40	14.88	16.05	15.34	12.06	12.18
FeO*	4.56	3.69	6.04	3.57	3.99	4.15	2.68	4.17	1.31	1.70	1.64
MnO	0.13	0.13	0.24	0.08	0.11	0.13	0.09	0.13	0.07	0.04	0.08
MgO	0.24	0.48	0.66	0.12	1.23	1.21	0.31	1.91	0.19	0.00	0.09
CaO	1.27	1.57	2.63	0.70	3.82	3.09	1.06	3.34	1.36	0.52	0.42
Na2O	11.00	8.50	7.60	5.88	5.44	5.25	4.79	4.61	6.25	4.75	4.31
K2O	5.34	6.13	5.36	6.58	4.84	5.47	5.74	4.82	5.11	4.71	4.39
P2O5	0.11	0.16	0.26	0.09	0.53	0.52	0.06	0.37	0.05	0.00	0.07
H2O-	0.14	0.19	0.30	0.10	0.16	0.30	0.15	0.10	0.08	0.12	0.13
LOI	0.65	0.92	1.10	0.17	0.39	0.79	0.29	0.71	0.40	0.31	0.36
Total	100.88	101.19	99.53	99.75	99.48	99.26	100.34	99.29	100.16	100.62	100.46
ppm											
Zn	41	60	99	54	72	72	50	82	36	27	109
Cu	0	<4	5	<5	18	12	<5	10	<3	0	3
Ni	3	<5	<4	<4	<4	5	<4	24	<5	2	5
Co	0	5	4	<4	6	5	5	7	<4	2	0
Mo	6	13	6	<3	<4	6	6	4	<2	2	2
Nb	57	254	438	137	124	132	217	122	65	55	72
Zr	204	480	740	294	395	401	511	458	54	163	146
Y	21	46	52	60	40	48	97	55	31	15	35
Sr	31	167	119	134	1047	741	77	450	13	146	177
Rb	151	144	180	238	140	204	190	159	197	333	330
U	0	8	12	25	7	<5	13	6	5	16	7
Th	17	31	34	113	19	22	59	26	14	37	54
Pb	18	42	38	41	18	22	28	28	16	13	38
Cr	6	<14	<8	<13	<8	<8	<8	35	<10	17	6
V	<15	<8	<9	<11	<12	<16	6	31	<6	<10	<4
Ba	<13	66	66	52	2094	1800	177	1385	<12	238	235
Sc	<10	<6	<10	<5	<4	9	5	<8	<4	<9	<4
F	881	1560	1660	810	1650	2070	3530	1550	4130	2332	1700
Cl	6300	1100	515								
La	83.11			285.40	95.45	113.73	230.60	120.68		54.24	148.63
Ce	151.61			502.24	193.16	233.64	429.80	238.99		69.49	246.71
Pr	14.27			44.48	20.91	24.45	42.92	24.84		8.22	20.31
Nd	43.80			125.50	72.10	81.90	136.10	82.50		24.83	56.20
Sm	6.10			17.79	11.84	13.11	23.73	13.59		3.25	7.35
Eu	0.69			0.99	3.89	3.38	0.80	2.66		0.49	0.93
Gd	4.14			12.74	9.26	10.14	19.70	10.92		2.60	5.08
Dy	3.76			12.39	8.12	9.22	20.22	10.58		2.50	5.05
Ho	0.68			2.26	1.45	1.68	3.66	1.95		0.63	0.93
Er	1.95			6.06	4.13	4.89	10.37	5.71		1.86	2.72
Yb	2.43			5.62	4.02	4.89	9.94	5.80		2.41	3.34
Lu	0.44			0.75	0.61	0.74	1.46	0.88			0.50

FeO* = all Fe as FeO

13-14	Clinopyroxene-rich foyaite (MKC)	19	Alkali-feldspar syenite (MKC)
15	Amphibole-rich foyaite (MKC)	20	Feldspar porphyry (MKC)
16	Alkali-syenite (MKC)	21	Alkali-granite (MKC)
17	Monzonite (MKC)	22-23	Alkali-granite -Marinkas Kwela Granite
18	Granite (MKC)		body (MKC)

Table 5.2. CIPW norms for representative whole-rock analyses given in Table 8.1.

	ORS 133	ORS 102	ORS 108	ORS 99	ORS 112	ORS 92	ORS 62	ORS 130	ORG 11	ORS 14	ORF 30	ORF 46
[wt%]	1	2	3	4	5	6	7	8	9	10	11	12
Q		2.74		1.95	0.60	5.70	1.61	6.62	12.43	27.37		
C		0.12				1.37	0.11	0.20				
or	16.78	24.76	29.31	31.38	31.50	31.32	31.20	30.91	30.14	26.06	19.21	28.72
ab	30.29	42.22	51.82	48.74	53.65	46.20	51.87	45.44	46.37	40.88	39.92	47.17
an	19.28	15.29	8.34	5.18	4.53	7.16	7.16	7.49	1.24		14.69	3.18
ne	2.06		0.81								2.03	10.16
kp												
ac										1.39		
ns										1.44		
wo												
di	10.92		0.70	3.15	0.23				2.65	1.17	7.34	4.48
hy		7.94		4.23	5.38	3.51	4.13	4.33	2.40	1.11		
ol	7.96		3.43								7.48	1.77
mt	4.60	2.84	2.38	3.31	3.04	1.83	1.84	1.93	1.87		4.39	1.97
il	3.42	2.28	1.12	0.38	0.19	1.67	1.84	1.03	0.47	0.08	2.77	0.78
ap	3.08	1.85	0.62		0.19	0.50	1.02	0.45	0.21	0.17	2.37	0.38

	ORF 6	ORF 24	ORF 23	MKS 67	MKS 66	MKS 59	MKS 61	MKS 29	MKS 43	MKG 16	MKG38
[wt%]	13	14	15	16	17	18	19	20	21	22	23
Q				1.75	0.60	1.35	17.23	7.97	12.46	31.02	33.48
C				0.45							
or	31.56	36.22	31.67	38.88	28.60	32.32	33.92	28.48	30.20	27.83	25.94
ab	26.31	32.34	31.24	49.75	46.03	44.42	40.53	39.01	50.45	35.81	36.47
an		1.07	3.65	2.88	11.79	7.76	2.15	8.87			0.92
ne	26.34	21.45	17.91								
kp											
ac	4.89								1.42	1.82	
ns	2.93								0.19	0.54	
wo									0.62		
di	4.90	4.85	6.62		3.04	3.44	2.33	4.30	4.24	2.30	0.61
hy				3.45	4.03	3.89	1.77	5.55		0.91	1.48
ol	2.70	1.43	2.76								
mt		1.99	3.25	1.91	2.15	2.23	1.44	2.23			0.88
il	0.38	0.51	0.65	0.32	1.61	1.71	0.49	1.37	0.04	0.02	0.08
ap	0.26	0.38	0.62	0.21	1.26	1.23	0.14	0.88	0.12		0.17

Assumed Fe^{2+}/Fe^{3+} = 2/1 (molecular)

Table 5.2. Distribution coifficients for various trace-elements within nepheline-bearing and mafic rocks (A) and granitic rocks (B). Most values in (C) are from Nash and Crecraft (1985)

		Plagioclase	Alkali-feldspar	Nepheline	Clinopxroxene	Amphibole	Biotite	Sphene	Apatite	Ti-magnetite
A	Ba	0.2 - 0.3	0.4 - 9.8	0.09 - 0.42	0.001 - 0.3	0.04 - 0.4		1.5 - 150		0.12
	Sr	2.2 - 4.4	2.3 - 8.2	0.25	0.07 - 0.5	0.02 - 0.5		8 - 21	1.1 - 5	
	Rb	0.04 - 0.07	0.32 - 1.25	0.44 - 1.5	0.001 - 0.1	0.01 - 0.3				
	Th		0.001 - 0.007		0.01 - 0.55	0 - 0.041		0.01 - 8.0	1.2	0.01 - 2.2
	Pb		0.21	0.15	0.102 - 0.126					16.5
	Nb		0.004	0.011	0.029 - 0.025			2.3 - 93		24.6
	Zr		0.003 - 0.01	0.005	0.24 - 1.0	0 - 1.77		2.5 - 19		1.8
	Y		0.017		0.66 - 1.12			29		1.4
	Zn		0.06		2.5	0 - 3.3		14 - 31		0.01 - 29.6
	Cr		0.08		0 - 6.16	0 - 3.1				
	La	0.2 - 0.343	0.219 - 0.31	0.12	0.06 - 0.46	0.31 - 1.44		10.8 - 26.8	1 - 24	0.071 - 0.34
	Ce	0.042 - 0.212	0.173 - 0.24	0.14	0.18 - 0.96	0.49 - 2.06		16.2 - 53.9	1.1 - 24.3	0.044 - 0.31
	Sm	0.04 - 0.213	0.139 - 0.17	0.22	0.48 - 5.33	1.07 - 7.29		30.3 - 154.7	1.4 - 95.5	0.2 - 0.98
	Eu	0.919 - 4.65	1.32 - 1.72	0.26	0.58 - 7.83	1.09 - 9.39		21 - 150.3	1.1 - 102	0.59
	Gd	0.127	0.132 - 0.17	0.33	0.61	1.16		30.5	1.6 - 28	
	Er	0.078	0.128 - 0.14	0.33	0.71	0.96		58.7	1.2 - 12	
	Yb	0.062	0.116 - 0.13	0.33	0.398 - 2.63	0.33 - 2.06		13 - 43.9	0.9 - 8.8	0.75
B	Ba	0.3 - 0.36	6.12		0.131	0.044 - 0.054	6.36 - 10			
	Sr	1.45 - 4.4	3.87		0.516	0.094 - 0.22	0.12			
	Rb	0.016 - 0.048	0.66		0.032	0.065 - 0.081	2 - 3.26			
	Th									
	Pb									
	Nb									
	Zr									
	Y									
	Zn									
	Cr									
	La				0.362		0.32		16.6	
	Ce				1.62		0.26		20.7	
	Sm				1.11		0.24		14.5	
	Eu								21.7	
	Gd				2.25				14.1	
	Er				2.01		0.33		9.4	
	Yb									
C	Ba	0.56 - 3.3	7.2 - 24		0.3 - 2.3*		5.6 - 36			
	Sr	6.8 - 33	4.5 - 7.3				0.29 - 0.53			
	Rb	0.06 - 0.19	1.2 - 1.8				2.3 - 4.1			
	Th	0.03 - 0.04	0.02		0.09 - 0.23	0 - 0.041*	0.27 - 2.0			0.09 - 13.1
	Pb	0.42 - 1.3	0.99 - 3.2				0.6 - 1.6			
	Nb						4 - 9.5			
	Zr	0.04 - 0.36	0.01 - 0.05			0 - 1.77*	0.79 - 1.8			
	Y	0.04 - 0.21					1.0 - 1.4			
	Zn	1.0 - 6.1			7.2 - 21*	0 - 3.3*	42 - 230			105 - 110
	Cr					0 - 3.1*	8.3 - 31			54 - 164
	La	0.3 - 0.45	0.07 - 0.08		0.76 - 1.7		0.76 - 15.1			0.8 - 1.9
	Ce	0.21 - 0.34	0.02 - 0.04		1.2 - 2.9	1.03 - 4.49*	0.86 - 11			1.02 - 2.7
	Sm	0.11 - 0.23	0.02		3.6 - 8.3	1.61 - 8.0*	1.0 - 4.3			1.9 - 4.5
	Eu	3.8 - 7.9	3.3 - 6.5		3.2 - 5.8	1.39 - 5.1*	0.59 - 4.7			0.77 - 2.1
	Gd					2.0*				
	Er					2.38 - 11.2*				
	Yb	0.06 - 0.13	0.03		3.5 - 11.6	1.89 - 9.0*	0.32 - 3			1.0 - 2.2

From:

(A) Watson and Green (1981); Nagasawa (1980); Onuma (1981); Horner et al.(1983); Larsen (1979); Giannetti and Luhr (1983) Wolff (1984); Berlin and Henderson (1969); Sun and Hanson (1976); Ewart (1982).

(B) Nagasawa and Schnetzler (1971); Hanson (1978); Cox et al. (1979); Philpotts and Schnetzler (1970).

(C) Nash and Crecraft (1985), except those ranges marked with '*' which are for high-silica rhyolites and are taken from Mahood (1981); Mahood and Hildreth (1983); Leeman and Phelps (1981).

feldspar, it is necessary to employ a chemical parameter which is itself sensitive to the removal or addition of feldspar. Because both Sr and Ba have $D^{fsp} > 1$ (Hanson, 1978; Nash and Crecraft, 1985), their concentrations would be suitable monitors; both, indeed, have been used elsewhere as such (*e.g.*, by Johnson *et al.*,1989). In the present study, Sr has been preferred to Ba. The latter has two relative disadvantages; it is not strongly partitioned into plagioclase (D_{Ba}^{plag} 0.2-0.3 - Nagasawa and Schnetzler, 1971), but it is strongly partitioned into biotite (D_{Ba}^{biot} 6.36 - Philpotts and Schnetzler, 1970).

5.2 Relationships In Petrogeny's Residua System

When plotted in terms of Bowen's (1937) 'Petrogeny's Residua System' (***Q-ne-ks***), the critically saturated rocks of the GPC and MKC fall about the ***ab-or*** join, close to the syenite minimum (Fig. 5.1).

Except for the rocks of the larvikite - pulaskite series, which also fall very close to the ***ab-or*** join, the Si-undersaturated rocks show a distinct trend towards the phonolitic minimum. The trend, which is most pronounced for the clinopyroxene-rich foyaite, strongly suggests a liquid line of descent controlled by alkali-feldspar fractionation. The clinopyroxene-rich and amphibole-rich foyaites cannot be discriminated on a normative basis; both contain some ***ac***-normative samples. Rocks of the alkali-melasyenite - nepheline syenite series are depleted in the ***ks*** component compared to the foyaites.

Rocks of the monzonite - granite series show a trend from the ***ab-or*** join towards, but on the K-rich side of, the granitic minimum, and this is also indicative of alkali-feldspar fractionation. The K-rich nature of the monzonite - granite series is consistent with early appearance of biotite in these rocks. By contrast, alkali-granites tend to cluster close to the granitic minimum, although some alkali-granite from the GPC does fall between that minimum and the ***ab-or*** join.

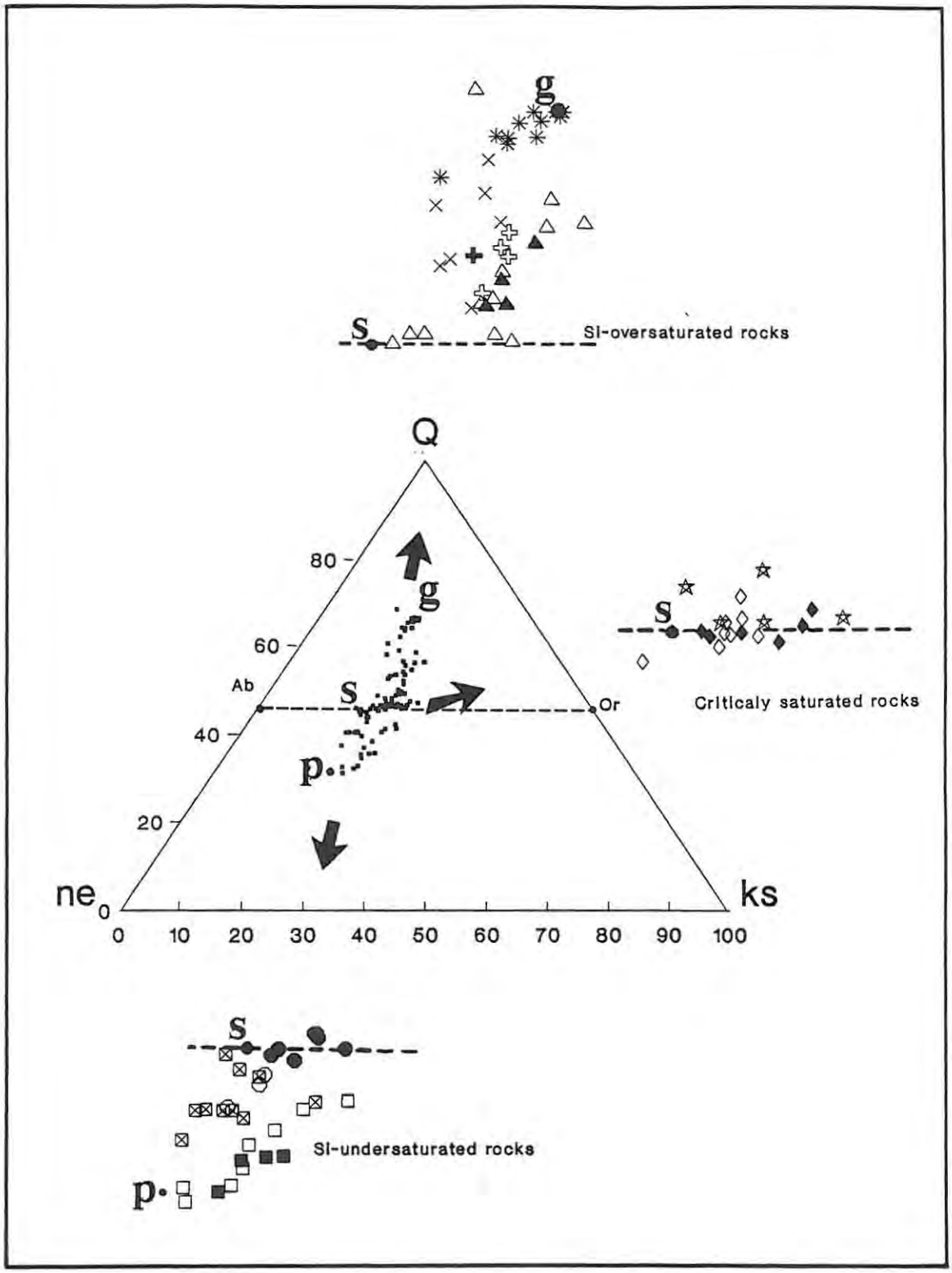

Figure 5.1 Petrogeny's Residua System (Bowen, 1937) with plotted compositions of rocks from the GPC and MKC. Symbols as in Table 2.1. CIPW norms are presented in Appendix 4.2. The letters **g, s** and **p** mark the positions of the granite, syenite and phonolite minima respectively, at 1Kb $P(H_2O)$(Tuttle and Bowen, 1958; Hamilton and Mackenzie, 1965).

5.3 Major-Element Variations (Fig 5.2)

The atomic ratio Na+K/Al of rocks in the GPC and MKC is as low as 0.52 (monzodiorite). In most of the other series/types it falls in a range from around 0.7 to around 1.0. Only in the foyaites and alkali-granites does it commonly exceed unity and even then it never exceeds 1.17. Thus, the GPC and the MKC are only mildly peralkaline. In this regard they are similar to other alkaline complexes such as the Red Hill Complex of New Hampshire (Foland and Friedman, 1977; Henderson *et al.*, 1989); the Marangudzi Complex of Zimbabwe (Foland and Henderson, 1976); the Qôroq Centre in Greenland (Stephenson, 1976); and the Tugtutôq Younger Giant Dyke Complex, also in Greenland (Upton and Thomas, 1980).

In the **Si-undersaturated rocks,** the ratio Na + K/Al increases with decreasing concentrations of Sr from monzodiorite (1530 - 1610ppm Sr) to foyaite (<320ppm Sr). The larvikite - pulaskite series and the alkali-melasyenite - nepheline syenite series overlap with one another while falling in the intermediate range of 310 to 1420ppm Sr.

As well as having the highest concentrations of Sr, monzodiorite has the highest concentrations of 'mafic' oxides (FeO, MgO, CaO, TiO_2 and P_2O_5), and the lowest concentrations of 'felsic' oxides (SiO_2, Al_2O_3, Na_2O and K_2O). While monzodiorite also has the highest Mg# [MgO/(MgO + FeO*) = 0.32-0.37], the values are substantially lower than those that would indicate of equilibrium with mantle material.

Over a similar range of Sr concentrations, the alkali melasyenite - nepheline syenite series has higher concentrations of Na_2O, and lower concentrations of MgO and CaO, than does the larvikite - pulaskite series. In both series, however, the concentrations of 'mafic' oxides decrease systematically with decreasing Sr concentrations, and the 'felsic' oxides systematically increase in concentration. The marked decrease in Sr concentrations clearly implies an evolutionary process

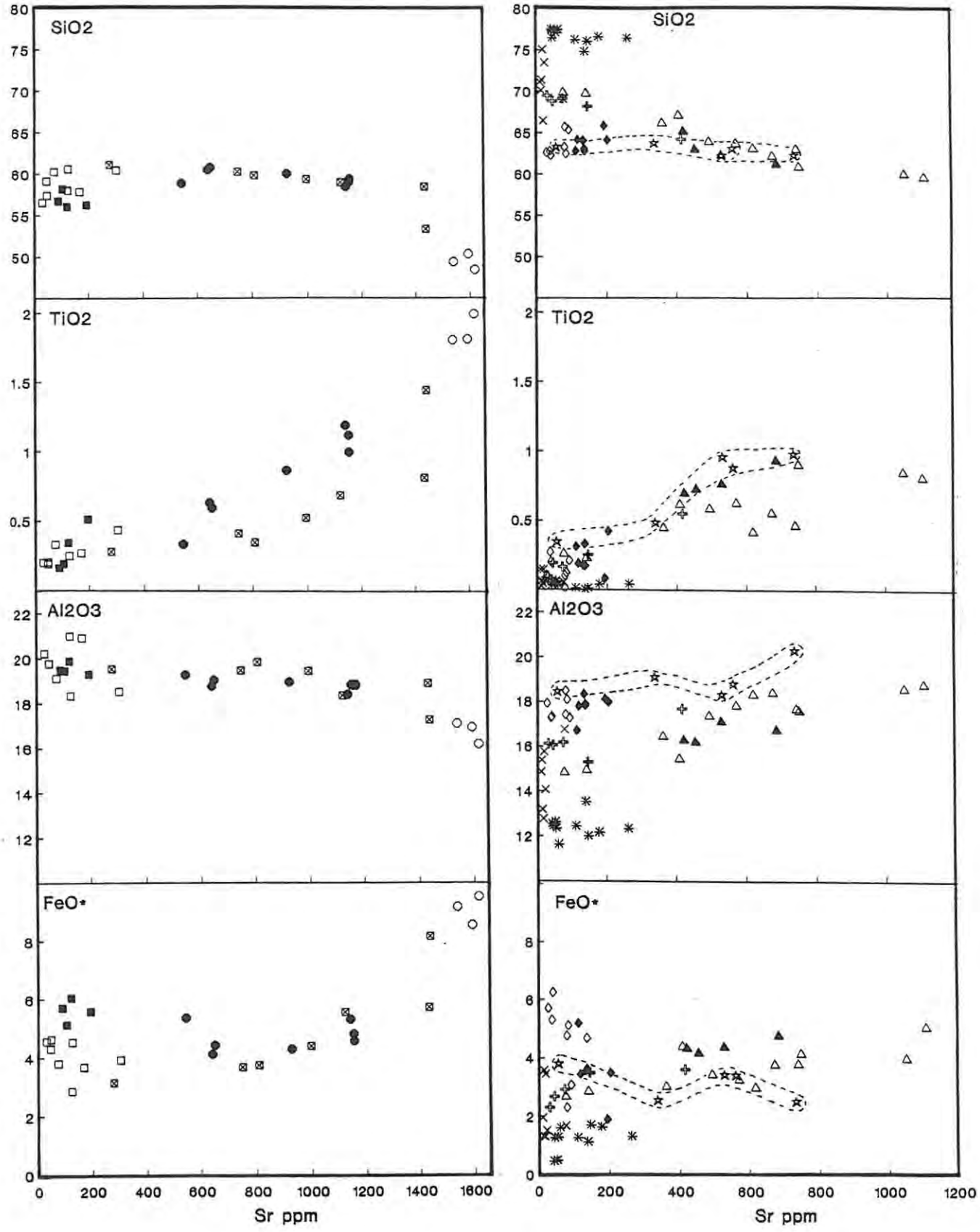

Figure 5.2 Major element geochemistry of the rocks of the GPC and MKC. **Si-undersaturated** rocks are presented on the left hand side of the figure, and **Si-oversaturated** and **critically saturated** rocks on the right hand side. For comparative purposes, the scale of the Y-axis is identical on both sides of the figure. The field defined by the dotted line encloses data for the alkali-feldspar syenite. Symbols as in Table 2.1. FeO* = all Fe as FeO.

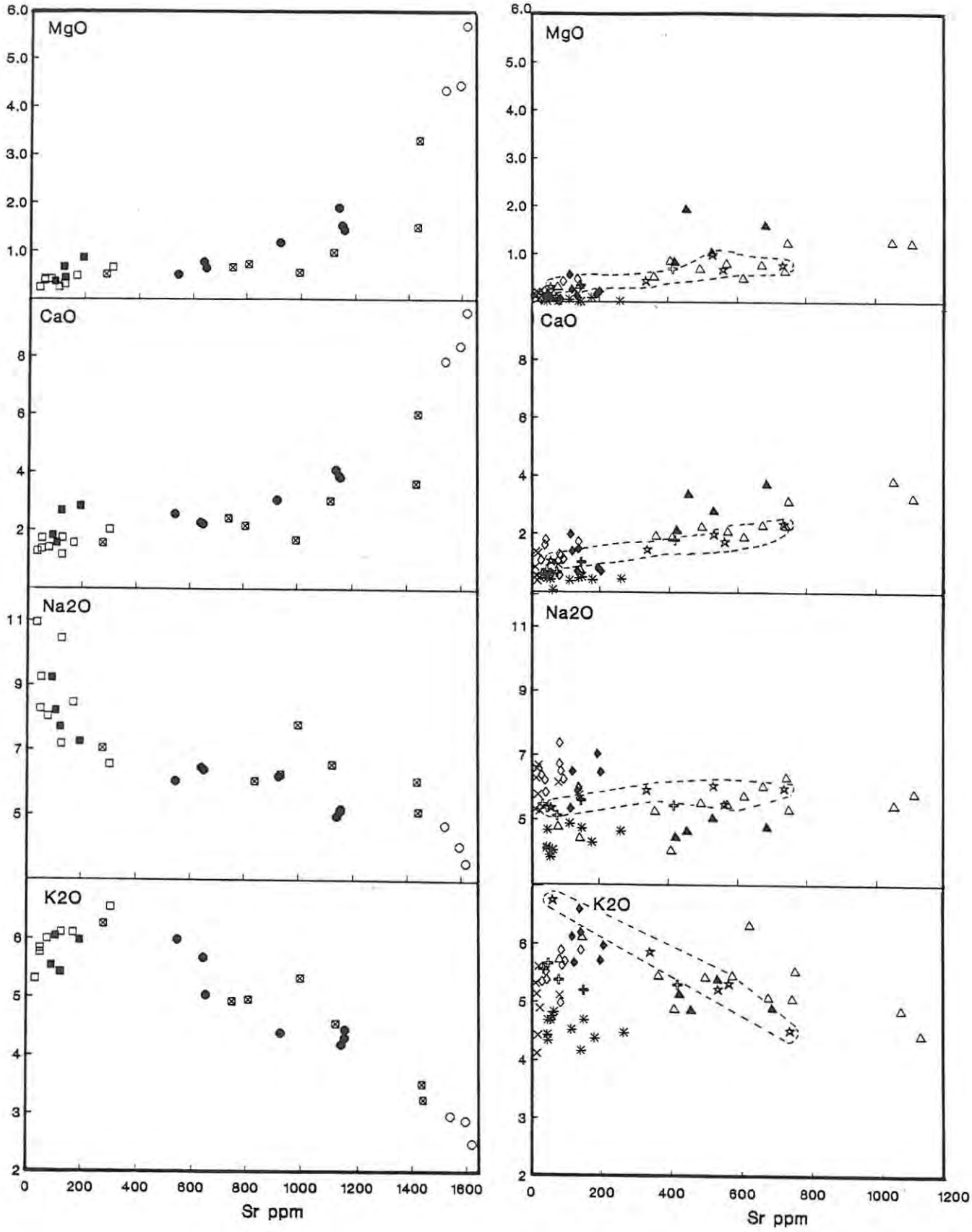

Figure 5.2 Continued.

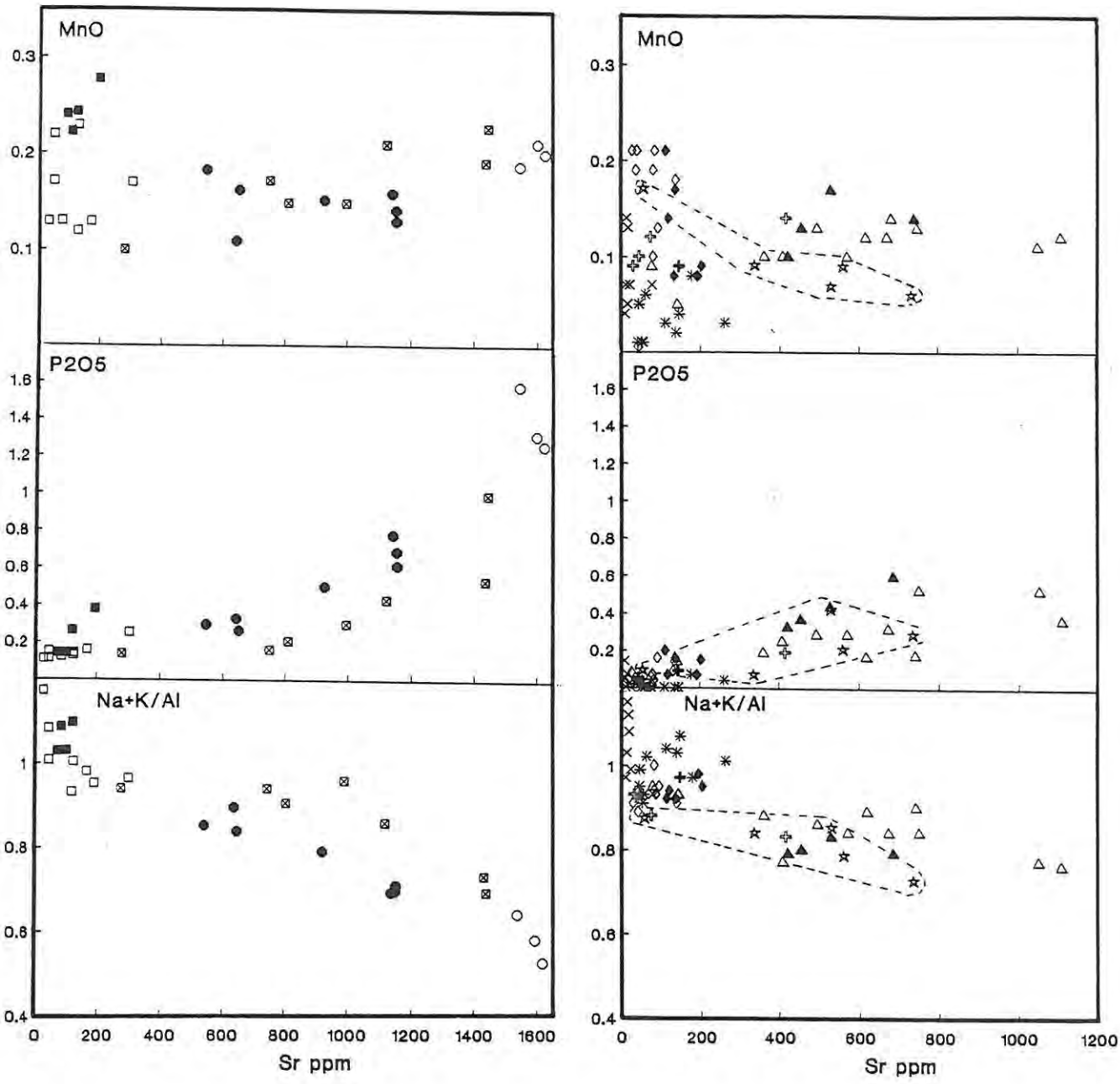

Figure 5.2 Continued.

involving feldspar. But, because the bulk composition of the rock types closely approximates that of feldspar, the precise nature of the process - whether accumulation or fractionation - cannot be determined on the basis of major-element data alone. Which ever is the case (feldspar accumulation or fractionation), trends to lower concentrations of mafic elements suggest that fractionation of mafic minerals took place.

With decreasing concentrations of Sr, the clinopyroxene-rich foyaite shows weak trends towards higher concentrations of Al_2O_3 and Na_2O, and lower concentrations of SiO_2, TiO_2, MgO and K_2O. Not all of these trends are evident in the amphibole-rich foyaite. At similar concentrations of Sr, the amphibole-rich foyaite has higher concentrations of FeO and generally lower concentrations of SiO_2 and K_2O than does the clinopyroxene-rich foyaite. Such compositional differences suggest the possibility that the two types of foyaite may not be directly related genetically.

The **critically-saturated** alkali-syenites show only a narrow range in the concentrations of major elements, probably because of the evolved nature of the rocks. Nevertheless there is a tendency for SiO_2 and K_2O to decrease in concentration, and for FeO and CaO to increase in concentration, with decreasing Sr. The alkali-feldspar syenite shows increasing K_2O, FeO and MnO and decreasing Al_2O_3, Na_2O, MgO, CaO, TiO_2 and P_2O_5 with increasing Sr. The trend for K_2O is especially pronounced.

The most primitive rocks of the monzonite - granite and larvikite - pulaskite series are virtually identical in terms of major-element composition, reflecting the very similar mineralogy noted in Chapter 3. The two series, however, evolved to very different compositions. With decreasing concentrations of Sr, the monzonite - granite series shows decreasing concentrations of Al_2O_3 and Na_20 (both of which showed an increase in the larvikite - pulaskite series); and a marked increase in the concentration of $Si0_2$. The compositional trends in the monzonite - granite series, taken together with relationships in

Petrogeny's Residua System, suggest that evolution here was dominated by fractionation of alkali-feldspar along with mafic phases.

The feldspar porphyries show slight enrichments in CaO, FeO, MgO, TiO_2 and P_2O_5, and depletions in Na_2O, compared with the associated hypidiomorphic granular rocks of the monzonite - granite series.

The alkali-granite of the Marinkas Kwela Granite body is generally more silicic than the alkali-granite of the dykes and plugs, and has lower concentrations of $Ti0_2$, Al_2O_3 and Na_2O at higher overall Sr concentrations. The differences in silica concentrations are significant and form the basis for subdividing the alkali-granites into high- and low-silica varieties - a distinction relevant to later chapters. The alkali-granite in the dykes and plugs has very low Sr concentrations but seems to be compositionally continuous with the most evolved rocks of the monzonite - granite series for all major elements except Na_2O, which is in higher concentrations in the alkali-granite, and K_2O and FeO, which are in lower concentrations.

5.4 Trace Element Variations

5.4 a Transition Metals: Cu, Cr, Ni, V, and Co (Fig. 5.3)

The low concentrations recorded for these elements is unsurprising given the highly leucocratic nature of the GPC and MKC in general. Together with similarly low Mg#, they suggest that the rocks of both complexes underwent considerable compositional evolution before emplacement. The elements are in especially low concentrations in the foyaites, the alkali-syenites and the alkali-granites (not shown on Fig. 5.3). Their positive correlations with Sr (Fig. 5.3) are consistent with major-element data which showed that fractionation of mafic phases was a part of the compositional evolution.

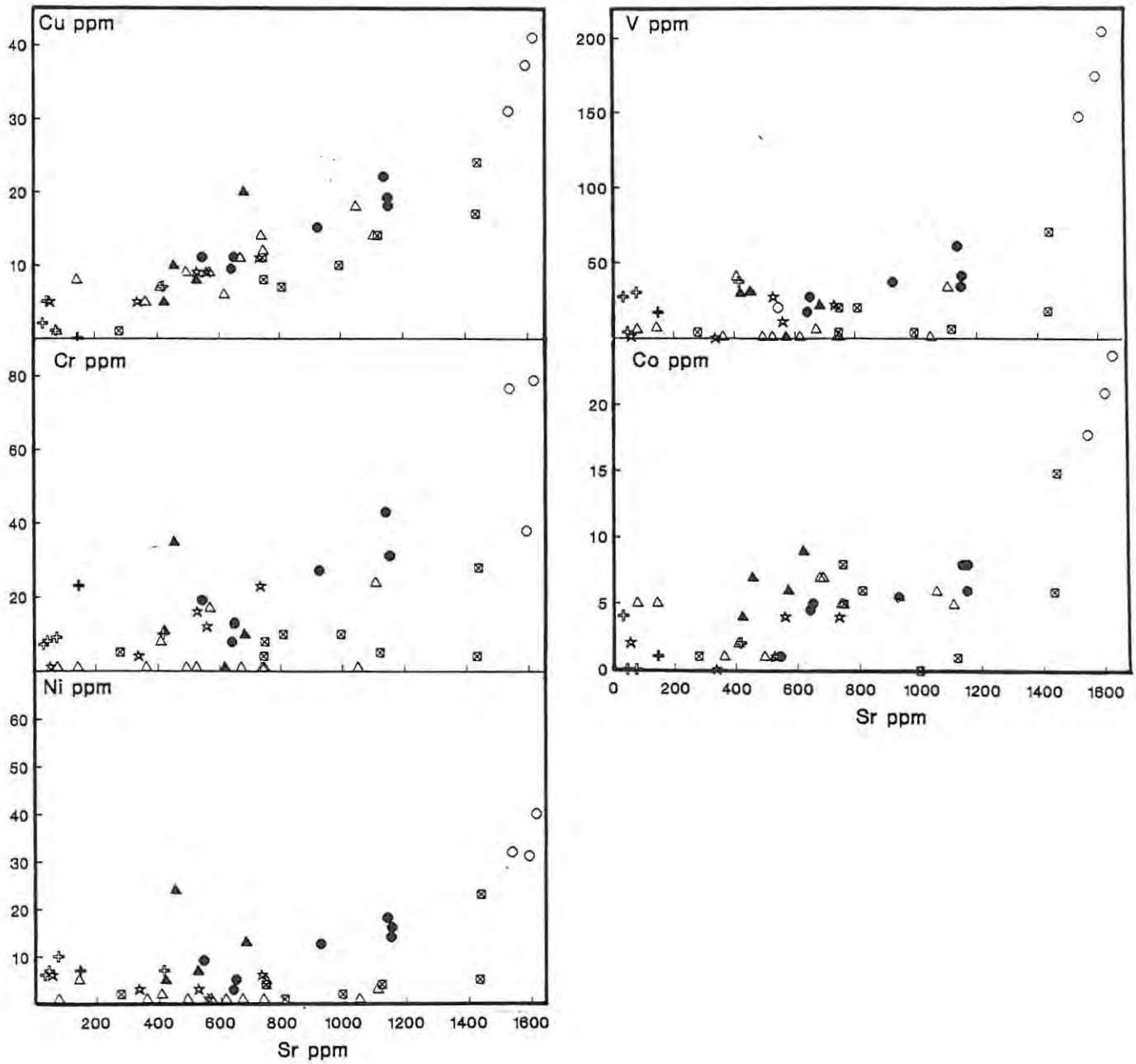

Figure 5.3 Transition element geochemistry for the rocks of the GPC and MKC. Because of very low concentrations for both Sr and the transition elements, data for the alkali-granites and the foyaites have been omitted. Symbols as in Table 2.1.

5.4.b Ba and Sr (Fig. 5.4)

Because alkali-feldspar concentrates both Sr and Ba (D_{Sr} = 2.3 - 8.2, D_{Ba} = 0.4 - 9.8 - Table 5.3), these two elements generally show a positive co-variation over a very wide range of bulk compositions. Maximum Ba concentrations of ± 2000ppm occur in the monzodiorite, larvikite, alkali-melasyenite, monzonite and alkali-feldspar syenite.

5.4.c Rb (Fig 5.4)

Rb concentrates in biotite (D_{Rb} = 2 - 3.26 - Table 5.3) and sometimes also in alkali-feldspar (D_{Rb} = 0.32 - 1.25). It is incompatible in most other phases crystallising from melts.

In the rocks of the GPC and MKC, the concentration of Rb increases (*vs* decreasing Sr) from 80ppm to 180ppm in the larvikite - pulaskite series; from 90ppm to 140ppm in the alkali-melasyenite - nepheline syenite series; from 120ppm to 210ppm in the foyaites; and from 120ppm to 280ppm in the monzonite - granite series. It remains relatively constant at ±120ppm in alkali-feldspar syenite. Data for alkali-syenites are generally scattered, although those for alkali-syenite in the GPC show a decrease in the concentrations of Rb (210ppm down to 100ppm) with decreasing Sr.

The highest concentrations of Rb (300ppm - 500ppm) occur in the alkaline rocks of the Marinkas Kwela Granite body and alkali-feldspar granite of the Grootpenseiland Granite body. The high concentrations of Rb (and Nb) in the latter distinguish it from other alkaline-related rocks of the Monzonite - Granite series. The other alkali-granites - those in dykes and plugs - contain significantly lower concentrations of Rb (±220ppm), similar to Rb concentrations in the evolved members of the monzonite - granite series.

With one exception, K/Rb ratios are within the limits of scatter considered by Ahrens *et al.* (1952) and Shaw (1968) to be typical of

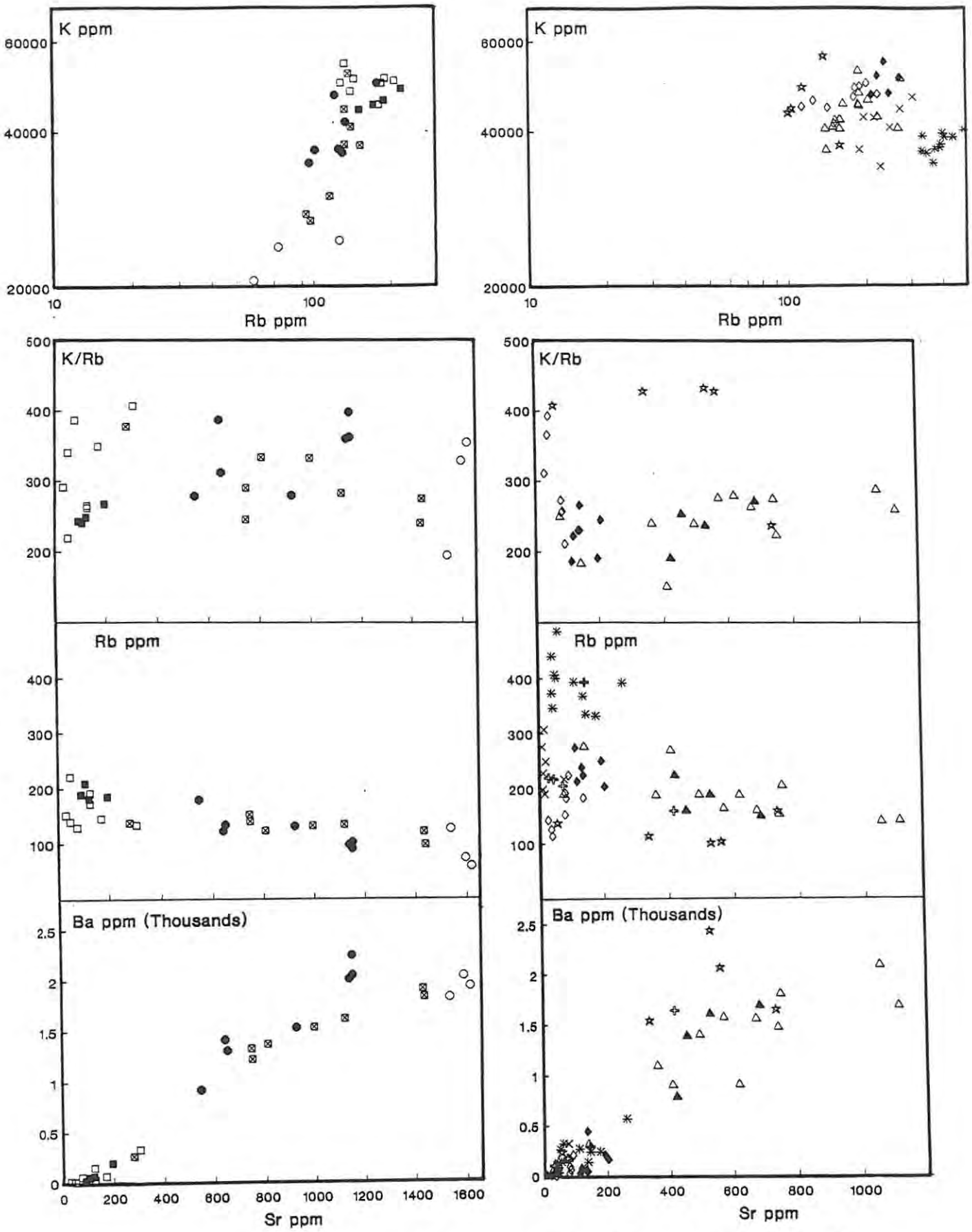

Figure 5.4 Variation of K *vs.* Rb and of K/Rb, Rb and Ba *vs.* Sr for the rocks of the GPC and MKC. **Si-undersaturated** rocks are presented on the left hand side of the figure, and **Si-oversaturated** and **critically saturated** rocks on the right hand side. For comparative purposes, the scale of the Y-axis is identical on both sides of the figure. Symbols as in Table 2.1.

continental crustal rocks. The exception is the ratio for alkali-granites of the Marinkas Kwela Granite body. These rocks are distinctly enriched in Rb relative to K, possibly as a result of protracted feldspar fractionation. In the larvikite - pulaskite series, the foyaites and the monzonite - granite series, K/Rb ratios decrease with differentiation. Similar trends are observed elsewhere (see, *e.g.*, Taylor, 1965; Stephenson, 1976). The K/Rb ratio for alkali-feldspar syenite appears to remain more or less constant, while the ratio for the alkali-melasyenite - nepheline syenite series appears to be constant or increases slightly with differentiation. Accumulation of alkali-feldspar is one process that could cause increasing K/Rb ratios.

5.4.d Zr, Nb, Y, Zn and Mo (Fig. 5.5)

These elements do not readily enter into common rock-forming minerals and usually concentrate in residual melts until suitable host minerals crystallise. Data on concentrations in each of the rock series/types are collated in Table 5.4. In general, concentrations are positively correlated with one another (Fig.5.6), although the data are often rather scattered.

As regards the **Si-undersaturated rocks,** the most notable feature is the contrasting behaviour that Zn, Zr and Nb display in the larvikite - pulaskite series on the one hand, and in the alkali-melasyenite - nepheline syenite series on the other. In the former, their concentrations increase with decreasing concentration of Sr; in the latter, the opposite obtains. Also of note is that, while concentrations of the elements in the foyaites show no systematic variation against Sr, most concentrations are higher in the amphibole-rich foyaites than in the clinopyroxene-rich foyaites. (Mo provides the exception.)

Data for the **critically saturated** alkali-syenites are very scattered and yield no discernible trend against Sr, although it is noteworthy that these rocks, taken as a whole, are more enriched in the five

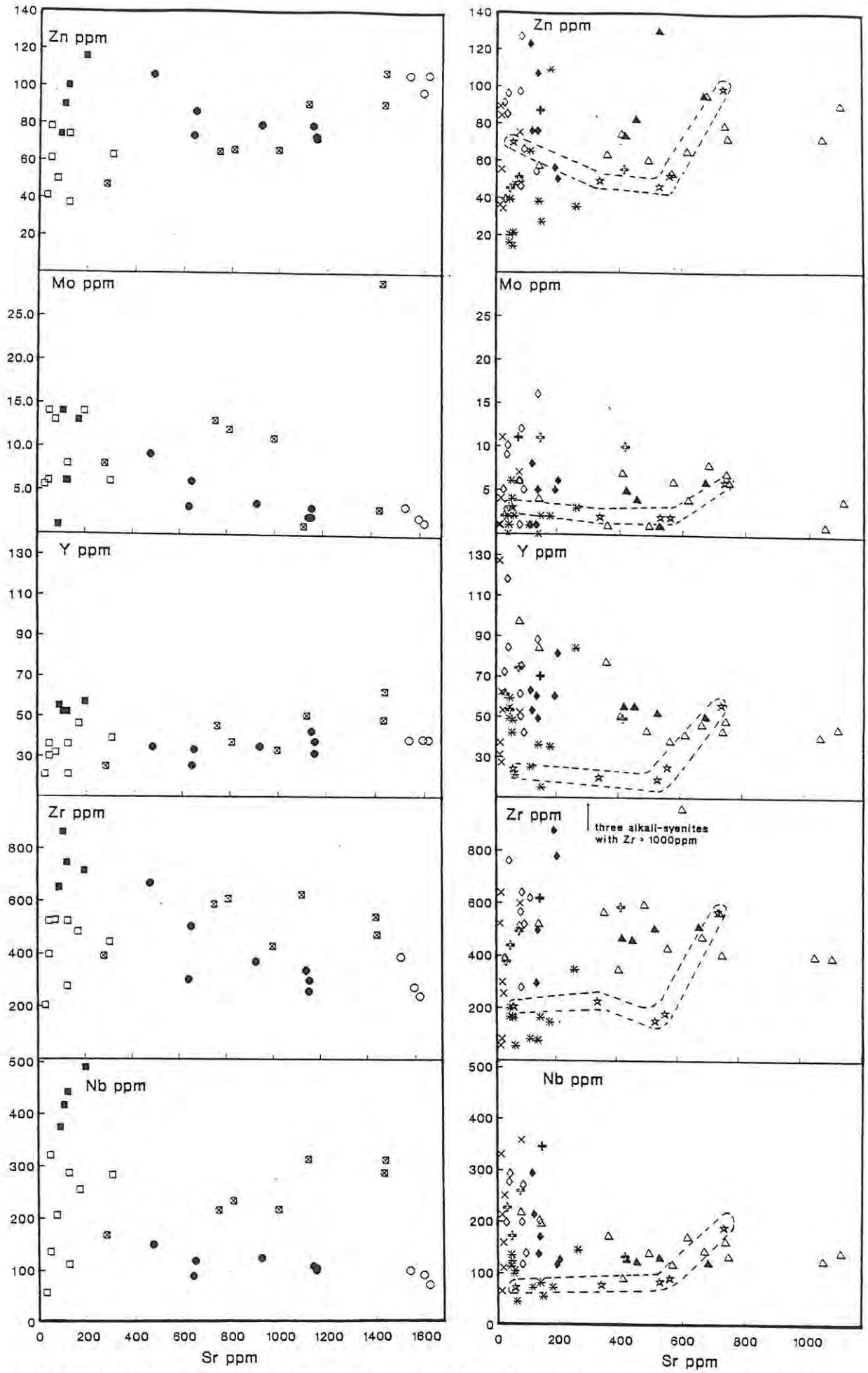

Figure 5.5 Variation of Zn, Mo, Y, Zr and Nb (all in ppm) *vs.* Sr (ppm) for the rocks of the GPC and MKC. **Si-undersaturated** rocks are presented on the left hand side of the figure and **Si-oversaturated** and **critically saturated** rocks on the right hand side. For comparative purposes, the scale of the Y-axis is identical on both sides of the figure. The field defined by the dotted line encloses data for alkali-feldspar syenites. Symbols as in Table 2.1.

Table 5.4 Approximate variations in the concentrations of Nb, Zr, Y, Mo and Zn (all in ppm) and the sence of variations against Sr (ppm) (see Fig.5.5)

	Nb	Zr	Y	Mo	Zn
Monzodiorite	60 ↗ 88	200 ↗ 380	38	1 ↗ 3	95 - - - - 105
Larvikite – Pulaskite series	80 ↗ 140	240 ↗ 650	25 — 40	1 ↗ 8	70 ↗ 105
Alkali–melasyenite – Nepheline–syenite	320 ↘ 160	380 - - - 640	65 ↘ 22	1 ↗ 13	105 ↘ 45
Foyaites	50 - - - - 500	200 - - - - 880	20 - - - - 55	1 - - - - 14	35 - - - - 115
Alkali–syenite	100 - - - - 280	250 - - - - 720	40 - - - - 120	1 - - - - 15	45 - - - - 125
Alkali–feldspar syenite	60 — 200	150 — 600	10 — 55	2 — 7	40 — 100
Monzonite – Granite series	100 ↗ 210	350 ↗ 600	35 ↗ 95	1 ↗ 6	50 90
Alkali–granite	40 - - - - 350	50 - - - - 620	15 - - - - 125	1 - - - - 11	10 - - - - 110

↗ increasing against Sr — constant

↘ decreasing against Sr - - - - no trend

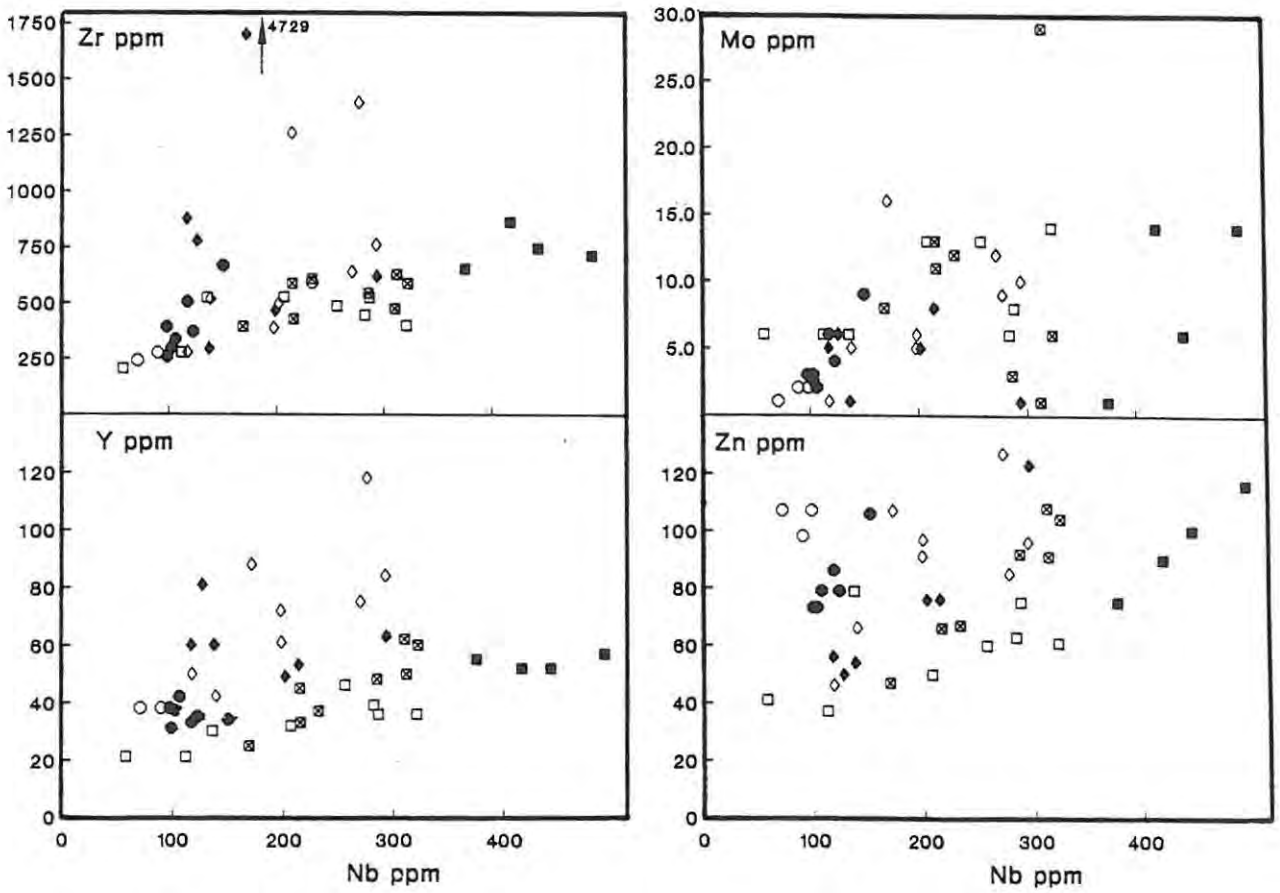

Figure 5.6 Variation of Zr, Y, Mo and Zn *vs.* Nb (all in ppm) for the Si-undersaturated and critically saturated rocks of the GPC and MKC. Symbols as in Table 2.1.

elements than is any other rock type. By contrast, alkali-feldspar syenite is amongst the least enriched and, apart from a single sample, shows the least variation as regards concentrations of the five elements.

As regards the **Si-oversaturated rocks,** the monzonite - granite series shows systematic trends in Figure 5.5, and the alkali-granites do not. In the former, concentrations of Zr, Nb, Y and Mo all increase with decreasing Sr (although Zn displays the opposite tendency). A reflection of these increases is the late-stage appearance of accessory phases such as zircon and allanite, noted in Chapter 3.3.a.

5.3 e Pb, Th and U (Fig. 5.7)

Data on concentrations of these elements in each of the rock series/types are collated in Table 5.5. All three elements display residual behaviour in the larvikite - pulaskite and monzonite - granite series. In the alkali-melasyenite - nepheline syenite series, Th and possibly U show residual behaviour while the concentrations of Pb show positive correlation with those of Sr.

Data for the other rock types yield no well-defined trends excepting in one notable respect: concentrations of Th are positively correlated in alkali-syenite *of the MKC*, but negatively correlated in alkali-syenite *of the GPC*. It may be useful here to recall the differences that were noted earlier between the alkali-syenites of the two complexes in regard to their amphibole compositions (Chap 4.3).

Like the previous group of elements, Pb, Th and U are present in alkali-feldspar syenite only in low and fairly constant concentrations compared with concentrations in other rock types. This feature of alkali-feldspar syenite is unsurprising given the rarity of accessory minerals (Chap 3.2.a), and can also be seen as characteristic of feldspar cumulates.

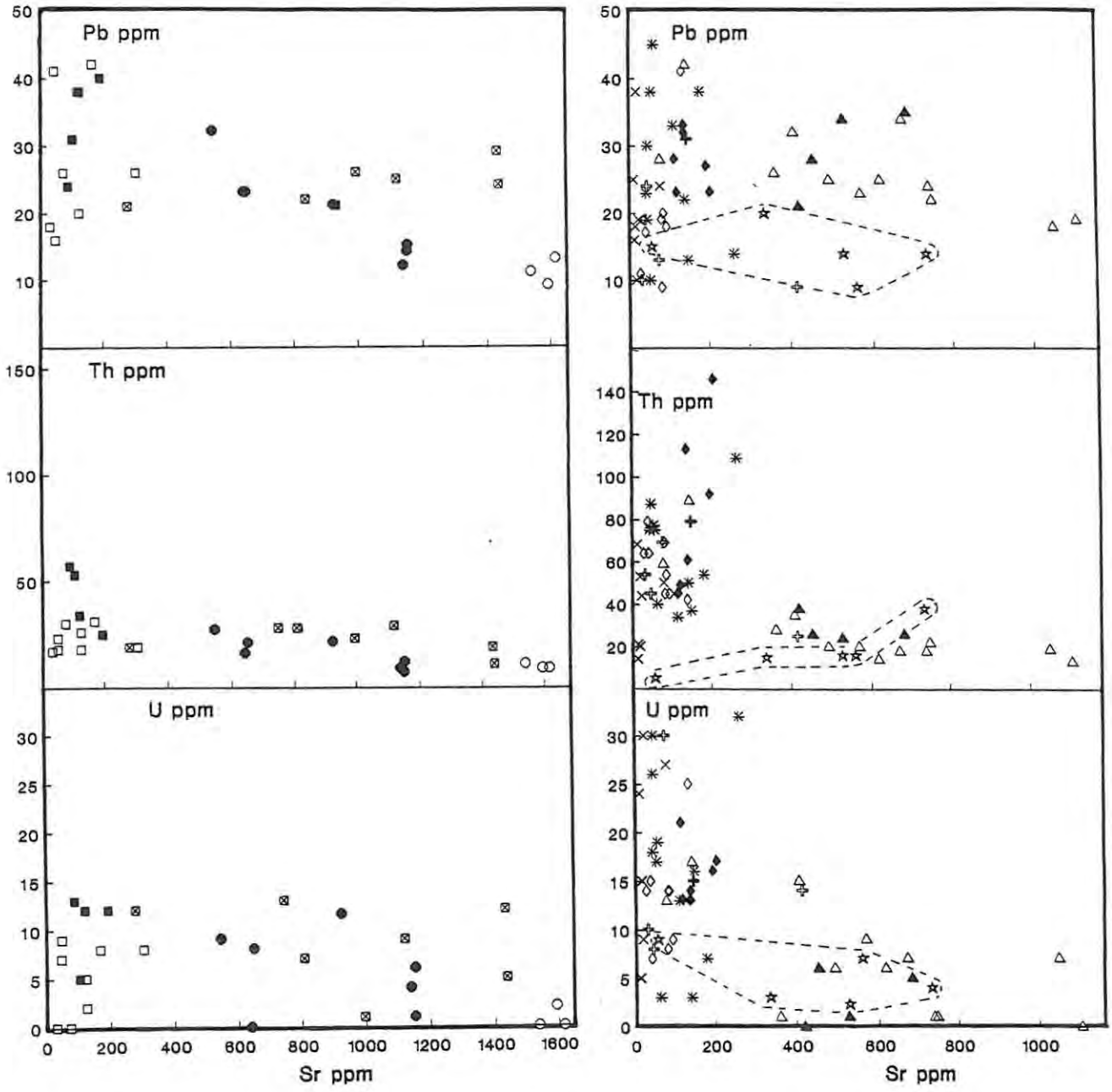

Figure 5.7 Variation of Pb, Th and U (all in ppm) *vs.* Sr for the rocks of the GPC and MKC. **Si-undersaturated** rocks are presented on the left hand side of the figure, and **Si-oversaturated** and **critically saturated** rocks on the right hand side. For comparative purposes, the scale of the Y-axis is identical on both sides of the figure. The field defined by the dotted line encloses data for the alkali-feldspar syenite. Symbols as in Table 2.1.

Table 5.5 Approximate variations in the concentrations of Pb, Th and U (all in ppm) and the sence of variations against Sr (ppm) (see Fig.5.7)

	Pb	Th	U
Monzodiorite	8 - - - 14	10	1 - - - 2
Larvikite – Pulaskite series	12 / 33	5 / 30	1 / 11
Alkali–melasyenite – Nepheline–syenite	30 \ 20	6 / 31	1 - - - 12
Foyaites	15 - - - 42	20 - - - 60	1 - - - 14
Alkali–syenite	8 - - - 44	42 - - - 145	25 \ 7
Alkali–feldspar syenite	6 — 20	40 \ 5	2 — 9
Monzonite – Granite series	17 / 42	12 / 90	1 / 18
Alkali–granite	10 - - - 45	30 - - - 110	3 - - - 32

/ increasing against Sr — constant

\ decreasing against Sr - - - no trend

5.4.f F and Cl (Figs. 5.8 & 5.9)

The concentration of F decreases against Sr in all rock types except those of monzonite - granite series, where it increases to a maximum of ±3500ppm. Data for Cl is available only for the Si-undersaturated rocks. In respect of those, and with the exception of the foyaites, Cl tends to be very erratic. The positive correlation with Na_2O that the element shows in the foyaites (Fig. 5.8.c) is to be expected, given that sodalite forms a significant portion of some of those rocks. Chlorine also shows a negative correlation with Nb, Y and Zr for both types of foyaite (Fig.5.9).

5.4.g Rare Earth Elements (REE)

Many of the common rock-forming minerals have unique REE mineral-melt distribution coefficient patterns, but these coefficients are not large and so the REE behave incompatibly in most melts. Accessory minerals such as apatite, sphene, allanite and monazite commonly have very high partition coefficients for REE and it is often

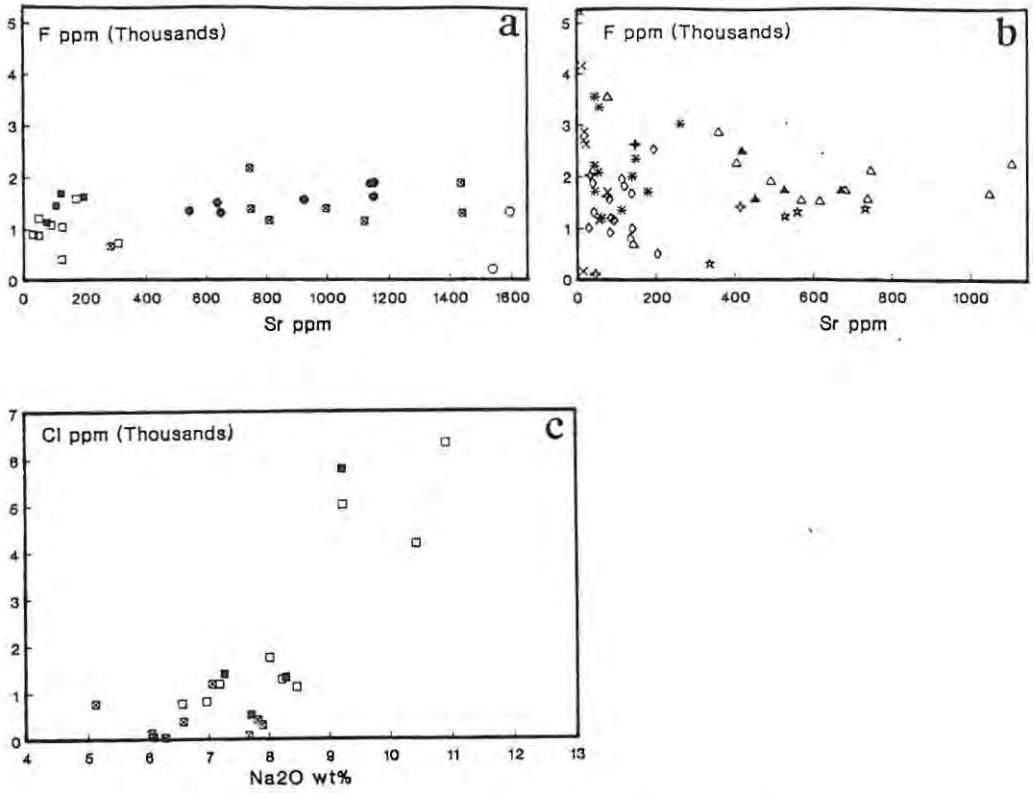

Figure 5.8 Variation of F (ppm) *vs.* Sr (ppm) for **(a)** the Si-undersaturated rocks, **(b)** Si-oversaturated and critically saturated rocks and **(c)** Cl (ppm) *vs.* Na_2O (wt%) for the foyaites and the alkali-melasyenite - nepheline syenite series. Symbols as in Table 2.1.

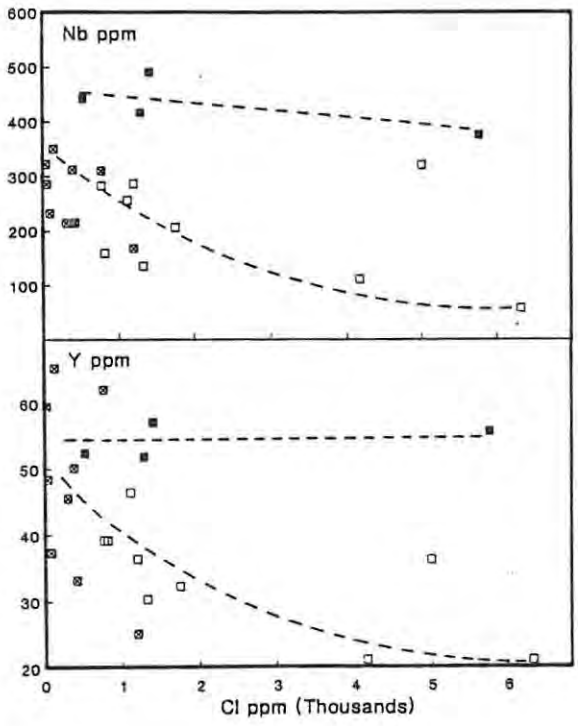

Figure 5.9 Variation of Nb and Y *vs.* Cl (all in ppm) for the foyaites and alkali-melasyenite - nepheline syenite series. Symbols as in Table 2.1.

these phases that determine the relative concentrations of REE in a rock or magma.

In the discussion that follows, all ratios amongst REE with the exception of those involving Eu have been calculated using measured concentrations. Chondrite-normalised values were used to assess anomalous concentrations of Eu with respect to the normalised concentrations of Sm and Gd. The extent of the anomaly is defined by the ratio Eu/Eu* where Eu is the concentration of europium and Eu* is the value obtained at the europium position by straight line interpolation between the plotted points for chondrite-normalised Sm and Gd. Where this ratio exceeds unity the Eu anomaly is positive, whereas negative Eu anomalies have Eu/Eu* <1.

A general feature to be noted about all rock types in both the GPC and the MKC is that there is a general decrease in the La/Yb ratio with increasing Na+K/Al (Fig 5.10).

Si-undersaturated rocks have high absolute REE abundances and are distinctly enriched in light Rare Earth Elements (LREE) at 260-760 x chondrite, compared with heavy Rare Earth Elements (HREE) at 11-29 x chondrite. Such steeply inclined chondrite-normalised REE profiles are a characteristic of alkaline rocks (Neuman *et al.*,1977; Môller *et al.*, 1980; Price *et al.*,1985; Bouabdli *et al.*,1988).

The least evolved rocks of the alkali-melasyenite - nepheline syenite series show the highest absolute REE abundances and have a slight negative Eu anomaly (Eu/Eu* = 0.72). With decreasing concentration of Sr, the abundance of LREE and middle Rare Earth Elements (MREE) steadily decreases and the Eu anomaly disappears, or becomes slightly positive, in nepheline syenite (Fig.5.10.a). There is also a corresponding decrease in the La/Yb ratio from 39 to 17.

One monzodiorite was analysed for REE. It showed concentrations within the range for the alkali-melasyenite, but with no Eu anomaly and a distinctly higher La/Yb ratio of ±70.

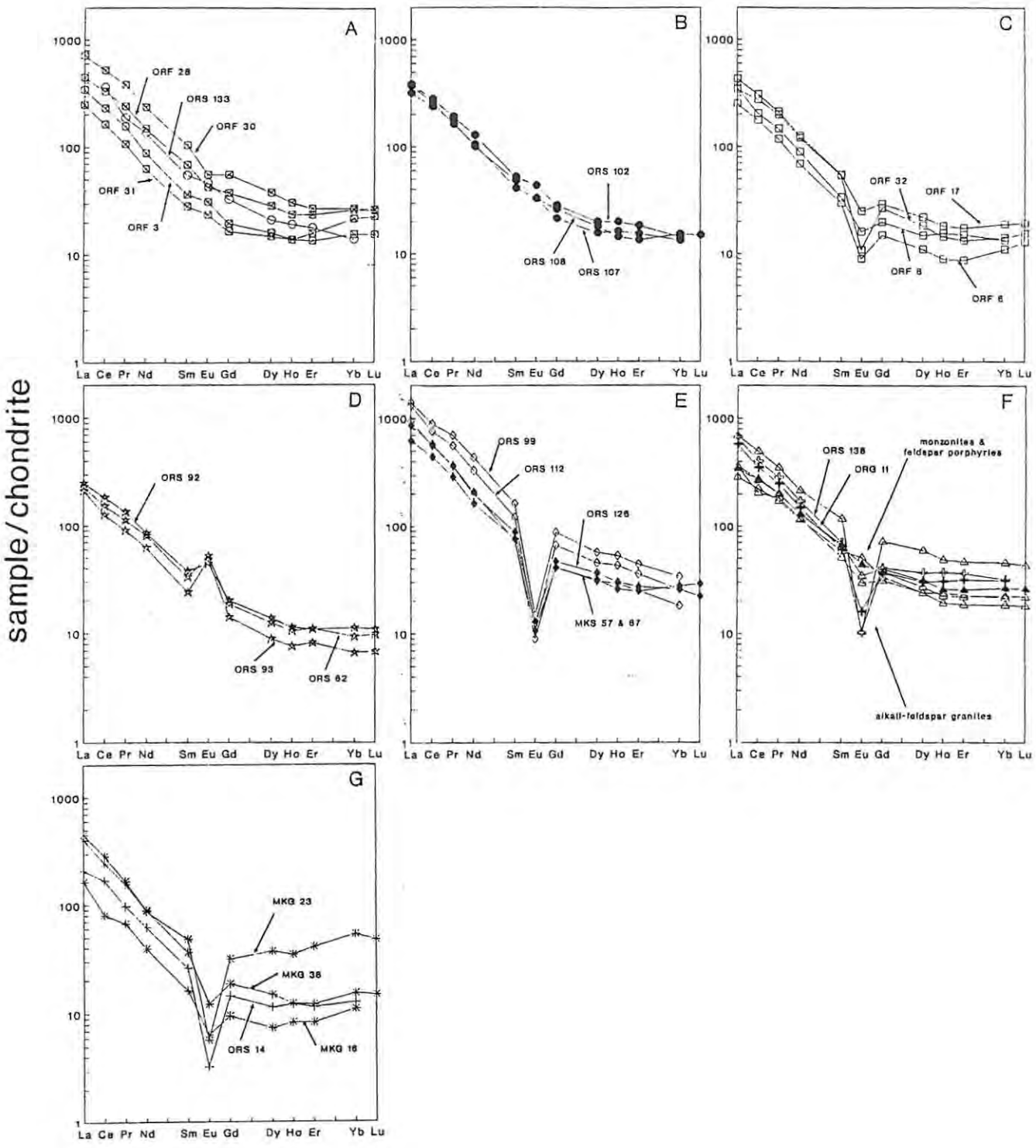

Figure 5.10 REE patterns, normalised against chondritic abundance data from Nakamura (1974), for the rocks of **(A)** the alkali-melasyenite - nepheline syenite series and the monzodiorite, **(B)** the larvikite - pulaskite series, **(C)** the clinopyroxene-rich foyaite, **(D)** the alkali-feldspar syenite, **(E)** the alkali-syenites, **(F)** the monzonite - granite series and **(G)** the alkali-granites. Symbols as in Table 2.1.

The larvikite - pulaskite series (Fig. 5.10.b) and the foyaites (Fig. 5.10.c) show a very narrow range of REE abundances, with La/Yb ratios varying between 31 and 41, and 34 and 40, respectively. The clinopyroxene-rich foyaite shows a systematic decrease in REE concentrations with differentiation, and negative Eu anomalies become more pronounced (Eu/Eu* = 0.62 - 0.42).

The **critically saturated** alkali-feldspar syenite (Fig. 5.10.d) is the only rock type to display a significant positive Eu anomaly (Eu/Eu* = 1.6), but otherwise the rock shows high absolute REE abundances and La/Yb ratios (34) like those found in Si-undersaturated rocks. In contrast, the alkali-syenites (Fig. 5.10.e) show a strong enrichment in LREE abundances (which is especially marked in the alkali-syenite from the GPC), and large negative Eu anomalies (Eu/Eu* = 0.12-0.17). La/Yb ratios vary between 34 and 79.

The more evolved rocks of the **Si-oversaturated** monzonite - granite series show slightly higher REE abundances, and more pronounced negative Eu anomalies, than do the less evolved rocks of the series (Fig. 5.10.f). Ratios for Eu/Eu* in the more evolved rocks are 0.11 in the MKC, 0.19 in the GPC and 0.34 in the Grootpenseiland Granite body; in the less evolved rocks, the figure is about unity. Patterns of REE abundance in the less evolved rocks, including the feldspar porphyries, are very similar to those of the larvikite - pulaskite series, but show slightly lower La/Yb ratios (20-25).

Finally, the most notable feature of the alkali-granites in terms of REE concentrations are the flat chondrite-normalised HREE (Gd-Dy) patterns that they display. Alkali-granites are the only rocks in either complex to show this characteristic.

CHAPTER 6: ISOTOPE GEOCHEMISTRY AND AGE DETERMINATIONS FOR THE GPC AND THE MKC

6.1 Introduction

Radiogenic and stable isotopic analyses were undertaken in order to constrain the age of emplacement of the GPC and MKC, and to help characterise the source-rocks of the various magma types. Sr, Nd and Pb isotopic analyses were carried out at the Council for Scientific and Industrial Research (C.S.I.R.) in Pretoria, and oxygen isotopic analyses at the University of Cape Town. The results are presented in Tables 6.1 to 6.3. Analytical procedures are presented in Appendix 3. A general discussion covering isotope systematics was not considered necessary here in view of the wealth of such information elsewhere (*e.g.* Faure, 1986).

6.2 Rb/Sr Isotopic Age For The GPC And The MKC

Field evidence noted in Chapter 2 showed that the rocks of the larvikite - pulaskite series were amongst the earliest to be emplaced in either complex. These rocks were selected for age-determinations in this study because, as Chapter 5 shows, they display geochemical coherence as a suite, and have a wide range of Rb/Sr ratios relative to other Si-undersaturated rocks. Whole-rock Rb/Sr isotopic data were obtained for seven samples (Table 6.1). One data-point (ORS 61) was omitted from the data-set because it alone deviated significantly from a line of best fit on an isochron diagram (Fig. 6.1), and because similar deviations were frequently observed in numerous other variation diagrams (for example, of Sr *vs* Zr, Nb and U).

Table 6.1. Sr and O isotopic analyses.

	Rb	Sr	$^{87}Rb/^{86}Sr$	$^{87}Sr/^{86}Sr$	I_{Sr}	$\delta^{18}O_{(SMOW)}$ feldspar	quartz
Monzodiorites							
ORS 133	74	1599	0.1342	0.705583 ±9	0.7045 ±1 *		
Alkali melasyenites-nepheline syenites							
ORF 49	118	925	0.3691	0.707644 ±31	0.7048 ±11 !		
Larvikites-pulaskites							
ORS 61	127	638	0.5761	0.709643 ±13	0.7052 ±2 *		
ORS 90	87	1153	0.2203	0.706358 ±10	0.7046 ±1 *		
ORS 94	104	1158	0.2612	0.706712 ±8	0.7047 ±1 *		
ORS 102	98	1158	0.2442	0.706551 ±12	0.7047 ±1 *		
ORS 107	128	923	0.4029	0.707996 ±9	0.7049 ±1 *		
ORS 108	133	648	0.5961	0.709230 ±19	0.7047 ±1 *	8.14	
ORS 158	123	501	0.7107	0.710041 ±17	0.7046 ±2 *		
Foyaites							
ORF 17	138	296	1.3450	0.714106 ±23	0.7043 ±3 !	7.66	
ORF 32	139	46◦	8.8697	0.766042 ±23	0.7017 ±18 !		
ORF 33	186	121	4.4439	0.739095 ±19	0.7065 ±9 !		
ORF 40	191	87	6.3458	0.757681 ±26	0.7111 ±13 !		
Alkali-syenites							
ORS 60	152	83	5.3220	0.742729 ±10	0.7037 ±11 !		
ORS 99	114	37	8.8610	0.773071 ±13	0.7081 ±17 !	7.62	
ORS 126	192	87	6.4140	0.752943 ±10	0.7059 ±12 !	8.05	
MKS 57	218	121	5.2044	0.740629 ±20	0.7025 ±10 !	7.74	
MKS 67	237	134	5.1475	0.740879 ±21	0.7031 ±10 !		
Alkali-feldspar syenites							
ORS 62	102	537	0.5521	0.709009 ±11	0.7049 ±1 !		
Monzonites-granites							
MKG 6	268	405	1.9168	0.719587 ±20	0.7055 ±4 !	8.31	9.41
MKS 3	144	1107	0.3767	0.707351 ±21	0.7045 ±1 !		
MKS 36	194	497	1.1270	0.712773 ±22	0.7044 ±2 !		
MKS 53	164	672	0.7052	0.710400 ±25	0.7052 ±2 !	8.48	
MKS 54	194	623	0.9012	0.710681 ±15	0.7040 ±2 !		
MKS 59	209	734	0.8250	0.711395 ±23	0.7057 ±1 !		
MKS 61	191	75	7.3577	0.755831 ±24	0.7019 ±15 !		
MKS 63	192	356	1.5665	0.716364 ±21	0.7049 ±3 !		
MKS 66	142	1037	0.3955	0.707326 ±22	0.7044 ±1 !		
ORS 130	160	407	1.1380	0.713314 ±23	0.7049 ±3 !		
ORS 138	204	73	8.1285	0.762333 ±22	0.7027 ±16 !		
ORG 11 porphyries	390	144	7.8785	0.763406 ±23	0.7056 ±16 !		
MKS 16	225	418	1.5587	0.716359 ±21	0.7049 ±3 !		
MKS 29	161	455	1.0243	0.713065 ±19	0.7055 ±2 !		
Alkali-granites							
ORS 14	197	15◦	39.6700	0.961922 ±39	0.6713 ±79 !		
ORF 48	313	17◦	55.5090	1.067573 ±44	0.6609 ±111 !		
MKS 43	204	11◦	54.2910	1.064905 ±35	0.6671 ±108 !		
MKG 16	332	144	6.7052	0.760868 ±19	0.7117 ±13 !	7.92	9.79
MKG 38	327	175	5.4246	0.742333 ±20	0.7025 ±11 !	7.50	
MKG 36						7.95	11.92
MKG 23						7.86	
MKG 13						7.53	

! calculated at 514Ma

* calculated at 529Ma

Present day ratios quoted at 2σ level

Initial ratios quoted at 1σ level

Decay constant = $1.42 \times 10^{-11} y^{-1}$

◦ Determined by isotope dilution - otherwise by XRF.

$^{87}Sr/^{86}Sr$ for NBS SRM 987 = 0.710275 ±16

Assumed Bulk Earth: $^{87}Sr/^{86}Sr = 0.7047$; $^{87}Rb/^{86}Sr = 0.0847$.

The resulting data-set of six analyses defines an isochron with an inferred late Pan-African age of 529 ± 24Ma. This result is consistent with all previous isotopic work on rocks of the Kuboos - Bremen Igneous Province (Allsopp *et al.*,1979), which has indicated equivalent emplacement ages of 525 ± 60Ma (U-Pb zircon) for the Kuboos pluton, 518 ± 15Ma (Rb/Sr errochron and U-Pb zircon concordia) for the Younger Bremen Complex, and 491 ± 8Ma (Rb/Sr isochron) for the Garub pyroclastic sill. Hence, 529 ± 24Ma is accepted as a reasonable emplacement age for the earliest intrusive rocks of the GPC.

Near the other end of the emplacement history of the complexes are the rocks of the monzonite - granite series, which are intruded only by alkali-granites. In the MKC, the series appears to be geochemically coherent (see Chapter 5), and it exhibits a wide range of Rb/Sr ratios. Of the eleven samples chosen from the MKC, one datum point (for MKS 59) is anomalous (Fig.6.2) in that it lies well above the line of best fit for the remaining data. When this sample is disregarded, the remaining data still define only an errorchron* on an isochron diagram (Fig.6.2) with an inferred age of 514 ± 26Ma. The apparent geochemical coherence of the series does not on its own necessarily require that the rocks were derived from a single magma batch but, when taken in conjunction with the close spatial relationships between the rocks, it does indicate a common parentage. In the ideal case, isochron relationships would then be expected. The 'excess' or 'geological' scatter in the isochron diagram in Figure 6.2 can only be attributed to a degree of open system evolution. In any case the 514 ± 26Ma errorchron can confidently be accepted as an approximation of the age at which the monzonite - granite series was emplaced in the MKC.

---

*Where data points for a related suite of rocks deviate from a line of best fit by more than the estimated analytical uncertanty then the data set is described as having excess, or geological, scatter and defines an errorchron, as opposed to an isochron (Brooks et al.,1972).

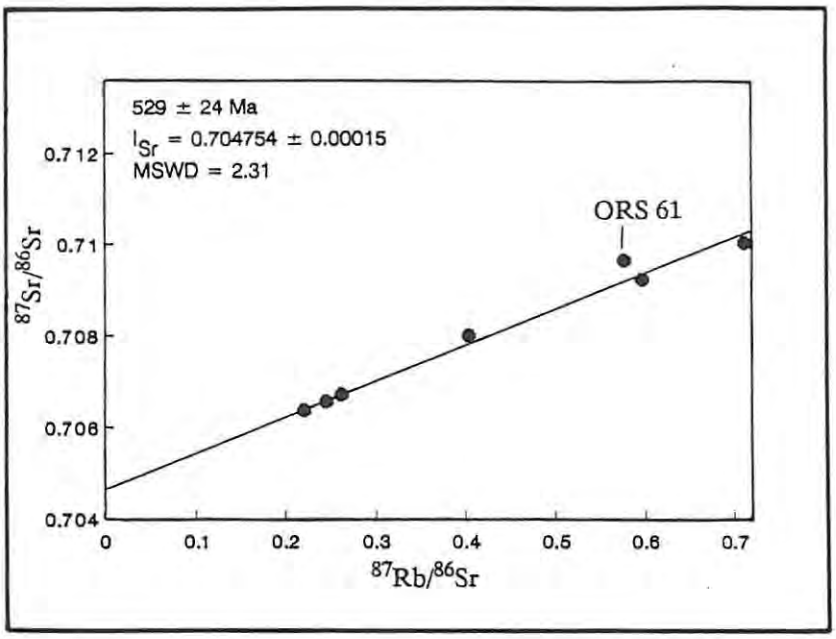

Figure 6.1 Rb/Sr isochron diagram for rocks of the larvikite - pulaskite series. Removing the one anomalous data point (ORS 61) yields an isochron with an inferred age of 529 ± 24Ma. Errors quoted at the 2σ level.

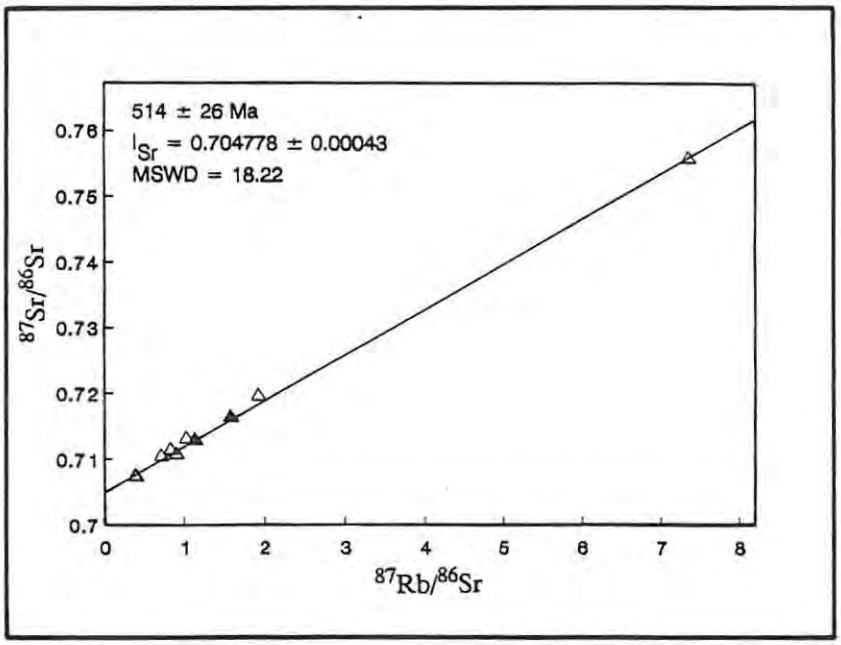

Figure 6.2 Rb/Sr isochron diagram for rocks of the monzonite - granite series of the MKC. Removing the anomalous data point (MKS 59) yields an errorchron with an inferred age of 514 ± 26Ma. Errors quoted at the 2σ level.

This errorchron age is not significantly altered when either the high $^{87}Rb/^{86}Sr$ sample (MKC 61 - an alkali-feldspar granite) or the two feldspar porphyry samples (MKC 16 and MKC 29) are omitted. Neither is it changed by adding data for three samples taken from the monzonite - granite series of the GPC (including one sample from the Grootpenseiland Granite body).

Indeed, setting aside data for the alkali-granites, *all* combinations of data-sets from the various rock series of both intrusive complexes define errorchron regression lines that indicate emplacement ages equivalent to those of the rocks of the larvikite - pulaskite series (Fig.6.3). Because of low sample numbers and the uncertainty of genetic links between the complexes, the lines of best fit in Figure 6.3. cannot be regarded as true errorchrons. Nevertheless the data do suggest that the intrusive history of the GPC and the MKC was relatively short.

Data for the ***alkali-granites*** of both intrusive complexes define a line of lower slope and higher initial ratio than the 514Ma errorchron (Fig.6.4). While these results are consistent with the fact that the alkali-granites were the last major phases of both complexes, the ± 460Ma age obtained is very low in relation to ages obtained for other intrusive units. It seems most likely that these alkali-granites are not directly related to one another (compositional differences have already been noted in Chapter 5), or else did not evolve within a closed system.

6.3 Initial Sr-Isotope Ratios

Disregarding the alkali-granites, for which the minimum age of intrusion cannot be constrained, the range in I_{Sr} for all rock types having Sr concentrations <200ppm, and assumed intrusive ages between 529Ma and 514Ma, lies between 0.7011 and 0.7111. The scatter in the data suggests that some I_{Sr} ratios have been disturbed. Ancient loss of Rb (i.e. through subsolidus alteration) could result in low apparent I_{Sr} ratios while the high ratios (>0.706) may reflect interaction with a high $^{87}Sr/^{86}Sr$ component such as the crust.

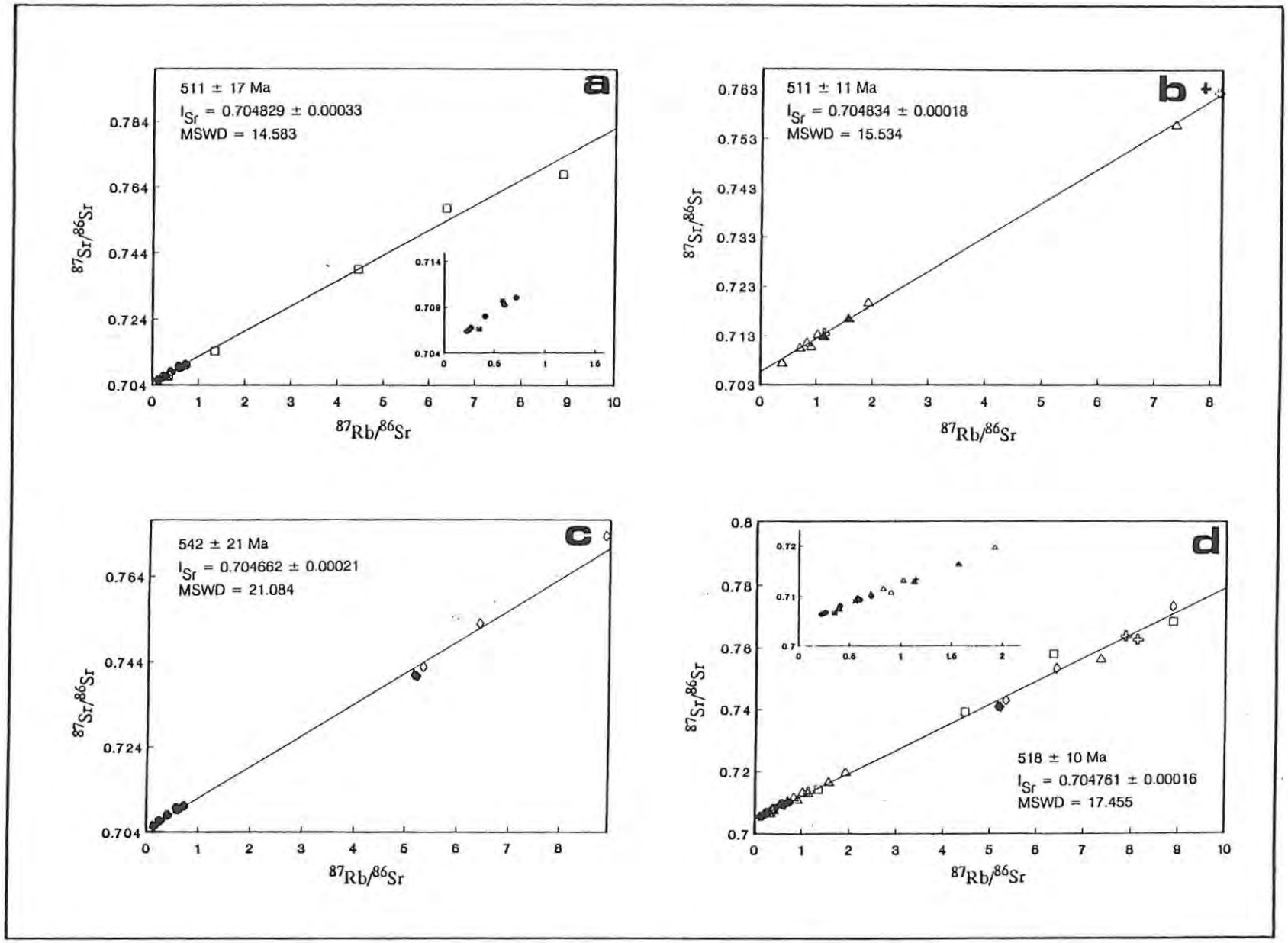

Figure 6.3 Rb/Sr isochron diagram for various combinations of rock-types in the GPC and the MKC: **a)** all data for Si-undersaturated rocks, **b)** all data for rocks of the monzonite - granite series (GPC and MKC), **c)** all data for the larvikite - pulaskite series and the alkali-syenites and **d)** combination of **a**, **b** and **c**. Inserts show more clearly the spread of data with low $^{87}Rb/^{86}Sr$. Note that all combinations give equivalent ages and I_{Sr} ratios. Symbols as in Table 2.1. Errors quoted at the 2σ level.

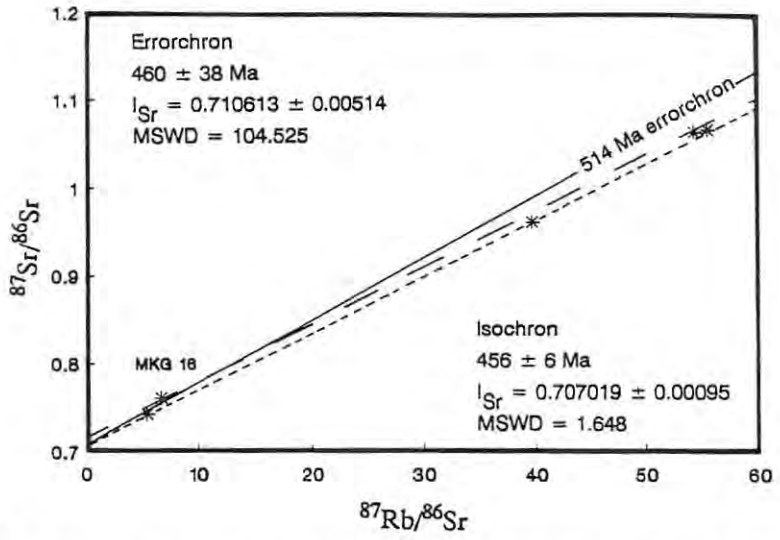

Figure 6.4 Rb/Sr isochron diagram for alkali-granites of the GPC and MKC. The two data points with lowest $^{87}Rb/^{86}Sr$ are for alkali-granites from the Marinkas Kwela Granite body. Retaining all five data points yields a line with errorchron statistics (large dashed line) while eliminating the data point for MKC 16 yields a line with isochron statistics (small dashed line). Both regression lines have a significantly lower gradient than the 514Ma reference line (see text for detail). Errors quoted at the 2σ level.

However, the majority of samples, including all those with Sr concentrations >200ppm, show a narrow range in I_{Sr} that lies between 0.704 and 0.706. Rocks of the larvikite - pulaskite series and the monzonite - granite series share equivalent initial $^{87}Sr/^{86}Sr$ ratios (I_{Sr}) of 0.704754 ± 0.00007 (2σ) and 0.704778 ± 0.00043 (2σ) respectively (Figs. 6.1 & 6.2). Such values are only slightly higher than that of Bulk Earth at 529Ma (approximately 0.7039). They probably reflect a large component of mantle-derived Sr but another possible explanation, discussed in Chapter 10.1, is that Sr was derived, at least in part, from lower crustal regions having low $^{87}Sr/^{86}Sr$ ratios.

While the age of the alkali-granites is not well constrained, the rocks have to be younger than 514 ± 26Ma, which is the age established for the rocks of the monzonite - granite series (Chap. 6.2.) into which the alkali-granites were intruded. This defines a minimum I_{Sr} of 0.7047, and the maximum value obtained for these rocks is 0.7157.

6.4 Sm/Nd Isotopic Compositions

Sm/Nd isotopic data were obtained for only five samples, one from each of the larvikite - pulaskite series (ORS 107), the foyaites (ORF 17), and the monzonite - granite series (MKS 36); and two from the alkali-syenites (ORS 99 and ORS 60). The initial $^{143}Nd/^{144}Nd$ ratios (I_{Nd}) for the first three samples lie between 0.51231 and 0.51250 (ε_{Nd} = +0.9 to +3.5 - Table 6.2), which indicates derivation from a source region that, compared to CHUR, had a slight time-integrated depletion of Nd relative to Sm. The data contrast with the Sr isotopic results (above) which, while also suggesting a mantle source, are slightly enriched (I_{Sr} mostly > 0.704) relative to Bulk Earth (I_{Sr} 0.7039 at 529Ma). The first alkali-syenite analysed gave a significantly higher I_{Nd} of 0.512545 ± 0.000064 (2σ) and initial ε_{Nd} of +9.8. Such values, which are close to those of present-day MORB, are inexplicably high, particularly considering the high accompanying I_{Sr} ratios (0.7081). It is considered most likely that they reflect an analytical problem. A second alkali-syenite sample was analysed and gave more reasonable results, with an I_{Nd} ratio of 0.512242 ± 0.000064 (2s) and ε_{Nd} of +5.2.

6.5. Pb-Pb Isotopic Composition

Eight samples were analysed for their Pb isotopic composition and the results are in Table 6.3. The samples were selected from the larvikite - pulaskite series (ORS 107), the foyaite series (ORF 17), the alkali-syenite series (ORS 99), the monzonite - granite series (MKS 29, MKS 36 and ORG 11, the last coming from the Grootpenseiland Granite body) and two alkali-granites (ORF 48 and MKG 16).

The data show a very narrow range in $^{207}Pb/^{204}Pb$ ratios but comparatively large ranges in the ratios of $^{206}Pb/^{204}Pb$ and $^{208}Pb/^{204}Pb$, which reach values of 22.54 and 48.674 respectively. When regressed,

Table 6.2 Nd isotopic analyses.

	Sm(ppm)	Nd(ppm)	$^{147}Sm/^{144}Nd$	$^{143}Nd/^{144}Nd$	$\in_{Nd}^{CHUR}$
ORS 107	36.41	244.0	0.0902	0.512322 ±10	+1.0 *
ORF 17	54.19	363.3	0.0902	0.512367 ±11	+1.7 I
ORS 99	44.96	338.0	0.0803	0.512754 ±19	+9.9 I
ORS 60	29.28	211.4	0.0836	0.512524 ±09	+5.2 I
MKS 36	84.97	511.4	0.1003	0.512498 ±16	+3.5 I

* calculated at 529Ma

I calculated at 514Ma

Present day ratios quoted at 2σ level.

Decay constant = $6.54 \times 10^{-12} y^{-1}$.

$^{143}Nd/^{144}Nd$ normalized to $^{144}Nd/^{146}Nd = 0.7219$

Analyses of Johnson Matthey standard yields $^{143}Nd/^{144}Nd = 0.511803 \pm 15$

$I^{o}_{CHUR} = 0.51264$.

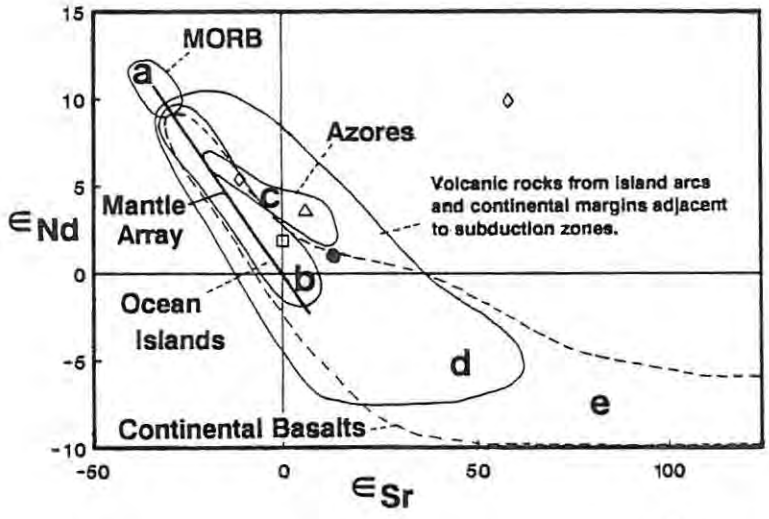

Figure 6.5 Plot of ε_{Nd} *vs.* ε_{Sr} comparing data for the rocks of the GPC and MKC to fields for various other igneous rocks (Fields **a - c** and '**Mantle Array**' are from DePaolo, 1981; fields **d - e** are from Faure, 1986)

the data-set defines an isochron with an inferred age of 524^{+255}_{-304} (Fig.6.6). The degree of uncertainty may be unacceptably large but, interestingly, the inferred age is equivalent to Rb/Sr ages. More importantly, the results indicate that the source region for the magmas forming the complexes was isotopically homogeneous in terms of its Pb isotopic signature.

The ratio $^{238}U/^{204}Pb$ (*i.e.*, μ value) for the source region of a rock can be calculated knowing the age and $^{206}Pb/^{207}Pb$ of both that rock and the primeval source of Pb (Faure, 1986). Because the age of emplacement for the bulk of the GPC and MKC can confidently be constrained to around 514 - 529Ma, the μ value of $9.87^{+0.07}_{-0.08}$ associated with the Pb-Pb isochron (Fig.6.6) can also be accepted with confidence, assuming the two-stage terrestrial Pb evolution model of Stacey and Kramers (1975). For the samples considered here, individual model μ values for ages between 514 Ma and 529Ma are within error of each other (Table 6.3) and of the abovementioned isochron μ value, and this consideration reinforces the point already made about homogeneity in the Pb-isotopic composition of the source region for each sample.

The μ values obtained are only slightly higher than an 'average Earth' μ value of 9.74 (Stacey and Kramers, 1975) and lie between values for Pb-isotopic growth in orogenic and mantle environments (Zartman and Doe, 1981)(Fig.6.6). On a diagram of initial $^{206}Pb/^{204}Pb$ *vs.* initial $^{207}Pb/^{204}Pb$ (Fig. 6.7) the data lie close to the fields for crustal Pb, dut are also very similar to the data for such ocean islands as Gough and Tristan de Cunha. A mantle origin for Pb would be consistent with the data for Sr and Nd isotopes. However, the primitive rocks of the GPC and MKC contain much lower concentrations of Pb than they do of Sr and Nd. Hence, interaction between mantle melts and the crust may have readily altered the isotopic composition of Pb but have had little effect on the isotopic compositions of Sr anf Nd. Consequently, the combined isotopic data are not sufficient to rule out the presence of a crustal component.

Table 6.3 Pb isotopic analyses.

	$^{206}Pb/^{204}Pb$	$^{207}Pb/^{204}Pb$	$^{208}Pb/^{204}Pb$	$\mu \pm 0.12$	Initial ratios (single stage)	
					$^{206}Pb/^{204}Pb$	$^{207}Pb/^{204}Pb$
Larvikite ORS 107	19.437	15.693	40.155	9.84	18.62	15.56
Foyaite ORF 17	19.724	15.726	39.627	9.91	18.67	15.60
Alkali-syenite ORS 99	22.549	15.862	48.674	9.78	18.56	15.73
Granite MKS 36	18.888	15.660	39.721	9.83	18.61	15.54
Porphyry MKS 29	18.791	15.665	39.813	9.88	18.64	15.54
Granite ORG 11	20.376	15.753	42.378	9.86	18.63	15.62
Alkali-granite ORF 48	18.467	15.641	39.918	9.86	18.63	15.51
Alkali-granite MKG 16	21.026	15.827	43.120	10.02	18.78	15.70

1σ uncertainties;
$^{206}Pb/^{204}Pb$ = 0.09%
$^{207}Pb/^{204}Pb$ = 0.09%
$^{208}Pb/^{204}Pb$ = 0.15%

Decay constants;
$^{238}U = 1.55125 \times 10^{-10} y^{-1}$
$^{235}U = 9.8485 \times 10^{-10} y^{-1}$
$^{232}Th = 4.9475 \times 10^{-11} y^{-1}$

Error correlation between $^{206}Pb/^{204}Pb$ and $^{207}Pb/^{204}Pb$ = 0.91.

μ = Model μ values calculated for an assumed age of 529Ma - based on the model of Stacey and Kramers (1975).

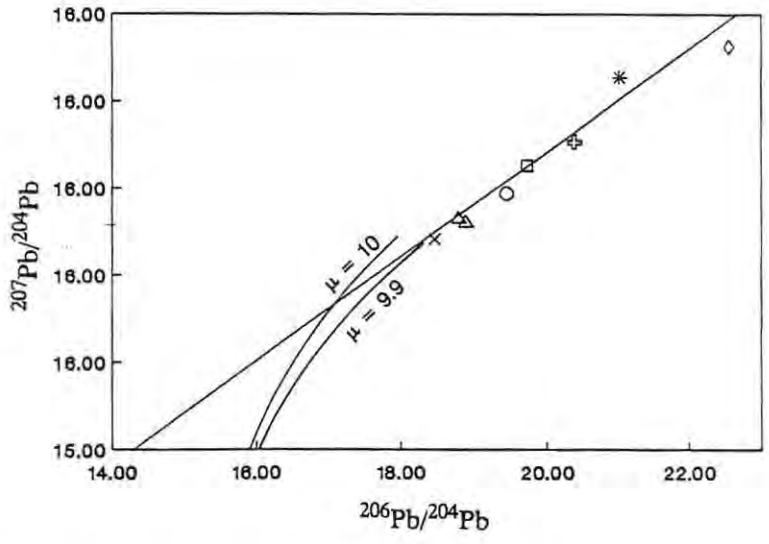

Figure 6.6 Plot of $^{207}Pb/^{204}Pb$ *vs.* $^{206}Pb/^{204}Pb$ showing data for rocks of the GPC and MKC (symbols as in Table 2.1). The regression line yields isochron statistics (see text for details) and μ - values of 9.87.

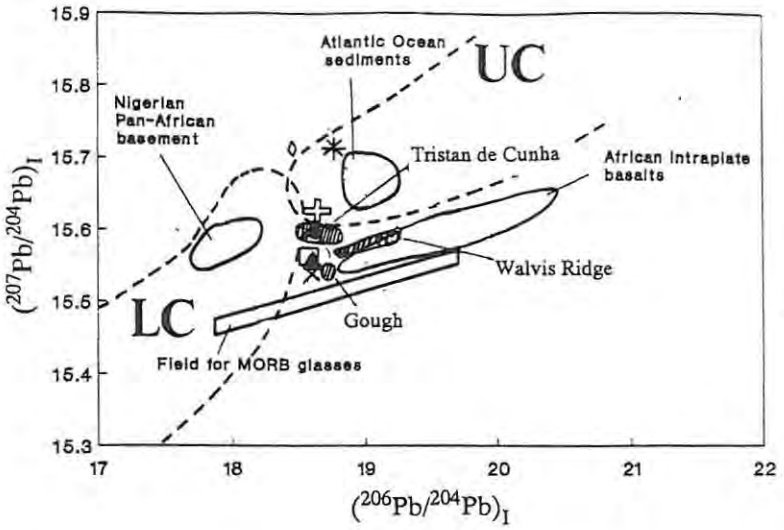

Figure 6.7 Plot of initial $^{207}Pb/^{204}Pb$ *vs.* initial $^{206}Pb/^{204}Pb$ (at 529Ma) comparing data for the rocks of the GPC and MKC to fields for basaltic rocks, Pan-African basement from Nigeria, Atlantic Ocean sediments (Halliday *et al.*, 1988) and the fields for Upper crustal (**UC**) and Lower crustal (**LC**) rocks (Zartman and Doe, 1981). Symbols as in Table 2.1.

6.6 Oxygen Isotopic Composition

The O-isotopic composition of quartz was determined for two samples (Table 6.1), one from the monzonite - granite series (MKG 6) and the other from an alkali-granite (MKG 16). The O-isotopic composition of feldspar (Table 6.1) was determined for rocks of the larvikite - pulaskite series (ORS 107), the foyaites (ORF 17), the alkali-syenites (ORS 99 & MKS 57), the monzonite - granite series (MKG 6 & MKS 53) and the Marinkas Kwela Granite body (five samples).

No significant difference could be detected between the $\delta^{18}O$ values for feldspars from the foyaites, alkali-syenites and Marinkas Kwela Granite. The feldspar values have a combined range of between 7.50‰ and 8.05‰. Feldspar from the pulaskite (ORS 107) is slightly enriched in ^{18}O, and feldspars from rocks of the monzonite - granite series display an even higher degree of enrichment ($\delta^{18}O$ = 8.31 - 8.48‰).

Where low temperature exchange of O isotopes has not occurred the $\delta^{18}O$ value of feldspar should be higher than that of any co-existing mineral except quartz (Taylor and Sheppard, 1986). Since there is no evidence for alteration of the Si-undersaturated rocks, the observed range in $\delta^{18}O$ for feldspar (7.66 - 8.14‰) may represent a maximum whole-rock value. It is possible that the actual whole-rock values are lower than that range and

possibly within the range for uncontaminated rocks of mantle origin, which according to Kyser (1986) is 5.7 to 7.5‰.

Quartz from MKG 16 and MKG 6 has higher $\delta^{18}O$ values (9.79‰ and 9.41‰ respectively) than have co-existing feldspars. The quartz-feldspar O-isotope fractionation for the rocks of the monzonite - granite series (1.12‰) is typical of magmatic values, considered by Sheppard and Harris (1985) to approximate unity. These rocks appear to have undergone little low temperature exchange of O-isotopes. However, because the rocks of the monzonite - granite series and the alkali-granites are quartz-rich, it is quite likely that their whole-rock $\delta^{18}O$ values would exceed those of uncontaminated rocks of mantle origin. It is possible that the melts the gave rise to these Si-oversaturated rocks interacted with a high $\delta^{18}O$ source such as the crust.

6.7 Discussion

In Chapter 5, compositional similarities between the primitive rocks of the larvikite - pulaskite series and the monzonite - granite series were frequently observed. It is inviting here to emphasise that the radiogenic isotope data presented in this chapter are consistent with those observations. Indeed, setting aside data for alkali-granites and the unusually high ε_{Nd} for the sample of alkali-syenite (ORS 99), the data presented here suggest that all of the observed rock series were derived at the same time and from source regions that were isotopically very similar. A single common source region cannot be ruled out on the basis of Sr, Nd and Pb isotopic data. These data point strongly towards a mantle source region with isotopic characteristics lying within, or close to, those of the Mantle Array. Available O-isotopic data are also consistent with a mantle origin for the Si-undersaturated rocks and alkali-syenites although it is difficult to substantiate this based on $\delta^{18}O$ data for feldspar alone. Whole-rock $\delta^{18}O$ values for the Si-oversaturated rocks probably exceed those of the Si-undersaturated rocks and possibly exceed the range for uncontaminated rocks of mantle origin. Accordingly, the possibility exists for a crustal component in the Si-oversaturated rocks. Like the isotopic composition of Pb, and in contrast to that of Sr and Nd, O-isotopes may be highly sensitive to the presence of a crustal component, in which $^{18}O/^{16}O$ fractionations may be very large (Taylor and Sheppard, 1986).

CHAPTER 7: THE EVOLUTION OF THE SILICA-UNDERSATURATED ROCKS OF THE GROOTPENSEILAND AND MARINKAS KWELA COMPLEXES

7.1 Introduction

Of the four Si-undersaturated series or types, only one - foyaite - is a major component of either complex, at least at present levels of exposure. In Chapter 2.3 it was shown that the other three types occurred as xenoliths or screens. This applies to both the Si-undersaturated components of the GPC, one of which - the monzodiorite - is of such compositional homogeneity and limited outcrop (Chap. 3.1.a) that its evolution cannot realistically be assessed. It is sufficient here to note that (1) the monzodiorite is the earliest and compositionally most primitive phase observed in the GPC (if not in both complexes); (2) mineralogical evidence (Chap 4.5) suggests that it is not directly related to the larvikite - pulaskite series; and (3) its low I_{Sr} ratio (Chap. 6.3) is indicative of a mantle origin for Sr at least.

In the sections that follow, the larvikite - pulaskite series and the alkali-melasyenite - nepheline-syenite series are discussed together. This is not meant to imply that they are genetically related. Rather, their similarities give rise to virtually identical problems in geochemical modelling which for the sake of brevity are discussed in detail only once.

7.2 The Larvikite - Pulaskite And Alkali-melasyenite - Nepheline Syenite Series

The main characteristics of the larvikite - pulaskite series that have an immediate bearing on its evolution are as follows:

> The elongated outcrop shows a progressive mineralogical variation that parallels the northwest trending long axis (Chap. 2.3). Mineralogical changes are from a perthite+plagioclase+ clinopyroxene+biotite-bearing assemblage (larvikite) in the southwest, to a perthite+clinopyroxene+amphibole+nepheline-bearing assemblage (pulaskite) in the northeast (Chap. 3.1.b). The Mg# of clinopyroxene decreases from larvikite to pulaskite (Chap 4.2), as does the abundance of accessory apatite, sphene and Ti-rich magnetite (Chap. 3.1.b). Nepheline, which is invariably a late crystallising phase, occurs only in pulaskite (Chap. 3.1.b). Larvikite is generally of a slightly finer grain-size than pulaskite (Chap. 2.3). Whole-rock inter-element variations (Chap. 5) are well constrained.

The alkali-melasyenite - nepheline syenite series also undergoes a mineralogical variation that parallels the long axis of its narrow outcrop.

> The transition in this instance is from nepheline-rich alkali-melasyenite in the south to nepheline syenite in the north (Chap. 3.1.c). Compositional variations, including a decrease in the Mg# of clinopyroxene, are of the same general nature as in the larvikite-pulaskite series (Chap. 5). However, one exception relates to trends in the trace-elements Nb, Zr and Zn (Chap 5.4.d; Fig. 5.5).

These combinations of features indicate that the rocks in each individual series are internally related genetically (*i.e.*, are comagmatic). More particularly, the data are consistent in both cases with progressive crystallisation of a magma body inwards

from the chamber walls - *i.e.*, the rocks have formed through *in situ* crystallisation.

During *in situ* crystallisation, phases crystallise within a 'solidification zone' and generate evolved liquids that continuously migrate, or are convected, back to the evolving body of magma (Langmuir, 1989; Nielsen, 1990). The crystallised solids are separated from the evolving melt and may be viewed as cumulates. To be noted is that both series resemble side-wall cumulates found elsewhere in alkaline complexes - for example, at Ilimaussaq and Klokken in Greenland (Ronsbo, 1989; Parsons and Brown, 1988).

7.2.a Some Problems Concerning The Modelling Of Cumulates.

Cumulate rocks commonly represent a mixture of liquidus or near-liquidus minerals together with phases that crystallised from residual evolved liquids trapped between crystallising solids. The quantitative evaluation of models that may account for the compositional evolution of such rocks would require accurate knowledge of the bulk composition of the cumulus assemblage (at the time of crystallisation) and the precise compositions of residual and parental liquids. In practice, such data are seldom obtainable, particularly for medium- to coarse-grained holocrystalline rocks such as those considered here. In addition, Langmuir (1989) and Nielsen (1990) suggest that, where *in situ* crystallisation was the cause of compositional evolution, crystallisation of phases below the liquidus may also effect compositional trends. This is because, with decreasing proportions of liquid migrating back from the solidification zone, the composition of that liquid and of the bulk solid (crystals) residue should reflect equilibrium at increasing degrees of equilibrium crystallisation, rather than reflect liquidus phase proportions and compositions (Langmuir, 1989).

Nevertheless, it must be expected that, in the larvikite - pulaskite and alkali-melasyenite - nepheline syenite series, crystallisation

of the major modal phases (alkali-feldspar, clinopyroxene and amphibole) exerted the dominant control over compositional trends. This proposition will be discussed in Chapter 7.2.b below. Subsequent sections will examine the nature of interstitial liquids and examine the effects that crystallisation of accessory phases may have had on whole rock compositions.

7.2.b Crystallisation Of The Major Mineral Phases

To examine the effects of the crystallisation of the major modal phases, the approach used by Tindle and Pearce (1981) to study rocks derived through *in situ* crystallisation was followed here. Appropriate values for $D_{Sr, Ba, Rb}$ (Table 5.3) were used to estimate the control that crystallisation of major modal phases exerted on whole-rock trends. Both Rayleigh and equilibrium fractional crystallisation were assumed (Fig. 7.1.a and b). Additional aims were to assess the effects of crystallisation of the less abundant phases (plagioclase, biotite) as well as non-liquidus phases, notably nepheline.

It will be seen that, in terms of Ba *vs.* Sr and Rb, the trends are similar for both series and consistent with the crystallisation of the assemblage alkali-feldspar+clinopyroxene+amphibole. The whole-rock trends are not markedly influenced by crystallisation of plagioclase and this is consistent with the presence of this phase only in the most primitive rocks. However, the crystallisation of biotite, at least a minor phase in most rocks, may explain why the larvikite - pulaskite series shows larger depletions in Ba than are accounted for (in terms of the D values selected) by crystallisation of alkali-feldspar alone. No evidence is provided by Figure 7.1.a and b that crystallisation of nepheline influenced whole-rock trends for Rb, Ba and Sr.

Steady decreases throughout both series in whole-rock concentrations of P_2O_5 and TiO_2 (Fig 5.2) indicate that apatite and sphene and/or Ti-magnetite also crystallised continuously. All

Distribution Coefficients

Element	Mineral						
	K-fsp	plag	neph	cpx	amph	biot	sph
Rb	0.78	0.05	0.97	0.05	0.15	2.63	
Ba	5.10	0.25	0.25	0.15	0.22	8.18	76.00
Sr	5.20	3.30	0.25	0.28	0.26	0.12	14.00
Cr	0.08			3.10	1.50		

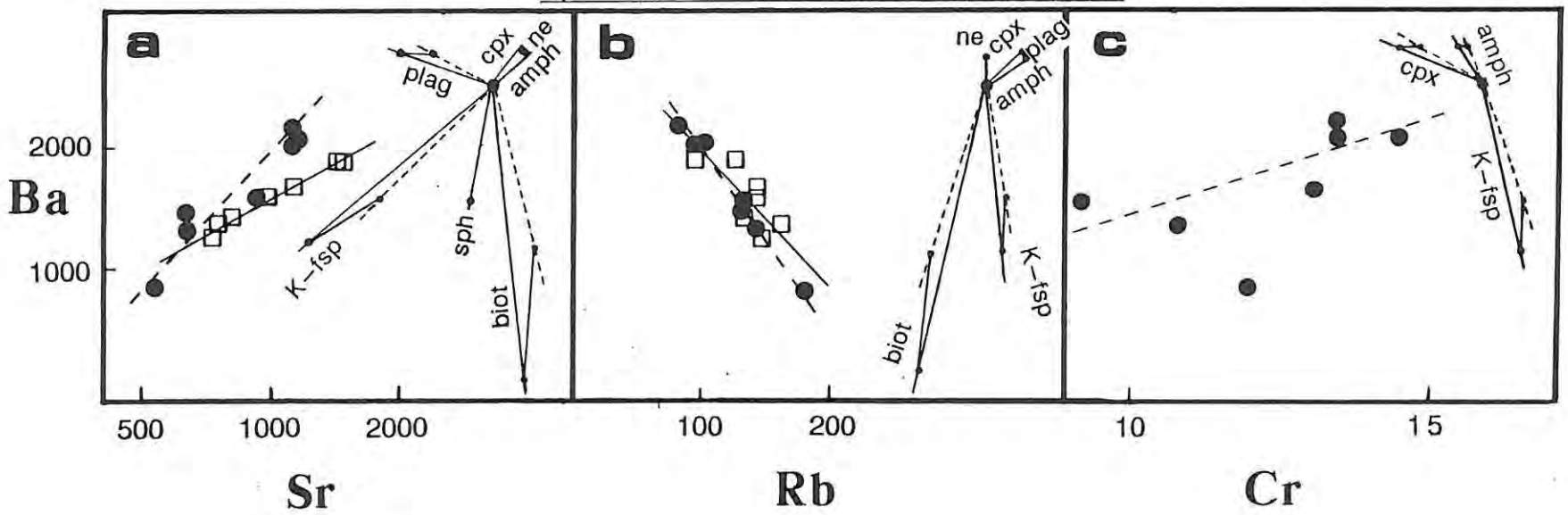

Figure 7.1 Plots of Ba *vs.* Sr(**a**), Rb(**b**) and Cr(**c**) for the rocks of the larvikite - pulaskite series and the alkali-melasyenite - nepheline syenite series. Symbols as in Table 2.1. Mineral control vectors have been constructed assuming both Rayleigh fractionation (solid line) and equilibrium fractionation (dashed line). Relevant D values were obtained by averaging the respective range of values from Table 5.3.

three form inclusions in feldspar or amphibole (Chap. 3.1.b and c) and are likely to represent near-liquidus phases.

7.2.c The Interstitial Liquid

Whole-rock trends (Fig 7.1.a and b) for the larvikite - pulaskite series reflect crystallisation of an assemblage having clinopyroxene+amphibole / alkali-feldspar ratios close to or slightly less than unity. Although such estimates are critically dependent upon the selected D values, particularly $D^{K\text{-feld}}$, similarly high ratios are predicted on a plot of Cr *vs.* Ba (Fig 7.1.c). These ratios are considerably higher than the observed modal ratios, which range between 0.2 to 0.3 (obtained by point counts on 500 points). The difference between observed and estimated ratios can be reconciled to some extent in terms of 'excess' alkali-feldspar derived from trapped residual liquids, as distinct from abundant liquidus (or near-liquidus) alkali-feldspar. This 'excess' alkali-feldspar would have no effect on subsequent whole-rock compositional trends.

Observed clinopyroxene+amphibole / alkali-feldspar ratios for the alkali-melasyenite - nepheline syenite series (0.3 to 0.4) are closer to values estimated from Figure 7.1.a and b (around 0.75) which may thus be more reasonable reflections of liquidus phase proportions for these rocks. They suggest that the interstitial liquids crystallised comparatively less alkali-feldspar than did those in the larvikite - pulaskite series.

Nepheline is the last phase to crystallise in both Si-undersaturated series and lies interstitially to alkali-feldspar (Chap. 3.1.b and c). Its abundance in the alkali-melasyenite - nepheline syenite series contrasts with its relative paucity in the larvikite - pulaskite series. It follows that residual liquids trapped during accumulation of the alkali-melasyenite - nepheline syenite series were more Si-undersaturated than liquids trapped during accumulation of the larvikite - pulaskite series. In the latter series, nepheline crystallised from trapped liquids only in the

more evolved rocks, and even then only after substantial interstitial alkali-feldspar had crystallised.

7.2.d Crystallisation Of The Accessory Mineral Phases

With evolution from larvikite to pulaskite, Zn, Zr and Nb show trends to higher concentrations. By contrast, evolution from alkali-melasyenite to nepheline syenite shows no tendency for Zr to increase in concentration, and Zn and Nb (and also REE) actually decrease in concentration (Fig. 5.5).

The accessory phases sphene, apatite and bastnaesite may concentrate Zn, Zr, Nb and REE (Table 5.3). Of these minerals, ?bastnaesite occurs only as inclusions within nepheline (Chap. 3.1.b and c) and reflects REE- and Th-enriched residual liquids. Crystallisation of this phase is unlikely to have influenced whole-rock compositional trends.

Because $D^{ap}_{Gd} > D^{ap}_{Yb}$ and $D^{sph}_{Nb} > D^{sph}_{Zr}$ (Table 5.3), observed whole-rock trends to lower Gd/Yb with decreasing P_2O_5, and to higher Zr/Nb with decreasing TiO_2 (Fig 7.2.), suggest that crystallisation of apatite and sphene influenced whole-rock trends for Zr, Nb and REE. It is proposed that the modal proportions of apatite and sphene underwent a more significant decrease during accumulation of the alkali-melasyenite - nepheline syenite series than they did during accumulation of the larvikite - pulaskite series. This is reflected by more pronounced decreases in whole-rock P_2O_5 and TiO_2 concentrations in the former series, and led to decreasing concentrations of Nb and REE.

The proportions of apatite+sphene and alkali-feldspar that crystallised would also have had a large control over the relative REE concentrations in the rocks. All of these minerals may fractionate Eu^{2+} relative to REE^{3+}, but the effect of apatite and sphene ($D_{Eu} < D_{Sm,Gd}$ - Table 5.3) is opposite to that of alkali-feldspar ($D_{Eu} > D_{Sm,Gd}$ - Table 5.3). The increase in the Eu/Eu* ratios within the alkali-melasyenite - nepheline syenite series

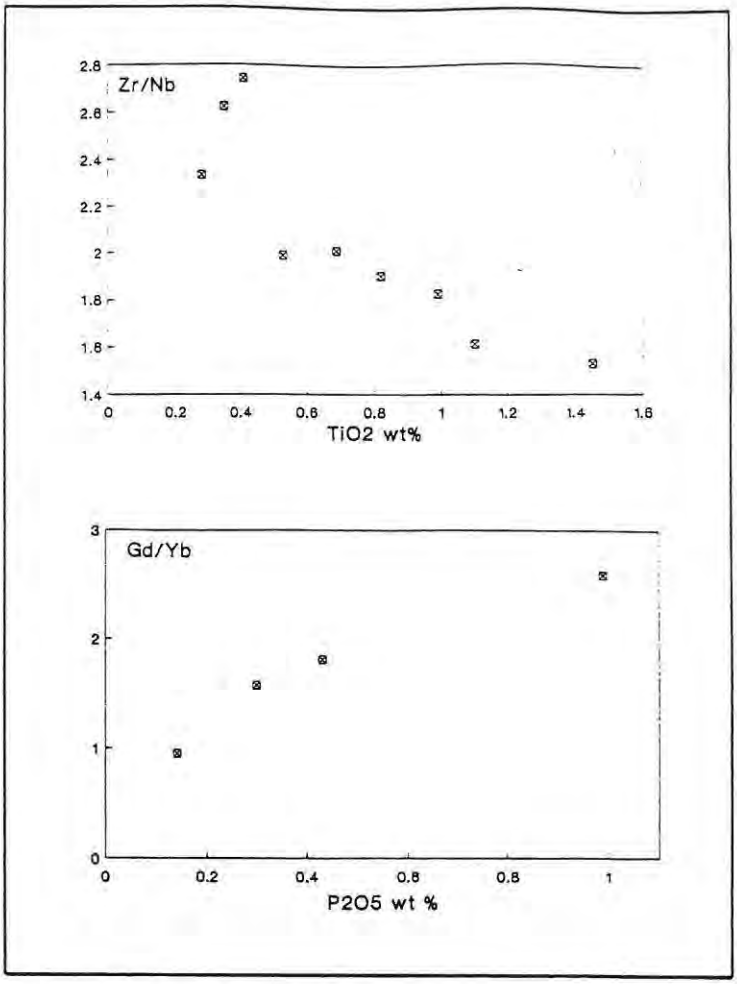

Figure 7.2 Plots of Zr/Nb *vs.* TiO_2 (wt%) and Gd/Yb *vs.* P_2O_5 (wt%) for the rocks of the alkali-melasyenite - nepheline syenite series of the MKC.

(Chap. 5.4.g; Fig. 5.10) may then be linked to progressive decreases in the whole-rock concentrations of TiO_2 and P_2O_5 (Fig. 7.3), reflected by increasing alkali-feldspar/apatite+sphene ratios.

7.2.e The Degree Of Crystallisation

The concentrations of Th increase systematically with increasing Sr (Fig 5.7), *i.e.*, with compositional evolution (Chap. 5.1) across the outcrop width of each series. Such correlations suggest that the changing concentrations of Th reflect crystal/liquid equilibrium rather than changing proportions of cumulus phases and interstitial liquids. This is to be expected because in both series, accessory sphene is the only early crystallising phase in which Th concentrates (D_{Th}^{sph} = 0.01-8.0, Table 5.3). It is likely that Th concentrated in residual liquids until ?bastnaesite crystallised.

Assuming then that bulk $D_{Th} \approx 0$, the 3.5- to 4-fold enrichments that occur in both series in the concentrations of Th (Fig. 5.7) should reflect a minimum of 70-75% crystallisation of the respective parental magmas.

The amount of crystallisation/accumulation of a magma may vary amongst different sites within a chamber (*e.g.* Wiebe, 1988; Weinstein *et al.*,1988). Still, the large degrees of crystallisation seemingly required to derive the Th concentrations of the pulaskite and nepheline syenite suggest the possibility in each case of an origin within a magma chamber of small volume. In this connection it is worth noting that other Si-undersaturated rocks related to the larvikite - pulaskite series are not observed (Chap. 2). However, the alkali-melasyenite - nepheline syenite series is directly related, at least spatially (Chap. 2.3), to the large body of foyaite. If the former crystallised in a small chamber then direct genetic links are possible only to a small portion of the foyaites and the foyaite body itself must represent a multiple intrusion.

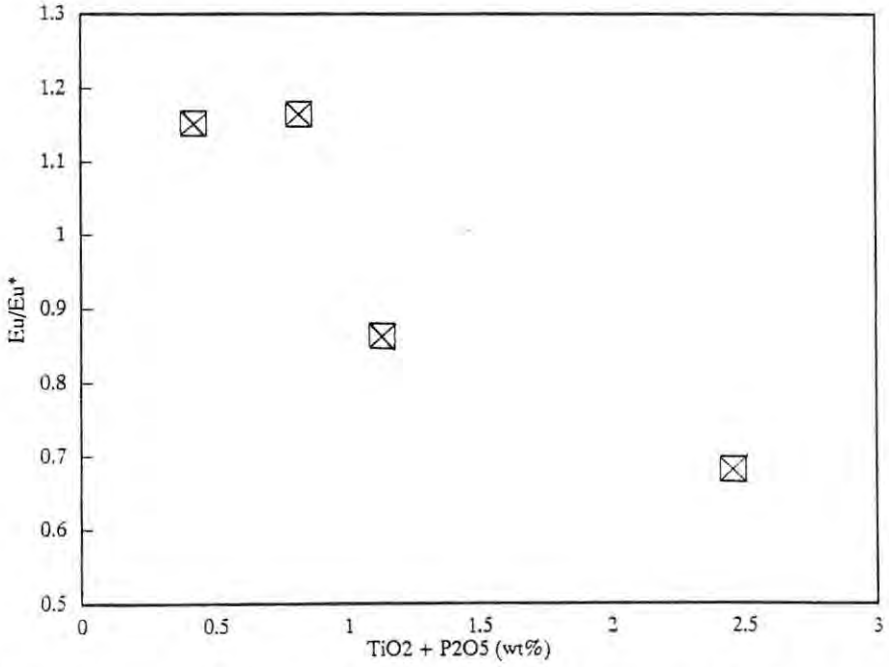

Figure 7.3 Plot of $TiO_2+P_2O_5$ (wt%) *vs.* Eu/Eu* for the alkali-melasyenite - nepheline syenite series.

7.2.f. Crystallisation of The Larvikite.

An interesting feature of the larvikite is that it shows almost no compositional variation except in regard to Th, one sample having almost double the Th concentration of others (Figs. 5.2 - 5.7 and 7.4). Assuming, as suggested above, that this variation reflects crystal/liquid equilibrium, it would follow that, while evolution from larvikite to pulaskite reflects fractionation controlled by crystallisation of alkali-feldspar+clinopyroxene+amphibole, evolution amongst the larvikites themselves was different.

Langmuir (1989) and Nielsen (1990) note that *in situ* crystallisation should cause more change in the concentration of incompatible trace elements, relative to major elements, than would fractional crystallisation. The contrast should be greater where only small proportions of magma entering the solidification zone return from that zone to the chamber. The phenomenon arises because the total solid composition near the solidus is closer to the initial liquid composition than is the bulk solid composition on the liquidus (Langmuir, 1989).

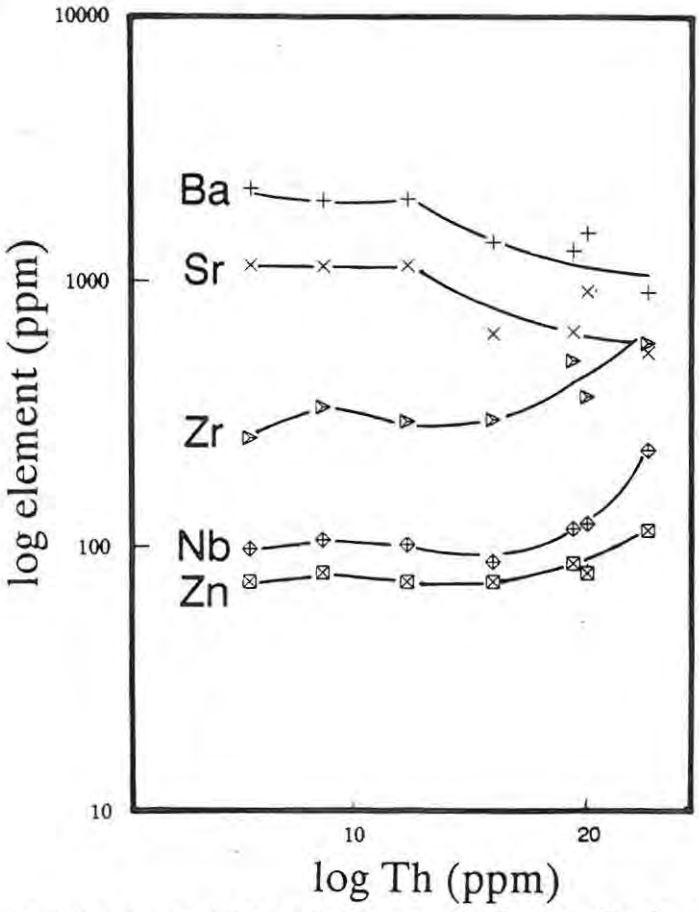

Figure 7.4 Variations in the concentrations of Th *vs.* Ba, Sr, Zr, Nb, and Zn (all in ppm) for larvikite of the GPC.

A possible implication for the larvikite - pulaskite series is that only a small and highly fractionated (Th-rich) portion of residual liquids returned from the solidification zone into the remaining magma during accumulation of the larvikites. At compositions corresponding to approximately 12ppm Th, the proportion of returning residual liquids increased and led to increased compositional differentiation amongst the later rocks.

If that happened, a possible explanation is that the larvikite cooled, or accumulated, faster than did the pulaskite. The finer grain-size of the former (Chap. 2.3) is consistent with this explanation.

7.3 The Foyaites

Important features of the foyaites that bear on their genesis are as follows:

> Two main types have been identified: clinopyroxene-rich and amphibole-rich (Chap 2.3). The latter tend to occur either in the central portions of the foyaite body or as late-stage dykes (Chap 2.3). Compared with the amphibole-rich variety, clinopyroxene-rich foyaite is generally depleted in FeO, MgO, CaO, Nb, Zr, Y, REE, Zn, Th, Pb, Rb and F, and enriched in SiO_2 and P_2O_5 (Chap 5).

The importance of fractional crystallisation in the compositional evolution of the clinopyroxene-rich foyaite can readily be demonstrated. Well-defined trends towards the phonolite minimum in 'Petrogeny's Residua System' were noted in Chapter 5.2 (Fig. 5.1) and indicate that the rocks were derived through fractionation of feldspar. Supporting evidence includes large negative Eu anomalies (Chap. 5.4.g; Fig. 5.10) and trends to lower concentrations of Sr and Ba with differentiation (Chap. 5, Figs. 5.2 - 5.7). Decreasing whole-rock concentrations of MgO and CaO (Fig. 5.2) and decreasing Mg# within clinopyroxene also indicate that at least some fractionation of clinopyroxene occurred (Chap. 5.3).

The data available for the amphibole-rich foyaite are few and this hampers comprehensive petrogenetic assessment. What data there are approximate the whole-rock trends for clinopyroxene-rich foyaite in terms of Na_2O, K_2O and Al_2O_3 (Fig. 5.2) and on that basis it appears that the rocks may also have undergone substantial fractionation of alkali-feldspar.

7.3.a Relationship Between The Two Types Of Foyaite

Because of close spatial relationships it is inviting to seek a genetic link between the two types of foyaite and between them and the alkali-melasyenite - nepheline syenite series. Four processes that could explain compositional differences between the foyaites are discussed below.

(1) *Volatile complexing within a vapour phase during and after crystallisation of the melt.*

Processes of vapour/liquid fractionation are possibly amongst the hardest to recognise or constrain because they commonly lead to the loss of various components. No firm basis was found to implicate them here. Although amphibole-rich foyaite invariably displays a high volatile content, the zeolitisation of sodalite and nepheline is common to both types, as is late-stage replacement of nepheline by sodalite. High 'loss on ignition' in amphibole-rich foyaite, compared with the clinopyroxene-rich variety (Table 5.1), relates to the presence of amphibole alone and not to more extensive alteration.

(2) *Separate magma inputs*

The two types of foyaite may have derived from at least two independent magma batches, perhaps related at depth to a common chamber. A complex intrusive history is consistent with suggestions made in the previous section that the alkali-melasyenite - nepheline-syenite series could have crystallised in a

small chamber. It is also consistent with the compositional scatter observed for the amphibole-rich foyaite in particular (Figs. 5.2 - 5.7). The isotopic compositions of Sr may point in the same direction. The range of I_{Sr} ratios for the clinopyroxene-rich foyaite is 0.701 to 0.705 (Chap. 6.3, Table 6.1), which is significantly lower than the I_{Sr} of the single amphibole-rich foyaite analysed (0.7098). However it should be noted that the sample in question (ORF 40) contains only 87ppm Sr and so the possibility exists of selective contamination by crustal Sr, particularly given that xenoliths of Nama dolomite occur in the foyaites (Chap. 1.2).

(3) *Crystal/liquid fractionation*

As regards a possible relationship through crystal/liquid fractionation, it is notable that the amphibole-rich foyaite occurs either centrally to the clinopyroxene-rich foyaite or as late dykes. It also shows relative enrichments in Rb, Th and U (Fig. 5.7) and is the most fractionated rock within the body. However, both types of foyaite appear *prima facie* to evolve to lower concentrations of Nb and Zn (and Y also decreases with evolution of the clinopyroxene-rich foyaite) (Fig. 7.5), but the concentrations of these trace elements in the amphibole-rich foyaite are similar to or higher than those in the clinopyroxene-rich foyaite. Accordingly, closed system crystal/liquid equilibrium alone cannot explain the compositional differences between the foyaites.

(4) *Contamination.*

The wide range of I_{Sr} and the presence of the dolomite xenoliths already noted above may suggest more generally that some of the compositional differences amongst the foyaites relate to selective contamination.

Nama xenoliths are found in many rocks of both complexes (Chap. 1.2) and are invariably rimmed by a skarn assemblage of andradite+hedenbergite+ wollastonite. Chemical analyses of the skarns (Table 7.1) show them to be highly variable in composition,

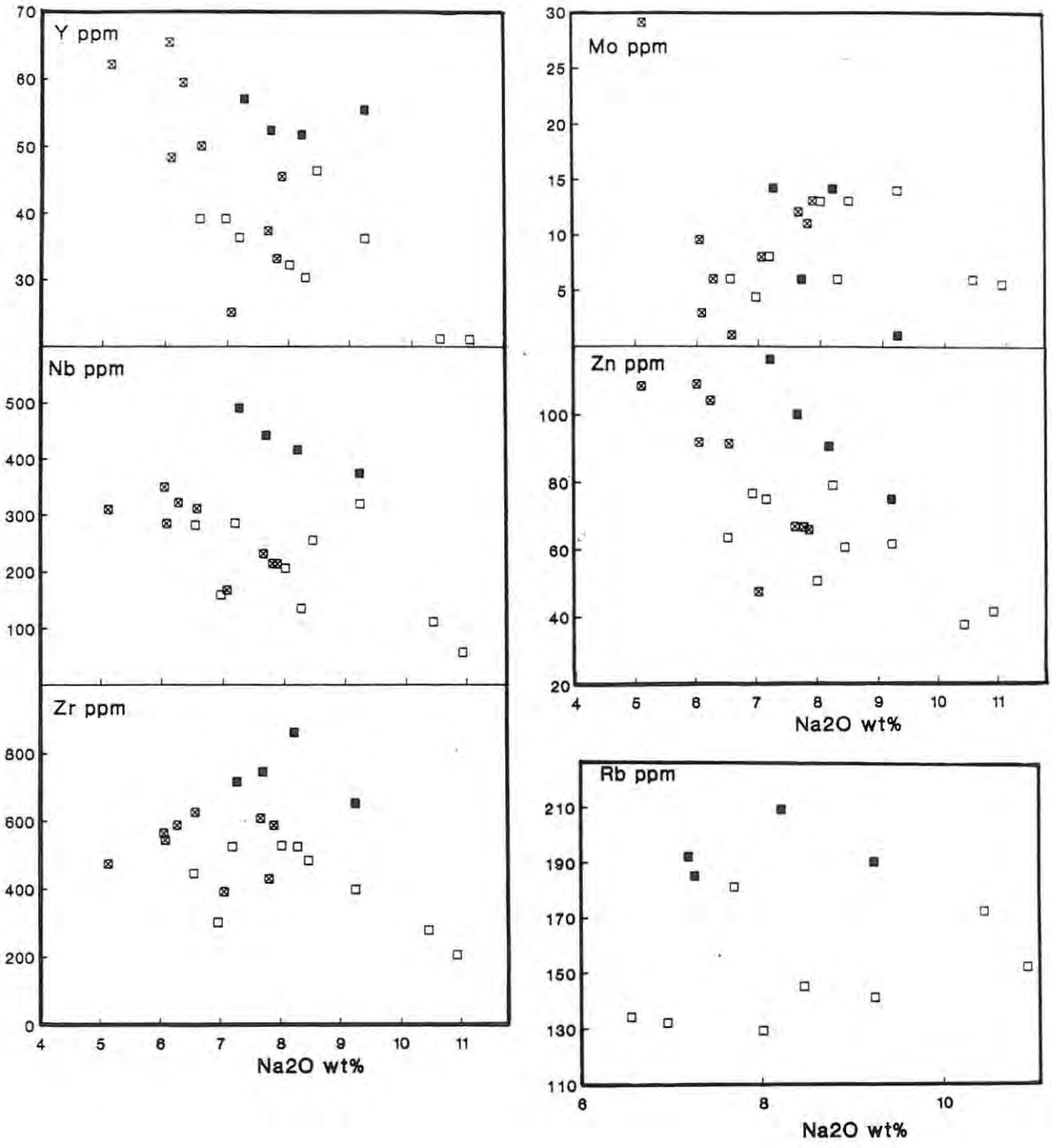

Figure 7.5 Various trace elements (ppm) plotted against Na_2O (wt%) for both types of foyaite and the alkali-melasyenite - nepheline syenite series.

TABLE 7.1 Chemical analyses of Dolomite xenoliths (Nama), altered 'skarn' rims and host rocks.

	CARBONATE XENOLITHS		SKARN RIMS						AVERAGE SKARN	HOST ROCKS ALKALI-SYENITES			
	ORS X1	ORS X2	ORS S1	ORS S2	ORS S3	ORS S4	ORS S5	ORS S6		ORS 60	ORS 110	ORS 112	ORS 126
[wt%]													
SiO2	0.23	0.35	24.67	37.11	40.77	37.05	40.56	45.00	37.53	64.54	61.49	62.40	65.24
TiO2	0.01	0.01	0.06	0.01	0.40	0.12	0.37	0.22	0.20	0.10	0.12	0.10	0.01
Al2O3	0.02	0.10	0.55	3.20	10.09	10.94	10.47	8.63	7.31	17.77	17.81	17.86	18.35
Fe2O3	0.11	0.02	0.20	2.35	1.62	0.98	1.06	0.67	1.15	0.60	0.62	0.70	0.28
FeO	0.77	0.13	1.42	16.93	11.70	7.04	7.65	4.82	8.26	4.31	4.46	5.05	2.03
MnO	0.19	0.09	0.62	0.62	1.03	0.49	0.58	0.40	0.62	0.19	0.21	0.21	0.10
MgO	17.81	2.36	0.35	0.39	2.39	0.21	0.52	0.43	0.72	0.03	0.05	0.02	0.00
CaO	40.94	51.92	44.58	32.08	29.09	30.97	35.10	36.28	34.68	1.32	1.22	1.07	0.56
Na2O	0.08	0.05	0.09	0.14	0.53	0.38	0.50	0.30	0.32	7.51	6.39	6.34	6.66
K2O	0.02	0.00	0.01	0.00	0.32	2.25	0.10	0.46	0.52	5.08	5.53	5.33	5.85
P2O5	0.00	0.00	0.16	0.04	0.17	0.02	0.00	0.00	0.07	0.07	0.04	0.08	0.01
H2O-	0.07	0.03	0.09	0.11	0.12	0.13	0.04	0.07	0.09	0.11	0.11	0.13	0.07
LOI	41.24	43.57	25.86	5.43	1.26	9.02	2.25	2.15	7.66	0.25	0.73	0.46	0.52
Tot	101.49	98.63	98.66	98.41	99.49	99.60	99.20	99.43	99.13	101.88	98.78	99.75	99.68
[ppm]													
Zn	15	7	73	86	194	111	39	43	91	97	127	91	46
Cu	6	13	12	17	11	10	6	11	11	0	7	2	0
Ni	1	2	n.d.	3	15	8	7	23	9	2	7	9	4
Co	n.d.	3	1	n.d.	n.d.	n.d.	n.d.	n.d.	0	1	0	0	2
Mo	n.d.	1	n.d.	2	7	24	8	9	8	6	12	5	1
Nb	4	3	1381	123	30	292	68	46	323	198	269	19	117
Zr	37	52	80	24	491	1422	535	534	514	567	637	388	276
Y	6	7	46	13	53	86	57	48	51	61	75	72	50
Sr	746	1258	1044	196	107	812	95	127	397	81	85	29	82
Rb	n.d.	n.d.	n.d.	n.d.	22	105	9	37	29	152	181	143	191
U	n.d.	n.d.	6	n.d.	5	6	n.d.	n.d.	3	8	14	14	14
Th	1	n.d.	14	14	13	59	16	7	21	69	54	64	45
Pb	n.d.	1	29	44	16	21	18	14	24	19	20	11	9
Cr	57	70	71	64	66	17	42	122	64	10	<11	<12	<12
V	26	21	46	23	69	22	44	50	42	2	31	32	29
Ba	20	18	29	15	172	370	30	10	104	<28	62	46	92
Sc	11	13	12	10	22	22	10	10	14	<10	<8	<8	<10
F	2670	1959	34070	2240	2055	14455	2967	2523	9718	1563	1198	1003	913

n.d. = not detected

but notably they are enriched in Nb, Zr, Y and Zn compared both to the unaltered cores of the xenoliths and, in many cases, to the host-rock (alkali-syenite in the case of the skarns analysed) It is likely that large dolomite xenoliths with a density of around 2.9g/cm^3 (Deer *et al.*, 1980) would settle through a syenitic liquid, particularly when much of the material had been converted to a dense skarn assemblage (andradite = 3.86g/cm^3, hedenbergite = 3.56g/cm^3, wollastonite = 2.87-3.09g/cm^3). In this connection it is interesting that Nama xenoliths are exposed at levels below the inferred paleosurface of Nama sedimentation (*viz*, the unconformity between the Nama and rocks of the Richtersveld Subprovince).

Many of the observed compositional differences amongst the foyaites may then relate to the degree of interaction between the Si-undersaturated melts and the xenoliths. At higher levels, melts may have become depleted in Nb, Zr, Y and Zn during interaction with the xenoliths. As the xenoliths settled, further interaction (now between melt and skarn) may have caused the same trace elements to become enriched within the melt at deeper levels. If that were the case, the concentrations of these trace elements should increase directly in proportion to increasing I_{Sr}. While there are insufficient data to prove such trends, Figure 7.6. shows a positive correlation, at least in the case of Zr, with the amphibole-rich foyaite (ORF 40) having the highest value for both Zr and I_{Sr}.

7.3.b Conclusion

As discussed above, contamination could account for the enrichment in Nb and Zn which seemed to exclude crystal fractionation as an explanation for the compositional differences amongst the foyaites. These trace elements would be significantly enriched in a melt that incorporated altered xenolith (skarn) material. The concentrations in the melt of such trace elements as Rb, which show only low concentrations within the skarn, should be unaffected by such a process and may reflect fractional

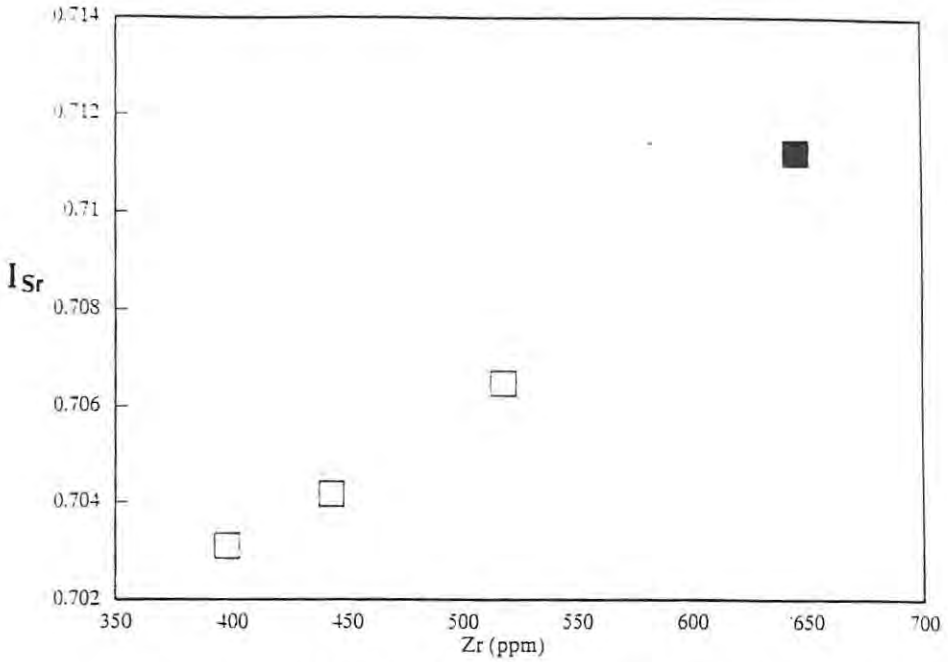

Figure 7.6 Plot of I_{Sr} vs. Zr (ppm) for the foyaites.

crystallisation alone. Accordingly, fractional crystallisation accompanied by trace element and isotopic exchange between the melt and altered dolomite xenoliths (skarns) is a plausible means of relating the two types of foyaites, and is the explanation most consistent with the given data.

7.4 Relationships Amongst The Si-undersaturated Rocks

The I_{Sr} ratios for the Si-undersaturated rocks are generally low and, combined with high ε_{Nd} values, are indicative of a mantle origin. There is little, or no, evidence for interaction with the continental crust (Chaps. 6.3 and 6.4). All rock types in the GPC and the MKC are, however, compositionally far removed from primary magmas which could have been in equilibrium with the mantle. Accordingly, initial features of the parental melts and the mantle source region are hard to assess.

The Ba/Sr ratio is significantly higher in both the monzodiorite and the alkali-melasyenite, compared with the larvikite. It is

possible, therefore, that the melts that gave rise to the first two rock types may have fractionated significantly higher proportions of plagioclase ($D_{Ba<Sr}$) or lower proportions of biotite ($D_{Ba>Sr}$) than did the melt that gave rise to the larvikite. Greater degrees of plagioclase fractionation would explain the more alkaline compositions of the alkali-melasyenite and monzodiorite compared with the larvikite. The occurrence of slightly negative Eu anomalies in the alkali- melasyenite, and the general absence of such anomalies in the larvikite, are consistent with this proposition.

It was indicated in the last section that it is possible that the foyaites and the alkali-melasyenite - nepheline syenite series share a genetic link. A direct relationship between the later series and the clinopyroxene-rich foyaite is favoured by close mutual contacts. The clinopyroxene-rich foyaite and the nepheline syenite are also mineralogically very similar and are distinguished only by the more intergranular textures of the former.

On a plot of Na_2O *vs.* K_2O, the clinopyroxene-rich foyaite and the rocks of the alkali melasyenite - nepheline syenite series diverge strongly (Fig. 7.7) and within the system ***Q-ne-ks*** they evolve towards the phonolite minimum, but on opposites sides of the thermal trough (Fig. 5.1). There is also a sharp contrast in their

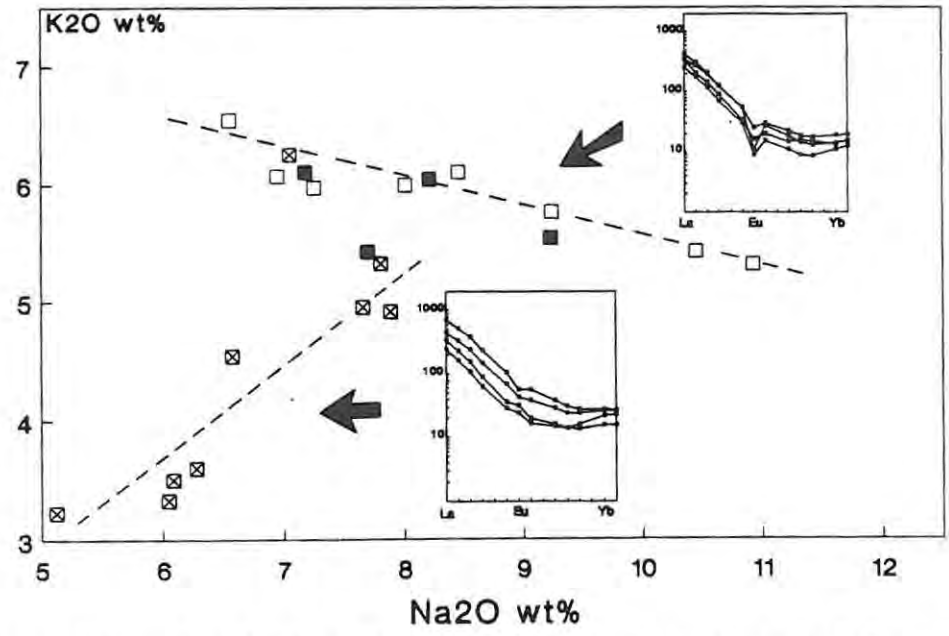

Figure 7.7 Plot of K_2O *vs.* Na_2O (wt%) showing the contrasting whole-rock trends between the alkali-melasyenite - nepheline syenite series and the foyaites. The insets show the contrasting chondrite-normalised REE patterns.

Eu/Eu* ratios. It is suggested here that the alkali-melasyenite - nepheline syenite series represents a sequence of cumulates (now preserved as a screen) which crystallised *in situ* along a side-wall during fractionation of the foyaites.

CHAPTER 8: THE EVOLUTION OF THE CRITICALLY SATURATED ROCKS OF THE GROOTPENSEILAND AND MARINKAS KWELA COMPLEXES

Principal differences noted in earlier chapters between the two critically saturated rock types are as follows:

> Quartz is present in alkali-feldspar syenite and absent from the alkali-syenites, even though the latter are more evolved (Chap. 3. 2.a). The compositions of their clinopyroxene, amphibole and biotite are different (Chaps. 4.2, 4.3 and 4.4). The alkali-feldspar syenite shows a range to higher concentrations of K_2O and Sr, compared with the alkali-syenites (Chap.5), and has higher K/Rb ratios (Fig. 5.4.). The alkali-feldspar syenite also has distinctly lower concentrations of Y, Zr, Nb and Th (Chap. 5. 4. d) and lower Eu/Eu* ratios (Fig. 5.10) than have the alkali-syenites.

These differences suggest that the two rock types are not directly related by crystal-liquid equilibrium. It remains to consider the petrogenesis of each type separately.

8.1 The Alkali-syenites

These rocks are essentially bimineralic, with amphibole lying interstitally to coarsely exsolved perthite; minor to accessory amounts of magnetite also occur (Chap. 3.2.b). A significant geochemical feature of the rocks is their highly evolved compositions as indicated by large negative Eu anomalies (Fig. 5.10.d) and low concentrations of Sr and Ba (Fig. 5.4). These features and, in the

alkali-syenite of the GPC, the correlation between decreasing Sr (and Ba) and Eu/Eu* (Fig. 8.1), indicate that feldspar fractionation was important in controlling compositional evolution. However, the scatter of compositional data shown on most variation diagrams in Chapter 5 cannot rationally be explained in terms of simple closed-system fractionation alone.

In Chapter 7.3. it was suggested that the composition of a syenitic melt may be altered through interaction with dolomite xenoliths. Such xenoliths were most commonly observed within the alkali-syenites and it is possible that much of the compositional scatter may relate to incorporation of xenolithic material.

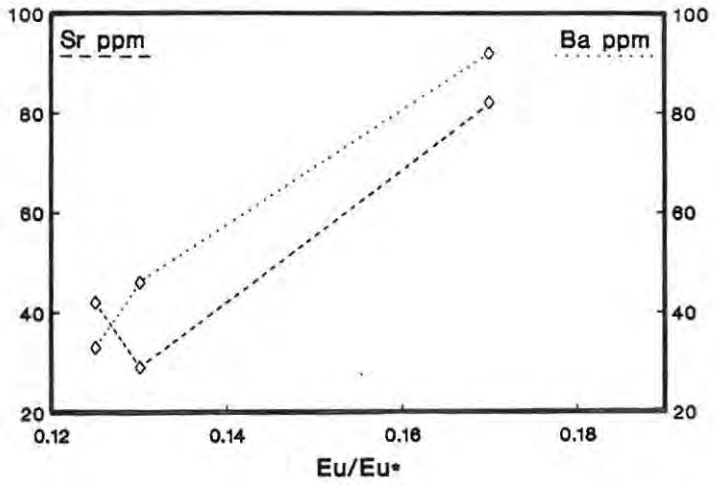

Figure 8.1 Plot of Sr (dashed line) and Ba (dotted line) *vs.* Eu/Eu* for the alkali-syenite of the GPC.

A further explanation for the observed compositional scatter relates to the modal layering observed in the rocks (Chaps. 2.4 and 3.2.b). When the compositional effects of fractional crystallisation and an additional process that may lead to modal layering are superimposed, poorly constrained inter-element relationships are a rational result.

The highly interstitial habit of amphibole also limits the number of possible processes through which the modal layering itself might have occurred. Mechanical separation of amphibole from feldspar is unlikely. Processes like differential cooling are more probable.

8.1.a Relationship Between The Alkali-syenites In The Two Complexes

Chapter 2.7 noted the possibility that some co-genetic magma series could be common to both the GPC and the MKC, and that the alkali-syenites were one of the three series/types that might qualify. While the major and trace element compositions of the alkali-syenites of both complexes overlap extensively (Chap.5), differences exist for some elements (*e.g.*, P_2O_5 and Th). The range of amphibole compositions also differs (Chap. 4.3). Given these differences, it seems highly unlikely that the alkali-syenites of the two complexes are directly related genetically.

8.1.b Relationship To Other Rock Types

Syenites and trachytes are generally considered to be either the products of fractional crystallisation, or primary partial melts. Compositional evolution towards the syenite minimum in the system **Q-ne-ks** is dominated by alkali-feldspar fractionation and follows a compositional path lying close to the **ab-or** join. Most of the rock types in the GPC and MKC show compositional trends leading away from the syenite minimum. Thus they are unlikely to be parental to the alkali-syenites.

An additional point is that, relative to other rock series/types analysed for Sm/Nd isotopic data (Chap. 6.4), ε_{Nd} values for the alkali-syenites are high, at least as regards those in the GPC (Fig. 6.5). Given the high concentrations of REE in the alkali-syenites (Chap. 5.4.g), it is likely that their ε_{Nd} values are primary. Consequently, the alkali-syenites (at least in the case of the GPC) derive from a source that is isotopically very distinct from those of all other rocks analysed (Chap.6.7) and which has a higher time-integrated Sm/Nd ratio than that of the other sources.

8.2 The Alkali-feldspar Syenite

Features of this rock that have bearing on its compositional evolution are as follows:-

> Compositions are characterised by prominent positive Eu anomalies (Fig.5.10.d). Only small major element variations occur, except for K_2O which systematically increases from about 4.5wt% in less evolved samples to about 7wt% in more evolved samples (Fig. 5.2). The concentrations of CaO, FeO and MgO, as well as of the trace elements Zn, Mo, Nb, Zr, Y, Pb and Th, are constant and very low (Chap.5).

Alkali-feldspar accumulation is clearly suggested by the positive Eu anomalies. The low and constant concentrations of many trace elements is also a common feature of cumulates.

The alkali-feldspar syenite is in contact with rocks of the larvikite - pulaskite series, with the monzonite - granite series, with alkali-granites and with alkali-syenites. But a genetic relationship with the latter has already been ruled out, and the presence of quartz in the alkali-feldspar syenite rules out a relationship to the Si-undersaturated larvikites-pulaskites (Chaps. 2.4 and 3.2.a). The

alkali-granites can also be excluded given the inferred sequence of intrusions (Chap. 2.7).

This leaves only the monzonite - granite series as a likely candidate for the magma from which the alkali-syenite accumulated. This possibility was explored using trace elements.

The REE concentrations of a parental liquid from which the alkali-feldspar syenites accumulated were calculated from the REE concentration in the most primitive alkali feldspar syenite by assuming a process of Rayleigh fractionation and Bulk $D_{REE} = D_{REE}^{K\text{-}fsp}$. The latter assumption was considered to be justified given the extremely high modal proportion of alkali-feldspar (up to 90% - Chap. 3.2.a) in the syenites, and the interstitial nature of mafic phases.

The calculated hypothetical parental liquid for alkali-feldspar syenite has La/Yb ratios between 17 and 24, Gd/Yb ratios between 1.91 and 2.22 and a large negative Eu anomaly (Eu/Eu* = 0.16 - 0.27) (Fig.8.2). In these respects, rocks of the monzonite - granite series display virtually identical characteristics, with La/Yb ratios of 20 to 25, Gd/Yb ratios of 1.9 to 2.3 and Eu/Eu* ratios that vary from near-unity down to 0.11. It seems, therefore, that the alkali-feldspar syenite accumulated from a melt that was compositionally very similar, in terms of REE concentrations, to the rocks of the monzonite - granite series. Equivalent I_{Sr} ratios for the alkali-feldspar syenite and the rocks of the monzonite - granite series (approximately 0.7048) support this proposition (Chap. 6.3; Table 6.1).

In Chapter 2.7, the chronological relationship between alkali-feldspar syenite and the alkali-syenites in the GPC was left unresolved because the contact between the two is not exposed (Chap. 2.4). If, as suggested above, there is a direct relationship between the alkali-feldspar syenite and the monzonite - granite series, that relationship would tend to indicate that accumulation of the alkali-feldspar syenite postdated crystallisation of the alkali-syenites.

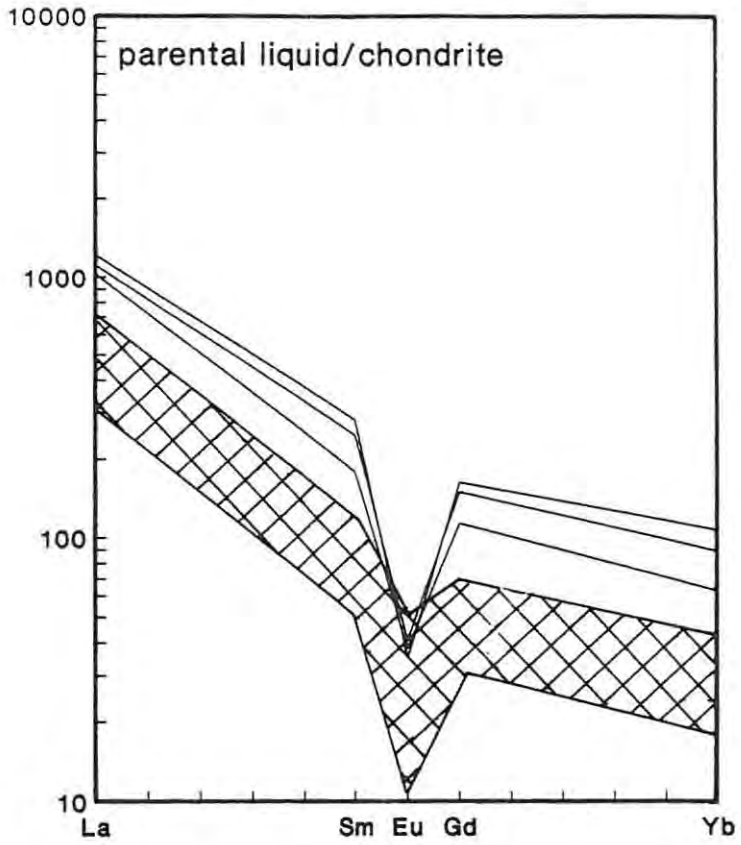

Figure 8.2 Chondrite-normalised REE patterns for the parental liquids of the alkali-feldspar syenite, estimated assuming Bulk D_{REE} = D_{REE} (K-fsp) and using D values from Table 5.3. These patterns are compared with the range of patterns from the monzonite - granite series (hatched field), and show prominent negative Eu anomalies, in contrast with alkali-feldspar syenite whole-rock patterns which have prominent positive Eu anomalies (*cf.* Fig. 5.10.D).

CHAPTER 9: THE EVOLUTION OF THE SILICA-OVERSATURATED ROCKS OF THE GROOTPENSEILAND AND MARINKAS KWELA COMPLEXES

9.1 The Monzonite - Granite Series

These rocks comprise the only 'series' (as defined in this study) having members in both complexes. Evidence is lacking that would conclusively distinguish the GPC rocks (*viz*, the Grootpenseiland Granite and the dykes and plugs of granite and alkali-feldspar granite) from those of the MKC. To be recalled, however, is that only one fresh sample was obtained from the Grootpenseiland Granite, and this sample has higher Rb and Nb concentrations than the other alkali-feldspar granites (Chap. 5.4.c). These differences may relate to alteration (Chap. 3.4.b), but it is also possible that the Grootpenseiland body crystallised from a magma slightly different from the one that gave rise to the ring dyke in the MKC.

Because the monzonite - granite series exhibits a wider compositional range in the MKC than in the GPC (Chap. 2. 5, Chap. 4.3 and Chap. 5, Fig. 5.2), discussion of the geochemical evolution of the series is based on data pertaining to the suite of rocks in the MKC. Key features relating to compositional evolution are as follows.

In the MKC, the rocks of the series were intruded as a sequence of successively more evolved magmas collectively forming a ring dyke (Chap 2.5 and Fig. 2.1). Trends towards the granitic minimum in Petrogeny's Residua System are indicative of alkali-feldspar fractionation (Chap. 5.2 and Fig. 5.1). The most primitive rocks (*viz*, monzonites) are Sr- and Ba-rich (Chap

5.4.b). Both these elements decrease rapidly with increasing differentiation (Fig.5.4), also suggesting a major role for the fractionation of alkali-feldspar, along with plagioclase. Feldspar fractionation is further suggested by the development of a large negative Eu anomaly (Fig. 5.10.f) in the more evolved rocks (Chap 5.4.g). The presence of alkali-feldspar porphyries (Chap. 2.5) suggests the early crystallisation of alkali-feldspar, and from this petrographic evidence alkali-feldspar fractionation may also be inferred. Additionally, decreasing concentrations of FeO, MgO and MnO (Chap. 5.3) require removal of mafic phases. Textural evidence indicates that the monzonitic magmas crystallised biotite before amphibole (Chap. 3.3.a and Chap 4.5), and it is likely that biotite fractionation accounts for much of the initial change in the concentrations of FeO, MgO, K_2O, TiO_2 and Ba (D_{Ba}^{biot} = 5.6 - 36: Table 5.3).

9.1.a Major Elements: Least-squares Mixing Calculations

Least-squares mixing calculations were carried out to investigate a fractional crystallisation origin for compositional variation in the series. The data used (Table 9.1) were average mineral compositions along with whole-rock compositions estimated by fitting trend-lines to Sr *vs.* oxide plots and reading oxide concentrations at high, medium and low Sr ppm.

The mixing calculations gave remarkably good results ($\Sigma r^2 < 0.2$ and commonly < 0.03) consistent with petrographic observations (Table 9.2). The results indicate that the early stages of fractional crystallisation involved plagioclase (An_{27}), smaller amounts of biotite and very minor amounts of clinopyroxene + apatite + sphene. Evolution through the intermediate and evolved compositional ranges (800-100 ppm Sr, 61-70 wt% SiO_2) involved crystallisation of alkali-feldspar (Or_{58-38}) + plagioclase (An_{11}) + amphibole + Ti-magnetite. The results also showed that approximately 95% crystallisation of a monzonitic melt is required to generate the most

Table 9.1 Estimated whole-rock compositions of the monzonite - granite series and average mineral compositions.

	Whole-rock compositions				Mineral compositions		
	A	B	C	D			
ppm Sr	1100	800	400	100	Plag a	Plag b	CPX
[wt%]							
SiO2	59.00	61.50	66.00	70.00	61.17	64.77	50.29
TiO2	0.80	0.58	0.48	0.25	0.00	0.00	0.25
Al2O3	18.80	18.50	16.40	14.90	24.01	21.44	0.86
FeO*	4.80	4.00	3.10	2.80	0.22	0.12	14.15
MgO	1.20	0.75	0.50	0.30	0.00	0.00	8.79
CaO	3.50	2.50	1.60	0.90	5.85	2.45	22.94
Na2O	5.80	5.80	5.00	4.40	8.27	10.49	0.74
K2O	4.60	5.20	5.50	5.90	0.44	0.10	0.00
P2O5	0.47	0.38	0.20	0.10	0.00	0.00	0.00
Total	98.97	99.21	98.78	99.55	99.96	99.37	98.02
				n.	16	7	22

	Mineral compositions								
	Amph a	Amph b	Amph c	Biot a	Biot b	Ti-mgt	Ilm	Apatite	Sphene
[wt%]									
SiO2	38.98	40.46	40.37	34.72	35.17	0.00	0.00	0.44	30.40
TiO2	2.93	2.55	1.62	3.82	4.12	16.97	0.52	0.00	32.01
Al2O3	10.54	8.09	7.68	13.68	12.43	0.21	0.19	0.00	2.22
FeO*	23.73	27.26	31.97	26.51	25.81	81.00	99.00	0.00	1.77
MgO	5.59	4.60	1.97	7.32	7.77	0.00	0.00	0.00	0.00
CaO	10.78	9.15	9.52	0.01	0.00	0.00	0.00	54.95	27.31
Na2O	2.78	2.17	2.14	0.23	0.16	0.00	0.00	0.00	0.00
K2O	1.41	1.04	1.00	8.89	8.78	0.00	0.00	0.00	0.00
P2O5	0.00	0.00	0.00	0.00	0.00	0.00	0.00	38.51	0.00
Total	96.74	95.32	96.27	95.18	94.24	98.18	99.71	93.90	93.71
n.	5	5	5	5	5	5	3	4	2

FeO* = Total Fe as FeO

Table 9.2 Results of least-squares mixing tests for the monzonite - granite series.

(For mineral compositions see Table 10.5.)

Composition A to B						
	observed	estimated	Difference	Mixture wt%		Std-Dev
SiO2	59.00	59.02	0.02	B	74.33	1.43
TiO2	0.80	0.80	0.00	Plag a	17.21	1.19
Al2O3	18.80	18.78	-0.02	Biot a	6.45	0.40
FeO*	4.80	4.84	0.04	cpx	0.83	0.45
MgO	1.20	1.10	-0.10	Sphene	0.39	0.26
CaO	3.50	3.48	-0.02	Apatite	0.57	0.19
Na2O	5.80	5.76	-0.04			
K2O	4.60	4.51	-0.09	Total	99.78	
P2O5	0.47	0.50	0.03	Σr^2	0.02	
Composition B to C						
	observed	estimated	Difference	Mixture wt%		Std-Dev
SiO2	61.50	61.50	0.00	C	15.66	4.62
TiO2	0.58	0.57	-0.01	Plag b	24.71	8.13
Al2O3	18.50	18.46	-0.04	Or*	27.00	1.77
FeO*	4.00	4.00	0.00	Ab*	20.01	9.53
MgO	0.75	0.72	-0.03	Amph a	11.48	1.85
CaO	2.50	2.53	0.03	Ti-mag	0.94	0.41
Na2O	5.80	5.89	0.09	Apatite	0.79	0.24
K2O	5.20	5.26	0.06			
P2O5	0.38	0.34	-0.04	Total	100.06	
				Σr^2	0.02	
Composition C to D						
	observed	estimated	Difference	Mixture wt%		Std-Dev
SiO2	66.00	66.00	0.11	D	54.67	2.76
TiO2	0.48	0.49	-0.19	Or*	14.72	1.49
Al2O3	16.40	16.35	-0.02	Ab*	23.61	1.69
FeO*	3.10	3.12	0.08	Amph b	6.03	0.69
MgO	0.50	0.43	-0.06	Apatite	0.80	0.26
CaO	1.60	1.60	-0.11			
Na2O	5.00	5.12	0.14	Total	99.83	
K2O	5.50	5.58	0.09	Σr^2	0.11	
P2O5	0.20	0.36	0.16			

* Or and Ab = pure orthoclase and albite respectively (analyses from Deer et al.,1980).

fractionated alkali-feldspar granite. Interestingly, this is roughly proportional to the relative outcrop area of these evolved rock types.

9.1.b Trace Element Calculations

Using mineral proportions and values for the fraction of liquid remaining (F) obtained from the mixing calculations, the results of the major element modelling were tested using trace elements and the Rayleigh fractionation equation. The approach adopted was to use the observed values for C^o, C^l and F to calculate Bulk D. The latter were then evaluated using mineral proportions from the mixing calculations and mineral/melt D from the literature (Table 5.3).

Data for mineral/melt D for Si-rich rocks are less comprehensive than those for mafic and Si-undersaturated rocks. Moreover, numerous studies have emphasised the large variability of mineral/melt D in Si-rich rocks (Watson, 1977; Mahood and Hildreth, 1983; Nash and Crecraft, 1985; Mahood and Stimac, 1990). The variability arises because partitioning between phenocrysts and melts is governed primarily by crystal structure constraints in less silicic, dacitic melts, whereas the structure and volatile content of the melt are important considerations in very high silica systems (Nash and Crecraft, 1985). In addition, increasing peralkalinity and increasing concentrations of Fe offset the effects of increasing SiO_2 content on melt polymerisation, and consequently affect D values (Mahood and Stimac, 1990).

Because the rocks of the monzonite - granite series are neither peralkaline nor 'high-silica', the selection of appropriate D was restricted where possible to data from studies of rocks of near-dacitic compositions by Hanson (1978), Nagasawa and Schnetzler (1971) and Philpotts and Schnetzler (1970). Where no data were available for near-dacitic rocks, data of Nash and Crecraft (1985), which are intermediate to those reported from dacites and high silica

rhyolites, were used. Finally, data for mafic and Si-undersaturated rocks were used in preference to those for high silica rhyolites.

The results of trace element modelling are presented in Table 9.3. They show that variations in the concentrations of Ba, Sr and Pb are consistent with D in the literature (Table 5.3) and with fractionating mineral proportions in Table 9.2. The same can also be said for variations in Rb, Zr and Y concentrations, whilst those relating to Th and Nb are very nearly consistent within the less evolved compositional range of the rock series. For the intermediate compositional range, the value for bulk D_{Rb} required to account for observed variation in the concentration of Rb is only within the calculated range of D when the data of Nash and Crecraft (1985) are used ($D_{Rb}^{K\text{-}fsp}$ = 1.2 - 1.8). Similarly, the calculated ranges of bulk $D_{Nb,Y,Zr}$ are less than values required to account for observed variation in those elements for intermediate and evolved whole-rock compositional ranges. Data for D_{Nb}^{amph} and D_{Y}^{ap} are, however, lacking. These three elements need further consideration.

Table 9.3. Bulk D's required to account for observed trace-element variations compared to values calculated using fractionating assemblages determined by least-squares mixing calculations. Values for D are from Table 5.3 and do not include those for high-Si rhyolites (see text for details).

Fractionation Step	A to B		B to C		C to D	
F*	0.74		0.15		0.54	
Bulk D	Required	Calculated	Required	Calculated	Required	Calculated
Sr	2.11	1.20-3.51	1.35	1.71-3.44	4.10	1.97-6.33
Ba	1.46	1.81-4.99	1.25	0.73-3.50	3.40	0.86-5.21
Rb	0.61	0.51-0.85	0.92	0.36-0.39	0.69	0.56-0.57
Pb	0.14	0.43-1.27	0.94	0.82-2.30	0.67	0.84-2.72
Th	0.80	0.11-0.67	0.64	0.03-0.04	0.00	0.04-0.046
Nb	0.76	1.03-3.76	0.93	0.24	0.64	0.003
Zr	0.59	0.27-1.01	0.97	0.03-0.38	0.90	0.008-0.27
Y	0.91	0.73-0.96	0.80	0.03-0.08	0.14	0.014

F* = Fraction of liquid remaining as determined from least-squares mixing calculations.

Values for D_Y^{amph} and D_Y^{ap} can be estimated by extrapolating between respective D for Gd and Er and by assuming $D_{Ho \approx Y}$ (Table 5.3). Values thus obtained are high (D_Y^{amph} = 2.4-8.6, D_Y^{ap} = 1.3-16) and increase the maximum calculated bulk D_Y for both intermediate and evolved whole-rock compositional ranges to 1.3, so bracketing the required value. Furthermore, small errors in the abundance of sphene (D_{Nb} 2.3-93), Ti-magnetite (D_{Nb} 24.6) and biotite (D_{Nb} 4-9.5) in the calculated extract assemblages would have a large effect on the bulk D_{Nb}.

The discrepancy between calculated and required D_{Zr} is perhaps less readily reconciled. Zirconium concentrates predominantly in zircon, which appears to be a late phase to crystallise (Chaps. 3.3.a). In this respect Zr is like Th, which concentrates in late-stage allanite, but unlike the whole-rock data for Th, those for Zr exhibit a great deal of scatter with no obvious tendency to increase in concentration (Figs. 5.5 and 5.7). The occurrence of zircon in small fractures (Chap. 4.8.d) suggests that concentrations of Zr may not reflect crystal/liquid processes alone.

While the concentrations of Zr may thus have been affected by sub-solidus processes of hydrothermal alteration, there is no reason to suggest that other components have been similarly affected. Their concentrations, as well as major element concentrations, are consistent with fractional crystallisation alone.

9.2 The Alkali-granites

In Chapter 5.3, the alkali-granites were subdivided into high-silica and low-silica varieties. This section examines the causes of compositional variation amongst, and the possibility of a direct relationship between, the two varieties. Key features of the rocks are as follows:

The low-silica variety (SiO_2 < 75 wt%) intrudes as small dykes and plugs in both intrusive complexes, and the high-silica variety (SiO_2 > 75 wt%) forms the Marinkas Kwela Granite body (Chaps. 2.5 and 5.3). Compared with the low-silica alkali-granite, the high-silica variety exhibits a narrow range in composition, has lower concentrations of Al_2O_3, K_2O, Na_2O, Nb and Zr, and higher concentrations of FeO and Rb (Chap.5). The two varieties also display some petrographic differences (Chap. 3.3.b).

Phase relationships within the system **Q-ab-or** provide a suitable means for investigating petrological relationships in the two rocks, which are highly leucocratic and never highly peralkaline.

The high-silica alkali-granite lies between the granitic minimum at 1 kbar (F-free) and the granitic minimum at 1 kbar + 1 wt% F (Fig. 9.1). For granites, such compositions reflect either extensive fractionation of feldspar or low-temperature partial melts (minimum melts) of a crustal source region. Both possibilities are consistent with the large negative Eu anomalies (Fig. 5.10.f) and low K/Rb ratios (±10 - Fig. 5.4) exhibited by the high-silica alkali-granite.

The low-silica alkali-granite exhibits a large degree of scatter in the system **Q-ab-or** and, compared with the high-silica variety, is displaced towards **Q**-poor compositions (Fig. 9.1). It also shows large negative Eu anomalies (Fig. 5.10.f), as well as low K/Rb ratios that lie between those for the high-silica variety and those of all other rocks in both complexes. These features can also be attributed either to feldspar fractionation or to partial melting of a crustal source.

The two processes can be distinguished by plotting the concentration of a magmatophile element (*e.g.* Th) against the ratio of that element to a hypermagmatophile element (Allégre and Minster, 1978). The distinctions arise primarily because, for incompatible elements,

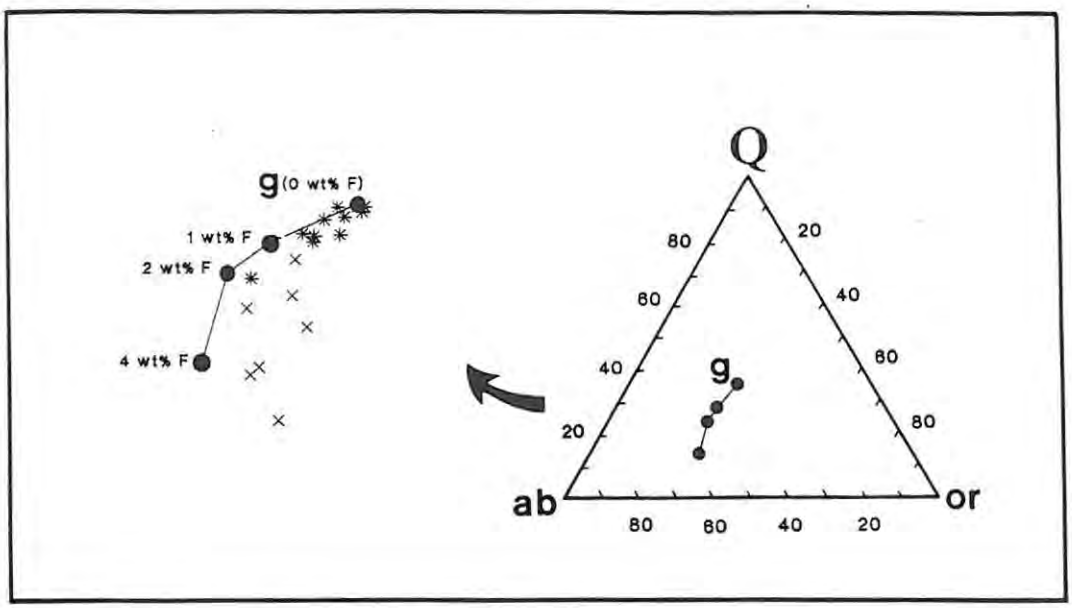

Figure 9.1 The system *Q-ab-or* showing the compositions of the high-silica (double crosses) and low-silica (single crosses) alkali-granites in relation to the granitic minimum at 1 kbar and with varying concentrations of fluorine (Data for the granitic minimum from Manning, 1981).

fractional crystallisation is less sensitive to small changes in D than is partial melting except where $F \rightarrow 0$. Thus

$$C_l^H / C_l^M = C_{o\,l}^H / C_{o\,l}^M = \text{constant}$$

for fractional crystallisation, but during equilibrium partial melting

$$C_l^H = C_{o\,s}^H / F$$

and

$$C_l^M = C_{o\,s}^M / (D_o^M + F)$$

where C^M and C^H represent the concentrations of a magmatophile and hypermagmantophile trace element respectively in the liquid (C_l), initial liquid ($C_{o,l}$) or initial solid ($C_{o,s}$), D_o is the bulk partition coefficient for the initial assemblage and F is the weight proportion of melted material (Allégre and Minster, 1978).

Thus in a (C_l^H /C_l^Mvs. C_l^M) diagram, rocks that are related through fractional crystallisation will define a horizontal line while rocks related through partial melting will define a straight line with a slope determined by the ratio

$$D_o^M / C_{os}^M .$$

Figure 9.2 was constructed to test an hypothesis that compositional features in the alkali-granites reflect fractional crystallisation. For the high-silica variety, plots for Nb/Th *vs.* Nb and Y/Th *vs.* Y show horizontal trends which are consistent with fractional crystallisation. The development of large negative Eu anomalies and of low K/Rb ratios in these rocks may also be ascribed to feldspar fractionation. For the low-silica variety, the data are too scattered to allow any conclusion to be drawn. The scatter may indicate that Y, Nb and Th do not conform to magmatophile or hypermagmatophile behaviour, but equally likely suggests that the individual intrusions of low-silica alkali-granite are not directly related genetically to each other.

The two varieties of alkali-granite show very different ranges in the ratios Nb/Th and Y/Th. The low-silica variety also shows a wide range in Y/Nb ratios, with values generally lower than the narrow range for the high-silica variety. Because of these compositional differences, it appears unlikely that the two varieties are directly related genetically. In any case, if they were related their relative abundances would require that the low-silica variety was derived from the high-silica variety - but the latter is clearly the more fractionated in terms both of the system **Q-ab-or**, and of K/Rb ratios.

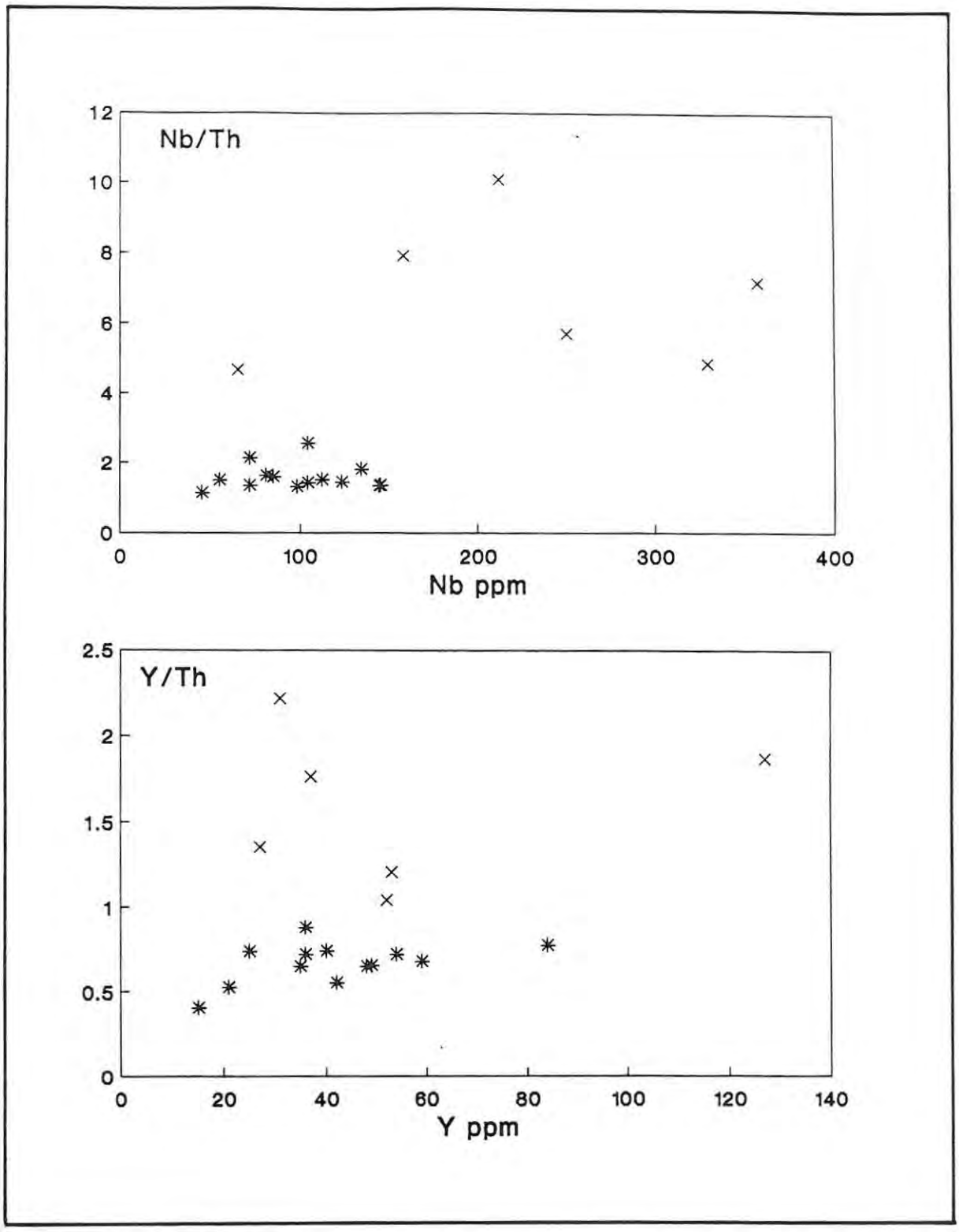

Figure 9.2 Plots of Nb/Th *vs.* Nb and Y/Th *vs.* Y for the alkali-granites. (symbols as in Table 2.1).

9.3 Sr- And O-isotopes And The Relationship Between The Si-oversaturated Rock Types.

Peralkaline Si-oversaturated rocks such as alkali-granite can result from differentiation of sub-alkalic and commonly metaluminous liquids, with or without volatile transfer of components (Macdonald, 1974), or from partial melting of crustal material under volatile-rich conditions (Bailey,1980; Davies and Macdonald, 1987). Therefore it is possible that the liquids that gave rise to the monzonite - granite series were parental also to the alkali-granites. This possibility was investigated using isotopic data. It is clear from the outset that significant differences between the two ranges of I_{Sr} ratios (Table 6.1) rule out a relationship through closed system fractional crystallisation alone.

9.3.a Isotopic Constraints On The Sources Of Alkali-Granites

It is not possible to accurately determine I_{Sr} ratios for the alkali-granites. It seems very likely that the samples with high Rb/Sr ratios (Table 6.1) have been disturbed in some way, however, two samples show low Rb/Sr and high I_{Sr} ratios which may suggest the presence of a crustal component in these alkali-granites at least.

Oxygen isotopic data possibly point in the same direction. The $\delta^{18}O$ values obtained for feldspar and quartz in the high-silica alkali-granite are 7.92‰ and 9.79‰ respectively (Table 6.1). The corresponding quartz-feldspar fractionation of 1.87 exceeds typical magmatic values which Sheppard and Harris (1985) considered to be ±1.0. Because feldspar exchanges O-isotopes much more readily than does quartz (Taylor and Sheppard, 1986; Faure, 1986), and given the subsolidus alteration associated with the alkali-granites (Chap. 3.4), it seems likely that the $\delta^{18}O$ of feldspar in the alkali-granite has been significantly reduced.

Because feldspar-melt $^{18}O/^{16}O$ fractionations are very low (Taylor and Sheppard, 1986), the melts from which the high-silica alkali-granites crystallised must have had $\delta^{18}O$ values at least as high as around 7.9‰. The true value may be as high as 8.9‰, assuming magmatic quartz-feldspar fractionations and that the isotopic composition of quartz has not been altered. This range of values would exceed the range expected through closed system fractional crystallisation ot a mantle melt.

According to Taylor and Sheppard (1986), it is only in the near-surface sedimentary and hydrothermal environments that $^{18}O/^{16}O$ fractionations are large enough to increase $\delta^{18}O$ values greatly above mantle values. Consequently, it is possible that material that once resided at or near the earth's surface made a contribution to the parental magma of the alkali-granite.

9.3.b Isotopic Constraints On The Source For The Monzonite - Granite Series

While the $\delta^{18}O$ for feldspar of the rocks of the monzonite - granite series are relatively high (8.3‰ - 8.5‰), quartz-feldspar fractionation of only ±1.12 implies that these values are primary. Because $\delta^{18}O_{feldspar} \approx \delta^{18}O_{melt}$ (Taylor and Sheppard, 1986), $\delta^{18}O$ values for the melts that crystallised the monzonite - granite series would have exceeded the range for uncontaminated rocks of mantle origin. Consequently, the oxygen isotope data allow for the presence of a crustal component in the rocks also of the monzonite - granite series. While the I_{Sr} for the series are equivalent to those for the Si-undersaturated rocks, the exact values and range are greater than those for the larvikite - pulaskite series (Chap.6.3). They also allow for a degree of crustal contamination in the monzonites/granites, but significantly less than in the alkali-granites.

9.4 Chemical Characterisation Of The Si-oversaturated Rocks

In terms of tectonic discrimination diagrams (Pearce *et al.*,1984), these rocks fall into the field for within-plate granites (Fig.9.4). They also exhibit geochemical characteristics of A-type magmas such as low Al_2O_3, CaO, MgO, Ba and Sr, and high FeO, Na_2O, K_2O, F, Zr, Nb and REE, relative to calc-alkaline and strongly peraluminous granitoids (Collins *et al.*,1982; Clemens *et al.*,1986; Whalen *et al.*,1987; Sheraton and Black, 1988).

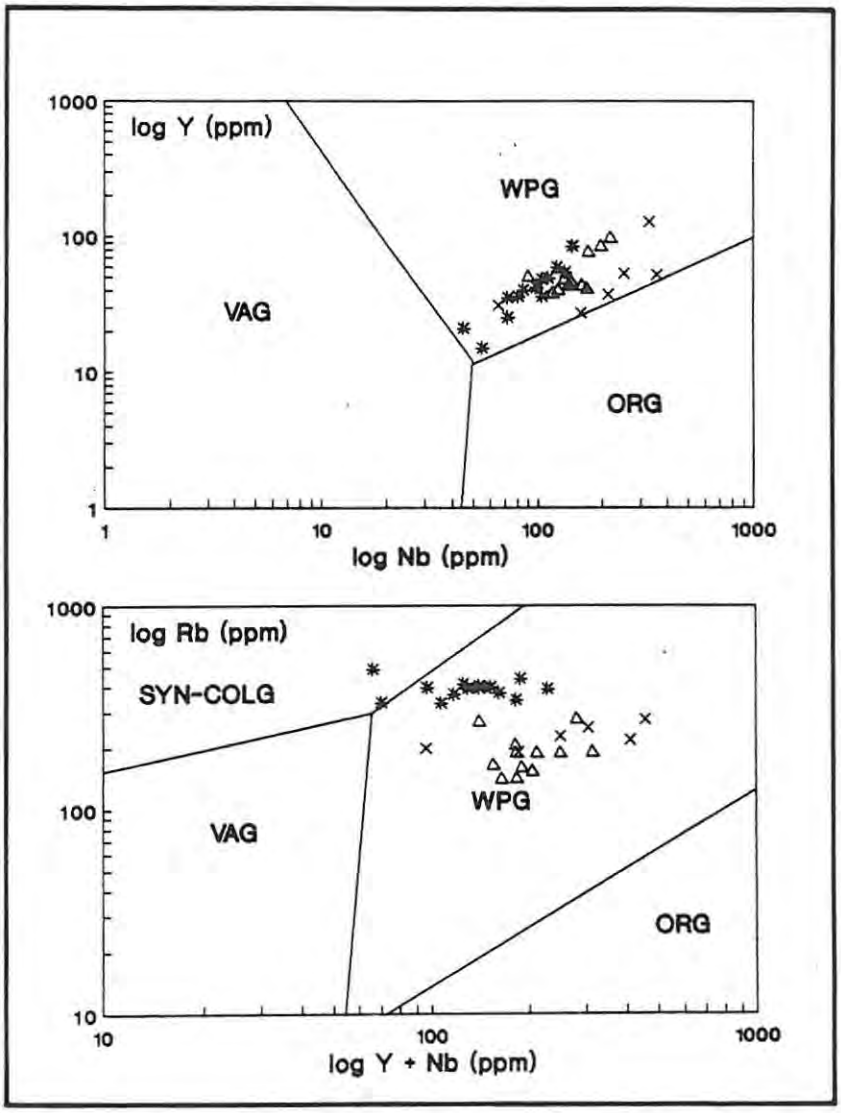

Figure 9.4 Tectonic discrimination diagrams using Y *vs.* Nb and Rb *vs.* Y+Nb (after Pearce *et al.*, 1984) showing the data for the Si-oversaturated rocks of the GPC and MKC. Symbols as in Table 2.1. **VAG** = volcanic-arc granites, **WPG** = within plate granites, **ORG** = ocean ridge granites and **SYN-COLG** = syn-collisional granites.

A-type granites are emplaced into anorogenic tectonic settings and may show a wide range of intrusive forms and associations. Some may occur as individual large bodies (plutons), commonly not associated with intermediate rock types (Collins *et al.*,1982). Others occur in alkaline provinces, either as isolated bodies or in direct association with a range of other alkaline igneous rocks, some of which may be Si-undersaturated.

Loiselle and Wones (1979) suggest that A-type magmas result when basaltic magmas interact with granulite-facies lower crust, or fractionate directly with no crustal interaction. On the basis of the generally anhydrous nature and high K/Rb ratios of most A-type granites, Collins *et al.* (1982) suggest that fractional crystallisation is not a general explanation for their origin, although some may have evolved in this way. In the case of the A-type granites of southeastern Australia, in particular, those authors favour the direct partial melting of a melt-depleted I-type source in the lower crust. Sheraton and Black (1988) also prefer partial melting of anhydrous granulite as a petrogenic process producing A-type granite magmas, but question the need for a highly refractory residual component. A current problem with the classification of A-type granitic rocks is that the term does not yet enjoy the same genetic significance as the terms I-type and S-type which, according to Chappell and White (1974), derive from well defined source regions. As a group, A-type granites show a very variable range of I_{Sr} ratios, the highest recorded being 0.720 for the Younger Granites of Nigeria (van Breeman *et al.*,1975). Hence, the basis for the A-type classification appears to hinge on broad compositional and tectonic similarities which may be the result of a number of unrelated genetic processes.

In the case of the Si-oversaturated rocks of the GPC and the MKC, a contribution of mantle-derived material to the genesis of magmas with A-type characteristics is clearly implied.

CHAPTER 10: SOURCE REGIONS AND RELATIONSHIPS BETWEEEN THE ROCKS OF THE GROOTPENSEILAND AND MARINKAS KWELA COMPLEXES

10.1 Magma Sources For The Rocks Of The GPC And The MKC

The petrogenesis of alkaline rocks has been ascribed by such authors as Weaver *et al.* (1972) and Price *et al.* (1985) to protracted fractional crystallisation of a mantle-derived basaltic magma with little, if any, crustal contribution. Woolley and Symes (1976) and Bailey (1989) have put forward alternative views which regard alkaline felsic magmas as primary melts of the lower crust. Davies and Macdonald (1988) have pointed out that in some provinces, the relative volume of basaltic and peralkaline sialic magma, and the dearth of intermediate compositions, seem inconsistent with closed-system fractional crystallisation; accordingly, they propose that both the mantle and the lower crust contribute to the magmatism. Reid (in press) has pointed in a similar direction in regard to the source regions for rocks of the Kanabeam Complex, which lies to the northeast of the MKC.

In the context of these different proposals, isotopic evidence was used to investigate the relative contributions made by mantle and crustal material to the melts that gave rise to the GPC and MKC.

The most ambiguous isotopic data are those for Sr, for which a wide range of I_{Sr} ratios were obtained (Chap. 6.3). The relatively high I_{Sr} ratios for the Si-oversaturated rocks may indicate the presence of a high $^{87}Sr/^{86}Sr$ crustal component. Despite the relatively low I_{Sr} ratios for the Si-undersaturated rocks, a crustal source could also have made a major contribution to those rocks (Chap. 6.3). It has been shown that regions

of Proterozoic lower crust, now observed in granulite terranes (Cohen *et al,* 1984; McMillan and Dungan, 1988) and as xenoliths in kimberlite (Rogers and Hawkesworth, 1982), also have $^{87}Sr/^{86}Sr$ ratios that are appropriately low for the source of the Si-undersaturated rocks. Melting of the lower crust, possibly accompanying or following metasomatism, has been suggested as a means of producing Si-undersaturated melts (*e.g.* by Bailey, 1974; Marsh, 1987). Taken on its own, the entire range of I_{Sr} ratios for the GPC and MKC could conceivably reflect mixtures of high and low $^{87}Sr/^{86}Sr$ crustal components.

Less ambiguous, however, are the isotopic compositions of Nd, which invariably show high $^{143}Nd/^{144}Nd$ ratios ($\varepsilon_{Nd} > 0$), reflecting a mantle source that has been depleted in Nd relative to Sm (Chap. 6.4). They indicate little or no contribution, at least of Nd, from regions of old continental crust which, like the lower crustal regions discussed above (Rogers and Hawkesworth, 1982; Cohen et al, 1984; McMillan and Dungan, 1988; DePaolo, 1981), should have low $^{143}Nd/^{144}Nd$ ratios ($\varepsilon_{Nd} < 0$). It seems likely, then, that the low I_{Sr} for the Si-undersaturated rocks likewise reflect mantle derivation - from a region with Nd and Sr isotopic compositions similar to those of the Mantle Array (Fig. 6.5).

The isotopic data for Pb are consistent with a mantle origin for the rocks of the GPC and MKC. The data may reflect derivation from a source with similar Pb isotopic compositions as the source for such oceanic islands as Gough, Tristan de Cunha and the Walvis Ridge. The data, however, are also consistent with crustal interaction, a possibility that draws limited support from Sr isotopic compositions and the O-isotopic compositions of the Si-oversaturated rocks.

The sensitivity of the various isotopic systems to interaction with crustal material appears to decrease in the order (Pb) > Sr, O > Nd. This can be attributed to the high concentrations of Sr and REE (and low Sm/Nd ratios) in the primitive magmas.

10.2 Relationship Between Si-undersaturated And Si-oversaturated Rocks

Close spatial relationships between Si-oversaturated and Si-undersaturated rocks are observed in the GPC and MKC. Such close relationships are also features of many other alkaline complexes (Pankhurst *et al.*, 1976; Upton and Thomas, 1980; Fletcher and Beddoe-Stephens, 1987; Woolley and Jones, 1987; Henderson *et al.*,1988).

It has been proposed - for example by Foland and Henderson (1976) and Eby (1987) - that in such situations the two magma types may be genetically related to each other.

The question of a common (mantle) source for all the rocks of the GPC and MKC remains equivocal on the basis of isotopic data presented here although similarities must be noted in terms of ϵ_{Nd} and ϵ_{Sr}. It must also be remembered that the most primitive rocks of the larvikite - pulaskite series and the alkali-melasyenite - nepheline-syenite series, although occurring in different complexes, are virtually identical in all compositional and mineralogical respects. These similarities, in conjunction with the close spatial relationships, also provide a strong case for relating those rocks genetically at Grootpenseiland and Marinkas Kwela.

The main problem with this hypothesis is that it requires a parental magma to evolve in composition across a thermal barrier which, in Petrogeny's Residua System, is represented by the ***ab-or*** join. Processes invoked to overcome this problem include (1) fractionation of amphibole from critically undersaturated magmas to produce Si-oversaturated trends (Foland and Henderson, 1976); (2) movement of ground water into, and the removal of SiO_2 from, a Si-oversaturated magma to produce Si-undersaturated trends (Pankhurst *et al.*, 1976); and (3)

crustal contamination of critically undersaturated trachytic magma so as to initiate Si-oversaturated trends (Eby, 1987).

The fractionation of a magma (at other than mantle pressures) across the thermal barrier has never been proved. Accordingly, the viability of amphibole fractionation as a means of initiating a Si-oversaturated trend in originally Si-undersaturated magmas cannot be assessed. Such a process, however, seems unlikely. In any case, evidence from mineral textures at Grootpenseiland and Marinkas Kwela (Chap. 3) is that amphibole does not appear on the liquidus for the primitive rocks of any series.

The possible role of ground water has been documented by Pankhurst *et al.* (1976) in regard to the Kangerdlugssuaq intrusion in East Greenland. Their study presents evidence that is consistent with the production of Si-undersaturated trends through the interaction of circulating meteoric waters with Si-oversaturated melts. Meteoric waters commonly have low $d^{18}O$ (Taylor, 1979). At Kangerdlugssuaq, they also had a $^{87}Sr/^{86}Sr$ ratio slightly higher than that of the Si-oversaturated melt. The circulating waters are thought by Pankhurst *et al.* to have caused 'de-silication' as well as reduced $d^{18}O$ values and increased $^{87}Sr/^{86}Sr$ ratios in the melts with which they interacted. However, in the GPC and MKC the Si-undersaturated rocks crystallised before the Si-oversaturated rocks, compared with which they show similar, or lower, $^{87}Sr/^{86}Sr$ ratios and higher (inferred) whole-rock $d^{18}O$. Consequently the model developed by Pankhurst *et al.* (1976) is clearly not applicable to the range of rock types observed in the GPC and the MKC.

Other processes involving circulating ground water/melt interactions could be more applicable. Hildreth *et al.* (1984) describe the effects caused where ground water and rhyolitic magmas interact. Such processes may be more common than is currently recognised, although the particular effects described by Hildreth *et al.* (1984) also involve

substantial depletions of ^{18}O in the melts - no evidence for which is observed in the GPC or the MKC.

Study of the GPC and MKC affords limited support for the proposition by Eby (1987) that liquid lines of descent can be differentially affected by crustal contamination. The isotopic data for the Si-oversaturated rocks allows that a proportion of crustal material interacted with the mantle melts. It is proposed here that the diverging trends shown by the respective rock series were caused through the interaction of these melts with crustal material. Where no interaction occurred, the melts fractionated towards successively more Si-undersaturated compositions to produce foyaitic or phonolitic residuals - and incorporation of a 'granitic' component resulted in a critically saturated or Si-oversaturated trends.

10.3 A Review

By way of concluding Chapters 3 to 10, dealing in detail with the two silicate complexes, it is useful to refer back to Chapter 2.7 where the field evidence was summarised, a *provisional* sequence was proposed and some uncertainties were noted.

As regards the **Si-undersaturated rocks of the GPC,** the summary in Chapter 2.7 requires no modification - two different magmas produced first the monzodiorite and later the larvikite - pulaskite series .It may be added here that, being a sidewall sequence (Chap 7.2), the larvikite - pulaskite series must have crystallised in a chamber of considerably greater extent than that of the present outcrop of Si-undersaturated rocks.

Chapter 2.7 requires refinement as regards its presentation of the **Si-undersaturated rocks of the MKC.** The evidence elaborated subsequently suggests that only one magma was involved and it gave rise to both the clinopyroxene- and amphibole-rich foyaite *together with* the alkali-melasyenite - pulaskite series (Chap 7.4).

Two apparently very similar **critically saturated rock types** were recognised in Chapter 2. The evidence of subsequent chapters is that (1) the differences between them make it unlikely that they are directly related (Chap. 8.1.b); (2) rather, the alkali-feldspar syenite is probably related genetically to the Si-oversaturated monzonite - granite series (Chap 8.2); and (3) a genetic relationship between the alkali-syenite of the GPC, and that of the MKC, is highly unlikely (Chap. 8.1.a).

Of the **Si-oversaturated rocks,** it has been shown that the alkali-granites comprise high- and low-silica varieties, with the former restricted to the MKC. Low-silica alkali-granites occur in both complexes and cannot be subdivided (Chap 9.2)

CHAPTER 11: PETROGRAPHY, MINERALOGY AND GEOCHEMISTRY OF THE MARINKAS KWELA CARBONATITE COMPLEX

11.1 Introduction

In Chapter 2.6 the geology and field relationships of the carbonatite complex were discussed and are summarised here. There are five main rock types, nepheline syenite, sôvite, beforsite, and ferrocarbonatite/Mn-rich ferrocarbonatite, and field relationships indicate that they were intruded in that order. The sôvite body was probably emplaced as a number of independent magma pulses, and contains silicate-rich and silicate-poor varieties of carbonatite. There are two large bodies of beforsite - a circular one in the south, and an elongated body to the east. Ferrocarbonatite dykes crop out only in the eastern beforsite, in contrast with dykes of Mn-rich ferrocarbonatite which surround the complex.

In this chapter and the one that follows, the carbonatite complex will be discussed in detail. This chapter is essentially descriptive, while Chapter 12 will assess the evolution of individual rock types and the complex as a whole.

11.2 Petrography

11.2.a Nepheline syenite

Nepheline syenite in the carbonatite complex has been fenitised by subsequent intrusions of carbonatite, and is commonly also brecciated. Biotite, alkali-feldspar, calcite, aegirine and cancrinite are

the predominate fenite minerals, and all of them, except possibly cancrinite and calcite, also occur as primary phases.

The rock is porphyritic. Phenocrysts of perthite, nepheline, aegirine-augite, biotite and pyrochlore lie in a groundmass of fine-grained alkali-feldspar, cancrinite and aegirine. Perthite phenocrysts are sometimes euhedral but more commonly have angular crystal faces which are attributable to brecciation. Fresh nepheline is not encountered, but large cancrinite aggregates with euhedral hexagonal faces are probably psuedomorphs after nepheline. It is also possible that groundmass cancrinite is a fenitisation product of a groundmass nepheline phase.

11.2.b Sövite

Commonly white in colour, the sövite is medium- to fine-grained and contains up to 98% calcite as the sole carbonate phase. Silicate-rich sövite is commonly porphyritic, containing large (up to 3cm) euhedral phenocrysts of aegirine-augite and/or alkali-amphibole (ferro-richterite) as the main silicate phases, with lesser amounts of phlogopite and aegirine as rims around aegirine-augite. The groundmass consists mainly of calcite with up to 20% apatite and some minor pyrochlore and magnetite. Textural characteristics show that at least some of the apatite crystallised before calcite. The silicate phenocrysts are commonly cross-cut by calcite-filled fractures.

Silicate-poor sövite is predominantly medium-grained and equigranular. It is commonly a monomineralic rock (calcite), but sövite remnants found in the eastern beforsite body contain stringers of apatite ± pyrochlore ± ankerite, and sôvite located near, or within, the nepheline syenite may contain phenocrysts of perthite.

11.2.c Beforsites

11.2.c (a) The Southern Beforsite

The southern beforsite, including associated radial dykes, consists largely of medium- to coarse-grained dolomite or ferroan dolomite (terminology after Deer *et al.*,1962). It is mostly equigranular, but an early (and phenocrystic?) phase of dolomite is sometimes found. Adcumulate textures are well developed; Le Bas (1987) records that such features are common in beforsites in general. Magnetite ± pyrite is the only primary opaque phase. It forms anhedral to euhedral crystals that occur within carbonate grains or along grain-boundaries.

Irregular blebs and discontinuous veins (or stringers) of magnetite ± pyrite occur and are now partly decomposed to hematite, goethite ± limonite. In thin section, the stringers and blebs can be seen to parallel a weak alignment of carbonate grains, suggesting they are of primary (magmatic) origin.

11.2.c (b) The Eastern Beforsite

This rock consists predominantly of ferroan dolomite although some samples consist mostly of ankerite. It displays allotriomorphic granular textures but with a distinct preferred alignment of carbonate grains, paralleled by fractures which form networks up to 2cm wide that are continuous for many metres. Brecciation commonly occurs along these fractures. Apatite constitutes up to 20% of the rock and is a late phase to crystallise, concentrating in the fracture networks as semi-continuous stringers of sub-rounded grains (Plate 11.1). Garson (1955) interpreted similar features in plutonic carbonatites to be flow structures. The apatite may be accompanied by euhedral pyrochlore ±magnetite, bastnaesite,

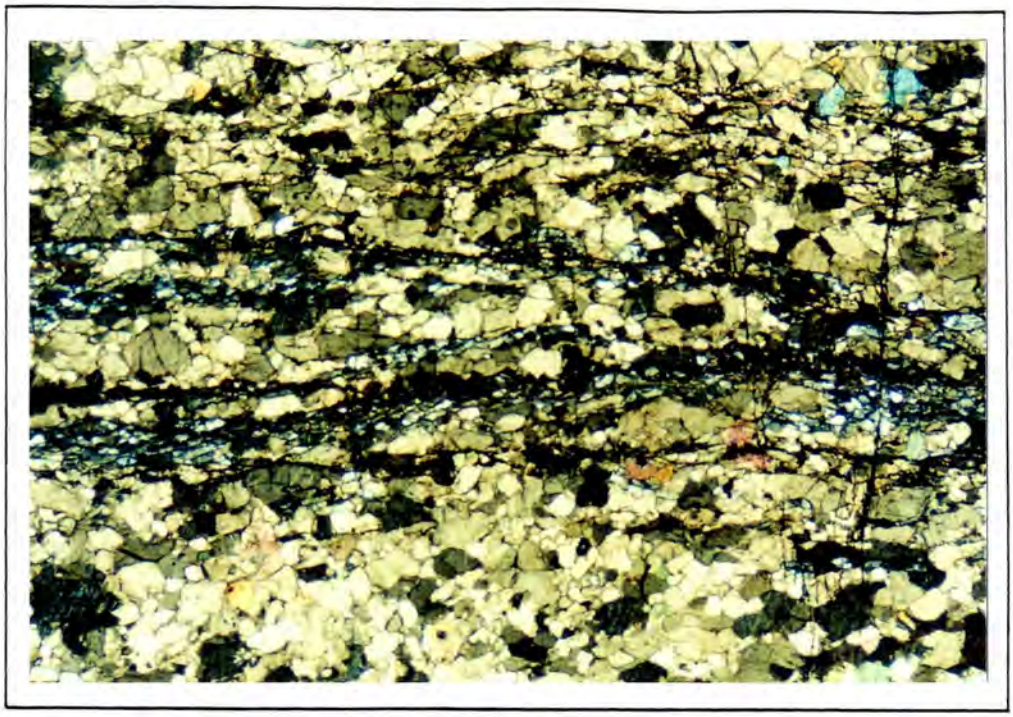

Plate 11.1 Photomicrograph of eastern beforsite showing apatite-rich layers or fractures within carbonate. (XP. x20).

phlogopite, fluorite and fine-grained euhedral needles of a colourless amphibole, eckermanite. Alignment of the carbonate grains and stringers is interpreted here as a flow alignment.

11.2.d Ferrocarbonatite

The ferrocarbonatite is a medium-grained, light-brown rock comprising an assemblage of ankerite ± magnetite, pyrochlore and bastnaesite. It shows well developed adcumulate textures. Despite its Fe-rich nature, the rock is free from Fe-staining, presumably because Fe has remained bound within carbonate.

11.2.e Mn-rich Ferrocarbonatite

The complex mineralogy of the Mn-rich carbonatite dykes is commonly obscured by a dark stain caused by the presence of abundant goethite. Most dykes are brecciated; large, irregular and ferrugenised clasts are surrounded by a groundmass of ankerite or

manganoan dolomite. In a few dykes, a coarse-grained assemblage of manganoan calcite, heavily dusted with magnetite, is intruded by veins of manganoan dolomite which contain aggregates of magnetite, phlogopite, chlorite, bastnaesite, synchisite and pyrochlore. Sphalerite also occurs in some of the unbrecciated Mn-rich carbonatite dykes; sample MKC 27 provides an example. In contrast to beforsite and ferrocarbonatite, Mn-rich ferrocarbonatite contains neither apatite nor pyrochlore. The complex mineralogy, and particularly the presence of a manganoan carbonate, are what distinguish the rock from all other carbonatites in the complex.

11.3 Mineralogy

Carbonate in the rocks of the Marinkas Kwela Carbonatite body belongs mostly to the calcite - dolomite - ankerite series. No siderite, rhodocrosite, magnesite or alkali-carbonate was found. Variations in carbonate compositions are summarised in Figure 11.1, using symbols given in Table 11.1, and typical analyses are presented in Table 11.2. The classification of carbonate follows Deer *et al.,* (1962), who used the term ankerite for carbonate with Mg:Fe < 4:1.

Calcite from the sövite, including that from the remnant sôvite in the eastern beforsite body, shows compositional variations that are consistent with Ca $\leftrightharpoons$ Mg substitution.

Carbonate in the beforsites ranges from dolomite to ankerite in the southern body, and from ferroan-dolomite to ankerite in the eastern body. With maximum FeO and MnO contents of around 5wt% and 2wt% respectively, the carbonate is very similar to ferroan-dolomite from the Fen Complex, described by Andersen (1984). The possible phenocrysts referred to in Chapter 11.2.c above are of dolomite, but they contrast with co-existing adcumulate dolomite in showing no Fe $\leftrightharpoons$Mg substitution and in containing only minor amounts of FeO (0.08wt%) and MnO (0.02wt%). It is possible that they crystallised

Table 11.1 Symbols used for whole-rock and mineral data

✙	Sövites
◊	Remnant sövites
○	Southern beforsite body
□	Eastern beforsite body
⊠	Ferrocarbonatites
✳	Mn-rich ferrocarbonatites
✡	Massive magnetite blebs

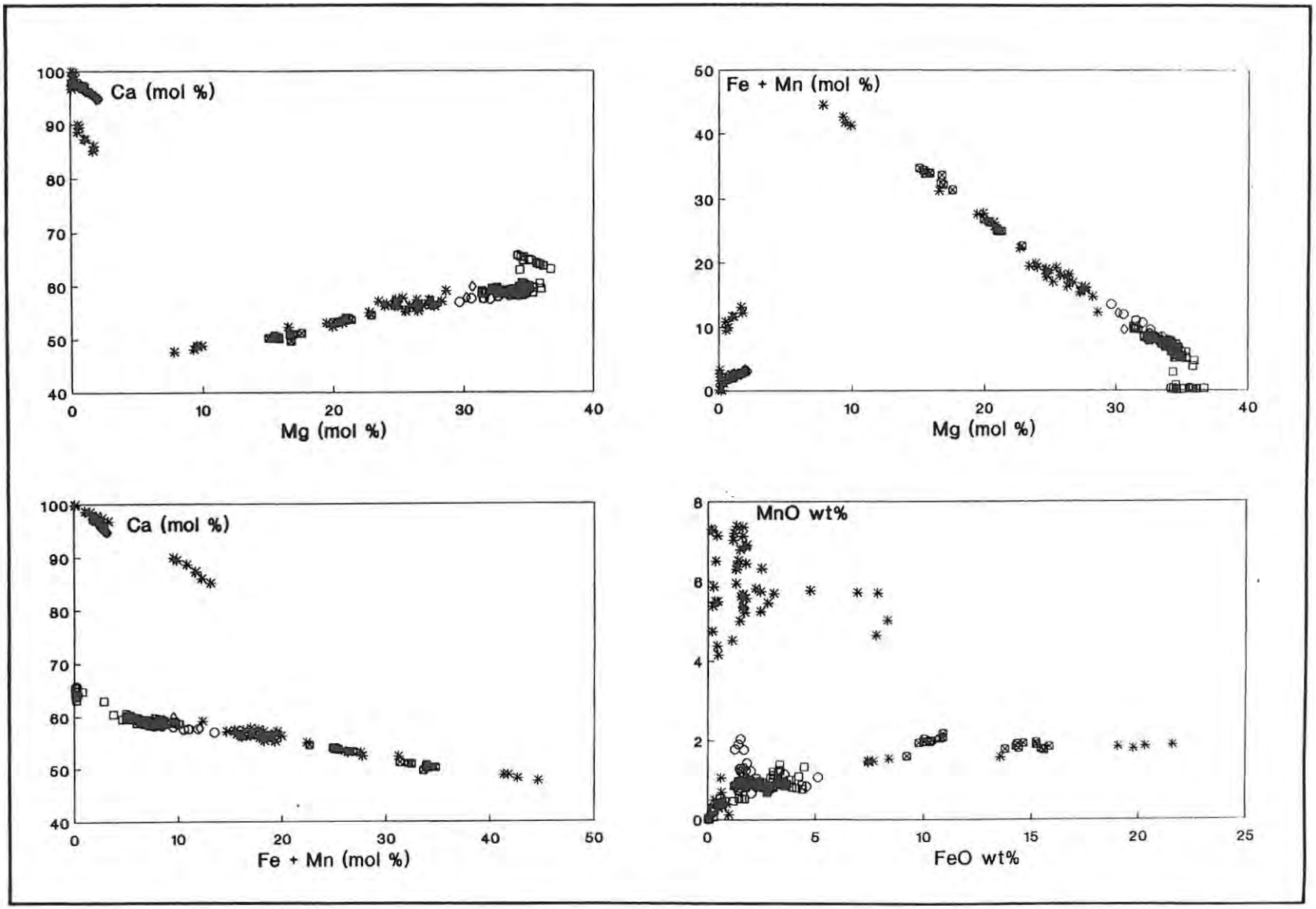

Figure 11.1 Plots showing the variations in the composition of carbonate within and between the carbonatites at Marinkas Kwela. Symbols as in Table 11.1.

Table 11.2. Typical partial analyses of carbonate phases in carbonatites.

[wt%]	MKC 29 1	MKC 32 2	MKC 48 3	MKC 44 4	MKC 6 5	MKC 62 6	MKC 17 7	MKC 16 8	MKC 54 9
FeO	0.64	10.42	14.84	4.35	1.67	3.22	1.54	0.28	0.54
MnO	0.71	1.75	1.85	1.25	0.79	1.20	6.66	5.19	0.36
MgO	1.00	13.20	10.46	17.47	19.51	18.12	14.69	0.89	0.53
CaO	51.88	27.78	27.55	28.65	28.25	28.18	27.84	47.91	52.45
Total	54.23	53.15	54.70	51.72	50.22	50.72	50.73	54.27	53.88
mol%									
Mg	1.56	21.37	16.20	29.80	34.75	31.68	25.24	1.37	0.83
Ca	95.74	53.28	50.53	57.90	59.62	58.38	56.68	87.78	97.36
Fe+Mn	2.69	25.35	33.27	12.30	5.63	9.93	18.09	10.85	1.82

1 calcite - remnant sövite
2 ankerite - Eastern beforsite body
3 ankerite - ferrocarbonatite
4 dolomite - Eastern beforsite body
5-6 dolomite - Southern beforsite body
7 dolomite - Mn-rich ferrocarbonatite
8 calcite - Mn-rich ferrocarbonatite
9 calcite - sövite

from an earlier 'parental' magma. Alternatively, they may represent xenocrysts from the sedimentary dolomites of the Nama Group. Similar xenocrysts are commonly found in rocks of the nearby GPC and MKC.

In the ferrocarbonatite, ankerite is the only carbonate to occur. It is distinctly richer in FeO than is the ankerite of the beforsite (Fig. 11.1).

Carbonate in the Mn-rich ferrocarbonatite mainly falls in the dolomite - ankerite compositional range, but some is calcitic. Both kinds are commonly manganoan. On a plot of Mg *vs.* Fe+Mn, most of the manganoan dolomite and manganoan ankerite falls in the compositional gap that separates ankerite in the beforsites from ankerite in the ferrocarbonatite. This comes about primarily because of the Mn-rich nature of carbonate in the Mn-rich ferrocarbonatite,

in contrast with the main dolomite-ankerite trend which is towards Fe enrichment.

11.4 Geochemistry

11.4. a Nepheline Syenite

Whole-rock geochemical analyses of the nepheline syenite are presented in Table 11.3, and some compositional features are plotted in Figures 11.2 and 11.3. Compared with the Si-undersaturated rocks of the GPC and MKC, the rock is unusually rich in CaO and is distinctly peralkaline, notwithstanding its higher Sr concentrations. It is also distinctly depleted in LREE, with no Eu anomaly (Fig.11.4). Unfortunately all samples collected for analysis show petrographic evidence of fenitisation so the effects of this process on the chemical compositions of the nepheline syenites cannot be quantitatively determined.

11.4.b Carbonatites

In discussions of the geochemistry of carbonatites, comparisons are often drawn with an 'average carbonatite composition' (*e.g.*, Gold, 1966). Such comparisons are not entirely satisfactory, for two main reasons. First, a characteristic feature of carbonatites is their very wide chemical variation (Hoy and Kwong, 1986; Woolley, 1982), particularly in respect of those elements for which high concentrations are regarded as typical (*e.g.*, Sr, Ba, Nb and the REE - Barber, 1974). Second, average analyses are commonly drawn from numerous individual publications, many of which report (or are biased towards) unusual geological features. Addressing these problems, Woolley and Kempe (1989) have produced average analyses for the main carbonatite types, trying where possible not to bias those averages by over-representing rocks of unusual

Table 11.3 Geochemical analyses of silicate rocks from the Marinkas Kwela Carbonatite Complex.

[wt%]	RS 112	RS 113	RS 114	RS 115	RS 117	RS 120
SiO2	49.61	50.98	50.45	53.45	54.65	54.57
TiO2	0.91	0.72	0.69	0.72	0.81	0.69
Al2O3	17.11	17.15	16.71	17.78	18.26	17.87
FeO*	4.55	5.53	5.20	5.48	2.16	5.62
MnO	0.17	0.12	0.10	0.39	0.16	0.17
MgO	1.29	0.78	0.85	1.10	0.21	1.19
CaO	5.42	5.05	4.70	3.70	4.04	4.88
Na2O	5.59	9.04	10.10	10.40	8.39	4.86
K2O	7.41	5.22	4.64	4.66	5.62	4.99
P2O5	0.60	0.78	0.43	0.41	0.34	0.40
Cr2O3	0.00	0.00	0.00	0.00	0.00	0.02
NiO	0.00	0.01	0.01	0.00	0.00	0.00
H2O-	0.17	0.13	0.11	0.12	0.14	0.11
LOI	5.96	5.12	4.50	2.40	4.20	4.32
Total	98.85	100.70	98.55	100.68	99.01	99.76
[ppm]						
Zn	87	46	57	198	16	92
Cu	20	17	15	19	25	15
Ni	<6	<5	3	5	4	7
Co	6	<4	5	6	10	4
Mo	3	5	6	8	<3	8
Nb	470	461	386	330	547	351
Zr	1003	1055	1103	1199	67	1126
Y	13	18	17	38	11	15
Sr	2063	1542	1203	869	1926	1098
Rb	255	162	155	165	121	175
U	49	23	20	10	23	6
Th	9	9	7	19	6	10
Pb	4	8	5	9	10	<3
Cr	<17	<7	<9	<8	<7	<16
V	102	153	116	39	16	100
Ba	2775	2261	1839	1224	2115	2218
Sc	<12	<12	<10	<12	<13	<10
F	1850	1300	700	890	300	680
Na+K/Al	1.01	1.20	1.29	1.25	1.09	0.75
[ppm]						
La			25.18			33.66
Ce			54.46			67.29
Pr			6.54			7.96
Nd			27.10			32.30
Sm			4.52			5.12
Eu			1.40			1.53
Gd			3.69			4.03
Dy			3.28			3.16
Ho			0.58			0.54
Er			1.70			1.59
Yb			1.77			1.60
Lu			0.31			0.31

FeO* = all Fe as FeO
LOI = Loss On Ignition

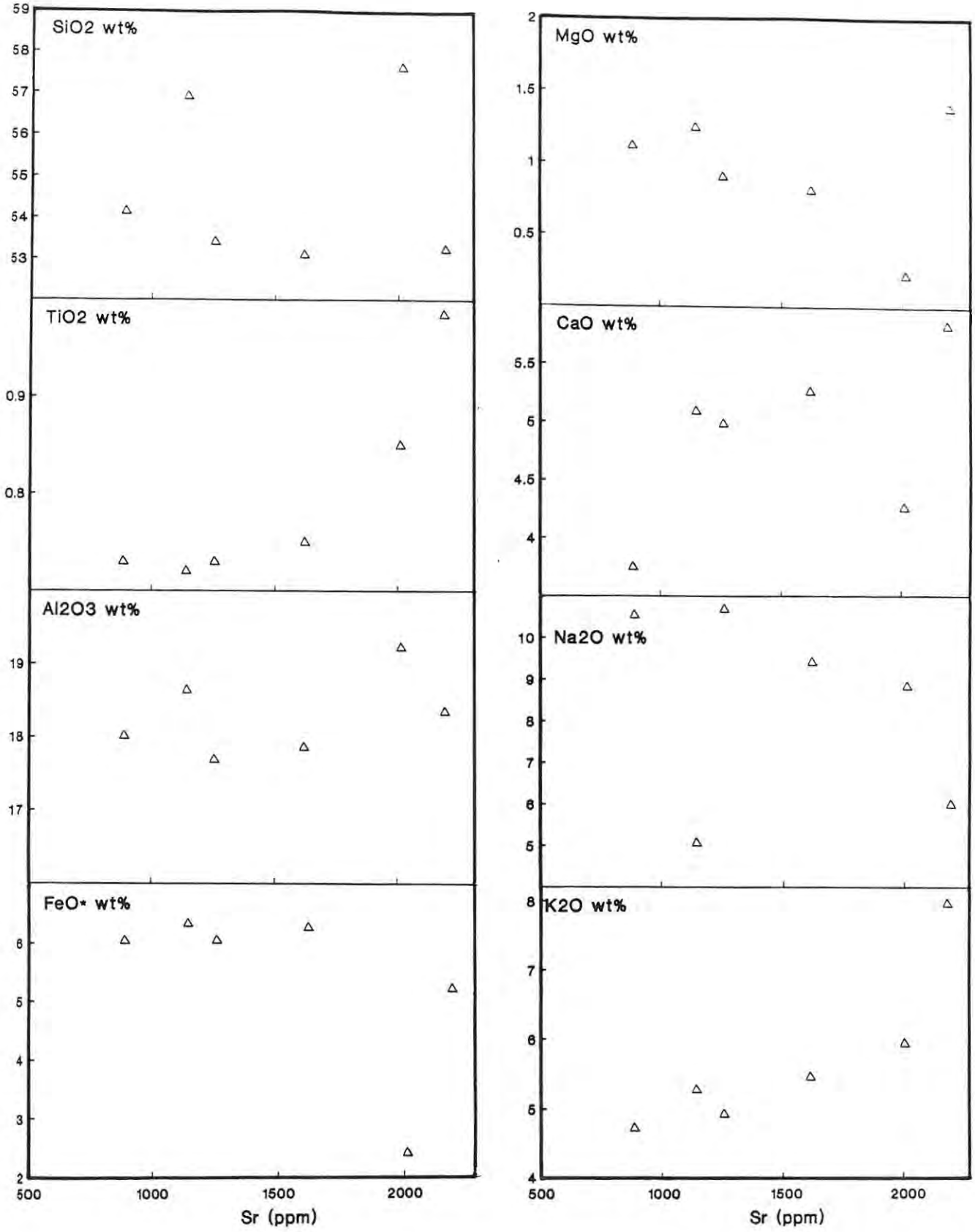

Figure 11.2 Variation of the major elements *vs.* Sr for the nepheline syenite.

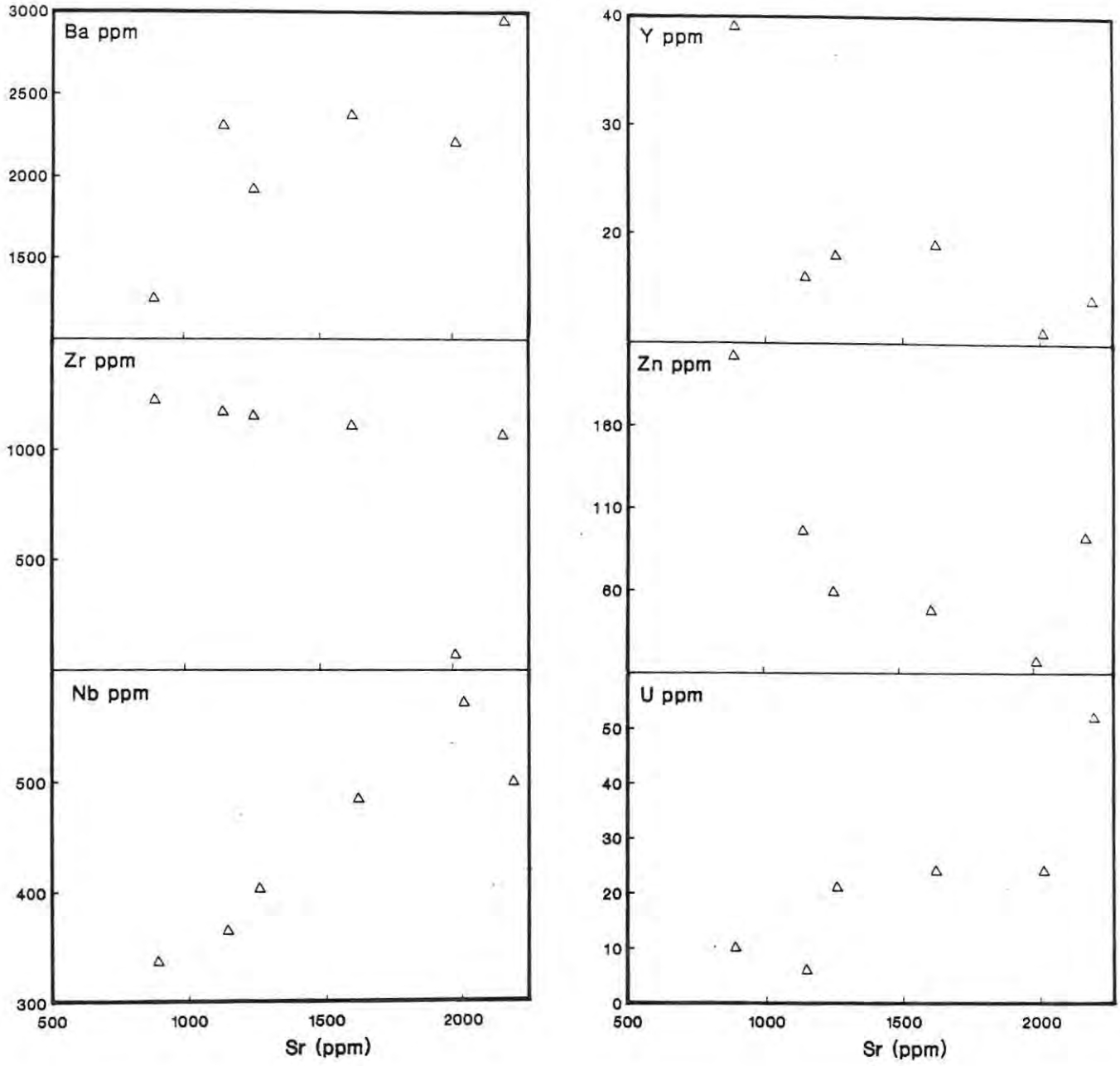

Figure 11.3 Variation of various trace elements *vs.* Sr for the nepheline syenite.

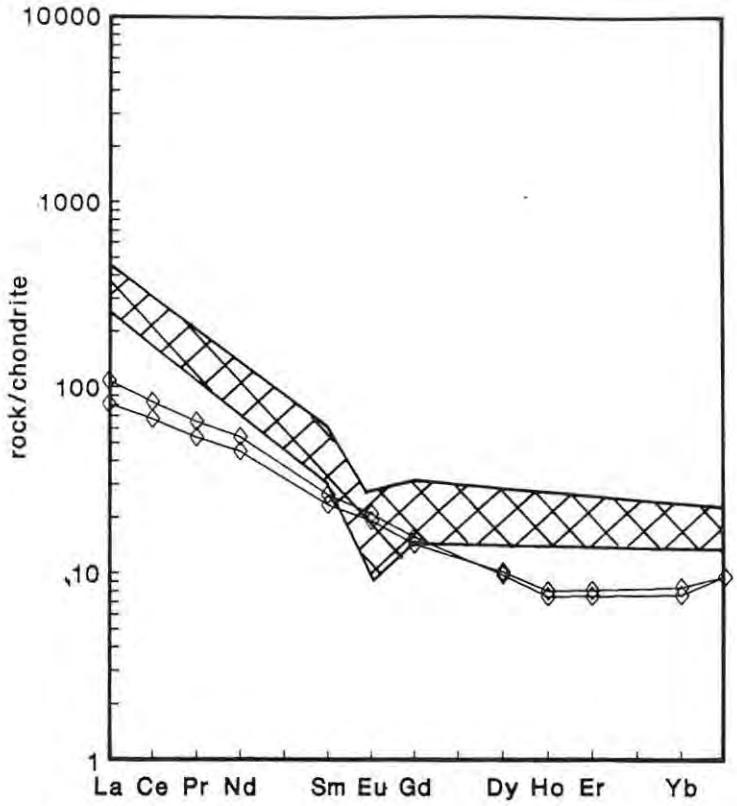

Figure 11.4 REE patterns for the nepheline syenite, normalised against chondritic abundance data from Nakamura (1974). For comparison, data for the nepheline syenite and foyaites of the MKC are also plotted (hatch field).

composition. Nevertheless, the range associated with each average value is still very large and, for comparative purposes, not entirely satisfactory.

Analyses of carbonatites from Marinkas Kwela are presented in Table 11.4. The carbonatites mostly have low SiO_2 and Al_2O_3 (<3wt% and <1wt% respectively) although silicate-rich sövite and phlogopite-rich beforsite (Chap.2.6) are exceptional in this respect. The concentration of P_2O_5 is conspicuously low in most rock types (<0.5wt%) but apatite-rich exceptions include sôvite and the eastern beforsite.

A magmatic sequence from sövite to beforsites to ferrocarbonatite has already been noted in Chapter 2.7. According to Woolley (1982) and Le Bas (1981), sequences of this kind are a feature of many carbonatite complexes. At Marinkas Kwela, an initial trend of MgO-enrichment is followed by enrichment in FeO+MnO, with the Mn-rich

ferrocarbonatite dykes representing a case of extreme Fe- and Mn-enrichment (Fig.11.5). However, it must be noted that some of the Mn-rich ferrocarbonatite dykes actually have lower MnO concentrations than those of the ferrocarbonatite. They are classified here as 'Mn-rich ferrocarbonatite' by virtue of their characteristic complex mineralogy and the presence of a manganoan carbonate (11.2.e above)

The southern beforsite is generally more FeO-rich than the eastern beforsite, although the carbonate of the former is relatively poor in FeO. This feature can be attributed to the abundance of magnetite in the southern beforsite. It is possible that some of the magnetite exsolved from the carbonate itself.

In a general survey of the trace element geochemistry of carbonatites, Nelson *et al.* (1988) described carbonatites as having high concentrations of Ba, Th, LREE, and Sr; variable concentrations of Nb, Ta and P; and low concentrations of Cr, Rb, K, Ti and HREE. According to Barber (1974) and Le Bas (1981), the concentration of Sr should decrease, and that of Ba and the REE (±Zn Pb and V) should increase, with fractionation of a carbonatite magma. Barber (1974) also found that Ti, Zr and Nb were most concentrated in the 'middle' carbonatite stage of the Homa and Wasaki carbonatite series from Kenya, and the data of Woolley and Kempe (1989) suggest that Nd is usually depleted in the Mg-rich 'middle' stages.

Carbonatites at Marinkas Kwela exhibit most of these general characteristics, although Ba is present in low concentrations (<800 ppm) in all varieties except the Mn-rich ferrocarbonatite, which is also richer in Sr, Zn, Th and LREE compared with the other rocks. Relatively high concentrations of Nb (600-2020 ppm) occur in sôvite and the eastern beforsite. Generally speaking, the concentrations of most trace elements are very variable, even within a particular rock-type. Some of the observed scatter is possibly related to fenitisation. Vapour/melt fractionations are undoubtedly an important feature of carbonatite evolution and could also lead to extreme ranges in the

Table 11.4. Geochemical analyses of carbonatites from the Marinkas Kwela Carbonatite Complex.

	MKC 4	MKC 6	MKC 7	MKC 9	MKC 18	MKC 35	MKC 55A	MKC 62	MKC 25	MKC 56	MKC 34	MKC 45	MKC 46
[wt%]	1	2	3	4	5	6	7	8	9	10	11	12	13
SiO2	0.13	0.54	0.62	0.39	0.20	0.15	0.29	0.12	5.03	7.31	0.38	0.13	1.12
TiO2	0.01	0.00	0.02	0.02	0.00	0.00	0.00	0.00	0.05	0.08	0.07	0.02	0.06
Al2O3	0.03	0.18	0.12	0.12	0.01	0.00	0.10	0.06	1.12	2.12	0.05	0.04	0.05
FeO*	4.34	8.46	7.48	5.98	5.92	5.04	7.81	6.44	4.48	4.17	3.08	3.67	7.76
MnO	0.85	1.20	2.22	0.98	0.93	1.00	1.81	1.10	0.86	0.74	0.75	0.89	0.79
MgO	20.51	19.66	18.10	20.56	19.20	19.54	17.87	17.36	18.98	20.01	18.00	17.34	16.66
CaO	28.01	27.97	29.51	27.63	28.90	28.80	28.92	29.16	27.69	25.49	30.24	32.42	30.72
Na2O	0.04	0.01	0.04	0.02	0.00	0.00	0.06	0.09	0.05	0.18	0.09	0.30	0.46
K2O	0.00	0.00	0.00	0.08	0.00	0.00	0.00	0.00	0.62	0.87	0.00	0.00	0.00
P2O5	0.00	0.03	0.00	0.04	0.00	0.00	0.00	0.00	0.53	0.40	1.62	3.92	3.19
Cr2O3	0.01	0.02	0.03	0.01	0.00	0.02	0.01	0.01	0.02	0.00	0.02	0.01	0.01
NiO	0.01	0.00	0.00	0.01	0.00	0.00	0.00	0.00	0.01	0.00	0.00	0.00	0.01
H2O-	0.02	0.17	0.08	0.04	0.07	0.03	0.11	0.14	0.08	0.22	0.14	0.09	0.13
LOI	44.99	42.22	42.56	44.26	43.87	43.66	42.44	43.89	40.63	37.88	44.36	41.07	39.26
Total	99.00	100.56	100.87	100.21	99.17	98.30	99.52	98.45	100.21	99.52	98.84	99.95	100.32
[ppm]													
Zn	45	50	130	82	214	39	108	0	88	96	28	43	47
Cu	67	26	61	81	72	72	69	86	143	74	45	62	57
Ni	4	1	4	0	6	4	7	3	6	3	2	6	6
Co	1	7	3	3	16	3	0	0	2	0	6	0	0
Mo	5	24	0	9	26	15	64	879	1	1	0	0	0
Nb	716	1008	785	91	17	106	551	1	50	86	611	2029	1737
Zr	0	78	33	11	0	0	0	0	0	1	49	6	48
Y	4	19	7	3	0	0	1	2	0	0	16	30	25
Sr	6103	2195	5331	7708	7618	7397	6015	7663	6580	6779	4715	5192	4923
Rb	0	2	0	0	0	0	0	0	30	41	0	0	0
U	1	9	2	0	0	0	0	0	0	0	0	0	0
Th	3	18	8	2	3	6	15	13	0	0	0	4	7
Pb	13	21	31	15	112	5	35	10	12	3	1	11	4
Cr	10	30	22	<6	42	54	7	<7	51	9	37	20	<10
V	23	42	34	24	34	29	<5	<5	<10	4	<10	<5	43
Ba	241	702	62	132	499	485	213	65	149	217	79	<15	40
Sc	<8	<8	<9	0	<8	<8	11	14	8	16	9	7	18
F	0	0	0	0	25	209	0	0	2013	0	335	0	0
La			127.60	115.97		84.26			62.36		153.75	175.20	
Ce			163.80	159.00		104.41			95.65		204.51	392.02	
Pr			18.44	18.76		12.40			12.14		25.06	48.04	
Nd			58.56	60.51		39.26			38.79		94.26	204.60	
Sm			6.08	6.52		4.45			4.83		13.26	30.47	
Eu			1.54	1.73		1.21			1.34		4.13	8.30	
Gd			4.02	4.17		2.67			3.72		9.85	21.47	
Dy									2.29		5.72	11.40	
Ho			0.67	0.53		0.41			0.53		1.02	1.74	
Er			1.46	1.08		0.89			1.21		2.05	4.40	
Yb			0.69	0.57		0.52			0.62		1.09	1.73	
Lu												0.22	

FeO* = all Fe as FeO
LOI = Loss On Ignition
1-8 Southern beforsite body
9-10 Southern beforsite body- phlogopite-rich
11-13 Eastern beforsite body

Table 11.4. Continued

	MKC 29	MKC 47	MKC 48	MKC 15	MKC 16	MKC 17	MKC 20A	MKC 20B	MKC 27	MKC 52	MKC 54	MKC 55B	MKC 59
[wt%]	14	15	16	17	18	19	20	21	22	23	24	25	26
SiO2	1.36	0.39	3.02	2.57	0.80	0.63	1.68	1.35	0.24	3.97	22.16	0.45	3.27
TiO2	0.01	0.46	0.01	0.00	0.00	0.00	0.00	0.00	0.00	0.07	0.85	0.00	0.00
Al2O3	0.02	0.12	0.93	0.03	0.01	0.03	0.61	0.41	0.05	0.33	1.65	0.23	0.73
FeO*	2.16	10.38	15.13	22.81	24.15	18.98	20.27	14.79	11.18	2.85	11.79	41.85	44.76
MnO	0.74	2.04	1.83	7.74	6.79	5.57	1.63	1.34	5.09	0.23	0.34	2.77	4.96
MgO	1.68	14.19	10.33	1.13	6.04	6.84	5.53	6.12	11.87	1.31	1.48	11.05	6.35
CaO	51.42	29.92	28.38	33.06	29.07	29.72	26.94	25.40	28.95	49.42	31.87	18.70	15.13
Na2O	0.01	0.06	0.24	0.35	0.20	0.07	0.07	0.13	0.07	0.25	1.84	0.07	0.05
K2O	0.00	0.05	0.04	0.08	0.00	0.00	0.04	0.00	0.00	0.07	0.24	0.00	0.08
P2O5	2.20	0.00	0.00	0.01	0.00	0.01	0.20	0.21	0.69	2.37	7.45	0.00	0.00
Cr2O3	0.02	0.01	0.04	0.03	0.03	0.02	0.02	0.00	0.02	0.04	0.04	0.01	0.00
NiO	0.01	0.00	0.00	0.01	0.01	0.00	0.00	0.00	0.00	0.00	0.00	0.01	0.00
H2O-	0.10	0.08	0.33	1.16	0.29	0.18	0.28	0.36	0.03	0.24	0.28	0.32	0.96
LOI	39.69	42.52	38.63	27.99	29.23	32.05	33.54	32.43	38.91	36.68	18.99	23.80	21.80
Total	99.45	100.35	99.10	97.25	96.92	94.33	91.06	82.72	97.24	97.87	99.13	99.80	98.64
[ppm]													
Zn	19	38	75	7184	3883	1488	164	244	832	24	38	627	453
Cu	65	19	89	76	58	83	146	385	78	33	37	55	56
Ni	8	5	15	8	13	16	15	29	8	7	19	13	11
Co	11	0	0	0	0	0	0	0	5	0	7	0	0
Mo	0	0	9	13	2	2	0	0	10	0	7	54	67
Nb	1982	378	324	7	190	196	64	71	5	950	236	252	1387
Zr	0	2	12	58	50	0	0	0	0	71	847	0	4
Y	92	13	51	44	56	90	64	54	11	70	445	0	8
Sr	6922	1268	7513	1575	4632	8363	15579	43778	7377	2745	2466	3546	3011
Rb	0	2	0	0	0	0	10	0	0	7	11	3	0
U	5	0	1	2	7	0	0	0	0	30	40	0	0
Th	28	0	86	137	196	412	712	1015	9	25	49	3	108
Pb	8	12	19	32	27	205	127	160	20	13	32	35	23
Cr	79	40	47	<10	53	19	<10	<10	30	<5	83	15	8
V	32	45	30	<10	<10	<10	<10	<11	<10	46	1021	20	48
Ba	455	<21	141	203	510	584	16303	26229	5390	345	282	157	655
Sc	<8	19	25	<10	<9	<8	<9	<9	<8	46	94	9	23
F	1711	0	0	1719	933	1714	2354	3565	217	500	500	0	1800
La	239.84	46.07		1545.90	532.97				1190.06	242.00	193.85		
Ce	417.54	77.10		3376.86	1135.50				1949.97	480.46	402.04		
Pr	56.83	7.46		519.79	174.80				245.71	53.39	48.95		
Nd	216.17	27.60		1931.98	661.55				833.04	217.10	217.20		
Sm	33.15	3.35		203.04	75.51				76.06	33.06	42.56		
Eu	10.38	0.90		47.59	20.71				17.35	9.51	14.39		
Gd	26.28	2.42		80.03	38.23				29.59	25.62	51.42		
Dy	20.55	2.71								17.50	80.28		
Ho	4.00	0.54		5.97	3.50				2.75	2.97	15.27		
Er	9.60	1.86		10.05	6.45				4.70	8.01	41.14		
Yb	6.80	1.96		2.88	2.70				1.38	5.18	31.70		
Lu		0.29								0.74	4.28		

FeO* = all Fe as FeO
LOI = Loss On Ignition
14 Remnant sovite
15-16 Ferrocarbonatites
17-22 Mn-rich ferrocarbonatites
23-24 Sovites
25-26 Massive magnetite bleb

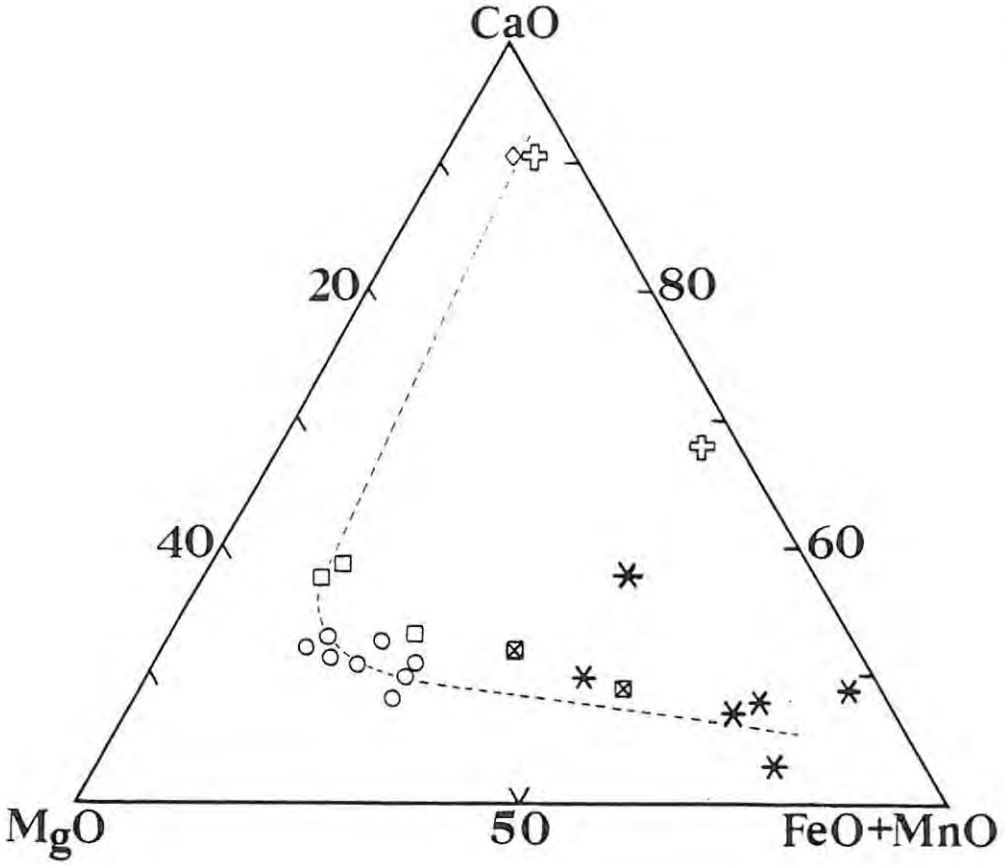

Figure 11.5 Plot of CaO - MgO - FeO*+MnO showing the compositions of the carbonatites at Marinkas Kwela. Symbols as in Table 11.1. FeO* = all Fe as Fe^{2+}.

concentrations of certain trace elements. Moreover, trace elements which do not readily enter the major carbonate phases tend to concentrate in discrete accessory phases (*e.g.*, Nb into pyrochlore) which themselves are very irregularly distributed. The Mn-rich ferrocarbonatite dykes, in particular, are modally very inhomogeneous, as is obvious on a comparison between analyses of two samples (MKC 20 a & b) taken from a single hand specimen (Table 11.4).

Amongst the trace elements, coherent compositional trends can be observed only for Th, Nb and Y (Fig.11.6). Considering the complex as a whole, there appears to be a tendency for the concentration of Th to increase, and that of Nb to decrease, with increasing concentration of FeO (*i.e.*, with differentiation). Yttrium shows high concentrations (13-445 ppm) in the apatite-rich lithologies but is depleted in the southern beforsite. Ferrocarbonatite and Mn-rich ferrocarbonatite also show high concentrations of Y.

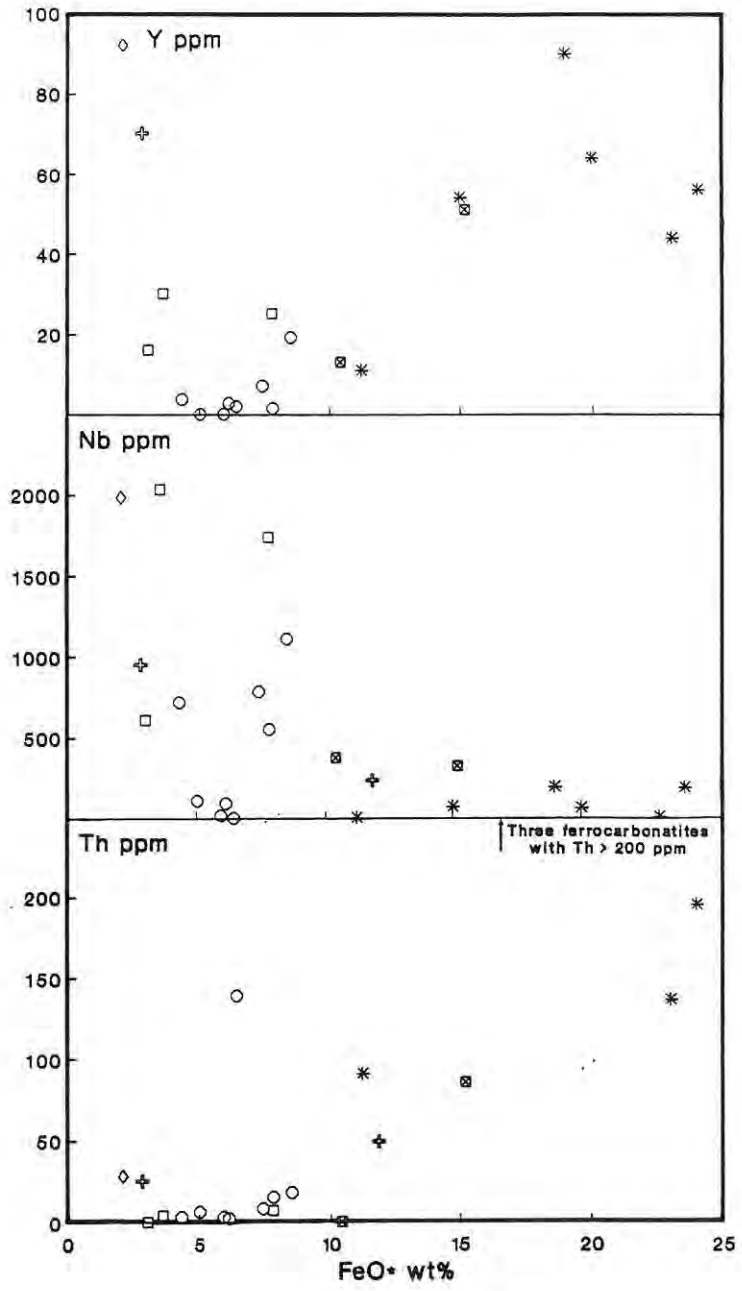

Figure 11.6 Concentrations of Y, Nb and Th (ppm) *vs.* FeO* for the carbonatites at Marinkas Kwela. Symbols as in Table 11.1. FeO* = all Fe as Fe^{2+}.

Chondrite-normalised REE concentrations for the carbonatite complex are plotted in Figure 11.7 and show characteristically high LREE/HREE ratios and large total enrichments for carbonatites relative to nepheline syenite. Total REE concentrations in the carbonatites increase in the order ferrocarbonatite, southern beforsite, eastern beforsite, sövite, Mn-rich ferrocarbonatite. The La/Yb ratio also increases in the same order, from as low as 23 in the ferrocarbonatite to as high as 860 in the Mn-rich ferrocarbonatite

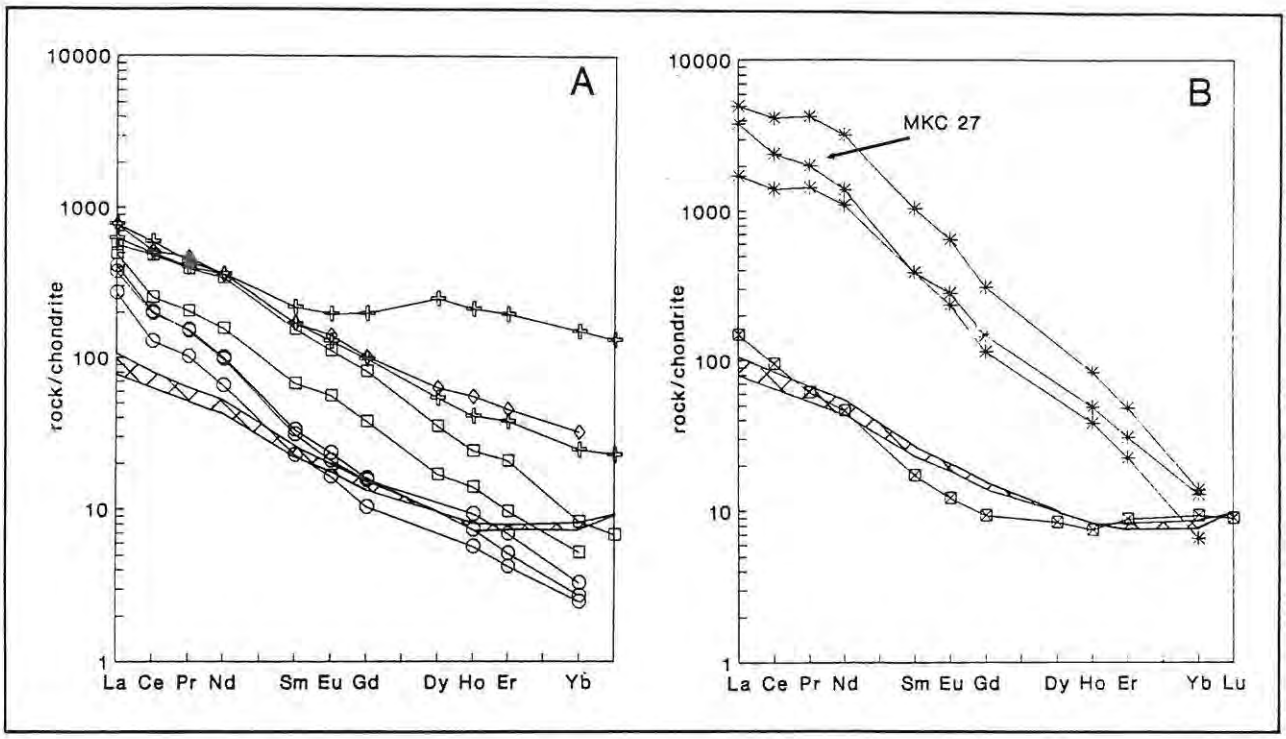

Figure 11.7 REE patterns for (A) the sövite and beforsites and (B) the ferrocarbonatite and Mn-rich ferrocarbonatite dykes, normalised against chondritic abundance data from Nakamura (1974). Symbols as in Table 11.1. For comparison, data for the nepheline syenite are also plotted (hatch field)

CHAPTER 12: GEOCHEMICAL EVOLUTION OF THE MARINKAS KWELA CARBONATITE COMPLEX

12.1. Nepheline Syenite Of The Marinkas Kwela Carbonatite Complex.

The high Sr, low Ni and low Mg# that are characteristic of this rock may reflect clinopyroxene fractionation - a process that Le Bas (1987) considers important in the evolution of silicate magmas associated with carbonatite complexes. However, petrogenetic processes are difficult to establish with certainty at Marinkas Kwela because of the evident effects of fenitisation (Chap. 11.2.a).

12.2. Carbonatites Of The Marinkas Kwela Carbonatite Complex

12.2.a. The 'Normal' Carbonatite Trend - A Discussion

According to Le Bas (1981) and Woolley (1982), field relationships suggest that a magmatic succession exists within carbonatite complexes, from early sôvite to beforsite to late-stage ferrocarbonatite. This sequence also corresponds to the crystallisation differentiation sequence determined experimentally by Wyllie (1965).

More recent studies have raised some doubts as to whether carbonatite complexes necessarily all fit the 'normal' trend with the simplicity suggested above. For example, Eggler (1989) and Gittins (1989) have shown that Mg-rich carbonatite melts may possibly

evolve independently of Ca-rich carbonatite melts through partial melting of a carbonated peridotite mantle. Magnesium-rich melts may also evolve through immiscible separation from a silicate melt at greater depths than those proposed for the immiscible separation of Ca-rich carbonatite melts (Le Bas, 1989). It seems, therefore, that a sövite melt is not a necessary precursor to a beforsite. Furthermore, beforsite need not fractionate to ferrocarbonatite. Fe-enrichment in a carbonatite is dictated by evolving oxygen fugacity, which is a complex function of the cooling history and rate of ascent of the magma (Gittins, 1989). Carbonatites are thought to have initial oxygen fugacities as low as the Ni-NiO buffer (Wyllie, 1989). Under these conditions, Fe partitions preferentially into ankerite rather than magnetite (Le Bas, 1989), and Fe-enrichment occurs in the carbonatite melt. If oxygen fugacity rises to the stage where magnetite crystallises, Fe-depletion will occur. Gittins (1989), however, suggests that rapid cooling may terminate Fe-depletion by diverting Fe into ankerite and hematite.

Nevertheless, the intrusive sequence from sövite through beforsite to ferrocarbonatite is commonly observed, and is still generally attributed to crystal fractionation whereby accumulation of calcite, calcite ± dolomite, and then dolomite, produces the more common coarse-grained carbonatites, whereas the residual liquids evolve to ferrocarbonatites. The sections below will examine the Marinkas Kwela Carbonatite Complex for evidence pertaining to this general scheme. Important issues that need to be addressed are:-

- the relationship between mineralogically different kinds of sövite, and their relationships to the beforsites;

- mineralogical and geochemical differences between the southern and eastern beforsite; and

- the relationship between Mn-rich ferrocarbonatite dykes and other carbonatites.

12.2.b The Parental? Sövite

Two alternative theories can be offered in regard to the origins of sövite at Marinkas Kwela. (1) Mineralogically, the rocks differ principally in the absolute and relative abundance of their phenocryst phases. Compositions similar to the silicate-poor sövite can be derived from those corresponding to silicate-rich sövite, *via* removal of the phenocryst phases. (2) Fenite that surrounds the sövite indicates that the latter was probably more alkali-rich than it is now. The silicate phases in the sövite are also rich in alkalies (*e.g.* alkali-amphiboles and -clinopyroxene). Consequently, the sequence from silicate-rich sövite to silicate-poor sövite may reflect fluid/melt (or vapour/melt) fractionation, since continuous loss of alkalies *via* an exsolved aqueous phases is thought to accompany the intrusion of melts that give rise to sövite (Le Bas, 1981,1987, 1989; Woolley, 1982; Gittins, 1989; Twyman and Gittins, 1987).

The possibility of a genetic relationship between the various types of sövite, and between them and beforsite, can be investigated by considering phases that are common to all of them. Apatite is such a phase. In a plot of P_2O_5 against Y (Fig.12.1), the three types of sövite form an array with a gradient that is distinctly higher than the one defined by the eastern beforsite, which is the only other apatite-rich lithology. The arrays probably reflect the control of apatite on the concentration of Y and imply that the different sövites may be related to one another but are probably unrelated to the eastern beforsite.

The liquidus for carbonatites has been placed as high as ±900°C (Twyman and Gittins, 1987), but is generally held to be within the range of 400 - 800°C (*e.g.*, Suwa *et.al.*, 1975; Le Bas, 1981). Within this temperature range, the calcite-dolomite solvus is steeply inclined (Fig.12.2) so that, at the high-temperature end of the range, a significant proportion (± 10 - 15 mole %) of $MgCO_3$ is in solid solution with calcite. At low temperatures, this Mg-rich calcite will

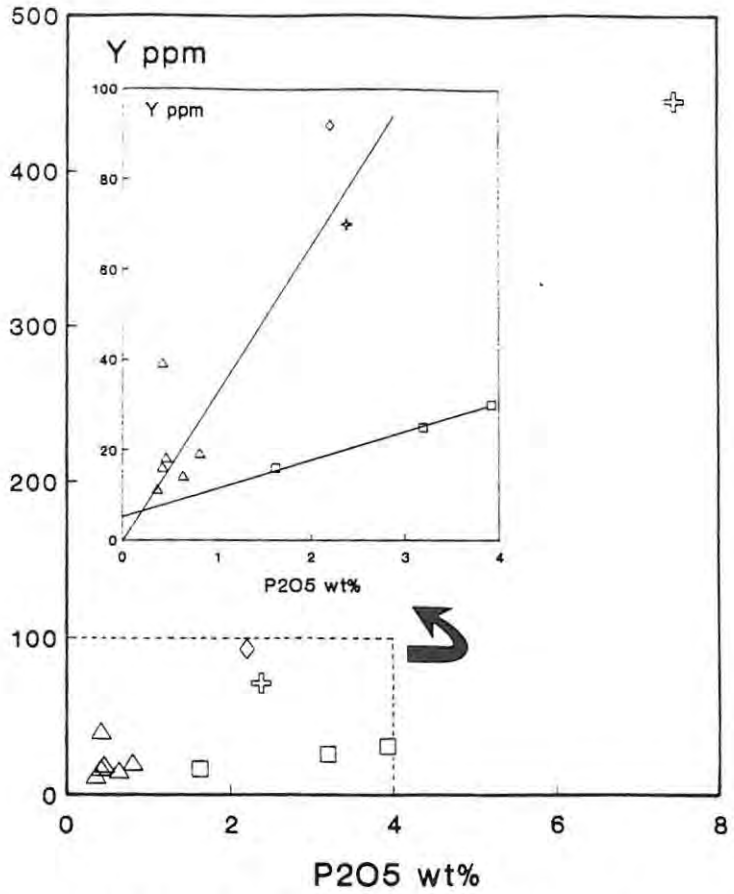

Figure 12.1 Plot of Y *vs.* P_2O_5 for apatite from the sövites and eastern beforsite. Symbols as in Table 11.1.

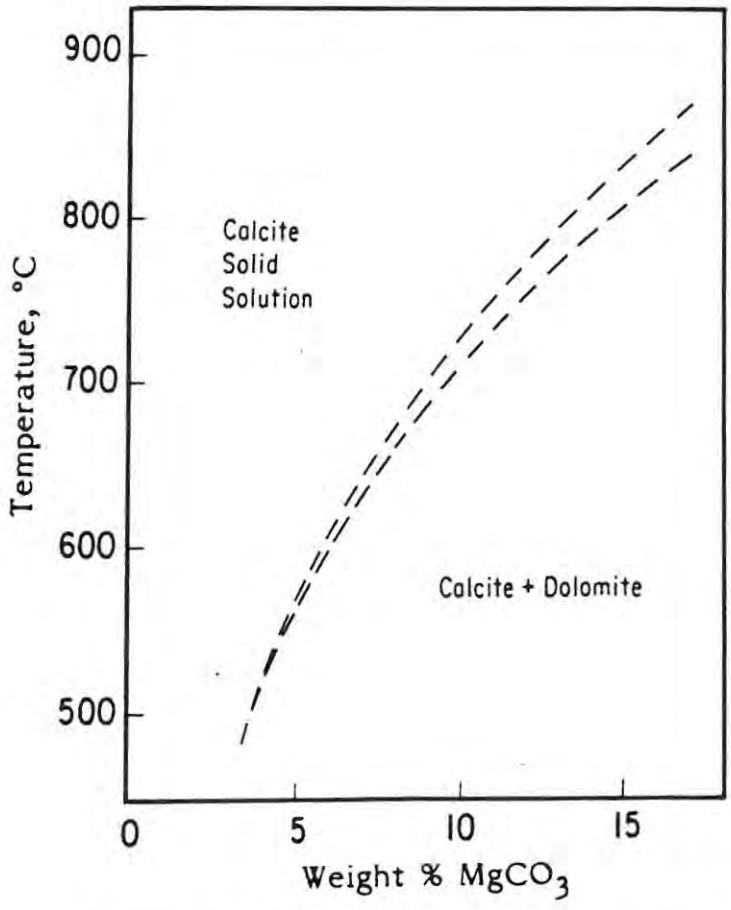

Figure 12.2 A portion of the calcite limb of the calcite - dolomite solvus (after Goldsmith and Heard, 1961).

exsolve into Mg-poor calcite and dolomite, and this is probably the origin for many calcite-dolomite carbonatites. No exsolution features, however, are observed in carbonatites from Marinkas Kwela (although remnant sôvite in the eastern beforsite has whole-rock MgO values which, at 1.7wt%, significantly exceed the MgO content of co-existing calcite and suggest that minor dolomite may be present). Consequently, the sövite and beforsites are separated by a marked geochemical compositional gap that is hard to reconcile with a crystal fractionation relationship at low pressures and at temperatures above ±500°C.

The findings immediately above, taken together with the Y/ P_2O_5 ratios in apatite (Fig 12.1), provide little evidence for a genetic relationship at Marinkas Kwela between sôvite and the beforsites.

12.2.c The Beforsite - Ferrocarbonatite Trend

Whole-rock Fe-enrichment is virtually continuous from the eastern beforsite to the southern beforsite to the ferrocarbonatite, and reflects a sequence to more evolved rock types. However, carbonate accounts for all whole-rock Fe in the eastern beforsite and the ferrocarbonatite, whereas in the southern beforsite dolomite is depleted in FeO compared with whole-rock values (Fig. 12.3). The 'excess' whole rock FeO in the southern beforsite occurs as magnetite dispersed within and between dolomite grains.

This contrasting distribution of Fe does not necessarily invalidate an hypothesis relating whole-rock Fe-enrichment to a genetic process Three ways to reconcile the differences can be advanced. First, they may reflect differences in fO_2.prevailing during crystallisation of each beforsite. Second, they may reflect different rates of cooling. According to Gittins (1989), rapid cooling favours Fe partitioning into carbonate. If the eastern beforsite cooled more rapidly than did the southern beforsite - and the amalgamated dyke-like form (see Chap.2.6) suggests it did - then crystallisation of magnetite may have

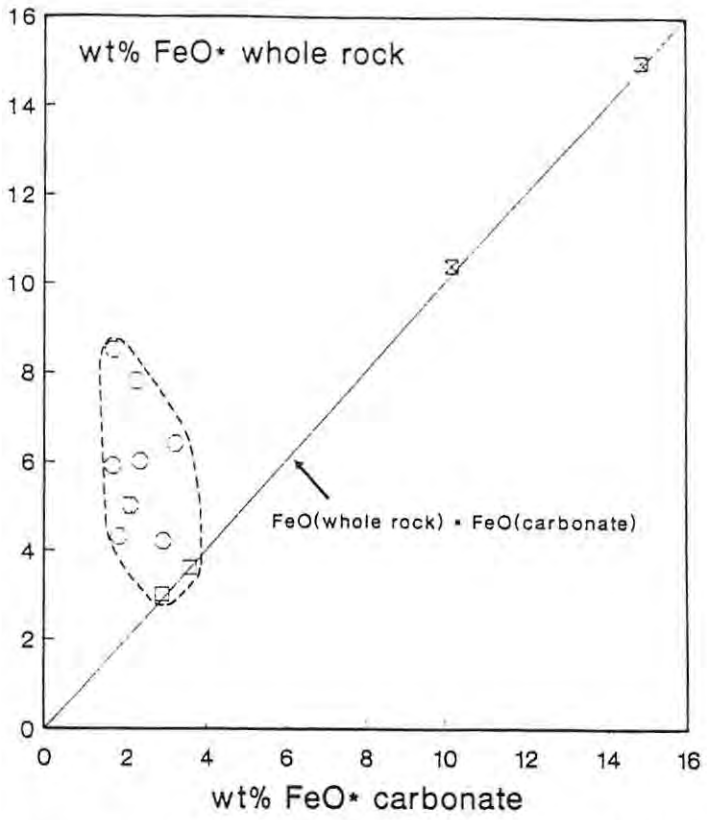

Figure 12.3 Whole rock FeO* *vs.* FeO* in carbonate, showing the compositions of the beforsites and the ferrocarbonatite. The solid line has a gradient of 1 (i.e. all whole rock Fe accounted for in carbonate). Symbols as in Table 11.1. FeO* = all Fe as Fe^{2+}.

been more inhibited in the eastern beforsite. Third, the differences may reflect a maximum solubility of FeO in carbonate - FeO that could not be fixed in carbonate crystallised as magnetite

The Fe-enrichment trend from the eastern beforsite to the southern beforsite to the ferrocarbonatite correlates with trends in certain trace element concentrations, notably those of Nb and Y (Chap. 11.4.b and Fig 11.6). The progressive decrease in the concentrations of Nb correlate with a decreasing modal abundance of pyrochlore and reflect fractionation of that mineral. In the case of Y, early decreases in concentration are followed by increasing concentrations at higher whole-rock FeO values. The early decrease can be attributed to apatite fractionation (D_Y^{ap} for carbonatite melts not available but >1 at least for silicate melts). At subsequently low concentrations of P_2O_5, apatite crystallisation would have ceased, leading to enrichments in Y in the more evolved Fe-rich rocks. Trends for Nb and Y thus seem consistent with an hypothesis that genetically links both varieties of beforsite and the ferrocarbonatite.

From the considerations above it seems probable that the eastern beforsite and the ferrocarbonatite are related through fractionation. It also seems likely that the southern beforsite relates to the same parental magma, but crystallised under physical conditions that were different from those that prevailed during the crystallisation of the eastern beforsite.

12.2.d The Mn-rich Ferrocarbonatite

The Mn-rich ferrocarbonatite dykes are commonly enriched in Fe, Y and Th, and depleted in Nb, compared with ferrocarbonatite and beforsite (Table 11.4, Fig.11.6). Accordingly, they could be related to those carbonatites through extreme fractionation. Figure 12.4 shows that the dykes can be divided into two groups - Group I having Mn concentrations of 1-2wt% and Group II having especially high Mn concentrations (>5wt%)

According to Rosenberg and Foit (1979), Mn concentrates more readily in dolomite than does Fe. Hence, the Mn/Fe ratio of a carbonatite melt should decrease with compositional evolution controlled by fractionation of dolomite. The composition of Group I Mn-rich ferrocarbonatites, which have the lowest MnO/FeO ratios (< 0.1) of all the carbonatites analysed from Marinkas Kwela, may thus reflect fractionation of dolomite. The Group II rocks, however, have some of the highest MnO/FeO ratios and so cannot be related to the other carbonatites through dolomite fractionation alone.

The key to the origin of the Group II rocks may lie with the crystallisation of magnetite in the southern beforsite body. Here, magnetite forms anhedral to euhedral grains, often included in carbonate (Chap.11.2.c), and was clearly an early phase to crystallise. It has lower MnO/FeO ratios than co-exsisting whole-rock values (Fig.12.4), and so magnetite crystallisation could have led to a

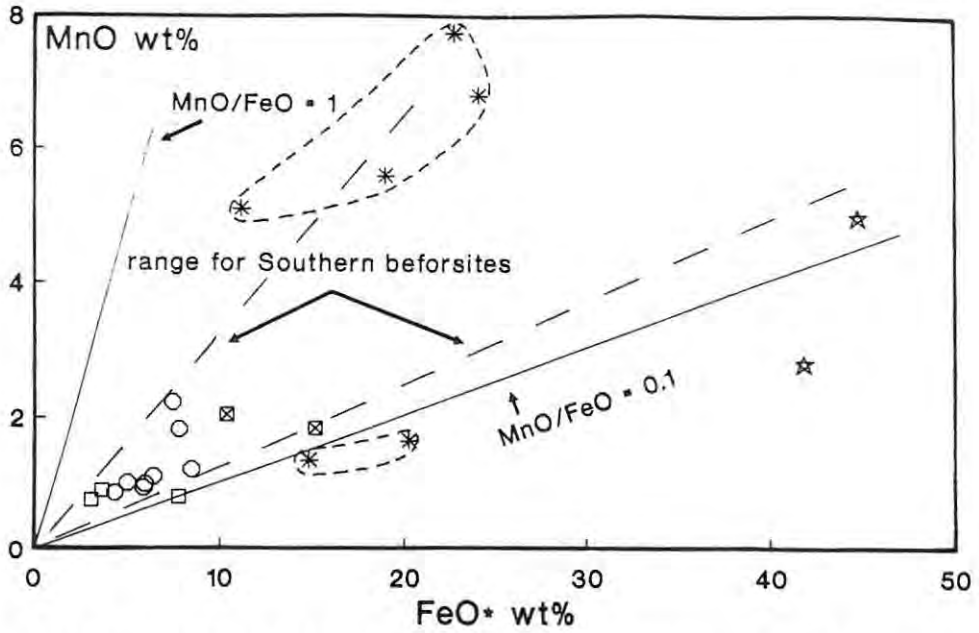

Figure 12.4 Plot of MnO *vs.* FeO* showing the compositions of the carbonatites at Marinkas Kwela. The fields enclose data for the Mn-rich ferrocarbonatite dykes. Symbols as in Table 11.1. FeO* = all Fe as Fe^{2+}.

residual melt with MnO/FeO ratios similar to those of the Group II dykes. The amount of magnetite fractionation required would have been small - large amounts would have depleted residual melts in both FeO and MnO, even if accompanying fractionation of dolomite offset the effect.to some extent

Therefore, whilst the ferrocarbonatite and Group I dykes may represent fractionated members of a series that did not involve crystallisation of magnetite, the Group II dykes may be the result of the more unusual situation where crystallisation of small amounts of magnetite increased the MnO/FeO ratio of residual melts.

Circumstantial evidence supports this proposition. Ferrocarbonatite occurs only in close spatial association with the eastern beforsite, in which magnetite did not crystallise, while at least three of the five Group II dykes identified are radial to the southern beforsite in which magnetite did crystallise. It is proposed here that the eastern beforsite, ferrocarbonatite and Group I Mn-rich dykes are genetically related through carbonate fractionation, and that a genetic

relationship also exists between the southern beforsite and the Group II dykes.

12.3. The Genesis Of Carbonatites And Related Silicate Rocks

The origins of carbonatite magma are controversial and central to this controversy is the connection between carbonatites and the Si-undersaturated alkaline rocks with which they are commonly associated. Although the data available here do not allow detailed evaluation of the issue, it is inviting to comment on features observed at Marinkas Kwela in context of more recent theories on the genesis of carbonatites and associated silicate rocks. The three principal theories are outlined immediately below.

- **Carbonatites evolve *via* crystal fractionation, at crustal pressures, of a mantle-derived alkali-rich silicate melt** (Watkinson and Wyllie, 1971). This is no longer a favoured hypothesis, on account of the rarity of rock-types intermediate between the silicate and carbonatite rocks.

- **Carbonatites are the direct result of melting of dolomite-peridotite within the mantle** (*e.g.*, Wyllie, 1987; Wyllie and Huang, 1975; Gittins, 1989; Twyman and Gittins, 1987; Eggler, 1989). The discovery that near-solidus melts of dolomite-peridotite have compositions corresponding to those of carbonatites suggests that some carbonatites might be primary. According to Gittins (1989), parental carbonatite magmas that reach the surface are likely to be dominantly calcitic, with a wide range in Ca:Mg ratios, and modestly alkalic. If the primary carbonatite melt is hydrous, alkali loss will occur through an exsolved aqueous phase, but under dry conditions crystallisation of calcite and dolomite will lead to residual compositions similar to the alkali-rich 'natrocarbonatites' of Oldoinyo Lengai, Tanzania (Twyman and

Gittins, 1987). Nephelinites and carbonatites are held to be derived sequentially or simultaneously from the carbonated mantle (Gittins, 1989).

- **Carbonatites are derived *via* immiscible separation of a carbonatite liquid from an originally homogeneous carbonated silicate melt** (Le Bas, 1981, 1987, 1989; Freestone and Hamilton, 1980; Kjarsgaard and Hamilton, 1988, 1989; Wyllie, 1989). Evidence for liquid immiscibility is derived from experimental work and from the occurrence in nature of spheres or droplets of carbonate within silicate melts. Carbonatite melts rich in Ca and Mg will separate immiscibly from primitive melilitite or melanephelinite melts, while alkali-rich carbonatites will separate from more evolved phonolite or nepheline syenite melts (Kjarsgaard and Hamilton, 1988). Le Bas (1987) further contends that alkali-rich carbonatites will also give rise to calcite and dolomite carbonatites by alkali loss through an exsolved aqueous phase - hence fenitisation of country-rocks. Wyllie (1987) adds that in most alkali complexes, volume relationships and the time sequence of intrusion appear to favour a derived origin for carbonatites.

Against this background, three observations on the Marinkas Kwela Carbonatite Complex are offered below.

First, the sövite at Marinkas Kwela contains silicate phenocrysts that are similar to phenocrysts in the associated nepheline syenite. The rock resembles, in many respects, the peralkaline sövites of the Fen Complex which, on mineralogical grounds, are considered by Andersen (1988) to be related to associated ijolites *via* immiscibility.

Second, and in opposition to the first, no petrological features that are indicative of immiscibility were seen in the nepheline syenite at Marinkas Kwela. This may well be because the nepheline syenite has been fenitised. Still, if the carbonatites had formed through immiscible separation from a silicate melt then, in accordance with

the findings of Kjarsgaard and Hamilton (1988), the calcitic nature of the sôvite would dictate that the conjugate silicate melt should have been very basic in composition, possibly melanephelenitic. By contrast, the silicate rock that does co-exist with sövite at Marinkas Kwela has a felsic and highly alkaline composition (although, again, note fenitisation). Two possible explanations for the co-existence of nepheline syenite and sövite are (1) that sövite separated from a silicate melt at a very early stage (but, if it did, the silicate magma must subsequently have undergone considerable fractionation to produce the nepheline syenite); and (2) that the sövite had a considerably more alkali-rich composition than is now observed. Fenitisation of country rocks points in latter direction.

Third, according to Wyllie (1989), most carbonatite complexes have a high ratio of silicate to carbonatite rocks. The reverse appears to be the case at Marinkas Kwela. If immiscible separation of carbonatite from a silicate melt had occurred there, a large body of silicate rocks, considerably less felsic than those that crop out, should underlie or have overlain the area.

The data are insufficient to make a confident judgement as to whether the relationship between the silicate magma and carbonatites came about through immiscible separation or direct melting of a dolomite-peridotite. The ratio of rock types in the complex is, however, difficult to reconcile with the immiscibility hypothesis

CHAPTER 13: TECTONIC SETTING OF THE CENTRAL PORTION OF THE KUBOOS - BREMEN IGNEOUS PROVINCE

Isotopic age determinations for the GPC and the MKC (Chap. 6), and for other complexes in the Kuboos - Bremen Igneous Province (Allsopp *et al.*,1979), indicate that the province was emplaced within the time span of the Pan-African orogeny. The latter was an igneous, metamorphic and deformational event of about 500-600Ma that affected much of the African continent (Rogers *et al.*1978). It has been described variously in terms of crustal extension, compressional remobilisation, continental collision and subduction of oceanic or continental crust. According to Rogers *et al.* (1978), no general agreement has been reached and it seems likely that different processes characterised different areas.

During the Pan-African orogeny the southwest margin of Africa saw the development of a 6000km chain of geosynclines, now preserved as a series of re-entrants known as the Gariep Province, the Saldanian Province and the coastal branch of the Damara Province (Fig. 13.1). The Damara Province, including both coastal and intracontinental branches, was the keystone of this Pan-African tectonism and represents an asymmetrical triple junction that developed between ≈1000Ma and 460Ma (Tankard *et al.* 1982).

To the south of the Damara Province outcrops the Gariep Group, a volcanosedimentary pile that constitutes the main lithological unit of the Gariep Province. Within a poorly constrained period between 980Ma and 550Ma (Tankard *et al.* 1982), this pile was accumulated and subsequently deformed when the Kalahari Plate was subducted

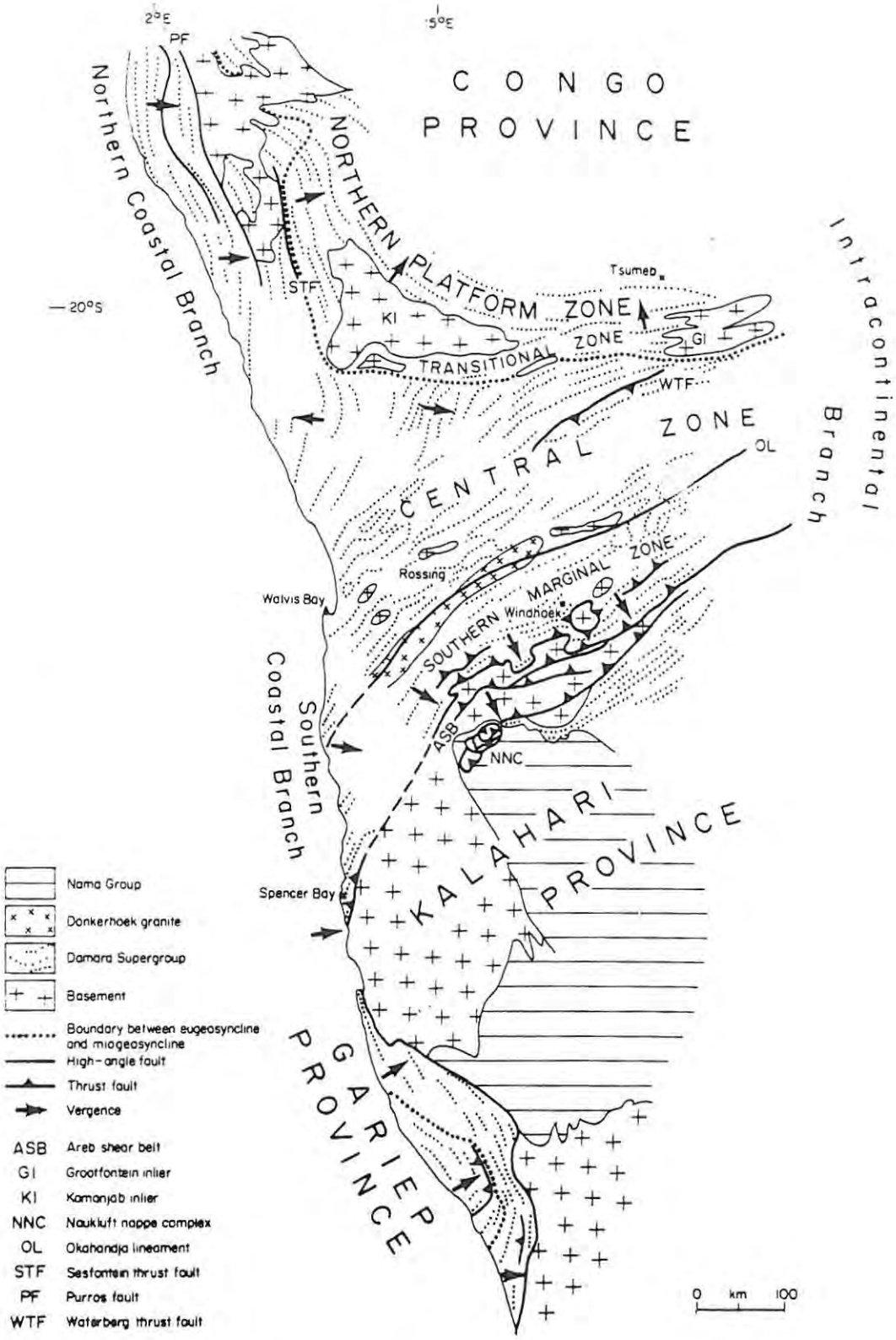

Figure 13.1 Geological map showing Pan-African tectonic elements of southwestern Africa (from Tankard *et al.*, 1982).

westward beneath the Brazilian Plate (Porada, 1979). Complementary to the Gariep Group are the stable platform sediments of the Nama Group which crop out to the northwest.

Into this tectonic framework were emplaced the intrusive phases of the Kuboos - Bremen Province at around 500 - 550Ma. In the southwest, the Swartbank and Kuboos plutons intruded the deformed Gariep Group. The Nama Group too was intruded by igneous complexes (including the GPC and MKC) during or immediately subsequent to the waning stages of sedimentation.

Notwithstanding that the Kuboos - Bremen Province shows a very close spatial and temporal relationship to the other Pan-African rocks of the region, it is not orientated parallel to any other known tectonic element of the Pan-African or of the Proterozoic basement. Consequently, the tectonic process that may link the rocks of the province to other Pan-African rocks remains unclear. Krôner (1975) postulated subduction of the Brazilian Plate beneath the Gariep geosyncline and the existence of a Kuboos - Bremen magmatic arc. However, the Kuboos - Bremen intrusions are chemically distinct from arc-related rocks and, subsequent to Krôner's postulation, Porada (1979) suggested that the relative abundance of granitoids between the respective continental plates argued for west-facing, rather than east-facing, subduction.

Another view is that of Martin and Porada (1977), who suggested that the Kuboos - Bremen Province formed when the lithosphere drifted over a mantle hot-spot or plume. This explanation would require that the age of the respective intrusions show a systematic relationship to the orientation of the province in general. The available isotopic age-dating (Allsopp *et al.* 1979; this study, Chap. 6) is insufficient to demonstrate such a relationship. Still, the idea of a mantle plume does draw merit from the fact that a regional thermal event with its focus on the central part of the Damara Province took place around 570 - 540Ma (Tankard *et al.* 1982), more or less synchronous with the intrusion of the Kuboos - Bremen complexes. The idea must, however,

be viewed against some current conceptions as to the nature of mantle plumes and associated magmatism. The following summary draws upon the work of White and McKenzie (1989).

- Mantle plumes generate mushroom-shaped thermal anomalies beneath the lithosphere.

- The diameter of the anomalies is typically 1500 - 2000km and temperatures are of the order of 100 - 150°C above 'normal'.

- The plumes cause the lithosphere to be uplifted and thinned.

- The underlying asthenosphere wells up to fill the space, decompresses and partially melts.

- The volume of melt generated depends only on the amount of lithospheric thinning and the temperature of the underlying asthenosphere.

- Thickest igneous sections are formed on rifted continent margins over the central head of the plume, but rifting in regions peripheral to the head will produce localised magmatism on a smaller scale.

- As the amount of lithospheric thinning and the temperature of the asthenosphere decrease away from the plume head, associated magmatism becomes more alkaline.

Accepting the regional scale that White and McKenzie (1989) attribute to mantle plumes, it seems unlikely that the linearity of the Kuboos - Bremen Province could be attributed to the trace of the thermal anomaly underlying a migrating continental plate, as was suggested by Martin and Porada (1977). It is, however, possible that the province is the result of magmatism originating in regions peripheral to the head of a plume centred on the Damara Province. This magmatism may have utilised a pre-existing crustal weakness, giving linearity to the

igneous province and explaining the absence of closely related magmatism. That crustal weakness possibly had origins with the rifting and subsequent subduction events that moulded the Gariep Province.

CHAPTER 14 : CONCLUSIONS

The initial basis for recognising two separate silicate complexes at Grootpenseiland and Marinkas Kwela was the repetition, along two separate loci, of a sequence from Si-undersaturated rocks in the southwest to Si-oversaturated rocks in the northeast. The general morphology and lithological range of the two complexes are similar, but most of the rock types in each complex are unique to that complex and at Marinkas Kwela the rocks that initiate and terminate the intrusive sequence are more alkaline than their analogues in the GPC (Chap.2).

Isotopic age determinations show that the GPC and MKC were emplaced at around 520Ma and this is in accord with all published data on the Kuboos - Bremen Province (Chap.6). The lack of chilled margins also suggests that the intrusive history of the complexes was short.

Development of the two complexes began with the intrusion of Si-undersaturated magmas having an I_{Sr} of around 0.7047 and ε_{Nd} between +0.9 and +3.5, indicating a mantle source region (Chap.6). Low Mg# and low concentrations of transition elements point to considerable fractionation before emplacement at present levels.

Evidence remains of three such magmas. The earliest and least fractionated of these formed the monzodiorite of the GPC. Of two subsequent magmas, one is now represented only in remnant form by rocks of the larvikite - pulaskite series, which formed a sidewall sequence in the GPC. The other, which is the first known intrusive phase of the MKC, led to the formation of the alkali-melasyenite - nepheline syenite sidewall crystallisation sequence (now a screen). At the same time it crystallised a large body of foyaites.

The two sidewall sequences developed through *in situ* accumulation from the respective magmas which evolved *via* crystallisation

dominated by alkali-feldspar, clinopyroxene and amphibole (Chap. 7.2). The foyaites, which evolve from clinopyroxene- to amphibole-rich, owe their compositional diversity to fractional crystallisation probably accompanied by differential assimilation of dolomitic country rock (Chap. 7.3).

In both complexes, critically saturated alkali-syenitic magma intruded after and to the northeast of the Si-undersaturated rocks. In general, the resulting highly felsic rocks in each complex are very similar in composition, but some differences (*e.g.*, in trends for Th) suggest that they crystallised from two separate magma batches (Chap. 8.1). Evidence of extensive fractionation before emplacement includes low Mg#, low Eu/Eu* and low concentrations of transition elements. Feldspar was the dominant phase removed. Later trends were complicated to some extent by processes that led to modal layering (Chap 8.1).

Subsequently, Si-oversaturated alkaline-related magmas (the 'monzonite - granite series') intruded the alkali-syenite in each complex. In the complex ring-dyke of the MKC, each successive pulse of Si-oversaturated magma was more evolved than its predecessor. The different rocks can be related by a process of fractional crystallisation dominated by alkali-feldspar. Isotopic compositions of O (and possibly Sr), indicate the possibility that a crustal component was involved in the genesis of these rocks.

The compositionally primitive members of the Si-oversaturated series, and of the Si-undersaturated larvikite - pulaskite series, are very similar in composition. Parental magmas of the two series are thought to have a common or very similar origin, with the diverging differentiation trends possibly being due to interaction with a crustal component (Chap 10. 2). The critically-saturated alkali-feldspar syenite in the GPC probably represents cumulates related to and intruded by rocks of the monzonite - granite series, notwithstanding close mineralogical similarities to the alkali-syenites.

The youngest intrusive rocks in both complexes are alkali-granites. They appear to have evolved independently from the monzonite - granite

series, and independently from one another. Isotopic data indicate the possibility that a crustal component was also involved in the genesis of these rocks.

While the alkali-syenite of each complex probably crystallised from different magmas and the alkali-granites certainly did, there are no clear compositional criteria for making a similar distinction between corresponding rocks of the monzonite-granite series that occur in each complex. The one possible exception relates to the alkali-feldspar granite that comprises the Grootpenseiland Granite stock which, however, is extensively altered (Chaps 3 and 5).

Intrusion of the carbonatite complex pre-dates the emplacement of the Marinkas Kwela Granite. Emplacement of the complex began with nepheline syenite but these highly fenitised rocks appear to show no genetic relationship to subsequent carbonatites. Neither is the sôvite parental to the beforsites.

Within the compositional range of beforsite to Mn-rich ferrocarbonatite, two lineages are observed. The main lineage is from eastern beforsite through ferrocarbonatite to Mn-rich ferrocarbonatite dykes and results essentially from fractionation of carbonate alone. The subsidiary lineage from southern beforsite to Mn-rich ferrocarbonatite dykes results from fractionation of magnetite as well as carbonate, and consequently the dykes have substantially higher MnO/FeO ratios than those related to the main lineage (Chap. 12).

LIST OF REFERENCES

Allégre, C.J. and Minster, J.F. (1978) Quantitative models of trace element behaviour in magmatic processes. **Earth Planet. Sci. Lett.** 38: 1-25.

Allsopp, H.L., Kostlin, E.O., Welke, H.J., Burger, A.J., Kröner, A. and Blignault, H.J. (1979) Rb-Sr and U-Pb Geochronology of late Precambrian - early Paleozoic igneous activity in the Richtersveld (South Africa) and southern South West Africa. **Trans. Geol. Soc.S.Afr.** 82: 185-204.

Andersen, T. (1984) Secondary processes in carbonatites: petrology of "rodberg" (hematite-calcite-dolomite carbonatite) in the Fen central complex, Telemark (South Norway). **Lithos.** 17: 227-245.

Andersen, T. (1988) Evolution of peralkaline calcite carbonatite magma in the Fen complex, southeast Norway. **Lithos.** 22: 99-112.

Ahrens, L.H., Pinson, W.H. and Kearns, M.M. (1952) Association of Rb and K and their abundance in common igneous rocks and meteorites. **Geochim. Cosmochim. Acta.** 2: 229-242.

Bailey, D.K. (1974) Origin of alkaline magmas as a result of anatexis: melting in the deep crust. In: Sorensen, H. (Ed), **The Alkaline Rocks.** Wiley, London. pp.436-442.

Bailey, D.K. (1980) Volcanism, Earth degassing and replenished lithospheric mantle. **Phil. Trans. R. Soc. London.** A297: 309-322

Bailey, D.K. (1989) Carbonatite melt from the mantle in the volcanoes of south-east Zambia. **Nature.** 338: 415-418.

Baker, B.H., Goles, G.G., Leeman, W.P. and Lindstrom, M.M. (1977) Geochemistry and Petrogenesis of a Basalt - Benmoreite - Trachyte Suite from the Southern Part of the Gregory Rift, Kenya. **Contrib. Mineral. Petrol.** 64: 303-332.

Baker, B.H. and McBirney, A.R. (1985) Liquid fractionation: Pt. III- Geochemistry of zoned magmas and the compositional effects of liquid fractionation. **J. Volcanol. geotherm. Res.** 24: 55-81.

Barber, C. (1974) The geochemistry of carbonatites and related rocks from two carbonatite complexes, south Nyanza, Kenya. **Lithos.** 7: 53-63.

Barker, D.S. and Nixon, P.H. (1989) High-Ca, low-alkali carbonatite volcanism at Fort Portal, Uganda. **Contrib. Mineral. Petrol.** 103: 166-177.

Berlin, R. and Henderson, C.M.B. (1969) The distribution of Sr and Ba between the alkali feldspar, plagioclase and groundmass phases of porphyritic trachytes and phonolites. **Geochim. Cosmochim. Acta.** 33: 247-255.

Binsted, N. (1981) The system Ab-Ne-NaCl-H_2O. **Prog. Exp. Petrol.NERC Ser. D.** 5: 34-36

Blignault, H.J. (1977) Structural - metamorphic imprint on part of the Namaqua Mobile Belt in South West Africa. **Precambrian Res. Unit.University of Cape Town Bull. No. 23.**

Bouabdli, A. Dupuy, C. and Dostal, J. (1988) Geochemistry of Mesozoic alkaline Lamprophyres and related rocks from the Tamazert massif, High Atlas (Morocco). **Lithos**. 22: 43-58.

Bowen, N.L. (1922) The reaction principle in petrogenesis. **J. Geol.** 30: 177-198.

Bowen, N.L. (1937) Recent high-temperature research on silicates and its significance in igneous geology. **Am. J. Sci.** 33: 1-21.

Brooks, C., Hart, S.R. and Wendt, I. (1972) Realistic use of two-error regression treatments as applied to rubidium - strontium data. **Rev. Geophys. Space Physics.** 10: 551-577.

Burnham, C.W. (1979) Magmas and Hydrothermal Fluids. In: Barnes, H.L. (Ed) **Geochemistry of Hydrothermal Ore Deposits - 2nd Edition. John Wiley and sons.** 1979 pp 798.

Chappell, B. and White, A.J.R. (1974) Two contrasting granite types. **Pacific Geology**.8: 173-174.

Clemens, J.D., Holloway, J.R. and White, A.J.R. (1986) Origin of an A-type granite; Experimental constraints. **American Mineralogist**. 71: 317-324.

Cohen, R.S., O'Nions, R.K. and Dawson, J.B. (1984) Isotope geochemistry of xenoliths from East Africa: implications for development of mantle reservoirs and their interactions. **Earth Planet, Sci, Let.** 68: 209-220.

Collins, W.J., Beams, S.D., White, A.J.R. and Chappell, B.W. (1982) Nature and Origin of A-Type Granites with particular reference to Southeastern Australia. **Contrib. Mineral. Petrol**. 80: 189-200.

Cox, K.G., Bell, J.D. and Pankhurst, R.J. (1979) **The Interpretation of Igneous Rocks**. George Allen & Unwin, London. 450pp.

Cullers, R.L. and Graf, J.L. (1984) Rare earth elements in igneous rocks of the continental crust: predominantly basic and ultrabasic rocks. In: Henderson, P. (editor) **Rare Earth Element Geochemistry**. Elsevier Science Publishing Company, INC., 510p

Cullers, R.L. and Medaris, Jr. G. (1977) Rare Earth Elements in Carbonatite and Cogenetic Alkaline Rocks: Examples from Seabrook Lake and Callander Bay, Ontario. **Contrib. Mineral. Petrol**. 65: 143-153.

Davies, G.R. and Macdonald, R. (1987) Crustal influence in the petrogenesis of the Naivasha basalt - comendite complex: combined trace element and Sr-Nd-Pb isotope constraints. **J. Petrol.** 28: 1009-1031.

Deer, W.A., Howie, R.A. and Zussman, J. (1962) **Rock-forming Minerals. Vol. 5 Non-Silicates.** Longmans, Green and Co. Ltd., 371p.

Deer, W.A., Howie, R.A. and Zussman, J. (1980) **An introduction to the Rock-forming Minerals**. Longmans Group Ltd., 528p.

Deer, W.A., Howie, R.A. and Zussman, J. (1982) **Rock-forming Minerals. Vol 1a. Orthosilicates**. Longmans Group Ltd., 919p

DePaolo, D.J. (1981) Trace element and isotopic effects of combined wallrock assimilation and fractional crystallization. **Earth Planet, Sci, Let.** 53: 189-202.

DePaolo, D.J. (1981) Neodymium isotopes in the Colorado Front Range and crust-mantle evolution in the Proterozoic. **Nature.** 291 193-196

Dickenson, M.P. and Hess, P.C. (1986) The structural role and homogeneous redox equilibria of iron in peraluminous, metaluminous and peralkaline silicate melts. **Contrib, Mineral, Petrol.** 92: 207-217.

Droop, G.T.R. (1987) A general equation for estimating Fe^{3+} concentrations in ferromagnesian silicates and oxides from microprobe analyses, using stoichiometric criteria. **Min. Mag.** 51: 431-435.

Eby, G.N. (1987) The Monteregian Hills and White Mountains alkaline igneous province, eastern North America. In: Fitton, J.G. and Upton, B.G.J. (editors) **Alkaline Ingneous Rocks, Geological Society Special Publication.** 30: 433-447.

Eggler, D.H. (1989) Carbonatites, Primary melts and mantle dynamics: In, Bell, K. (editor) **Carbonatites. Genesis and evolution.** Unwin Hyman Ltd (1989). 618p.

Eglington, B.M., Harmer, R.E and Kerr, A. (1989) Isotope and Geochemical Constraints on Proterozoic Crustal Evolution in South-Eastern Africa. **Precambrian Research.** 45: 159-174.

Eglington, B.M. and Harmer, R.E. (1989) GEODATE: a program for the processing and regression of isotope data using IBM - compatible microcomputors. **CSIR Manual.** EMA-H 8901, 57p.

Ewart, A. (1982) Petrogenesis of Tertiary anorogenic volcanic scenes of southern Queensland, Australia, in the light of trace element geochemistry and O, Sr and Pb isotopes. **J. Petrol.** 23: 344-382.

Exley, R.A. (1980) Microprobe studies of REE-rich accessory minerals: implications for Skye granite petrogenesis and REE mobility in hydrothermal systems..**Earth Planet. Sci. Lett.** 48: 97-110.

Faure, G. (1986) **Principles of Isotope Geology (2nd edition).** John Wiley and Sons, Inc. 589p

Ferguson, A.K. (1978) The crystallization of pyroxenes and amphiboles in some alkaline rocks and the presence of a pyroxene compositional gap. **Contrib. Mineral. Petrol.** 67: 11-15.

Fleischer, M.G. (1978) Relation of the relative concentrations of lanthanides in titanite to type of host rocks. **American Mineralogist.** 63: 869-873.

Fletcher, C.J.N. and Beddoe-Stephens, B. (1987) The petrology, chemistry and crystallization history of the Velasco alkaline province, eastern Bolivia. In: Fitton, J.G. and Upton, B.G.J. (editors) **Alkaline Igneous Rocks. Geological Society Special Publication.** 30: 403-413.

Foland, K.A. and Friedman, I. (1977) Application of Sr and O Isotope Relations to the Petrogenesis of the Alkaline Rocks of the Red Hill Complex, New Hampshire, USA. **Contrib. Mineral. Petrol.** 65: 213-225.

Foland, K.A. and Henderson G.M.B. (1976) Application of age and Sr isotope data to the petrogenesis of the Marangudzi Ring Complex, Rhodesia. **Earth Planet. Sci. Lett.** 29: 291-301.

Freestone, I.C. and Hamilton, D.L. (1980) The Role of Liquid Immiscibility in the Genesis of Carbonatites - An Experimental Study. **Contib. Mineral. Petrol.** 73: 105-117.

Garson, M.S. (1955) Flow phenomena in carbonatites in southern Nyasaland. **Colonial Geology and Mineral Resources**.5(3): 311-318.

Germs, G.J.B. (1972) The stratigraphy and palaentology of the lower Nama Group, South West Africa. **Precambrian Res. Unit.University of Cape Town, Bull. No. 12.**

Gianetti, B. and Luhr, J.F. (1983) The white trachytic tuff of Roccamonfina Volcano (Roman Region, Italy). **Contrib. Mineral. Petrol.** 84: 235-252.

Giret, M., Bonin, B. and Leger, J.M. (1980) Amphibole compositional trends in oversaturated and undersaturated alkaline plutonic ring-complexes. **Canadian Mineral.** 18: 481-495.

Gittins, J. (1989) The origin and evolution of carbonatite magmas. In, Bell, K. (1989) **Carbonatites. Genesis and evolution.** Unwin Hyman Ltd. 663p.

Gold, D.P. (1966) The average and typical chemical composition of carbonatites. **Mineral. Soc. India, IMA**. 83-91.

Goldsmith, J.R. and Heard, H.C. (1961) Subsolidus phase relations in the system $CaCO_3$ - $MgCO_3$. **J. Geology**. 69: 45-74.

Haggerty, S.E. (1976) The chemistry and genesis of opaque minerals in kimberlites. **Phys. Chem. Earth**. 9: 295-307.

Halliday, A.N., Dickin, A.P., Fallick, A.E. and Fitton, J.G. (1988) Mantle dynamics; a Nd, Sr, Pb and O isotopic study of the Cameroon line volcanic chain. **J. Petrol.** 29:181-211.

Hamilton, D.L. and MacKenzie, W.S. (1965) Phase-equilibrium studies in the system $NaAlSiO_4$ (nepheline) - $KAlSiO_4$ (kalsilite) - SiO_2 - H_2O. **Mineral. Mag.** 34: 214-231.

Hanson, G.N. (1978) The application of trace elements to the petrogenesis of igneous rocks of granitic composition. **Earth Planet. Sci. Let**.38: 26-43.

Hartnady, C., Joubert, P. and Stowe, C. (1985) Proterozoic Crustal Evolution in Southwestern Africa. **Episodes**. 8: 236-244.

Henderson, C.M.B. and Gibb, F.G.F. (1986) The petrology of the Lugar sill, S.W. Scotland.**Trans. R.Soc. Edinburgh, Earth Sci.** 77: 325-347.

Henderson, C.M.B., Pendlebury, K. and Foland, K.A. (1989) Mineralogy and Petrology of the Red Hill Alkaline Igneous Complex, New Hampshire, U.S.A. **J. Petrol.** 30: 627-666.

Henderson, P. (1980) Rare Earth Element Partitioning Between Sphene. Apatite and other Coexisting Minerals of the Kangerdlugssuaq Intrusion, E. Greenland.**Contrib. Mineral. Petrol.** 72: 81-85.

Hildreth, W., Christiansen, R.L. and O'Neil, J.R. (1984) Catastrophic Isotopic Modification of Rhyolitic Magma at Times of Caldera Subsidence, Yellowstone Plateau Volcanic Field. **J. Geophys Res.** 89: 8399-8369.

Hoy, T. and Kwong, Y.T.J. (1986) The Moint Grace Carbonatite - a Nb and Light Rare Earth Element Enriched Marble of Probable Pyroclastic Origin in the Shuswap Complex, Southeastern British Colombia. **Econ. Geol.** 81: 1374-1386.

Johnson, C.M., Czamanske, G.K. and Lipman, P.W. (1989) Geochemistry of the intrusive rocks associated with the Latir volcanic field, New Mexico, and contrasts between evolution of plutonic and volcanic rocks. **Contrib. Mineral. Petrol.** 103: 90-109.

Joubert, P. (1986) Namaqualand - A model of Proterozoic accretion ?.**Trans. Geol. Soc.S.Afr.** 89: 79-96.

Killick, A.M. and Odell, J. (1980) The Marinkas Kwela alteration body - a porphyry-type system associated with the Kuboos-Bremen Line, SWA/Namibia. **Trans. Geol. Soc. S. Afr.** 83: 207-212.

Kjarsgaard, B.A. and Hamilton, D.L. (1988) Liquid immiscibility and the origin of the alkali-poor carbonatites. **Mineral. Mag.** 52: 43-55.

Kjarsgaard, B.A. and Hamilton, D.L. (1989) The genesis of carbonatites by immiscibility. In: Bell, K. (Ed.) **Carbonatites, Genesis and Evolution.** Unwin Hyman Ltd. 618p.

Kröner, A. (1975) Late Precambrian formations in the western Richtersveld, northern Cape Province. **Roy. Soc. S. Africa. Trans.** 41: 375-437

Kröner, A. and Blignault, H.J. (1976) Towards a definition of some tectonic and igneous provinces in western South Africa and southern South West Africa. **Trans. Geol. Soc. S. Afr.** 79: 232-238.

Kyser, T.K. (1986) Stable isotope variation in the mantle. In, Valley, J.W., Taylor, H.R.Jr. and O'Neil, J.R. (Eds.). **Reviews in Mineralogy**. 16, Stable isotopes and high temperature geological processes, 570p.

Langmuir, C.L. (1989) Geochemical consequences of *in situ* crystallization. **Nature**. 340: 199-205

Larsen, L.M. (1976) Clinopyroxene and Coexisting Mafic Minerals from the Alkaline Ilimaussaq Intrusion, South Greenland. **J. Petrol**. 17: 258-290.

Larsen, L.M. (1979) Distribution of REE and other trace elements between phenocrysts and peralkaline undersaturated magmas exemplified by rocks from the Gardar igneous province, south Greenland. **Lithos**. 12: 303-315.

Leake, B.E. (1978) Nomenclature of amphiboles. **Mineral. Mag:** 42, 533-563.

Le Bas, M.J. (1977) **Cabonatite-Nephelinite Volcanism**. Wiley, London.

Le Bas, M.J. (1981) Carbonatite magmas. **Mineral. Mag.** 44: 33-40.

Le Bas, M.J. (1987) Nephelinites and carbonatites. In: Fitton, J.G. and Upton, B.G.J. (editors) Alkaline Igneous Rocks, **Geological Society Special Publication**, No. 30: 53-83.

Le Bas, M.J. (1989) Diversification of Carbonatite. In: Bell, K. (Ed.) **Carbonatites, Genesis and Evolution.** Unwin Hyman Ltd. 618p.

Leeman, W.P. and Phelp, D.W. (1981) Partitioning of rare earths and other trace elements between sanidine and coexisting volcanic glass. **J. Geophys. Res.** 86:10193-10199.

Loiselle, M.C. and Wones, D.R. (1979) Characteristics and origin of anorogenic granites. **Geol. Soc. Am. Abstr. with Progr.**, 11, 468p.

Macdonald, R. (1974) The role of fractional crystallization in the formation of alkaline rocks. In, Sorensen, H. (editor) **The Alkaline Rocks**. Wiley, London, 442-458.

Mahood, G.A. (1981) Chemical Evolution of a Pleistocene Rhyolitic Center: Sierra La Primavera, Jalisco, Mexico. **Contrib. Mineral. Petrol.** 77: 129-149.

Mahood, G.A. and Hildreth, W. (1983) Large partition coefficients for trace elements in high-silica rhyolites. **Geochim. Cosmochim Acta.** 47: 11-30.

Mahood, G.A. and Stimac, J.A. (1990) Trace-element partitioning in pantellerites and trachytes. **Geochim. Cosmochim. Acta.** 54: 2257-2276.

Manning, D.A.C. (1981) The effect of fluorine on liquidus phase relationships in the system Qz-Ab-Or with excess water at 1kbar. **Contrib. Mineral. Petrol.** 76: 206-215.

Marsh, J.S. (1987) Evolution of a strongly differentiated suite of phonolites from the Klinghardt Mountains, Namibia. **Lithos**, 20: 41-58.

Martin, H. (1965) The Precambrian geology of South West Africa and Namaqualand. **Precambrian Res. Unit, University of Cape Town.** 159p.

Martin, H. and Porada, H. (1977) The intracratonic branch of the Damara orogen in South West Africa. Part II. Discussion of relationships with the Pan - African mobile belt system. **Precambr. Res.** 5: 339-357.

McMillan, N.J. and Dungan, M.A. (1988) Open system magma evolution of the Taus Plateau volcanic field, northern New Mexico, 3. Andersites and Dacites. **J. Petrol.** 29: 527-557

Middlemost, E. (1967) Petrology of the Bremen Granite-Syenite Complex, South West Africa. **Trans. Geol.Soc.S.afr.** 70: 117-134.

Möller, P., Morteani, G. and Schley, F. (1980) Discussion of REE distribution patterns of carbonatites and alkalic rocks. **Lithos.** 13: 171-179.

Morimoto, N., Fabries, J., Ferguson, A.K., Ginzburg, I.V., Ross, M., Seifert. F.A., Zussman, J., Aoki, K. and Gottardi, G. (1988) Nomenclature of pyroxenes. **Am. Mineral.** 73: 1123-1133.

Nagasawa, H., Schreiber, H.D. and Morris, R.V. (1980) Experimental mineral/liquid partition coefficients of the rare earth elements (REE), Sc and Sr for perovskite, spinel and melilite. **Earth Planet. Sci. Lett.** 46: 431-437.

Nagasawa, H. and Schnetzler, C.C. (1971) Partition of rare earth, alkali and alkaline earth elements between phenocrysts and acidic igneous magma. **Geochim. Cosmochim. Acta.** 35: 953-968.

Nakamura, N. (1974) Determination of REE, Ba, Fe, Mg, Na anf K in carbonaceous and ordinary chondrites. **Geochim. Cosmochim. Acta.** 38: 575-775.

Nash, W.P. (1972) Apatite chemistry and phosphorous fugacity in a differentiated igneous intrusion. **Am. Mineral.** 57: 877-886.

Nash, W.P. and Wilkinson, J.F.G. (1970) Shonkin Sag Laccolith, Montana. I. Mafic Minerals and Estimates of Temperature, Pressure, Oxygen Fugacity and Silica Activity. **Contrib. Mineral. Petrol.** 25: 241-269.

Nash, W.P. and Crecraft, H.R. (1985) Partition coefficients for trace elements in silicic magmas. **Geochim. Cosmochim. Acta.** 49: 2309-2322.

Nelson, D.R., Chivas, A.R., Chappell, B.W. and McCulloch, M.T. (1988) Geochemical and isotopic systematics in carbonatites and implications for the evolution of ocean-island sources. **Geochim. Cosmochim. Acta.** 52: 1-17.

Neuman, E-R., Brunfelt, A.O. and Finstad, K.G. (1977) Rare Earth Elements in some igneous rocks in the Oslo rift, Norway. **Lithos.** 10: 311-314.

Nicholls, J. and Carmichael, J.S.E. (1969) Peralkaline acid liquids: a petrological study. **Contrib. Mineral. Petrol.** 20: 268-294.

Nicolaysen, L.O. and Burger, A.J. (1965) Note on an extensive zone of 1000 million-year old metamorphic and igneous rocks in southern Africa. **Sci. Terre.** 10: 497-516.

Nielsen, R.H. (1990) Simulation of Igneous Differentiation Processes. In: Nicholls, J. and Russell, J.K. (Eds.), **Reviews in Mineralogy Vol. 24**; Mineralogical Society of America. pp 65-107.

Onuma, N., Ninomiya, S. and Nagasawa, H. (1981) Mineral/groundmass partition coefficients for nepheline, melilite, clinopyroxene and perovskite in melilite-nepheline basalt, Nyiragongo, Zaire. **Geochem. J.** 15: 221-228.

Pankhurst, R.J., Beckinsale, R.D. and Brooks, C.K. (1976) Stromtium and Oxygen Isotopic Evidence Relating to the Petrogenesis of the Kangerdlugssuaq Alkaline Intrusion, East Greenland. **Contrib. Mineral. Petrol.** 54: 17-42.

Parsons, I. and Brown, W.L. (1988) Sidewall crystallization in the Klokken intrusion: zoned ternary feldspars and coexisting minerals. **Contrib. Mineral. Petrol.** 98: 431-443.

Pearce, J.A., Harris, N.B.W. and Tindle, A.G. (1984) Trace Element Discrimination Diagrams for the Tectonic Interpretation of Granitic Rocks. **J. Petrol.** 25: 956-983.

Philpotts, J.A. and Schnetzler, C.C. (1970) Phenocryst matrix partition coefficients for K, Rb, Sr and Ba with applications to anorthosite and basalt genesis. **Geochim. Cosmochim. Acta.** 34: 307.

Pollard, P.J. (1983) Magmatic and postmagmatic processes in the formation of rocks associated with rare-element deposits. **Trans. Inst. Min. Metall. (Sect. B).** 92: 1-9.

Porada, H (1979) The Damara-Ribeira orogen of the Pan-African Brasiliana cycle in Namibia (South West Africa) and Brazil as interpretes in terms of continetal collision. **Tectonophysics.** 57: 237-265.

Price, R.C., Johnson, R.W., Gray, C.M. and Frey, F.A. (1985) Geochemistry of phonolites and trachytes from the summit region of Mt. Kenya. **Contrib. Mineral. Petrol.** 89: 394-409.

Reid, D.L. (1979a) Age relationships within the Mid-Proterozoic Vioolsdrif Batholith, Lower Orange River region. **Trans. Geol. Soc. S. Afr.** 82: 305-311.

Reid, D.L. (1979b) Petrogenesis of calc-alkaline metalavas in the Mid-Proterozoic Haib Volcanic Subgroup; Lower Orange River region. **Trans. Geol. Soc. S. Afr.** 82: 109-131.

Reid, D.L. (1982) Age relationships within the Vioolsdrif Batholith, Lower Orange River region, II. A two stage emplacement history and the extent of Kibaran overprinting. **Trans. Geol. Soc. S. Afr.** 85: 108-110.

Reid, D.L. (in press) Alkaline rocks in the Kuboos-Bremen Igneous Province, Southern Namibia: The Kanabeam Multiple Ring Complex. **Communs Geol. Surv. Namibia.** 5: 5-17.

Rock, N.M.S. (1982) The Late Cretaceous alkaline igneous province in the Iberian Peninsula, and its tectonic significance. **Lithos.** 15: 111-131.

Rogers, J.J.W., Ghume, M.A., Nagy, R.M., Geenberg, J.K. anf Fullagar, P.D. (1978) Plutonism in Pan - African belts and geologic evolution of northeastern Africa. **Earth Planet. Sci. Lett.** 39: 109-117.

Rogers, N.W. and Hawkesworth, C.J. (1982) Proterozoic age and cumulate origin for granulite xenoliths, Lesotho. **Nature.** 299: 409-413.

Ronsbo, J.G. (1989) Coupled substitutions involving REEs and Na and Si in apatite in alkaline rocks from the Ilimaussaq intrusion, South Greenland, and the petrological implications. **Am. Mineral.** 74: 896-901.

Rosenberg, P.E. and Foit, F.F. (1979) The stability of transition metal dolomites in carbonate systems: a discussion. **Geochim. Cosmochim. Acta.** 43: 951-955.

Sack, R.O., Carmichael, I.S.E., Rivers, M. and Ghiorso, M.S. (1980) Ferric-ferrous equilibria in natural silicate liquides at 1 bar. **Contrib. Mineral. Petrol.**75: 369-376.

Sawka, W.N. and Chappell, B.W. and Kistler, R.W. (1990) Granitoid Compositional Zoning by Side-wall Boundary Layer Differentiation: Evidence from the Palisade Crest Intrusive Suite, Central Sierra Nevada, California. **J. Petrol.** 31: 519-553.

Schommarz, R.E. (1988) Preliminary report on the Marinkas Quelle Carbonatite Complex. **Department of Economic Affairs, Namibia, Economic Mineral Report.**(unpublished).

Shand, S.J. (1922) The problem of the alkaline rocks. **Proc. Geol. Soc. S. Afr.** 25: 19-33.

Shaw, D.M. (1968) A review of K-Rb fractionation trends by covariance analysis. **Geochim. Cosmochim. Acta.** 32: 573-601.

Sheppard, S.M.F. and Harris, C. (1985) Hydrogen and oxygen geochemistry of Ascention Island lavas and granites: variation with crystal fractionation and interaction with sea water. **Contrib. Mineral. Petrol.** 91: 74-81.

Sheraton, J.W. and Black, L.P. (1988) Chemical evolution of granitic rocks in the East Antarctic Shield, with particular reference to post-orogenic granites. **Lithos.** 21: 37-52.

Söhnge, P.G. and De Villiers, J. (1948) The Kuboos pluton and its associated line of intrusives. **Trans. Geol. Soc. S. Afr.** 51: 1-31.

Sorensen, H, (1974) **The Alkaline Rocks.**John Wiley and Sons, London. 622p.

Stacey, J.S. and Kramers, J.D. (1975) Approximation of terrestrial lead isotope evolution by a two-stage model. **Earth Planet. Sci. Lett.** 26: 707-721.

Stephenson, D. (1972) Alkali clinopyroxenes from nepheline syenites of the South Qôroq Centre, South Greenland. **Lithos.** 5: 187-201.

Stephenson, D. (1976) The South Qöroq Centre nepheline syenites, South Greenland. **Grønl. Geol. Unders. Bull.** 118, 55p.

Streckeisen, A. (1976) To each plutonic rock its proper name. **Earth Science Review.** 12: 1-33.

Sun, S.S. and Hanson, G.N. (1976) Rare earth element evidence for differentiation of McMurdo volcanics, Ross Island, Antarctica. **Contrib. Mineral. Petrol.** 54: 139-155.

Suwa, K., Oana, S., Wada, H. and Osaki, S. (1975) Isotope geochemistry and petrology of African carbonatites. **Phys. Chem. Earth.** 9: 735-745

Tankard, A.J., Jackson, M.P.A., Eriksson, K.A., Hobday, D.K., Hunter, D.R. and Minter, W.E.L. (1982) **Crustal Evolution of Southern Africa. 3.8 Billion Years of Earth History.** Springer - Verlag. New York, Inc. 523p.

Taylor, H.P.Jr (1979) Oxygen and Hydrogen Isotope Relationships in Hydrothermal Ore Deposits. In: Barnes, H.L. (Ed) **Geochemistry of Hydrothermal Ore Deposits - 2nd Edition. John Wiley and sons.** 1979 pp 798.

Taylor, H.P.Jr. and Sheppard, S.M.F. (1986) Igneous rocks: I. processes of isotope fractionation and isotope systematics. In. Valley, J.W., Taylor. H.P.Jr. and O'Neil, J.R.(Eds.) **Reviews in Mineralogy.16, Stable Isotopes in high temperature geological processes. Mineralogical Society of America.** 570p.

Taylor, S.R. (1965) The application of trace-element data to problems in petrology.**Phys. Chem. Earth.** 6: 133-213.

Tindle, A.G. and Pearce, J.A. (1981) Petrogenetic Modelling of in situ Fractional Crystallization in the Zoned Loch Doon Pluton, Scotland. **Contrib. Mineral. Petrol.** 78: 196-207.

Tuttle, O.F. and Bowen, n.l. (1958) Origin of granite in the light of experimental studies. **Mem. Geol. Soc. Am.** 74.

Twyman, J.D. and Gittins, J. (1987) Alkalic carbonatite magmas: parental or derived ?. In: Fitton, J.G. and Upton, B.G.J. (editors) **Alkaline Igneous Rocks. Geological Society Special Publication.** 30, 85-94.

Tyler, R.C. and King, B.C. (1967) The pyroxenes of the alkaline igneous complexes of eastern Uganda.**Mineral. Mag.**36: 5-21.

Upton, B.G.J., Stephenson, D. and Martin, A.R. (1985) The Tugtutôq older giant dyke complex: mineralogy and geochemistry of an alkali gabbro-augite-syenite-foyaite association in the Gardar Province of South Greenland. **Mineral. Mag.** 49: 623-642.

Upton, B.G.J. and Thomas, J.E. (1980) The Tugtutôq Younger Giant Dyke Complex, South Greenland: Fractional Crystallization of Transitional Olivine Basalt Magma. **J. Petrol.** 21: 167-198.

van Breemen, O., Hutchinson, J.and Bowen, P. (1975) Age and origin of the Nigerian Mesozoic granites: a Rb-Sr isotopic study. **Contrib. Mineral. Petrol.**50: 157-172.

Walsh, J.N., Buckley, F. and Barker, J. (1981) The Simultaneous Determination of the Rare-Earth Elements in Rock Using Inductively Coupled Plasma Source Spectrometry. **Chemical Geology**. 33: 141-153.

Watkinson, D.H. and Wyllie, P.J. (1971) Experimental study on the join $NaAlSiO_4$-$CaCO_3$-H_2O and the genesis of alkalic rock-carbonatite complexes. **J. Petrol**. 12: 357-378.

Watson, E.B. (1977) Partitioning of manganese between forsterite and silicate liquid. **Geochim. Cosmochim. Acta**.41: 1363-1374.

Watson, E.B. and Green, T.H. (1981) Apatite/liquid partition coefficients for the rare earth elements and strontium. **Earth Planet. Sci. Lett**. 56: 405-421.

Weaver, S.P., Sceal, J.S.C. and Gibson, I.L. (1972) Trace element data relevant to the origin of trachytic and pantelleritic lavas in the East African R.H. System. **Contrib. Mineral. Petrol**. 36: 181-194.

Weinstein, S.A., Yuen, D.A. and Olson, P.L. (1988) Evolution of crystal-settling in magma-chamber convection. **Earth Planet. Sci. Lett.** 87: 237-248.

Whalen, J.B., Currie, K.L. and Chappell, B.W. (1987) A-type granites: geochemical characteristics, discrimination, and petrogenesis. **Contrib. Mineral. Petrol.** 95: 407-419.

White, R. and McKenzie, D. (1989) Magmatism at Rift Zones: The Generation of Volcanic Continental Margins and Flood Basalts: **J. Geophys. Res.** 94, B6: 7685-7729.

Wiebe, R.A. (1988) Structural and Magmatic Evolution of a Magma Chamber: The Network Island Layered Intrusion, Nain, Labrador. **J. Petrol**. 29: 383-411.

Wolff, J.A. (1984) Variation in Nb/Ta during differentiation of phonolite magma, Tenerife, Canary Islands. **Geochim. Cosmochim. Acta**. 48: 1345-1348.

Wones, D.R. and Gilbert, M.C. (1982) Amphiboles in the igneous environment. In: Veblen, D.R. and Ribbe, P.H. (editors) **Amphiboles: petrology and experimental phase relations. Reviews in Mineralogy 9B. Mineralogical Society of America.**

Woolley, A.R. and Symes, R.F. (1976) The analcime-phyric phonlites (blairmorites) and associated analcime kenytes of the Lupata Gorge, Mocambique. **Lithos**. 9: 9-15.

Woolley, A.R. (1982) A discussion of carbonatite evolution and nomenclature and the generation of sodic and potassic fenites. **Mineral. Mag.** 46: 13-17.

Woolley, A.R. and Jones, G.C. (1987) The petrochemistry of the northern part of the Chilwa alkaline province, Malawi. In: Fitton, J.G. and Upton, B.G.J. (editors) **Alkaline Igneous Rocks, Geological Society Special Publication.** 30: 335-355.

Woolley, A.R. and Kempe, D.R.C. (1989) Carbonatites: nomenclature, average chemical compositions, and element distribution. In: Bell, K. (Ed.) **Carbonatites, Genisis and Evolution.** Unwin Hyman Ltd. 618p

Wörner, G., Beusen, J.-M., Duchateau, N., Gijbels, R. and Schminke, H.-V. (1983) Trace element abundances and mineral/ melt distribution coefficients in phonolites from the Laacher See Volcano (Germany). **Contrib. Mineral. Petrol.** 84: 152-173.

Wörner, G. and Schmincke, H. U. (1984) Mineralogical and Chemical Zonation of the Laacher See Tephra Sequence (East Eifel, W. Germany) **J. Petrol.** 25: 805-835.

Wyllie, P.J. (1965) Melting Relationships in the System CaO-MgO-CO_2-H_2O with Petrological Applications. **J. Petrol.** 6: 101-123.

Wyllie, P.J. (1987) Transfer of subcratonic carbon into kimberlites and rare earth carbonatites. In: Mysen, B.O. (Ed.) Magmatic Processes. Physicochemical Principles. **The Geochemical Society. Spec. Pub.** 1: 107-119.

Wyllie, P.J. (1989) Origins of carbonatites: evidence from phase equilibrium studies. In: Bell, K. (ed) **Carbonatites. Genesis and evolution.** Unwin Hyman Ltd. 618p.

Wyllie, P.J. and Huang, H.-L. (1975) Peridotite kimberlite and carbonatite examined in the system CaO-MgO-SiO_2-CO_2. **Geology.** 3: 621-624.

Zartman, R.E. and Doe, B.R. (1981) Plumbotectonics - the model. **Tectonophysics.** 75: 135-162.

APPENDIX 1: WHOLE ROCK SAMPLE DESCRIPTIONS AND LOCATIONS

See locality maps

Sample Number	Rock Type	Complex
Larvikite - pulaskite series		
ORS 61	pulaskite	GPC
ORS 90	larvikite	GPC
ORS 94	larvikite	GPC
ORS 101	pulaskite	GPC
ORS 102	larvikite	GPC
ORS 107	larvikite	GPC
ORS 108	pulaskite	GPC
Foyaites		
ORF 6	clinopyroxene-rich foyaite	MKC
ORF 7	amphibole-rich foyaite	MKC
ORF 8	clinopyroxene-rich foyaite	MKC
ORF 14	clinopyroxene-rich foyaite	MKC
ORF 17	clinopyroxene-rich foyaite	MKC
ORF 21	amphibole-rich foyaite	MKC
ORF 22	clinopyroxene-rich foyaite	MKC
ORF 23	amphibole-rich foyaite	MKC
ORF 24	clinopyroxene-rich foyaite	MKC
ORF 32	clinopyroxene-rich foyaite	MKC
ORF 33	clinopyroxene-rich foyaite	MKC
ORF 40	amphibole-rich foyaite	MKC
ORF 41	clinopyroxene-rich foyaite	MKC
Alkali-melasyenite - nepheline syenite series		
ORF 3	nepheline syenite	MKC
ORF 12	nepheline syenite	MKC
ORF 28	alkali-melasyenite	MKC
ORF 29	alkali-melasyenite	MKC
ORF 30	alkali-melasyenite	MKC

ORF 31	nepheline syenite	MKC
ORF 43	nepheline syenite	MKC
ORF 44	nepheline syenite	MKC
ORF 46	nepheline syenite	MKC
ORF 49	nepheline syenite	MKC

Monzodiorite

ORS 133		GPC
ORS 175		GPC
ORS 176		GPC

Alkali-syenites

ORS 60		GPC
ORS 99		GPC
ORS 110		GPC
ORS 112		GPC
ORS 126		GPC
ORS 171		GPC
ORS 189		GPC
ORS 193		GPC
MKS 35		MKC
MKS 49		MKC
MKS 57		MKC
MKS 64		MKC
MKS 67		MKC
MKS 69		MKC

Alkali-feldspar syenite

ORS 62		GPC
ORS 92		GPC
ORS 93		GPC
ORS132		GPC
ORS173		GPC

Monzonite - granite series

ORS 129	alkali-feldspar granite	GPC
ORS 130	granite	GPC
ORS 138	alkali-feldspar granite	GPC
ORS 172	alkali-feldspar granite	GPC
ORG 11	alkali-feldspar granite	GPC
MKS 3	monzonite	MKC
MKS 21	granite	MKC

MKS 27	alkali-feldspar granite	MKC
MKS 34	granite	MKC
MKS 36	granite	MKC
MKS 52	syenite	MKC
MKS 53	syenite	MKC
MKS 54	syenite	MKC
MKS 59	syenite	MKC
MKS 61	alkali-feldspar granite	MKC
MKS 63	granite	MKC
MKS 66	monzonite	MKC
MKG 6	granite	MKC
MKS 16	feldspar porphyry	MKC
MKS 29	feldspar porphyry	MKC
MKS 39	feldspar porphyry	MKC
MKS 46	feldspar porphyry	MKC

Alkali-granites

ORS 14	alkali-granite (low-Si)	GPC
ORS 95	alkali-granite (low-Si)	GPC
ORS 178	alkali-granite (low-Si)	GPC
ORS 190	alkali-granite (low-Si)	GPC
MKS 43	alkali-granite (low-Si)	MKC
ORF 19	alkali-granite (low-Si)	MKC
ORF 48	alkali-granite (low-Si)	MKC
MKG 12	quartz-feldspar porphyry (high-Si)	MKC
MKG 13	quartz-feldspar porphyry (high-Si)	MKC
MKG 16	alkali-granite (high-Si)	MKC
MKG 19	alkali-granite (high-Si)	MKC
MKG 23	quartz-feldspar porphyry (high-Si)	MKC
MKG 25	alkali-granite (high-Si)	MKC
MKG 31	alkali-granite (high-Si)	MKC
MKG 33	alkali-granite (high-Si)	MKC
MKG 34	quartz-feldspar porphyry (high-Si)	MKC
MKG 38	alkali-granite (high-Si)	MKC

Rocks of the Marinkas Kwela Carbonatite Complex

MKC 4	magnetite-rich beforsite	S beforsite
MKC 6	magnetite-rich beforsite	S beforsite
MKC 7	magnetite-rich beforsite	S beforsite
MKC 9	magnetite-rich beforsite	S beforsite
MKC 15	Mn-rich ferrocarbonatite	E of Complex

MKC 16	Mn-rich ferrocarbonatite	E of Complex
MKC 17	Mn-rich ferrocarbonatite	E of Complex
MKC 18	magnetite-rich beforsite	S beforsite
MKC 20A	Mn-rich ferrocarbonatite	In sôvite
MKC 20B	Mn-rich ferrocarbonatite	In sôvite
MKC 25	mgt-, phlogopite-rich beforsite	S beforsite
MKC 27	Mn-rich ferrocarbonatite	S of Complex
MKC 29	remnant sôvite	E beforsite
MKC 34	apatite-rich beforsite	E beforsite
MKC 35	magnetite-rich beforsite	S beforsite
MKC 45	apatite-rich beforsite	E beforsite
MKC 46	apatite-rich beforsite	E beforsite
MKC 47	ferrocarbonatite	E beforsite
MKC 48	ferrocarbonatite	E beforsite
MKC 52	clinopyroxene-rich sôvite	Mid Complex
MKC 54	amphibole-rich sôvite	Mid Complex
MKC 55A	magnetite-rich beforsite	S beforsite
MKC 55B	magnetite bleb	S beforsite
MKC 56	mgt-, phlogopite-rich beforsite	S beforsite
MKC 59	magnetite bleb	S beforsite
MKC 62	magnetite-rich beforsite	S beforsite
RS 112	nepheline syenite	N of Complex
RS 113	nepheline syenite	N of Complex
RS 114	nepheline syenite	N of Complex
RS 115	nepheline syenite	N of Complex
RS 117	nepheline syenite	N of Complex
RS 120	nepheline syenite	N of Complex

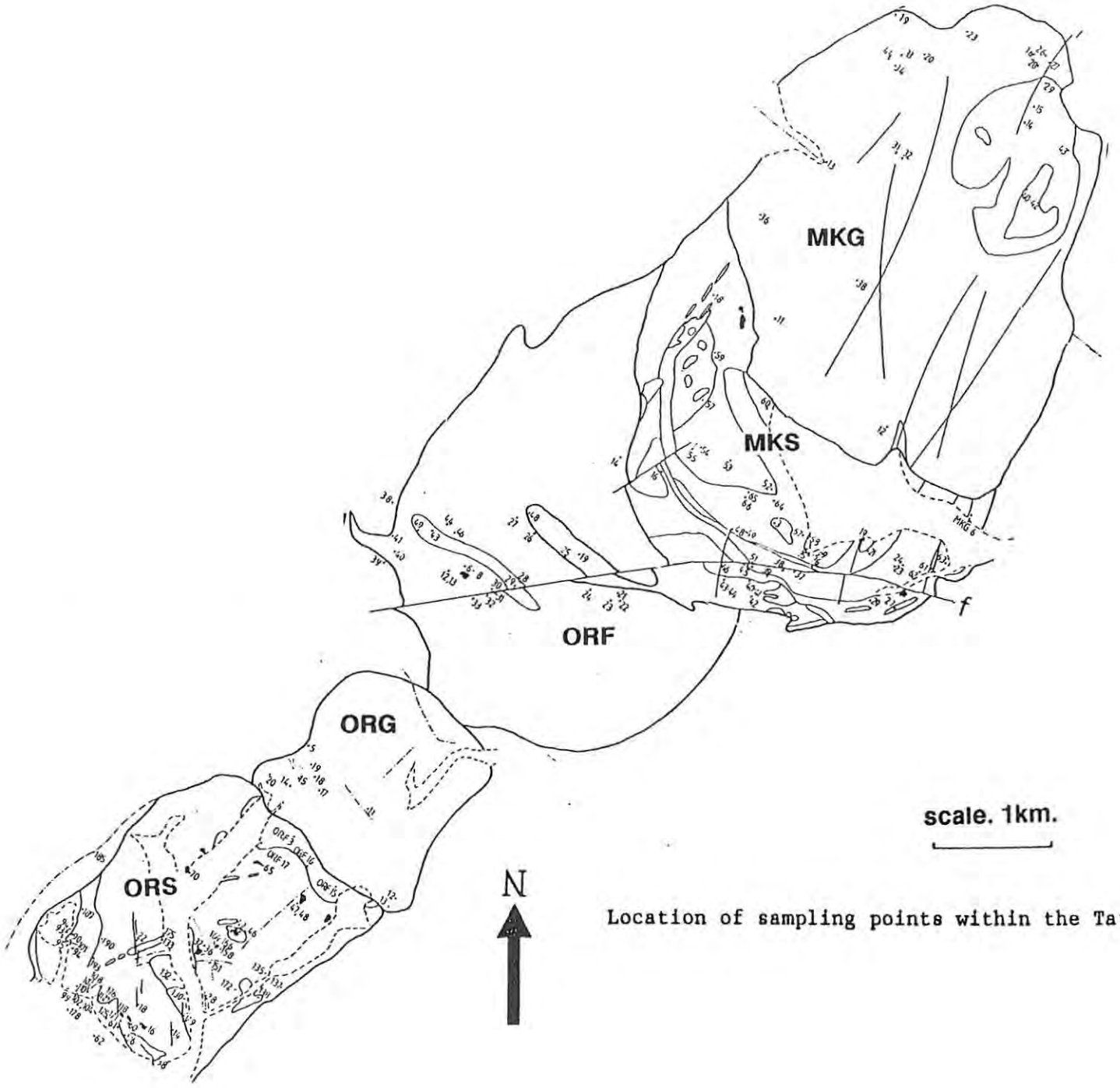

Location of sampling points within the Tatasberg Complex.

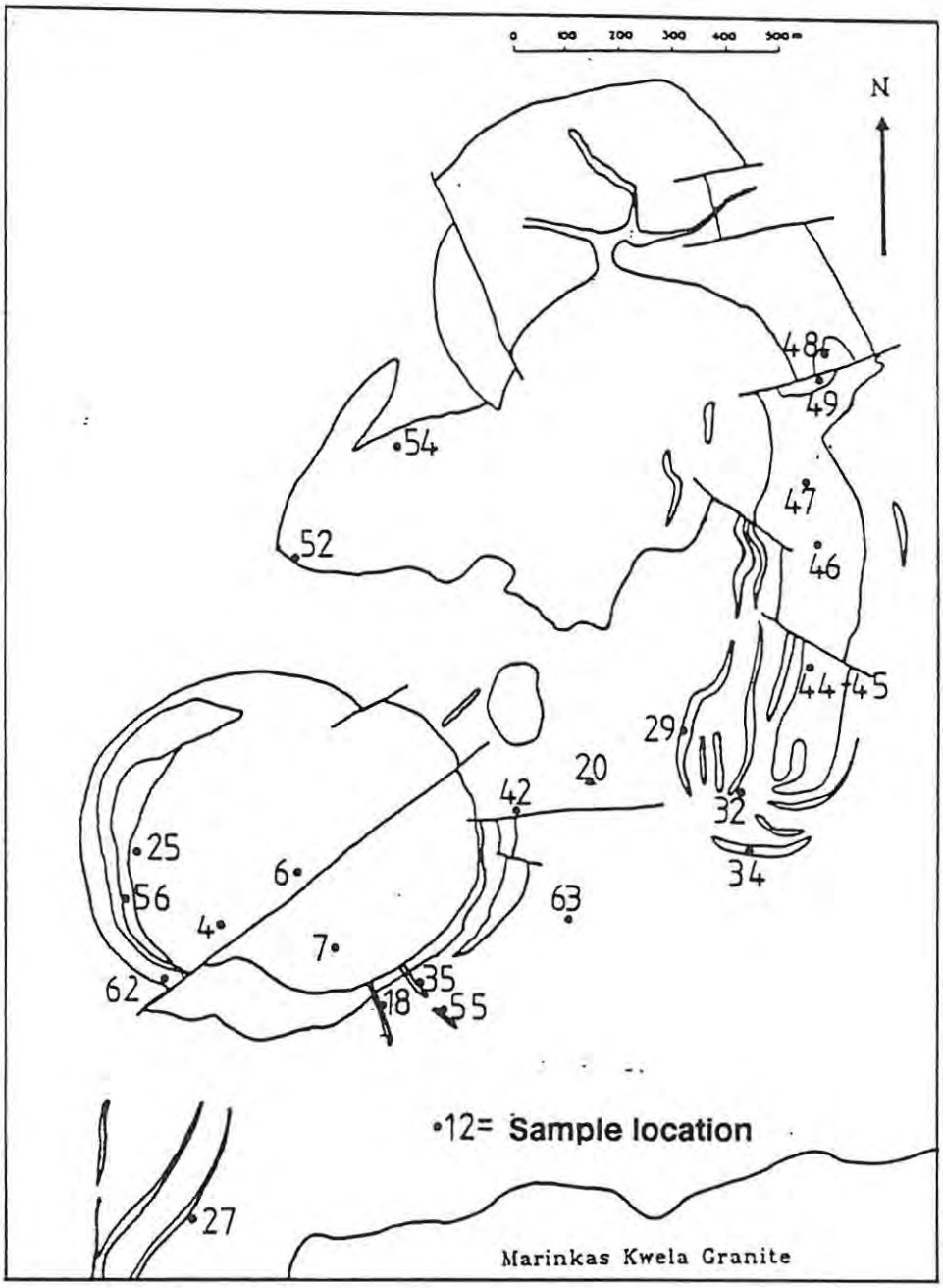

Location of sampling points within the Marinkas Kwela Carbonatite Complex.

APPENDIX 2: MINERAL CHEMISTRY

Fe^{2+}/Fe^{3+} ratios for clinopyroxenes and for amphiboles have been caluclated according to the method of Droop (1987).

Structural formulae are calculated on the basis of

6 oxygens for clinopyroxene
23 oxygens for amphibole
22 oxygens for biotite.

Larvikite - pulaskite series

ORS61 CLINOPYROXENE

	1	2	3	4	5	6	7	8	9	10
SiO2	50 17	50 12	49 84	51 32	51 69	51 64	51 74	51.75	51 77	51 35
TiO2	0 18	0 21	0.31	0.26	0 22	0 30	0 17	0 27	0 24	0 30
Al2O3	1 41	1 61	1 68	1 38	1 25	1 43	0 90	1 38	1 28	1 29
Cr2O3	0 00	0 00	0 00	0 00	0 00	0 00	0 00	0 00	0 00	0 00
Fe2O3	4 65	4 40	4 91	3 47	3 63	3 61	3 21	3 88	3 28	4 53
FeO	15 01	14 22	14 40	9 52	8 90	8 34	10 41	8 60	9 21	8 80
MnO	0 93	0 95	0 82	0 74	0 71	0 76	0 81	0 74	0 75	0 77
MgO	4 84	5.42	5.12	9 94	10 66	10 28	9 45	10 10	10 00	9 95
CaO	20 97	21 01	20 63	22 62	22 59	22 69	22 91	23 09	22 89	22 76
Na2O	1 88	1 80	1 96	1 00	0 96	1 19	0 99	1 12	1 08	1 12
Total	100 03	99 74	99 67	100 25	100 61	100 24	100 59	100 93	100.50	100 88
Si	1 9649	1.9603	1.9541	1.9489	1.9495	1.9518	1.9656	1.9477	1.9576	1.9394
Al	0 0000	0 0000	0 0000	0 0000	0 0000	0 0000	0 0000	0 0000	0 0000	0 0000
Fe3+	0 0000	0 0000	0 0000	0 0000	0 0000	0 0000	0 0000	0 0000	0 0000	0 0000
Al	0 0651	0 0742	0 0777	0 0618	0 0556	0 0637	0 0404	0 0612	0 0571	0 0574
Fe3+	0 1371	0 1295	0 1450	0 0992	0 1031	0 1028	0 0917	0 1099	0 0933	0 1288
Ti	0 0053	0 0062	0 0091	0 0074	0 0062	0 0085	0 0048	0 0076	0 0068	0 0085
Cr	0 0000	0 0000	0 0000	0 0000	0 0000	0 0000	0 0000	0 0000	0 0000	0 0000
Mg	0 2825	0 3159	0 2992	0 5626	0 5989	0 5791	0 5350	0 5664	0 5637	0 5601
Fe2+	0 4918	0 4651	0 4691	0 2690	0 2362	0 2459	0 3281	0 2548	0 2792	0 2452
Mn	0 0182	0 0089	0 0000	0 0000	0 0000	0 0000	0 0000	0 0000	0 0000	0 0000
Mg	0 0000	0 0000	0 0000	0 0000	0 0000	0 0000	0 0000	0 0000	0 0000	0 0000
Fe2+	0 0000	0 0000	0 0031	0 0332	0 0446	0 0177	0 0028	0 0158	0 0121	0 0328
Mn	0 0127	0 0225	0 0272	0 0238	0 0228	0 0243	0 0260	0 0235	0 0239	0 0247
Ca	0 8800	0 8805	0 8667	0 9204	0 9129	0 9189	0 9326	0 9313	0 9273	0 9211
Na	0 1424	0 1367	0 1490	0 0736	0 0702	0 0872	0 0729	0 0817	0 0792	0 0820
Total	4 0000	4 0000	4 0000	4 0000	4 0000	4 0000	4 0000	4 0000	4 0000	4 0000

ORS90 CLINOPYROXENE

	1	2	3	4	5	6	7	8	9	10	11	12	13
SiO2	51.75	51 52	51 09	52 05	51 20	51 77	51 23	51 94	52 45	51 45	51 19	51 46	51 08
TiO2	0 26	0 27	0 18	0 04	0 28	0 17	0 38	0 44	0 23	0 02	0 09	0 07	0 10
Al2O3	1 09	1 02	0 99	0 58	1 13	0 80	1 25	1 31	0 98	0 52	0 77	0 58	0 67
Cr2O3	0 00	0 00	0 00	0 00	0 00	0 01	0 00	0 00	0 00	0 00	0 00	0 00	0 00
Fe2O3	1 49	1 24	2 08	1 73	1 51	1 69	1 50	0 55	0 66	3 90	3 68	3 42	4 39
FeO	12 00	12 87	11 88	10 31	12 87	11 78	11 69	10 90	11 11	8 63	8 30	8 79	8 54
MnO	0 94	1 04	1 03	0 92	1 14	0 96	0 96	0 84	0 83	0 50	0 87	1 01	1 04
MgO	9 63	9 28	9 03	10 55	8 97	9 50	9 60	10 96	10 50	10 40	10 82	10 95	10 17
CaO	21 98	21 79	22 08	22 55	21 35	22 12	21 78	21 51	22 10	23 53	22 90	23 15	23 27
Na2O	0 83	0 75	0 85	0 72	0 89	0 87	0 84	0 79	0 85	0 71	0 75	0 67	0 79
Total	99 96	99 77	99 22	99 44	99 33	99 67	99 23	99 24	99 70	100 06	99 37	99 60	100 04
Si	1 9772	1.9791	1 9736	1 9879	1 9775	1 9850	1 9705	1 9794	1 9934	1 9583	1 9550	1 9606	1 9484
Al	0.0000	0.0000	0 0000	0 0000	0 0000	0 0000	0 0000	0 0000	0 0000	0 0000	0 0000	0 0000	0 0000
Fe3+	0.0000	0 0000	0 0000	0 0000	0 0000	0 0000	0 0000	0 0000	0 0000	0 0000	0 0000	0 0000	0 0000
Al	0 0489	0 0460	0 0453	0 0260	0 0514	0 0363	0 0565	0 0589	0 0440	0 0233	0 0347	0 0262	0 0299
Fe3+	0 0429	0 0358	0 0606	0 0496	0 0438	0 0487	0 0434	0 0158	0 0189	0 1116	0 1057	0 0982	0 1259
Ti	0 0074	0 0077	0 0053	0 0011	0 0082	0 0049	0 0110	0 0125	0 0064	0 0006	0 0026	0 0021	0 0028
Cr	0 0001	0 0000	0 0001	0 0000	0 0001	0 0003	0 0000	0 0000	0 0000	0 0000	0 0000	0 0000	0 0000
Mg	0 5486	0 5314	0 5197	0 6003	0 5161	0 5426	0 5506	0 6222	0 5947	0 5900	0 6161	0 6216	0 5779
Fe2+	0 3521	0 3791	0 3690	0 3230	0 3804	0 3672	0 3386	0 2906	0 3360	0 2745	0 2408	0 2520	0 2635
Mn	0 0000	0 0000	0 0000	0 0000	0 0000	0 0000	0 0000	0 0000	0 0000	0 0000	0 0000	0 0000	0 0000
Mg	0 0000	0 0000	0 0000	0 0000	0 0000	0 0000	0 0000	0 0000	0 0000	0 0000	0 0000	0 0000	0 0000
Fe2+	0 0313	0 0344	0 0147	0 0062	0 0353	0 0104	0 0376	0 0569	0 0172	0 0003	0 0242	0 0121	0 0088
Mn	0 0304	0 0339	0 0337	0 0299	0 0372	0 0311	0 0313	0 0270	0 0266	0 0291	0 0282	0 0325	0 0337
Ca	0 9000	0 8870	0 9142	0 9225	0 8834	0 9086	0 8979	0 8782	0 9001	0 9597	0 9369	0 9451	0 9510
Na	0 0611	0 0556	0 0638	0 0535	0 0667	0 0650	0 0628	0 0584	0 0626	0 0526	0 0557	0 0497	0 0581
Total	4 0000	4 0000	4 0000	4 0000	4 0000	4 0000	4 0000	4 0000	4 0000	4 0000	4 0000	4 0000	4 0000

ORS94 CLINOPYROXENE

	1	2	3	4	5	6	7	8	9	10	11	12	13	14	15	16	17	18	19	20	21	22	23	24
SiO2	51 33	52.78	53 04	52.49	52 34	53.03	53.08	52.59	52.57	52 67	52 40	52.29	52.26	52 29	52 74	51 59	50.87	51 42	50 69	50 70	49 17	50 48	49 52	51 04
TiO2	0.48	0.28	0.20	0.35	0.43	0.24	0.14	0.40	0.36	0.33	0 38	0.30	0.34	0 38	0 39	0 19	0.27	0 15	0 54	0.45	0 75	0 45	0 64	0 29
Al2O3	1.24	0.95	0.84	1.12	1.35	0.92	0.85	1.31	1.18	1.15	1.24	1.17	1.17	1 21	1 28	0 75	1.34	1 12	2 38	2.83	4 14	2 38	3 11	1 38
Cr2O3	0.01	0.00	0.00	0.00	0.00	0.00	0.01	0.00	0.00	0.00	0.00	0.00	0.00	0 00	0 00	0 00	0.00	0 00	0 34	0.19	0 20	0 18	0 29	0 00
Fe2O3	1.63	0.00	0.00	0.00	0.60	0.07	0.66	0.00	0.00	0.00	0.00	0.00	0.31	0 00	0 00	3 72	4 56	4 14	4 43	3 96	4 29	4 14	5 29	3 33
FeO	11.36	12.64	12.21	12 68	12 40	12 00	12.38	12.27	12.30	13 24	12 62	13.35	13 18	12 67	13.22	7 76	8 86	9 57	6 97	5 78	5 94	7 34	7 64	9 95
MnO	0.87	0.95	0.84	1.01	0.95	0.90	0.92	0.85	0.87	0 88	0.83	0.99	1 03	0 95	0 89	0 99	0 93	1 09	0 78	0 75	0 81	0 79	0 84	0 82
MgO	9.56	9.48	10.36	9.51	9 95	10 42	9.53	10.15	10 23	9.59	10 07	9.23	9 56	9 83	9 70	11 21	10.19	9 82	10 80	11 30	10 71	10 83	10 00	10 08
CaO	22.08	21.85	21.87	21.73	21.55	21.99	21.50	21.52	21.15	21.41	21.48	21.61	21.69	21 55	21 73	23 29	22.76	22 77	23 24	24 06	23 83	23 59	21 61	22 29
Na2O	0.91	0.76	0.64	0.81	0.92	0 86	1.24	0.83	0.79	0 87	0.79	0.88	0.81	0 85	0 84	0.71	0 85	0 92	0 93	0.76	0 67	0 67	1 25	0 86
Total	99.46	99.69	99.98	99.67	100.48	100.43	100 29	99.92	99.45	100 14	99 81	99.82	100 34	99 73	100.79	100.21	100.63	101 01	101 10	100 78	100 50	100 84	100 19	100 04
Si	1 9685	2 0203	2 0166	2 0085	1 9829	2 0031	2 0133	1 9995	2 0083	2 0062	1 9969	2 0012	1 9894	1 9957	1 9954	1 9508	1 9286	1 9455	1 8986	1 8942	1 8478	1 8977	1 8782	1 9447
Al	0 0000	0 0000	0 0000	0 0000	0 0000	0 0000	0 0000	0 0000	0 0000	0 0000	0 0000	0 0000	0 0000	0 0000	0 0000	0 0000	0 0000	0 0000	0 0000	0 0000	0 0000	0 0000	0 0000	0 0000
Fe3+	0 0000	0 0000	0 0000	0 0000	0 0000	0 0000	0 0000	0 0000	0 0000	0 0000	0 0000	0 0000	0 0000	0 0000	0 0000	0 0000	0 0000	0 0000	0 0000	0 0000	0 0000	0 0000	0 0000	0 0000
Al	0 0562	0 0430	0 0377	0 0507	0 0603	0 0408	0 0378	0 0588	0 0531	0 0515	0 0558	0 0529	0 0524	0 0545	0 0571	0 0334	0 0599	0 0500	0 1051	0 1246	0 1834	0 1055	0 1331	0 0620
Fe3+	0 0470	0 0000	0 0000	0 0000	0 0172	0 0019	0 0187	0 0000	0 0000	0 0000	0 0000	0 0000	0 0090	0 0000	0 0000	0 1059	0 1302	0 1180	0 1248	0 1112	0 1213	0 1170	0 1519	0 0956
Ti	0 0137	0 0082	0 0057	0 0102	0 0122	0 0069	0 0039	0 0115	0 0104	0 0095	0 0107	0 0085	0 0096	0 0110	0 0111	0 0054	0 0076	0 0043	0 0152	0 0126	0 0212	0 0127	0 0184	0 0083
Cr	0 0003	0 0000	0 0000	0 0000	0 0000	0 0000	0 0003	0 0000	0 0000	0 0000	0 0000	0 0000	0 0000	0 0000	0 0000	0 0001	0 0000	0 0000	0 0101	0 0056	0 0059	0 0053	0 0087	0 0000
Mg	0 5463	0 5408	0 5869	0 5421	0 5617	0 5868	0 5386	0 5750	0 5825	0 5445	0 5721	0 5266	0 5425	0 5592	0 5471	0 6315	0 5757	0 5539	0 6029	0 6292	0 5998	0 6068	0 5693	0 5724
Fe2+	0 3365	0 4046	0 3697	0 3970	0 3487	0 3636	0 3928	0 3548	0 3540	0 3945	0 3613	0 4121	0 3864	0 3753	0 3848	0 2237	0 2265	0 2739	0 1420	0 1167	0 0683	0 1527	0 1176	0 2618
Mn	0 0000	0 0034	0 0000	0 0000	0 0000	0 0000	0 0079	0 0000	0 0000	0 0000	0 0000	0 0000	0 0000	0 0000	0 0000	0 0000	0 0000	0 0000	0 0000	0 0000	0 0000	0 0000	0 0000	0 0000
Mg	0 0000	0 0000	0 0000	0 0000	0 0000	0 0000	0 0000	0 0000	0 0000	0 0000	0 0000	0 0000	0 0000	0 0000	0 0000	0 0000	0 0000	0 0000	0 0000	0 0000	0 0000	0 0000	0 0000	0 0000
Fe2+	0 0280	0 0000	0 0184	0 0080	0 0441	0 0156	0 0000	0 0355	0 0390	0 0274	0 0410	0 0153	0 0331	0 0292	0 0337	0 0218	0 0545	0 0290	0 0764	0 0639	0 1183	0 0781	0 1246	0 0553
Mn	0 0284	0 0275	0 0269	0 0326	0 0306	0 0288	0 0215	0 0274	0 0282	0 0284	0 0266	0 0319	0 0332	0 0306	0 0285	0 0317	0 0299	0 0349	0 0247	0 0237	0 0257	0 0252	0 0270	0 0265
Ca	0 9073	0 8960	0 8908	0 8911	0 8748	0 8900	0 8740	0 8765	0 8660	0 8740	0 8771	0 8863	0 8847	0 8815	0 8808	0 9439	0 9246	0 9231	0 9327	0 9632	0 9596	0 9503	0 8782	0 9150
Na	0 0679	0 0563	0 0473	0 0598	0 0676	0 0626	0 0912	0 0611	0 0586	0 0640	0 0583	0 0653	0 0596	0 0630	0 0616	0 0518	0 0625	0 0675	0 0675	0 0551	0 0486	0 0488	0 0919	0 0615
Total	4 0000	4 0000	4 0000	4 0000	4 0000	4 0000	4 0000	4 0000	4 0000	4 0000	4 0000	4 0000	4 0000	4 0000	4 0000	4 0000	4 0000	4 0000	4 0000	4 0000	4 0000	4 0000	4 0000	4 0000

ORS102 CLINOPYROXENE

	1	2	3	4	5	6	7	8	9	10	11	12	13	14	15	16	17	18	19	20	21
															c	m	r		c	m	r
SiO2	50 91	50 95	51 04	51 18	51 07	51 34	51 70	51 55	51 47	51 21	52 16	50 92	50 33	49 71	52 64	53 53	53 23	52 05	52 72	51 22	51 27
TiO2	0 15	0 17	0 16	0 16	0 15	0 12	0 21	0 14	0 03	0 20	0 01	0 22	0 18	0 13	0 45	0 17	0 12	0 28	0 24	0 31	0 28
Al2O3	0 94	0 96	0 95	0 91	0 89	1 60	1 69	0 86	0 95	1 01	0 29	1 06	0 96	1 13	1 19	0 68	0 52	0 95	0 76	1 16	1 06
Cr2O3	0 00	0 00	0 00	0 00	0 00	0 09	0 09	0 00	0 00	0 00	0 00	0 00	0 00	0 09	0 00	0 00	0 01	0 01	0 00	0 02	0 00
Fe2O3	3 79	3 22	3 06	3 57	2 38	3 91	3 88	3 29	3 99	3 96	10 71	3 77	3 82	6 81	0 51	0 59	0 00	1 46	1 18	2 40	2 31
FeO	10 19	10 41	10 75	10 34	10 55	5 14	4 62	8 23	8 15	8 82	6 93	10 14	9 95	9 87	10 58	8 09	9 77	11 61	9 62	11 58	11 77
MnO	1 15	1 03	1 09	1 08	1 02	0 60	0 53	0 84	0 85	0 93	0 91	1 01	1 04	0 80	0 85	0 73	0 88	0 97	0 92	1 01	1 04
MgO	9 58	9 60	9 59	9 61	9 85	12 46	12 83	11 36	10 66	10 51	7 50	9 64	9 45	7 41	11 20	13 28	12 76	10 10	11 68	9 36	9 29
CaO	22 32	22 26	22 27	22 37	22 52	24 41	24 57	22 62	23 31	22 71	18 52	22 48	22 37	21 59	21 89	22 18	21 42	22 28	22 41	21 93	21 90
Na2O	0 86	0 86	0 80	0 89	0 69	0 49	0 54	0 74	0 80	0 82	3 76	0 85	0 83	1 73	0 84	0 70	0 55	0 72	0 69	0 89	0 89
Total	99 90	99 47	99 70	100 11	99 13	100 16	100 66	99 63	100 21	100 19	100 77	100 09	98 92	99 26	100 14	99 95	99 26	100 44	100 21	99 87	99 81
Si	1 9517	1 9589	1 9593	1 9566	1 9669	1 9227	1 9211	1 9572	1 9504	1 9453	1 9788	1 9470	1 9483	1 9343	1 9845	1 9973	2 0108	1 9763	1 9847	1 9632	1 9677
Al	0 0000	0 0000	0 0000	0 0000	0 0000	0 0000	0 0000	0 0000	0 0000	0 0000	0 0000	0 0000	0 0000	0 0000	0 0000	0 0000	0 0000	0 0000	0 0000	0 0000	0 0000
Fe3+	0 0000	0 0000	0 0000	0 0000	0 0000	0 0000	0 0000	0 0000	0 0000	0 0000	0 0000	0 0000	0 0000	0 0000	0 0000	0 0000	0 0000	0 0000	0 0000	0 0000	0 0000
Al	0 0425	0 0434	0 0432	0 0409	0 0404	0 0705	0 0741	0 0384	0 0424	0 0451	0 0130	0 0477	0 0439	0 0518	0 0527	0 0301	0 0233	0 0425	0 0336	0 0522	0 0479
Fe3+	0 1094	0 0930	0 0883	0 1027	0 0690	0 1103	0 1085	0 0941	0 1138	0 1133	0 3057	0 1084	0 1112	0 1993	0 0144	0 0165	0 0000	0 0418	0 0334	0 0691	0 0668
Ti	0 0045	0 0051	0 0046	0 0046	0 0042	0 0034	0 0057	0 0039	0 0009	0 0058	0 0002	0 0063	0 0054	0 0039	0 0128	0 0047	0 0033	0 0079	0 0069	0 0090	0 0080
Cr	0 0000	0 0000	0 0000	0 0000	0 0000	0 0027	0 0027	0 0000	0 0000	0 0000	0 0000	0 0000	0 0000	0 0028	0 0001	0 0000	0 0002	0 0004	0 0000	0 0005	0 0001
Mg	0 5471	0 5503	0 5488	0 5473	0 5653	0 6953	0 7103	0 6427	0 6018	0 5952	0 4241	0 5495	0 5450	0 4295	0 6290	0 7387	0 7181	0 5717	0 6554	0 5346	0 5313
Fe2+	0 2965	0 3083	0 3151	0 3045	0 3210	0 1179	0 0986	0 2208	0 2412	0 2406	0 2198	0 2881	0 2945	0 3126	0 2911	0 2101	0 2551	0 3357	0 2707	0 3345	0 3460
Mn	0 0000	0 0000	0 0000	0 0000	0 0000	0 0000	0 0000	0 0000	0 0000	0 0000	0 0291	0 0000	0 0000	0 0000	0 0000	0 0000	0 0000	0 0000	0 0000	0 0000	0 0000
Mg	0 0000	0 0000	0 0000	0 0000	0 0000	0 0000	0 0000	0 0000	0 0000	0 0000	0 0000	0 0000	0 0000	0 0000	0 0000	0 0000	0 0000	0 0000	0 0000	0 0000	0 0000
Fe2+	0 0301	0 0265	0 0300	0 0281	0 0189	0 0431	0 0451	0 0406	0 0171	0 0397	0 0000	0 0363	0 0276	0 0087	0 0424	0 0425	0 0536	0 0330	0 0322	0 0367	0 0319
Mn	0 0374	0 0334	0 0353	0 0349	0 0334	0 0191	0 0166	0 0272	0 0274	0 0301	0 0000	0 0326	0 0339	0 0263	0 0272	0 0232	0 0281	0 0310	0 0292	0 0329	0 0338
Ca	0 9168	0 9170	0 9162	0 9184	0 9291	0 9795	0 9784	0 9203	0 9465	0 9242	0 7527	0 9212	0 9277	0 9002	0 8843	0 8866	0 8668	0 9064	0 9039	0 9009	0 9006
Na	0 0641	0 0642	0 0592	0 0680	0 0517	0 0356	0 0389	0 0548	0 0587	0 0606	0 2767	0 0628	0 0624	0 1304	0 0616	0 0504	0 0406	0 0532	0 0501	0 0663	0 0660
Total	4 0000	4 0000	4 0000	4 0000	4 0000	4 0000	4 0000	4 0000	4 0000	4 0000	4 0000	4 0000	4 0000	4 0000	4 0000	4 0000	4 0000	4 0000	4 0000	4 0000	4 0000

ORS107 CLINOPYROXENE

	1	2	3	4	5	6	7	8	9	10	11	12	13	14	15
	c	m	c	m	r		c	m	m	r					
SiO2	51 91	51 36	51 94	52 38	52 05	51 29	52 75	52 73	51 70	51 51	51 99	53 22	51 41	51 03	51 06
TiO2	0 38	0 37	0 40	0 41	0 33	0 26	0 50	0 47	0 43	0 34	0 39	0 34	0 30	0 34	0 27
Al2O3	1 01	1 05	1 08	1 10	1 08	1 36	1 31	1 28	1 16	1 08	1 15	1 21	1 24	1 16	1 26
Cr2O3	0 00	0 00	0 00	0 00	0 00	0 04	0 03	0 00	0 01	0 00	0 00	0 00	0 00	0 01	0 00
Fe2O3	1 66	1 72	1 76	1 20	1 40	2 99	2 15	1 01	1 31	1 22	0 00	3 45	2 29	1 31	2 98
FeO	11 18	12 76	11 01	10 22	11 09	13 49	7 57	8 80	12 13	13 20	12 41	6 04	13 44	14 32	13 41
MnO	0 80	0 94	0 82	0 82	0 81	0 87	0 74	0 79	0 85	0 89	0 83	0 79	0 92	1 01	1 03
MgO	10 21	8 98	10 14	11 71	10 24	8 80	11 95	12 25	9 37	8 67	10 19	12 00	8 00	7 62	7 46
CaO	21 99	22 02	22 31	21 90	22 34	21 08	22 79	21 58	21 98	21 92	21 38	22 12	22 21	22 22	21 83
Na2O	0 87	0 83	0 86	0 65	0 81	1 74	1 01	0 95	0 94	0 92	0 78	1 59	1 01	0 85	1 21
Total	100 01	100 01	100 30	100 38	100 16	99 90	100 82	99 86	99 87	99 75	99 13	100 75	100 82	99 86	100 50
Si	1 9751	1 9714	1 9713	1 9709	1 9762	1 9827	1 9632	1 9786	1 9775	1 9823	1 9933	1 9733	1 9678	1 9762	1 9854
Al	0 0000	0 0000	0 0000	0 0000	0 0000	0 0000	0 0000	0 0000	0 0000	0 0000	0 0000	0 0000	0 0000	0 0000	0 0000
Fe3+	0 0000	0 0000	0 0000	0 0000	0 0000	0 0000	0 0000	0 0000	0 0000	0 0000	0 0000	0 0000	0 0000	0 0000	0 0000
Al	0 0452	0 0476	0 0475	0 0487	0 0482	0 0621	0 0574	0 0565	0 0522	0 0489	0 0521	0 0527	0 0560	0 0531	0 0570
Fe3+	0 0474	0 0498	0 0503	0 0341	0 0401	0 0869	0 0603	0 0285	0 0376	0 0355	0 0000	0 0963	0 0658	0 0382	0 0863
Ti	0 0108	0 0107	0 0114	0 0115	0 0095	0 0074	0 0140	0 0133	0 0122	0 0098	0 0114	0 0095	0 0087	0 0098	0 0078
Cr	0 0000	0 0000	0 0000	0 0000	0 0000	0 0013	0 0010	0 0000	0 0003	0 0001	0 0000	0 0000	0 0000	0 0002	0 0001
Mg	0 5791	0 5134	0 5736	0 6568	0 5795	0 3915	0 6629	0 6852	0 5342	0 4972	0 5824	0 6628	0 4561	0 4398	0 4278
Fe2+	0 3175	0 3785	0 3172	0 2490	0 3226	0 4361	0 2043	0 2165	0 3634	0 4085	0 3542	0 1786	0 4133	0 4590	0 4210
Mn	0 0000	0 0000	0 0000	0 0000	0 0000	0 0146	0 0000	0 0000	0 0000	0 0000	0 0000	0 0000	0 0000	0 0000	0 0000
Mg	0 0000	0 0000	0 0000	0 0000	0 0000	0 0000	0 0000	0 0000	0 0000	0 0000	0 0000	0 0000	0 0000	0 0000	0 0000
Fe2+	0 0383	0 0310	0 0321	0 0726	0 0294	0 0000	0 0314	0 0598	0 0247	0 0162	0 0438	0 0086	0 0169	0 0048	0 0108
Mn	0 0259	0 0305	0 0264	0 0261	0 0261	0 0138	0 0234	0 0252	0 0274	0 0291	0 0270	0 0247	0 0298	0 0332	0 0335
Ca	0 8963	0 9058	0 9070	0 8830	0 9086	0 8730	0 9089	0 8676	0 9008	0 9037	0 8781	0 8789	0 9109	0 9223	0 9004
Na	0 0644	0 0614	0 0631	0 0474	0 0597	0 1305	0 0731	0 0688	0 0696	0 0687	0 0579	0 1146	0 0747	0 0635	0 0899
Total	4 0000	4 0000	4 0000	4 0000	4 0000	4 0000	4 0000	4 0000	4 0000	4 0000	4 0000	4 0000	4 0000	4 0000	4 0000

ORS108 CLINOPYROXENE

	1	2	3	4	5	6	7
SiO2	52 56	51 27	50 00	51 87	51 27	51 57	51 91
TiO2	0 30	0 15	0 24	0 31	0 27	0 26	0 33
Al2O3	0 76	0 90	1 26	1 03	0 79	1 16	1 36
Cr2O3	0 00	0 00	0 01	0 00	0 00	0 00	0 00
Fe2O3	2 71	3 03	4 01	3 58	3 29	4 32	5 04
FeO	7 71	11 95	14 38	7 90	11 85	7 66	6 39
MnO	0 80	0 86	1 15	0 87	0 97	0 89	0 75
MgO	11 69	8 34	5 72	10 99	8 38	10 57	11 01
CaO	22 56	22 21	21 15	22 39	21 81	22 76	21 78
Na2O	1 05	1 14	1 55	1 13	1 26	1 15	1 66
Total	100 14	99 87	99 45	100 07	99 89	100 34	100 23
Si	1 9745	1 9738	1 9634	1 9588	1 9735	1 9474	1 9496
Al	0 0000	0 0000	0 0000	0 0000	0 0000	0 0000	0 0000
Fe3+	0 0000	0 0000	0 0000	0 0000	0 0000	0 0000	0 0000
Al	0 0337	0 0410	0 0584	0 0457	0 0358	0 0516	0 0601
Fe3+	0 0766	0 0878	0 1184	0 1017	0 0954	0 1229	0 1426
Ti	0 0086	0 0043	0 0069	0 0089	0 0079	0 0075	0 0094
Cr	0 0000	0 0001	0 0002	0 0000	0 0000	0 0000	0 0000
Mg	0 6544	0 4785	0 3349	0 6184	0 4807	0 5951	0 6162
Fe2+	0 2267	0 3848	0 4721	0 2252	0 3801	0 2230	0 1717
Mn	0 0000	0 0034	0 0090	0 0000	0 0000	0 0000	0 0000
Mg	0 0000	0 0000	0 0000	0 0000	0 0000	0 0000	0 0000
Fe2+	0 0154	0 0000	0 0000	0 0244	0 0012	0 0189	0 0291
Mn	0 0256	0 0247	0 0291	0 0278	0 0315	0 0283	0 0239
Ca	0 9079	0 9163	0 8898	0 9060	0 8995	0 9210	0 8765
Na	0 0766	0 0852	0 1177	0 0829	0 0942	0 0843	0 1209
Total	4 0000	4 0000	4 0000	4 0000	4 0000	4 0000	4 0000

ORS108 CLINOPYROXENE

	8	9	10	11	12	13	14	15	16	17	18	19	20	21	22	23
SiO2	51 82	52 34	52 81	52 29	52.35	51 99	52 52	51 22	50 59	52 10	52 06	52 13	51 85	51 62	51 64	50 59
TiO2	0 32	0 24	0 20	0 27	0 29	0 28	0 14	0 27	0 36	0 37	0 45	0 48	0 41	0 44	0 38	0 49
Al2O3	1 34	0 87	1 01	1 13	1 15	1 04	0 89	1 28	1 06	3 26	1 22	1 30	1 11	1 31	1 00	1 35
Cr2O3	0 00	0 00	0 00	0 00	0 00	0 00	0 00	0 00	0 00	0 00	0 00	0 00	0 00	0 00	0 00	0 01
Fe2O3	5 08	4 40	4 34	3 40	3 72	4 17	3 62	4 55	3 78	2 53	5 72	6 61	5 58	5 81	5 16	4 97
FeO	5 47	5 47	5 41	6 40	6 08	5 63	6 79	7 49	12 00	8 79	4 81	4 54	4 47	4 72	6 08	8 95
MnO	0 78	0 78	0 85	0 79	0 81	0 79	0 85	0 87	1 12	0 81	0 80	0 77	0 81	0 87	0 86	0 88
MgO	11 42	11 81	12 59	12 11	12 09	11 96	12 47	10 29	8 73	10 43	12 50	11 98	12 53	12 73	12 56	9 35
CaO	21 77	22 77	22 18	22 39	22 26	22 60	21 71	22 37	20 43	20 08	21 99	21 64	22 24	21 65	22 15	22 75
Na2O	1 67	1 36	1 34	1 14	1 27	1 23	1 13	1 32	1 28	1 88	1 42	1 81	1 35	1 32	0 94	1 14
Total	99 68	100 04	100 73	99 93	100 04	99.70	100 12	99 64	99 35	100 23	100 98	101 26	100 35	100 46	100 79	100 47
Si	1.9501	1 9618	1 9596	1 9610	1.9600	1.9548	1.9663	1.9473	1.9585	1.9504	1 9319	1 9310	1.9346	1 9250	1.9289	1 9265
Al	0 0000	0 0000	0 0000	0 0000	0.0000	0 0000	0.0000	0.0000	0.0000	0.0000	0 0000	0 0000	0.0000	0 0000	0.0000	0 0000
Fe3+	0 0000	0.0000	0 0000	0 0000	0 0000	0 0000	0.0000	0.0000	0.0000	0.0000	0.0000	0.0000	0.0000	0.0000	0 0000	0 0000
Al	0 0596	0 0383	0 0442	0.0499	0.0507	0.0459	0.0392	0.0575	0.0484	0.1437	0.0534	0 0570	0.0487	0 0575	0 0442	0 0604
Fe3+	0 1438	0.1242	0 1213	0.0960	0.1049	0.1179	0.1019	0.1301	0.1101	0.0712	0 1599	0 1842	0.1566	0 1630	0 1450	0 1426
Ti	0 0091	0 0068	0 0057	0.0077	0.0083	0.0080	0.0040	0.0076	0.0103	0.0104	0 0125	0 0133	0 0116	0 0124	0.0106	0 0139
Cr	0 0000	0 0000	0 0000	0 0000	0 0000	0.0001	0 0000	0 0000	0 0000	0 0000	0 0000	0 0000	0.0000	0 0000	0 0000	0.0004
Mg	0 6402	0.6594	0 6963	0 6768	0.6748	0.6705	0.6959	0.5828	0.5036	0.5816	0.6915	0 6613	0.6967	0 7075	0 6991	0 5304
Fe2+	0 1472	0 1713	0.1328	0 1697	0 1613	0.1576	0.1590	0.2220	0.3275	0.1931	0 0827	0 0842	0.0863	0 0595	0 1010	0 2524
Mn	0.0000	0.0000	0.0000	0.0000	0 0000	0.0000	0.0000	0.0000	0.0000	0.0000	0 0000	0.0000	0.0000	0.0000	0 0000	0.0000
Mg	0 0000	0 0000	0 0000	0 0000	0 0000	0 0000	0.0000	0.0000	0.0000	0.0000	0.0000	0.0000	0.0000	0.0000	0.0000	0.0000
Fe2+	0.0249	0.0001	0 0355	0 0311	0.0290	0.0196	0.0538	0.0161	0.0610	0.0820	0.0665	0.0564	0.0532	0.0876	0.0890	0 0327
Mn	0.0250	0.0248	0.0268	0.0251	0.0258	0.0252	0.0271	0.0280	0.0368	0.0258	0.0252	0.0241	0 0256	0.0274	0.0272	0 0283
Ca	0.8780	0.9144	0.8821	0.8996	0.8930	0.9107	0.8710	0.9112	0.8475	0.8053	0.8744	0.8587	0.8889	0.8648	0.8866	0.9282
Na	0 1220	0.0992	0.0961	0.0832	0.0922	0.0897	0.0818	0.0973	0.0961	0.1365	0.1020	0 1297	0.0977	0.0953	0.0683	0 0842
Total	4.0000	4.0000	4.0000	4.0000	4 0000	4.0000	4.0000	4.0000	4.0000	4.0000	4.0000	4.0000	4.0000	4 0000	4.0000	4 0000

ORS61 AMPH

	1	2	3	4	5	6	7	8	9	10
						c	r		c	r
SiO2	38.72	38.84	38.01	37.70	38.27	39.32	39.85	38.46	37.69	38.65
TiO2	2.38	3.44	3.44	2.90	1.92	2.97	3.81	3.01	2.24	2.17
Al2O3	11.12	10.51	10.92	11.52	11.33	10.66	10.96	11.52	12.28	10.91
Fe2O3	3.67	1.49	2.99	3.87	4.53	3.26	0.39	1.99	4.20	2.96
FeO	22.89	23.83	23.06	22.93	22.51	21.59	22.26	22.31	22.16	23.71
MnO	0.75	0.86	0.85	0.84	0.82	0.85	0.71	0.77	0.79	0.85
MgO	4.42	4.51	4.23	3.88	4.19	5.45	6.18	5.30	4.29	4.07
CaO	10.55	10.56	10.44	10.39	10.54	10.59	10.96	10.99	10.77	10.55
Na2O	3.07	2.99	2.95	2.97	3.02	3.02	3.02	2.94	2.86	3.08
K2O	1.46	1.45	1.42	1.52	1.49	1.37	1.41	1.51	1.62	1.49
Tot	99.04	98.48	98.31	98.52	98.62	99.09	99.55	98.79	98.89	98.43
Si	6.0822	6.1339	6.0228	5.9740	6.0489	6.1233	6.1412	6.0235	5.9321	6.1289
ivAl	1.9178	1.8661	1.9772	2.0260	1.9511	1.8767	1.8588	1.9765	2.0679	1.8711
Fe3+	0.0000	0.0000	0.0000	0.0000	0.0000	0.0000	0.0000	0.0000	0.0000	0.0000
Ti4+	0.0000	0.0000	0.0000	0.0000	0.0000	0.0000	0.0000	0.0000	0.0000	0.0000
viAl	0.1417	0.0907	0.0634	0.1259	0.1601	0.0804	0.1324	0.1506	0.2105	0.1685
Ti	0.2812	0.4086	0.4097	0.3456	0.2282	0.3478	0.4416	0.3543	0.2651	0.2588
Fe3+	0.4342	0.1772	0.3571	0.4614	0.5391	0.3824	0.0451	0.2341	0.4969	0.3527
Fe2+	3.0077	3.1473	3.0554	3.0382	2.9758	2.8124	2.8687	2.9217	2.9160	3.1445
Mg	1.0348	1.0615	0.9997	0.9162	0.9870	1.2649	1.4194	1.2371	1.0062	0.9619
Mn	0.1003	0.1148	0.1147	0.1127	0.1098	0.1121	0.0929	0.1022	0.1053	0.1136
Mg	0.0000	0.0000	0.0000	0.0000	0.0000	0.0000	0.0000	0.0000	0.0000	0.0000
Fe2+	0.0000	0.0000	0.0000	0.0000	0.0000	0.0000	0.0000	0.0000	0.0000	0.0000
Mn	0.0000	0.0000	0.0000	0.0000	0.0000	0.0000	0.0000	0.0000	0.0000	0.0000
Ca	1.7759	1.7870	1.7719	1.7640	1.7847	1.7671	1.8093	1.8443	1.8162	1.7926
Na	0.2241	0.2130	0.2281	0.2360	0.2153	0.2329	0.1907	0.1557	0.1838	0.2074
Na	0.7110	0.7019	0.6783	0.6764	0.7102	0.6790	0.7117	0.7371	0.6889	0.7393
K	0.2926	0.2922	0.2871	0.3073	0.3005	0.2722	0.2772	0.3017	0.3253	0.3004

ORS107 AMPH

	1	2	3	4	5	6	7	8	9	10	11	12
SiO2	39.97	39.88	39.41	39.46	39.49	39.49	39.55	39.29	38.40	39.17	39.40	39.01
TiO2	3.48	2.51	1.51	3.45	3.48	3.41	3.49	3.45	2.90	2.87	3.00	2.95
Al2O3	9.68	10.10	10.58	10.02	10.07	10.03	10.09	10.05	11.24	11.10	11.05	11.25
Fe2O3	0.00	2.31	4.21	1.00	1.17	1.43	1.48	0.42	0.00	1.34	0.15	0.30
FeO	23.49	22.31	20.72	22.68	22.48	22.22	22.20	22.96	23.07	22.29	22.36	22.48
MnO	0.91	0.95	0.95	0.93	0.98	0.93	0.90	0.90	0.77	0.80	0.75	0.72
MgO	5.45	5.40	5.48	5.78	5.85	5.96	5.87	5.80	5.48	5.66	5.73	5.69
CaO	10.41	10.32	10.24	10.67	10.83	10.76	10.76	11.02	11.35	11.17	10.99	11.03
Na2O	3.26	3.27	3.21	3.22	3.06	3.15	3.06	2.99	2.88	2.76	2.76	2.87
K2O	1.51	1.52	1.57	1.49	1.49	1.44	1.36	1.43	1.48	1.50	1.44	1.51
Tot	98.16	98.57	97.87	98.71	98.90	98.81	98.77	98.33	97.57	98.86	97.63	97.81
Si	6.2955	6.2520	6.2113	6.1808	6.1699	6.1703	6.1752	6.1788	6.0922	6.1225	6.1955	6.1394
ivAl	1.7045	1.7480	1.7887	1.8192	1.8301	1.8297	1.8248	1.8212	1.9078	1.8775	1.8045	1.8606
Fe3+	0.0000	0.0000	0.0000	0.0000	0.0000	0.0000	0.0000	0.0000	0.0000	0.0000	0.0000	0.0000
Ti4+	0.0000	0.0000	0.0000	0.0000	0.0000	0.0000	0.0000	0.0000	0.0000	0.0000	0.0000	0.0000
viAl	0.0935	0.1161	0.1777	0.0317	0.0240	0.0179	0.0329	0.0427	0.1945	0.1679	0.2441	0.2269
Ti	0.4121	0.2964	0.1784	0.4068	0.4093	0.4002	0.4098	0.4083	0.3458	0.3377	0.3548	0.3489
Fe3+	0.0000	0.2728	0.4997	0.1180	0.1381	0.1683	0.1738	0.0495	0.0000	0.1580	0.0177	0.0358
Fe2+	3.0940	2.9247	2.7315	2.9712	2.9377	2.9039	2.8982	3.0196	3.0606	2.9130	2.9410	2.9587
Mg	1.2791	1.2614	1.2863	1.3495	1.3611	1.3869	1.3659	1.3601	1.2957	1.3180	1.3422	1.3342
Mn	0.1213	0.1266	0.1264	0.1228	0.1297	0.1228	0.1194	0.1199	0.1034	0.1054	0.1001	0.0955
Mg	0.0000	0.0000	0.0000	0.0000	0.0000	0.0000	0.0000	0.0000	0.0000	0.0000	0.0000	0.0000
Fe2+	0.0000	0.0000	0.0000	0.0000	0.0000	0.0000	0.0000	0.0000	0.0000	0.0000	0.0000	0.0000
Mn	0.0000	0.0000	0.0000	0.0000	0.0000	0.0000	0.0000	0.0000	0.0000	0.0000	0.0000	0.0000
Ca	1.7574	1.7329	1.7290	1.7904	1.8131	1.8016	1.8004	1.8570	1.9300	1.8711	1.8520	1.8604
Na	0.2426	0.2671	0.2710	0.2096	0.1869	0.1984	0.1996	0.1430	0.0700	0.1289	0.1480	0.1396
Na	0.7515	0.7270	0.7095	0.7669	0.7397	0.7547	0.7274	0.7688	0.8163	0.7062	0.6926	0.7362
K	0.3034	0.3044	0.3159	0.2986	0.2964	0.2868	0.2706	0.2867	0.3003	0.2989	0.2885	0.3034

ORS107 AMPH

	13	14	15	16	17	18	19	20	21	22	23	24
	c	r				c	m	r				
SiO2	39.43	39.15	39.07	39.44	38.88	39.37	39.36	40.01	39.86	39.87	39.53	38.87
TiO2	2.94	2.50	2.03	1.81	2.07	2.95	2.51	3.20	3.39	3.03	1.97	2.11
Al2O3	10.86	11.48	11.24	11.04	10.88	11.22	10.94	10.50	10.34	10.43	10.87	11.63
Fe2O3	0.00	0.35	1.77	3.50	5.47	2.20	2.75	0.83	1.05	2.55	2.72	3.63
FeO	22.25	22.64	22.33	21.86	20.70	21.14	21.86	21.90	21.63	22.09	21.55	20.91
MnO	0.80	0.88	0.80	0.92	0.78	0.78	0.96	0.88	0.91	0.91	0.90	0.84
MgO	5.80	5.40	5.01	4.91	4.56	5.68	5.32	6.02	5.90	5.30	5.38	5.35
CaO	11.06	10.90	10.53	10.34	9.49	10.78	10.66	10.67	10.39	10.35	10.29	10.69
Na2O	2.84	2.95	2.95	2.92	3.20	2.58	2.95	3.07	3.07	3.17	3.24	2.91
K2O	1.50	1.64	1.63	1.61	1.59	1.52	1.57	1.35	1.31	1.31	1.54	1.50
Tot	97.58	97.88	97.35	98.24	97.63	98.21	98.89	98.43	97.95	99.01	97.98	98.44
Si	6.2134	6.1644	6.1945	6.1976	6.1519	6.1471	6.1491	6.2333	6.2485	6.2056	6.2164	6.0823
ivAl	1.7866	1.8356	1.8055	1.8024	1.8481	1.8529	1.8509	1.7667	1.7515	1.7944	1.7836	1.9177
Fe3+	0.0000	0.0000	0.0000	0.0000	0.0000	0.0000	0.0000	0.0000	0.0000	0.0000	0.0000	0.0000
Ti4+	0.0000	0.0000	0.0000	0.0000	0.0000	0.0000	0.0000	0.0000	0.0000	0.0000	0.0000	0.0000
viAl	0.2498	0.2956	0.2963	0.2431	0.1817	0.2124	0.1629	0.1620	0.1541	0.1201	0.2321	0.2282
Ti	0.3483	0.2958	0.2416	0.2251	0.2465	0.3459	0.2948	0.3749	0.3988	0.3547	0.2325	0.2477
Fe3+	0.0000	0.0411	0.2109	0.4140	0.6519	0.2582	0.3233	0.0968	0.1237	0.2987	0.3218	0.4279
Fe2+	2.9324	2.9812	2.9606	2.8449	2.7393	2.7596	2.8554	2.8535	2.8284	2.8762	2.8343	2.7365
Mg	1.3632	1.2683	1.1834	1.1501	1.0756	1.3211	1.2370	1.3965	1.3748	1.2305	1.2589	1.2478
Mn	0.1064	0.1180	0.1072	0.1228	0.1049	0.1030	0.1266	0.1164	0.1203	0.1198	0.1195	0.1117
Mg	0.0000	0.0000	0.0000	0.0000	0.0000	0.0000	0.0000	0.0000	0.0000	0.0000	0.0000	0.0000
Fe2+	0.0000	0.0000	0.0000	0.0000	0.0000	0.0000	0.0000	0.0000	0.0000	0.0000	0.0000	0.0000
Mn	0.0000	0.0000	0.0000	0.0000	0.0000	0.0000	0.0000	0.0000	0.0000	0.0000	0.0000	0.0000
Ca	1.8677	1.8391	1.7896	1.7416	1.6099	1.8027	1.7843	1.7818	1.7411	1.7255	1.7336	1.7916
Na	0.1323	0.1609	0.2104	0.2584	0.3901	0.1973	0.2157	0.2182	0.2589	0.2745	0.2664	0.2084
Na	0.7366	0.7384	0.6950	0.6313	0.5903	0.5844	0.6787	0.7081	0.6732	0.6813	0.7229	0.6746
K	0.3006	0.3298	0.3305	0.3222	0.3214	0.3034	0.3122	0.2682	0.2618	0.2594	0.3082	0.2999

ORS108 AMPH

	1	2	3	4	5	6	7	8	9	10
	c	r						c	r	
SiO2	39.37	39.11	38.21	38.57	39.29	38.50	38.27	38.36	38.69	38.54
TiO2	3.93	3.92	2.84	3.80	3.97	2.55	3.16	2.31	3.75	3.50
Al2O3	10.16	10.36	10.56	10.29	10.20	10.64	10.71	10.51	10.02	9.88
Fe2O3	0.86	0.38	2.35	0.00	0.36	2.31	2.68	2.59	1.38	1.61
FeO	21.47	22.02	24.42	22.87	21.91	23.24	24.05	23.12	24.21	24.39
MnO	0.80	0.78	0.83	0.87	0.87	0.83	0.86	0.92	0.99	0.90
MgO	6.12	5.99	3.60	5.46	6.22	4.55	3.81	4.33	4.24	3.97
CaO	10.63	10.75	10.86	10.77	10.73	10.71	10.53	10.27	10.22	10.17
Na2O	2.79	2.91	2.67	3.02	3.06	2.94	2.86	3.19	3.21	3.11
K2O	1.38	1.34	1.38	1.36	1.38	1.42	1.41	1.48	1.41	1.38
Tot	97.51	97.57	97.52	97.10	97.99	97.68	98.35	97.07	98.12	97.44
Si	6.1892	6.1580	6.1277	6.1423	6.1615	6.1320	6.0815	6.1563	6.1515	6.1782
ivAl	1.8108	1.8420	1.8723	1.8577	1.8385	1.8680	1.9185	1.8437	1.8485	1.8218
Fe3+	0.0000	0.0000	0.0000	0.0000	0.0000	0.0000	0.0000	0.0000	0.0000	0.0000
Ti4+	0.0000	0.0000	0.0000	0.0000	0.0000	0.0000	0.0000	0.0000	0.0000	0.0000
viAl	0.0724	0.0813	0.1246	0.0732	0.0468	0.1303	0.0871	0.1449	0.0290	0.0442
Ti	0.4641	0.4647	0.3427	0.4553	0.4685	0.3057	0.3781	0.2791	0.4488	0.4214
Fe3+	0.1016	0.0453	0.2835	0.0000	0.0426	0.2766	0.3207	0.3127	0.1655	0.1939
Fe2+	2.8227	2.8994	3.2757	3.0586	2.8732	3.0962	3.1965	3.1033	3.2189	3.2701
Mg	1.4330	1.4049	0.8608	1.2963	1.4532	1.0798	0.9014	1.0355	1.0039	0.9486
Mn	0.1061	0.1043	0.1128	0.1167	0.1157	0.1114	0.1162	0.1245	0.1339	0.1218
Mg	0.0000	0.0000	0.0000	0.0000	0.0000	0.0000	0.0000	0.0000	0.0000	0.0000
Fe2+	0.0000	0.0000	0.0000	0.0000	0.0000	0.0000	0.0000	0.0000	0.0000	0.0000
Mn	0.0000	0.0000	0.0000	0.0000	0.0000	0.0000	0.0000	0.0000	0.0000	0.0000
Ca	1.7901	1.8142	1.8327	1.8378	1.8025	1.8278	1.7935	1.7654	1.7412	1.7458
Na	0.2099	0.1858	0.1673	0.1622	0.1975	0.1722	0.2065	0.2346	0.2588	0.2542
Na	0.6410	0.7020	0.6643	0.7703	0.7336	0.7342	0.6747	0.7501	0.7512	0.7180
K	0.2774	0.2698	0.2820	0.2763	0.2761	0.2877	0.2903	0.3045	0.2851	0.2840

	ORS108 AMPH													
	11	12	13	14	15	16	17	18	19	20	21 c	22 r	23	24
SiO2	38 75	38 96	39 03	38 34	38 98	38 97	39 22	38 71	39 45	39 05	39 12	38 60	38 11	37 88
TiO2	2 92	3 65	3 48	1 69	3 99	3 54	4 03	2 94	1 95	3 85	3 89	3 85	3 38	2 98
Al2O3	10 14	10 00	10 11	10 82	10 14	10 44	10 13	10 33	10 37	10 15	10 07	10 18	10 35	11 04
Fe2O3	2 17	0 58	1 12	5 29	0 03	1 94	0 73	2 78	3 64	0 00	0 00	0 00	0 83	1 11
FeO	23 19	24 26	24 51	22 15	22 70	21 53	22 38	21 40	23 95	23 83	22 74	23 22	24 20	25 14
MnO	0 98	0 94	0 87	0 92	0 67	0 73	0 76	0 76	0 92	0 93	0 95	0 84	1 04	1 09
MgO	4 38	4 49	4 37	4 00	6 30	6 22	6 23	5 94	3 94	5 12	5 40	5 14	4 16	3 48
CaO	10 26	10 28	10 56	10 15	10 99	10 74	10 82	10 83	10 26	10 65	10 95	10 92	10 53	10 68
Na2O	3 06	3 22	3 05	3 05	3 18	3 25	3 20	3 05	3 20	3 10	2 98	3 03	3 01	3 01
K2O	1 30	1 39	1 41	1 51	1 50	1 42	1 50	1 43	1 58	1 43	1 42	1 43	1 40	1 55
Tot	97 14	97 78	98 50	97 92	98 49	98 77	99 00	98 17	99 25	97 92	97 52	97 22	97 01	97 96
Si	6 1974	6 1993	6 1761	6 1075	6 1121	6 0818	6 1133	6 0935	6 2119	6 1844	6 2183	6 1727	6 1315	6 0720
ivAl	1 8026	1 8007	1 8239	1 8925	1 8738	1 9182	1 8626	1 9065	1 7881	1 8156	1 7817	1 8273	1 8685	1 9280
Fe3+	0 0000	0 0000	0 0000	0 0000	0 0141	0 0000	0 0241	0 0000	0 0000	0.0000	0 0000	0.0000	0 0000	0 0000
Ti4+	0.0000	0 0000	0.0000	0.0000	0 0102	0 0000	0 0000	0 0000	0 0000	0.0000	0 0000	0.0000	0 0000	0 0000
viAl	0 1094	0 0751	0 0617	0.1395	0.0000	0.0022	0 0000	0 0111	0.1380	0.0799	0.1054	0 0911	0 0953	0.1573
Ti	0 3511	0 4367	0.4144	0 2027	0.4604	0.4151	0.4726	0 3476	0.2310	0 4587	0 4651	0.4634	0.4088	0.3587
Fe3+	0 2612	0 0694	0 1332	0.6342	−0.0102	0.2273	0.0616	0 3295	0 4308	0 0000	0.0000	0.0000	0.1008	0.1335
Fe2+	3 1019	3.2280	3.2431	2.9503	2.9771	2.8108	2.9178	2 8165	3.1538	3 1295	3.0234	3.1059	3 2568	3 3705
Mg	1.0443	1.0639	1.0310	0.9488	1.4733	1.4476	1.4479	1 3944	0.9237	1 2073	1.2785	1.2253	0.9965	0.8318
Mn	0 1321	0.1268	0 1166	0 1245	0 0892	0.0971	0.1001	0 1009	0 1226	0.1247	0.1276	0.1142	0.1417	0.1481
Mg	0 0000	0.0000	0.0000	0.0000	0.0000	0.0000	0.0000	0 0000	0.0000	0.0000	0.0000	0.0000	0.0000	0 0000
Fe2+	0 0000	0 0000	0 0000	0.0000	0.0000	0 0000	0 0000	0 0000	0 0000	0 0000	0 0000	0 0000	0 0000	0 0000
Mn	0 0000	0 0000	0.0000	0.0000	0.0000	0 0000	0 0000	0 0000	0 0000	0.0000	0 0000	0.0000	0 0000	0 0000
Ca	1 7575	1.7527	1.7905	1 7328	1.8457	1.7964	1.8074	1.8265	1.7317	1.8078	1.8644	1.8711	1.8145	1.8345
Na	0.2425	0.2473	0.2095	0.2672	0.1543	0.2036	0 1926	0.1735	0.2683	0.1922	0.1356	0.1289	0.1855	0.1655
Na	0 7068	0.7470	0.7254	0 6742	0 8112	0.7794	0 7745	0 7577	0.7081	0 7606	0.7822	0.8096	0 7535	0 7685
K	0.2655	0.2830	0.2844	0 3064	0.2999	0.2828	0.2980	0.2865	0.3175	0.2898	0.2888	0.2910	0.2867	0.3167

ORS90 BIOTITE

	1	2	3	4	5	6	7	8	9
SiO2	35 15	34 99	35 23	34 88	34 99	35 22	34 96	35 09	34 96
TiO2	5 35	6 08	5 74	5 21	5 39	4 87	4 52	5 12	4 28
Al2O3	12 76	13 16	13 13	13 31	13 01	12 91	13 06	12 92	12 85
FeO	24 16	22 26	22 52	24 54	24 37	24 28	24 07	24 04	23 69
MnO	0 47	0 53	0 49	0 50	0 53	0 55	0 53	0 51	0 54
MgO	8 78	9 31	9 42	8 39	8 48	8 80	8 97	8 75	9 51
CaO	0 00	0 00	0 00	0 00	0 00	0 00	0 00	0 00	0 01
Na2O	0 25	0 23	0 32	0 23	0 11	0 19	0 18	0 18	0 13
K2O	8 70	8 76	8 50	9 00	9 03	8 91	8 90	8 86	9 02
Tot	95 62	95 31	95 35	96 07	95 88	95 72	95 18	95 48	95 00
Si	5 5083	5 4536	5 4838	5 4594	5 4828	5 5212	5 5091	5 5088	5 5165
Ti	0 6306	0 7129	0 6721	0 6134	0 6347	0 5736	0 5358	0 6041	0 5081
Al	2 3578	2 4176	2 4102	2 4566	2 4027	2 3866	2 4257	2 3919	2 3904
Fe2+	3 1657	2 9020	2 9310	3 2127	3 1934	3 1834	3 1724	3 1563	3 1259
Mn	0 0628	0 0695	0 0641	0 0668	0 0702	0 0724	0 0709	0 0681	0 0723
Mg	2 0503	2 1629	2 1857	1 9569	1 9792	2 0549	2 1065	2 0466	2 2364
Ca	0 0005	0 0000	0 0000	0 0000	0 0000	0 0000	0 0000	0 0000	0 0024
Na	0 0744	0 0701	0 0962	0 0695	0 0322	0 0581	0 0535	0 0560	0 0398
K	1 7382	1 7427	1 6880	1 7964	1 8043	1 7819	1 7902	1 7745	1 8164
Tot	15 5886	15 5312	15 5311	15 6318	15 5994	15 6319	15 6641	15 6063	15 7082

ORS94 BIOTITE

	1	2	3	4
	c	r		
SiO2	35 64	34 89	35 02	35 20
TiO2	4 89	5 31	4 92	5 50
Al2O3	12 82	12 91	12 92	12 67
FeO	23 88	23 42	23 80	23 49
MnO	0 51	0 61	0 56	0 55
MgO	9 01	8 41	8 72	8 80
CaO	0 00	0 16	0 00	0 00
Na2O	0 32	0 38	0 25	0 35
K2O	8 96	8 47	8 77	8 58
Tot	96 02	94 55	94 95	95 13
Si	5 5545	5 5157	5 5237	5 5272
Ti	0 5737	0 6310	0 5830	0 6490
Al	2 3555	2 4054	2 4019	2 3452
Fe2+	3 1128	3 0960	3 1389	3 0850
Mn	0 0673	0 0813	0 0752	0 0730
Mg	2 0917	1 9821	2 0498	2 0597
Ca	0 0000	0 0268	0 0000	0 0000
Na	0 0964	0 1174	0 0752	0 1050
K	1 7809	1 7075	1 7646	1 7191
Tot	15 6327	15 5631	15 6123	15 5633

ORS102 BIOTITE

	1	2	3	4	5	6	7
		c	r			c	r
SiO2	35 41	35 54	35 05	35 37	35 57	35 68	35 23
TiO2	5 08	5 31	5 64	4 59	4 57	3 54	2 65
Al2O3	13 27	13 37	13 37	13 39	13 12	13 09	12 50
FeO	23 59	23 45	24 66	24 35	23 00	23 70	27 94
MnO	0 53	0 49	0 56	0 52	0 47	0 50	0 90
MgO	8 92	9 04	8 20	8 71	9 41	9 71	6 88
CaO	0 00	0 00	0 00	0 00	0 03	0 00	0 00
Na2O	0 26	0 27	0 29	0 28	0 30	0 26	0 09
K2O	8 81	8 79	8 66	8 63	8 56	8 50	8 71
Tot	95 83	96 25	96 42	95 84	95 02	94 97	94 91
Si	5 5161	5 5030	5 4555	5 5234	5 5643	5 5992	5 6740
Ti	0 5923	0 6185	0 6600	0 5391	0 5371	0 4153	0 3211
Al	2 4367	2 4411	2 4527	2 4650	2 4187	2 4223	2 3740
Fe2+	3 0741	3 0367	3 2105	3 1794	3 0083	3 1104	3 7641
Mn	0 0693	0 0637	0 0738	0 0689	0 0619	0 0658	0 1232
Mg	2 0699	2 0867	1 9016	2 0267	2 1943	2 2712	1 6522
Ca	0 0000	0 0000	0 0000	0 0000	0 0050	0 0002	0 0000
Na	0 0797	0 0799	0 0875	0 0857	0 0922	0 0778	0 0292
K	1 7501	1 7365	1 7204	1 7192	1 7072	1 7022	1 7894
Tot	15 5882	15 5661	15 5621	15 6075	15 5890	15 6644	15 7272

ORS107 BIOTITE

	1	2	3	4	5	6	7
	c	m	r				
SiO2	35 52	34 91	34 84	34 53	35 41	35 27	35 19
TiO2	2 91	4 50	4 13	4 11	3 93	4 35	3 18
Al2O3	12 74	13 49	13 48	13 29	13 41	13 04	13 55
FeO	25 99	26 87	26 87	27 03	27 65	26 90	26 54
MnO	0 69	0 71	0 80	0 74	0 72	0 73	0 65
MgO	8 95	7 10	7 05	7 22	7 02	8 95	7 20
CaO	0 00	0 00	0 00	0 00	0 00	0 00	0 00
Na2O	0 36	0 25	0 24	0 28	0 27	0 27	0 24
K2O	8 41	8 69	8 84	8 47	8 96	8 83	8 78
Tot	95 59	96 53	96 25	95 67	97 36	96 34	95 31
Si	5 6088	5 4905	5 5041	5 4879	5 5399	5 5627	5 5929
Ti	0 3454	0 5324	0 4907	0 4918	0 4621	0 5156	0 3802
Al	2 3715	2 5006	2 5099	2 4903	2 4728	2 4242	2 5387
Fe2+	3 4321	3 5342	3 5510	3 5930	3 6186	3 5474	3 5275
Mn	0 0928	0 0951	0 1071	0 0998	0 0954	0 0980	0 0875
Mg	2 1065	1 6638	1 6596	1 7111	1 6373	1 6322	1 7043
Ca	0 0000	0 0000	0 0000	0 0000	0 0000	0 0000	0 0000
Na	0 1108	0 0771	0 0735	0 0851	0 0819	0 0832	0 0730
K	1 6949	1 7431	1 7821	1 7177	1 7891	1 7761	1 7798
Tot	15 7629	15 6368	15 6780	15 6785	15 6971	15 6393	15 6840

ORS108 BIOTITE

	1	2	3	4	5	6	7	8
SiO2	34 38	34 36	33 99	33 75	34 68	33 66	34 05	34 27
TiO2	3 99	4 27	3 58	3 78	4 36	4 10	4 69	4 04
Al2O3	13 05	13 28	13 51	13 27	13 49	13 62	13 16	13 31
FeO	29 82	30 17	30 10	30 50	30 58	30 32	30 14	29 25
MnO	0 66	0 73	0 70	0 73	0 77	0 70	0 80	0 64
MgO	4 84	4 81	5 09	4 74	4 81	4 71	4 44	4 99
CaO	0 00	0 00	0 00	0 00	0 00	0 00	0 00	0 00
Na2O	0 24	0 22	0 16	0 16	0 20	0 17	0 24	0 23
K2O	8 78	8 72	8 68	8 48	8 96	8 57	8 63	7 92
Tot	95 75	96 54	95 81	95 42	97 86	95 84	96 15	94 63
Si	5 5458	5 5011	5 4859	5 4834	5 4854	5 4383	5 4815	5 5491
Ti	0 4840	0 5143	0 4351	0 4617	0 5186	0 4980	0 5679	0 4916
Al	2 4817	2 5061	2 5702	2 5415	2 5161	2 5951	2 4979	2 5410
Fe2+	4 0229	4 0407	4 0632	4 1445	4 0454	4 0969	4 0579	3 9610
Mn	0 0896	0 0983	0 0961	0 1005	0 1029	0 0953	0 1088	0 0874
Mg	1 1640	1 1471	1 2249	1 1483	1 1347	1 1339	1 0642	1 2046
Ca	0 0000	0 0000	0 0000	0 0000	0 0000	0 0000	0 0000	0 0000
Na	0 0758	0 0668	0 0504	0 0507	0 0613	0 0517	0 0752	0 0716
K	1 8069	1 7809	1 7866	1 7576	1 8082	1 7661	1 7714	1 6368
Tot	15 6707	15 6554	15 7124	15 6883	15 6727	15 6751	15 6249	15 5430

ORS102 ALKALI-FELDSPAR

	1	2	3	4	5
	c	m	r		
SiO2	66.16	66.94	64.43	64.73	66.94
Al2O3	21.10	19.75	18.49	18.26	19.75
FeO	0.05	0.07	0.07	0.07	0.07
CaO	2.02	0.62	0.08	0.07	0.62
Na2O	10.59	9.41	1.72	1.26	9.41
K2O	0.20	2.74	14.95	15.52	2.74
Total	100.12	99.54	99.74	99.91	99.53
An	9.42	2.98	0.38	0.33	2.97
Ab	89.50	81.42	14.80	10.97	81.44
Or	1.08	15.60	84.82	88.70	15.60
Na+K/Al	0.84	0.93	1.03	1.03	0.93

ORS107 ALKALI-FELDSPAR

	1	2	3	4	5	6	7	8	9	10	11	12	13	14
						c	m	r						
SiO2	64.84	65.38	66.45	66.93	65.32	67.01	65.19	66.31	67.92	65.54	65.39	66.09	66.05	66.03
Al2O3	18.35	18.42	19.19	19.15	18.75	19.29	18.96	19.01	19.37	18.92	18.45	18.95	19.03	18.91
FeO	0.07	0.04	0.05	0.09	0.05	0.01	0.01	0.09	0.04	0.04	0.05	0.07	0.07	0.05
CaO	0.00	0.01	0.19	0.24	0.12	0.36	0.18	0.17	0.32	0.18	0.07	0.18	0.19	0.17
Na2O	0.96	1.42	6.91	7.58	4.39	7.71	5.25	5.86	10.90	4.49	2.62	5.91	6.07	5.39
K2O	16.24	15.09	7.41	6.15	11.30	6.07	10.00	8.89	1.33	10.69	13.46	8.52	8.50	9.51
Total	100.46	100.35	100.20	100.14	99.92	100.44	99.59	100.33	99.88	99.86	100.03	99.73	99.92	100.07
An	0.00	0.05	0.90	1.13	0.54	1.66	0.86	0.81	1.47	0.83	0.32	0.87	0.91	0.80
Ab	8.23	12.51	58.12	64.47	36.95	64.81	43.98	49.63	91.20	38.61	22.78	50.89	51.60	45.68
Or	91.77	87.44	40.97	34.40	62.50	33.54	55.16	49.56	7.33	60.56	76.90	48.24	47.50	53.53
Na+K/Al	1.04	1.01	1.01	1.00	1.04	1.00	1.03	1.01	1.00	1.00	1.02	1.00	1.01	1.01

ORS90 PLAGIOCLASE

	1	2	3	4	5	6	7
	c	m	r				
SiO2	62.44	65.10	64.48	62.44	65.45	64.90	61.86
Al2O3	22.79	18.80	18.66	23.37	18.92	18.82	23.47
FeO	0.21	0.11	0.10	0.15	0.10	0.12	0.13
CaO	4.54	0.44	0.64	4.74	0.38	0.54	5.07
Na2O	8.67	4.83	4.45	8.92	5.45	4.84	8.71
K2O	0.37	9.87	10.64	0.46	9.01	9.83	0.38
Total	99.02	99.15	99.16	100.08	99.31	99.05	99.62
An	21.95	2.09	2.98	22.12	1.82	2.55	23.85
Ab	75.89	41.76	37.70	75.31	47.02	41.72	74.03
Or	2.15	56.15	59.33	2.57	51.16	55.73	2.12

ORS94 PLAGIOCLASE

	1	2	3	4	5	6	7	8	9	10	11	12
						c	m	r	c	m	r	
SiO2	62.38	64.73	65.32	62.84	64.99	64.06	64.58	65.11	60.20	65.47	66.49	63.17
Al2O3	24.30	21.95	22.09	23.14	21.87	22.41	21.75	20.81	24.73	21.36	20.45	22.41
FeO	0.32	0.11	0.14	0.13	0.18	0.17	0.19	0.36	0.14	0.19	0.06	0.09
CaO	1.42	3.19	3.09	3.99	2.92	3.69	2.86	2.09	6.28	2.57	1.54	3.83
Na2O	8.15	9.92	9.91	8.82	9.93	9.42	9.55	10.34	7.91	10.04	9.51	8.48
K2O	2.65	0.16	0.24	0.63	0.27	0.44	0.88	0.53	0.37	0.48	0.13	0.22
Total	99.22	100.06	100.78	99.55	100.16	100.19	99.80	99.23	99.63	100.11	98.18	98.20
An	7.34	14.97	14.50	19.27	13.78	17.34	13.51	9.74	29.87	12.05	8.15	19.71
Ab	76.34	84.14	84.18	77.09	84.72	80.22	81.57	87.31	68.05	85.25	91.03	78.96
Or	16.32	0.89	1.32	3.64	1.50	2.44	4.93	2.96	2.09	2.70	0.81	1.33

ORS94 PLAGIOCLASE

	13	14	15	16	17	18	19	20	21	22	23	24	25	26	27	28	29	30	31	32	33	34
										c	m	m	r									
SiO2	67.65	69.04	65.82	65.96	66.95	66.65	66.00	66.24	63.88	64.10	64.83	64.90	65.35	68.78	64.42	64.85	64.93	65.30	65.51	67.63	66.61	66.82
Al2O3	20.33	19.57	21.11	21.04	21.66	21.70	21.79	21.72	22.14	22.27	21.95	21.98	21.59	22.31	22.18	22.19	22.00	21.83	21.41	21.03	21.51	21.70
FeO	0.06	0.06	0.15	0.17	0.12	0.11	0.08	0.13	0.11	0.12	0.11	0.12	0.16	0.16	0.11	0.15	0.13	0.18	0.14	0.14	0.15	0.13
CaO	0.40	0.54	2.39	2.56	2.67	2.72	2.92	2.82	3.58	3.80	3.40	3.19	2.71	3.21	3.54	3.43	3.25	3.09	2.75	2.02	2.66	2.70
Na2O	9.70	9.87	8.55	8.46	9.80	9.73	9.84	9.69	8.80	8.84	9.15	9.35	9.28	6.78	8.82	9.12	9.04	9.15	8.96	9.28	9.52	9.40
K2O	0.37	0.15	0.27	0.25	0.19	0.17	0.14	0.17	0.43	0.38	0.31	0.24	0.55	0.21	0.20	0.18	0.49	0.61	0.57	0.68	0.22	0.15
Total	98.50	99.24	98.30	98.45	101.39	101.09	100.76	100.76	98.94	99.52	99.75	99.79	99.65	101.45	99.27	99.93	99.85	100.15	99.34	100.77	100.67	101.00
An	2.15	2.92	13.14	14.10	12.96	13.23	13.96	13.72	17.92	18.76	16.72	15.63	13.45	20.40	17.93	17.02	16.10	15.15	14.02	10.27	13.22	13.57
Ab	95.45	96.10	85.10	84.23	85.93	85.77	85.23	85.32	79.55	78.99	81.49	82.95	83.28	77.97	80.86	81.91	81.03	81.28	82.54	85.58	85.49	85.51
Or	2.40	0.98	1.76	1.67	1.10	1.00	0.81	0.96	2.53	2.25	1.79	1.42	3.27	1.62	1.21	1.07	2.87	3.57	3.44	4.15	1.30	0.91

ORS102 PLAGIOCLASE

	1	2	3	4	5	6	7	8	9	10	11	12	13	14	15	16	17	18	19	20	21	22	23	24
					c	m	r	c	m	r						c	m	m	r					
SiO2	66.16	65.21	63.80	63.98	61.93	63.93	65.17	64.00	63.62	60.04	57.98	62.13	60.03	59.35	57.52	57.09	60.00	62.81	65.59	64.70	65.35	62.51	61.45	61.87
Al2O3	21.10	21.90	21.96	22.44	23.68	22.56	21.62	21.99	22.53	26.72	26.34	23.54	24.94	25.31	26.50	26.78	25.41	23.58	22.09	22.42	22.19	23.62	24.13	23.82
FeO	0.05	0.17	0.12	0.11	0.06	0.11	0.08	0.11	0.15	0.04	0.07	0.13	0.13	0.10	0.04	0.08	0.07	0.13	0.14	0.12	0.06	0.12	0.13	0.10
CaO	2.02	2.68	3.39	3.69	5.07	3.64	2.47	2.89	3.54	8.70	8.57	5.15	6.73	7.24	8.70	8.80	7.24	5.14	3.41	3.59	3.27	4.78	5.63	4.88
Na2O	10.59	10.16	9.87	9.59	8.61	9.57	10.25	9.91	9.45	5.25	6.62	8.15	7.74	7.30	6.60	6.70	7.36	8.46	9.27	9.41	9.69	8.65	8.26	8.13
K2O	0.20	0.27	0.15	0.16	0.14	0.24	0.12	0.19	0.26	0.06	0.08	0.14	0.11	0.10	0.07	0.11	0.07	0.11	0.09	0.21	0.14	0.23	0.25	0.25
Total	100.12	100.39	99.29	99.97	99.49	100.03	99.71	99.07	99.55	100.82	99.65	99.24	99.68	99.39	99.45	99.55	100.15	100.23	100.60	100.45	100.70	99.91	99.85	99.05
An	9.42	12.52	15.83	17.39	24.35	17.15	11.66	13.72	16.91	47.61	41.51	25.67	32.26	35.18	41.96	41.78	35.09	24.98	16.80	17.22	15.57	23.08	26.96	24.53
Ab	89.50	85.95	83.32	81.73	74.85	81.53	87.66	85.22	81.59	51.98	58.03	73.49	67.09	64.22	57.62	57.61	64.49	74.37	82.66	81.59	83.63	75.60	71.62	73.97
Or	1.08	1.52	0.85	0.88	0.81	1.32	0.69	1.06	1.49	0.41	0.45	0.84	0.65	0.60	0.42	0.61	0.42	0.65	0.54	1.19	0.80	1.32	1.42	1.51

ORS102 PLAGIOCLASE

	25	26	27	28	29	30	31	32	33	34	35	36	37	38	39	40	41	42	43	44	45	46	47	48
												c	m	r		c	m	r						
SiO2	62.25	59.70	61.90	56.97	60.35	58.01	58.74	58.29	62.08	60.34	60.91	55.83	59.13	59.66	57.25	58.21	63.46	65.78	66.99	66.37	66.64	66.41	64.74	65.57
Al2O3	23.61	26.74	23.86	27.06	25.06	26.36	25.84	26.35	23.92	25.07	24.26	27.68	25.56	25.14	26.70	26.20	23.33	21.85	21.38	21.54	21.13	21.53	22.24	22.31
FeO	0.08	0.04	0.10	0.06	0.02	0.01	0.10	0.07	0.02	0.09	0.10	0.13	0.07	0.12	0.11	0.09	0.16	0.12	0.07	0.12	0.23	0.16	0.13	0.06
CaO	5.04	8.86	5.54	9.32	6.79	8.33	7.78	8.36	5.58	6.70	5.88	11.66	7.50	7.17	8.83	8.26	4.70	2.99	2.57	2.66	2.17	2.14	2.68	2.99
Na2O	8.74	4.91	8.21	6.34	7.44	6.68	6.88	6.95	8.16	7.64	7.88	4.53	7.17	7.23	6.40	6.71	8.27	9.35	9.20	9.46	9.19	9.91	9.24	10.41
K2O	0.16	0.11	0.24	0.10	0.17	0.13	0.13	0.13	0.13	0.13	0.16	0.10	0.13	0.14	0.11	0.14	0.13	0.14	0.12	0.11	0.39	0.20	0.23	0.11
Total	99.87	100.36	99.85	99.84	99.83	99.50	99.47	100.16	99.89	99.97	99.19	99.94	99.56	99.46	99.40	99.60	100.03	100.23	100.32	100.25	99.76	100.35	99.47	101.45
An	23.94	49.55	26.81	44.57	33.22	40.49	38.15	39.64	27.20	32.42	28.94	58.36	36.37	35.12	42.98	40.16	23.72	14.91	13.28	13.36	11.25	10.52	14.49	13.63
Ab	75.15	49.71	71.82	54.86	65.81	58.78	61.08	59.65	72.04	66.84	70.15	41.07	62.87	64.06	56.40	59.06	75.53	84.28	85.97	85.95	86.33	88.29	84.12	85.77
Or	0.91	0.74	1.38	0.57	0.97	0.73	0.77	0.71	0.76	0.74	0.91	0.57	0.76	0.82	0.63	0.78	0.76	0.82	0.75	0.68	2.42	1.20	1.39	0.60

ORS107 PLAGIOCLASE

	1	2	3	4	5	6	7	8	9
SiO2	67.04	66.95	66.82	67.14	66.65	67.92	65.98	67.16	66.49
Al2O3	21.08	20.82	20.56	20.42	20.79	19.37	21.05	20.56	20.48
FeO	0.06	0.07	0.03	0.07	0.09	0.04	0.05	0.06	0.04
CaO	1.96	1.49	1.46	1.25	1.64	0.32	1.99	1.23	1.34
Na2O	10.61	10.89	11.08	11.28	10.83	10.90	10.60	11.04	10.86
K2O	0.10	0.31	0.09	0.07	0.16	1.33	0.19	0.19	0.45
Total	100.84	100.53	100.04	100.23	100.17	99.88	99.86	100.23	99.67
An	9.20	6.91	6.75	5.73	7.66	1.47	9.28	5.71	6.23
Ab	90.26	91.36	92.76	93.87	91.45	91.20	89.67	93.22	91.29
Or	0.54	1.73	0.50	0.40	0.89	7.33	1.05	1.06	2.48

ORS108 PLAGIOCLASE

	1	2	3	4
SiO2	66.60	66.87	66.80	66.50
Al2O3	19.97	20.71	20.28	20.15
FeO	0.04	0.06	0.10	0.07
CaO	0.85	1.42	1.11	0.88
Na2O	10.49	11.00	10.33	11.39
K2O	1.85	0.16	1.55	0.13
Total	99.79	100.23	100.17	99.11
An	3.86	6.60	5.13	4.04
Ab	86.15	92.50	86.35	95.26
Or	10.00	0.90	8.52	0.70

	ORS101 NEPHELINE			ORS107 NEPHELINE			ORS108 NEPHELINE							
	1	2	3	1	2	3	1	2	3	4	5	6	7	8
SiO2	44 87	45 20	44 58	48.18	47 05	47 18	45 70	45 57	45 97	48 76	46 52	45 96	45 81	45 22
Al2O3	32 99	32 35	32 69	32 56	32 45	32 59	32 35	32 49	32 60	33 79	32 38	32 51	32 21	32 35
FeO	0 30	0 38	0 32	0 23	0 26	0 22	0 25	0 23	0 20	0 19	0 18	0 21	0 23	0 23
CaO	0 36	0 51	0 49	0 42	0 30	0 57	0 54	0 65	0 57	0 55	0 55	0 53	0 56	0 53
Na2O	16 15	15 70	16 24	15.71	16 81	15 10	16 58	16 73	16 64	13 59	16 18	16 57	16 17	15 86
K2O	5 89	5 41	5 35	5.07	5.09	4 76	5 15	5.18	5 20	4 46	4 73	4 66	4 67	4 82
Total	100 56	99 54	99 67	102 18	101 95	100.43	100 56	100 84	101 18	101 34	100 53	100 44	99 65	99 01
An	0 98	1 45	1 36	1 21	0.82	1 70	1 48	1 74	1 54	1 80	1 54	1 47	1.57	1 52
Ab	79 87	80 34	81.08	81.49	82 72	81.44	81 80	81 63	81 66	80 78	82 58	83 15	82 72	82 06
Or	19 15	18 21	17.57	17.30	16.46	16 86	16 72	16 63	16 80	17 42	15 88	15 38	15 71	16 42
Na+K/Al	1 00	0 98	0 99	0.96	1.02	0 92	1 02	1 02	1 01	0 80	0 98	0 99	0 98	0 97

	ORS102 OPAQUES			ORS107 OPAQUES				ORS108 OPAQUES								ORS94 OPAQUES				
	1	2	3	1	2	3	4	1	2	3	4	5	6	7	8	1	2	3	4	5
TiO2	1 27	0 25	20.33	0.06	33 38	11.29	0.42	1 21	12 95	10 04	49 24	0 84	0 37	0 60	47 71	47 55	47 65	47 86	0 23	47 44
Al2O3	0 21	0 12	2 02	0 12	0.03	0.17	0 91	0 15	0 55	0 04	0 01	0 12	0 20	0 12	0 01	0 00	0 00	0 00	0 07	0 00
Cr2O3	0 05	0 08	0 05	0.00	0 00	0 00	0 01	0 00	0 01	0 00	0 00	0 07	0 09	0 09	0 00	0 00	0 00	0 00	0 10	0 00
Fe2O3	66 01	68 46	18 02	56.58	19 96	45 62	63 71	66 50	42 28	48 43	6 93	69 05	65 52	69 15	9 24	10 04	7 57	8 41	69 40	7 68
FeO	31 72	31 24	39 15	25.60	22 69	38 07	29 93	31 93	40 39	38 16	38 18	32 53	30 23	32 15	36 35	36 54	36 15	35 41	31 63	35 02
MnO	0 43	0 13	6 87	0.03	7.22	2.81	0 09	0 22	2 26	1 71	6 02	0 14	0 08	0 12	6 44	6 13	6 59	7 51	0 08	7 54
CaO	0.00	0 00	0 00	0.03	0.02	0.03	0.04	0.04	0 03	0 00	0.00	0 03	0.02	0.05	0.04	0 01	0 03	0.02	0 02	0 00
MgO	0.00	0 00	0.01	0.26	0.03	0.01	0.00	0.00	0 02	0.01	0 03	0.00	0 00	0.00	0.06	0 08	0 02	0 01	0 02	0 01
Tot	99.70	100.29	86.44	82.43	83.29	97.98	95.10	100.06	98.47	98.38	100.38	102.79	96.51	102.26	99.79	100.27	97 99	99 21	101 52	97 67
Al	0.0776	0 0420	0.8174	0.0532	0.0009	0.0607	0.3441	0.0552	0.2011	0 0154	0 0002	0.0429	0 0741	0.0412	0 0003	0 0000	0 0000	0 0000	0 0234	0 0000
Cr	0 0113	0 0204	0.0139	0.0000	0.0000	0 0000	0.0020	0.0000	0.0025	0 0000	0 0000	0 0160	0 0216	0 0204	0.0000	0 0001	0 0000	0 0000	0 0235	0 0000
Fe3+	15.3210	15.8224	4 6617	15.9105	0.4603	10.6642	15.4520	15 3868	9 7979	11 3008	0 1315	15.5617	15.7252	15 6671	0 1766	0 1910	0 1473	0 1616	15 8488	0 1498
Ti	0.2950	0.0576	5 2535	0.0182	0.7694	2 6375	0.1009	0.2790	2 9992	2.3419	0.9341	0 1897	0.0896	0 1357	0 9115	0 9044	0 9264	0 9192	0 0521	0 9251
Mg	0.0015	0 0000	0.0035	0.1424	0.0013	0.0060	0.0022	0.0015	0.0069	0 0027	0.0010	0.0000	0 0000	0.0000	0.0024	0 0030	0 0006	0 0004	0 0102	0 0004
Fe2+	8.1819	8 0237	11.2536	8.0007	0.5815	9.8907	8.0660	8.2102	10.4023	9.8940	0.8055	8.1467	8.0618	8 0945	0.7722	0.7729	0.7815	0.7563	8 0267	0 7595
Mn	0 1131	0 0339	1.9999	0.0080	0.1874	0 7397	0.0239	0.0580	0 5901	0 4479	0.1286	0 0363	0.0219	0.0303	0 1386	0 1314	0 1442	0 1625	0 0214	0 1656
Ni	0.0000	0.0000	0.0000	0.0095	0.0004	0.0072	0.0111	0 0108	0.0068	0 0000	0.0000	0 0067	0 0059	0.0109	0 0008	0 0001	0 0006	0 0005	0 0040	0 0000
Tot	24.0015	24.0000	24.0035	24.1424	2.0013	24.0060	24.0022	24.0015	24.0069	24 0027	2 0010	24.0000	24 0000	24.0000	2.0024	2.0030	2 0006	2 0004	24 0102	2 0004

Alkali-melasyenite - nepheline-syenite

ORF3 AMPHIBOLE

	1	2	3	4
	c	r		
SiO2	38 67	37 88	37 86	38 37
TiO2	1.41	1 81	1 57	2.31
Al2O3	10.02	10 51	10 62	10.56
Fe2O3	5 93	5.52	7 21	4.72
FeO	22 97	23 42	21.91	21 01
MnO	1.18	1 11	1.14	1 08
MgO	3 28	2 99	3 11	4 52
CaO	9 26	9 34	9 13	9.53
Na2O	3 71	3 79	3 58	3 49
K2O	1 56	1 47	1 53	1.35
Tot	97.98	97 82	97.65	96.94
Si	6.1992	6.0971	6.0827	6 1329
ivAl	1.8008	1 9029	1.9173	1.8671
Fe3+	0.0000	0.0000	0.0000	0.0000
viAl	0 0919	0.0916	0.0945	0 1228
Ti	0 1700	0.2191	0.1891	0.2777
Fe3+	0 7151	0.6683	0.8715	0.5678
Fe2+	3.0791	3.1523	2.9449	2.8088
Mg	0.7836	0.7173	0.7448	1.0767
Mn	0.1602	0.1513	0.1552	0.1462
Mg	0.0000	0.0000	0.0000	0.0000
Fe2+	0 0000	0.0000	0.0000	0.0000
Ca	1.5906	1.6103	1.5720	1.6322
Na	0.4094	0.3897	0.4280	0.3678
Na	0.7441	0.7926	0.6873	0.7131
K	0.3191	0.3019	0.3137	0.2759
Tot	16.0632	16.0945	16.0010	15.9890

ORF21 AMPHIBOLE

	1	2	3	4	5	6	7	8	9
					c	r			
SiO2	42 99	46 90	46 04	46 93	48 77	45 96	40 72	51 47	40 44
TiO2	2.19	1 85	2 01	2 12	1 40	1 94	2 94	0 50	2 94
Al2O3	11 10	7 04	8 10	7 24	5 68	7 36	10 49	1 54	10 37
Fe2O3	0.00	0 00	0.00	0.00	0 00	0 00	2 33	0 00	2 61
FeO	12 15	9 80	10 18	9 15	8 50	12 85	18 55	13 31	18 35
MnO	0 43	0 47	0 40	0.38	0.44	0 55	0 77	0 71	0 72
MgO	11 66	11 33	11 15	11 34	12 10	10 42	7 65	9 55	7 58
CaO	14 40	19 28	18 44	20 09	20 66	17 08	10 37	21 06	10 26
Na2O	2 88	1 84	2 06	1 79	1 62	2 45	3 26	1 56	3 22
K2O	0 64	0 25	0 28	0 15	0 13	0 49	1 29	0 00	1 29
Tot	98 44	98 76	98 65	99 18	99 29	99 11	98 36	99 71	97 77
Si	6.5265	7 4288	7.2491	7 4462	7 7294	7 2127	6 2570	8 4019	6 2523
ivAl	1.4735	0 5712	0 7509	0.5538	0.2706	0 7873	1 7430	0 0000	1 7477
Fe3+	0.0000	0.0000	0 0000	0.0000	0.0000	0.0000	0.0000	0.0000	0.0000
viAl	0 5132	0 7425	0 7522	0 7997	0.7903	0 5743	0.1564	0.6985	0.1429
Ti	0.2502	0.2202	0 2378	0.2527	0.1667	0.2294	0 3392	0.0616	0 3413
Fe3+	0.0000	0.0000	0.0000	0.0000	0.0000	0.0000	0.2691	0 0000	0 3032
Fe2+	1.5425	1.2985	1.3402	1.2143	1.1266	1.6863	2 3832	1.8173	2 3724
Mg	2.6382	2 6755	2.6164	2.6826	2.8570	2 4370	1.7518	2 3238	1.7463
Mn	0.0559	0.0632	0.0534	0.0507	0.0593	0.0730	0.1003	0.0988	0.0940
Mg	0.0000	0.0000	0.0000	0.0000	0.0000	0.0000	0.0000	0 0000	0.0000
Fe2+	0.0000	0.0000	0.0000	0.0000	0.0000	0.0000	0.0000	0.0000	0.0000
Ca	2.0000	2 0000	2.0000	2.0000	2.0000	2.0000	1.7080	2.0000	1.6998
Na	0.0000	0.0000	0.0000	0.0000	0.0000	0 0000	0.2920	0.0000	0.3002
Na	0.8472	0.5639	0 6278	0.5497	0.4982	0.7462	0.6790	0.4943	0.6649
K	0.1240	0.0506	0.0563	0.0301	0.0253	0.0986	0.2521	0.0000	0.2544
Tot	16.3144	16 8859	16.7955	16.9950	17.0321	16.7168	15.9311	17.5793	15.9192

ORF28 AMPHIBOLE

	1	2	3	4	5	6	7
					c	m	r
SiO2	37 21	36 91	37 28	37 29	37 73	36 74	37 09
TiO2	2 83	2 66	2 81	2 40	3 23	3 13	2 82
Al2O3	10 90	11 52	11.39	11 07	11 21	11 21	11 77
Fe2O3	1 91	3 54	2 87	3.69	2 30	1 87	3 35
FeO	23 83	23 30	22 55	23 16	21 94	22 35	22 32
MnO	0 82	0 88	0 85	0 90	0 91	0 76	0 92
MgO	3 69	3 25	3 89	3 34	4 77	4 41	3 98
CaO	10 20	10 00	10 00	9 85	10 28	10 08	10 24
Na2O	3 11	3 09	3 07	3 16	3 08	3 17	3 08
K2O	1 46	1 51	1 48	1 46	1 45	1 54	1 47
Tot	95 96	96 67	96 17	96 32	96 89	95 25	97 05
Si	6.0645	5 9809	6 0311	6 0570	6 0313	5 9977	5 9530
ivAl	1.9355	2 0191	1.9689	1 9430	1 9687	2 0023	2 0470
Fe3+	0 0000	0 0000	0 0000	0.0000	0 0000	0 0000	0 0000
viAl	0 1589	0 1809	0 2034	0 1777	0 1441	0 1548	0 1805
Ti	0 3474	0 3246	0 3414	0 2932	0 3877	0 3845	0 3410
Fe3+	0 2345	0 4322	0 3494	0 4516	0 2761	0 2303	0 4050
Fe2+	3 2489	3 1581	3 0511	3 1456	2 9332	3 0512	2 9961
Mg	0 8968	0 7839	0 9378	0 8085	1 1359	1 0739	0 9528
Mn	0 1135	0 1203	0 1169	0 1233	0 1229	0 1054	0 1247
Mg	0 0000	0 0000	0 0000	0 0000	0 0000	0 0000	0 0000
Fe2+	0 0000	0 0000	0 0000	0 0000	0 0000	0 0000	0 0000
Ca	1 7812	1 7365	1 7333	1 7151	1 7616	1 7627	1 7605
Na	0 2188	0 2635	0 2667	0 2849	0 2384	0 2373	0 2395
Na	0 7632	0 7072	0 6955	0 7093	0 7166	0 7653	0 7183
K	0 3029	0 3130	0 3046	0 3029	0 2949	0 3203	0 3007
Tot	16 0661	16 0202	16.0001	16 0122	16 0115	16 0857	16 0190

ORF28 AMPHIBOLE

	8	9	10	11	12	13	14	15
			c	r		c	r	
SiO2	37.90	38 45	38.14	37.64	38.16	38.39	37 50	37.87
TiO2	3.26	3.38	3.34	1.72	3.12	3.35	3 08	2 04
Al2O3	10.45	10.25	10.54	10.31	9.93	10.51	10.75	10 75
Fe2O3	4.56	2.97	4.44	6.12	3.67	1.85	2 04	3 53
FeO	19.87	20 10	19.26	20.64	21.45	23.66	23.79	22.69
MnO	0.85	0 77	0.85	0.94	0.90	0.99	0.98	0.98
MgO	4.68	5.23	4.98	3.61	3.96	3.95	3.71	3.88
CaO	9.09	9.18	8.99	8.98	8.86	10.05	10.18	10 14
Na2O	3.07	3.18	3.07	3.02	3.17	3.08	3 10	2 99
K2O	1.43	1.42	1.42	1.58	1.42	1.43	1.44	1.49
Tot	95.16	94.92	95.02	94.56	94.64	97.27	96.56	96.35
Si	6.1272	6.2043	6.1468	6.1835	6.2339	6.1455	6 0728	6 1295
ivAl	1.8728	1.7957	1.8532	1.8165	1.7661	1.8545	1.9272	1 8705
Fe3+	0.0000	0.0000	0.0000	0.0000	0.0000	0.0000	0.0000	0.0000
viAl	0.1189	0 1542	0.1494	0.1802	0.1464	0 1289	0.1251	0 1808
Ti	0.3964	0.4102	0.4048	0.2125	0.3833	0.4033	0.3751	0.2483
Fe3+	0.5546	0.3601	0.5379	0.7568	0.4510	0.2233	0.2481	0 4298
Fe2+	2.6861	2.7127	2.5958	2.8358	2.9305	3.1679	3.2218	3 0708
Mg	1 1276	1.2577	1 1961	0.8838	0 9641	0.9424	0 8959	0 9359
Mn	0 1164	0 1051	0 1159	0.1308	0.1245	0.1342	0 1340	0 1344
Mg	0 0000	0 0000	0 0000	0 0000	0 0000	0 0000	0 0000	0 0000
Fe2+	0 0000	0 0000	0 0000	0 0000	0 0000	0 0000	0 0000	0 0000
Ca	1 5746	1 5872	1 5525	1.5807	1.5509	1.7238	1 7664	1 7586
Na	0 4254	0 4128	0 4475	0 4193	0 4491	0 2762	0 2336	0 2414
Na	0 5370	0 5821	0 5118	0 5427	0 5551	0 6798	0 7398	0 6970
K	0 2949	0 2917	0 2920	0 3311	0 2980	0 2920	0 2975	0 3077
Tot	15 8319	15 8738	15 8038	15 8738	15.8510	15 9719	16 0373	16 0046

ORF29 AMPHIBOLE

	1	2	3	4	5	6	7	8	9	10	11	12	13	14	15
	c	m	m	r											
SiO2	41.01	39.83	39.34	39.27	38 11	38.37	38 54	38 50	37 84	38 72	38 87	38 07	39 09	39 04	37 99
TiO2	2.57	3.31	3 66	3.39	2 46	2 74	2 48	2 93	1 87	3 22	2 93	1 94	2 57	2 80	2 54
Al2O3	10.03	10 49	9.99	10.59	12 00	11 42	11 41	11 31	11.99	10 37	10 60	11 76	10 80	10 56	11 19
Fe2O3	2.97	0.70	0.88	1.35	3.75	2.67	3 24	1 55	4 44	1 41	1 92	4 55	2 46	2 34	3 62
FeO	18.68	19.69	19 85	21.04	20.73	21 90	21 32	22 16	20 40	22 16	21 94	20 34	21 36	21 93	20 61
MnO	0.61	0.63	0.65	0.69	0.71	0.68	0.72	0 87	0 69	0 70	0 72	0 79	0 74	0 78	0 77
MgO	7.61	7.42	7.11	6.12	5.33	5.34	5.50	5 35	5 42	5 44	5 36	5 30	5 59	5 38	5 25
CaO	10.41	10.54	10 31	10 28	10.59	10 77	10 80	10 80	10 83	10 44	10 50	10 66	10 60	10 45	10 26
Na2O	3.03	3.18	3 12	3 14	3 00	3 04	2 99	3 00	2 91	3 08	2 95	2 92	2 98	3.10	2 96
K2O	1.44	1 45	1 43	1.46	1 57	1 57	1 53	1 54	1.59	1.39	1 39	1 50	1 34	1 42	1 53
Tot	98.37	97.24	96 34	97 33	98.26	98.49	98 53	98 00	97.97	96.90	97 19	97 83	97 52	97 81	96 73
Si	6.3100	6 2180	6.2155	6 1789	5.9823	6 0283	6 0413	6 0711	5 9666	6 1634	6 1650	6 0067	6 1646	6.1611	6 0588
ivAl	1.6900	1.7820	1.7845	1.8211	2.0177	1 9717	1 9587	1.9289	2 0334	1 8366	1 8350	1 9933	1 8354	1 8389	1 9412
Fe3+	0.0000	0.0000	0.0000	0.0000	0.0000	0.0000	0 0000	0.0000	0.0000	0 0000	0.0000	0 0000	0.0000	0.0000	0.0000
viAl	0.1289	0 1475	0.0769	0 1428	0.2036	0.1433	0 1495	0 1734	0 1948	0 1095	0 1466	0 1945	0 1729	0 1264	0 1618
Ti	0 2972	0 3887	0.4353	0 4009	0 2909	0 3238	0 2929	0 3480	0.2215	0 3851	0 3496	0 2300	0 3049	0 3321	0 3048
Fe3+	0.3443	0 0819	0.1044	0 1600	0 4427	0 3155	0 3827	0 1834	0 5273	0 1685	0 2294	0 5397	0 2923	0 2781	0 4339
Fe2+	2.4039	2 5710	2.6230	2.7689	2.7209	2 8769	2 7949	2 9232	2 6898	2 9504	2 9101	2 6842	2 8171	2 8941	2 7485
Mg	1.7462	1.7272	1 6732	1 4349	1 2474	1 2507	1 2848	1 2562	1 2740	1 2916	1 2678	1 2458	1 3134	1 2655	1 2468
Mn	0 0793	0 0836	0 0873	0 0925	0 0945	0 0898	0 0952	0 1157	0 0926	0 0948	0 0984	0 1058	0 0994	0 1038	0 1042
Mg	0 0000	0 0000	0 0000	0 0000	0 0000	0 0000	0 0000	0 0000	0 0000	0 0000	0 0000	0 0000	0 0000	0 0000	0 0000
Fe2+	0 0000	0 0000	0 0000	0 0000	0 0000	0 0000	0 0000	0 0000	0 0000	0 0000	0 0000	0 0000	0 0000	0 0000	0 0000
Ca	1 7170	1 7623	1 7444	1 7323	1 7815	1 8124	1 8137	1 8245	1 8299	1 7813	1 7848	1 8020	1 7905	1 7674	1 7538
Na	0 2830	0 2377	0 2556	0 2677	0 2185	0 1876	0 1863	0 1755	0 1701	0 2187	0 2152	0 1980	0 2095	0 2326	0 2462
Na	0 6222	0 7234	0 7002	0 6904	0 6841	0 7373	0 7219	0 7410	0 7181	0 7256	0 6929	0 6944	0 7005	0 7161	0 6701
K	0 2830	0 2894	0 2881	0 2938	0 3141	0 3156	0 3051	0 3105	0 3204	0 2814	0 2820	0 3028	0 2695	0 2865	0 3120
Tot	15.9052	16.0128	15 9883	15 9842	16 0082	16 0529	16 0270	16 0514	16 0385	16 0069	15 9749	15 9971	15 9700	16 0026	15 9821

ORF30 AMPHIBOLE

	1	2	3	4 c r	5	6	7	8	9	10	11	12 c	13 m	14 r	15	16	17	18	19	20
SiO2	38 93	38 95	39 30	39 31	38 71	39 06	39 44	39 68	39 13	39 31	40 35	39 40	39 11	39 57	39 37	39 48	39 14	39 21	39 60	39 26
TiO2	3 29	3 35	2 55	2 94	2 53	2 58	2 95	2 98	2 75	3 28	3 12	3 12	3 21	3 46	3 29	3 13	3 26	3 25	3 12	2 58
Al2O3	11 18	11 16	11 47	10 98	11 49	11 45	11 23	11 43	11 35	11 40	10 46	10 58	10 37	10 52	11 03	11 55	11 66	11 85	11 57	12 15
Fe2O3	0 81	0 28	1 44	1 27	1 08	1 98	1 08	0 22	0 81	0 68	0 65	2 71	1 65	1 01	1 24	0 00	0 00	0 00	0 00	0 69
FeO	20 11	19 30	19 68	19 46	20 65	19 28	19 27	18 75	19 95	19 74	19 57	17 49	17 98	18 88	19 32	19 91	19 89	19 71	19 76	19 30
MnO	0 61	0 57	0 62	0 62	0 63	0 56	0 58	0 54	0 56	0 61	0 54	0 48	0 49	0 56	0 56	0 60	0 55	0 56	0 60	0 53
MgO	6 86	7 54	7 20	7 34	6 49	7 16	7 57	8 20	7 24	7 26	7 57	7 80	7 85	7 60	7 27	7 47	7 45	7 43	7 45	7 37
CaO	10 89	10 98	11 11	11 01	11 08	10 99	11 12	11 23	11 18	11 07	10 73	10 30	10 45	10 45	10 66	11 25	11 25	11 35	11 25	11 10
Na2O	2 93	2 93	2 94	2 90	2 87	2 90	2 89	2 95	2 93	2 86	2 91	2 92	2 89	3 01	2 95	2 99	3 02	2 94	2 94	2 90
K2O	1 34	1 33	1 54	1 38	1 53	1 50	1 41	1 45	1 47	1 40	1 43	1 44	1 46	1 45	1 48	1 48	1 57	1 58	1 55	1 57
Tot	96 93	96 41	97 84	97 22	97 06	97 44	97 53	97 42	97 37	97 62	97 34	96 24	95 45	96 50	97 16	97 85	97 80	97 89	97 82	97 46
Si	6 1156	6 1231	6 1155	6 1455	6 1037	6 0994	6 1336	6 1474	6 1188	6 1148	6 2722	6 1772	6 1903	6 2038	6 1487	6 1288	6 0903	6 0921	6 1496	6 1033
ivAl	1 8844	1 8769	1 8845	1 8545	1 8963	1 9006	1 8664	1 8526	1 8812	1 8852	1 7278	1 8228	1 8097	1 7962	1 8513	1 8712	1 9097	1 9079	1 8504	1 8967
Fe3+	0 0000	0 0000	0 0000	0 0000	0 0000	0 0000	0 0000	0 0000	0 0000	0 0000	0 0000	0 0000	0 0000	0 0000	0 0000	0 0000	0 0000	0 0000	0 0000	0 0000
viAl	0 1871	0 1906	0 2202	0 1696	0 2393	0 2069	0 1920	0 2344	0 2107	0 2052	0 1896	0 1320	0 1249	0 1475	0 1792	0 2418	0 2298	0 2635	0 2670	0 3307
Ti	0 3883	0 3959	0 2988	0 3453	0 3000	0 3032	0 3455	0 3469	0 3229	0 3841	0 3643	0 3679	0 3818	0 4074	0 3864	0 3651	0 3820	0 3802	0 3645	0 3016
Fe3+	0 0957	0 0334	0 1686	0 1498	0 1286	0 2327	0 1262	0 0255	0 0958	0 0794	0 0760	0 3203	0 1969	0 1194	0 1458	0 0000	0 0000	0 0000	0 0000	0 0802
Fe2+	2 6418	2 5377	2 5621	2 5447	2 7232	2 5178	2 5061	2 4294	2 6096	2 5685	2 5445	2 2940	2 3794	2 4749	2 5235	2 5849	2 5886	2 5615	2 5661	2 5095
Mg	1 6065	1 7666	1 6690	1 7091	1 5245	1 6659	1 7536	1 8928	1 6867	1 6828	1 7543	1 8222	1 8511	1 7769	1 6909	1 7294	1 7275	1 7207	1 7234	1 7077
Mn	0 0807	0 0758	0 0814	0 0814	0 0844	0 0734	0 0766	0 0710	0 0744	0 0801	0 0713	0 0637	0 0659	0 0739	0 0743	0 0789	0 0721	0 0742	0 0790	0 0704
Mg	0 0000	0 0000	0 0000	0 0000	0 0000	0 0000	0 0000	0 0000	0 0000	0 0000	0 0000	0 0000	0 0000	0 0000	0 0000	0 0000	0 0000	0 0000	0 0000	0 0000
Fe2+	0 0000	0 0000	0 0000	0 0000	0 0000	0 0000	0 0000	0 0000	0 0000	0 0000	0 0000	0 0000	0 0000	0 0000	0 0000	0 0000	0 0000	0 0000	0 0000	0 0000
Ca	1 8325	1 8500	1 8531	1 8449	1 8717	1 8384	1 8523	1 8634	1 8737	1 8457	1 7869	1 7303	1 7714	1 7547	1 7831	1 8713	1 8755	1 8889	1 8720	1 8488
Na	0 1675	0 1500	0 1469	0 1551	0 1283	0 1616	0 1477	0 1366	0 1263	0 1543	0 2131	0 2697	0 2286	0 2453	0 2169	0 1287	0 1245	0 1111	0 1260	0 1512
Na	0 7250	0 7435	0 7402	0 7241	0 7497	0 7169	0 7243	0 7489	0 7627	0 7097	0 6639	0 6169	0 6578	0 6698	0 6754	0 7707	0 7863	0 7750	0 7559	0 7219
K	0 2677	0 2676	0 3048	0 2754	0 3070	0 2993	0 2805	0 2864	0 2925	0 2771	0 2829	0 2875	0 2951	0 2901	0 2951	0 2930	0 3118	0 3130	0 3068	0 3120
Tot	15 9927	16 0111	16 0450	15 9995	16 0567	16 0162	16 0049	16 0353	16 0552	15 9868	15 9467	15 9044	15 9529	15 9598	15 9704	16 0637	16 0981	16 0880	16 0627	16 0339

ORF43 AMPHIBOLE

	1 c	2 r	3	4	5
SiO2	39 67	38 42	38 44	39 21	40 30
TiO2	2 46	2 52	2 42	2 33	2 08
Al2O3	8 54	9 85	9 81	9 10	8 35
Fe2O3	3 89	3 70	4 17	5 36	3 11
FeO	21 98	22 15	21 61	20 68	22 15
MnO	1 16	1 13	1 10	1 11	1 12
MgO	4 78	4 21	4 34	4 69	4 93
CaO	8 92	9 05	9 02	8 73	8 83
Na2O	3 96	3 86	3 79	3 79	4 00
K2O	1 41	1 49	1 46	1 41	1 43
Tot	96 79	96 39	96 17	96 41	96 30
Si	6 3647	6 2059	6 2123	6 2967	6 4785
ivAl	1 6164	1 7941	1 7877	1 7033	1 5215
Fe3+	0 0189	0 0000	0 0000	0 0000	0 0000
viAl	0 0000	0 0822	0 0810	0 0194	0 0605
Ti	0 2973	0 3064	0 2946	0 2817	0 2511
Fe3+	0 4512	0 4495	0 5069	0 6479	0 3758
Fe2+	2 9500	2 9928	2 9205	2 7780	2 9781
Mg	1 1437	1 0139	1 0462	1 1223	1 1820
Mn	0 1579	0 1552	0 1508	0 1507	0 1525
Mg	0 0000	0 0000	0 0000	0 0000	0 0000
Fe2+	0 0000	0 0000	0 0000	0 0000	0 0000
Ca	1 5337	1 5670	1 5614	1 5018	1 5211
Na	0 4663	0 4330	0 4386	0 4982	0 4789
Na	0 7663	0 7751	0 7480	0 6817	0 7690
K	0 2894	0 3074	0 3012	0 2892	0 2928
Tot	16 0557	16 0826	16 0492	15 9709	16 0618

ORF44 AMPHIBOLE

	1	2	3	4	5	6 c	7 r	8
SiO2	38 42	37 88	37 95	37 94	39 44	39 35	39 02	38 52
TiO2	2 25	2 16	1 97	2 01	1 92	2 64	2 58	2 36
Al2O3	9 39	9 36	9 38	9 35	10 19	10 25	10 54	10 52
Fe2O3	5 23	6 17	5 19	5 51	3 28	2 77	2 20	4 34
FeO	22 59	21 76	22 41	22 48	20 56	19 97	20 93	20 61
MnO	1 34	1 34	1 34	1 28	1 19	1 06	1 15	1 20
MgO	3 04	2 98	3 02	2 93	5 79	6 07	5 89	4 94
CaO	8 92	8 70	8 92	8 86	10 09	9 96	10 18	9 85
Na2O	3 36	3 32	3 37	3 39	3 57	3 42	3 46	3 30
K2O	1 35	1 33	1 34	1 34	1 30	1 23	1 28	1 37
Tot	95 89	94 99	94 89	95 09	97 33	96 72	97 03	97 00
Si	6 2684	6 2373	6 2629	6 2532	6 2378	6 2272	6 1861	6 1387
ivAl	1 7316	1 7627	1 7371	1 7468	1 7622	1 7728	1 8139	1 8613
Fe3+	0 0000	0 0000	0 0000	0 0000	0 0000	0 0000	0 0000	0 0000
viAl	0 0745	0 0543	0 0879	0 0700	0 1378	0 1395	0 1560	0 1152
Ti	0 2761	0 2675	0 2445	0 2491	0 2284	0 3142	0 3076	0 2829
Fe3+	0 6423	0 7642	0 6451	0 6839	0 3908	0 3293	0 2623	0 5199
Fe2+	3 0828	2 9966	3 0925	3 0985	2 7189	2 6433	2 7753	2 7468
Mg	0 7392	0 7305	0 7428	0 7197	1 3647	1 4316	1 3444	1 1733
Mn	0 1852	0 1869	0 1873	0 1787	0 1594	0 1421	0 1544	0 1620
Mg	0 0000	0 0000	0 0000	0 0000	0 0000	0 0000	0 0000	0 0000
Fe2+	0 0000	0 0000	0 0000	0 0000	0 0000	0 0000	0 0000	0 0000
Ca	1 5594	1 5350	1 5773	1 5647	1 7099	1 6889	1 7293	1 6811
Na	0 4406	0 4650	0 4227	0 4353	0 2901	0 3111	0 2707	0 3189
Na	0 6223	0 5949	0 6557	0 6481	0 8047	0 7383	0 7929	0 7008
K	0 2810	0 2794	0 2821	0 2818	0 2623	0 2483	0 2583	0 2785
Tot	15 9033	15 8743	15 9378	15 9298	16 0670	15 9866	16 0512	15 9794

ORF49 AMPHIBOLE

	1	2	3	4	5	6	7	8	9	10	11	12	13	14	15
	c	r	c	r	c	m	r							c	r
SiO2	39 78	39 35	40 55	39 74	39 69	39 37	39 27	39 70	39 54	39 18	39 03	38 79	39 29	39 14	39 36
TiO2	3 63	2 47	2 10	2 21	3 06	3 24	2 78	1 74	2 96	2 89	3 05	2 88	3 10	2 98	2 95
Al2O3	10 22	10 12	7 99	8 69	9 30	9 55	9 28	9 58	10 14	10 45	10 25	10 29	10 33	10 45	10 22
Fe2O3	1 69	2 35	3 64	3 81	2 62	2 16	2 51	2 96	0 00	0 59	0 96	1 35	0 66	1 17	1 01
FeO	17 81	20 02	21 86	22 07	19 09	19 17	20 22	19 47	21 28	20 64	20 64	19 97	20 83	20 37	21 31
MnO	0 83	0 90	1 20	1 14	0 74	0 78	0 80	0 71	0 99	0 93	1 01	0 98	0 80	0 83	1 00
MgO	8 32	6 51	5 19	4 79	6 56	6 61	5 70	6 13	6 63	6 67	6 61	6 68	6 83	6 82	6 35
CaO	10 76	10 59	8 96	9 01	9 49	9 55	9 40	9 59	10 73	10 70	10 77	10 45	10 67	10 67	10 59
Na2O	3 06	2 97	3 98	3 94	3 21	3 34	3 21	3 21	3 21	3 18	3 06	3 25	3 38	3 31	3 31
K2O	1 26	1 38	1 39	1 47	1 26	1 20	1 23	1 27	1 42	1 39	1 44	1 36	1 33	1 29	1 48
Tot	97 36	96 66	96 88	96 87	95 02	94 96	94 39	94 36	96 91	96 62	96 82	96 00	97 22	97 02	97 58
Si	6 1696	6 2301	6 4811	6 3711	6 3462	6.3009	6 3604	6 4067	6.2496	6 2036	6 1804	6 1815	6 1851	6 1686	6 2002
ivAl	1 8304	1.7699	1 5061	1 6289	1.6538	1.6991	1 6396	1.5933	1.7504	1.7964	1.8196	1.8185	1 8149	1 8314	1 7998
Fe3+	0 0000	0.0000	0.0128	0.0000	0.0000	0.0000	0.0000	0.0000	0.0000	0.0000	0.0000	0.0000	0 0000	0.0000	0.0000
viAl	0.0374	0.1194	0.0000	0.0145	0.1001	0.1020	0.1320	0.2301	0.1394	0.1533	0.0934	0.1141	0 1027	0.1101	0.0981
Ti	0.4238	0.2940	0.2529	0.2669	0.3675	0.3896	0.3386	0.2109	0.3523	0.3442	0.3626	0.3452	0 3675	0.3538	0.3492
Fe3+	0.1974	0.2797	0.4255	0.4596	0.3148	0.2599	0.3058	0.3591	0.0006	0.0698	0.1149	0.1622	0 0777	0 1387	0.1203
Fe2+	2.3098	2.6506	2.9223	2.9591	2.5529	2.5659	2.7387	2.6279	2.8125	2.7330	2.7335	2.6614	2 7427	2.6857	2.8070
Mg	1.9221	1.5351	1.2372	1.1457	1.5639	1.5787	1.3757	1.4743	1.5626	1.5745	1.5601	1.5854	1 6025	1 6013	1 4913
Mn	0.1096	0.1212	0 1620	0.1543	0.1009	0.1059	0.1093	0.0976	0.1327	0.1252	0.1353	0.1317	0 1070	0.1104	0 1340
Mg	0.0000	0.0000	0.0000	0.0000	0.0000	0.0000	0.0000	0.0000	0.0000	0.0000	0.0000	0.0000	0 0000	0.0000	0.0000
Fe2+	0.0000	0.0000	0.0000	0.0000	0.0000	0.0000	0.0000	0.0000	0.0000	0.0000	0.0000	0.0000	0.0000	0.0000	0.0000
Ca	1.7885	1.7965	1.5349	1.5486	1.6261	1.6385	1.6311	1.6581	1.8178	1.8148	1.8280	1.7848	1 8006	1 8028	1.7869
Na	0.2115	0.2035	0.4651	0.4514	0.3739	0.3615	0.3689	0.3419	0.1822	0.1852	0.1720	0.2152	0 1994	0.1972	0.2131
Na	0.7097	0.7070	0.7689	0.7720	0.6210	0.6735	0.6398	0.6635	0.8019	0.7896	0.7670	0.7905	0.8312	0.8139	0.7984
K	0.2499	0.2794	0.2838	0.3004	0.2569	0.2460	0.2538	0.2607	0.2863	0.2806	0.2910	0.2764	0.2677	0 2584	0.2976
Tot	15.9596	15.9864	16.0526	16.0724	15.8779	15.9195	15.8935	15.9242	16.0881	16.0702	16.0580	16.0669	16.0989	16 0723	16.0960

ORF12 BIOTITE

	1	2	3	4	5	6
					c	r
SiO2	35 30	34 97	35 57	35 66	35.84	35 81
TiO2	4 44	4 55	4 62	4 64	4.54	4 14
Al2O3	13 26	13 42	13 76	13 73	13 46	13 45
FeO	22 06	22 07	22 00	21 67	21 38	22 03
MnO	0 56	0 56	0 54	0 50	0 60	0 52
MgO	9 70	9 73	10 05	10 09	10 21	10 18
CaO	0 07	0 11	0 04	0 05	0 06	0 06
Na2O	0 35	0 34	0 33	0 33	0 25	0 33
K2O	8 70	8.63	8.90	9 02	9 00	9 00
Tot	94 43	94 38	95 84	95 69	95 35	95 51
Si	5 5449	5 4991	5.4986	5.5130	5 5542	5.5563
Ti	0 5248	0.5384	0 5371	0.5393	0 5293	0 4826
Al	2 4547	2 4881	2 5082	2.5023	2.4597	2.4606
Fe2+	2 8974	2 9021	2 8444	2.8021	2.7713	2.8591
Mn	0.0745	0.0742	0.0713	0.0660	0.0783	0 0680
Mg	2.2715	2.2797	2.3160	2.3258	2.3568	2.3536
Ca	0 0114	0 0184	0 0070	0.0087	0.0100	0 0105
Na	0 1051	0 1046	0.0994	0.0992	0.0738	0.0994
K	1.7427	1.7321	1.7556	1.7795	1.7802	1.7807
Tot	15 6269	15 6368	15 6377	15.6358	15.6136	15.6709

OHF28 BIOTITE

	1	2
	c	r
SiO2	34 40	34 50
TiO2	3 29	3 40
Al2O3	13 77	13 38
FeO	27 31	27 69
MnO	0 77	0 75
MgO	6 39	6 12
CaO	0 01	0 01
Na2O	0 31	0 20
K2O	8 83	9 06
Tot	95 08	95.12
Si	5 5217	5 5530
Ti	0.3972	0.4116
Al	2.6058	2.5390
Fe2+	3.6662	3.7274
Mn	0.1046	0.1023
Mg	1.5286	1.4685
Ca	0.0016	0.0026
Na	0.0962	0.0628
K	1.8088	1.8604
Tot	15.7307	15.7275

ORF39 BIOTITE

	1	2	3	4	5	6	7
		c	r	c	r		
SiO2	35 28	35 22	34 92	34 72	34 21	34 24	34 64
TiO2	3 62	3 43	3 70	3 63	3 82	4 31	4 00
Al2O3	14 25	14 09	14 26	14 16	14 05	13 40	13 77
FeO	25 95	25 44	26 04	25 75	26 05	25 45	25 56
MnO	0 59	0 59	0 56	0 61	0 66	0 65	0 61
MgO	7 97	8 08	7 76	7 99	6 95	7 09	7 54
CaO	0 00	0 03	0 00	0 04	0 00	0 00	0 00
Na2O	0 30	0 26	0 31	0 28	0 29	0 27	0 25
K2O	9 05	8 91	9 04	8 83	8 66	8 37	8 80
Tot	97 02	96 05	96 59	96 02	94 69	93 78	95 17
Si	5 4910	5.5229	5 4675	5.4623	5 4728	5 5121	5 4971
Ti	0 4239	0.4045	0.4362	0.4295	0.4596	0 5218	0 4774
Al	2 6149	2.6051	2 6319	2.6255	2.6499	2 5432	2 5762
Fe2+	3.3777	3 3358	3.4094	3.3877	3.4853	3 4264	3 3923
Mn	0.0781	0 0786	0.0737	0 0818	0 0894	0 0886	0 0820
Mg	1 8482	1 8880	1 8115	1.8731	1 6570	1 7010	1 7832
Ca	0 0001	0 0046	0.0000	0.0060	0 0000	0 0000	0 0000
Na	0.0901	0 0789	0.0954	0 0864	0.0896	0 0840	0 0769
K	1 7974	1.7822	1.8047	1.7726	1.7675	1 7190	1 7816
Tot	15.7214	15 7007	15 7303	15 7250	15.6712	15 5961	15 6667

ORF 30 BIOTITE

	1	2	3	4	5	6
	c	m	r			
SiO2	34 91	34 71	35 45	34 63	34 10	34 85
TiO2	2 95	3 98	3 19	3 69	4 72	3 72
Al2O3	14 72	14 06	13 21	14 26	14 28	14 53
FeO	22 21	23 70	24 78	22 71	22 59	23 51
MnO	0 45	0 47	0 58	0 46	0 45	0 45
MgO	10 15	9 39	9 27	9 78	9 10	9 10
CaO	0 00	0 00	0 00	0 00	0 00	0 00
Na2O	0 20	0 30	0 17	0 26	0 21	0 19
K2O	9 02	8 97	9 09	8 58	8 83	9 10
Tot	94 61	95 58	95 74	94 37	94 28	95 45
Si	5 4734	5 435[illegible]	5 5685	5 4531	5 3884	5 4537
Ti	0 3478	0 4687	0 3769	0 4370	0 5609	0 4378
Al	2 7208	2 5956	2 4463	2 6473	2 6603	2 6806
Fe2+	2 9123	3 1037	3 2554	2 9908	2 9854	3 0769
Mn	0 0598	0 0623	0 0772	0 0614	0 0602	0 0596
Mg	2 3717	2 1913	2 1701	2 2952	2 1430	2 1223
Ca	0 0005	0 0000	0 0000	0 0000	0 0000	0 0000
Na	0 0599	0 0911	0 0524	0 0794	0 0643	0 0577
K	1 8042	1 7920	1 8217	1 7237	1 7801	1 8168
Tot	15 7504	15 7399	15 7685	15 6878	15 6427	15 7054

ORF44 BIOTITE

	1	2	3	4
		c	r	
SiO2	36 08	36.05	34.73	36.27
TiO2	2 68	2.54	2.88	2.76
Al2O3	12 47	12.43	13.21	12.98
FeO	24 85	24.97	26.24	24.04
MnO	0 84	0 89	0 84	0.86
MgO	8 70	8 56	7.71	8.34
CaO	0 01	0 01	0.01	0.03
Na2O	0 31	0 25	0.31	0.23
K2O	8.29	8 52	8.36	8.49
Tot	94 23	94.22	94.30	94.00
Si	5.7391	5.7479	5.5788	5.7581
Ti	0.3206	0.3046	0.3480	0.3295
Al	2.3385	2.3365	2.5019	2.4294
Fe2+	3.3059	3.3297	3.5255	3.1919
Mn	0.1132	0.1202	0.1143	0.1156
Mg	2.0631	2.0341	1.8459	1.9733
Ca	0.0024	0.0011	0.0009	0.0047
Na	0.0944	0.0773	0.0986	0.0705
K	1.6822	1.7331	1.7175	1.7196
Tot	15.6593	15.6844	15.7293	15.5927

ORF49 BIOTITE

	1	2	3
SiO2	34 42	35.14	35.13
TiO2	3 01	3.00	3.66
Al2O3	13.58	13.64	14.46
FeO	23.52	23.90	26.14
MnO	0.77	0.71	0.56
MgO	9 02	9 35	7.83
CaO	0.02	0.00	0.01
Na2O	0 33	0.29	0.26
K2O	8.97	9 18	9.05
Tot	93.64	95.20	97.08
Si	5.5181	5.5390	5.4673
Ti	0.3634	0.3556	0.4285
Al	2.5674	2.5346	2.6523
Fe2+	3 1540	3 1506	3.4022
Mn	0 1039	0.0951	0.0742
Mg	2.1559	2 1960	1.8151
Ca	0.0030	0.0000	0.0012
Na	0.1030	0 0892	0.0779
K	1.8348	1.8458	1.7965
Tot	15.8037	15.8057	15.7152

ORF12 CLINOPYROXENE

	1	2	3	4	5	6	7	8	9	10	11	12	13	14	15	16	17	18	19	20	21	22
	c	r					c	m	r	c	m	m	r									
SiO2	51 34	51 01	51 00	50 76	46 25	45 53	46 10	50 76	50 69	52 00	50 86	51 04	50 46	51 16	50 77	50 82	51 10	52 75	51 49	52 17	52 36	52 21
TiO2	0 37	0 30	0 31	0 26	1 72	1 65	1 72	0 26	0 33	0 17	0 32	0 38	0 23	0 32	0 32	0 34	0 26	0 67	0 28	0 30	0 35	0 27
Al2O3	1 77	2 07	1 76	1 56	7 80	8 79	8 38	1 65	1 51	1 08	1 63	1 63	1 40	1 67	1 73	1 75	1 36	1 64	1 41	1 67	1 75	1 62
Cr2O3	0 01	0 00	0 01	0 02	0 01	0 03	0 03	0 02	0 11	0 01	0 04	0 03	0 00	0 01	0 00	0 00	0 00	0 00	0 00	0 00	0 01	0 00
Fe2O3	4 95	7 11	6 50	6 61	8 59	9 18	8 28	5 44	6 11	4 14	5 34	5 39	6 43	4 89	5 03	4 43	4 29	2 24	3 13	3 43	2 06	2 78
FeO	6 00	5 45	5 35	6 18	1 79	0 51	0 17	7 75	6 45	5 77	7 07	7 49	6 41	7 13	7 17	7 82	7 90	7 58	9 49	9 05	9 24	9 54
MnO	0 83	0 79	0 76	0 79	0 44	0 46	0 34	0 81	0 78	0 64	0 79	0 79	0 77	0 75	0 80	0 77	0 76	0 67	0 81	0 82	0 66	0 78
MgO	11 26	9 98	10 71	9 85	10 78	11 49	11 78	9 80	9 66	11 73	9 82	9 58	9 50	10 31	10 35	10 17	10 30	12 01	10 03	10 03	10 76	10 05
CaO	22 79	22 05	22 73	22 06	20 88	20 17	22 17	21 92	21 44	22 76	21 63	21 28	22 01	22 02	21 96	21 68	22 16	21 96	21 74	22 07	22 13	21 89
Na2O	1 21	1 93	1 50	1 75	1 87	1 86	1 45	1 47	1 94	1 26	1 73	1 89	1 78	1 50	1 39	1 42	1 27	1 27	1 25	1 43	1 18	1 38
Total	100 51	100 69	100 64	99 85	100 14	99 67	100 43	99 88	99 02	99 56	99 21	99 49	98 98	99 76	99 51	99 20	99 40	100 78	99 62	100 97	100 52	100 52
Si	1 9247	1 9158	1 9147	1 9273	1 7266	1 6984	1 7057	1 9315	1 9387	1 9584	1 9412	1 9444	1 9351	1 9392	1 9312	1 9398	1 9475	1 9598	1 9616	1 9581	1 9650	1 9673
Al	0 0000	0 0000	0 0000	0 0000	0 0000	0 0000	0 0000	0 0000	0 0000	0 0000	0 0000	0 0000	0 0000	0 0000	0 0000	0 0000	0 0000	0 0000	0 0000	0 0000	0 0000	0 0000
Fe3+	0 0000	0 0000	0 0000	0 0000	0 0000	0 0000	0 0000	0 0000	0 0000	0 0000	0 0000	0 0000	0 0000	0 0000	0 0000	0 0000	0 0000	0 0000	0 0000	0 0000	0 0000	0 0000
Al	0 0781	0 0916	0 0780	0 0699	0 3434	0 3865	0 3657	0 0741	0 0682	0 0480	0 0727	0 0732	0 0631	0 0746	0 0776	0 0788	0 0611	0 0718	0 0634	0 0739	0 0774	0 0720
Fe3+	0 1395	0 2009	0 1835	0 1890	0 2414	0 2579	0 2305	0 1558	0 1758	0 1174	0 1533	0 1545	0 1855	0 1395	0 1440	0 1274	0 1231	0 0625	0 0897	0 0970	0 0581	0 0789
Ti	0 0103	0 0084	0 0089	0 0074	0 0484	0 0463	0 0480	0 0073	0 0095	0 0048	0 0092	0 0109	0 0067	0 0090	0 0092	0 0097	0 0074	0 0187	0 0079	0 0085	0 0100	0 0077
Cr	0 0003	0 0000	0 0003	0 0006	0 0004	0 0009	0 0009	0 0007	0 0033	0 0002	0 0011	0 0010	0 0000	0 0002	0 0000	0 0000	0 0000	0 0000	0 0000	0 0001	0 0003	0 0000
Mg	0 6290	0 5586	0 5991	0 5575	0 3664	0 3084	0 3550	0 5559	0 5507	0 6586	0 5588	0 5440	0 5427	0 5826	0 5870	0 5783	0 5852	0 6648	0 5695	0 5605	0 6018	0 5641
Fe2+	0 1428	0 1406	0 1303	0 1757	0 0000	0 0000	0 0000	0 2061	0 1926	0 1711	0 2049	0 2164	0 2020	0 1941	0 1823	0 2059	0 2232	0 1821	0 2695	0 2601	0 2524	0 2774
Mn	0 0000	0 0000	0 0000	0 0000	0 0000	0 0000	0 0000	0 0000	0 0000	0 0000	0 0000	0 0000	0 0000	0 0000	0 0000	0 0000	0 0000	0 0000	0 0000	0 0000	0 0000	0 0000
Mg	0 0000	0 0000	0 0000	0 0000	0 2334	0 3302	0 2948	0 0000	0 0000	0 0000	0 0000	0 0000	0 0000	0 0000	0 0000	0 0000	0 0000	0 0000	0 0000	0 0000	0 0000	0 0000
Fe2+	0 0454	0 0308	0 0379	0 0207	0 0560	0 0158	0 0054	0 0404	0 0138	0 0108	0 0206	0 0221	0 0035	0 0318	0 0460	0 0439	0 0285	0 0534	0 0330	0 0240	0 0376	0 0233
Mn	0 0262	0 0253	0 0243	0 0255	0 0138	0 0146	0 0107	0 0261	0 0252	0 0204	0 0255	0 0254	0 0250	0 0242	0 0256	0 0248	0 0247	0 0211	0 0260	0 0261	0 0216	0 0248
Ca	0 9157	0 8875	0 9144	0 8977	0 8352	0 8063	0 8790	0 8937	0 8787	0 9185	0 8848	0 8687	0 9043	0 8942	0 8950	0 8865	0 9051	0 8742	0 8873	0 8878	0 8899	0 8838
Na	0 0880	0 1407	0 1088	0 1288	0 1351	0 1347	0 1044	0 1083	0 1436	0 0919	0 1279	0 1393	0 1321	0 1106	0 1022	0 1051	0 0942	0 0915	0 0921	0 1041	0 0859	0 1008
Total	4 0000	4 0000	4 0000	4 0000	4 0000	4 0000	4 0000	4 0000	4 0000	4 0000	4 0000	4 0000	4 0000	4 0000	4 0000	4 0000	4 0000	4 0000	4 0000	4 0000	4 0000	4 0000

ORF30 CLINOPYROXENE

	1	2	3	4	5	6	7	8	9
SiO2	50 42	50 22	48 61	48 84	49 62	50 36	51 10	50 88	51 06
TiO2	0 16	0 15	0 48	0 41	0 19	0 24	0 18	0 24	0 21
Al2O3	1 28	1 19	2 68	1 92	1 31	1 76	1 43	1 43	1 50
Cr2O3	0 00	0 00	0 00	0 00	0 00	0 02	0 02	0 02	0 00
Fe2O3	5 79	6 20	9 41	7 80	7 27	6 03	6 74	5 87	5 78
FeO	8 76	9 42	8 11	7 94	7 48	8 04	4 42	5 66	5 41
MnO	0 71	0 73	0 72	0 70	0 72	0 64	0 60	0 50	0 54
MgO	8 86	8 35	7 77	8 14	8 91	11 11	11 79	11 15	11 29
CaO	23 47	22 53	19 73	22 71	23 28	23 30	23 76	23 36	23 55
Na2O	1 10	1 35	2 28	1 41	1 20	0 88	1 03	1 09	1 08
Total	100 55	100 14	99 80	99 87	99 89	100 38	101 07	100 21	100 41
Si	1 9242	1 9295	1 8740	1 8838	1 9047	1 9003	1 9059	1 9181	1 9185
Al	0 0000	0 0000	0 0000	0 0000	0 0000	0 0000	0 0000	0 0000	0 0000
Fe3+	0 0000	0 0000	0 0000	0 0000	0 0000	0 0000	0 0000	0 0000	0 0000
Al	0 0575	0 0540	0 1219	0 0871	0 0592	0 0782	0 0629	0 0634	0 0663
Fe3+	0 1662	0 1792	0 2730	0 2266	0 2100	0 1713	0 1893	0 1666	0 1634
Ti	0 0046	0 0043	0 0139	0 0119	0 0055	0 0069	0 0051	0 0067	0 0058
Cr	0 0000	0 0000	0 0000	0 0000	0 0000	0 0006	0 0007	0 0005	0 0001
Mg	0 5041	0 4783	0 4465	0 4677	0 5097	0 6247	0 6552	0 6266	0 6323
Fe2+	0 2677	0 2842	0 1447	0 2067	0 2156	0 1183	0 0868	0 1363	0 1321
Mn	0 0000	0 0000	0 0000	0 0000	0 0000	0 0000	0 0000	0 0000	0 0000
Mg	0 0000	0 0000	0 0000	0 0000	0 0000	0 0000	0 0000	0 0000	0 0000
Fe2+	0 0119	0 0184	0 1169	0 0493	0 0247	0 0723	0 0510	0 0423	0 0378
Mn	0 0228	0 0239	0 0236	0 0230	0 0234	0 0205	0 0188	0 0159	0 0171
Ca	0 9599	0 9274	0 8151	0 9387	0 9576	0 9424	0 9496	0 9437	0 9481
Na	0 0812	0 1008	0 1705	0 1052	0 0896	0 0645	0 0748	0 0800	0 0784
Total	4 0000	4 0000	4 0000	4 0000	4 0000	4 0000	4 0000	4 0000	4 0000

ORF44 NEPHELINE

	1	2	3	4	5	6	7	8	9	10	11	12	13	14	15	16
SiO2	44.86	44.79	44.35	44.86	44.34	43.89	45.32	43.93	44.69	44.61	44.51	44.48	44.63	44.68	44.48	44.57
Al2O3	32.68	32.26	32.71	32.24	32.69	32.61	32.34	32.58	32.47	32.74	32.65	32.46	32.46	32.67	32.58	32.60
FeO	0.26	0.31	0.29	0.30	0.31	0.30	0.33	0.29	0.18	0.19	0.22	0.22	0.24	0.15	0.24	0.23
CaO	0.27	0.26	0.32	0.27	0.30	0.27	0.28	0.29	0.26	0.29	0.24	0.23	0.23	0.27	0.25	0.24
Na2O	16.23	16.52	16.55	16.49	16.73	16.58	16.58	16.66	16.55	16.73	16.73	16.92	16.92	16.85	16.77	16.88
K2O	5.35	5.11	5.31	5.17	5.33	5.47	5.18	5.33	5.34	5.34	5.47	5.42	5.48	5.39	5.37	5.35
Total	99.65	99.25	99.53	99.33	99.70	99.12	100.03	99.08	99.49	99.90	99.82	99.73	99.96	100.01	99.69	99.87
Qz	6.64	6.29	5.53	6.34	5.12	4.80	6.57	4.87	5.81	5.36	5.08	4.73	4.79	5.11	5.11	5.00
Ne	75.20	76.40	76.49	76.17	76.93	76.67	76.03	77.07	76.18	76.71	76.57	77.16	76.95	76.88	76.86	77.10
Ks	18.16	17.31	17.98	17.49	17.95	18.53	17.40	18.06	18.01	17.94	18.34	18.11	18.26	18.02	18.03	17.90

ORF30 NEPHELINE

	1	2	3
SiO2	43.91	43.83	44.33
Al2O3	32.61	32.80	32.57
FeO	0.33	0.29	0.29
CaO	0.21	0.21	0.19
Na2O	16.63	16.60	16.69
K2O	6.04	6.22	5.91
Total	99.73	99.95	99.98
Qz	3.94	3.68	4.39
Ne	75.87	75.57	75.9[illegible]
Ks	20.19	20.74	19.69

ORF28 SODALITE

	1	2	3	4	5
SiO2	39.43	38.69	38.59	37.90	37.40
Al2O3	31.98	31.84	31.71	31.67	31.23
FeO	0.10	0.14	0.11	0.07	0.25
CaO	0.19	0.19	0.16	0.11	0.15
Na2O	24.61	26.46	26.13	26.38	25.93
K2O	0.02	0.01	0.00	0.04	0.02
Total	96.32	97.33	96.70	96.17	94.99

ORF43 SODALITE

	1	2	3
SiO2	38.01	37.78	36.89
Al2O3	31.66	31.71	30.87
FeO	0.12	0.17	0.17
CaO	0.16	0.19	0.23
Na2O	26.17	26.43	26.43
K2O	0.03	0.03	0.00
Total	96.14	96.30	94.59

ORF12 PLAGIOCLASE

	1	2	3	4	5	6	7	8	9	10	11	12	13	14	15	16
SiO2	68.48	68.27	67.94	68.18	68.33	68.03	68.57	67.97	68.71	66.36	66.10	68.62	67.66	68.13	67.17	68.20
Al2O3	20.20	20.65	20.60	20.07	20.09	20.29	20.32	20.13	20.06	20.47	20.46	20.00	20.48	20.05	20.03	20.34
FeO	0.05	0.03	0.04	0.08	0.08	0.12	0.04	0.08	0.10	0.05	0.08	0.11	0.07	0.06	0.06	0.16
CaO	0.82	1.16	1.23	0.83	0.74	0.97	0.84	0.87	0.77	1.52	1.19	0.72	1.35	0.85	0.64	0.98
Na2O	11.30	11.41	11.31	11.29	11.37	11.07	11.43	11.43	11.53	11.27	11.33	11.60	11.45	11.74	12.11	11.42
K2O	0.29	0.12	0.11	0.18	0.16	0.45	0.13	0.17	0.15	0.14	0.13	0.37	0.16	0.35	0.13	0.43
Total	101.14	101.64	101.23	100.63	100.77	100.93	101.32	100.65	101.33	99.83	101.29	101.43	101.17	101.18	100.13	101.53
An	3.77	5.28	5.64	3.87	3.46	4.52	3.85	4.01	3.54	6.86	5.45	3.27	6.06	3.76	2.80	4.41
Ab	94.63	94.07	93.75	95.15	95.65	93.00	95.45	95.05	95.64	92.37	93.85	94.74	93.09	94.36	96.53	93.29
Or	1.60	0.66	0.61	0.97	0.89	2.49	0.70	0.94	0.82	0.76	0.70	1.99	0.84	1.87	0.67	2.29

ORF29 PLAGIOCLASE

	1	2	3	4
SiO2	65.74	65.14	66.11	65.95
Al2O3	21.45	20.61	21.04	21.66
FeO	0.06	0.05	0.07	0.06
CaO	2.40	2.18	2.53	2.52
Na2O	10.66	10.90	10.79	10.74
K2O	0.15	0.29	0.17	0.15
Total	100.48	99.17	100.71	101.08
An	10.98	9.80	11.38	11.40
Ab	88.19	88.66	87.70	87.81
Or	0.83	1.54	0.92	0.79

ORF12 ALKALI-FELDSPAR

	1	2	3	4	5	6	7	8	9	10	11
SiO2	63.76	69.19	66.71	67.43	65.96	68.36	67.38	64.57	68.13	68.20	67.46
Al2O3	18.09	19.44	19.55	20.04	19.84	20.14	19.00	18.11	20.05	20.34	20.00
FeO	0.03	0.01	0.04	0.05	0.08	0.09	0.07	0.05	0.06	0.16	0.11
CaO	0.46	0.09	0.42	0.85	0.52	0.75	0.19	0.04	0.85	0.98	0.89
Na2O	0.93	10.51	9.36	9.20	10.15	11.22	6.99	0.30	11.74	11.42	11.14
K2O	15.10	1.84	3.68	3.22	2.97	0.98	7.15	15.62	0.35	0.43	0.87
Total	98.37	101.07	99.75	100.78	99.52	101.54	100.78	98.70	101.18	101.53	100.48
An	2.28	0.40	1.92	4.00	2.33	3.39	0.90	0.22	3.76	4.41	4.03
Ab	8.36	89.33	77.93	78.05	81.89	91.34	59.27	2.83	94.36	93.29	91.27
Or	89.36	10.26	20.15	17.95	15.78	5.27	39.83	96.94	1.87	2.29	4.70

ORF29 ALKALI-FELDSPAR

	1	2	3	4	5	6	7	8	9	10	12	13
SiO2	66.13	65.14	66.06	65.62	66.21	66.09	64.89	65.30	65.51	65.49	64.61	65.56
Al2O3	20.95	20.61	20.87	18.62	19.52	18.86	18.44	18.64	18.62	18.68	18.38	18.80
FeO	0.08	0.05	0.08	0.07	0.05	0.06	0.05	0.04	0.01	0.00	0.01	0.00
CaO	2.31	2.18	2.22	0.18	0.79	0.33	0.21	0.22	0.20	0.25	0.12	0.22
Na2O	10.55	10.90	10.23	3.38	6.53	4.46	2.74	3.18	4.17	4.65	3.03	4.72
K2O	0.62	0.29	1.02	11.62	7.00	9.79	12.71	11.97	10.75	10.08	12.17	9.90
Total	100.65	99.17	100.48	99.49	100.10	99.59	99.04	99.34	99.26	99.14	98.32	99.20
An	10.43	9.60	10.13	0.91	3.78	1.62	1.02	1.08	0.99	1.23	0.62	1.07
Ab	86.22	88.66	84.36	30.39	56.43	40.27	24.43	28.44	36.70	40.70	27.31	41.59
Or	3.35	1.54	5.51	68.70	39.80	58.11	74.55	70.48	62.31	58.07	72.08	57.34

ORF29 ALKALI-FELDSPAR

	14	15	16	17	18	19	20
SiO2	65.47	65.81	65.42	65.98	65.52	64.94	64.05
Al2O3	18.97	19.32	19.01	18.71	18.87	18.44	18.60
FeO	0.03	0.03	0.03	0.03	0.08	0.02	0.05
CaO	0.15	0.63	0.57	0.22	0.44	0.20	0.30
Na2O	4.61	5.90	5.02	5.63	5.05	4.17	3.47
K2O	10.24	7.91	9.17	8.70	9.25	10.79	11.67
Total	99.46	99.62	99.21	99.26	99.21	98.56	98.14
An	0.70	3.04	2.76	1.04	2.13	0.96	1.46
Ab	40.37	51.52	44.19	49.08	44.40	36.66	30.64
Or	58.93	45.43	53.05	49.88	53.48	62.38	67.90

ORF28 ALKALI-FELDSPAR

	1	2	3	4	5	6	7	8	9
SiO2	65.20	66.39	65.30	65.35	64.21	67.49	66.86	65.79	65.75
Al2O3	18.37	18.77	18.27	18.35	17.99	19.28	19.20	18.67	18.77
FeO	0.03	0.05	0.07	0.09	0.03	0.04	0.08	0.07	0.10
CaO	0.17	0.40	0.15	0.27	0.06	0.26	0.26	0.23	0.16
Na2O	4.28	6.31	4.37	4.15	0.54	9.18	7.91	4.91	4.31
K2O	10.57	7.71	10.40	10.42	15.30	3.79	5.26	9.51	10.33
Total	98.62	99.63	98.56	98.63	98.14	100.04	99.57	99.38	99.42
An	0.83	1.91	0.71	1.34	0.33	1.21	1.25	1.12	0.79
Ab	37.79	54.39	38.69	37.20	5.05	77.69	68.70	43.48	38.51
Or	61.38	43.71	60.59	61.46	94.62	21.10	30.06	55.40	60.70

Monzodiorite

ORS175 AMPHIBOLE

	1 c	2 m	3 r	4	5	6	7	8
SiO2	39.90	39.93	39.63	40.60	40.27	40.17	39.75	39.86
TiO2	3.67	3.33	3.17	4.40	4.45	4.35	3.95	3.62
Al2O3	11.17	11.24	11.32	10.55	10.85	10.92	11.14	11.36
Fe2O3	0.00	0.49	0.86	0.00	0.00	0.00	0.00	0.31
FeO	17.42	17.91	17.97	17.79	17.86	17.88	18.33	18.21
MnO	0.28	0.31	0.37	0.34	0.29	0.38	0.33	0.37
MgO	9.45	9.07	8.87	9.24	9.23	9.14	8.95	8.86
CaO	11.56	11.53	11.55	11.58	11.51	11.40	11.62	11.59
Na2O	2.76	2.77	2.80	2.83	2.87	2.87	2.69	2.74
K2O	1.47	1.48	1.48	1.36	1.31	1.21	1.40	1.37
Tot	97.69	98.07	98.02	98.69	98.64	98.32	98.15	98.28
Si	6.1231	6.1209	6.0921	6.1888	6.1336	6.1289	6.0941	6.1004
ivAl	1.8769	1.8791	1.9079	1.8112	1.8664	1.8711	1.9059	1.8996
Fe3+	0.0000	0.0000	0.0000	0.0000	0.0000	0.0000	0.0000	0.0000
Ti4+	0.0000	0.0000	0.0000	0.0000	0.0000	0.0000	0.0000	0.0000
viAl	0.1435	0.1518	0.1433	0.0840	0.0815	0.0920	0.1074	0.1495
Ti	0.4238	0.3841	0.3662	0.5044	0.5101	0.4989	0.4553	0.4161
Fe3+	0.0000	0.0569	0.0999	0.0000	0.0000	0.0000	0.0000	0.0356
Fe2+	2.2358	2.2955	2.3109	2.2675	2.2755	2.2807	2.3502	2.3305
Mg	2.1608	2.0716	2.0313	2.1003	2.0955	2.0789	2.0448	2.0207
Mn	0.0361	0.0402	0.0483	0.0438	0.0374	0.0495	0.0423	0.0477
Mg	0.0000	0.0000	0.0000	0.0000	0.0000	0.0000	0.0000	0.0000
Fe2+	0.0000	0.0000	0.0000	0.0000	0.0000	0.0000	0.0000	0.0000
Mn	0.0000	0.0000	0.0000	0.0000	0.0000	0.0000	0.0000	0.0000
Ca	1.9016	1.8941	1.9026	1.8909	1.8785	1.8639	1.9083	1.9013
Na	0.0984	0.1059	0.0974	0.1091	0.1215	0.1361	0.0917	0.0987
Ca	0.0000	0.0000	0.0000	0.0000	0.0000	0.0000	0.0000	0.0000
Na	0.7232	0.7178	0.7384	0.7288	0.7246	0.7116	0.7088	0.7135
K	0.2887	0.2903	0.2912	0.2652	0.2541	0.2356	0.2736	0.2676
Tot	16.0118	16.0081	16.0296	15.9939	15.9788	15.9472	15.9824	15.9811

ORS176 AMPHIBOLE

	1	2	3	4	5	6	7	8	9	11	12	13	14	15
SiO2	39.97	40.08	39.97	39.65	39.59	39.54	39.14	39.42	39.98	39.58	39.16	39.05	39.14	40.05
TiO2	2.86	3.07	3.31	3.08	2.35	3.59	3.50	3.95	4.49	1.25	3.42	3.52	3.46	3.40
Al2O3	11.31	10.78	10.81	11.21	12.04	11.97	12.52	12.04	11.93	12.71	11.48	11.60	11.44	11.41
Fe2O3	0.00	0.85	0.18	0.84	0.22	0.05	0.66	0.00	0.00	3.35	0.63	0.77	1.11	0.00
FeO	20.91	20.56	20.51	20.26	20.32	20.39	20.36	19.34	17.17	18.47	20.63	20.63	20.42	21.42
MnO	0.38	0.35	0.41	0.35	0.35	0.33	0.36	0.36	0.27	0.28	0.43	0.37	0.39	0.37
MgO	7.15	7.20	7.35	7.26	7.17	7.51	6.87	7.46	8.65	7.13	6.92	6.95	7.03	6.99
CaO	11.19	10.86	10.95	10.94	11.07	11.30	11.09	11.05	10.90	10.92	10.97	10.98	10.98	11.20
Na2O	3.06	3.00	2.97	3.03	3.13	3.17	3.12	3.17	3.12	3.05	3.07	3.08	3.06	3.11
K2O	1.47	1.52	1.46	1.51	1.49	1.28	1.21	1.17	1.27	1.48	1.44	1.53	1.44	1.49
Tot	98.30	98.28	97.91	98.12	97.74	99.12	98.84	97.95	97.78	98.22	98.49	98.55	98.46	99.44
Si	6.1918	6.2049	6.2021	6.1464	6.1490	6.0541	6.0141	6.0883	6.1212	6.1011	6.0884	6.0940	6.0930	6.1466
ivAl	1.8082	1.7951	1.7979	1.8536	1.8510	1.9459	1.9859	1.9117	1.8788	1.8989	1.9196	1.9554	1.9370	1.8534
Fe3+	0.0000	0.0000	0.0000	0.0000	0.0000	0.0000	0.0000	0.0000	0.0000	0.0000	0.0000	0.0000	0.0000	0.0000
Ti4+	0.0000	0.0000	0.0000	0.0000	0.0000	0.0000	0.0000	0.0000	0.0000	0.0000	0.0000	0.0000	0.0000	0.0000
viAl	0.2569	0.1733	0.1791	0.1951	0.3538	0.2140	0.2819	0.2799	0.2752	0.4112	0.1820	0.1787	0.1522	0.2119
Ti	0.3338	0.3579	0.3865	0.3588	0.2748	0.4132	0.4042	0.4593	0.5173	0.1448	0.3991	0.4098	0.4028	0.3930
Fe3+	0.0000	0.0995	0.0207	0.0980	0.0262	0.0059	0.0766	0.0000	0.0000	0.3884	0.0809	0.0902	0.1293	0.0000
Fe2+	2.7091	2.6616	2.6613	2.6258	2.6400	2.6111	2.6162	2.4977	2.1983	2.3812	2.6791	2.6707	2.6450	2.7490
Mg	1.6510	1.6619	1.6987	1.6767	1.6593	1.7134	1.5738	1.7162	1.9742	1.6374	1.6024	1.6023	1.6199	1.5984
Mn	0.0492	0.0457	0.0537	0.0456	0.0460	0.0424	0.0473	0.0470	0.0351	0.0369	0.0565	0.0483	0.0507	0.0478
Mg	0.0000	0.0000	0.0000	0.0000	0.0000	0.0000	0.0000	0.0000	0.0000	0.0000	0.0000	0.0000	0.0000	0.0000
Fe2+	0.0000	0.0000	0.0000	0.0000	0.0000	0.0000	0.0000	0.0000	0.0000	0.0000	0.0000	0.0000	0.0000	0.0000
Mn	0.0000	0.0000	0.0000	0.0000	0.0000	0.0000	0.0000	0.0000	0.0000	0.0000	0.0000	0.0000	0.0000	0.0000
Ca	1.8576	1.8024	1.8205	1.8176	1.8425	1.8535	1.8256	1.8285	1.7888	1.8033	1.8254	1.8211	1.8227	1.8422
Na	0.1424	0.1976	0.1795	0.1824	0.1575	0.1465	0.1744	0.1715	0.2112	0.1967	0.1746	0.1789	0.1773	0.1578
Ca	0.0000	0.0000	0.0000	0.0000	0.0000	0.0000	0.0000	0.0000	0.0000	0.0000	0.0000	0.0000	0.0000	0.0000
Na	0.7768	0.7041	0.7155	0.7269	0.7843	0.7959	0.7554	0.7768	0.7141	0.7148	0.7488	0.7446	0.7422	0.7689
K	0.2899	0.3000	0.2890	0.2984	0.2947	0.2504	0.2380	0.2306	0.2476	0.2914	0.2844	0.3012	0.2850	0.2923
Tot	16.0687	16.0041	16.0045	16.0253	16.0790	16.0462	15.9934	16.0074	15.9617	16.0062	16.0332	16.0459	16.0272	16.0612

ORS133 BIOTITE

	1 c	2 r	3	4	5	6	7
SiO2	35.34	35.67	35.44	34.86	34.10	34.56	34.65
TiO2	3.55	4.46	4.54	4.36	4.77	4.11	4.07
Al2O3	14.46	14.50	14.04	14.54	14.58	14.63	14.66
FeO	19.69	19.88	19.40	19.58	19.73	19.65	19.91
MnO	0.43	0.45	0.41	0.45	0.42	0.43	0.43
MgO	12.37	11.37	11.87	11.97	11.24	11.86	11.78
CaO	0.00	0.00	0.00	0.00	0.00	0.00	0.00
Na2O	0.21	0.25	0.30	0.28	0.30	0.25	0.23
K2O	9.14	8.54	9.08	8.69	8.34	8.73	8.80
Tot	95.19	95.11	95.06	94.74	93.47	94.21	94.54
Si	5.4409	5.4751	5.4573	5.3852	5.3448	5.3748	5.3761
Ti	0.4111	0.5144	0.5261	0.5066	0.5617	0.4805	0.4753
Al	2.6241	2.6240	2.5485	2.6482	2.6940	2.6828	2.6853
Fe2+	2.5358	2.5518	2.4978	2.5303	2.5867	2.5555	2.5841
Mn	0.0565	0.0586	0.0531	0.0585	0.0556	0.0568	0.0563
Mg	2.8394	2.6012	2.7241	2.7564	2.6244	2.7487	2.7242
Ca	0.0000	0.0000	0.0000	0.0000	0.0000	0.0000	0.0000
Na	0.0612	0.0741	0.0881	0.0845	0.0909	0.0757	0.0680
K	1.7952	1.6723	1.7829	1.7132	1.6679	1.7327	1.7413

ORS175 BIOTITE

	1	2 c	3 r	4
SiO2	34.76	35.83	35.54	35.74
TiO2	3.71	4.37	4.42	4.26
Al2O3	14.84	14.57	14.68	14.50
FeO	21.97	19.81	20.04	20.07
MnO	0.26	0.24	0.25	0.23
MgO	10.98	12.06	11.90	11.97
CaO	0.04	0.00	0.00	0.00
Na2O	0.10	0.18	0.16	0.16
K2O	8.13	9.21	9.25	9.42
Tot	94.80	96.37	96.24	96.35
Si	5.3987	5.4412	5.4130	5.4411
Ti	0.4334	0.4987	0.5062	0.4876
Al	2.7183	2.6082	2.6359	2.6015
Fe2+	2.8542	2.5288	2.5532	2.5558
Mn	0.0346	0.0311	0.0320	0.0300
Mg	2.5416	2.7297	2.7007	2.7166
Ca	0.0067	0.0000	0.0000	0.0000
Na	0.0316	0.0532	0.0469	0.0469
K	1.6113	1.7833	1.7965	1.8291

ORS133 CLINOPYROXENE

	1	2	3	4	5	6	7	8	9	10	11	12	13	14	15	16	17	18	19	20	21	22	23
					c	m	r						c	m	r								
SiO2	49 49	52 63	50 70	52 00	49 42	51 42	51 88	51 85	51 74	51 98	51 53	51 53	49 41	51 24	51 28	51 46	51 26	50 80	51 37	53 43	52 85	50 46	49 53
TiO2	1 68	0 12	0 85	0 49	0 92	0 81	0 74	0 45	0 20	0 72	0 74	0 97	1 16	0 79	0 31	0 56	0 70	0 53	0 23	0 10	0 13	1 13	1 25
Al2O3	4 02	1 39	2 71	1 83	5 73	2 21	1 85	1 87	1 49	1 88	2 03	2 19	4 32	1 91	1 73	2 12	2 10	2 16	1 79	0 26	1 05	3 10	3 88
Cr2O3	0 01	0 01	0 05	0 01	0 13	0 01	0 01	0 03	0 00	0 01	0 01	0 01	0 01	0 00	0 00	0 00	0 00	0 00	0 00	0 00	0 00	0 00	0 00
Fe2O3	4 95	2 89	5 61	4 75	5 18	4 63	4 80	3 49	4 55	3 60	3 31	4 26	6 52	4 30	5 15	4 90	4 45	5 44	5 21	2 68	3 72	4 77	6 03
FeO	3 57	6 00	3 71	4 11	0 16	4 54	6 18	4 10	5 69	4 26	6 35	4 24	0 00	4 04	5 23	5 04	5 18	5 31	5 58	2 90	4 03	2 07	1 42
MnO	0 32	0 43	0 43	0 46	0 17	0 47	0 52	0 41	0 51	0 40	0 44	0 45	0 21	0 39	0 49	0 48	0 41	0 44	0 49	0 46	0 46	0 22	0 30
MgO	12 31	12 75	12 49	12 91	14 47	12 59	11 52	13 61	12 06	13 28	12 30	13 09	14 27	13 01	11 81	11 91	12 17	11 49	11 63	15 71	13 81	13 70	13 69
CaO	22 75	23 11	22 86	22 63	22 65	22 95	22 58	23 08	23 02	23 20	21 97	22 95	22 81	23 34	23 18	23 34	23 02	22 82	23 02	23 30	23 70	24 05	22 45
Na2O	1 23	0 92	1 23	1 30	1 03	1 16	1 32	0 88	1 05	1 03	1 17	1 09	1 21	0 96	1 11	1 16	1 11	1 24	1 15	0 60	0 86	0 83	1 18
Total	100 32	100 24	100 65	100 49	99 86	100 80	100 89	99 77	100 30	100 35	99 84	100 77	99 91	99 98	100 28	100 96	100 40	100 24	100 47	99 44	100 70	100 33	99 73
Si	1 8401	1 9591	1 8821	1 9267	1 8140	1 9057	1 9327	1 9286	1 9356	1 9255	1 9300	1 9051	1 8213	1 9104	1 9206	1 9113	1 9119	1 9055	1 9225	1 9756	1 9525	1 8643	1 8385
Al	0 0000	0 0000	0 0000	0 0000	0 0000	0 0000	0 0000	0 0000	0 0000	0 0000	0 0000	0 0000	0 0000	0 0000	0 0000	0 0000	0 0000	0 0000	0 0000	0 0000	0 0000	0 0000	0 0000
Fe3+	0 0000	0 0000	0 0000	0 0000	0 0000	0 0000	0 0000	0 0000	0 0000	0 0000	0 0000	0 0000	0 0000	0 0000	0 0000	0 0000	0 0000	0 0000	0 0000	0 0000	0 0000	0 0000	0 0000
Al	0 1764	0 0608	0 1187	0 0801	0 2479	0 0967	0 0811	0 0821	0 0657	0 0819	0 0894	0 0953	0 1876	0 0837	0 0764	0 0927	0 0923	0 0955	0 0790	0 0113	0 0456	0 1352	0 1698
Fe3+	0 1384	0 0808	0 1568	0 1326	0 1430	0 1293	0 1344	0 0976	0 1280	0 1004	0 0934	0 1186	0 1917	0 1205	0 1452	0 1370	0 1248	0 1537	0 1468	0 0747	0 1033	0 1326	0 1684
Ti	0 0469	0 0032	0 0236	0 0135	0 0254	0 0226	0 0068	0 0127	0 0055	0 0200	0 0209	0 0269	0 0322	0 0222	0 0087	0 0156	0 0196	0 0150	0 0064	0 0028	0 0036	0 0314	0 0349
Cr	0 0002	0 0002	0 0016	0 0003	0 0038	0 0004	0 0004	0 0009	0 0000	0 0003	0 0003	0 0003	0 0002	0 0000	0 0001	0 0000	0 0000	0 0000	0 0000	0 0000	0 0000	0 0000	0 0000
Mg	0 6381	0 7072	0 6908	0 7128	0 5800	0 6954	0 6394	0 7547	0 6724	0 7329	0 6866	0 7212	0 5883	0 7229	0 6592	0 6593	0 6765	0 6423	0 6487	0 8657	0 7589	0 7008	0 6270
Fe2+	0 0000	0 1477	0 0085	0 0607	0 0000	0 0556	0 1379	0 0521	0 1283	0 0645	0 1093	0 0378	0 0000	0 0507	0 1104	0 0954	0 0867	0 0935	0 1192	0 0455	0 0885	0 0000	0 0000
Mn	0 0000	0 0000	0 0000	0 0000	0 0000	0 0000	0 0000	0 0000	0 0000	0 0000	0 0000	0 0000	0 0000	0 0000	0 0000	0 0000	0 0000	0 0000	0 0000	0 0000	0 0000	0 0000	0 0000
Mg	0 0439	0 0000	0 0000	0 0000	0 2115	0 0000	0 0000	0 0000	0 0000	0 0000	0 0000	0 0000	0 1955	0 0000	0 0000	0 0000	0 0000	0 0000	0 0000	0 0000	0 0000	0 0536	0 1304
Fe2+	0 1111	0 0392	0 1087	0 0666	0 0050	0 0852	0 0546	0 0754	0 0498	0 0675	0 0896	0 0933	0 0000	0 0754	0 0533	0 0611	0 0748	0 0731	0 0554	0 0440	0 0358	0 0639	0 0440
Mn	0 0099	0 0135	0 0136	0 0145	0 0053	0 0147	0 0164	0 0130	0 0161	0 0126	0 0139	0 0140	0 0065	0 0123	0 0154	0 0151	0 0130	0 0140	0 0155	0 0144	0 0143	0 0069	0 0093
Ca	0 9061	0 9217	0 9091	0 8987	0 8908	0 9114	0 9013	0 9199	0 9225	0 9208	0 8816	0 9092	0 9009	0 9324	0 9303	0 9289	0 9200	0 9172	0 9231	0 9231	0 9364	0 9521	0 8929
Na	0 0890	0 0665	0 0885	0 0935	0 0734	0 0831	0 0950	0 0631	0 0760	0 0736	0 0850	0 0783	0 0865	0 0694	0 0804	0 0835	0 0803	0 0902	0 0834	0 0428	0 0611	0 0592	0 0849
Total	4 0000	4 0000	4 0000	4 0000	4 0000	4 0000	4 0000	4 0000	4 0000	4 0000	4 0000	4 0000	4 0107	4 0000	4 0000	4 0000	4 0000	4 0000	4 0000	4 0000	4 0000	4 0000	4 0000

ORS175 CLINOPYROXENE

	1	2	3	4	5	6	7	8	9	10	11	12	13	14
			c	r				c	r			c	m	r
SiO2	51 50	48 25	48 34	47 57	49 64	49 90	50 17	54 02	53 92	53 44	53 36	53 27	51 46	51 07
TiO2	0 43	0 73	1 09	0 91	0 82	0 65	0 69	0 11	0 14	0 13	0 12	0 13	0 87	0 99
Al2O3	2 23	6 33	6 11	5 57	4 07	2 95	2 41	0 28	0 63	0 63	0 58	0 57	2 29	2 87
Cr2O3	0 00	0 00	0 03	0 04	0 04	0 00	0 00	0 00	0 00	0 00	0 00	0 00	0 02	0 00
Fe2O3	4 34	6 00	5 49	7 67	5 14	6 09	6 00	3 19	3 23	3 32	3 32	3 75	5 03	4 52
FeO	4 34	1 28	1 39	2 57	2 40	3 72	3 20	2 29	3 69	3 12	3 40	3 08	2 62	3 61
MnO	0 34	0 22	0 19	0 33	0 27	0 34	0 37	0 31	0 34	0 31	0 30	0 30	0 29	0 27
MgO	12 95	12 61	12 50	11 39	12 41	11 59	11 97	16 18	14 53	14 72	14 87	14 45	13 32	12 75
CaO	23 42	23 89	24 51	21 90	23 86	23 51	23 81	24 01	24 59	24 34	23 77	24 29	23 94	24 16
Na2O	0 91	0 81	0 76	1 39	1 02	1 17	1 12	0 54	0 68	0 68	0 70	0 77	1 08	0 95
Total	100 46	100 11	100 40	99 33	99 68	99 92	99 72	100 92	101 75	100 69	100 41	100 60	100 92	101 19
Si	1 9112	1 7871	1 7870	1 7919	1 8516	1 8729	1 8834	1 9664	1 9625	1 9611	1 9634	1 9595	1 8947	1 8814
Al	0 0000	0 0000	0 0000	0 0000	0 0000	0 0000	0 0000	0 0000	0 0000	0 0000	0 0000	0 0000	0 0000	0 0000
Fe3+	0 0000	0 0000	0 0000	0 0000	0 0000	0 0000	0 0000	0 0000	0 0000	0 0000	0 0000	0 0000	0 0000	0 0000
Al	0 0977	0 2765	0 2665	0 2472	0 1791	0 1303	0 1065	0 0119	0 0272	0 0274	0 0250	0 0246	0 0993	0 1249
Fe3+	0 1213	0 1673	0 1527	0 2174	0 1444	0 1720	0 1694	0 0874	0 0884	0 0917	0 0919	0 1039	0 1394	0 1253
Ti	0 0120	0 0203	0 0302	0 0259	0 0231	0 0184	0 0194	0 0030	0 0037	0 0037	0 0032	0 0037	0 0242	0 0273
Cr	0 0000	0 0000	0 0009	0 0011	0 0011	0 0000	0 0000	0 0000	0 0000	0 0000	0 0000	0 0000	0 0006	0 0000
Mg	0 7160	0 5359	0 5497	0 5084	0 6523	0 6485	0 6698	0 8775	0 7883	0 8049	0 8153	0 7921	0 7307	0 7001
Fe2+	0 0531	0 0000	0 0000	0 0000	0 0000	0 0308	0 0349	0 0202	0 0924	0 0724	0 0646	0 0757	0 0059	0 0224
Mn	0 0000	0 0000	0 0000	0 0000	0 0000	0 0000	0 0000	0 0000	0 0000	0 0000	0 0000	0 0000	0 0000	0 0000
Mg	0 0000	0 1603	0 1391	0 1312	0 0377	0 0000	0 0000	0 0000	0 0000	0 0000	0 0000	0 0000	0 0000	0 0000
Fe2+	0 0817	0 0391	0 0429	0 0811	0 0748	0 0860	0 0655	0 0497	0 0200	0 0235	0 0400	0 0189	0 0749	0 0889
Mn	0 0108	0 0070	0 0060	0 0105	0 0085	0 0109	0 0118	0 0094	0 0104	0 0097	0 0093	0 0094	0 0090	0 0084
Ca	0 9311	0 9480	0 9707	0 8639	0 9534	0 9452	0 9579	0 9363	0 9589	0 9571	0 9371	0 9574	0 9444	0 9535
Na	0 0653	0 0585	0 0544	0 1014	0 0740	0 0850	0 0815	0 0382	0 0481	0 0487	0 0502	0 0549	0 0770	0 0677
Total	4 0000	4 0000	4 0000	4 0000	4 0000	4 0000	4 0000	4 0000	4 0000	4 0000	4 0000	4 0000	4 0000	4 0000

ORS133 PLAGICLASE

	1	2	3	4	5	6	7	8	9	10	11	12	13	14	15	16	17	18	19	20	21	22	23
						c	m	m	r														
SiO2	63 11	63 79	64 25	64 43	63 78	63 21	63 70	66 30	67 74	59 48	65 58	65 91	64 22	57 62	48 60	50 04	50 50	52 05	54 74	65 83	59 03	58 59	62 42
Al2O3	22 38	21 91	22 03	22 14	22 04	23 09	21 84	21 42	20 40	20 77	22 45	22 23	23 08	26 65	30 59	31 97	30 14	30 56	28 96	22 19	26 24	26 54	24 14
FeO	0 17	0 25	0 27	0 18	0 18	0 12	0 17	0 03	0 04	0 48	0 14	0 11	0 11	0 07	0 10	0 16	0 07	0 13	0 11	0 17	0 10	0 18	0 15
CaO	3 87	3 38	3 16	3 45	3 53	4 80	3 62	2 56	1 49	8 28	3 52	3 67	4 73	9 32	17 09	15 09	15 52	13 48	11 13	3 29	8 04	8 32	5 82
Na2O	9 44	9 72	9 89	9 76	9 64	8 32	8 81	10 01	9 95	7 81	9 44	8 93	8 59	6 15	2 49	3 18	3 33	4 20	5 47	9 59	7 31	7 10	8 53
K2O	0 33	0 48	0 42	0 18	0 34	0 13	0 37	0 16	0 07	0 05	0 24	0 14	0 13	0 06	0 20	0 05	0 05	0 05	0 09	0 26	0 12	0 12	0 23
Total	99 30	99 53	100 01	100 14	99 52	99 66	98 51	100 47	99 70	96 87	101 37	100 99	100 86	99 87	99 07	100 49	99 61	100 47	100 51	101 33	100 84	100 84	101 30
An	18 13	15 68	14 66	16 19	16 52	23 96	18 10	12 27	7 62	36 83	16 86	18 37	23 13	45 40	78 28	72 21	71 83	63 77	52 66	15 70	37 55	39 04	27 04
Ab	80 05	81 67	83 01	82 82	81 58	75 24	79 71	86 81	91 94	62 88	81 77	80 82	76 09	54 22	20 63	27 52	27 90	35 96	46 85	82 80	61 79	60 29	71 67
Or	1 82	2 65	2 33	0 99	1 90	0 80	2 19	0 92	0 43	0 29	1 37	0 81	0 78	0 38	1 09	0 26	0 26	0 27	0 49	1 50	0 67	0 67	1 29

ORS175 PLAGIOCLASE

	1	2	4	5	6	7	8	9	11	13	14	15	16	17	20	1	3	4	6	8	9
							c	m	r		c	m	m	m	r						
SiO2	48 01	47 03	47 53	47 43	46 93	46 75	46 91	55 39	64 94	47 43	47 70	47 56	47 61	48 41	64 30	66 23	66 06	62 70	61 60	60 15	58 92
Al2O3	31 69	32 63	33 22	33 18	33 48	33 29	33 46	28 08	23 89	33 02	33 05	33 08	33 16	31 67	22 72	23 87	21 46	23 51	23 52	24 62	25 58
FeO	0 26	0 14	0 09	0 15	0 12	0 14	0 16	0 11	0 15	0 15	0 08	0 14	0 11	0 15	0 19	0 13	0 03	0 09	0 15	0 10	0 06
CaO	18 69	15 73	17 33	17 18	17 79	17 82	17 79	10 80	5 53	17 27	17 02	16 84	16 99	13 50	4 17	5 06	1 23	5 03	5 54	6 41	7 60
Na2O	0 91	1 81	1 95	2 11	1 82	1 78	1 85	5 69	5 66	2 07	2 01	2 21	2 09	2 24	8 53	4 21	9 42	8 16	7 39	7 14	6 71
K2O	1 74	1 45	0 07	0 10	0 03	0 05	0 03	0 15	0 37	0 05	0 05	0 03	0 07	2 16	0 34	0 22	0 52	0 19	0 43	0 26	0 24
Tot	101 29	98 80	100 19	100 16	100 17	99 83	100 20	100 23	100 54	99 98	99 93	99 85	100 03	98 14	100 26	99 72	98 71	99 68	98 63	98 68	99 11
An	83 42	75 88	82 75	81 32	84 26	84 48	84 06	50 77	34 12	81 93	82 11	80 70	81 45	67 06	20 82	39 05	6 51	25 12	28 50	32 62	37 94
Ab	7 32	15 80	16 87	18 11	15 57	15 24	15 78	48 42	63 16	17 78	17 59	19 13	18 15	20 15	77 16	58 88	90 21	73 73	68 89	65 81	60 67
Or	9 26	8 32	0 38	0 57	0 17	0 28	0 16	0 81	2 71	0 28	0 30	0 17	0 39	12 80	2 02	2 07	3 28	1 16	2 61	1 57	1 40

ORS176 PLAGIOCLASE

	1	2	3	4	5	6	7	8	9	10	11	12	13	14	15	16	17	18	19	20	21	22	23	24
SiO2	65.62	65.36	59.77	60.48	60.25	65.13	64.94	65 39	60.21	63.62	62 58	60.78	60.54	59 76	61 30	60.16	65.24	65 23	65 62	64 89	65 15	65 24	65 57	65 43
Al2O3	21.87	21.75	25.14	24.54	24.89	22.01	21.92	22 08	24.87	24.54	23.20	24.49	24.38	23.89	24.54	24.74	21 33	21.95	21 64	21 37	21 46	21 72	21 46	21 75
FeO	0.16	0.11	0.05	0.05	0.03	0.11	0.18	0 09	0.07	0.05	0.04	0.02	0.09	1 02	0.04	0.02	0.13	0.17	0 14	0 08	0 18	0 08	0 07	0 05
CaO	3.02	2.97	6.92	6.11	6.59	3.17	3.01	3 16	6.54	6.25	4.68	6.23	5.98	6 27	6.02	6 38	2 62	3 15	2 95	2 96	2 99	3 20	2 63	3 00
Na2O	9.73	9.63	7.61	7.99	7.85	9.79	10.05	9 65	7.81	8.35	8.97	8.24	8.33	8.20	8.19	8.13	10.09	9.83	9 77	10.01	10.16	9.54	10.33	10.12
K2O	0.17	0.10	0.06	0.11	0.12	0.09	0.08	0 22	0.18	0.13	0.13	0.12	0.14	0.21	0.12	0.16	0 19	0 23	0 20	0 21	0 16	0 15	0 07	0 10
Tot	100.57	99.92	99.56	99.28	99.73	100.30	100.19	100.59	99.66	100.94	99.59	99.87	99.46	99.45	100.21	99.59	99.60	100 56	100 31	99 52	100 10	99.94	100 13	100 45
An	14.49	14.50	33.28	29.54	31.47	15.12	14.15	15.11	31.31	34.90	22.22	29.28	28.20	29.35	28.69	30.00	12 44	14 82	14 15	13 87	13 85	15 51	12 28	13 99
Ab	84.51	84.93	66.29	69.83	67.85	84.35	85.36	83.64	67.68	64.23	77.08	70.07	71.02	69.50	70.60	69.13	86 50	83 68	84 74	84 94	85 29	83 60	87 32	85 46
Or	1.00	0.57	0.43	0.63	0.68	0.53	0.47	1.25	1.01	0.87	0.71	0.65	0.78	1 16	0.70	0.88	1 06	1 30	1 12	1 19	0 86	0 89	0 40	0 55

Foyaites

ORF7 AMPHIBOLE

	1	2	3	4	5	6	7	8	9	10	11	12	13
		c	r						c	m	r		
SiO2	38 13	37 95	37 94	38 88	39 16	39 40	39 00	38 42	38 58	37 96	37 86	38 62	39 19
TiO2	1 14	1 28	1.27	1 30	1.39	1 45	1 40	1 46	1 45	1 32	1 16	1 20	1 41
Al2O3	10 04	9 53	9 98	9 50	8 76	8 29	8 71	9 10	8 84	9 77	10 09	9 48	8 86
Fe2O3	7 28	7 01	7 70	6 62	7 57	7 81	6 28	7 43	7 63	7 81	8 75	7 79	7 82
FeO	23 78	23 64	23 41	24 23	23 96	22 69	23 27	22 62	22 67	22 74	22 71	23 43	23 42
MnO	1.47	1 48	1 46	1 61	1 57	1 49	1 56	1 54	1.43	1 41	1 42	1 38	1.43
MgO	1 88	2 03	1 98	1 98	2 04	2 08	2 07	1 98	2 07	1 91	1 88	1 95	2 14
CaO	8 56	8 43	8 51	8 27	8 14	7 36	7 63	7 60	7 49	7 99	8 51	8 36	8 16
Na2O	4 08	4 05	4 04	4 35	4 24	4 08	4 12	4 09	4.19	4 00	3 81	3 90	3 99
K2O	1 49	1 58	1 57	1 55	1 54	1 54	1.54	1 55	1.57	1 56	1 44	1 47	1 49
Tot	97 85	96 98	97 86	98 29	98 38	96 19	95 58	95 78	95 92	96 47	97 64	97 58	97 91
Si	6 1776	6 2076	6 1482	6 2694	6 3127	6 4442	6 4247	6 3218	6 3412	6 2144	6 1357	6 2576	6 3233
IVAl	1 8224	1 7924	1 8518	1 7306	1 6648	1 5558	1 5753	1 6782	1 6588	1 7856	1 8643	1 7424	1 6767
Fe3+	0 0000	0 0000	0 0000	0 0000	0 0225	0 0000	0 0000	0 0000	0 0000	0 0000	0 0000	0 0000	0 0000
VIAl	0 0954	0 0454	0 0548	0 0753	0 0000	0 0427	0 1163	0 0871	0 0542	0 1000	0 0635	0 0685	0 0086
Ti	0 1389	0 1575	0 1548	0 1577	0 1685	0 1784	0 1734	0 1807	0 1790	0 1625	0 1414	0 1462	0 1711
Fe3+	0 8871	0 8627	0 9396	0 8034	0 8963	0 9613	0 7789	0 9196	0 9438	0 9619	1 0675	0 9493	0 9495
Fe2+	3 2228	3 2344	3 1722	3 2679	3 2307	3 1042	3 2055	3 1125	3 1169	3 1140	3 0786	3 1756	3 1608
Mg	0 4540	0 4949	0 4782	0 4758	0 4901	0 5070	0 5082	0 4655	0 5071	0 4660	0 4541	0 4709	0 5146
Mn	0 2018	0 2051	0 2004	0 2199	0 2144	0 2064	0 2177	0 2148	0 1991	0 1955	0 1949	0 1894	0 1954
Mg	0 0000	0 0000	0 0000	0 0000	0 0000	0 0000	0 0000	0 0000	0 0000	0 0000	0 0000	0 0000	0 0000
Fe2+	0 0000	0 0000	0 0000	0 0000	0 0000	0 0000	0 0000	0 0000	0 0000	0 0000	0 0000	0 0000	0 0000
Ca	1 4861	1 4775	1 4770	1 4289	1 4060	1 2899	1 3468	1 3400	1 3191	1 4016	1 4778	1 4514	1 4108
Na	0 5139	0 5225	0 5230	0 5711	0 5940	0 7101	0 6532	0 6600	0 6809	0 5984	0 5222	0 5486	0 5892
Na	0 7679	0 7620	0 7463	0 7889	0 7313	0 5838	0 6628	0 6448	0 6545	0 6713	0 6750	0 6767	0 6590
K	0 3080	0 3297	0 3246	0 3189	0 3167	0 3214	0 3237	0 3254	0 3292	0 3258	0 2977	0 3039	0 3067
Tot	16 0759	16 0918	16 0709	16 1078	16 0480	15 9052	15 9865	15 9702	15 9837	15 9971	15 9727	15 9806	15 9657

ORF8 AMPHIBOLE

	1	2	3	4	5
	m	r			
SiO2	41 12	40 47	40 69	39 86	40 68
TiO2	1 85	1 75	1 82	1 89	1 21
Al2O3	8 73	8 44	8 40	9 37	8 54
Fe2O3	7 53	7 87	7 89	8 14	8 38
FeO	19 12	21 18	19 79	20 22	20 25
MnO	1 22	1 16	1 20	1 19	1 16
MgO	5 38	3 84	4 83	4 00	4 26
CaO	8 29	7 49	8 03	7 90	7 77
Na2O	4 08	4 55	4 16	4 19	4 33
K2O	1 43	1 55	1 47	1 47	1 50
Tot	98 76	98 28	98 48	98 21	98 07
Si	6 4001	6 4105	6 4142	6 2946	6 4309
IVAl	1 5999	1 5752	1 5539	1 7054	1 5691
Fe3+	0 0000	0 0143	0 0320	0 0000	0 0000
VIAl	0 0020	0 0000	0 0000	0 0382	0 0233
Ti	0 2170	0 2080	0 2151	0 2244	0 1441
Fe3+	0 8824	0 9233	0 8995	0 9672	0 9968
Fe2+	2 4893	2 8050	2 5962	2 6701	2 6771
Mg	1 2479	0 9074	1 1300	0 9411	1 0032
Mn	0 1614	0 1562	0 1593	0 1591	0 1556
Mg	0 0000	0 0000	0 0000	0 0000	0 0000
Fe2+	0 0000	0 0000	0 0000	0 0000	0 0000
Ca	1 3825	1 2709	1 3488	1 3368	1 3161
Na	0 6175	0 7291	0 6512	0 6632	0 6839
Na	0 6148	0 6670	0 6136	0 6186	0 6423
K	0 2842	0 3123	0 2938	0 2958	0 3024
Tot	15 8990	15 9793	15 9074	15 9144	15 9447

ORF14 AMPHIBOLE

	1	2	3	4
	c	m	m	r
SiO2	39 30	39 53	39 25	38 57
TiO2	3 07	2 74	2 71	2 72
Al2O3	9 71	9 65	9 69	9 66
Fe2O3	2 48	3 07	3 64	3 69
FeO	20 86	21 17	20 21	22 41
MnO	0 96	1 04	0 96	1 07
MgO	6 05	5 57	6 02	4 27
CaO	10 04	9 94	9 92	9 53
Na2O	3 40	3 38	3 42	3 40
K2O	1 46	1 34	1 36	1 48
Tot	97 29	97 43	97 18	96 81
Si	6 2164	6 2541	6 2124	6 2056
IVAl	1 7836	1 7459	1 7876	1 7944
Fe3+	0 0000	0 0000	0 0000	0 0000
VIAl	0 0264	0 0546	0 0213	0 0374
Ti	0 3652	0 3258	0 3222	0 3295
Fe3+	0 2952	0 3657	0 4338	0 4473
Fe2+	2 7593	2 8011	2 6755	3 0160
Mg	1 4260	1 3135	1 4189	1 0234
Mn	0 1260	0 1393	0 1284	0 1465
Mg	0 0000	0 0000	0 0000	0 0000
Fe2+	0 0000	0 0000	0 0000	0 0000
Ca	1 6981	1 6841	1 6827	1 6433
Na	0 3019	0 3159	0 3173	0 3567
Na	0 7394	0 7200	0 7315	0 7045
K	0 2941	0 2698	0 2740	0 3030
Tot	16 0335	15 9898	16 0055	16 0075

ORF14 AMPHIBOLE

	5	6	7	8	9	10	11	12	13	14	15	16
					c	m	m	r				
SiO2	39 52	39 20	38 97	39 48	39 34	40 06	40 10	39 63	39 19	39 40	39 49	39 35
TiO2	3.50	3.11	3.41	3 39	3.38	1 90	1.65	1.95	3 01	3 60	3.17	2 08
Al2O3	9 53	9 66	9 57	9 46	9 59	8 27	8 04	7 98	7 83	7 61	9 11	9 41
Fe2O3	2 23	2 91	0 16	0 78	2 11	6 52	6 37	7 50	5 81	4 61	2 26	4 47
FeO	21 84	21 46	22 37	21 72	20 64	18 25	18 56	18 03	19 14	19 20	22 60	22 83
MnO	0 96	1 06	0 95	0 91	0 87	0 97	0 93	0 96	1 00	1 01	1 05	1 11
MgO	5 66	5 34	5 84	5 96	6 20	5 87	5 83	5 59	5 31	5 91	4 97	3 97
CaO	9 91	9 82	10 34	10 11	9 96	8 83	8 80	8 62	8 54	8 72	9 66	9 43
Na2O	3 52	3 45	3 38	3 29	3 32	3 32	3 41	3 25	3 26	3 32	3 48	3 47
K2O	1 39	1 31	1 32	1 32	1 36	1 24	1 25	1 28	1 31	1 34	1 38	1 48
Tot	98 05	97 31	96 30	96 42	96 77	95 22	94 94	94 79	94 40	94 72	97 17	97 60
Si	6 2211	6 2199	6 2426	6 2907	6 2356	6 4316	6 4669	6 4100	6 3825	6 3811	6 2983	6 2906
IVAl	1 7694	1 7801	1 7574	1 7093	1 7644	1 5653	1 5286	1 5217	1 5034	1 4530	1 7017	1 7094
Fe3+	0 0095	0 0000	0 0000	0 0000	0 0000	0 0031	0 0045	0 0683	0 1142	0 1659	0 0000	0 0000
VIAl	0 0000	0 0272	0 0494	0 0679	0 0285	0 0000	0 0000	0 0000	0 0000	0 0000	0 0113	0 0640
Ti	0 4142	0 3712	0 4106	0 4067	0 4032	0 2294	0 2001	0 2372	0 3687	0 4385	0 3802	0 2501
Fe3+	0 2543	0 3480	0 0188	0 0940	0 2518	0 7841	0 7681	0 8443	0 5984	0 3960	0 2713	0 5373
Fe2+	2 8751	2 8484	2 9969	2 8940	2 7358	2 4501	2 5036	2 4395	2 6068	2 6009	3 0140	3 0525
Mg	1 3282	1 2625	1 3951	1 4141	1 4639	1 4045	1 4012	1 3475	1 2878	1 4265	1 1813	0 9458
Mn	0 1283	0 1427	0 1292	0 1233	0 1168	0 1319	0 1270	0 1315	0 1384	0 1381	0 1419	0 1503
Mg	0 0000	0 0000	0 0000	0 0000	0 0000	0 0000	0 0000	0 0000	0 0000	0 0000	0 0000	0 0000
Fe2+	0 0000	0 0000	0 0000	0 0000	0 0000	0 0000	0 0000	0 0000	0 0000	0 0000	0 0000	0 0000
Ca	1 6717	1 6689	1 7750	1 7255	1 6915	1 5190	1 5207	1 4940	1 4901	1 5133	1 6509	1 6153
Na	0 3283	0 3311	0 2250	0 2745	0 3085	0 4810	0 4793	0 5060	0 5099	0 4867	0 3491	0 3847
Na	0 7448	0 7289	0 8244	0 7409	0 7112	0 5525	0 5869	0 5132	0 5195	0 5558	0 7270	0 6909
K	0 2797	0 2646	0 2688	0 2677	0 2750	0 2540	0 2572	0 2641	0 2722	0 2769	0 2808	0 3018
Tot	16 0244	15 9935	16 0932	16 0086	15 9862	15 8065	15 8441	15 7773	15 7917	15 8327	16 0078	15 9927

ORF17 AMPHIBOLE

	1	2	3	4	5	6	7	8	9	10
		c	m	r						
SiO2	38 95	38 51	38 59	38 28	38 27	37 61	38 42	38 33	38 12	39 32
TiO2	2 40	2 45	2.42	1 92	2.35	1 86	2 51	2 49	2 32	1 49
Al2O3	10 71	10.74	10.78	10 11	10.51	10 01	10 42	10 47	10 20	9 36
Fe2O3	5 35	5.19	4.90	6.79	6.28	6 35	4 52	3 80	4.39	5 64
FeO	20.89	20.46	21.23	22.61	21.89	22.60	22 12	22 50	23 58	22 99
MnO	1 03	1.04	1.03	1.14	1.12	1 07	1 10	1 11	1 07	1 09
MgO	4.66	4.78	4.63	3.08	3.57	3 14	4 09	4 14	3 18	3 55
CaO	9 33	9 46	9 70	9.08	9 23	9.05	9 54	9 58	9 30	9 00
Na2O	3 68	3 54	3.51	3.61	3.51	3 80	3 53	3 69	3 65	3 86
K2O	1.51	1.41	1 46	1.57	1 53	1 42	1 44	1 44	1.45	1 52
Tot	98 51	97.58	98.24	98.17	98.26	96 91	97 71	97 55	97 25	97 82
Si	6 1232	6 1026	6.0934	6 1284	6.0873	6 1063	6 1263	6 1262	6 1528	6 2986
IVAl	1.8768	1 8974	1 9066	1.8716	1 9127	1 8937	1 8737	1 8738	1 8472	1 7014
Fe3+	0 0000	0 0000	0 0000	0.0000	0.0000	0 0000	0 0000	0 0000	0 0000	0 0000
VIAl	0 1089	0 1089	0 0995	0 0359	0 0576	0 0226	0 0855	0 0991	0 0927	0 0659
Ti	0 2839	0 2925	0 2870	0 2307	0 2813	0 2271	0 3011	0 2993	0 2822	0 1794
Fe3+	0 6329	0 6193	0 5822	0 8178	0 7512	0 7760	0 5425	0 4571	0 5328	0 6798
Fe2+	2 7460	2 7110	2 8042	3 0271	2 9125	3 0687	2 9498	3 0081	3 1826	3 0796
Mg	1 0910	1 1283	1 0895	0 7342	0 8461	0 7588	0 9[illegible]2	0 9865	0 7639	0 8480
Mn	0 1373	0 1400	0 1375	0 1543	0 1513	0 1468	0 1489	0 1499	0 1458	0 1472
Mg	0 0000	0 0000	0 0000	0 0000	0 0000	0 0000	0 0000	0 0000	0 0000	0 0000
Fe2+	0 0000	0 0000	0 0000	0 0000	0 0000	0 0000	0 0000	0 0000	0 0000	0 0000
Ca	1 5710	1 6067	1 6405	1 5578	1 5740	1 5752	1 6[illegible]92	1 6408	1 6088	1 5437
Na	0 4290	0 3933	0 3595	0 4422	0 4260	0 4248	0 3708	0 3592	0 3912	0 4563
Na	0 6934	0 6930	0 7154	0 6790	0 6572	0 7711	0 7208	0 7835	[illegible]497	0 7430
K	0 3028	0 2845	0 2949	0 3198	0 3102	0 2946	0 2935	0 2946	[illegible]69	0 3102
Tot	15 9962	15 9775	16 0103	15 9988	15 9674	16 0656	16 0143	16 0781	16 0486	16 0531

	ORF17 AMPHIBOLE						
	11	12	13	14	15	16	17
	c	m	m	m	r		
SiO2	38.71	38.34	38.50	38.17	38.17	38.39	38.34
TiO2	2.16	2.27	2.34	2.34	2.20	2.31	1.83
Al2O3	10.73	10.80	10.79	10.66	10.61	10.57	10.19
Fe2O3	5.82	5.90	6.09	6.10	4.71	5.01	6.24
FeO	20.78	20.67	20.83	21.29	22.54	22.66	23.42
MnO	0.98	0.94	0.99	1.02	1.01	0.98	1.12
MgO	4.55	4.49	4.44	4.10	3.67	3.73	2.82
CaO	9.32	9.38	9.50	9.45	9.40	9.62	9.19
Na2O	3.69	3.54	3.54	3.53	3.62	3.52	3.67
K2O	1.46	1.48	1.42	1.44	1.42	1.40	1.50
Tot	98.21	97.81	98.45	98.13	97.36	98.20	98.34
Si	6.1104	6.0798	6.0702	6.0589	6.1223	6.1078	6.1401
ivAl	1.8896	1.9202	1.9298	1.9411	1.8777	1.8922	1.8599
Fe3+	0.0000	0.0000	0.0000	0.0000	0.0000	0.0000	0.0000
viAl	0.1066	0.0977	0.0753	0.0580	0.1279	0.0911	0.0637
Ti	0.2560	0.2709	0.2780	0.2799	0.2650	0.2764	0.2207
Fe3+	0.6920	0.7041	0.7228	0.7289	0.5691	0.5994	0.7526
Fe2+	2.7434	2.7404	2.7473	2.8268	3.0235	3.0156	3.1370
Mg	1.0712	1.0603	1.0441	0.9688	0.8774	0.8855	0.6740
Mn	0.1309	0.1266	0.1326	0.1376	0.1371	0.1320	0.1520
Mg	0.0000	0.0000	0.0000	0.0000	0.0000	0.0000	0.0000
Fe2+	0.0000	0.0000	0.0000	0.0000	0.0000	0.0000	0.0000
Ca	1.5768	1.5934	1.6042	1.6082	1.6163	1.6397	1.5775
Na	0.4232	0.4066	0.3958	0.3918	0.3837	0.3603	0.4225
Na	0.7072	0.6832	0.6849	0.6939	0.7435	0.7258	0.7186
K	0.2950	0.3000	0.2865	0.2923	0.2911	0.2834	0.3061
Tot	16.0022	15.9832	15.9715	15.9862	16.0346	16.0091	16.0247

	ORF21 AMPHIBOLE							
	1	2	3	4	5	6	7	8
SiO2	39.23	39.06	39.20	38.64	39.38	39.50	39.10	38.87
TiO2	1.40	1.64	1.60	1.88	1.97	1.98	1.96	0.97
Al2O3	9.12	9.26	9.27	9.94	8.61	8.86	9.28	9.45
Fe2O3	5.29	5.52	5.59	6.06	5.42	4.01	5.31	6.57
FeO	22.52	22.86	22.72	21.70	22.21	22.95	22.23	22.40
MnO	1.71	1.78	1.75	1.67	1.51	1.64	1.59	1.39
MgO	3.61	3.31	3.33	3.64	3.78	3.89	3.76	3.27
CaO	9.56	9.60	9.55	9.61	9.46	9.61	9.55	9.47
Na2O	3.35	3.30	3.29	3.29	3.08	3.30	3.24	3.26
K2O	1.45	1.46	1.41	1.37	1.37	1.51	1.46	1.48
Tot	97.25	97.79	97.74	97.80	96.78	97.25	97.50	97.11
Si	6.3209	6.2756	6.2918	6.1771	6.3548	6.3526	6.2709	6.2804
ivAl	1.6791	1.7244	1.7082	1.8229	1.6374	1.6474	1.7291	1.7196
Fe3+	0.0000	0.0000	0.0000	0.0000	0.0078	0.0000	0.0000	0.0000
viAl	0.0537	0.0287	0.0453	0.0500	0.0000	0.0321	0.0255	0.0801
Ti	0.1692	0.1979	0.1937	0.2258	0.2387	0.2389	0.2363	0.1177
Fe3+	0.6417	0.6678	0.6758	0.7293	0.6501	0.4859	0.6413	0.7987
Fe2+	3.0339	3.0716	3.0502	2.9014	2.9968	3.0871	2.9815	3.0267
Mg	0.8676	0.7926	0.7971	0.8669	0.9082	0.9319	0.8988	0.7868
Mn	0.2339	0.2415	0.2379	0.2266	0.2062	0.2240	0.2166	0.1899
Mg	0.0000	0.0000	0.0000	0.0000	0.0000	0.0000	0.0000	0.0000
Fe2+	0.0000	0.0000	0.0000	0.0000	0.0000	0.0000	0.0000	0.0000
Ca	1.6498	1.6529	1.6428	1.6462	1.6364	1.6561	1.6411	1.6404
Na	0.3502	0.3471	0.3572	0.3538	0.3636	0.3439	0.3589	0.3596
Na	0.6965	0.6804	0.6680	0.6658	0.5997	0.6857	0.6489	0.6603
K	0.2990	0.2988	0.2888	0.2799	0.2816	0.3098	0.2997	0.3046
Tot	15.9955	15.9792	15.9569	15.9457	15.8813	15.9955	15.9486	15.9649

	ORF22 AMPHIBOLE							
	1	2	3	4	5	6	7	
SiO2	41.00	40.02	40.35	39.54	40.33	40.69	40.29	
TiO2	1.71	1.62	1.65	1.62	1.65	1.65	1.57	
Al2O3	8.19	8.48	8.05	8.06	8.03	7.95	8.28	
Fe2O3	4.30	5.34	4.63	5.46	5.20	4.12	6.91	
FeO	22.20	21.24	21.96	20.99	21.50	22.17	20.37	
MnO	1.44	1.53	1.43	1.57	1.54	1.50	1.53	
MgO	4.62	4.60	4.60	4.54	4.63	4.57	4.63	
CaO	8.72	8.71	8.72	8.64	8.59	8.56	8.20	
Na2O	4.15	4.10	4.13	3.97	4.23	4.21	4.26	
K2O	1.35	1.39	1.38	1.39	1.33	1.42	1.47	
Tot	97.68	97.02	96.89	95.79	97.04	96.83	97.51	
Si	6.5125	6.4095	6.4770	6.4231	6.4614	6.5288	6.4145	
ivAl	1.4875	1.5905	1.5227	1.5437	1.5173	1.4712	1.5535	
Fe3+	0.0000	0.0000	0.0004	0.0332	0.0212	0.0000	0.0320	
viAl	0.0458	0.0101	0.0000	0.0000	0.0000	0.0330	0.0000	
Ti	0.2037	0.1957	0.1994	0.1981	0.1991	0.1994	0.1883	
Fe3+	0.5140	0.6440	0.5584	0.6346	0.6059	0.4973	0.7953	
Fe2+	2.9485	2.8445	2.9477	2.8519	2.8801	2.9743	2.7125	
Mg	1.0939	1.0975	1.0996	1.0997	1.1054	1.0925	1.0974	
Mn	0.1941	0.2082	0.1949	0.2157	0.2095	0.2035	0.2065	
Mg	0.0000	0.0000	0.0000	0.0000	0.0000	0.0000	0.0000	
Fe2+	0.0000	0.0000	0.0000	0.0000	0.0000	0.0000	0.0000	
Ca	1.4836	1.4940	1.5000	1.5033	1.4746	1.4717	1.3994	
Na	0.5164	0.5060	0.5000	0.4967	0.5254	0.5283	0.6006	
Na	0.7626	0.7671	0.7840	0.7542	0.7886	0.7799	0.7157	
K	0.2742	0.2838	0.2819	0.2887	0.2712	0.2905	0.2985	
Tot	16.0368	16.0509	16.0659	16.0429	16.0599	16.0704	16.0142	

	ORF22 AMPHIBOLE			
	8	9	10	11
SiO2	41.04	40.87	40.65	40.91
TiO2	1.54	1.61	1.67	1.63
Al2O3	7.77	8.01	8.09	7.92
Fe2O3	6.14	5.80	2.91	3.12
FeO	20.64	21.14	22.56	22.21
MnO	1.38	1.42	1.56	1.55
MgO	4.80	4.65	4.54	4.70
CaO	8.06	8.24	8.61	8.54
Na2O	4.23	4.22	4.22	4.18
K2O	1.42	1.48	1.40	1.44
Tot	97.03	97.45	96.22	96.19
Si	6.5410	6.5021	6.5576	6.5891
ivAl	1.4590	1.4979	1.4424	1.4109
Fe3+	0.0000	0.0000	0.0000	0.0000
viAl	0.0014	0.0050	0.0965	0.0933
Ti	0.1848	0.1931	0.2020	0.1974
Fe3+	0.7368	0.6948	0.3537	0.3760
Fe2+	2.7506	2.8131	3.0433	2.9921
Mg	1.1396	1.1029	1.0906	1.1284
Mn	0.1867	0.1911	0.2138	0.2108
Mg	0.0000	0.0000	0.0000	0.0000
Fe2+	0.0000	0.0000	0.0000	0.0000
Ca	1.3773	1.4046	1.4889	1.4729
Na	0.6227	0.5954	0.5111	0.5271
Na	0.6859	0.7065	0.8102	0.7770
K	0.2880	0.3008	0.2890	0.2949
Tot	15.9739	16.0073	16.0992	16.0719

	ORF23 AMPHIBOLE			
	1	2	3	4
SiO2	38.70	38.53	38.53	38.82
TiO2	1.65	1.77	1.69	1.62
Al2O3	9.27	9.67	9.47	9.13
Fe2O3	8.08	7.94	9.44	8.46
FeO	20.98	20.77	19.97	20.87
MnO	1.24	1.21	1.26	1.32
MgO	3.23	3.30	3.24	3.24
CaO	8.20	8.27	8.09	8.21
Na2O	3.75	3.70	3.58	3.68
K2O	1.49	1.51	1.53	1.57
Tot	96.58	96.67	96.80	96.92
Si	6.2615	6.2182	6.2092	6.2644
ivAl	1.7385	1.7818	1.7908	1.7356
Fe3+	0.0000	0.0000	0.0000	0.0000
viAl	0.0288	0.0578	0.0086	0.0007
Ti	0.2004	0.2152	0.2046	0.1963
Fe3+	0.9833	0.9644	1.1455	1.0269
Fe2+	2.8387	2.8029	2.6917	2.8166
Mg	0.7782	0.7938	0.7774	0.7787
Mn	0.1706	0.1659	0.1722	0.1808
Mg	0.0000	0.0000	0.0000	0.0000
Fe2+	0.0000	0.0000	0.0000	0.0000
Ca	1.4208	1.4303	1.3968	1.4203
Na	0.5792	0.5697	0.6032	0.5797
Na	0.5976	0.5865	0.5164	0.5730
K	0.3071	0.3104	0.3142	0.3222
Tot	15.9048	15.8989	15.8306	15.8953

	ORF40 AMPHIBOLE			
	1	2	3	4
			c	r
SiO2	39.26	39.00	37.86	38.44
TiO2	1.13	1.25	1.20	1.28
Al2O3	8.53	8.45	8.84	8.64
Fe2O3	7.70	7.95	9.81	7.68
FeO	23.71	24.02	21.86	23.95
MnO	1.37	1.39	1.37	1.29
MgO	1.58	1.49	1.62	1.45
CaO	7.13	7.25	6.91	7.19
Na2O	4.42	4.44	4.39	4.54
K2O	1.64	1.67	1.57	1.59
Tot	96.47	96.90	95.42	96.05
Si	6.4359	6.3880	6.2766	6.3530
ivAl	1.5641	1.6120	1.7234	1.6470
Fe3+	0.0000	0.0000	0.0000	0.0000
viAl	0.0847	0.0204	0.0036	0.0364
Ti	0.1390	0.1539	0.1491	0.1588
Fe3+	0.9496	0.9798	1.2243	0.9552
Fe2+	3.2510	3.2907	3.0308	3.3111
Mg	0.3859	0.3629	0.3998	0.3580
Mn	0.1897	0.1923	0.1924	0.1805
Mg	0.0000	0.0000	0.0000	0.0000
Fe2+	0.0000	0.0000	0.0000	0.0000
Ca	1.2516	1.2722	1.2279	1.2737
Na	0.7484	0.7278	0.7721	0.7263
Na	0.6566	0.6824	0.6377	0.7284
K	0.3436	0.3496	0.3317	0.3358
Tot	16.0001	16.0319	15.9694	16.0642

	ORF14 BIOTITE				
	1	2	3	4	5
SiO2	35.05	35.00	34.27	33.31	33.52
TiO2	3.29	3.42	3.55	3.43	3.44
Al2O3	12.36	12.41	12.75	12.62	12.73
FeO	28.54	28.86	29.52	29.65	30.15
MnO	0.92	0.91	0.78	0.77	0.83
MgO	6.21	5.88	5.83	5.71	5.48
CaO	0.00	0.00	0.00	0.00	0.00
Na2O	0.30	0.29	0.29	0.32	0.26
K2O	8.91	9.09	8.78	8.67	8.76
Tot	95.58	95.86	95.76	94.47	95.17
Si	5.6374	5.6272	5.5293	5.4734	5.4766
Ti	0.3980	0.4135	0.4308	0.4239	0.4227
Al	2.3437	2.3522	2.4255	2.4448	2.4520
Fe2+	3.8390	3.8805	3.9841	4.0747	4.1196
Mn	0.1253	0.1234	0.1065	0.1066	0.1149
Mg	1.4885	1.4089	1.4020	1.3978	1.3344
Ca	0.0000	0.0000	0.0000	0.0000	0.0000
Na	0.0936	0.0904	0.0907	0.1010	0.0833
K	1.8283	1.8645	1.8069	1.8176	1.8256

	ORF17 BIOTITE	
	1	2
SiO2	34.41	33.61
TiO2	3.56	3.15
Al2O3	12.15	11.23
FeO	29.12	34.26
MnO	0.89	1.41
MgO	6.30	2.51
CaO	0.13	0.03
Na2O	0.30	0.18
K2O	7.41	8.25
Tot	94.27	94.62
Si	5.5947	5.6494
Ti	0.4353	0.3983
Al	2.3289	2.2257
Fe2+	3.9596	4.8167
Mn	0.1226	0.2005
Mg	1.5266	0.6294
Ca	0.0225	0.0054
Na	0.0943	0.0587
K	1.5366	1.7694

ORF6 (CPX–RICH FOYAITE) CLINOPYROXENE

	1	2	3	4	5	6	7	8	9	10	11	12	13	14	15	16	17	18	19	20
SiO2	49 73	50 03	49 69	49 28	49 57	49 75	48 86	49 95	49 61	49 41	50 51	50 34	50 36	51 27	50 34	50 57	50 21	49 98	49 81	50 11
TiO2	0 16	0 16	0 16	0 15	0 19	0 11	0 25	0 15	0 11	0 23	0 19	0 21	0 13	0 16	0 18	0 12	0 21	0 27	0 17	0 17
Al2O3	1 24	1 28	1 27	1 34	1 36	1 49	1 25	1 14	1 31	1 23	1 53	1 22	1 41	1 14	1 18	1 50	1 17	1 32	1 25	1 24
Cr2O3	0 00	0 01	0 00	0 00	0 00	0 00	0 00	0 00	0 00	0 00	0 00	0 00	0 00	0 00	0 00	0 00	0 00	0 00	0 00	0 00
Fe2O3	11 53	9 12	9 13	8 48	6 92	6 40	8 61	9 74	7 27	9 39	7 69	6 50	6 91	10 14	6 50	6 33	7 17	9 42	8 60	5 94
FeO	9 72	10 55	10 13	11 43	12 24	12 26	13 51	10 19	11 86	11 71	13 21	15 00	13 22	11 58	14 36	12 29	14 04	12 46	10 78	13 24
MnO	1 34	1 39	1 36	1 42	1 35	1 47	1 38	1 43	1 52	1 29	1 48	1 49	1 50	1 25	1 49	1 71	1 35	1 32	1 46	1 61
MgO	3 95	5 06	5 15	4 94	5 28	5 08	3 05	4 68	4 86	3 54	4 23	3 97	4 91	4 19	4 22	5 52	3 82	3 45	5 20	4 52
CaO	16 86	18 78	18 65	20 09	20 47	19 81	18 24	18 17	19 71	17 73	18 00	19 06	19 20	16 47	19 22	19 43	18 78	17 33	19 02	20 18
Na2O	4 29	3 22	3 23	2 51	2 20	2 46	3 22	3 58	2 61	3 72	3 29	2 67	2 64	4 32	2 66	2 55	3 01	3 85	2 98	2 28
Total	98 81	99 60	98 78	99 64	99 57	98 84	98 37	99 03	98 86	98 24	100 13	100 46	100 28	100 53	100 15	100 03	99 76	99 41	99 27	99 69
Si	1 9594	1 9535	1 9538	1 9349	1 9446	1 9611	1 9582	1 9615	1 9582	1 9672	1 9707	1 9712	1 9622	1 9837	1 9727	1 9655	1 9753	1 9687	1 9525	1 9654
Al	0 0000	0 0000	0 0000	0 0000	0 0000	0 0000	0 0000	0 0000	0 0000	0 0000	0 0000	0 0000	0 0000	0 0000	0 0000	0 0000	0 0000	0 0000	0 0000	0 0000
Fe3+	0 0000	0 0000	0 0000	0 0000	0 0000	0 0000	0 0000	0 0000	0 0000	0 0000	0 0000	0 0000	0 0000	0 0000	0 0000	0 0000	0 0000	0 0000	0 0000	0 0000
Al	0 0576	0 0589	0 0589	0 0620	0 0629	0 0692	0 0591	0 0528	0 0610	0 0578	0 0704	0 0563	0 0648	0 0520	0 0545	0 0687	0 0543	0 0613	0 0578	0 0573
Fe3+	0 3418	0 2681	0 2702	0 2507	0 2042	0 1899	0 2596	0 2879	0 2158	0 2813	0 2259	0 1917	0 2026	0 2954	0 1916	0 1852	0 2123	0 2794	0 2538	0 1754
Ti	0 0047	0 0047	0 0047	0 0043	0 0055	0 0034	0 0075	0 0044	0 0032	0 0069	0 0056	0 0062	0 0038	0 0047	0 0053	0 0036	0 0062	0 0080	0 0050	0 0050
Cr	0 0000	0 0003	0 0001	0 0000	0 0000	0 0000	0 0000	0 0000	0 0001	0 0000	0 0000	0 0000	0 0000	0 0000	0 0000	0 0000	0 0000	0 0000	0 0000	0 0000
Mg	0 2319	0 2945	0 3018	0 2891	0 3087	0 2984	0 1822	0 2738	0 2859	0 2100	0 2460	0 2317	0 2852	0 2416	0 2465	0 3197	0 2240	0 2025	0 3038	0 2876
Fe2+	0 3202	0 3445	0 3332	0 3754	0 4015	0 4042	0 4530	0 3348	0 3916	0 3898	0 4310	0 4911	0 4308	0 3748	0 4708	0 3996	0 4618	0 4106	0 3534	0 4344
Mn	0 0437	0 0290	0 0311	0 0185	0 0172	0 0349	0 0386	0 0463	0 0424	0 0435	0 0212	0 0230	0 0128	0 0316	0 0313	0 0231	0 0414	0 0382	0 0263	0 0403
Mg	0 0000	0 0000	0 0000	0 0000	0 0000	0 0000	0 0000	0 0000	0 0000	0 0000	0 0000	0 0000	0 0000	0 0000	0 0000	0 0000	0 0000	0 0000	0 0000	0 0000
Fe2+	0 0000	0 0000	0 0000	0 0000	0 0000	0 0000	0 0000	0 0000	0 0000	0 0000	0 0000	0 0000	0 0000	0 0000	0 0000	0 0000	0 0000	0 0000	0 0000	0 0000
Mn	0 0010	0 0169	0 0142	0 0287	0 0276	0 0142	0 0082	0 0013	0 0084	0 0000	0 0277	0 0264	0 0367	0 0094	0 0181	0 0332	0 0036	0 0058	0 0222	0 0132
Ca	0 7118	0 7857	0 7857	0 8452	0 8604	0 8367	0 7833	0 7646	0 8336	0 7564	0 7527	0 7997	0 8016	0 6828	0 8071	0 8092	0 7916	0 7314	0 7989	0 8481
Na	0 3277	0 2438	0 2463	0 1912	0 1673	0 1880	0 2502	0 2726	0 1998	0 2872	0 2489	0 2027	0 1994	0 3241	0 2021	0 1922	0 2295	0 2940	0 2265	0 1734
Total	4 0000	4 0000	4 0000	4 0000	4 0000	4 0000	4 0000	4 0000	4 0000	4 0000	4 0000	4 0000	4 0000	4 0000	4 0000	4 0000	4 0000	4 0000	4 0000	4 0000

ORF8 (CPX–RICH FOYAITE) CLINOPYROXENE

	1	2	3	4	5	6	7	8	9	10	11	12	13	14	15	16
SiO2	49 89	50 78	50 36	51 33	50 87	51 05	51 14	50 97	50 56	51 91	51 69	51 38	51 84	51 93	51 61	51 43
TiO2	0 38	0 22	0 23	0 22	0 23	0 19	0 21	0 21	0 30	0 23	0 23	0 26	0 25	0 22	0 32	0 20
Al2O3	1 75	1 43	1 44	1 45	1 58	1 54	1 51	1 49	1 47	1 13	1 02	1 57	1 50	1 44	1 31	1 35
Cr2O3	0 00	0 00	0 00	0 00	0 00	0 00	0 00	0 00	0 00	0 00	0 00	0 00	0 00	0 00	0 00	0 01
Fe2O3	7 55	6 14	6 46	5 94	6 00	5 71	5 35	5 75	7 08	4 16	7 61	5 16	4 16	3 49	7 78	4 60
FeO	9 75	9 22	9 46	7 82	8 66	9 01	8 94	8 76	10 64	10 57	10 60	11 22	10 15	11 09	10 53	10 41
MnO	1 22	1 04	1 20	1 01	1 08	1 04	0 97	1 01	1 13	1 07	1 18	1 11	0 92	0 96	1 23	1 12
MgO	6 97	8 05	7 72	9 29	8 71	8 76	9 07	8 92	6 81	8 53	6 43	7 11	8 62	8 82	6 10	8 06
CaO	20 92	21 38	21 68	22 07	22 12	22 02	22 13	22 03	20 63	21 78	19 08	20 68	21 91	21 69	17 94	21 41
Na2O	2 11	1 92	1 77	1 70	1 60	1 58	1 49	1 56	2 24	1 62	3 09	2 19	1 66	1 45	3 53	1 80
Total	100 55	100 19	100 33	100 83	100 85	100 90	100 80	100 69	100 84	101 01	100 93	100 69	101 01	101 09	100 34	100 39
Si	1 9187	1 9442	1 9334	1 9394	1 9313	1 9367	1 9387	1 9361	1 9394	1 9684	1 9753	1 9641	1 9612	1 9651	1 9801	1 9642
Al	0 0000	0 0000	0 0000	0 0000	0 0000	0 0000	0 0000	0 0000	0 0000	0 0000	0 0000	0 0000	0 0000	0 0000	0 0000	0 0000
Fe3+	0 0000	0 0000	0 0000	0 0000	0 0000	0 0000	0 0000	0 0000	0 0000	0 0000	0 0000	0 0000	0 0000	0 0000	0 0000	0 0000
Al	0 0793	0 0645	0 0652	0 0646	0 0707	0 0689	0 0675	0 0665	0 0665	0 0505	0 0460	0 0708	0 0669	0 0642	0 0593	0 0608
Fe3+	0 2186	0 1770	0 1867	0 1689	0 1715	0 1629	0 1525	0 1644	0 2043	0 1188	0 2189	0 1485	0 1183	0 0995	0 2247	0 1323
Ti	0 0110	0 0063	0 0066	0 0062	0 0065	0 0055	0 0060	0 0059	0 0085	0 0065	0 0066	0 0075	0 0071	0 0063	0 0092	0 0057
Cr	0 0000	0 0000	0 0000	0 0000	0 0000	0 0000	0 0000	0 0000	0 0000	0 0000	0 0000	0 0000	0 0000	0 0000	0 0000	0 0000
Mg	0 3995	0 4593	0 4417	0 5231	0 4928	0 4953	0 5124	0 5050	0 3890	0 4820	0 3662	0 4051	0 4860	0 4974	0 3488	0 4585
Fe2+	0 2916	0 2928	0 2998	0 2372	0 2585	0 2674	0 2616	0 2582	0 3317	0 3353	0 3388	0 3589	0 3212	0 3326	0 3378	0 3324
Mn	0 0000	0 0000	0 0000	0 0000	0 0000	0 0000	0 0000	0 0000	0 0000	0 0068	0 0235	0 0094	0 0005	0 0000	0 0202	0 0099
Mg	0 0000	0 0000	0 0000	0 0000	0 0000	0 0000	0 0000	0 0000	0 0000	0 0000	0 0000	0 0000	0 0000	0 0000	0 0000	0 0000
Fe2+	0 0221	0 0025	0 0040	0 0101	0 0164	0 0186	0 0218	0 0199	0 0097	0 0000	0 0000	0 0000	0 0000	0 0183	0 0000	0 0000
Mn	0 0397	0 0337	0 0390	0 0323	0 0347	0 0334	0 0311	0 0325	0 0367	0 0276	0 0147	0 0266	0 0290	0 0308	0 0197	0 0263
Ca	0 8621	0 8771	0 8918	0 8934	0 8998	0 8951	0 8989	0 8968	0 8477	0 8849	0 7813	0 8470	0 8681	0 8795	0 7376	0 8761
Na	0 1573	0 1425	0 1318	0 1248	0 1178	0 1162	0 1094	0 1149	0 1665	0 1191	0 2287	0 1623	0 1218	0 1064	0 2626	0 1333
Total	4 0000	4 0000	4 0000	4 0000	4 0000	4 0000	4 0000	4 0000	4 0000	4 0000	4 0000	4 0000	4 0000	4 0000	4 0000	4 0000

ORF17 (CPX–RICH FOYAITE) CLINOPYROXENE

	1	2	3	4	5	6	7
SiO2	48 28	48 54	48 48	48 62	48 27	49 15	49 21
TiO2	0 36	0 37	0 36	0 41	0 46	0 23	0 30
Al2O3	1 79	1 72	1 73	1 75	1 94	1 17	1 21
Cr2O3	0 00	0 00	0 00	0 00	0 00	0 00	0 00
Fe2O3	7 63	8 54	6 81	8 05	7 76	9 40	9 92
FeO	11 30	11 00	12 10	11 25	11 84	12 03	11 43
MnO	1 26	1 19	1 17	1 23	1 18	1 24	1 19
MgO	5 41	5 29	5 15	5 03	4 94	3 78	3 81
CaO	21 46	20 75	21 27	20 19	20 91	18 50	17 73
Na2O	1 79	2 19	1 85	2 41	2 05	3 29	3 66
Total	99 31	99 58	98 92	98 95	99 35	98 79	98 46
Si	1 9030	1 9065	1 9185	1 9197	1 9045	1 9519	1 9553
Al	0 0000	0 0000	0 0000	0 0000	0 0000	0 0000	0 0000
Fe3+	0 0000	0 0000	0 0000	0 0000	0 0000	0 0000	0 0000
Al	0 0832	0 0796	0 0807	0 0815	0 0902	0 0548	0 0567
Fe3+	0 2263	0 2523	0 2029	0 2393	0 2304	0 2811	0 2967
Ti	0 0107	0 0109	0 0107	0 0122	0 0136	0 0069	0 0090
Cr	0 0000	0 0000	0 0000	0 0000	0 0000	0 0000	0 0000
Mg	0 3178	0 3097	0 3037	0 2960	0 2904	0 2237	0 2256
Fe2+	0 3621	0 3475	0 4005	0 3711	0 3753	0 3995	0 3798
Mn	0 0000	0 0000	0 0015	0 0000	0 0000	0 0341	0 0321
Mg	0 0000	0 0000	0 0000	0 0000	0 0000	0 0000	0 0000
Fe2+	0 0103	0 0138	0 0000	0 0005	0 0153	0 0000	0 0000
Mn	0 0427	0 0396	0 0377	0 0411	0 0394	0 0076	0 0079
Ca	0 9072	0 8733	0 9019	0 8542	0 8840	0 7872	0 7548
Na	0 1368	0 1668	0 1419	0 1845	0 1568	0 2533	0 2820
Total	4 0000	4 0000	4 0000	4 0000	4 0000	4 0000	4 0000

	ORF22 (CPX-RICH FOYAITE) CLINOPYROXENE							
	1	2	3	4	5	6	7	8
SiO2	50.08	49.32	50.11	49.85	49.93	49.59	49.92	50.93
TiO2	0.22	0.22	0.26	0.22	0.16	0.21	0.29	0.21
Al2O3	1.52	1.14	1.64	1.57	1.12	1.75	1.50	1.28
Cr2O3	0.00	0.00	0.00	0.00	0.00	0.00	0.02	0.01
Fe2O3	6.89	8.82	6.37	6.63	7.44	7.91	7.95	4.10
FeO	8.22	10.71	7.68	7.84	8.14	8.79	12.34	11.72
MnO	1.26	1.50	1.10	1.14	1.26	1.23	1.48	1.29
MgO	8.07	5.12	8.51	8.39	7.66	6.68	4.54	7.42
CaO	21.45	19.62	21.86	21.45	21.25	20.41	17.35	19.94
Na2O	1.88	2.74	1.76	1.81	2.06	2.46	3.41	2.00
Total	99.59	99.19	99.30	98.89	99.03	99.03	98.79	98.90
Si	1.9296	1.9407	1.9288	1.9290	1.9386	1.9305	1.9686	1.9799
Al	0.0000	0.0000	0.0000	0.0000	0.0000	0.0000	0.0000	0.0000
Fe3+	0.0000	0.0000	0.0000	0.0000	0.0000	0.0000	0.0000	0.0000
Al	0.0690	0.0530	0.0746	0.0716	0.0512	0.0802	0.0697	0.0587
Fe3+	0.1998	0.2611	0.1845	0.1930	0.2175	0.2317	0.2359	0.1200
Ti	0.0063	0.0066	0.0075	0.0065	0.0047	0.0062	0.0086	0.0061
Cr	0.0000	0.0000	0.0000	0.0000	0.0000	0.0000	0.0005	0.0002
Mg	0.4634	0.3004	0.4882	0.4839	0.4432	0.3878	0.2668	0.4299
Fe2+	0.2615	0.3524	0.2452	0.2451	0.2643	0.2863	0.4069	0.3810
Mn	0.0000	0.0266	0.0000	0.0000	0.0192	0.0078	0.0116	0.0041
Mg	0.0000	0.0000	0.0000	0.0000	0.0000	0.0000	0.0000	0.0000
Fe2+	0.0032	0.0000	0.0021	0.0087	0.0000	0.0000	0.0000	0.0000
Mn	0.0412	0.0233	0.0360	0.0372	0.0222	0.0328	0.0379	0.0384
Ca	0.8856	0.8273	0.9014	0.8896	0.8841	0.8513	0.7330	0.8306
Na	0.1404	0.2087	0.1317	0.1355	0.1551	0.1854	0.2605	0.1511
Total	4.0000	4.0000	4.0000	4.0000	4.0000	4.0000	4.0000	4.0000

	ORF21 (AMPH-RICH FOYAITE) CLINOPYROXENE				ORF23 (AMPH-RICH FOYAITE) CLINOPYROXENE				ORF40 (AMPH-RICH FOYAITE) CLINOPYROXENE							
	1	2	3	4	1	2	3	4	1	2	3	4	5	6	7	8
SiO2	49.46	48.70	49.84	49.10	48.66	49.00	48.40	48.42	49.98	50.27	50.24	50.35	50.44	49.87	49.86	49.99
TiO2	0.24	0.26	0.24	0.34	0.30	0.31	0.28	0.36	0.27	0.37	0.29	0.23	0.27	0.30	0.30	0.24
Al2O3	1.10	1.18	1.10	1.52	1.27	1.30	1.26	1.45	0.92	0.93	0.93	0.86	0.97	0.98	1.12	0.96
Cr2O3	0.00	0.00	0.00	0.00	0.00	0.01	0.00	0.00	0.00	0.00	0.00	0.00	0.00	0.00	0.00	0.00
Fe2O3	6.06	6.80	5.11	5.39	9.93	10.15	9.96	9.13	12.37	13.79	13.34	14.26	13.47	14.17	11.31	14.61
FeO	14.70	14.60	15.49	15.98	14.01	13.83	13.77	13.22	13.67	12.49	12.92	12.05	12.54	11.75	14.28	11.30
MnO	1.89	1.89	1.65	1.83	1.53	1.44	1.42	1.39	1.36	1.36	1.24	1.40	1.23	1.27	1.34	1.25
MgO	4.21	3.75	4.18	3.56	2.90	2.94	2.71	3.56	1.02	0.95	1.08	1.07	1.13	1.09	1.14	1.12
CaO	18.68	18.73	18.64	18.47	18.22	18.17	18.21	18.95	12.97	12.19	12.59	12.13	12.35	12.30	13.66	12.26
Na2O	2.44	2.43	2.44	2.41	3.11	3.25	3.18	2.80	5.72	6.31	6.06	6.36	6.24	6.29	5.33	6.41
Total	98.78	98.34	98.69	98.60	99.92	100.40	99.19	99.28	98.28	98.66	98.69	98.72	98.64	98.02	98.34	98.15
Si	1.9704	1.9562	1.9847	1.9663	1.9325	1.9340	1.9355	1.9265	2.0058	2.0041	2.0036	2.0047	2.0082	1.9985	2.0011	1.9987
Al	0.0000	0.0000	0.0000	0.0000	0.0000	0.0000	0.0000	0.0000	0.0000	0.0000	0.0000	0.0000	0.0000	0.0000	0.0000	0.0000
Fe3+	0.0000	0.0000	0.0000	0.0000	0.0000	0.0000	0.0000	0.0000	0.0000	0.0000	0.0000	0.0000	0.0000	0.0000	0.0000	0.0000
Al	0.0517	0.0559	0.0516	0.0718	0.0596	0.0604	0.0593	0.0681	0.0435	0.0437	0.0439	0.0404	0.0455	0.0463	0.0530	0.0452
Fe3+	0.1817	0.2055	0.1530	0.1624	0.2968	0.3016	0.2996	0.2733	0.3736	0.4136	0.4002	0.4274	0.4036	0.4275	0.3417	0.4397
Ti	0.0072	0.0077	0.0072	0.0102	0.0089	0.0091	0.0084	0.0107	0.0081	0.0111	0.0086	0.0069	0.0081	0.0090	0.0089	0.0073
Cr	0.0000	0.0000	0.0000	0.0000	0.0000	0.0003	0.0000	0.0001	0.0000	0.0000	0.0000	0.0000	0.0000	0.0000	0.0000	0.0000
Mg	0.2498	0.2245	0.2481	0.2125	0.1714	0.1731	0.1617	0.2112	0.0610	0.0564	0.0642	0.0635	0.0670	0.0651	0.0682	0.0667
Fe2+	0.4896	0.4905	0.5160	0.5353	0.4634	0.4555	0.4606	0.4367	0.4588	0.4166	0.4309	0.4014	0.4175	0.3937	0.4793	0.3779
Mn	0.0200	0.0158	0.0240	0.0079	0.0000	0.0000	0.0104	0.0000	0.0462	0.0459	0.0419	0.0472	0.0415	0.0431	0.0456	0.0423
Mg	0.0000	0.0000	0.0000	0.0000	0.0000	0.0000	0.0000	0.0000	0.0000	0.0000	0.0000	0.0000	0.0000	0.0000	0.0000	0.0000
Fe2+	0.0000	0.0000	0.0000	0.0000	0.0018	0.0008	0.0000	0.0031	0.0000	0.0000	0.0000	0.0000	0.0000	0.0000	0.0000	0.0000
Mn	0.0438	0.0484	0.0316	0.0541	0.0515	0.0482	0.0377	0.0468	0.0000	0.0000	0.0000	0.0000	0.0000	0.0000	0.0000	0.0000
Ca	0.7974	0.8061	0.7953	0.7925	0.7752	0.7686	0.7801	0.8079	0.5577	0.5207	0.5380	0.5175	0.5269	0.5282	0.5874	0.5252
Na	0.1885	0.1893	0.1884	0.1871	0.2391	0.2484	0.2468	0.2157	0.4451	0.4878	0.4686	0.4910	0.4817	0.4887	0.4148	0.4969
Total	4.0000	4.0000	4.0000	4.0000	4.0000	4.0000	4.0000	4.0000	4.0000	4.0000	4.0000	4.0000	4.0000	4.0000	4.0000	4.0000

	ORF22 NEPHELINE				ORF23 NEPHELINE																
	1	2	3	4	1	2	3	4	5	6	7	8	9	10	11	12	13	14	15	16	17	18	19
SiO2	44 72	44 77	45 19	45 13	45 91	45 79	45 10	45 21	45 13	45 34	45 34	45 73	45 21	45 01	45 91	45 79	45 10	49 41	45 21	45 13	46 08	45 12	45 23
Al2O3	31 67	31 86	31 88	31 99	32 12	32 04	32 53	32 30	32 09	32 85	32 86	32 84	32 96	32 87	32 13	32 04	32 53	35 48	32 30	32 09	31 87	32 65	32 56
FeO	0 57	0 56	0 60	0 52	0 17	0 27	0 13	0 29	0 39	0 28	0 26	0 33	0 31	0 34	0 17	0 27	0 13	0 42	0 29	0 39	0 51	0 48	0 44
CaO	0 23	0 27	0 23	0 24	0 36	0 44	0 43	0 46	0 45	0 19	0 20	0 20	0 20	0 28	0 36	0 44	0 43	0 49	0 46	0 45	0 07	0 11	0 11
Na2O	16 81	17 03	17 02	16 93	16 58	16 60	16 77	16 95	16 64	16 89	16 99	17 01	16 64	16 88	16 59	16 61	16 77	18 35	16 95	16 64	16 75	16 51	16 45
K2O	5 25	5 31	5 27	5 26	4 80	4 69	5 18	5 21	5 07	5 71	5 58	5 39	5 56	5 77	4 81	4 69	5 18	5 70	5 21	5 07	5 07	5 60	5 51
Total	99 25	99 79	100 19	100 06	99 94	99 83	100 13	100 42	99 76	101 26	101 23	101 50	100 88	101 16	99 96	99 85	100 14	109 85	100 42	99 76	100 33	100 47	100 30
Qz	5 42	4 94	5 40	5 56	7 65	7 66	5 97	5 65	6 42	5 20	5 18	5 75	5 80	4 85	7 63	7 64	5 96	5 98	5 65	6 42	7 07	5 94	6 29
Ne	76 99	77 40	77 11	76 93	76 19	76 51	76 68	77 02	76 50	75 99	76 41	76 49	75 68	76 09	76 20	76 52	76 68	76 59	77 02	76 50	76 07	75 35	75 25
Ks	17 59	17 67	17 49	17 51	16 16	15 83	17 35	17 33	17 08	18 80	18 41	17 76	18 52	19 06	16 17	15 83	17 36	17 43	17 33	17 08	16 86	18 72	18 46

	ORF23 NEPHELINE								
	20	21	22	23	24	25	26	27	28
SiO2	45 48	46 37	45 15	44 83	45 29	46 08	46 02	44 47	45 31
Al2O3	32 29	31 80	32 81	32 83	32 54	31 35	31 87	32 56	31 69
FeO	0 40	0 51	0 46	0 46	0 39	0 29	0 39	0 12	0 39
CaO	0 15	0 07	0 14	0 11	0 08	0 05	0 08	0 23	0 09
Na2O	16 44	16 57	15 95	16 77	16 89	16 35	16 24	16 11	16 3
K2O	5 16	4 53	5 39	5 43	5 50	4 81	4 51	5 65	5 42
Total	99 92	99 85	99 90	100 43	100 69	98 93	99 10	99 14	99 20
Qz	7 04	8 49	7 45	5 36	5 45	8 30	8 93	6 08	6 81
Ne	75 58	76 24	74 18	76 50	76 34	75 45	75 69	74 72	74 94
Ks	17 36	15 27	18 36	18 15	18 21	16 26	15 38	19 19	18 25

	ORF17 SODALITE					ORF22 SODALITE		ORF6 SODALITE											
	1	2	3	4	5	1	2	1	2	3	4	5	6	7	8	9	10	11	12	13
SiO2	40 64	39 96	37 98	38 22	38 07	38 23	37 00	39 62	38 48	38 57	38 21	38 67	37 34	38 05	38 02	38 30	39 29	37 98	38 85	38 56
Al2O3	32 08	31 05	31 17	31 31	31 37	31 37	30 61	31 94	31 86	31 47	31 29	31 60	31 39	31 36	31 52	31 59	31 90	31 39	31 64	31 53
FeO	0 19	0 20	0 18	0 17	0 15	0 29	0 24	0 20	0 17	0 19	0 16	0 26	0 25	0 26	0 22	0 17	0 22	0 20	0 23	0 25
CaO	0 17	0 40	0 15	0 13	0 16	0 23	0 20	0 13	0 08	0 14	0 13	0 14	0 13	0 13	0 11	0 08	0 12	0 10	0 09	0 11
Na2O	23 49	22 91	26 00	26 17	26 32	26 58	26 56	25 40	26 37	26 20	26 20	25 91	26 71	26 86	26 85	26 89	24 99	25 57	26 15	25 95
K2O	0 03	1 25	0 05	0 04	0 04	0 00	0 00	0 02	0 03	0 02	0 00	0 02	0 02	0 02	0 00	0 01	0 02	0 01	0 01	0 02
Total	96 61	95 77	95 54	96 04	96 10	96 69	94 61	97 32	96 98	96 60	95 98	96 60	95 84	96 68	96 72	97 04	96 53	95 25	96 97	96 42

	ORF14 SODALITE					ORF 7
	1	2	3	4	5	1
SiO2	38 35	38 05	38 23	38 17	39 09	36 25
Al2O3	32 17	32 01	32 08	32 06	31 86	31 01
FeO	0 14	0 14	0 10	0 10	0 27	0 27
CaO	0 13	0 16	0 14	0 14	0 20	0 23
Na2O	26 47	26 49	26 63	26 44	26 09	26 09
K2O	0 04	0 03	0 04	0 04	0 05	0 03
Total	97 30	96 88	97 22	96 95	97 56	93 87

Alkali-syenites

ORS99 AMPHIBOLE

	1	2	3	4	5	6	7	8
	c	m	r	c	m	r		
SiO2	38.24	38.60	38.00	38.80	38.06	38.89	39.91	38.50
TiO2	1.71	1.40	1.63	1.38	1.44	1.40	0.94	1.14
Al2O3	8.57	8.64	8.61	7.68	8.55	7.90	6.84	9.01
Fe2O3	6.10	5.66	5.50	5.72	4.73	5.92	8.98	6.58
FeO	26.98	27.27	27.37	27.57	27.55	27.80	25.33	27.18
MnO	1.22	1.16	1.09	1.21	1.20	1.19	1.88	1.08
MgO	0.57	0.71	0.66	0.75	0.76	0.66	0.42	0.74
CaO	8.78	8.89	8.94	8.61	8.95	8.90	6.79	9.35
Na2O	3.55	3.58	3.52	3.86	3.60	3.61	4.50	3.38
K2O	1.24	1.34	1.37	1.30	1.46	1.35	1.52	1.35
Tot	96.96	97.22	96.68	96.87	96.30	97.60	97.10	98.30
Si	6.3194	6.3577	6.3085	6.4333	6.3463	6.4043	6.5821	6.2812
ivAl	1.6702	1.6423	1.6846	1.5021	1.6537	1.5341	1.3302	1.7188
Fe3+	0.0103	0.0000	0.0069	0.0646	0.0000	0.0616	0.0877	0.0000
viAl	0.0000	0.0345	0.0000	0.0000	0.0259	0.0000	0.0000	0.0146
Ti	0.2126	0.1729	0.2039	0.1715	0.1802	0.1735	0.1162	0.1399
Fe3+	0.7486	0.7012	0.6808	0.6494	0.5931	0.6716	1.0265	0.8075
Fe2+	3.7292	3.7559	3.7995	3.8235	3.8415	3.8288	3.4931	3.7086
Mg	0.1392	0.1731	0.1631	0.1863	0.1898	0.1608	0.1020	0.1797
Mn	0.1704	0.1624	0.1527	0.1693	0.1696	0.1653	0.2622	0.1497
Mg	0.0000	0.0000	0.0000	0.0000	0.0000	0.0000	0.0000	0.0000
Fe2+	0.0000	0.0000	0.0000	0.0000	0.0000	0.0000	0.0000	0.0000
Ca	1.5538	1.5685	1.5903	1.5293	1.5995	1.5711	1.2005	1.6340
Na	0.4462	0.4315	0.4097	0.4707	0.4005	0.4289	0.7995	0.3660
Na	0.6916	0.7103	0.7221	0.7709	0.7643	0.7230	0.6393	0.7023
K	0.2612	0.2820	0.2904	0.2742	0.3106	0.2830	0.3192	0.2806

ORS110 AMPHIBOLE

	1	2	3	4	5	6	7	8
		c	m	r				
SiO2	39.26	39.60	39.27	39.58	39.34	39.98	38.88	39.22
TiO2	1.07	1.38	1.04	1.06	1.21	1.18	1.58	1.18
Al2O3	8.24	8.26	8.24	8.01	8.04	7.96	8.77	8.25
Fe2O3	7.61	8.43	8.31	7.08	7.52	8.35	7.48	8.66
FeO	25.79	25.93	25.53	26.30	25.91	25.39	24.88	24.75
MnO	1.37	1.33	1.47	1.45	1.70	1.46	1.47	1.43
MgO	0.80	0.46	0.76	0.78	0.73	0.66	1.11	0.74
CaO	7.83	6.93	7.84	7.74	7.88	7.06	7.72	6.93
Na2O	4.12	4.80	4.08	4.35	4.17	4.44	4.27	4.50
K2O	1.45	1.49	1.51	1.42	1.44	1.51	1.37	1.62
Tot	97.54	98.62	98.05	97.76	97.93	97.98	97.53	97.27
Si	6.4265	6.4176	6.4008	6.4700	6.4265	6.4971	6.3393	6.4245
ivAl	1.5735	1.5771	1.5839	1.5300	1.5485	1.5029	1.6607	1.5755
Fe3+	0.0000	0.0053	0.0153	0.0000	0.0251	0.0000	0.0000	0.0000
viAl	0.0159	0.0000	0.0000	0.0133	0.0000	0.0229	0.0249	0.0182
Ti	0.1311	0.1677	0.1270	0.1298	0.1480	0.1440	0.1932	0.1451
Fe3+	0.9379	1.0232	1.0042	0.8710	0.8990	1.0209	0.9177	1.0672
Fe2+	3.5306	3.5148	3.4806	3.5950	3.5397	3.4511	3.3929	3.3907
Mg	0.1949	0.1113	0.1846	0.1898	0.1787	0.1601	0.2687	0.1799
Mn	0.1897	0.1830	0.2035	0.2011	0.2347	0.2010	0.2026	0.1988
Mg	0.0000	0.0000	0.0000	0.0000	0.0000	0.0000	0.0000	0.0000
Fe2+	0.0000	0.0000	0.0000	0.0000	0.0000	0.0000	0.0000	0.0000
Ca	1.3729	1.2035	1.3692	1.3556	1.3790	1.2300	1.3491	1.2163
Na	0.6271	0.7965	0.6308	0.6444	0.6210	0.7700	0.6509	0.7837
Na	0.6812	0.7121	0.6578	0.7350	0.6994	0.6286	0.6976	0.6456
K	0.3034	0.3083	0.3140	0.2955	0.3001	0.3125	0.2850	0.3380

ORS112 AMPHIBOLE

	1	2	3	4	5	6
SiO2	38.46	38.91	38.70	39.44	39.48	39.17
TiO2	0.78	0.80	0.68	0.79	0.76	0.81
Al2O3	8.23	8.37	8.45	7.71	7.49	8.03
Fe2O3	6.43	9.12	8.30	6.40	7.85	8.57
FeO	27.06	25.51	25.96	27.35	27.04	26.37
MnO	1.38	1.23	1.30	1.34	1.31	1.32
MgO	0.25	0.23	0.25	0.24	0.20	0.22
CaO	8.17	7.06	7.70	8.05	7.41	7.41
Na2O	3.97	4.42	4.06	3.89	4.49	4.36
K2O	1.41	1.58	1.51	1.35	1.43	1.58
Tot	96.12	97.23	96.92	96.56	97.46	97.83
Si	6.4303	6.4063	6.4001	6.5470	6.5117	6.4310
ivAl	1.5697	1.5937	1.5999	1.4530	1.4571	1.5531
Fe3+	0.0000	0.0000	0.0000	0.0000	0.0312	0.0159
viAl	0.0528	0.0305	0.0482	0.0565	0.0000	0.0000
Ti	0.0981	0.0994	0.0851	0.0984	0.0947	0.1005
Fe3+	0.8092	1.1304	1.0333	0.7995	0.9432	1.0434
Fe2+	3.7835	3.5123	3.5899	3.7977	3.7299	3.6199
Mg	0.0615	0.0564	0.0609	0.0596	0.0494	0.0531
Mn	0.1949	0.1710	0.1827	0.1883	0.1828	0.1831
Mg	0.0000	0.0000	0.0000	0.0000	0.0000	0.0000
Fe2+	0.0000	0.0000	0.0000	0.0000	0.0000	0.0000
Ca	1.4628	1.2457	1.3640	1.4314	1.3098	1.3029
Na	0.5372	0.7543	0.6360	0.5686	0.6902	0.6971
Na	0.7489	0.6562	0.6657	0.6822	0.7445	0.6904
K	0.2997	0.3321	0.3186	0.2868	0.3013	0.3313

ORS126 AMPHIBOLE

	1	2	3	4	5	6	7	8
SiO2	41.05	42.30	41.20	41.78	41.72	40.26	40.67	40.79
TiO2	0.85	1.11	0.80	0.87	0.93	0.69	0.71	0.88
Al2O3	6.34	5.59	6.65	6.65	6.26	6.62	6.32	6.48
Fe2O3	8.62	7.59	9.10	7.82	7.87	9.23	7.18	8.00
FeO	25.78	27.45	25.89	26.98	26.53	25.44	26.77	26.91
MnO	1.65	1.74	1.61	1.47	1.75	1.67	1.80	1.51
MgO	0.42	0.41	0.39	0.34	0.54	0.38	0.40	0.38
CaO	6.20	6.28	6.00	6.08	6.32	6.24	6.85	6.82
Na2O	4.92	5.14	5.31	5.29	5.08	4.98	4.72	4.78
K2O	1.38	1.43	1.38	1.46	1.43	1.47	1.39	1.41
Tot	97.20	99.02	98.32	98.52	98.43	96.99	96.81	97.96
Si	6.7338	6.8334	6.6886	6.7597	6.7634	6.6424	6.7300	6.6735
ivAl	1.2270	1.0645	1.2717	1.2403	1.1964	1.2884	1.2322	1.2501
Fe3+	0.0392	0.1020	0.0396	0.0000	0.0402	0.0692	0.0378	0.0764
viAl	0.0000	0.0000	0.0000	0.0293	0.0000	0.0000	0.0000	0.0000
Ti	0.1051	0.1343	0.0978	0.1057	0.1139	0.0857	0.0887	0.1085
Fe3+	1.0257	0.8202	1.0719	0.9282	0.9205	1.0769	0.8561	0.9081
Fe2+	3.5373	3.7084	3.5144	3.6527	3.5966	3.5098	3.7043	3.6815
Mg	0.1029	0.0987	0.0948	0.0823	0.1293	0.0939	0.0991	0.0926
Mn	0.2290	0.2384	0.2211	0.2019	0.2398	0.2337	0.2517	0.2092
Mg	0.0000	0.0000	0.0000	0.0000	0.0000	0.0000	0.0000	0.0000
Fe2+	0.0000	0.0000	0.0000	0.0000	0.0000	0.0000	0.0000	0.0000
Ca	1.0894	1.0863	1.0428	1.0547	1.0975	1.1034	1.2143	1.1960
Na	0.9106	0.9137	0.9572	0.9453	0.9025	0.8966	0.7857	0.8040
Na	0.6531	0.6961	0.7145	0.7148	0.6955	0.6968	0.7286	0.7106
K	0.2878	0.2954	0.2866	0.3020	0.2953	0.3090	0.2936	0.2949

MKS49 AMPHIBOLE

	1	2	4	5	6	7	8
SiO2	40.52	40.17	40.27	40.49	41.46	40.33	39.77
TiO2	1.80	1.78	1.76	1.97	1.70	1.63	1.87
Al2O3	7.45	7.48	7.41	7.41	6.25	6.90	7.17
Fe2O3	6.47	6.42	6.50	6.49	2.69	5.61	6.38
FeO	24.99	25.13	24.98	25.01	27.43	25.00	24.44
MnO	1.19	1.19	1.22	1.20	1.31	1.21	1.18
MgO	2.29	2.28	2.21	2.31	2.42	2.25	2.21
CaO	8.64	8.88	8.68	8.44	8.77	8.38	8.44
Na2O	3.57	3.43	3.48	3.78	3.99	3.53	3.42
K2O	1.22	1.28	1.24	1.24	1.05	1.22	1.14
Tot	98.13	98.04	97.75	98.34	97.06	96.05	96.03
Si	6.5158	6.4806	6.5084	6.5010	6.7560	6.6205	6.5303
ivAl	1.4117	1.4231	1.4111	1.4029	1.2000	1.3349	1.3889
Fe3+	0.0725	0.0963	0.0804	0.0961	0.0440	0.0446	0.0808
viAl	0.0000	0.0000	0.0000	0.0000	0.0000	0.0000	0.0000
Ti	0.2176	0.2154	0.2137	0.2378	0.2083	0.2007	0.2315
Fe3+	0.7103	0.6837	0.7106	0.6877	0.2862	0.6479	0.7080
Fe2+	3.3605	3.3907	3.3758	3.3589	3.7385	3.4320	3.3558
Mg	0.5490	0.5477	0.5327	0.5526	0.5866	0.5509	0.5402
Mn	0.1627	0.1625	0.1672	0.1629	0.1804	0.1684	0.1645
Mg	0.0000	0.0000	0.0000	0.0000	0.0000	0.0000	0.0000
Fe2+	0.0000	0.0000	0.0000	0.0000	0.0000	0.0000	0.0000
Ca	1.4889	1.5344	1.5032	1.4528	1.5315	1.4748	1.4848
Na	0.5111	0.4656	0.4968	0.5472	0.4685	0.5252	0.5152
Na	0.6006	0.6080	0.5948	0.6297	0.7919	0.5990	0.5742
K	0.2493	0.2624	0.2555	0.2531	0.2179	0.2564	0.2397

MKS35 AMPHIBOLE

	1	2	3	4	5	6	7
SiO2	39.44	39.54	39.29	38.84	38.61	38.41	39.38
TiO2	2.49	2.71	2.77	1.68	1.58	1.51	1.55
Al2O3	10.25	10.26	9.96	10.81	10.49	10.54	9.77
Fe2O3	2.52	2.69	3.46	5.17	4.46	7.16	6.47
FeO	22.99	22.59	23.08	22.87	24.31	23.08	23.94
MnO	0.78	0.88	0.91	0.90	0.84	0.93	0.95
MgO	4.92	4.87	4.45	3.62	3.10	2.65	2.66
CaO	10.29	10.02	9.97	9.82	9.95	9.40	9.22
Na2O	3.41	3.41	3.48	3.35	3.31	3.27	3.41
K2O	1.33	1.34	1.25	1.42	1.45	1.43	1.47
Tot	98.41	98.31	98.63	98.50	98.10	98.38	98.81
Si	6.2142	6.2231	6.1959	6.1553	6.1820	6.1352	6.2648
ivAl	1.7858	1.7769	1.8041	1.8447	1.8180	1.8648	1.7352
Fe3+	0.0000	0.0000	0.0000	0.0000	0.0000	0.0000	0.0000
viAl	0.1174	0.1270	0.0485	0.1757	0.1619	0.1193	0.0975
Ti	0.2945	0.3205	0.3291	0.2004	0.1905	0.1811	0.1850
Fe3+	0.2989	0.3186	0.4109	0.6165	0.5378	0.8608	0.7742
Fe2+	3.0298	2.9740	3.0438	3.0311	3.2563	3.0834	3.1859
Mg	1.1549	1.1427	1.0466	0.8552	0.7389	0.6298	0.6599
Mn	0.1045	0.1172	0.1210	0.1211	0.1146	0.1257	0.1276
Mg	0.0000	0.0000	0.0000	0.0000	0.0000	0.0000	0.0000
Fe2+	0.0000	0.0000	0.0000	0.0000	0.0000	0.0000	0.0000
Ca	1.7365	1.6900	1.6844	1.6673	1.7065	1.6085	1.5717
Na	0.2635	0.3100	0.3156	0.3327	0.2935	0.3915	0.4283
Na	0.7773	0.7304	0.7498	0.6975	0.7340	0.6225	0.6245
K	0.2666	0.2700	0.2523	0.2870	0.2968	0.2916	0.2975

MKS35 AMPHIBOLE

	8	9	10	11	12	13
SiO2	39 30	39 11	39 03	39 35	39 25	38 90
TiO2	1 75	1 70	1 67	1 62	1 59	1 50
Al2O3	9 38	9 63	9 45	9 46	9 47	9 64
Fe2O3	6 39	6 49	4 84	5 87	4 75	4 78
FeO	24 52	24 37	25 41	24 58	25 40	25 46
MnO	0 99	1 01	1 13	1 17	1 12	1 13
MgO	2 32	2 38	2 38	2 44	2 42	2 25
CaO	8 98	9 27	9 53	9 29	9 42	9 57
Na2O	3 56	3 38	3 45	3 39	3 55	3 37
K2O	1 42	1 43	1 46	1 50	1 48	1 53
Tot	98 61	98 77	98 34	98 69	98 45	98 14
Si	6 2851	6 2457	6 2790	6 2893	6 3013	6 2728
ivAl	1 7149	1 7543	1 7210	1 7107	1 6987	1 7272
Fe3+	0 0000	0 0000	0 0000	0 0000	0 0000	0 0000
viAl	0 0529	0 0581	0 0705	0 0727	0 0927	0 1065
Ti	0 2105	0 2036	0 2016	0 1952	0 1923	0 1823
Fe3+	0 7694	0 7800	0 5858	0 7062	0 5742	0 5807
Fe2+	3 2797	3 2547	3 4187	3 2862	3 4095	3 4337
Mg	0 5528	0 5664	0 5696	0 5812	0 5791	0 5418
Mn	0 1346	0 1371	0 1538	0 1585	0 1523	0 1549
Mg	0 0000	0 0000	0 0000	0 0000	0 0000	0 0000
Fe2+	0 0000	0 0000	0 0000	0 0000	0 0000	0 0000
Ca	1 5387	1 5865	1 6432	1 5914	1 6198	1 6535
Na	0 4613	0 4135	0 3568	0 4086	0 3802	0 3465
Na	0 6436	0 6319	0 7196	0 6433	0 7240	0 7076
K	0 2891	0 2905	0 2988	0 3066	0 3035	0 3141

MKS57 AMPHIBOLE

	1	2	3	4	5	6	7	8	9	10	11	12	13	14	15	16	17
SiO2	38 63	38 37	37 99	38 36	38 37	38 56	38 00	38 32	38 42	38 33	38 65	38 31	38 34	38 20	38 03	38 36	38 21
TiO2	1 82	1 89	1 80	1 62	1 48	1 62	1 50	1 72	2 20	1 91	1 67	1 99	2 17	2 15	2 01	1 70	1 59
Al2O3	9 05	9 19	9 12	8 99	8 65	8 87	9 38	8 99	8 59	8 74	9 01	8 86	8 80	8 68	8 76	8 96	9 05
Fe2O3	6 30	6 26	6 39	6 55	7 48	6 57	6 77	5 16	6 20	6 64	5 44	6 51	7 06	6 47	5 77	6 56	5 38
FeO	25 83	25 86	26 05	26 14	25 54	26 23	25 82	27 08	26 46	26 55	26 94	26 26	26 34	26 55	26 39	26 21	26 80
MnO	1 12	1 11	1 12	1 11	1 22	1 16	1 14	1 20	1 18	1 20	1 32	1 21	1 25	1 17	1 23	1 26	1 32
MgO	1 21	1 19	1 01	0 89	0 99	0 90	0 91	0 89	0 86	0 89	0 94	0 85	0 86	0 81	0 90	0 88	0 93
CaO	9 39	9 47	9 47	9 37	9 27	9 26	9 39	9 52	9 22	9 44	9 53	9 43	9 44	9 33	9 45	9 44	9 63
Na2O	2 93	2 90	2 92	2 90	2 91	2 97	2 87	3 03	2 93	2 91	3 03	2 80	2 96	2 96	2 81	2 89	2 96
K2O	1 18	1 19	1 21	1 18	1 17	1 29	1 37	1 32	1 25	1 41	1 37	1 25	1 19	1 20	1 23	1 26	1 32
Tot	97 46	97 44	97 07	97 11	97 08	97 42	97 16	97 21	97 31	98 00	97 89	97 48	98 42	97 54	96 57	97 52	97 20
Si	6 2957	6 2603	6 2408	6 2944	6 3002	6 3109	6 2369	6 2999	6 2999	6 2588	6 3069	6 2707	6 2279	6 2605	6 2843	6 2771	6 2842
ivAl	1 7043	1 7397	1 7592	1 7056	1 6742	1 6891	1 7631	1 7001	1 6606	1 6822	1 6931	1 7106	1 6850	1 6769	1 7076	1 7229	1 7158
Fe3+	0 0000	0 0000	0 0000	0 0000	0 0256	0 0000	0 0000	0 0000	0 0395	0 0590	0 0000	0 0186	0 0871	0 0626	0 0081	0 0000	0 0000
viAl	0 0353	0 0281	0 0071	0 0337	0 0000	0 0221	0 0523	0 0425	0 0000	0 0000	0 0395	0 0000	0 0000	0 0000	0 0000	0 0064	0 0389
Ti	0 2229	0 2316	0 2222	0 1998	0 1833	0 1999	0 1852	0 2124	0 2711	0 2342	0 2046	0 2445	0 2652	0 2646	0 2497	0 2088	0 1972
Fe3+	0 7733	0 7691	0 7898	0 8086	0 8982	0 8090	0 8364	0 6381	0 7253	0 7569	0 6686	0 7836	0 7764	0 7359	0 7098	0 8074	0 6660
Fe2+	3 5202	3 5290	3 5784	3 5870	3 5067	3 5900	3 5438	3 7231	3 6291	3 6260	3 6765	3 5959	3 5786	3 6384	3 6478	3 5870	3 6858
Mg	0 2937	0 2895	0 2471	0 2172	0 2419	0 2184	0 2234	0 2172	0 2103	0 2163	0 2287	0 2077	0 2077	0 1985	0 2211	0 2150	0 2281
Mn	0 1546	0 1528	0 1554	0 1537	0 1699	0 1605	0 1589	0 1668	0 1643	0 1666	0 1822	0 1683	0 1721	0 1626	0 1716	0 1753	0 1839
Mg	0 0000	0 0000	0 0000	0 0000	0 0000	0 0000	0 0000	0 0000	0 0000	0 0000	0 0000	0 0000	0 0000	0 0000	0 0000	0 0000	0 0000
Fe2+	0 0000	0 0000	0 0000	0 0000	0 0000	0 0000	0 0000	0 0000	0 0000	0 0000	0 0000	0 0000	0 0000	0 0000	0 0000	0 0000	0 0000
Ca	1 6394	1 6560	1 6674	1 6481	1 6310	1 6236	1 6515	1 6771	1 6192	1 6512	1 6658	1 6533	1 6432	1 6387	1 6739	1 6558	1 6969
Na	0 3606	0 3440	0 3326	0 3519	0 3690	0 3764	0 3485	0 3229	0 3808	0 3488	0 3342	0 3467	0 3568	0 3613	0 3261	0 3442	0 3031
Na	0 5681	0 5748	0 5967	0 5698	0 5587	0 5660	0 5658	0 6418	0 5517	0 5720	0 6241	0 5418	0 5753	0 5808	0 5736	0 5730	0 6417
K	0 2443	0 2485	0 2539	0 2459	0 2454	0 2683	0 2867	0 2759	0 2617	0 2928	0 2859	0 2616	0 2469	0 2548	0 2590	0 2626	0 2778

MKS64 AMPHIBOLE

	1	2	4	6	7	9	11	12	13	14	15
SiO2	37 39	37 50	37 75	37 77	38 12	38 15	37 52	37 40	37 55	37 53	37 70
TiO2	1 50	1 56	1 60	1 59	1 80	1 94	1 70	1 67	2 09	1 81	1 61
Al2O3	9 75	9 70	9 70	9 47	9 44	9 55	9 93	9 90	10 09	9 84	9 59
Fe2O3	5 57	5 97	6 13	5 76	6 57	5 64	7 12	7 16	5 38	6 27	6 94
FeO	24 43	25 03	24 54	25 41	24 79	25 57	24 46	24 56	25 40	25 06	24 73
MnO	0 95	0 89	0 89	1 01	1 08	1 02	1 15	1 14	1 07	1 08	1 05
MgO	1 61	1 49	1 68	1 68	1 70	1 65	1 63	1 60	1 63	1 56	1 64
CaO	9 36	9 63	9 48	9 92	9 83	9 90	9 96	9 94	10 03	9 96	9 89
Na2O	2 70	2 66	2 71	2 77	2 59	2 67	2 55	2 61	2 62	2 62	2 60
K2O	1 35	1 35	1 30	1 25	1 23	1 34	1 33	1 35	1 39	1 29	1 29
Tot	94 61	95 78	95 77	96 64	97 14	97 43	97 35	97 32	97 25	97 01	97 05
Si	6 2448	6 2088	6 2302	6 2091	6 2152	6 2123	6 1181	6 1081	6 1290	6 1438	6 1680
ivAl	1 7552	1 7912	1 7698	1 7909	1 7848	1 7877	1 8819	1 8919	1 8710	1 8562	1 8320
Fe3+	0 0000	0 0000	0 0000	0 0000	0 0000	0 0000	0 0000	0 0000	0 0000	0 0000	0 0000
viAl	0 1650	0 1030	0 1171	0 0442	0 0294	0 0461	0 0266	0 0144	0 0710	0 0440	0 0184
Ti	0 1882	0 1943	0 1983	0 1964	0 2209	0 2373	0 2080	0 2055	0 2563	0 2229	0 1985
Fe3+	0 7005	0 7438	0 7608	0 7121	0 8067	0 6915	0 8740	0 8801	0 6608	0 7729	0 8550
Fe2+	3 4124	3 4663	3 3866	3 4942	3 3803	3 4826	3 3366	3 3545	3 4678	3 4308	3 3830
Mg	0 4001	0 3678	0 4124	0 4119	0 4135	0 4014	0 3956	0 3883	0 3961	0 3800	0 3990
Mn	0 1337	0 1248	0 1248	0 1412	0 1493	0 1411	0 1592	0 1571	0 1479	0 1494	0 1461
Mg	0 0000	0 0000	0 0000	0 0000	0 0000	0 0000	0 0000	0 0000	0 0000	0 0000	0 0000
Fe2+	0 0000	0 0000	0 0000	0 0000	0 0000	0 0000	0 0000	0 0000	0 0000	0 0000	0 0000
Ca	1 6754	1 7092	1 6765	1 7477	1 7169	1 7278	1 7405	1 7394	1 7549	1 7465	1 7333
Na	0 3246	0 2908	0 3235	0 2523	0 2831	0 2722	0 2595	0 2606	0 2451	0 2535	0 2667
Na	0 5493	0 5625	0 5448	0 6317	0 5349	0 5700	0 5473	0 5656	0 5827	0 5774	0 5588
K	0 2885	0 2843	0 2742	0 2624	0 2552	0 2778	0 2775	0 2813	0 2889	0 2695	0 2696

MKS67 AMPHIBOLE

	1	2	3	4	5	6	7	8	9	10
SiO2	37 23	37 72	36 62	36 62	37 08	37 44	36 71	36 70	31 25	31 35
TiO2	0 99	0 95	1 02	0 96	0 99	1 00	0 97	1 04	1 64	1 55
Al2O3	9 62	9 93	9 83	10 09	10 06	10 44	11 00	11 09	13 95	13 80
Fe2O3	7 25	8 13	7 77	8 79	8 56	6 37	6 18	7 77	38 45	38 72
FeO	24 07	23 64	23 57	23 30	23 28	24 35	24 11	22 46	0 00	0 00
MnO	1 45	1 40	1 38	1 42	1 42	1 45	1 54	1 52	1 13	1 12
MgO	1 76	1 67	1 64	1 60	1 58	1 47	1 50	1 92	2 48	2 48
CaO	9 91	9 70	9 87	9 85	9 74	9 92	10 14	9 92	0 01	0 00
Na2O	2 74	2 71	2 64	2 69	2 66	2 60	2 59	2 56	0 09	0 05
K2O	1 46	1 47	1 37	1 50	1 41	1 46	1 52	1 52	7 29	7 57
Tot	96 47	97 31	95 70	96 82	96 78	96 49	96 24	96 49	96 29	96 65
Si	6 1462	6 1527	6 0922	6 0312	6 0894	6 1554	6 0597	6 0141	4 9227	4 9355
ivAl	1 8538	1 8473	1 9078	1 9594	1 9106	1 8446	1 9403	1 9859	2 5907	2 5609
Fe3+	0 0000	0 0000	0 0000	0 0095	0 0000	0 0000	0 0000	0 0000	0 4866	0 5036
viAl	0 0189	0 0619	0 0194	0 0000	0 0376	0 1781	0 1996	0 1561	0 0000	0 0000
Ti	0 1232	0 1168	0 1275	0 1192	0 1227	0 1232	0 1205	0 1279	0 1938	0 1837
Fe3+	0 9002	0 9984	0 9724	1 0806	1 0583	0 7878	0 7673	0 9582	5 1929	5 1615
Fe2+	3 3237	3 2246	3 2802	3 2101	3 1980	3 3485	3 3290	3 0777	0 0000	0 0000
Mg	0 4319	0 4049	0 4065	0 3924	0 3866	0 3609	0 3685	0 4696	0 0000	0 0000
Mn	0 2021	0 1934	0 1939	0 1978	0 1969	0 2015	0 2151	0 2104	0 0000	0 0000
Mg	0 0000	0 0000	0 0000	0 0000	0 0000	0 0000	0 0000	0 0000	0 5829	0 5829
Fe2+	0 0000	0 0000	0 0000	0 0000	0 0000	0 0000	0 0000	0 0000	0 0000	0 0000
Ca	1 7523	1 6949	1 7590	1 7382	1 7139	1 7474	1 7927	1 7425	0 0014	0 0000
Na	0 2477	0 3051	0 2410	0 2618	0 2861	0 2526	0 2073	0 2575	0 0287	0 0161
Na	0 6288	0 5520	0 6111	0 5962	0 5610	0 5777	0 6202	0 5558	0 0000	0 0000
K	0 3072	0 3065	0 2907	0 3155	0 2946	0 3072	0 3195	0 3175	1 4652	1 5194

	MKS69 AMPHIBOLE							
	1	2	3	4	5	6	7	8
SiO2	38.33	37.87	38.08	37.89	37.77	37.85	38.01	37.13
TiO2	2.86	2.77	2.56	2.68	2.52	2.58	2.36	1.71
Al2O3	10.17	9.97	9.70	9.77	9.44	9.98	9.41	9.99
Fe2O3	3.27	3.25	3.32	3.77	3.82	4.13	3.68	4.17
FeO	23.80	23.89	23.94	24.06	24.65	24.79	25.59	24.88
MnO	1.01	1.01	1.06	1.07	1.17	1.18	1.20	1.24
MgO	3.79	3.62	3.45	3.29	3.02	2.65	2.35	2.13
CaO	10.24	10.11	9.98	9.99	9.98	9.96	9.90	9.84
Na2O	3.15	3.20	3.08	3.16	3.24	3.11	3.09	3.03
K2O	1.31	1.32	1.39	1.31	1.35	1.39	1.39	1.45
Tot	97.93	97.01	96.56	96.99	96.95	97.61	96.98	95.57
Si	6.1262	6.1248	6.1878	6.1425	6.1553	6.1246	6.2102	6.1597
ivAl	1.8738	1.8752	1.8122	1.8575	1.8137	1.8754	1.7898	1.8403
Fe3+	0.0000	0.0000	0.0000	0.0000	0.0310	0.0000	0.0000	0.0000
viAl	0.0425	0.0258	0.0460	0.0098	0.0000	0.0284	0.0228	0.1136
Ti	0.3438	0.3369	0.3128	0.3267	0.3089	0.3140	0.2900	0.2133
Fe3+	0.3932	0.3956	0.4066	0.4594	0.4371	0.5026	0.4521	0.5202
Fe2+	3.1811	3.2308	3.2531	3.2623	3.3591	3.3542	3.4969	3.4520
Mg	0.9028	0.8725	0.8355	0.7949	0.7335	0.6391	0.5722	0.5266
Mn	0.1367	0.1384	0.1459	0.1469	0.1615	0.1617	0.1661	0.1742
Mg	0.0000	0.0000	0.0000	0.0000	0.0000	0.0000	0.0000	0.0000
Fe2+	0.0000	0.0000	0.0000	0.0000	0.0000	0.0000	0.0000	0.0000
Ca	1.7537	1.7520	1.7377	1.7353	1.7427	1.7269	1.7332	1.7491
Na	0.2463	0.2480	0.2623	0.2647	0.2573	0.2731	0.2668	0.2509
Na	0.7298	0.7555	0.7081	0.7286	0.7665	0.7026	0.7121	0.7238
K	0.2671	0.2724	0.2882	0.2709	0.2807	0.2870	0.2897	0.3069

	ORS110 BIOTITE		ORS112 BIOTITE					MKS 69	
	1	2	1	2	3	4	5	1	2
SiO2	33 22	33 19	32 47	32 98	33 10	32 51	32 12	33 52	33 15
TiO2	2 10	2 58	2 33	3 88	3 03	2 56	2 46	3 46	3 37
Al2O3	10 89	10 98	10 95	10 83	11 03	11 10	11 24	12 43	12 29
FeO	35 20	37 22	37 68	36 12	37 51	37 91	38 38	31 91	31 35
MnO	1 68	1 22	1 18	1 07	1 02	1 12	1 15	0 95	1 01
MgO	1 48	0 69	0 21	0 39	0 46	0 30	0 28	3 61	3 99
CaO	0 06	0 03	0 06	0 11	0 09	0 11	0 08	0 01	0 08
Na2O	0 13	0 11	0 12	0 19	0 17	0 12	0 12	0 21	0 21
K2O	7 66	8 09	7 24	7 26	7 33	7 38	7 04	8 44	7 93
Tot	92 62	94 11	92 23	92 83	93 73	93 11	92 86	94 54	93 37
Si	5 7461	5 6969	5 6954	5 6868	5 6840	5 6517	5 6086	5 5575	5 5475
Ti	0 2737	0 3326	0 3079	0 5033	0 3910	0 3352	0 3234	0 4314	0 4241
Al	2 2219	2 2228	2 2641	2 2026	2 2331	2 2751	2 3138	2 4296	2 4247
Fe2+	5 0934	5 3432	5 5279	5 2088	5 3877	5 5120	5 6044	4 4246	4 3876
Mn	0 2755	0 1780	0 1750	0 1563	0 1481	0 1651	0 1693	0 1334	0 1432
Mg	0 3824	0 1752	0 0538	0 1005	0 1165	0 0780	0 0721	0 8920	0 9951
Ca	0 0102	0 0061	0 0105	0 0201	0 0171	0 0210	0 0153	0 0014	0 0137
Na	0 0423	0 0363	0 0408	0 0629	0 0573	0 0391	0 0402	0 0675	0 0681
K	1 6898	1 7725	1 6190	1 5973	1 6050	1 6357	1 5681	1 7852	1 6924
Tot	15 7352	15 7635	15 6946	15 5387	15 6396	15 7129	15 7152	15 7227	15 6963

	ORS99 CLINOPYROXENE		ORS110 CLINOPYROXENE					ORS112 CLINOPYROXENE			ORS126 CLINOPYROXENE
	1	2	1	2	3	4	5	1	2	3	1
SiO2	49 62	49 75	50 49	50 42	49 75	50 85	50.26	52 98	52 48	52 60	49 69
TiO2	0 00	0 01	0 29	0 18	0 10	0 15	0 32	0.37	0 39	0 24	0 14
Al2O3	0 51	0 42	0 75	1 06	0 38	0 50	0 69	2 36	2 16	2 52	1 01
Cr2O3	0 00	0 00	0 00	0 00	0 00	0 00	0 00	0.00	0 00	0 00	0 00
Fe2O3	11 14	11.95	12 27	13 35	7 31	10.22	13 72	28 67	26 85	29 06	18 22
FeO	15 97	15 45	14 41	13 97	18 08	15 20	13.26	0.84	2 72	0 19	11 09
MnO	1 72	1 64	1 62	1 30	2 22	1 63	1.49	0 26	0 38	0 24	1 29
MgO	0 24	0 24	0 83	0 69	1.00	1 80	0 71	0.05	0 08	0 05	0 29
CaO	14 04	13 86	13 76	13 12	17 38	15 11	13 13	1.23	2 30	1 21	11 84
Na2O	5 01	5 22	5 50	5 85	3 27	4 64	5 94	13 14	12 28	13 17	6 78
Total	98.24	98.54	99 92	99 93	99 49	100.10	99 51	99.88	99 62	99 27	100 35
Si	2 0146	2 0123	2.0019	1 9955	2 0053	2.0098	1.9979	2.0109	2 0091	2 0063	1 9615
Al	0 0000	0 0000	0 0000	0 0000	0 0000	0 0000	0 0000	0.0000	0.0000	0 0000	0 0000
Fe3+	0.0000	0 0000	0.0000	0.0000	0.0000	0.0000	0.0000	0.0000	0.0000	0 0000	0 0000
Al	0 0244	0 0202	0 0351	0 0496	0.0180	0.0234	0.0324	0.1054	0.0974	0.1134	0 0469
Fe3+	0.3404	0.3639	0.3660	0 3977	0.2216	0.3039	0.4104	0.8188	0.7734	0 8340	0 5412
Ti	0 0000	0 0002	0 0088	0 0053	0 0029	0 0044	0 0095	0.0105	0.0111	0.0068	0 0040
Cr	0 0000	0 0000	0 0000	0 0000	0 0000	0 0000	0.0000	0.0000	0 0000	0 0000	0 0000
Mg	0 0144	0 0143	0.0493	0 0408	0.0603	0.1058	0 0418	0.0025	0.0043	0 0029	0 0171
Fe2+	0.5422	0.5228	0 4778	0 4623	0.6096	0.5025	0.4408	0.0266	0.0870	0.0061	0 3661
Mn	0.0590	0.0563	0 0543	0 0435	0.0758	0.0545	0.0501	0.0084	0.0123	0.0076	0 0247
Mg	0 0000	0 0000	0 0000	0 0000	0 0000	0 0000	0 0000	0.0000	0 0000	0 0000	0 0000
Fe2+	0 0000	0 0000	0 0000	0 0000	0 0000	0 0000	0 0000	0.0000	0 0000	0 0000	0 0000
Mn	0 0000	0 0000	0 0000	0 0000	0 0000	0 0000	0 0000	0.0000	0 0000	0 0000	0 0185
Ca	0.6110	0 6009	0 5845	0 5565	0 7507	0 6399	0.5594	0.0498	0 0942	0.0494	0 5010
Na	0 3940	0 4091	0 4224	0 4489	0.2559	0 3557	0.4576	0.9670	0 9112	0 9736	0 5191
Total	4 0000	4 0000	4 0000	4 0000	4 0000	4 0000	4 0000	4 0000	4 0000	4 0000	4 0000

	MKS49 ILLMENITE			MKS57 ILLMENITE		MKS64 ILLMENITE		MKS49 MAGNETITE		MKS57 MAGNETITE			MKS64 MAGNETITE					
	1	2	5	4	5	8	10	1	2	1	2	3	1	2	3	4	5	7
TiO2	50 26	58 22	55 59	13 10	43 11	42 29	42 46	1 89	2.33	2 53	1 28	1 53	14 64	1 65	3 38	11 89	1 12	1 27
Al2O3	0 06	0 07	0 05	0 02	0 01	0 05	0 01	0 21	0.20	0 22	0 27	0 20	0 99	0 17	0 32	0 17	0 05	0 29
Cr2O3	0 00	0 00	0 00	0 00	0 00	0 00	0 00	0 03	0 02	0 00	0 00	0 00	0 00	0 00	0 00	0 00	0 01	0 00
Fe2O3	0 00	0 00	0 00	10 53	10 04	10 81	10 52	64 70	64 94	61 63	64 32	65 92	36 23	63 86	64 67	42 38	66 23	64 74
FeO	39 37	33 24	30 08	31 27	31 26	32 77	32 69	32 33	33 06	31 64	31 14	32 35	41 19	31 88	34 89	39 15	31 73	31 37
MnO	2 30	7 68	7 18	7 39	7 42	5 19	5 42	0 29	0 47	0 75	0 29	0 21	2 10	0 26	0 49	1 39	0 11	0 19
CaO	0 00	0 00	0 00	0 01	0 00	0 00	0 01	0 04	0 02	0 04	0 00	0 00	0 02	0 04	0 01	0 01	0 02	0 03
MgO	0 01	0 01	0 00	0 02	0 02	0 02	0 00	0 00	0 00	0 00	0 02	0 00	0 00	0 00	0 01	0 01	0 00	0 01
Tot	91 99	99 21	92 89	92 32	91 84	91 11	91 11	99 49	101.03	96 81	97 30	100 22	95 16	98 06	103 76	94 98	99 27	97 89
	0 0020	0 0021	0 0017	0 0007	0 0004	0 0018	0 0004	0 0755	0 0705	0 0833	0 1014	0 0741	0 3686	0 0645	0 1119	0 0628	0 0192	0 1057
Cr	0 0000	0 0000	0 0000	0 0000	0 0000	0 0000	0 0000	0 0075	0 0049	0 0000	0 0000	0 0000	0 0000	0 0000	0 0000	0 0000	0 0030	0 0000
Fe3+	0 0000	0 0000	0 0000	0 2177	0 2087	0 2265	0 2205	15 0405	14 8595	14 7114	15 2894	15 2182	8 6467	15 0623	14 3867	10 2115	15 4546	15 0967
Ti	1 0392	1 1201	1 1438	0 8908	0 8954	0 8858	0 8895	0 4383	0 5326	0 6027	0 3046	0 3539	3 4923	0 4366	0 7507	2 8628	0 2616	0 2988
Mg	0 0003	0 0005	0 0000	0 0007	0 0007	0 0006	0 0000	0 0000	0 0000	0 0000	0 0102	0 0017	0 0000	0 0000	0 0054	0 0027	0 0019	0 0046
Fe2+	0 9052	0 7113	0 6882	0 7186	0 7220	0 7635	0 7616	8 3514	8 4077	8 3917	8 2266	8 2988	10 9237	8 3570	8 6244	10 4839	8 2287	8 2388
Mn	0 0536	0 1665	0 1663	0 1720	0 1735	0 1224	0 1278	0 0761	0 1212	0 2014	0 0780	0 0551	0 5628	0 0703	0 1238	0 3770	0 0289	0 0516
Ni	0 0001	0 0000	0 0000	0 0002	0 0000	0 0000	0 0002	0 0108	0 0037	0 0095	0 0000	0 0000	0 0058	0 0093	0 0024	0 0020	0 0040	0 0085
Tot	2 0003	2 0005	2 0000	2 0007	2 0007	2 0006	2 0000	24 0000	24 0000	24 0000	24 0102	24 0017	24 0000	24 0000	24 0054	24 0027	24 0019	24 0046

	MKS67 MAGNETITE									MKS69 MAGNETITE										MKS35 MAGNETITE		
	1	2	3	4	5	6	7	8	9	1	2	3	4	5	6	7	8	9	10	1	2	3
TiO2	2 00	2 54	8 12	1 95	15 18	1 67	1 79	2.10	1.03	1 67	15 38	10 80	1 49	7 89	7 65	2 78	13 91	14 16	21 36	3 39	14 29	10 25
Al2O3	0 07	0 24	1 08	0 38	0 66	0 64	0 32	0 26	0 45	0 12	0 66	0 19	0 10	0 17	1 51	0 59	0 26	0 29	0 15	0 28	0 30	0 09
Cr2O3	0 00	0 01	0 00	0 00	0 00	0 00	0 00	0 00	0 02	0 00	0 00	0 00	0 00	0 00	0 00	0 00	0 00	0 00	0 00	0 00	0 00	0 00
Fe2O3	65 34	64 22	50 92	65 33	36 32	65 81	65 74	65 87	65 08	65 02	35 82	46 27	62 56	51 52	37 07	60 08	40 15	39 78	29 06	62 35	39 45	46 96
FeO	32 33	32 99	35 58	32 71	39 75	32 96	32 58	33 13	31 24	32 03	41 18	38 75	30 43	36 34	31 17	31 78	40 43	39 65	44 99	33 51	41 29	37 61
MnO	0 70	0 64	2 65	0 46	4 31	0 46	0 45	0 46	0 22	0 29	3 02	1 59	0 44	1 14	0 33	0 64	2 80	3 87	6 50	0 83	2 33	1 99
CaO	0 00	0 00	0 00	0 00	0 00	0 00	0 00	0 00	0 00	0 01	0 00	0 00	0 02	0 00	0 00	0 02	0 00	0 00	0 03	0 00	0 02	0 00
MgO	0 00	0 00	0 00	0 00	0 00	0 00	0 00	0 00	0 04	0 01	0 00	0 01	0 00	0 00	0 07	0 00	0 02	0 01	0 01	0 00	0 01	0 02
Tot	100 44	100 64	98 34	100 84	96 22	101 75	100 88	101 83	98 03	99 13	96 06	97 60	95 05	97 07	77 72	95 88	97 56	97 76	102 09	100 35	97 67	96 89
Al	0 0243	0 0857	0 3917	0 1371	0 2450	0 2262	0 1162	0 0940	0 1650	0 0434	0 2444	0 0687	0 0370	0 0642	0 6916	0 2222	0 0967	0 1064	0 0530	0 1003	0 1114	0 0342
Cr	0 0000	0 0013	0 0000	0 0000	0 0000	0 0000	0 0000	0 0000	0 0038	0 0000	0 0000	0 0000	0 0000	0 0000	0 0000	0 0000	0 0000	0 0000	0 0000	0 0008	0 0000	0 0000
Fe3+	15 0554	14 7460	11 8389	14 9680	8 5844	14 9244	15 0630	14 9538	15 3439	15 1797	8 4793	10 8644	15 2397	12 2001	10 8377	14 4421	9 3969	9 2869	6 4592	14 3416	9 2162	11 1172
Ti	0 4602	0 5835	1 8857	0 4474	3 5853	0 4247	0 4104	0 4761	0 2437	0 3885	3 6382	2 5334	0 3617	1 8679	2 2353	0 6679	3 2532	3 3033	4 7439	0 7786	3 3362	2 4243
Mg	0 0012	0 0004	0 0000	0 0000	0 0018	0 0000	0 0000	0 0000	0 0189	0 0030	0 0016	0 0047	0 0000	0 0019	0 0380	0 0000	0 0099	0 0065	0 0051	0 0000	0 0037	0 0081
Fe2+	8 2779	8 4173	9 1921	8 3285	10 4388	8 3066	8 2949	8 3589	8 1653	8 3109	10 8336	10 1120	8 2360	9 5645	10 1270	8 4905	10 5146	10 2865	11 1107	8 5647	10 7207	9 8943
Mn	0 1823	0 1662	0 6936	0 1189	1 1465	0 1180	0 1155	0 1172	0 0581	0 0759	0 8046	0 4215	0 1214	0 3033	0 1083	0 1731	0 7386	1 0168	1 6259	0 2139	0 6114	0 5300
Ni	0 0000	0 0000	0 0000	0 0000	0 0000	0 0000	0 0000	0 0000	0 0003	0 0016	0 0000	0 0000	0 0043	0 0000	0 0000	0 0042	0 0000	0 0000	0 0073	0 0000	0 0041	0 0000
Tot	24 0012	24 0004	24 0000	24 0000	24 0018	24 0000	24 0000	24 0000	24 0189	24 0030	24 0016	24 0047	24 0000	24 0019	24 0380	24 0000	24 0099	24 0065	24 0051	24 0000	24 0037	24 0081

Alkali-feldspar syenites

ORS92 AMPHIBOLE	1	2	3	4
			c	r
SiO2	42.73	44.73	43.32	42.78
TiO2	1.97	1.49	1.76	1.94
Al2O3	7.36	5.96	6.92	7.04
Fe2O3	6.64	7.35	7.14	4.21
FeO	18.56	17.43	17.68	19.66
MnO	0.91	0.83	0.89	0.90
MgO	6.73	7.63	7.31	6.70
CaO	10.44	10.22	10.53	10.49
Na2O	2.04	2.04	1.94	2.07
K2O	0.89	0.58	0.78	0.85
Tot.	98.29	98.26	98.27	96.64
Si	6.5961	6.8359	6.6570	6.7089
ivAl	1.3392	1.0738	1.2537	1.2911
Fe3+	0.0647	0.0903	0.0894	0.0000
viAl	0.0000	0.0000	0.0000	0.0106
Ti	0.2286	0.1713	0.2029	0.2291
Fe3+	0.7067	0.7552	0.7365	0.4970
Fe2+	2.3965	2.2285	2.2719	2.5782
Mg	1.5489	1.7378	1.6734	1.5651
Mn	0.1194	0.1073	0.1152	0.1201
Mg	0.0000	0.0000	0.0000	0.0000
Fe2+	0.0000	0.0000	0.0000	0.0000
Ca	1.7262	1.6736	1.7338	1.7631
Na	0.2738	0.3264	0.2662	0.2369
Na	0.3380	0.2793	0.3131	0.3926
K	0.1759	0.1135	0.1537	0.1697

ORS92 BIOTITE	1	2	3	4	5
SiO2	35.66	35.44	35.35	35.40	35.59
TiO2	4.21	4.61	4.98	5.18	4.50
Al2O3	12.24	12.89	12.57	12.76	12.19
FeO	26.48	25.89	26.11	24.63	26.42
MnO	0.38	0.44	0.44	0.39	0.29
MgO	8.31	7.87	7.57	8.67	7.85
CaO	0.00	0.00	0.00	0.00	0.02
Na2O	0.18	0.21	0.18	0.19	0.12
K2O	8.75	8.60	8.28	8.60	8.44
Tot	96.19	95.94	95.47	95.81	95.40
Si	5.6078	5.5674	5.5806	5.5369	5.6304
Ti	0.4975	0.5442	0.5914	0.6090	0.5355
Al	2.2696	2.3875	2.3392	2.3523	2.2740
Fe2+	3.4831	3.4015	3.4474	3.2216	3.4954
Mn	0.0505	0.0584	0.0583	0.0518	0.0391
Mg	1.9466	1.8416	1.7805	2.0198	1.8508
Ca	0.0000	0.0000	0.0000	0.0000	0.0025
Na	0.0549	0.0637	0.0551	0.0582	0.0353
K	1.7547	1.7244	1.6670	1.7151	1.7037
Tot	15.6646	15.5888	15.5195	15.5647	15.5666

ORS92 CLINOPYROXENE	1	2	3	4	5	6	7	8	9
				c	m	r			
SiO2	51.80	52.33	52.10	53.07	52.10	51.93	52.60	52.42	52.38
TiO2	0.42	0.43	0.46	0.06	0.43	0.44	0.42	0.28	0.43
Al2O3	0.98	1.05	1.12	0.43	0.98	1.24	1.11	0.88	1.16
Cr2O3	0.00	0.00	0.00	0.00	0.00	0.00	0.00	0.00	0.00
Fe2O3	0.92	0.42	0.65	0.00	0.30	0.46	0.00	0.10	0.00
FeO	11.64	11.51	10.66	10.63	11.27	10.96	11.21	11.56	11.29
MnO	1.02	0.90	0.94	0.91	0.87	0.92	0.96	1.03	0.90
MgO	11.14	11.57	12.36	12.12	11.92	12.24	12.03	11.39	12.12
CaO	21.03	21.01	20.55	21.52	20.73	20.31	21.01	21.56	20.43
Na2O	0.62	0.65	0.59	0.40	0.59	0.59	0.55	0.52	0.56
Total	99.57	99.86	99.43	99.14	99.20	99.10	99.89	99.74	99.27
Si	1.9754	1.9820	1.9743	2.0183	1.9830	1.9749	1.9861	1.9899	1.9894
Al	0.0000	0.0000	0.0000	0.0000	0.0000	0.0000	0.0000	0.0000	0.0000
Fe3+	0.0000	0.0000	0.0000	0.0000	0.0000	0.0000	0.0000	0.0000	0.0000
Al	0.0442	0.0469	0.0500	0.0194	0.0441	0.0554	0.0494	0.0395	0.0520
Fe3+	0.0264	0.0121	0.0187	0.0000	0.0086	0.0132	0.0000	0.0029	0.0000
Ti	0.0121	0.0123	0.0130	0.0018	0.0123	0.0127	0.0118	0.0079	0.0121
Cr	0.0000	0.0000	0.0000	0.0000	0.0000	0.0000	0.0000	0.0000	0.0000
Mg	0.6328	0.6533	0.6981	0.6867	0.6764	0.6939	0.6772	0.6445	0.6862
Fe2+	0.2845	0.2754	0.2202	0.2921	0.2587	0.2247	0.2616	0.3051	0.2497
Mg	0.0000	0.0000	0.0000	0.0000	0.0000	0.0000	0.0000	0.0000	0.0000
Fe2+	0.0867	0.0891	0.1176	0.0458	0.1001	0.1240	0.0924	0.0618	0.1089
Mn	0.0328	0.0287	0.0302	0.0293	0.0282	0.0297	0.0308	0.0330	0.0291
Ca	0.8593	0.8526	0.8346	0.8770	0.8455	0.8276	0.8501	0.8772	0.8313
Na	0.0457	0.0476	0.0433	0.0296	0.0432	0.0438	0.0406	0.0381	0.0414
Total	4.0000	4.0000	4.0000	4.0000	4.0000	4.0000	4.0000	4.0000	4.0000

Alkali-granites

HIGH Si ALKALI-GRANITES

MKG44 CLINOPYROXENE

	1	2	3	4	5	6	7	8	9	10	11	12	13	14	15
SiO2	52.67	52.33	52.01	52.50	52.25	52.09	52.42	52.25	51.22	51.38	52.20	52.25	51.80	52.09	52.40
TiO2	0.84	0.84	0.67	0.74	0.53	0.51	0.56	1.15	0.52	0.38	0.39	1.19	0.30	0.52	1.13
Al2O3	0.22	0.24	0.22	0.23	0.42	0.31	0.19	0.23	0.19	0.21	0.24	0.21	0.29	0.24	0.21
Cr2O3	0.05	0.06	0.05	0.06	0.05	0.04	0.04	0.06	0.01	0.00	0.01	0.01	0.01	0.00	0.00
Fe2O3	24.50	22.00	20.50	21.34	20.26	19.91	22.69	22.78	14.59	13.82	19.75	21.02	15.90	19.58	22.22
FeO	3.87	6.15	7.08	6.65	6.65	7.01	5.75	5.56	11.75	12.32	7.26	6.40	9.07	7.21	5.52
MnO	1.30	1.27	1.35	1.26	1.40	1.34	1.45	1.08	1.19	1.10	1.38	1.22	1.29	1.60	1.30
MgO	0.79	0.67	0.86	0.74	1.11	1.11	0.63	0.66	1.50	1.77	1.86	1.22	2.79	1.73	1.05
CaO	4.57	5.81	6.80	5.91	7.60	7.38	5.53	5.42	12.77	13.34	9.93	7.38	12.59	10.26	6.53
Na2O	11.06	10.19	9.51	10.06	9.31	9.26	10.30	10.51	6.41	6.06	8.21	9.55	6.63	8.13	10.05
Total	99.87	99.56	99.05	99.48	99.58	98.97	99.55	99.70	100.14	100.38	101.23	100.44	100.67	101.34	100.41
Si	2.0278	2.0312	2.0334	2.0390	2.0286	2.0352	2.0350	2.0231	2.0086	2.0103	2.0034	2.0126	2.0015	1.9995	2.0157
Al	0.0000	0.0000	0.0000	0.0000	0.0000	0.0000	0.0000	0.0000	0.0000	0.0000	0.0000	0.0000	0.0000	0.0000	0.0000
Fe3+	0.0000	0.0000	0.0000	0.0000	0.0000	0.0000	0.0000	0.0000	0.0000	0.0000	0.0000	0.0000	0.0000	0.0000	0.0000
Al	0.0100	0.0110	0.0101	0.0105	0.0192	0.0144	0.0087	0.0103	0.0088	0.0097	0.0109	0.0095	0.0132	0.0109	0.0094
Fe3+	0.7100	0.6426	0.6031	0.6238	0.5919	0.5854	0.6628	0.6637	0.4304	0.4070	0.5706	0.6092	0.4625	0.5651	0.6434
Ti	0.0243	0.0245	0.0196	0.0216	0.0155	0.0150	0.0163	0.0335	0.0153	0.0112	0.0113	0.0345	0.0088	0.0150	0.0327
Cr	0.0015	0.0018	0.0015	0.0018	0.0015	0.0013	0.0012	0.0018	0.0003	0.0000	0.0002	0.0003	0.0003	0.0000	0.0000
Mg	0.0453	0.0388	0.0501	0.0428	0.0642	0.0646	0.0364	0.0381	0.0878	0.1032	0.1064	0.0700	0.1604	0.0990	0.0602
Fe2+	0.1246	0.1998	0.2317	0.2159	0.2160	0.2292	0.1866	0.1801	0.3852	0.4031	0.2331	0.2061	0.2931	0.2313	0.1776
Mn	0.0424	0.0418	0.0447	0.0415	0.0460	0.0443	0.0477	0.0354	0.0395	0.0365	0.0449	0.0398	0.0422	0.0520	0.0424
Mg	0.0000	0.0000	0.0000	0.0000	0.0000	0.0000	0.0000	0.0000	0.0000	0.0000	0.0000	0.0000	0.0000	0.0000	0.0000
Fe2+	0.0000	0.0000	0.0000	0.0000	0.0000	0.0000	0.0000	0.0000	0.0000	0.0000	0.0000	0.0000	0.0000	0.0000	0.0000
Mn	0.0000	0.0000	0.0000	0.0000	0.0000	0.0000	0.0000	0.0000	0.0000	0.0000	0.0000	0.0000	0.0000	0.0000	0.0000
Ca	0.1885	0.2416	0.2847	0.2458	0.3162	0.3090	0.2300	0.2249	0.5366	0.5593	0.4084	0.3046	0.5213	0.4220	0.2692
Na	0.8256	0.7669	0.7209	0.7573	0.7008	0.7015	0.7753	0.7890	0.4874	0.4597	0.6110	0.7133	0.4967	0.6051	0.7495
Total	4.0000	4.0000	4.0000	4.0000	4.0000	4.0000	4.0000	4.0000	4.0000	4.0000	4.0000	4.0000	4.0000	4.0000	4.0000

MKG23 CLINOPYROXENE

	1	2	3	4	5	6	7	8
SiO2	52.13	51.24	50.69	52.43	52.43	52.26	52.56	51.53
TiO2	2.19	0.97	1.03	1.79	1.55	1.13	1.06	1.08
Al2O3	0.31	0.21	0.23	0.48	0.53	0.24	0.33	0.20
Cr2O3	0.00	0.00	0.07	0.07	0.06	0.00	0.00	0.01
Fe2O3	30.37	22.02	29.69	27.32	28.66	28.56	30.64	22.64
FeO	0.00	7.65	0.00	2.08	1.19	0.51	0.51	6.75
MnO	0.51	0.58	0.70	0.74	0.56	0.96	0.51	0.75
MgO	0.10	0.08	0.11	0.41	0.35	0.08	0.09	0.08
CaO	1.32	6.09	6.56	0.43	0.38	1.50	1.81	6.07
Na2O	13.42	9.91	12.38	12.98	13.22	13.32	13.00	10.17
Total	100.35	98.75	101.46	98.73	98.84	100.56	100.51	99.27
Si	1.9856	2.0185	1.9142	2.0251	2.0204	1.9874	2.0032	2.0160
Al	0.0000	0.0000	0.0000	0.0000	0.0000	0.0000	0.0000	0.0000
Fe3+	0.0000	0.0000	0.0000	0.0000	0.0000	0.0000	0.0000	0.0000
Al	0.0138	0.0098	0.0101	0.0218	0.0240	0.0108	0.0148	0.0092
Fe3+	0.8806	0.6528	1.0072	0.7940	0.8313	0.8175	0.8789	0.6665
Ti	0.0627	0.0287	0.0293	0.0520	0.0449	0.0895	0.0304	0.0317
Cr	0.0000	0.0000	0.0021	0.0021	0.0018	0.0001	0.0000	0.0002
Mg	0.0058	0.0048	0.0000	0.0236	0.0203	0.0044	0.0053	0.0047
Fe2+	0.0000	0.2519	0.0000	0.0672	0.0354	0.0161	0.0162	0.2208
Mn	0.0165	0.0194	0.0000	0.0243	0.0182	0.0309	0.0164	0.0249
Mg	0.0000	0.0000	0.0548	0.0000	0.0000	0.0000	0.0000	0.0000
Fe2+	0.0000	0.0000	0.0000	0.0000	0.0000	0.0000	0.0000	0.0000
Mn	0.0000	0.0000	0.0224	0.0000	0.0000	0.0000	0.0000	0.0000
Ca	0.0539	0.2571	0.2654	0.0178	0.0159	0.0611	0.0739	0.2545
Na	0.9911	0.7571	0.9065	0.9721	0.9878	0.9822	0.9609	0.7715
Total	4.0100	4.0000	4.1633	4.0000	4.0000	4.0000	4.0000	4.0000

MKG32 CLINOPYROXENE

	1	2	3	4	5	6	7	8
SiO2	53.48	53.31	52.32	52.92	52.74	52.94	52.99	53.42
TiO2	1.16	1.23	1.65	1.43	1.51	0.92	1.01	0.59
Al2O3	0.26	0.26	0.23	0.23	0.24	0.25	0.25	0.27
Cr2O3	0.00	0.00	0.00	0.00	0.00	0.00	0.00	0.00
Fe2O3	31.52	28.27	24.12	25.39	25.69	27.54	28.51	32.38
FeO	0.10	2.71	5.81	5.38	4.80	4.09	2.90	0.00
MnO	0.32	0.40	0.53	0.51	0.50	0.41	0.36	0.86
MgO	0.07	0.08	0.04	0.05	0.06	0.08	0.08	0.05
CaO	1.34	2.58	4.95	4.61	4.46	3.87	3.20	0.73
Na2O	13.53	12.57	11.06	11.36	11.49	11.76	12.24	13.87
Total	101.77	101.42	100.70	101.88	101.50	101.86	101.55	102.17
Si	2.0087	2.0177	2.0105	2.0094	2.0075	2.0075	2.0088	1.9965
Al	0.0000	0.0000	0.0000	0.0000	0.0000	0.0000	0.0000	0.0000
Fe3+	0.0000	0.0000	0.0000	0.0000	0.0000	0.0000	0.0000	0.0000
Al	0.0115	0.0116	0.0104	0.0103	0.0108	0.0112	0.0112	0.0118
Fe3+	0.8909	0.8054	0.6975	0.7256	0.7358	0.7858	0.8134	0.9671
Ti	0.0328	0.0350	0.0476	0.0408	0.0432	0.0264	0.0288	0.0166
Cr	0.0000	0.0000	0.0000	0.0000	0.0000	0.0000	0.0000	0.0000
Mg	0.0038	0.0045	0.0022	0.0025	0.0036	0.0043	0.0046	0.0028
Fe2+	0.0030	0.0857	0.1866	0.1708	0.1529	0.1298	0.0921	0.0000
Mn	0.0101	0.0130	0.0173	0.0165	0.0162	0.0132	0.0116	0.0017
Mg	0.0000	0.0000	0.0000	0.0000	0.0000	0.0000	0.0000	0.0000
Fe2+	0.0000	0.0000	0.0000	0.0000	0.0000	0.0000	0.0000	0.0000
Mn	0.0000	0.0000	0.0000	0.0000	0.0000	0.0000	0.0000	0.0254
Ca	0.0538	0.1046	0.2038	0.1876	0.1819	0.1572	0.1300	0.0292
Na	0.9853	0.9225	0.8241	0.8364	0.8480	0.8647	0.8997	1.0051
Total	4.0000	4.0000	4.0000	4.0000	4.0000	4.0000	4.0000	4.0563

MKG25 CLINOPYROXENE

	1	2	3	4	5	6
SiO2	52.42	53.19	53.29	53.02	52.22	52.62
TiO2	1.72	1.31	1.64	1.14	1.51	0.99
Al2O3	0.25	0.27	0.28	0.27	0.23	0.26
Cr2O3	0.00	0.00	0.00	0.00	0.00	0.00
Fe2O3	31.02	31.21	30.81	28.65	30.87	29.39
FeO	0.00	0.00	0.00	0.70	0.00	0.00
MnO	0.52	0.55	0.57	0.74	0.43	0.80
MgO	0.42	0.41	0.40	1.15	0.34	1.29
CaO	1.99	1.57	1.06	2.71	2.28	3.50
Na2O	13.22	13.42	13.67	12.39	12.99	12.22
Total	101.56	101.93	101.72	100.77	100.86	101.06
Si	1.9747	1.9928	1.9966	2.0082	1.9827	1.9890
Al	0.0000	0.0000	0.0000	0.0000	0.0000	0.0000
Fe3+	0.0000	0.0000	0.0000	0.0000	0.0000	0.0000
Al	0.0111	0.0119	0.0122	0.0121	0.0102	0.0115
Fe3+	0.9076	0.9036	0.8955	0.8166	0.8947	0.8496
Ti	0.0487	0.0369	0.0462	0.0325	0.0431	0.0281
Cr	0.0000	0.0000	0.0001	0.0000	0.0000	0.0000
Mg	0.0236	0.0229	0.0223	0.0649	0.0192	0.0726
Fe2+	0.0000	0.0000	0.0000	0.0222	0.0000	0.0000
Mn	0.0090	0.0175	0.0181	0.0237	0.0138	0.0257
Mg	0.0000	0.0000	0.0000	0.0000	0.0000	0.0000
Fe2+	0.0000	0.0000	0.0000	0.0000	0.0000	0.0000
Mn	0.0076	0.0000	0.0000	0.0000	0.0000	0.0000
Ca	0.0803	0.0630	0.0426	0.1100	0.0926	0.1418
Na	0.9656	0.9751	0.9934	0.9099	0.9563	0.8953
Total	4.0283	4.0238	4.0269	4.0000	4.0126	4.0136

LOW Si ALKALI-GRANITES

MKS43 CLINOPYROXENE

	1	2	3	4	5	6	7	8
SiO2	49.68	50.03	49.91	49.70	49.31	49.12	48.99	49.29
TiO2	0.14	0.17	0.19	0.21	0.19	0.22	0.20	0.21
Al2O3	0.17	0.18	0.17	0.16	0.23	0.17	0.27	0.17
Cr2O3	0.00	0.00	0.00	0.00	0.00	0.00	0.00	0.00
Fe2O3	5.53	5.89	5.76	5.88	5.16	6.47	7.15	5.84
FeO	20.64	20.62	21.29	20.96	20.96	20.05	19.32	20.84
MnO	1.47	1.41	1.49	1.56	1.43	1.48	1.40	1.50
MgO	1.12	1.23	1.24	1.17	1.41	1.19	1.29	1.19
CaO	14.75	15.01	15.54	15.95	16.38	15.47	14.74	15.64
Na2O	3.56	3.56	3.22	3.14	2.85	3.33	3.63	3.15
Total	97.06	98.10	98.81	98.74	97.92	97.50	96.98	97.84
Si	2.0481	2.0407	2.0290	2.0234	2.0223	2.0210	2.0216	2.0245
Al	0.0000	0.0000	0.0000	0.0000	0.0000	0.0000	0.0000	0.0000
Fe3+	0.0000	0.0000	0.0000	0.0000	0.0000	0.0000	0.0000	0.0000
Al	0.0081	0.0086	0.0081	0.0079	0.0113	0.0083	0.0131	0.0082
Fe3+	0.1717	0.1808	0.1761	0.1802	0.1594	0.2001	0.2219	0.1806
Ti	0.0043	0.0053	0.0058	0.0065	0.0057	0.0068	0.0061	0.0065
Cr	0.0000	0.0000	0.0000	0.0000	0.0000	0.0000	0.0000	0.0000
Mg	0.0687	0.0748	0.0751	0.0710	0.0862	0.0730	0.0793	0.0728
Fe2+	0.7117	0.7034	0.7238	0.7136	0.7190	0.6902	0.6668	0.7159
Mn	0.0355	0.0271	0.0110	0.0209	0.0184	0.0215	0.0148	0.0159
Mg	0.0000	0.0000	0.0000	0.0000	0.0000	0.0000	0.0000	0.0000
Fe2+	0.0000	0.0000	0.0000	0.0000	0.0000	0.0000	0.0000	0.0000
Mn	0.0158	0.0217	0.0403	0.0329	0.0312	0.0301	0.0361	0.0363
Ca	0.6516	0.6560	0.6769	0.6958	0.7199	0.6843	0.6516	0.6883
Na	0.2846	0.2816	0.2538	0.2479	0.2266	0.2558	0.2904	0.2509
Total	4.0000	4.0000	4.0000	4.0000	4.0000	4.0000	4.0000	4.0000

HIGH Si ALKALI-GRANITES

	MKG20 AMPHIBOLE			MKG23 AMPHIBOLE		MKG36 AMPHIBOLE	MKG38 AMPHIBOLE											
	1	2	3	1	2	1	1	2	3	4	5	6	7	8	9	10	11	12	13
SiO2	50 49	48 26	48 07	50 74	51 25	51 48	46 88	47 86	47 70	47 88	47 09	47 80	46 46	46 03	46 63	46 85	46 93	46 83	48 68
TiO2	0 22	0 40	0 38	0 62	0 82	0 33	0 77	1 56	1 61	1 54	1 78	1 58	1 11	0 87	0 50	0 79	1 26	1 39	1 22
Al2O3	1 12	0 83	0 81	0 45	0 31	0 85	1 97	1 34	1 41	1 41	2 01	1 47	2 31	2 27	2 32	2 25	1 97	1 75	1 21
Fe2O3	10 74	13 88	13 46	0 00	0 00	3 64	10 66	8 35	9 67	8 95	5 91	7 55	7 38	7 98	8 11	8 55	7 57	6 62	10 54
FeO	25 30	22 41	22 55	30 23	28 90	24 31	24 28	24 92	24 03	24 67	26 41	25 58	27 18	26 23	26 35	25 83	26 26	26 85	24 2[illegible]
MnO	1 17	2 35	2 45	1 22	1 06	2 47	1 96	2 22	2 13	2 18	2 04	2 17	1 87	1 86	1 96	2 03	2 14	2 09	1 37
MgO	0 07	0 45	0 44	0 32	0 67	1 87	0 94	1 28	1 24	1 25	1 14	1 20	0 66	0 70	0 79	0 74	1 02	1 05	0 73
CaO	2 28	3 91	4 48	1 36	1 33	0 59	5 68	4 88	4 43	4 49	5 77	5 00	6 20	5 84	6 23	5 97	6 00	5 99	3 27
Na2O	5 53	4 00	3 41	8 85	9 01	7 61	3 44	4 15	4 19	4 41	3 77	4 18	3 85	3 95	3 76	3 57	3 82	3 94	4 74
K2O	0 23	0 41	0 53	1 00	1 15	0 72	0 61	0 78	0 91	0 91	0 70	0 81	0 65	0 58	0 54	0 68	0 68	0 71	0 44
Tot	97 15	96 91	96 58	94 81	94 50	93 86	97 19	97 34	97 32	97 69	96 62	97 35	97 67	96 31	97 18	97 26	97 64	97 21	96 42
Si	7 9752	7 7084	7 7107	8 3984	8 5096	8 2948	7 5083	7 6311	7 5993	7 6121	7 5810	7 6325	7 4672	7 4872	7 5100	7 5233	7 5145	7 5427	7 7689
ivAl	0 0248	0 1561	0 1533	0 0000	0 0000	0 0000	0 3726	0 2525	0 2644	0 2645	0 3812	0 2760	0 4386	0 4360	0 4414	0 4268	0 3722	0 3323	0 2267
Fe3+	0 0000	0 1355	0 1360	0 0000	0 0000	0 0000	0 1192	0 1164	0 1363	0 1234	0 0377	0 0915	0 0941	0 0768	0 0486	0 0500	0 1133	0 1250	0 0044
viAl	0 1830	0 0000	0 0000	0 4861	0 5685	0 4564	0 0000	0 0000	0 0000	0 0000	0 0000	0 0000	0 0000	0 0000	0 0000	0 0000	0 0000	0 0000	0 0000
Ti	0 0262	0 0484	0 0462	0 0773	0 1030	0 0395	0 0924	0 1874	0 1934	0 1838	0 2150	0 1902	0 1348	0 1059	0 0604	0 0948	0 1512	0 1686	0 1465
Fe3+	1 2763	1 5333	1 4888	0 0000	0 0000	0 4409	1 1651	0 8858	1 0232	0 9468	0 6780	0 8155	0 7980	0 8999	0 9343	0 9828	0 7989	0 6775	1 2618
Fe2+	3 3415	2 9938	3 0260	4 1853	4 0130	3 2767	3 2521	3 3226	3 2017	3 2804	3 5561	3 4161	3 6533	3 5687	3 5489	3 4691	3 5165	3 6163	3 2321
Mg	0 0165	0 1072	0 1058	0 0797	0 1650	0 4489	0 2245	0 3044	0 2935	0 2951	0 2734	0 2848	0 1588	0 1687	0 1893	0 1778	0 2431	0 2526	0 1738
Mn	0 1565	0 3174	0 3331	0 1716	0 1495	0 3376	0 2659	0 2999	0 2881	0 2938	0 2775	0 2936	0 2552	0 2567	0 2671	0 2756	0 2903	0 2850	0 1858
Mg	0 0000	0 0000	0 0000	0 0000	0 0000	0 0000	0 0000	0 0000	0 0000	0 0000	0 0000	0 0000	0 0000	0 0000	0 0000	0 0000	0 0000	0 0000	0 0000
Fe2+	0 0000	0 0000	0 0000	0 0000	0 0000	0 0000	0 0000	0 0000	0 0000	0 0000	0 0000	0 0000	0 0000	0 0000	0 0000	0 0000	0 0000	0 0000	0 0000
Ca	0 3862	0 6695	0 7703	0 2419	0 2373	0 1025	0 9746	0 8333	0 7567	0 7646	0 9956	0 8562	1 0669	1 0177	1 0752	1 0265	1 0300	1 0331	0 5598
Na	1 6138	1 2384	1 0598	1 7581	1 7627	1 8975	1 0254	1 1667	1 2433	1 2354	1 0044	1 1438	0 9331	0 9823	0 9248	0 9735	0 9700	0 9669	1 4402
Na	0 0807	0 0000	0 0000	1 0831	1 1379	0 4792	0 0433	0 1169	0 0500	0 1245	0 1720	0 1500	0 2657	0 2627	0 2491	0 1382	0 2150	0 2648	0 0278
K	0 0461	0 0841	0 1076	0 2108	0 2436	0 1472	0 1240	0 1583	0 1840	0 1843	0 1433	0 1656	0 1326	0 1206	0 1106	0 1396	0 1392	0 1449	0 0887

Monzonite - granite series

MKS21 AMPHIBOLE

	1	2	3	4	5	6	7	8	9	10	11	12	13
					c	r		c	m	r			
SiO2	37 72	39 76	41 11	41 42	42 29	39 77	39 57	40 31	39 80	38 27	39 61	39 64	39 52
TiO2	3 50	3 07	2.45	2 00	1.72	1 83	2.37	2 02	2 68	4 03	2 25	2 54	2 33
Al2O3	8 13	8 58	8.26	8.05	7 44	8 84	9 33	8 99	8 83	8 63	9 01	8.78	8 57
Fe2O3	13 98	8 13	7 56	8 52	9 42	7 14	7 69	7 70	7 99	7 00	4 22	3 68	3 64
FeO	16 49	19 63	19 41	19 57	18 41	21 66	20 42	20 26	20 01	20 13	22 04	22 35	22 61
MnO	0 94	0 76	0 85	0 76	0 88	0 69	0 82	0 85	0 90	0 86	0 81	0 83	0 82
MgO	4 19	4 29	4 75	4 61	5 14	4 65	4 95	5 26	5 06	4 86	4 76	4 77	4 59
CaO	8 77	9 21	9 17	9 34	9 25	10 71	10 60	10 69	10 49	10 29	10 66	10 67	10 59
Na2O	2 11	2.17	2 30	2.18	2 07	2.29	2.25	2 20	2 11	2 01	2.20	2 17	2.22
K2O	1 07	1 14	1.05	0.99	0 94	1.24	1.23	1 24	1.17	1 15	1 24	1 24	1.22
Tot	96 90	96.74	96.91	97.43	97.57	98.84	99.23	99.52	99.04	97 23	96 80	96.66	96 11
Si	6 0317	6 3232	6.4849	6.5100	6.6039	6.2601	6.1762	6.2589	6.2130	6.1006	6 3329	6 3489	6.3771
ivAl	1 5323	1 6088	1 5151	1.4900	1.3704	1.6405	1.7168	1.6456	1.6251	1.6219	1 6671	1 6511	1 6229
Fe3+	0 4360	0 0680	0.0000	0.0000	0.0256	0.0994	0 1069	0.0955	0 1619	0 2775	0 0000	0 0000	0 0000
viAl	0 0000	0 0000	0 0204	0.0021	0 0000	0.0000	0.0000	0.0000	0 0000	0 0000	0.0304	0 0067	0 0074
Ti	0 4212	0 3666	0 2902	0.2362	0.2025	0.2166	0 2782	0 2359	0 3146	0 4831	0 2705	0 3060	0 2828
Fe3+	1 2470	0.9046	0 8979	1.0083	1.0815	0.7459	0.7959	0.8044	0.7768	0.5627	0 5082	0 4430	0.4422
Fe2+	2.2049	2.6101	2 5615	2.5720	2.4043	2.8539	2 6660	2.6308	2.6124	2.6834	2.9469	2.9941	3.0517
Mg	0.9996	1 0157	1 1159	1.0800	1.1958	1.0915	1 1514	1.2172	1.1772	1.1546	1.1342	1 1376	1.1038
Mn	0 1273	0 1029	0 1140	0 1013	0 1159	0.0920	0 1084	0 1118	0 1190	0 1161	0 1097	0,1126	0,1121
Mg	0.0000	0 0000	0.0000	0.0000	0.0000	0.0000	0 0000	0.0000	0.0000	0.0000	0 0000	0 0000	0 0000
Fe2+	0.0000	0 0000	0 0000	0.0000	0.0000	0.0000	0 0000	0.0000	0.0000	0.0000	0 0000	0 0000	0 0000
Ca	1.5033	1 5686	1 5503	1.5727	1.5478	1.8064	1.7728	1.7785	1.7546	1.7576	1 8262	1.8311	1.8310
Na	0.4967	0 4314	0.4497	0.4273	0.4522	0.1936	0.2272	0.2215	0.2454	0.2424	0.1738	0 1689	0 1690
Na	0 1582	0 2386	0.2550	0.2361	0.1752	0.5053	0.4537	0.4408	0.3933	0.3789	0 5082	0.5050	0.5256
K	0 2174	0 2317	0 2110	0 1984	0.1865	0.2490	0.2449	0 2456	0.2330	0.2339	0.2529	0 2534	0 2512

MKS29 AMPHIBOLE

	1	2	3	4	5	6	7	8	9	10
	c	m	m	r						
SiO2	42 71	42 07	42 83	41 85	43 00	42 91	42 94	43 02	44 92	43 40
TiO2	1 76	2 13	1 72	2.07	2 06	2 05	2 04	1 93	1 36	1 80
Al2O3	7 23	7 85	7 23	7 81	7 84	7 79	7 79	7 62	6 35	7 44
Fe2O3	5 37	5 73	6 02	4 99	6 84	6.14	6 91	6 88	5 97	6 34
FeO	16 68	16 43	15 98	17 06	16 40	16 73	16 49	15 93	16 52	14 64
MnO	0 48	0 51	0 49	0 51	0 57	0 60	0 60	0 63	0 58	0 58
MgO	8 40	8 15	8 69	8 06	8 38	8 18	8 30	8 37	8 87	9 48
CaO	10 56	10 37	10 48	10 47	10 64	10 54	10 62	10 42	10 76	10 63
Na2O	2.16	2 22	2 22	2 28	2 23	2 26	2 25	2 16	1 91	2 18
K2O	0 78	0 88	0 79	0 94	0 88	0 85	0 89	0 85	0 85	0 75
Tot	96 13	96 34	96 46	96 03	98 85	98 10	98 83	97 81	97 89	97 24
Si	6.6508	6.5451	6.6362	6.5481	6.5280	6.5633	6.5265	6.5826	6.8341	6.6251
ivAl	1.3278	1 4406	1 3208	1.4408	1.4032	1.4047	1 3959	1 3746	1 1390	1 3389
Fe3+	0.0215	0 0143	0.0430	0.0111	0 0688	0 0320	0 0777	0 0428	0 0270	0 0360
viAl	0.0000	0 0000	0.0000	0 0000	0 0000	0 0000	0 0000	0 0000	0 0000	0 0000
Ti	0.2059	0 2487	0.2002	0.2440	0 2352	0 2358	0 2332	0 2221	0 1556	0 2066
Fe3+	0.6079	0 6562	0 6585	0 5767	0 7132	0 6742	0 7126	0 7496	0 6568	0 6929
Fe2+	2.1730	2.1383	2 0705	2 2321	2 0824	2 1400	2 0965	2 0380	2 1016	1 8692
Mg	1.9494	1.8696	2 0061	1 8800	1.8960	1 8646	1 8803	1.9087	2 0112	2 1567
Mn	0.0638	0 0672	0,0647	0 0672	0 0733	0 0854	0 0775	0 0817	0 0747	0 0746
Mg	0.0000	0 0000	0 0000	0 0000	0.0000	0 0000	0 0000	0 0000	0 0000	0 0000
Fe2+	0.0000	0 0000	0 0000	0 0000	0 0000	0 0000	0 0000	0 0000	0 0000	0 0000
Ca	1 7620	1 7278	1.7403	1 7547	1 7308	1.7274	1 7296	1.7084	1 7541	1 7387
Na	0.2380	0 2722	0 2597	0 2453	0 2692	0.2726	0 2704	0 2916	0 2459	0 2613
Na	0.4135	0 3982	0 4076	0 4451	0 3872	0 3977	0 3926	0 3492	0 3176	0 3840
K	0.1541	0 1753	0 1571	0 1874	0 1704	0 1659	0 1724	0 1659	0 1262	0 1461

MKS36 AMPHIBOLE

	1	2	3	4	5	6	7	8	9	10	11	12	13	14	15	16
			c	m	r											
SiO2	37 84	39 50	38 91	39.62	37.91	42.01	42 47	42 43	42.51	42.46	47 61	39 60	39.66	41 84	40 14	40 04
TiO2	4 15	2 89	3 69	2.35	4 01	1.38	1 39	1 37	1.40	1.35	0 42	3 32	2.03	1 43	2 40	2 93
Al2O3	8 73	9 31	9 02	9 54	8.78	7.08	6.99	6.95	6.95	7.08	3 15	8.84	9 12	7 41	9 13	9.06
Fe2O3	7.01	1 91	5 60	4.11	6.76	6.66	6 16	7 20	6 98	6.39	6 27	7 20	7.32	7.68	6 67	4 42
FeO	21.01	24.28	21 62	22.39	21.08	22.48	22 70	21.72	21.88	22.13	18.96	21.21	21.09	21 32	21.63	23.58
MnO	0.96	0.75	0.96	0.78	0.94	0.94	0.96	1.03	1.00	1.00	0.89	0 89	0 92	0 98	0.86	0.85
MgO	4.31	4 17	4 65	4.60	4.35	4 54	4.53	4 73	4.70	4.77	7.77	4.56	4 38	4 60	4.54	4.06
CaO	10 29	10.73	10.46	10.63	10.30	10.34	10.33	10 22	10.21	10.53	10.91	10.39	10.30	10.14	10.53	10.62
Na2O	2.13	2.40	2 32	2.40	2.16	2.33	2.26	2.20	2.22	2.06	1.00	2 17	2.32	2.22	2 26	2.32
K2O	1 15	1 24	1 18	1.22	1.18	0.95	0 92	0 97	0.92	0.92	0.37	1.20	1 22	0 98	1.21	1.21
Tot	97 58	97 18	98 61	97.64	97.45	98.72	98 71	98.82	98.75	98.68	97 35	99.38	98 36	98 61	99.39	99 10
Si	6 0479	6 3205	6.1305	6.2834	6.0641	6.5978	6.6569	6.6330	6 6467	6.6430	7.3206	6.1850	6 2576	6.5567	6 2634	6 2907
ivAl	1.6450	1 6795	1 6755	1 7166	1.6557	1 3109	1 2917	1.2809	1.2802	1 3059	0 5710	1.6287	1 6961	1 3692	1.6790	1 6786
Fe3+	0.3071	0.0000	0.1940	0 0000	0.2802	0.0913	0 0514	0 0861	0.0731	0.0511	0 1084	0 1863	0.0463	0.0741	0.0576	0.0306
viAl	0.0000	0 0768	0 0000	0 0671	0 0000	0.0000	0 0000	0.0000	0.0000	0.0000	0 0000	0 0000	0 0000	0.0000	0 0000	0 0000
Ti	0 4988	0 3478	0 4609	0.2803	0.4824	0 1630	0.1639	0 1611	0 1646	0.1588	0 0486	0 3899	0 2413	0 1689	0 2820	0 3459
Fe3+	0.5361	0 2300	0 4698	0.4911	0.5337	0.6963	0 6747	0 7613	0 7461	0.7008	0 6166	0.6595	0 8233	0.8316	0.7260	0 4917
Fe2+	2 8087	3 2493	2 8493	2 9694	2 8195	2.9532	2 9758	2 8392	2 8617	2 8961	2 4384	2 7708	2 7833	2 7945	2 8228	3 0987
Mg	1 0266	0 9944	1 0919	1.0873	1.0370	1.0626	1 0582	1 1020	1.0952	1.1117	1 7805	1.0620	1 0289	1.0747	1.0555	0 9502
Mn	0 1298	0 1017	0 1281	0.1048	0.1274	0.1249	0.1275	0 1364	0 1324	0 1325	0 1159	0 1177	0 1232	0 1303	0 1138	0.1135
Mg	0 0000	0 0000	0 0000	0 0000	0.0000	0 0000	0.0000	0 0000	0.0000	0 0000	0 0000	0.0000	0 0000	0.0000	0 0000	0 0000
Fe2+	0 0000	0 0000	0 0000	0 0000	0.0000	0 0000	0.0000	0 0000	0.0000	0 0000	0 0000	0 0000	0 0000	0 0000	0 0000	0 0000
Ca	1 7619	1 8397	1.7659	1.8064	1 7654	1 7400	1 7349	1 7119	1.7105	1.7653	1 7975	1 7393	1.7410	1 7027	1.7609	1 7880
Na	0 2381	0 1603	0 2341	0 1936	0 2346	0.2600	0 2651	0 2881	0 2895	0.2347	0 2025	0.2607	0 2590	0.2973	0 2391	0 2120
Na	0 4220	0 5843	0.4747	0.5444	0.4353	0.4496	0 4218	0.3788	0.3836	0.3902	0 0956	0 3970	0 4502	0.3758	0 4452	0 4951
K	0 2345	0 2531	0.2372	0.2469	0.2367	0.1903	0 1840	0 1929	0.1839	0 1830	0 0726	0 2393	0 2452	0 1953	0.2406	0 2426

MKS46 AMPHIBOLE

	1	2	3	4	5
			c	m	r
SiO2	45 28	42 73	43 59	41 58	39 71
TiO2	1 25	1 78	1 39	2 32	3 08
Al2O3	5 36	7 08	6 47	7 52	9 77
Fe2O3	8 87	8 01	7 99	7 27	5 08
FeO	14 87	16 93	17 13	17 64	18 98
MnO	0 68	0.55	0 56	0 62	0 65
MgO	8 43	7 04	7.38	6 48	5 89
CaO	9 84	9 96	10 36	9 80	9 43
Na2O	1.70	1 88	1 77	2 05	2 89
K2O	0 50	0 81	0 63	0 87	1 43
Tot	96 77	96 77	97 27	96 16	96 91
Si	6 9427	6.6486	6 7400	6 5432	6 2521
ivAl	0 9689	1 2993	1 1790	1 3958	1 7479
Fe3+	0 0884	0.0521	0 0810	0 0610	0 0000
viAl	0 0000	0 0000	0 0000	0 0000	0 0656
Ti	0 1441	0 2082	0 1619	0 2751	0 3647
Fe3+	0 9346	0 8853	0 8493	0 8000	0 6016
Fe2+	1 9061	2 2025	2 2148	2 3224	2 4993
Mg	1 9271	1.6319	1 7006	1 5194	1 3821
Mn	0 0880	0 0721	0 0734	0 0831	0 0867
Mg	0 0000	0 0000	0 0000	0 0000	0 0000
Fe2+	0 0000	0 0000	0 0000	0 0000	0 0000
Ca	1 6161	1 6599	1 7161	1 6531	1 5909
Na	0 3839	0 3401	0 2839	0 3469	0 4091
Na	0 1209	0 2284	0 2463	0 2783	0 4731
K	0.0974	0 1614	0 1245	0 1750	0 2872

MKS52 AMPHIBOLE

	1	2	3	4	5	6	7	8	9
		c	m	m	c	m	r		
SiO2	40 06	40 15	39 98	40 07	39 99	39 27	39 14	38 46	38 11
TiO2	3 13	3 10	3 16	3 07	3 09	3 03	3 10	2 71	2 19
Al2O3	8 91	8 91	8 85	9 01	8 85	9 12	9 41	9 75	10 20
Fe2O3	5 90	7 24	6 06	6 47	5 30	2 27	2 75	3 16	3 16
FeO	18 45	17 44	18 30	18 55	19 58	22 96	23 57	24 17	24 27
MnO	0 81	0 73	0 73	0 76	0 79	0 88	0 96	1 04	0 92
MgO	6 08	6 15	6 08	5 82	5 48	4 99	4 28	3 61	3 44
CaO	9 50	9 17	9 40	9 39	9 42	10 61	10 54	10 57	10 75
Na2O	2 79	2 81	2 75	2 81	2 79	2 74	2 61	2 64	2 47
K2O	1 12	1 08	1 17	1 12	1 12	1 26	1 32	1 36	1 48
Tot	96 75	96 79	96 49	97 07	96 41	97 13	97 68	97 47	96 99
Si	6 3098	6 3031	6 3121	6 2982	6 3439	6 2723	6 2405	6 1846	6 1650
ivAl	1 6545	1 6491	1 6473	1 6696	1 6551	1 7173	1 7595	1 8154	1 8350
Fe3+	0 0357	0 0478	0 0407	0 0322	0 0010	0 0104	0 0000	0 0000	0 0000
viAl	0 0000	0 0000	0 0000	0 0000	0 0000	0 0000	0 0093	0 0330	0 1103
Ti	0 3708	0 3660	0 3752	0 3629	0 3687	0 3640	0 3717	0 3277	0 2664
Fe3+	0 6642	0 8081	0 6796	0 7337	0 6315	0 2627	0 3300	0 3823	0 3848
Fe2+	2 4300	2 2899	2 4170	2 4389	2 5981	3 0664	3 1423	3 2502	3 2830
Mg	1 4272	1 4389	1 4306	1 3633	1 2956	1 1878	1 0170	0 8651	0 8294
Mn	0 1078	0 0971	0 0976	0 1012	0 1062	0 1191	0 1297	0 1417	0 1261
Mg	0 0000	0 0000	0 0000	0 0000	0 0000	0 0000	0 0000	0 0000	0 0000
Fe2+	0 0000	0 0000	0 0000	0 0000	0 0000	0 0000	0 0000	0 0000	0 0000
Ca	1 6033	1 5425	1 5902	1 5814	1 6012	1 8158	1 8007	1 8213	1 8634
Na	0 3967	0 4575	0 4098	0 4186	0 3988	0 1842	0 1993	0 1787	0 1366
Na	0 4554	0 3979	0 4320	0 4363	0 4594	0 6644	0 6076	0 6444	0 6382
K	0 2257	0 2163	0 2357	0 2246	0 2267	0 2568	0 2685	0 2790	0 3055

MKS53 AMPHIBOLE

	1	2	3	4	5	6	7	8	9	10
					c	r				
SiO2	39 26	40 12	39 79	39 35	39 95	39 46	39 71	39 13	38 85	38 91
TiO2	2 85	2 16	3 13	3 10	3 06	3 11	3 15	2 96	3 00	2 94
Al2O3	8 69	8 54	8 70	8 87	8 75	9 22	9 31	9 37	9 51	9 59
Fe2O3	4 58	5 63	4 62	4 90	5 27	2 57	1 19	1 93	1 85	2 96
FeO	21 37	20 80	20 44	20 28	19 85	22 95	23 39	24 07	24 44	23 72
MnO	0 92	0 90	0 84	0 81	0 83	0 85	0 83	0 89	0 90	0 92
MgO	4 53	4 73	5 28	5 17	5 47	4 98	5 03	4 26	4 01	4 00
CaO	9 69	9 60	9 64	9 61	9 58	10 63	10 62	10 83	10 76	10 59
Na2O	2 55	2 52	2 68	2 67	2 69	2 71	2 74	2 38	2 53	2 49
K2O	1 29	1 38	1 24	1 26	1 26	1 27	1 26	1 35	1 30	1 31
Tot	95 74	96 38	96 35	96 02	96 71	97 75	97 23	97 17	97 15	97 43
Si	6 3397	6 4184	6 3433	6 3015	6 3345	6 2607	6 3178	6 2732	6 2441	6 2271
ivAl	1 6544	1 5816	1 6351	1 6746	1 6357	1 7246	1 6822	1 7268	1 7559	1 7729
Fe3+	0 0059	0 0000	0 0216	0 0238	0 0298	0 0147	0 0000	0 0000	0 0000	0 0000
viAl	0 0000	0 0291	0 0000	0 0000	0 0000	0 0000	0 0640	0 0441	0 0461	0 0365
Ti	0 3461	0 2599	0 3753	0 3734	0 3649	0 3711	0 3769	0 3566	0 3626	0 3539
Fe3+	0 5512	0 6781	0 5322	0 5673	0 5985	0 2920	0 1426	0 2327	0 2235	0 3564
Fe2+	2 8866	2 7832	2 7246	2 7156	2 6325	3 0451	3 1120	3 2279	3 2847	3 1744
Mg	1 0902	1 1277	1 2545	1 2339	1 2926	1 1775	1 1927	1 0178	0 9605	0 9540
Mn	0 1258	0 1220	0 1134	0 1099	0 1115	0 1142	0 1119	0 1209	0 1225	0 1247
Mg	0 0000	0 0000	0 0000	0 0000	0 0000	0 0000	0 0000	0 0000	0 0000	0 0000
Fe2+	0 0000	0 0000	0 0000	0 0000	0 0000	0 0000	0 0000	0 0000	0 0000	0 0000
Ca	1 6766	1 6456	1 6467	1 6490	1 6276	1 8072	1 8104	1 8604	1 8530	1 8160
Na	0 3234	0 3544	0 3533	0 3510	0 3724	0 1928	0 1896	0 1396	0 1470	0 1840
Na	0 4750	0 4273	0 4751	0 4780	0 4547	0 6408	0 6557	0 6002	0 6415	0 5887
K	0 2651	0 2817	0 2522	0 2574	0 2549	0 2571	0 2558	0 2761	0 2666	0 2675

MKS54 AMPHIBOLE

	1	2	3	4	5	6	7	8	9	10	11	12	13	14	15
SiO2	39 68	39 84	40 12	39 38	39 48	39 05	39 22	39 24	38 67	37 76	39 89	39 52	38 43	38 54	37 85
TiO2	3 20	3 25	3 15	3 10	3 04	2 98	2 90	2 88	2 85	1 51	3 08	3 20	2 77	2 36	1 99
Al2O3	9 02	9 30	9 02	8 84	9 13	9 79	9 91	9 92	10 10	10 85	9 08	9 17	9 48	10 02	10 56
Fe2O3	4 09	4 38	4 88	3 99	4 38	2 76	2 79	2 20	3 60	6 14	0 91	1 15	2 38	2 82	3 88
FeO	20 47	20 47	20 44	20 84	21 95	23 91	24 38	24 98	24 28	23 03	23 23	23 53	24 50	24 70	23 97
MnO	0 64	0 59	0 63	0 59	0 70	0 73	0 79	0 71	0 65	0 79	0 47	0 46	0 50	0 61	0 59
MgO	5 75	5 76	5 70	5 35	4 58	4 26	4 01	3 82	3 71	3 14	5 75	5 56	4 07	3 65	3 53
CaO	9 68	9 59	9 63	9 51	9 45	10 33	10 42	10 37	10 29	10 05	10 62	10 80	10 40	10 33	10 33
Na2O	3 07	3 19	3 10	2 98	3 06	3 04	3 01	3 02	2 92	2 94	3 05	2 97	2 99	2 92	2 91
K2O	1 27	1 36	1 28	1 31	1 38	1 35	1 36	1 43	1 50	1 60	1 31	1 27	1 33	1 60	1 60
Tot	96 87	97 73	97 95	95 89	97 15	98 20	98 79	98 57	98 57	97 80	97 39	97 62	96 86	97 55	97 22
Si	6 2885	6 2591	6 2901	6 3173	6 2896	6 2006	6 2013	6 2253	6 1444	6 0668	6 3246	6 2703	6 2092	6 1964	6 1104
ivAl	1 6853	1 7225	1 6672	1 6718	1 7104	1 7994	1 7987	1 7747	1 8556	1 9332	1 6754	1 7144	1 7908	1 8036	1 8896
Fe3+	0 0263	0 0184	0 0427	0 0108	0 0000	0 0000	0 0000	0 0000	0 0000	0 0000	0 0000	0 0153	0 0000	0 0000	0 0000
viAl	0 0000	0 0000	0 0000	0 0000	0 0044	0 0333	0 0486	0 0807	0 0364	0 1219	0 0223	0 0000	0 0146	0 0955	0 1206
Ti	0 3814	0 3840	0 3714	0 3740	0 3642	0 3559	0 3448	0 3436	0 3406	0 1825	0 3674	0 3813	0 3366	0 2852	0 2415
Fe3+	0 4610	0 4999	0 5331	0 4703	0 5255	0 3298	0 3325	0 2627	0 4306	0 7422	0 1086	0 1218	0 2898	0 3411	0 4716
Fe2+	2 7136	2 6890	2 6800	2 7965	2 9240	3 1748	3 2233	3 3144	3 2265	3 0940	3 0802	3 1215	3 3100	3 3215	3 2365
Mg	1 3581	1 3486	1 3318	1 2791	1 0874	1 0081	0 9449	0 9032	0 8785	0 7519	1 3584	1 3134	0 9800	0 8737	0 8495
Mn	0 0859	0 0785	0 0837	0 0802	0 0945	0 0982	0 1058	0 0954	0 0875	0 1075	0 0631	0 0620	0 0690	0 0829	0 0803
Mg	0 0000	0 0000	0 0000	0 0000	0 0000	0 0000	0 0000	0 0000	0 0000	0 0000	0 0000	0 0000	0 0000	0 0000	0 0000
Fe2+	0 0000	0 0000	0 0000	0 0000	0 0000	0 0000	0 0000	0 0000	0 0000	0 0000	0 0000	0 0000	0 0000	0 0000	0 0000
Ca	1 6438	1 6144	1 6178	1 6347	1 6131	1 7576	1 7654	1 7628	1 7519	1 7302	1 8043	1 8365	1 8002	1 7797	1 7867
Na	0 3562	0 3856	0 3822	0 3653	0 3869	0 2424	0 2346	0 2372	0 2481	0 2698	0 1957	0 1635	0 1998	0 2203	0 2133
Na	0 5871	0 5861	0 5602	0 5616	0 5584	0 6935	0 6882	0 6918	0 6515	0 6460	0 7412	0 7514	0 7382	0 6895	0 6983
K	0 2568	0 2726	0 2560	0 2681	0 2805	0 2735	0 2743	0 2894	0 3041	0 3280	0 2642	0 2575	0 2748	0 3273	0 3294

MKS59 AMPHIBOLE

	1	2	3	4	5	6	7	8
SiO2	40 55	39 44	39 93	39 58	39 47	39 95	39 80	39 99
TiO2	2 30	2 64	2 99	3 03	3 03	3 09	3 01	3 05
Al2O3	8 23	9 02	9 16	9 21	9 21	9 34	9 17	9 08
Fe2O3	2 92	1 03	2 63	2 43	2 48	3 45	3 56	3 45
FeO	21 41	22 36	21 87	21 72	22 14	21 96	21 84	22 00
MnO	0 66	0 67	0 67	0 66	0 68	0 62	0 71	0 68
MgO	6 15	5 57	5 69	5 62	5 52	5 56	5 59	5 54
CaO	10 71	10 69	10 70	10 59	10 75	10 80	10 84	10 77
Na2O	2 63	2 60	2 56	2 55	2 56	2 53	2 56	2 52
K2O	1 06	1 17	1 24	1 23	1 26	1 23	1 18	1 23
Tot	96 62	95 19	97 44	96 62	97 10	98 52	98 27	98 31
Si	6 4434	6 3766	6 3075	6 3019	6 2736	6 2533	6 2521	6 2775
ivAl	1 5417	1 6234	1 6925	1 6981	1 7255	1 7236	1 6982	1 6804
Fe3+	0 0148	0 0000	0 0000	0 0000	0 0009	0 0231	0 0497	0 0421
viAl	0 0000	0 0959	0 0133	0 0307	0 0000	0 0000	0 0000	0 0000
Ti	0 2749	0 3210	0 3552	0 3628	0 3622	0 3638	0 3556	0 3601
Fe3+	0 3346	0 1252	0 3127	0 2912	0 2958	0 3830	0 3714	0 3659
Fe2+	2 8453	3 0240	2 8896	2 8927	2 9429	2 8745	2 8609	2 8880
Mg	1 4564	1 3421	1 3395	1 3336	1 3076	1 2970	1 3087	1 2961
Mn	0 0888	0 0918	0 0896	0 0890	0 0916	0 0818	0 0945	0 0900
Mg	0 0000	0 0000	0 0000	0 0000	0 0000	0 0000	0 0000	0 0000
Fe2+	0 0000	0 0000	0 0000	0 0000	0 0000	0 0000	0 0000	0 0000
Ca	1 8235	1 8520	1 8111	1 8067	1 8309	1 8114	1 8246	1 8115
Na	0 1765	0 1480	0 1889	0 1933	0 1691	0 1886	0 1754	0 1885
Na	0 6338	0 6670	0 5951	0 5939	0 6198	0 5792	0 6043	0 5786
K	0 2149	0 2413	0 2499	0 2499	0 2555	0 2456	0 2365	0 2463

	MKS59 AMPHIBOLE						
	9	10	11	12	13	14	15
SiO2	39 84	39 68	40 51	40 51	39 84	40 18	41 70
TiO2	2 91	2 85	2 47	2 28	2 79	2 96	2 06
Al2O3	9 14	9 19	9 08	9 06	9 58	9 62	8 10
Fe2O3	4 07	4 20	1 36	0 96	2 41	2 45	2 88
FeO	22 12	21 89	23 74	24 00	21 42	21 54	21 28
MnO	0 65	0 63	0 43	0 44	0 38	0 43	0 42
MgO	5 34	5 33	5 32	5 40	6 12	6 05	6 51
CaO	10 78	10 75	11 09	11 21	10 92	10 79	10 79
Na2O	2 59	2 54	2 46	2 53	2 53	2 56	2 49
K2O	1 16	1 16	1 19	1 22	1 16	1 23	0 98
Tot	98 60	98 22	97 64	97 61	97 13	97 80	97 21
Si	6 2495	6 2448	6 2222	6 4129	6 2859	6 2955	6 5449
ivAl	1 6903	1 7051	1 7778	1 5871	1 7141	1 7045	1 4551
Fe3+	0 0602	0 0501	0 0000	0 0000	0 0000	0 0000	0 0000
viAl	0 0000	0 0000	0 0475	0 1045	0 0678	0 0727	0 0447
Ti	0 3433	0 3373	0 3224	0 2713	0 3310	0 3482	0 2431
Fe3+	0 4201	0 4470	0 2697	0 1149	0 2861	0 2888	0 3404
Fe2+	2 9019	2 8816	3 2139	3 1766	2 8264	2 8223	2 7931
Mg	1 2484	1 2501	1 0750	1 2742	1 4384	1 4116	1 5222
Mn	0 0864	0 0840	0 0715	0 0585	0 0503	0 0564	0 0565
Mg	0 0000	0 0000	0 0000	0 0000	0 0000	0 0000	0 0000
Fe2+	0 0000	0 0000	0 0000	0 0000	0 0000	0 0000	0 0000
Ca	1 8119	1 8128	1 8015	1 9019	1 8461	1 8116	1 8140
Na	0 1881	0 1872	0 1985	0 0981	0 1539	0 1884	0 1860
Na	0 5997	0 5879	0 7237	0 6769	0 6186	0 5896	0 5732
K	0 2321	0 2329	0 2906	0 2464	0 2335	0 2452	0 1965

	MKS61 AMPHIBOLE				
	1	2	3	4	5
SiO2	40 11	40 81	40 26	40 29	40 38
TiO2	1 50	1 29	1 62	1 87	1 84
Al2O3	7 83	7 73	7 60	7 65	7 58
Fe2O3	8 44	9 05	9 30	8 96	8 80
FeO	24 48	24 07	23 83	23 64	23 71
MnO	0 95	1 04	0 91	0 92	0 86
MgO	1 78	1 87	1 87	2 15	2 18
CaO	9 67	9 69	9 45	9 45	9 36
Na2O	2 12	2 06	2 09	2 18	2 26
K2O	1 06	0 90	1 00	1 02	1 01
Tot	97 94	98 51	97 93	98 13	97 98
Si	6 4561	6 5087	6 4682	6 4493	6 4705
ivAl	1 4863	1 4535	1 4386	1 4438	1 4318
Fe3+	0 0576	0 0377	0 0932	0 1069	0 0978
viAl	0 0000	0 0000	0 0000	0 0000	0 0000
Ti	0 1815	0 1547	0 1953	0 2251	0 2217
Fe3+	0 9654	1 0483	1 0313	0 9731	0 9630
Fe2+	3 2964	3 2112	3 2017	3 1644	3 1768
Mg	0 4271	0 4456	0 4478	0 5123	0 5213
Mn	0 1296	0 1401	0 1240	0 1250	0 1171
Mg	0 0000	0 0000	0 0000	0 0000	0 0000
Fe2+	0 0000	0 0000	0 0000	0 0000	0 0000
Ca	1 6685	1 6563	1 6259	1 6212	1 6076
Na	0 3315	0 3437	0 3741	0 3788	0 3924
Na	0 3295	0 2931	0 2781	0 2979	0 3092
K	0 2174	0 1841	0 2060	0 2082	0 2063

	MKS63 AMPHIBOLE									
	1	2	3	4	5	6 c	7 m	8 r	9	10
SiO2	41 29	41 33	41 61	41 41	41 72	42 48	41 64	41 32	40 95	41 11
TiO2	1 57	1 59	1 49	1 44	1 16	1 35	1 51	1 45	1 39	1 29
Al2O3	7 53	7 52	7 46	7 49	7 75	7 47	7 46	7 67	7 86	7 91
Fe2O3	4 10	6 33	6 70	6 67	6 81	6 09	5 61	5 68	5 75	5 38
FeO	24 01	22 82	22 81	22 86	22 67	23 18	23 21	23 22	23 10	23 22
MnO	0 72	0 76	0 74	0 79	0 77	0 83	0 73	0 83	0 79	0 74
MgO	3 92	3 98	4 05	3 97	4 15	4 22	4 01	3 88	3 94	3 86
CaO	10 21	10 16	10 19	10 17	10 28	10 37	10 27	10 29	10 33	10 29
Na2O	2 32	2 13	2 18	2 24	2 26	2 18	2 06	2 10	2 16	2 09
K2O	1 01	1 01	0 99	0 98	1 02	0 99	1 00	1 04	1 10	1 07
Tot	96 68	97 63	98 22	98 02	98 59	99 16	97 50	97 48	97 38	96 96
Si	6 6296	6 5668	6 5718	6 5615	6 5619	6 6325	6 6176	6 5801	6 5356	6 5774
ivAl	1 3704	1 4086	1 3891	1 3992	1 4371	1 3675	1 3824	1 4199	1 4644	1 4226
Fe3+	0 0000	0 0245	0 0390	0 0393	0 0010	0 0000	0 0000	0 0000	0 0000	0 0000
viAl	0 0549	0 0000	0 0000	0 0000	0 0000	0 0075	0 0154	0 0202	0 0145	0 0694
Ti	0 1896	0 1900	0 1770	0 1716	0 1372	0 1585	0 1805	0 1737	0 1668	0 1552
Fe3+	0 4950	0 7328	0 7579	0 7556	0 8047	0 7152	0 6712	0 6807	0 6908	0 6478
Fe2+	3 2246	3 0325	3 0128	3 0295	2 9827	3 0272	3 0849	3 0926	3 0840	3 1069
Mg	0 9380	0 9424	0 9534	0 9375	0 9728	0 9819	0 9498	0 9209	0 9371	0 9204
Mn	0 0979	0 1023	0 0990	0 1058	0 1026	0 1096	0 0983	0 1120	0 1068	0 1003
Mg	0 0000	0 0000	0 0000	0 0000	0 0000	0 0000	0 0000	0 0000	0 0000	0 0000
Fe2+	0 0000	0 0000	0 0000	0 0000	0 0000	0 0000	0 0000	0 0000	0 0000	0 0000
Ca	1 7565	1 7297	1 7246	1 7267	1 7325	1 7349	1 7489	1 7559	1 7665	1 7641
Na	0 2435	0 2703	0 2754	0 2733	0 2675	0 2651	0 2511	0 2441	0 2335	0 2359
Na	0 4788	0 3859	0 3922	0 4149	0 4217	0 3948	0 3837	0 4044	0 4350	0 4124
K	0 2061	0 2047	0 1995	0 1981	0 2047	0 1980	0 2023	0 2113	0 2240	0 2184

	MKS66 AMPHIBOLE										
	1	2	3	4	5	6 c	7 m	8 r	9	10	11	12
SiO2	39 29	39 04	38 57	39 03	38 96	39 27	38 40	38 27	37 82	38 94	39 32	39 19
TiO2	3 19	3 15	2 47	2 93	2 93	3 54	2 22	2 45	1 89	3 10	3 32	2 94
Al2O3	10 07	10 44	10 95	10 29	10 97	10 12	11 16	10 87	11 70	10 36	10 12	10 50
Fe2O3	1 52	1 06	2 20	2 00	2 29	4 92	6 99	5 24	7 09	1 67	1 27	1 82
FeO	22 61	22 71	21 77	21 77	21 65	19 71	18 52	19 82	18 23	22 48	22 77	22 20
MnO	0 47	0 45	0 48	0 47	0 47	0 64	0 63	0 62	0 57	0 65	0 67	0 62
MgO	5 53	5 40	5 50	5 85	5 69	5 43	5 06	4 84	4 82	5 46	5 55	5 66
CaO	10 68	10 72	10 91	10 80	10 81	9 40	9 56	9 65	9 44	10 72	10 88	10 84
Na2O	2 81	2 78	2 72	2 80	2 77	2 93	2 71	2 71	2 68	2 93	2 77	2 85
K2O	1 42	1 39	1 37	1 39	1 47	1 48	1 52	1 55	1 58	1 44	1 44	1 48
Tot	97 60	97 15	96 94	97 33	98 01	97 44	96 77	96 01	95 82	97 75	98 10	98 10
Si	6 2098	6 1933	6 1306	6 1731	6 1161	6 1740	6 0841	6 1285	6 0487	6 1564	6 1899	6 1620
ivAl	1 7902	1 8067	1 8694	1 8269	1 8839	1 8260	1 9159	1 8715	1 9513	1 8436	1 8101	1 8380
Fe3+	0 0000	0 0000	0 0000	0 0000	0 0000	0 0000	0 0000	0 0000	0 0000	0 0000	0 0000	0 0000
viAl	0 0859	0 1460	0 1815	0 0925	0 1463	0 0498	0 1686	0 1807	0 2548	0 0873	0 0681	0 1084
Ti	0 3791	0 3758	0 2951	0 3485	0 3465	0 4186	0 2645	0 2948	0 2273	0 3685	0 3931	0 3477
Fe3+	0 1810	0 1263	0 2635	0 2378	0 2707	0 5821	0 8331	0 6313	0 8528	0 1987	0 1507	0 2158
Fe2+	2 9889	3 0137	2 8935	2 8799	2 8427	2 5920	2 4544	2 6539	2 4389	2 9719	2 9973	2 9192
Mg	1 3024	1 2774	1 3021	1 3784	1 3313	1 2723	1 1948	1 1551	1 1489	1 2865	1 3021	1 3263
Mn	0 0628	0 0609	0 0642	0 0630	0 0626	0 0852	0 0846	0 0841	0 0772	0 0870	0 0888	0 0826
Mg	0 0000	0 0000	0 0000	0 0000	0 0000	0 0000	0 0000	0 0000	0 0000	0 0000	0 0000	0 0000
Fe2+	0 0000	0 0000	0 0000	0 0000	0 0000	0 0000	0 0000	0 0000	0 0000	0 0000	0 0000	0 0000
Ca	1 8083	1 8229	1 8584	1 8303	1 8177	1 5835	1 6230	1 6558	1 6177	1 8160	1 8352	1 8263
Na	0 1917	0 1771	0 1416	0 1697	0 1823	0 4165	0 3770	0 3442	0 3823	0 1840	0 1648	0 1737
Na	0 6706	0 6782	0 6974	0 6889	0 6621	0 4767	0 4549	0 4973	0 4488	0 7142	0 6807	0 6952
K	0 2863	0 2817	0 2783	0 2806	0 2941	0 2967	0 3072	0 3167	0 3224	0 2905	0 2892	0 2969

	ORS129 AMPHIBOLE		
	1	2	3
SiO2	41 27	41 89	43 19
TiO2	1 66	1 52	1 36
Al2O3	6 18	5 95	5 31
Fe2O3	5 45	5 60	12 00
FeO	26 99	26 94	21 79
MnO	1 34	1 25	1 12
MgO	2 01	2 02	2 35
CaO	9 77	9 63	6 93
Na2O	2 77	2 62	2 73
K2O	1 01	1 09	2 01
Tot	98 45	98 50	98 78
Si	6 6559	6 7352	6 8335
ivAl	1 1753	1 1278	0 9904
Fe3+	0 1688	0 1370	0 1761
viAl	0 0000	0 0000	0 0000
Ti	0 2008	0 1832	0 1615
Fe3+	0 4923	0 5409	1 2532
Fe2+	3 6405	3 6218	2 8829
Mg	0 4835	0 4835	0 5529
Mn	0 1829	0 1706	0 1496
Mg	0 0000	0 0000	0 0000
Fe2+	0 0000	0 0000	0 0000
Ca	1 6887	1 6590	1 1739
Na	0 3113	0 3410	0 8261
Na	0 5532	0 4760	0 0098
K	0 2083	0 2226	0 4066

	ORS130 AMPHIBOLE						
	1	2	3	4	5	6	7
SiO2	41 35	41 67	42 52	42 70	43 21	43 42	43 15
TiO2	2 02	2 02	1 98	1 42	1 50	1 17	1 32
Al2O3	7 99	7 68	7 40	5 78	5 87	5 55	5 83
Fe2O3	5 88	5 99	5 76	9 47	8 86	9 72	9 80
FeO	20 77	20 82	20 76	22 66	23 67	22 79	22 92
MnO	1 14	1 03	1 00	1 34	1 40	1 33	1 51
MgO	5 15	5 20	5 60	2 95	2 75	2 84	2 73
CaO	9 96	9 89	10 15	9 30	9 48	9 24	9 40
Na2O	2 72	2 66	2 47	2 09	2 16	1 98	2 01
K2O	0 85	0 84	0 82	0 78	0 74	0 75	0 76
Tot	97 84	97 81	98 45	98 47	99 62	98 79	99 44
Si	6 4968	6 5435	6 6101	6 7540	6 7677	6 8350	6 7659
ivAl	1 4804	1 4217	1 3565	1 0776	1 0838	1 0298	1 0782
Fe3+	0 0228	0 0347	0 0333	0 1684	0 1485	0 1352	0 1560
viAl	0 0000	0 0000	0 0000	0 0000	0 0000	0 0000	0 0000
Ti	0 2392	0 2387	0 2309	0 1685	0 1762	0 1390	0 1555
Fe3+	0 6725	0 6729	0 6410	0 9593	0 8956	1 0160	1 0005
Fe2+	2 7298	2 7347	2 6999	2 9975	3 1003	3 0010	3 0048
Mg	1 2069	1 2167	1 2964	0 6955	0 6419	0 6665	0 6384
Mn	0 1516	0 1371	0 1318	0 1793	0 1859	0 1775	0 2008
Mg	0 0000	0 0000	0 0000	0 0000	0 0000	0 0000	0 0000
Fe2+	0 0000	0 0000	0 0000	0 0000	0 0000	0 0000	0 0000
Ca	1 6774	1 6633	1 6906	1 5767	1 5904	1 5589	1 5793
Na	0 3226	0 3367	0 3094	0 4233	0 4096	0 4411	0 4207
Na	0 5054	0 4738	0 4343	0 2162	0 2458	0 1623	0 1904
K	0 1696	0 1691	0 1623	0 1568	0 1481	0 1498	0 1529

ORS138 AMPHIBOLE

	1	2	3	4
SiO2	43 55	41.97	42 47	42 75
TiO2	1 37	1 52	1 41	1 48
Al2O3	5 48	6 06	6 13	6 06
Fe2O3	9 48	8 32	7 00	7 03
FeO	23 29	23 85	24 27	24 52
MnO	1 43	1 48	1 39	1 46
MgO	2 80	2 67	2 65	2 58
CaO	9 31	9 55	9 50	9 51
Na2O	2 16	2 38	2 30	2 34
K2O	0 67	0 77	0 72	0 72
Tot	99 52	98 58	97 83	98 45
Si	6 8186	6 6778	6 7801	6 7861
ivAl	1 0120	1 1374	1 1529	1 1347
Fe3+	0 1695	0 1848	0 0670	0 0791
viAl	0 0000	0 0000	0 0000	0 0000
Ti	0 1607	0 1820	0 1690	0 1768
Fe3+	0 9472	0 8109	0 7739	0 7602
Fe2+	3 0506	3 1732	3 2396	3 2561
Mg	0 6525	0 6340	0 6302	0 6106
Mn	0 1890	0 1999	0 1873	0 1962
Mg	0 0000	0 0000	0 0000	0 0000
Fe2+	0 0000	0 0000	0 0000	0 0000
Ca	1 5614	1 6287	1 6247	1 6170
Na	0 4386	0 3713	0 3753	0 3830
Na	0 2171	0 3623	0 3376	0 3370
K	0 1342	0 1563	0 1456	0 1460

	MKS21 BIOTITE					MKS27 BIOTITE		MKS29 BIOTITE						MKS38 BIOTITE		MKS39 BIOTITE				
	1	2	3	4	5	1	2	1	2 c	3 m	4 r	5 c	6 r	1	2	1	2	3	4	5
SiO2	35 55	36 19	36 19	36 22	36 91	37 28	37 47	36 32	36 31	35 26	35 72	35 38	35 44	34 33	34 28	33 42	36 06	35 46	35 10	35 49
TiO2	3 58	3 47	3 63	3 17	3 07	2 92	2 91	4 05	4 19	4 03	4 12	4 11	3 76	2 89	2 90	3 49	3 58	3 70	3 57	4 24
Al2O3	11 78	11 76	11 61	11 80	11 63	11 34	11 14	12 39	12 41	12 25	12 44	12 38	11 71	15 14	15 05	11 27	11 43	11 65	11 86	12 04
FeO	27 94	28 41	28 78	27 90	25 65	24 67	24 83	23 50	23 55	23 37	23 62	23 40	27 13	27 86	27 56	25 87	26 58	26 79	26 99	25 43
MnO	0 40	0 40	0 45	0 45	0 39	0 39	0 35	0 21	0 22	0 24	0 22	0 26	0 36	0 77	0 71	0 34	0 33	0 36	0 27	0 25
MgO	6 41	6 95	6 91	7 03	8 78	9 86	9 82	9 69	9 62	9 26	9 36	9 22	7 26	3 92	3 94	6 83	7 59	7 21	7 47	7 77
CaO	0 00	0 00	0 01	0 07	0 01	0 00	0 01	0 00	0 00	0 03	0 01	0 02	0 03	0 00	0 00	2 99	0 00	0 00	0 03	0 01
Na2O	0 14	0 15	0 14	0 12	0 10	0 15	0 17	0 11	0 13	0 14	0 14	0 16	0 14	0 15	0 11	0 15	0 08	0 09	0 05	0 09
K2O	8 65	8 67	8 65	8 76	8 66	8 52	8 64	8 98	8 76	8 69	8 77	8 71	8 79	8 78	8 92	8 08	9 08	8 95	8 37	8 85
Tot	94 46	96 01	96 37	95 52	95 20	95 13	95 35	95 26	95 20	93 26	94 40	93 63	94 65	93 84	93 46	93 44	94 72	94 22	93 70	94 18
Si	5 7409	5 7473	5 7366	5 7727	5 8207	5 8480	5 8704	5 6764	5 6728	5 6418	5 6424	5 6364	5 6963	5 5811	5 5927	5 5445	5 7740	5 7219	5 6819	5 6803
Ti	0 4345	0 4144	0 4327	0 3800	0 3641	0 3445	0 3428	0 4761	0 4928	0 4853	0 4899	0 4922	0 4550	0 3528	0 3553	0 4358	0 4314	0 4487	0 4344	0 5109
Al	2 2433	2 2018	2 1697	2 2171	2 1622	2 0979	2 0584	2 2834	2 2861	2 3102	2 3164	2 3253	2 2192	2 9020	2 8948	2 2033	2 1570	2 2154	2 2637	2 2718
Fe2+	3 7738	3 7733	3 8155	3 7188	3 3830	3 2365	3 2536	3 0717	3 0771	3 1269	3 1207	3 1183	3 6473	3 7884	3 7601	3 5801	3 5588	3 6153	3 6538	3 4038
Mn	0 0547	0 0542	0 0602	0 0613	0 0526	0 0518	0 0463	0 0279	0 0291	0 0321	0 0297	0 0352	0 0490	0 1058	0 0979	0 0477	0 0446	0 0494	0 0367	0 0338
Mg	1 5426	1 6437	1 6329	1 6686	2 0635	2 3049	2 2934	2 2581	2 2406	2 2080	2 2035	2 1887	1 7432	0 9507	0 9579	1 6874	1 8104	1 7347	1 8031	1 8536
Ca	0 0007	0 0008	0 0016	0 0116	0 0012	0 0000	0 0022	0 0000	0 0003	0 0058	0 0018	0 0029	0 0056	0 0005	0 0002	0 5312	0 0006	0 0001	0 0060	0 0016
Na	0 0426	0 0465	0 0430	0 0368	0 0301	0 0456	0 0531	0 0336	0 0397	0 0423	0 0431	0 0488	0 0443	0 0458	0 0341	0 0483	0 0241	0 0293	0 0159	0 0279
K	1 7822	1 7569	1 7502	1 7808	1 7432	1 7045	1 7279	1 7912	1 7455	1 7732	1 7672	1 7705	1 8024	1 8219	1 8571	1 7095	1 8546	1 8430	1 7285	1 8060
Tot	15 6153	15 6391	15 6424	15 6476	15 6207	15 6338	15 6481	15 6182	15 5839	15 6255	15 6147	15 6184	15 6624	15 5490	15 5502	15 7969	15 6555	15 6578	15 6240	15 5898

	MKS46 BIOTITE			MKS51 BIOTITE			MKS53 BIOTITE		MKS59 BIOTITE					MKS61 BIOTITE		MKS66 BIOTITE			
	1	2	3	1	2	3	1	2	1	2	3	4	5	1	2	1	2	3	4
SiO2	35 47	35 00	34 95	37 93	38 08	37 70	34 20	34 91	34 87	34 84	35 23	35 42	35 50	34 55	34 60	34 58	35 07	34 42	34 80
TiO2	4 21	3 98	3 97	2 51	2 85	2 39	3 42	3 49	4 25	4 19	3 98	4 19	4 01	3 37	2 96	3 66	4 09	3 82	3 72
Al2O3	12 21	12 18	12 13	13 09	13 13	13 26	12 88	12 34	12 72	12 61	12 36	12 50	11 97	11 78	12 09	13 61	13 49	13 95	13 68
FeO	26 16	26 51	26 31	17 51	17 79	17 53	30 27	30 06	26 27	26 10	25 54	25 89	25 26	33 42	34 59	26 02	26 29	26 90	26 83
MnO	0 25	0 22	0 26	0 37	0 40	0 40	0 65	0 67	0 29	0 35	0 29	0 30	0 31	0 51	0 42	0 33	0 36	0 47	0 52
MgO	7 83	7 96	7 96	14 45	13 84	14 23	5 24	5 33	7 47	7 54	7 81	7 69	8 36	2 69	2 96	7 46	7 39	7 18	7 25
CaO	0 00	0 03	0 02	0 03	0 00	0 00	0 00	0 00	0 00	0 00	0 02	0 00	0 00	0 00	0 00	0 00	0 00	0 04	0 00
Na2O	0 10	0 08	0 09	0 12	0 12	0 16	0 12	0 11	0 14	0 20	0 15	0 15	0 15	0 05	0 02	0 24	0 32	0 19	0 18
K2O	8 98	8 36	8 62	9 31	9 38	9 40	8 72	8 68	8 82	8 63	8 59	8 91	8 94	8 19	8 00	8 77	8 75	8 97	9 06
Tot	95 21	94 32	94 32	95 33	95 56	95 06	95 50	95 59	94 83	94 46	93 97	95 05	94 50	94 56	95 62	94 68	95 76	95 94	96 04
Si	5 6361	5 6128	5 6115	5 7405	5 7526	5 7274	5 5454	5 6394	5 5694	5 5807	5 6493	5 6286	5 6637	5 7297	5 6871	5 5239	5 5375	5 4556	5 5069
Ti	0 5028	0 4798	0 4797	0 2853	0 3238	0 2730	0 4171	0 4240	0 5105	0 5048	0 4800	0 5008	0 4811	0 4203	0 3655	0 4395	0 4855	0 4554	0 4427
Al	2 2877	2 3031	2 2951	2 3352	2 3389	2 3755	2 4621	2 3500	2 3951	2 3813	2 3366	2 3418	2 2514	2 3030	2 3431	2 5627	2 5102	2 6067	2 5521
Fe2+	3 4770	3 5557	3 5332	2 2166	2 2486	2 2269	4 1046	4 0610	3 5091	3 4964	3 4251	3 4408	3 3704	4 6350	4 7559	3 4764	3 4710	3 5658	3 5508
Mn	0 0334	0 0303	0 0359	0 0470	0 0514	0 0514	0 0893	0 0915	0 0392	0 0474	0 0394	0 0404	0 0419	0 0709	0 0580	0 0450	0 0480	0 0631	0 0697
Mg	1 8535	1 9018	1 9054	3 2597	3 1169	3 2229	1 2663	1 2832	1 7781	1 8000	1 8664	1 8212	1 9877	0 6648	0 7252	1 7763	1 7391	1 6961	1 7098
Ca	0 0000	0 0059	0 0036	0 0053	0 0003	0 0004	0 0000	0 0000	0 0000	0 0007	0 0031	0 0000	0 0000	0 0000	0 0000	0 0000	0 0000	0 0065	0 0000
Na	0 0320	0 0234	0 0282	0 0357	0 0351	0 0465	0 0392	0 0358	0 0448	0 0621	0 0479	0 0456	0 0473	0 0167	0 0054	0 0748	0 0992	0 0590	0 0552
K	1 8215	1 7097	1 7655	1 7981	1 8082	1 8223	1 8039	1 7889	1 7972	1 7636	1 7573	1 8068	1 8191	1 7329	1 6767	1 7879	1 7619	1 8139	1 8291
Tot	15 6440	15 6225	15 6581	15 7235	15 6758	15 7463	15 7280	15 6739	15 6436	15 6368	15 6051	15 6259	15 6626	15 5733	15 6170	15 6866	15 6524	15 7221	15 7165

	MKS29 CLINOPYROXENE		MKS66 CLINOPYROXENE																	
	2	3	1	2	3	4	6	7	8	9	1	2	5	6	7	8	9	10	11	12	13	14	1
				c	m	r						c	m	r									
SiO2	51 07	51 85	50 86	50 92	50 35	49 63	49 96	49 77	50 01	49 82	50 92	50 86	51 33	50 01	50 12	50 04	49 80	50 11	50 38	50 45	50 42	50 18	51 12
TiO2	0 32	0 33	0 19	0 19	0 18	0 22	0 21	0 19	0 19	0 20	0 09	0 37	0 07	0 30	0 33	0 28	0 36	0 13	0 37	0 35	0 36	0 37	0 35
Al2O3	2 59	2 14	0 59	0 63	0 69	0 80	0 86	0 82	0 89	0 86	0 61	0 70	0 68	0 87	0 94	1 01	1 05	0 73	1 16	1 18	1 09	1 06	2 31
Cr2O3	0 29	0 23	0 00	0 00	0 00	0 02	0 00	0 00	0 00	0 00	0 00	0 00	0 00	0 00	0 00	0 00	0 00	0 00	0 01	0 01	0 00	0 00	0 21
Fe2O3	4 40	2 40	2 81	2 82	3 21	3 46	3 25	3 64	3 41	3 14	3 84	3 39	3 20	3 63	3 85	2 94	3 47	3 97	3 62	4 34	3 72	3 54	3 04
FeO	3 95	4 29	9 20	9 09	10 55	12 78	12 18	11 73	12 09	12 48	10 01	8 56	9 26	11 58	10 83	12 15	11 37	12 16	11 22	10 74	11 53	11 78	5 18
MnO	0 39	0 31	0 64	0 59	0 63	0 71	0 73	0 81	0 73	0 70	0 61	0 55	0 64	0 71	0 74	0 73	0 77	0 78	0 74	0 71	0 67	0 68	0 34
MgO	13 91	14 22	10 37	10 70	9 35	7 68	8 42	8 39	8 39	8 13	9 17	10 46	10 05	8 36	8 38	8 23	8 40	7 47	8 69	8 78	8 45	8 41	13 42
CaO	22 87	24 31	23 31	23 20	22 86	22 39	22 78	22 53	22 59	22 45	23 71	23 46	23 51	22 96	22 92	22 84	23 17	22 70	23 28	23 10	22 98	23 13	23 46
Na2O	0 63	0 26	0 60	0 56	0 70	0 79	0 61	0 71	0 70	0 71	0 78	0 72	0 76	0 75	0 94	0 70	0 66	1 01	0 71	0 85	0 84	0 70	0 42
Total	100 42	100 34	98 58	98 69	98 52	98 49	98 99	98 60	99 00	98 49	99 74	99 07	99 48	99 17	99 05	98 92	99 06	99 07	100 17	100 50	100 06	99 85	99 85
Si	1 8916	1 9167	1 9628	1 9601	1 9582	1 9534	1 9495	1 9489	1 9504	1 9550	1 9571	1 9511	1 9648	1 9462	1 9479	1 9521	1 9394	1 9592	1 9371	1 9322	1 9424	1 9398	1 9087
Al	0 0000	0 0000	0 0000	0 0000	0 0000	0 0000	0 0000	0 0000	0 0000	0 0000	0 0000	0 0000	0 0000	0 0000	0 0000	0 0000	0 0000	0 0000	0 0000	0 0000	0 0000	0 0000	0 0000
Fe3+	0 0000	0 0000	0 0000	0 0000	0 0000	0 0000	0 0000	0 0000	0 0000	0 0000	0 0000	0 0000	0 0000	0 0000	0 0000	0 0000	0 0000	0 0000	0 0000	0 0000	0 0000	0 0000	0 0000
Al	0 1131	0 0933	0 0269	0 0286	0 0316	0 0373	0 0395	0 0379	0 0408	0 0397	0 0277	0 0317	0 0305	0 0401	0 0430	0 0463	0 0482	0 0338	0 0524	0 0533	0 0495	0 0483	0 1017
Fe3+	0 1227	0 0669	0 0817	0 0816	0 0939	0 1026	0 0955	0 1072	0 1002	0 0928	0 1112	0 0979	0 0923	0 1063	0 1126	0 0862	0 1017	0 1168	0 1047	0 1251	0 1078	0 1031	0 0854
Ti	0 0089	0 0092	0 0055	0 0055	0 0053	0 0066	0 0060	0 0055	0 0056	0 0058	0 0025	0 0108	0 0019	0 0088	0 0096	0 0083	0 0107	0 0039	0 0107	0 0101	0 0103	0 0107	0 0098
Cr	0 0084	0 0067	0 0000	0 0000	0 0000	0 0006	0 0000	0 0000	0 0000	0 0000	0 0000	0 0000	0 0000	0 0000	0 0000	0 0000	0 0000	0 0000	0 0002	0 0002	0 0000	0 0000	0 0062
Mg	0 7469	0 7835	0 5962	0 6141	0 5421	0 4505	0 4894	0 4899	0 4876	0 4756	0 5252	0 5982	0 5731	0 4848	0 4853	0 4785	0 4875	0 4352	0 4980	0 5012	0 4852	0 4845	0 7468
Fe2+	0 0000	0 0406	0 2897	0 2702	0 3271	0 4023	0 3696	0 3595	0 3658	0 3861	0 3219	0 2615	0 2963	0 3600	0 3495	0 3808	0 3520	0 3977	0 3340	0 3102	0 3472	0 3534	0 0501
Mn	0 0000	0 0000	−0 0000	−0 0000	−0 0000	0 0000	−0 0000	−0 0000	0 0000	0 0000	0 0116	0 0000	0 0059	0 0000	−0 0000	0 0000	−0 0000	0 0125	0 0000	0 0000	0 0000	0 0000	−0 0000
Mg	0 0210	0 0000	0 0000	0 0000	0 0000	0 0000	0 0000	0 0000	0 0000	0 0000	0 0000	0 0000	0 0000	0 0000	0 0000	0 0000	0 0000	0 0000	0 0000	0 0000	0 0000	0 0000	0 0000
Fe2+	0 1223	0 0919	0 0071	0 0224	0 0161	0 0183	0 0278	0 0248	0 0287	0 0237	0 0000	0 0131	0 0000	0 0168	0 0025	0 0157	0 0182	0 0000	0 0269	0 0336	0 0244	0 0275	0 1116
Mn	0 0122	0 0097	0 0211	0 0192	0 0207	0 0236	0 0242	0 0269	0 0241	0 0233	0 0083	0 0179	0 0149	0 0233	0 0244	0 0241	0 0255	0 0131	0 0241	0 0230	0 0219	0 0222	0 0108
Ca	0 9077	0 9630	0 9639	0 9588	0 9526	0 9442	0 9524	0 9456	0 9439	0 9440	0 9765	0 9644	0 9642	0 9574	0 9545	0 9548	0 9668	0 9508	0 9591	0 9480	0 9486	0 9580	0 9386
Na	0 0452	0 0186	0 0452	0 0415	0 0525	0 0605	0 0461	0 0539	0 0530	0 0541	0 0580	0 0534	0 0561	0 0563	0 0707	0 0533	0 0500	0 0769	0 0529	0 0631	0 0627	0 0525	0 0304
Total	4 0000	4 0000	4 0000	4 0000	4 0000	4 0000	4 0000	4 0000	4 0000	4 0000	4 0000	4 0000	4 0000	4 0000	4 0000	4 0000	4 0000	4 0000	4 0000	4 0000	4 0000	4 0000	4 0000

	MKS21 OPAQUES								MKS27 OPAQUES				MKS61 OPAQUES		
	1	2	3	4	5	6	7	8	1	2	3	4	1	2	3
TiO2	2.02	3.31	0.68	47.08	47.35	46.48	49.40	49.28	1.92	1.39	0.49	3.86	14.76	1.37	1.60
Al2O3	0.20	0.27	0.22	0.01	0.00	0.01	0.02	0.01	0.42	0.32	0.23	0.67	0.21	0.26	0.30
Cr2O3	0.03	0.00	0.00	0.00	0.00	0.00	0.00	0.00	0.02	0.00	0.01	0.00	0.00	0.01	0.01
Fe2O3	64.89	63.42	68.66	9.22	9.21	9.70	5.77	6.64	64.86	67.21	69.50	62.04	38.47	65.49	65.33
FeO	32.79	34.41	32.23	40.30	40.62	39.65	40.78	40.65	32.65	32.77	32.23	34.63	42.51	31.97	32.27
MnO	0.18	0.26	0.04	2.01	1.93	2.12	3.60	3.62	0.29	0.16	0.08	0.69	1.46	0.15	0.21
CaO	0.01	0.00	0.00	0.00	0.00	0.00	0.00	0.00	0.00	0.03	0.00	0.00	0.02	0.00	0.00
MgO	0.00	0.01	0.01	0.03	0.02	0.02	0.01	0.01	0.00	0.00	0.00	0.00	0.00	0.01	0.02
Tot	100.12	101.67	101.83	98.62	99.11	97.96	99.57	100.19	100.15	101.88	102.54	101.89	97.44	99.25	99.72
Al	0.0735	0.0961	0.0789	0.0003	0.0000	0.0003	0.0006	0.0003	0.1525	0.1138	0.0814	0.2372	0.0771	0.0949	0.1090
Cr	0.0073	0.0000	0.0000	0.0000	0.0000	0.0000	0.0000	0.0000	0.0044	0.0000	0.0018	0.0000	0.0011	0.0023	0.0019
Fe3+	14.9868	14.4034	15.6120	0.1785	0.1773	0.1891	0.1104	0.1262	14.9586	15.2556	15.6956	14.0196	9.0118	15.2645	15.1482
Ti	0.4662	0.7503	0.1545	0.9106	0.9113	0.9053	0.9445	0.9367	0.4423	0.3153	0.1106	0.8716	3.4550	0.3191	0.3705
Mg	0.0011	0.0045	0.0024	0.0011	0.0008	0.0008	0.0004	0.0004	0.0000	0.0000	0.0000	0.0000	0.0000	0.0025	0.0092
Fe2+	8.4170	8.6841	8.1430	0.8668	0.8695	0.8588	0.8670	0.8592	8.3670	8.2672	8.0903	8.6961	11.0654	8.2797	8.3157
Mn	0.0468	0.0662	0.0115	0.0438	0.0418	0.0465	0.0775	0.0775	0.0753	0.0409	0.0203	0.1755	0.3849	0.0394	0.0548
Ni	0.0025	0.0000	0.0000	0.0000	0.0000	0.0000	0.0000	0.0000	0.0000	0.0073	0.0000	0.0000	0.0047	0.0000	0.0000
Tot	24.0011	24.0045	24.0024	2.0011	2.0008	2.0008	2.0004	2.0004	24.0000	24.0000	24.0000	24.0000	24.0000	24.0025	24.0092

MKS21 PLAGIOCLASE

	1	2	3	4	5	6	7	8	9	10	11	12	13	14	15
						c	m	m	m	m	m	r			
SiO2	60 55	63 52	66 16	65 91	63 31	63 14	63 42	63 21	63 58	64 94	65 15	65 90	64 78	64 71	65 25
Al2O3	22 90	22 79	21 14	21 21	21 89	22 30	22 32	22 29	21 90	22 19	21 84	21 14	22 29	22 13	21 57
FeO	0 81	0 29	0 13	0 06	0 08	0 11	0 12	0 09	0 13	0 14	0 13	0 10	0 13	0 13	0 13
CaO	4 78	2 53	1 33	2 40	3 33	4 06	3 89	3 83	3 49	3 34	3 21	1 76	3 49	3 54	3 12
Na2O	8 71	9 58	10 68	10 77	9 55	9 39	9 47	9 56	9 76	9 99	10 04	10 54	9 95	9 96	10 10
K20	1 01	0 97	0 58	0 04	0 59	0 31	0 34	0 31	0 31	0 37	0 28	0 78	0 30	0 32	0 31
Total	98 75	99 67	100 02	100 40	98 75	99 31	99 56	99 28	99 17	100 97	100 65	100 22	100 94	100 79	100 49
An	21 98	12 04	6 21	10 95	15 60	18 95	18 15	17 81	16 22	15 30	14 78	8 06	15 97	16 11	14 34
Ab	72 51	82 49	90 53	88 82	81 09	79 31	79 99	80 50	82 06	82 71	83 70	87 64	82 39	82 13	83 94
Or	5 51	5 48	3 26	0 23	3 32	1 74	1 86	1 69	1 72	1 99	1 51	4 28	1 65	1 76	1 72

MKS29 PLAGIOCLASE

	1	2	3	4	5	6	7
				c	m	m	r
SiO2	65 18	65 37	59 32	58 50	59 10	59 58	65 61
Al2O3	21 87	21 89	25 79	26 26	26 10	25 99	21 02
FeO	0 09	0 13	0 14	0 10	0 11	0 08	0 36
CaO	3 26	3 13	6 54	8 56	7 94	7 98	2 19
Na2O	10 09	10 11	7 25	6 90	7 21	7 28	10 50
K20	0 39	0 37	1 03	0 24	0 31	0 22	0 23
Total	100 88	101 00	100 07	100 56	100 77	101 13	99 91
An	14 83	14 32	31 31	40 13	37 18	37 26	10 20
Ab	83 06	83 69	62 82	58 53	61 09	61 52	88 52
Or	2 11	2 00	5 87	1 34	1 73	1 22	1 28

MKS36 PLAGIOCLASE

	1	2	3	4	5	6
			c	r		
SiO2	67 69	65 62	63 97	65 91	67 22	68 07
Al2O3	19 96	21 22	21 61	21 53	20 19	19 64
FeO	0 08	0 05	0 22	0 07	0 14	0 08
CaO	0 90	2 77	2 74	1 89	1 39	0 56
Na2O	11 93	10 79	10 25	10 86	11 67	12 15
K20	0 17	0 09	0 59	0 43	0 19	0 16
Total	100 73	100 54	99 38	100 70	100 81	100 65
An	3 99	12 35	12 47	8 58	6 12	2 45
Ab	95 14	87 16	84 32	89 11	92 90	96 74
Or	0 87	0 49	3 20	2 31	0 97	0 81

MKS59 PLAGIOCLASE

	1	2	3	4	5	6	7	8	9	10	11	12	13	14	15	16
							c	r								
SiO2	63 82	64 06	68 02	63 32	61 17	62 66	61 80	64 31	64 24	64 33	64 52	65 52	65 10	65 95	66 34	65 98
Al2O3	22 27	22 38	20 17	22 61	24 01	23 42	24 17	22 30	22 40	22 20	22 32	21 74	22 04	21 52	21 31	21 58
FeO	0 11	0 11	0 16	0 13	0 22	0 13	0 16	0 14	0 14	0 19	0 16	0 16	0 10	0 11	0 10	0 10
CaO	3 44	3 81	0 97	4 00	5 65	5 08	5 93	3 77	3 96	3 67	3 92	3 28	3 46	2 76	2 50	2 80
Na2O	9 69	9 48	11 59	9 42	8 27	8 74	8 19	9 50	9 29	9 48	9 50	10 00	10 03	10 52	10 66	10 42
K20	0 46	0 57	0 24	0 54	0 44	0 36	0 33	0 34	0 46	0 47	0 46	0 39	0 40	0 38	0 29	0 31
Total	99 79	100 41	101 15	100 02	99 95	100 40	100 58	100 36	100 49	100 33	100 88	101 09	101 13	101 24	101 19	101 18
An	15 98	17 61	4 35	18 44	27 43	23 81	28 03	17 64	18 57	17 17	18 12	15 02	15 60	12 41	11 30	12 72
Ab	81 50	79 27	94 35	78 58	70 12	74 19	70 10	80 46	78 89	80 23	79 37	82 85	82 18	85 54	87 12	85 62
Or	2 53	3 12	1 30	2 99	2 46	2 00	1 86	1 91	2 55	2 61	2 51	2 13	2 13	2 05	1 58	1 66

MKS63 PLAGIOCLASE

	1	2	3	4	5	6	7	8	9
						c	m	m	r
SiO2	65 02	67 01	65 95	64 18	63 05	64 77	65 97	67 43	66 88
Al2O3	22 00	20 57	20 88	22 29	22 56	21 44	21 28	20 49	20 63
FeO	0 06	0 08	0 08	0 25	0 53	0 12	0 06	0 10	0 12
CaO	3 24	1 63	2 09	1 71	1 33	2 45	2 44	1 66	1 78
Na2O	10 06	11 11	10 66	9 87	9 55	10 49	10 72	11 08	10 88
K20	0 25	0 19	0 27	1 04	1 03	0 10	0 16	0 28	0 24
Total	100 63	100 59	99 93	99 34	98 05	99 37	100 63	101 04	100 53
An	14 90	7 42	9 63	8 22	6 70	11 37	11 08	7 53	8 18
Ab	83 73	91 55	88 89	85 83	87 12	88 08	88 06	90 97	90 50
Or	1 37	1 03	1 48	5 95	6 18	0 55	0 86	1 50	1 31

MKS66 PLAGIOCLASE

	1	2	3	4	5	6	7	8	9	10	11	12	13
								c	m	r			
SiO2	66 65	64 01	63 12	64 37	65 37	65 04	67 73	63 11	65 92	67 47	64 82	63 51	63 18
Al2O3	20 89	22 08	22 45	21 97	21 78	21 70	22 56	22 87	20 10	19 79	21 82	22 43	22 63
FeO	0 00	0 03	0 09	0 04	0 10	0 05	0 02	0 07	0 03	0 18	0 12	0 07	0 10
CaO	1 68	3 30	4 31	3 60	3 33	3 17	3 74	4 44	2 50	1 70	3 29	4 02	4 37
Na2O	10 79	9 58	8 39	9 04	9 08	8 94	5 26	7 89	9 40	9 60	8 64	8 33	8 11
K20	0 02	0 25	0 45	0 29	0 35	0 18	0 37	0 48	0 07	0 07	0 21	0 44	0 51
Total	100 03	99 26	98 81	99 31	100 01	99 08	99 67	98 85	98 02	98 80	98 91	98 81	98 89
An	7 92	15 76	21 51	17 72	16 51	16 18	27 26	23 04	12 75	8 87	17 17	20 50	22 24
Ab	91 96	82 80	75 84	80 60	81 44	82 71	69 50	73 99	86 83	90 70	81 52	76 80	74 66
Or	0 13	1 44	2 65	1 69	2 05	1 11	3 24	2 97	0 43	0 43	1 31	2 69	3 10

	MKS66 PLAGIOCLASE																				
	14	15	16	17	18	19	20	21 c	22 m	23 m	24 m	25 r	26	27	28	29	30	31	32	33	34	35	36
SiO2	63 44	70 94	66 07	64 65	63 86	64 68	63 55	62 88	64 22	64 59	64 81	64 69	63 53	63 68	64 04	64 31	64 42	63 83	64 43	63 72	64 58	67 24	67 02
Al2O3	22 42	20 91	22 28	22 03	22 10	21 94	22 17	22 68	22 37	21 84	21 99	21 92	22 24	22 38	22 35	22 04	21 93	22 06	21 77	21 74	21 34	20 16	20 72
FeO	0 09	0 04	0 09	0 10	0 11	0 11	0 09	0 08	0 11	0 05	0 11	0 11	0 05	0 11	0 10	0 11	0 10	0 10	0 01	0 05	0 04	0 06	0 14
CaO	4 01	0 29	3 49	3 49	3 66	3 53	2 85	4 99	3 68	3 30	3 34	3 21	3 87	4 06	3 54	3 34	3 42	3 34	3 11	3 11	2 15	0 72	2 07
Na2O	8 15	5 93	8 21	8 12	7 66	7 64	9 68	9 33	9 92	10 12	10 08	10 07	9 56	9 38	9 96	9 92	9 98	9 71	10 19	10 00	10 41	11 21	10 69
K20	0 53	0 63	0 33	0 22	0 58	0 47	1 21	0 34	0 23	0 26	0 20	0 24	0 41	0 55	0 27	0 39	0 38	0 33	0 32	0 34	0 60	0 36	0 08
Total	98 63	98 74	100 48	98 62	97 97	98 37	99 55	100 31	100 53	100 16	100 53	100 22	99 67	100 17	100 25	100 10	100 24	99 38	99 82	98 98	99 08	99 74	100 71
An	20 67	2 48	18 63	18 92	20 12	19 73	13 06	22 38	16 80	15 04	15 29	14 77	17 88	18 72	16 18	15 33	15 60	15 68	14 17	14 48	9 77	3 34	9 61
Ab	76 11	91 16	79 27	79 63	76 06	77 17	80 36	75 78	81 97	83 56	83 59	83 93	79 86	78 26	82 34	82 52	82 32	82 46	84 10	83 67	86 94	94 69	89 95
Or	3 23	6 37	2 10	1 45	3 82	3 10	6 58	1 83	1 23	1 40	1 12	1 30	2 26	3 01	1 47	2 14	2 09	1 86	1 73	1 84	3 29	1 97	0 44

	MKS66 PLAGIOCLASE						
	37	38	39	40	41	42	43
SiO2	64 60	64 33	63 87	63 91	66 03	65 25	63 76
Al2O3	21 72	22 18	22 18	22 34	20 92	21 69	21 71
FeO	0 10	0 06	0 07	0 02	0 02	0 04	0 10
CaO	3 02	3 40	3 60	3 58	1 35	2 99	3 68
Na2O	10 11	9 77	9 51	9 66	10 50	9 94	9 64
K20	0 25	0 32	0 30	0 30	0 65	0 33	0 34
Total	99 78	100 06	99 54	99 80	99 47	100 25	99 24
An	13 97	15 85	17 01	16 72	6 41	13 99	17 08
Ab	84 66	82 39	81 29	81 62	89 92	84 16	81 04
Or	1 37	1 76	1 71	1 66	3 66	1 84	1 88

APATITE

	ORS108				ORS102					ORS107			MKS34							
	1	2	3	4	1	2	3	4	5	1	2	3	1	2	3	4	5	6	7	8
		c	r	gm	c	r	c	m	r	gm	c	r	c	m	r		c	r	c	r
SiO2	0 56	0 26	0 32	0.26	0 27	0 39	0 21	0 23	0 35	0 32	0 22	0 43	0 60	0 73	5 24	4 12	1 25	5 55	1 62	1 68
CaO	53 48	55 20	55 13	55 12	56 01	54 93	55 28	55 61	55 28	56 92	54 93	54 64	54 34	54 65	46 72	51 08	53 95	46 12	53 04	53 52
P2O5	39 04	39 56	39 54	39.78	38 72	37 40	38 74	39 07	39 01	39 49	38 75	38 66	38 99	38 38	30 24	35 95	38 18	30 62	37 24	36 88
La2O3	0 00	0 00	0 39	0 44	0 28	0 33	0 23	0 18	0 30	0 35	0 34	0 44	0 62	0 69	3 89	0 67	1 01	3 83	1 06	1 25
Ce2O3	2 75	0 73	0 72	0 79	0 43	0 46	0 46	0 65	0 72	0 77	0 76	0 77	1 12	1 24	6 34	1 25	1 78	6 27	2 40	2 26
Nd2O3	0 00	0 25	0 24	0 27	0 16	0 16	0 32	0 16	0 19	0 29	0 30	0 28	0 26	0 33	1 34	0 37	0 49	1 49	0 70	0 56
Sm2O3	0 00	0 13	0 00	0 00	0 00	0 00	0 00	0 00	0 00	0 00	0 00	0 00	0 00	0 00	0 11	0 00	0 00	0 18	0 00	0 00
Y2O3	0 00	0 00	0 08	0 08	0 07	0 00	0 11	0 00	0 00	0 08	0 07	0 09	0 13	0 15	1 00	0 16	0 20	0 98	0 29	0 24
F	5 61	6 22	6 47	6.96	6.61	5.27	6.21	7.08	6 12	5.54	5.97	5 77	6.24	6.25	5 88	7 15	5 65	5 11	5 61	5 77
Total	101 44	102 35	102 89	103.70	102 57	98 94	101 56	102 98	101 97	103 76	101 34	101 08	102 30	102 42	100 76	100 75	102 51	100 15	101 96	102 16
O=F	2 38	2 64	2 74	2.95	2 80	2 23	2 63	3 00	2 59	2 35	2 53	2 45	2 65	2 65	2 49	3 03	2 40	2 17	2 38	2 45
Total	99 06	99 71	100.15	100.75	99.77	96.71	98.93	99.98	99 38	101 41	98 81	98 63	99 65	99 77	98 27	97 72	100 11	97 98	99 58	99 71
Si	0 1040	0 0470	0 0570	0 0470	0 0490	0.0730	0.0390	0.0410	0 0640	0 0570	0.0400	0 0790	0 1090	0 1320	1 0330	0 7630	0 2280	1 0860	0 2990	0 3100
Ca	10 5510	10 7180	10 6570	10 6210	10.9130	11.0030	10.8380	10 8370	10.7770	10 8570	10.7760	10.7250	10 5780	10 6860	9 8790	10 1310	10 5080	9 6900	10 4670	10 5720
P	6 0870	6 0700	6 0400	6.0580	5.9600	5.9190	6.0000	6.0150	6 0090	5 9520	6 0070	5 9960	5 9970	5 9300	5 0520	5 6340	5 8760	5 0850	5 8060	5 7560
La	0 0000	0 0000	0 0260	0.0290	0.0190	0.0230	0.0150	0.0120	0.0200	0 0230	0.0230	0 0300	0 0420	0.0470	0 2830	0 0460	0 0670	0 2770	0 0720	0 0850
Ce	0 1850	0 0480	0 0480	0.0520	0.0290	0.0320	0.0310	0.0430	0 0480	0 0500	0.0510	0 0520	0 0740	0.0830	0 4580	0 0850	0 1180	0 4500	0 1620	0 1530
Nd	0 0000	0 0160	0 0150	0 0170	0.0120	0 0100	0 0210	0 0100	0 0130	0 0180	0 0200	0 0180	0 0170	0 0210	0 0950	0 0250	0 0320	0 1050	0 0460	0 0370
Sm	0 0000	0 0080	0 0000	0.0000	0.0000	0.0000	0.0000	0 0000	0 0000	0 0000	0 0000	0 0000	0 0000	0.0000	0 0070	0 0000	0 0000	0 0120	0 0000	0 0000
Y	0 0000	0.0000	0.0080	0 0080	0 0070	0.0000	0.0100	0.0000	0 0000	0 0070	0.0070	0 0080	0 0130	0 0140	0 1050	0 0160	0 0190	0 1030	0 0280	0 0240
F	3 2670	3 5640	3.6890	3.9600	3.8010	3.1160	3.5950	4.0720	3.5210	3.1180	3.4590	3.3440	3 5850	3.6080	3.6710	4.1880	3 2490	3 1660	3 2690	3 3650

	ORF17	ORS133			ORF28		MKS66		
	1	1	2	3	1	2	1	2	3
		c	r	gm	c	r	gm	c	r
SiO2	2 13	0 21	0.21	0 94	0 44	0.77	0 50	0 29	0 56
CaO	52 37	56.32	56.88	55.08	54.95	54 36	56 09	55.91	55.67
P2O5	36 51	38.77	39.11	38.70	38.51	37.92	39 00	39.50	39.18
La2O3	1 54	0 11	0.15	0.89	0.50	0.69	0 51	0 33	0 49
Ce2O3	2 75	0.17	0.20	0.73	0.87	1.20	0 75	0.68	0 90
Nd2O3	0 85	0.10	0.00	0.00	0.31	0 32	0 19	0.18	0 00
Sm2O3	0 00	0 00	0.00	0.00	0.00	0 00	0 00	0 00	0 00
Y2O3	0 24	0.00	0.00	0 00	0.08	0 09	0 10	0.07	0 08
F	5 42	4.19	4.36	4.78	7.10	7.26	5.26	4.94	4 62
Total	101 81	99 87	100 91	101.10	102.76	102.61	102 40	101 90	101.50
O=F	2 30	1.78	1.85	2.03	3.01	3.08	2 23	2 09	1.96
Total	99 51	98.09	99.06	99.07	99.75	99.53	100 17	99 81	99.54
Si	0 3940	0.0380	0.0370	0.1700	0.0800	0.1420	0 0900	0 0510	0.1000
Ca	10 3860	10 9760	11.0040	10.7180	10.7650	10.7230	10 8260	10 7610	10.7540
P	5 7210	5.9700	5.9780	5.9520	5.9610	5.9110	5.9470	6 0080	5.9800
La	0 1050	0 0080	0.0100	0.0590	0 0340	0.0470	0 0340	0 0220	0 0330
Ce	0 1860	0.0110	0.0130	0.0480	0.0580	0.0810	0 0490	0.0440	0 0600
Nd	0 0560	0 0070	0.0000	0.0000	0 0200	0.0210	0 0130	0.0120	0 0000
Sm	0 0000	0.0000	0.0000	0.0000	0 0000	0.0000	0 0000	0 0000	0 0000
Y	0 0240	0 0000	0 0000	0 0000	0 0070	0.0090	0 0100	0 0070	0 0080
F	3 1750	2.4090	2.4890	2.7470	4.1070	4.2250	2 9990	2 8080	2.6340

SPHENE

	ORS108		ORS102			MKS34	ORF17	ORS133		ORF28		MKS66		
	1	2	1	2	3	1	1	1	2	1	2	1	2	3
			c	m	r			c	r			c	r	
SiO2	30.69	30.93	29.93	29.91	29.64	30.97	30.12	30.47	30.26	30.40	30.45	30.41	30.41	30.42
TiO2	36.15	36.51	35.14	34.60	35.23	33.11	31.23	36.70	36.71	32.01	31.60	34.36	32.76	35.19
Al2O3	1.06	1.39	1.28	1.46	1.42	3.02	1.60	1.17	1.17	2.22	2.54	2.20	2.73	1.98
FeO	1.74	1.46	1.24	1.42	1.26	1.63	2.44	1.49	1.54	1.77	1.99	1.24	1.53	1.35
CaO	28.12	27.94	26.53	26.52	27.05	27.70	26.74	28.15	28.16	27.31	27.37	27.27	27.55	27.57
ZrO2	0.75	0.20	0.53	0.55	0.53	0.40	1.39	0.95	0.86	1.07	1.32	0.49	1.28	0.59
Nb2O5	0.58	0.36	1.08	0.88	0.79	0.84	3.38	0.49	0.42	2.96	2.26	1.09	0.88	1.06
La2O3	0.11	0.18	0.32	0.33	0.30	0.25	0.35	0.19	0.19	0.36	0.36	0.46	0.25	0.40
Ce2O3	0.13	0.97	1.07	1.28	0.85	0.88	0.85	0.60	0.54	0.87	0.82	1.04	0.67	0.88
Pr2O3	0.00	0.00	0.18	0.16	0.15	0.00	0.00	0.00	0.00	0.12	0.00	0.00	0.00	0.00
Nd2O3	0.09	0.17	0.52	0.53	0.35	0.20	0.30	0.29	0.24	0.27	0.27	0.25	0.23	0.27
Y2O3	0.00	0.10	0.33	0.28	0.23	0.15	0.14	0.13	0.10	0.19	0.21	0.19	0.18	0.15
ThO2	0.00	0.00	0.00	0.00	0.00	0.00	0.00	0.00	0.00	0.00	0.00	0.00	0.00	0.08
F	0.42	0.74	0.00	0.00	0.00	1.63	0.69	0.42	0.44	0.75	0.97	0.68	1.03	0.82
Total	99.84	100.95	98.15	97.92	97.80	100.78	99.23	101.05	100.63	100.30	100.16	99.68	99.50	100.76
O=F	0.18	0.31	0.00	0.00	0.00	0.69	0.29	0.18	0.19	0.32	0.41	0.29	0.44	0.35
Total	100.02	101.26	98.15	97.92	97.80	101.47	99.52	101.23	100.82	100.62	100.57	99.97	99.94	101.11
Si	4.0790	4.0850	4.0810	4.1010	4.0610	4.1260	4.1110	4.0240	4.0100	4.0810	4.1050	4.0820	4.1000	4.0450
Ti	3.6130	3.6260	3.6030	3.5680	3.6310	3.3170	3.2050	3.6450	3.6580	3.2310	3.2030	3.4690	3.3220	3.5180
Al	0.1660	0.2170	0.2050	0.2360	0.2290	0.4740	0.2570	0.1820	0.1820	0.3520	0.4040	0.3470	0.4340	0.3100
Fe	0.1940	0.1620	0.1410	0.1620	0.1450	0.1820	0.2780	0.1650	0.1710	0.1980	0.2240	0.1390	0.1730	0.1500
Ca	4.0040	3.9540	3.8750	3.8960	3.9710	3.9530	3.9100	3.9850	3.9980	3.9270	3.9520	3.9220	3.9810	3.9280
Zr	0.0490	0.0130	0.0350	0.0370	0.0360	0.0260	0.0920	0.0610	0.0560	0.0700	0.0870	0.0320	0.0840	0.0390
Nb	0.0350	0.0210	0.0660	0.0540	0.0490	0.0510	0.2090	0.0290	0.0250	0.1800	0.1380	0.0660	0.0540	0.0640
La	0.0050	0.0090	0.0160	0.0170	0.0150	0.0120	0.0180	0.0090	0.0090	0.0180	0.0180	0.0230	0.0130	0.0200
Ce	0.0060	0.0470	0.0530	0.0640	0.0420	0.0430	0.0420	0.0290	0.0260	0.0430	0.0410	0.0510	0.0330	0.0430
Pr	0.0000	0.0000	0.0090	0.0080	0.0080	0.0000	0.0000	0.0000	0.0000	0.0060	0.0000	0.0000	0.0000	0.0000
Nd	0.0050	0.0080	0.0250	0.0260	0.0170	0.0090	0.0150	0.0140	0.0110	0.0130	0.0130	0.0120	0.0110	0.0130
Y	0.0000	0.0070	0.0240	0.0210	0.0170	0.0110	0.0100	0.0090	0.0070	0.0140	0.0150	0.0140	0.0130	0.0110
Th	0.0000	0.0000	0.0000	0.0000	0.0000	0.0000	0.0000	0.0000	0.0000	0.0000	0.0000	0.0000	0.0000	0.0030
F	0.1760	0.3070	0.0000	0.0000	0.0000	0.6850	0.2970	0.1750	0.1860	0.3160	0.4150	0.2900	0.4410	0.3460

OTHER ACCESSORY MINERALS

	ORS 108	ORS 99	ORS 193 REE Sphenes				MKS27 Allanite	
			1	2	3	4	1	2
	Bastnaesite?	Bastnaesite?						
SiO2	11.92	7.78	32.94	33.11	26.90	27.31	33.17	33.00
TiO2	0.08	0.00	17.70	17.83	20.39	20.62	1.78	2.04
Al2O3	0.66	0.41	--	--	--	--	12.06	11.14
FeO	0.97	1.33	6.31	6.32	5.72	5.80	14.50	13.93
MnO	--	--	0.09	0.87	1.13	1.13	--	--
CaO	3.03	4.65	4.75	4.80	4.28	4.68	11.08	10.53
ZrO2	0.13	0.00	0.89	0.81	0.98	1.04	0.00	0.13
Nb2O5	0.00	0.00	7.15	7.19	8.03	8.13	0.00	0.85
La2O3	23.80	16.03	4.38	4.96	7.51	4.59	6.85	5.78
Ce2O3	28.28	25.86	12.88	12.06	12.05	14.78	11.98	11.27
Pr2O3	1.98	3.07	1.30	1.43	2.17	1.46	1.00	1.10
Nd2O3	6.96	9.71	3.27	3.74	3.61	4.07	2.78	3.01
Y2O3	0.80	1.55	0.45	0.37	0.53	0.55	0.20	0.46
ThO2	7.97	2.59	3.54	3.56	3.05	3.02	0.79	1.05
F	5.60	11.09	--	--	--	--	0.52	0.49
Total	92.18	84.07	95.64	97.04	96.34	97.17	96.71	94.78
O=F	2.37	4.70	0.00	0.00	0.00	0.00	0.22	0.21
Total	94.55	88.77	95.64	97.04	96.34	97.17	96.93	94.99

Carbonatites

SOVITES

MKC54 CARBONATES

	1	2	3	4	5	6	7	8	9	10	11	12
FeO	0 52	0 50	0 69	0 57	0 86	0 50	0 50	0 61	0 56	0 54	0 53	0 52
MnO	0 36	0 27	0 32	0 41	0 40	0 31	0 30	0 41	0 54	0 43	0 40	0 40
MgO	0 45	0 36	0 48	0 62	0 92	0 44	0 45	0 65	0 52	0 51	0 62	0 56
CaO	51 36	52 79	50 98	52 43	50 16	51 62	51 04	52 02	54 92	52 58	52 97	52 79
CO2	41 38	42 36	41 20	42 47	41 19	41 53	41 08	42 20	44 39	42 45	42 86	42 64
Tot	93 55	95 77	92 99	95 92	92 66	93 90	92 87	95 28	100 37	95 96	96 85	96 38
%Mg	0 72	0 57	0 77	0 97	1 49	0 70	0 73	1 02	0 78	0 79	0 96	0 87
%Ca	97 47	97 88	97 13	97 07	95 91	97 63	97 63	96 93	97 11	97 27	97 19	97 30
%Fe+Mn	1 81	1 55	2 09	1 95	2 60	1 66	1 64	2 04	2 11	1 94	1 85	1 83

MKC52 CARBONATE

	1	2	3	4	5	6	7	8	9	10	11
FeO	0 65	0 54	0 02	0 33	0 22	0 29	0 28	0 30	0 02	0 23	0 25
MnO	0 44	0 41	0 05	0 23	0 20	0 21	0 25	0 23	0 01	0 30	0 28
MgO	0 74	0 56	0 03	0 22	0 19	0 19	0 27	0 21	0 13	0 23	0 22
CaO	54 36	52 53	54 22	53 05	52 78	53 14	52 78	52 77	53 90	52 76	53 33
CO2	44 18	42 47	42 67	42 26	41 92	42 26	42 09	42 01	42 51	42 03	425 33
Tot	99 72	95 98	96 97	95 76	95 08	95 80	95 40	95 52	96 55	95 32	95 99
%Mg	1 12	0 88	0 04	0 35	0 29	0 30	0 43	0 33	0 21	0 37	0 34
%Ca	96 73	97 21	99 81	98 53	98 86	98 71	98 49	98 61	99 74	98 56	98 59
%Fe+Mn	2 10	1 91	0 15	1 12	0 84	0 99	1 08	1 06	0 05	1 07	1 06

REMNANT SOVITES

MKC29 CALCITE

	1	2	3	4	5	6	7	8	9	10	11	12	13	14	15	16	17	18	19	20	21	22	23	24
FeO	0 70	3 17	0 59	0 54	0 64	0 56	0 62	0 61	1 33	0 87	1 21	1 13	1 46	1 49	1 07	1 32	1 21	0 44	0 60	0 52	0 66	0 52	0 56	0 51
MnO	0 81	1 09	0 84	0 70	0 72	0 73	0 75	0 72	0 19	0 38	0 19	0 13	0 20	0 18	0 11	0 17	0 09	0 55	0 59	0 66	0 56	0 69	0 73	0 71
MgO	1 16	17 63	1 18	1 08	1 15	1 12	1 18	1 12	0 11	0 33	0 10	0 11	0 12	0 12	0 11	0 11	0 14	0 32	0 30	0 52	0 48	0 64	0 78	0 79
CaO	52 40	29 04	51 65	52 24	53 29	52.14	51 35	51 24	53 38	52 66	53 69	53 84	53.31	52 63	53 29	52 65	52 88	53 25	53 63	52 71	52 98	51 57	51 73	51 15
CO2	43 38	44 69	42 75	42 98	43 96	42 98	42 48	42 30	42 99	42 49	43 15	43 19	43 03	42.51	42 70	42 40	42 50	42 79	43 20	42 72	42 89	41 90	42 29	41 80
Total	97 76	92 44	96 41	97 00	99 12	96 97	95 76	95 38	96 68	95 85	97 12	97 27	96 67	95.44	96 21	95 34	95 61	96 91	97 72	96 61	96 91	94 86	95 53	94 45
%Mg	1 81	30 66	1 83	1 67	1 74	1 73	1 86	1 77	0 18	0 51	0 15	0 17	0 18	0 19	0 16	0 17	0 22	0 50	0 46	0 81	0 74	1 00	1 23	1 26
%Ca	95 22	59 81	95 31	95 87	95 60	95 70	95 38	95 54	96 84	97.00	97 10	97 36	96 55	96.47	97 49	96 83	97 18	97 55	97 19	96 82	96 84	96 54	96 16	96 26
%Fe+Mn	2 97	9 54	2 86	2 46	2 65	2 57	2 76	2 69	2 99	2 49	2 75	2 47	3 27	3 34	2 35	2 99	2 59	1 96	2 35	2 37	2 42	2 46	2 61	2 48

MKC29 CALCITE

	25	26	27	28	29	30	31	32	33	34	35	36	37	38	39	40	41	42	43	44	45	46	47	48
FeO	0 70	0 54	0 65	0 64	0 72	0 64	0 66	0 58	0 57	0 76	0 68	0 75	0 66	0 84	0 76	0 65	0 73	0 70	3 42	0 62	3 74	4 21	0 73	0 36
MnO	0 68	0 62	0 66	0 68	0 75	0 69	0 71	0 75	0 73	0 69	0 80	0 79	0 73	0.80	0 77	0 62	0 71	0 71	1 09	0 70	1 11	1 09	0 67	0 71
MgO	1 24	0 77	0 99	1 02	1 18	0 95	1 10	0 98	0 74	1 28	1 16	1 26	1 15	1 31	1 42	1 01	1 15	1 25	17 43	1 16	17 69	17 31	1 19	0 05
CaO	50 82	51 69	51 54	51 88	52 01	51 28	51 03	52 04	52 13	50 61	50 73	51 66	51 32	52 23	51 84	52 11	51 86	52 80	29 28	51 99	29 38	29 04	51 04	53 27
CO2	42 12	42 16	42 38	42 68	43 05	42 14	42 13	42 78	42 56	42 05	42 03	42 90	42 43	43.47	43 22	42 82	42 88	43 72	44 81	42 93	45 38	44 98	42 27	42 57
Total	94 86	95 24	95 57	96 26	96 98	95 06	94 97	96 55	96 16	94 62	94 72	96 61	95 62	97 82	97 26	96 56	96 60	98 48	92 61	96 79	93 57	92 42	95 17	96 60
%Mg	1 95	1 21	1 56	1 58	1 83	1 50	1 74	1 52	1 15	2 02	1 83	1 95	1 80	2 01	2 20	1 56	1 78	1 90	30 10	1 80	30 11	29 56	1 88	0 08
%Ca	95 24	96 44	95 81	95 77	95 27	95 80	95 48	95 82	96 25	95 03	95 15	94 98	95 40	94 76	94 78	95 90	95 35	95 32	59 90	95 55	59 26	58 77	95 28	97 79
%Fe+Mn	2 81	2 35	2 64	2 65	2 90	2 70	2 78	2 66	2 60	2 95	3 02	3 07	2 80	3 23	3 02	2 54	2 88	2 78	10 01	2 64	10 63	11 66	2 85	2 13

MKC44 CALCITE AND DOLOMITE

	3	4	5	1	2	3	4	5	6	7	8	9	10
FeO	3 93	0 37	4 10	4 07	0 11	4 49	0 37	4 64	0 31	5 03	4 33	4 24	0 35
MnO	1 04	0 67	1 08	1 16	0 32	1 25	0 65	1 30	0 70	1 62	1 29	1 24	0 67
MgO	17 69	0 07	17 50	17 75	0 12	17 37	0 05	17 39	0 06	16 90	17 57	17 61	0 19
CaO	28 62	53 44	28 73	28 64	53 82	28 61	53 41	28 58	53 50	28 82	28 82	28 41	52 79
CO2	44 86	42 70	44 86	45 10	42 68	44 97	42 64	45 09	42 72	45 18	45 28	44 92	42 31
Total	92 22	96 87	92 17	92 66	96 94	92 21	96 74	92 36	96 98	92 53	92 96	92 19	95 96
%Mg	30 50	0 11	30 06	30 38	0 19	29 61	0 07	29 52	0 10	28 35	29 80	30 19	0 30
%Ca	58 47	97 83	58 49	58 09	98 96	57 78	97 91	57 49	97 90	57 28	57 91	57 71	97 65
%Fe+Mn	11 03	2 07	11 45	11 53	0 86	12 61	2 02	13 00	2 00	14 37	12 29	12 10	2 05

EASTERN BEFORSITES

MKC34 CARBONATES

	1	2	3	4	5	6	7	8	9	10	11	12	13	14	15	16	17	18	19	20	21	22	23	24
FeO	3 04	3 01	2 79	2 91	2 91	2 75	2 79	2 87	0 02	0.09	0 06	1 99	1 48	1 92	0 08	0.06	0.28	1 97	2 17	0 79	1 42	1 68	0 08	0 02
MnO	0 80	0 83	0 84	0 79	0 79	0 67	0 72	0.76	0 03	0.03	0 04	0 99	0 79	0 91	0.00	0 01	0 06	0 99	0 90	0 47	0 98	1 07	0 05	0 01
MgO	18 83	18 43	18 45	18 34	18 46	18 40	18 70	18 60	20 72	20 38	19 46	19 00	19 86	19 26	20 24	20 24	19 94	19 46	19 42	19 62	19 71	19 70	19 61	19 58
CaO	29 09	28 67	28 67	28 64	28 39	28 51	28 98	28 80	31 21	31 00	31 55	28 06	28 88	27 91	30 73	30 22	31 51	28 10	28 15	30 35	28 38	27 99	31 46	31 19
CO2	45 78	45 01	44 89	44 80	44 74	44.59	45 34	45 16	47 18	46.69	46 10	44 63	45 77	44 69	46 30	45 89	46.74	45 14	45 21	46 03	45 30	44 69	46 29	45 90
Tot	94 52	92 95	92 84	92 57	92 38	92 17	93.73	93.33	99.17	98 19	97 21	94 68	96 78	94 68	97 35	96 42	98 54	95 66	95 85	97 25	95 79	94 65	97 39	96 69
%Mg	32 33	32.14	32 32	32 14	32 47	32.51	32 50	32 39	35 87	35 58	34 15	33 88	34 84	34 42	35 67	36 05	34 55	34 40	34 24	34 30	34 94	34 44	34 37	34 61
%Ca	59 17	59.23	59.51	59.50	59.15	59 71	59.66	59 45	64.02	64.14	65 62	59 28	60 03	59 09	64 15	63 79	64 69	58.87	58 80	62 88	59 60	59 21	65 36	65 33
%Fe+Mn	8 50	8 63	8 17	8 36	8 39	7 78	7.84	8 15	0.12	0.28	0.23	6 84	5 13	6 49	0 18	0.16	0 76	6 74	6 97	2 82	5 46	6 33	0 27	0 06

MKC34 CARBONATES

	25	26	27	28	29	30	31	32	33	34	35	36	37	38	39	40	41	42	43	44	45	46	47	48
FeO	0.08	1.18	1.46	1 59	1 71	1.96	0.08	0.09	2.03	0 05	0 05	2 36	4 11	2 38	2 36	2 44	2 53	2 43	2 22	2 33	2 49	2 21	2 35	2 30
MnO	0.01	0.46	0.52	0 51	0.51	0.96	0.02	0.00	0.95	0.00	0 00	0 85	0 78	0 89	0 89	0 92	0 92	0 81	0 87	0 86	0 87	0 90	0 88	0 84
MgO	20.42	20.11	19.87	19.44	19.46	19.33	20.89	20.53	19.37	19.69	20.01	19.62	18 11	19.37	19 11	19 19	18.92	18.99	19 04	18.96	19 08	19 24	19 05	19 07
CaO	30.77	28 64	27.73	27.73	28.31	27 50	30 34	30.53	27 88	30.82	31.10	27.92	27.93	27 87	27 81	27.56	28.07	27 82	28 22	27 89	27 92	28 01	27 80	27 95
CO2	46.53	45.47	44.69	44.31	44.85	44.52	46.71	46.46	44.89	45.74	46.32	45.33	44 72	45.05	44.72	44 67	44.83	44.59	44 86	44 57	44 83	44 93	44 63	44 71
Tot	97 82	95.85	94.27	93.58	94 84	94.27	98.05	97.62	95.13	96.29	97.49	96.08	95.66	95.55	94.89	94.77	95.27	94 64	95.22	94.61	95.20	95.29	94 72	94 87
%Mg	35 82	35.81	35.95	35.34	34 84	34.72	36.67	36.13	34 44	34.99	35 15	34 53	31 48	34 22	33 98	34.16	33.41	33 84	33 71	33 79	33 77	34 09	33 93	33 91
%Ca	63 97	60.42	59.45	59.73	60 05	58.52	63 11	63.66	58.73	64.90	64.73	58 21	57 55	58 35	58 58	58.14	58.75	58.73	59 22	58 89	58 57	58 81	58 65	58 89
%Fe+Mn	0 21	3.76	4.60	4 93	5 12	6.76	0 22	0.21	6 83	0.12	0.12	7.27	10.96	7 43	7 44	7 70	7 83	7 43	7 06	7 32	7 66	7 09	7 42	7 20

MKC34 CARBONATES

	49	50	51	52	53	54	55	56	57	58	59	60	61	62	63	64	65	66	67	68	69	70	71	72
FeO	1 82	2.24	1.67	1 98	1 67	1.46	5.08	2 50	4 54	3.53	2 02	3 22	1 26	1 53	1 81	1 77	1 48	1 55	1 50	1 42	1 67	1 88	1 56	1 78
MnO	0 87	0.81	1 28	1 21	1.75	1.27	1.06	0 80	0 82	1 14	0 65	0 92	1 76	1 20	1 42	1 23	1 29	1 28	2 03	1 89	0 95	0 94	0 92	0 94
MgO	19 29	18 93	19 75	19 18	19.15	19.67	17.40	19.00	17.74	18.29	19.21	18 33	19 44	19.58	19 31	19.57	19 43	19 23	19.65	19 13	19 70	19 33	19 35	19 47
CaO	27.86	27.67	28.27	28.35	27.69	28.07	28.21	28.13	28.20	27.73	28.10	27 49	27 72	27 88	27 93	28 37	28 21	28 17	28 16	27 83	28 65	28 30	28 44	28 19
CO2	44 60	44 29	45.60	45 17	44.77	45.22	44.94	44 87	44 81	44.62	44 70	44.15	44 87	44.97	45 02	45 50	45 09	44 88	45 76	44 79	45 63	45 07	44 99	45 08
Tot	94.44	93.94	96.57	95.88	95.03	95.69	96.69	95.30	96.11	95.31	94.68	94.11	95.05	95.16	95.49	96.44	95.51	95.11	97.10	95.05	96.60	95.52	95.26	95.46
%Mg	34.59	34.01	34.61	33.72	33 99	34.84	29.63	33.58	30.55	31.99	34.33	32 60	34 61	34 88	34.14	34.31	34.44	34 18	34 14	33 94	34 56	34 22	34 40	34 54
%Ca	59 21	58.93	58.72	59.06	58.21	58.93	56.90	58.92	57.56	57.49	59.52	57 92	58 47	58 86	58.51	58 94	59.24	59 33	57 97	58 52	59 53	59 36	59 92	59 26
%Fe+Mn	6 20	7.07	6.67	7 22	7.81	6.23	13.47	7 50	11.89	10.52	6.15	9 48	6 91	6 26	7.34	6.76	6.32	6 49	7 90	7 54	5 91	6 42	5 68	6 20

MKC46 CARBONATES

	1	2	3	4	5	6	7	8	9	10
FeO	3 85	3 33	4 36	4 20	3 31	3 90	3 40	3 58	3 61	4 39
MnO	1 00	0 92	0.87	1 08	0 92	0 82	0 96	0 87	0 83	0 77
MgO	17 90	17 99	17 91	19 39	18 16	17 81	17 90	17 92	17 92	17 55
CaO	28 89	28 47	27 36	31 22	28 56	28 74	28 39	28 69	28 86	28 59
CO2	45.22	44 62	44 26	48 95	44 87	44 93	44 53	44 85	44 97	44 79
Tot	93 00	92 01	90 39	100 65	92 51	92 30	91 79	92 33	92 59	91 70
%Mg	30 66	31 44	31 38	30 69	31 61	30 74	31 33	31 08	30 98	30 23
%Ca	58 64	58 98	56 81	58 55	58 91	58 77	58 86	58 97	59 12	58 34
%Fe+Mn	10 70	9 57	11 80	10 76	9 48	10 49	9 81	9 95	9 90	11 43

MKC45 CARBONATES

	1	2	3	4	5	6	7	8	9	10
	3 54	3 77	3 62	3 67	3 40	3 43	3 60	3 46	3 55	3 63
	0 93	1 00	0 85	0 89	0 90	0 88	0 89	0 94	0 85	0 87
	18 50	17 99	18 25	18 25	18 37	18 13	18 21	18 33	18 26	18 19
	28 99	28 60	28 75	28 79	28 72	28 81	28 53	28 97	28 70	28 63
	45 72	45 05	45 26	45 35	45 26	45 08	45 06	45 48	45 19	45 11
	94 15	92 64	93 11	93 29	93 24	92 90	92 69	93 71	93 00	92 79
	31 56	31 00	31 42	31 33	31 70	31 37	31 51	31 42	31 53	31 41
	58 61	58 41	58 66	58 57	58 74	59 04	58 47	58 65	58 70	58 59
	9 83	10 59	9 92	10 10	9 56	9 60	10 01	9 72	9 77	10 00

SOUTHERN BEFORSITE

MKC4 CARBONATES

	1	2	3	4	5
FeO	1.75	1.77	1.97	2.30	1.23
MnO	0.90	0.93	0.99	0.88	0.85
MgO	20.04	19.89	19.69	19.18	19.85
CaO	28.13	28.05	28.21	27.79	28.00
CO2	45.61	45.42	45.48	44.74	44.95
Tot	96.43	96.06	96.34	94.90	94.89
%Mg	35.30	35.14	34.59	34.12	35.63
%Ca	58.69	58.71	58.72	58.58	59.55
%Fe+Mn	6.01	6.15	6.69	7.30	4.82

MKC6 CARBONATES

	1	2	3	5	6	7	8	9	10	11	12	13	14	15	16	17	18	19
FeO	0.02	0.09	0.06	1.99	1.48	1.92	0.08	0.06	0.28	1.97	2.17	0.79	1.42	1.68	0.08	0.02	0.08	1.18
MnO	0.03	0.03	0.04	0.99	0.79	0.91	0.00	0.01	0.06	0.99	0.90	0.47	0.98	1.07	0.05	0.01	0.01	0.46
MgO	20.72	20.38	19.46	19.00	19.86	19.26	20.24	20.24	19.94	19.46	19.42	19.62	19.71	19.26	19.61	19.58	20.42	20.11
CaO	31.21	31.00	31.55	28.06	28.88	27.91	30.73	30.22	31.51	28.10	28.15	30.35	28.38	27.95	31.46	31.19	30.77	28.64
CO2	47.18	46.69	46.10	44.63	45.77	44.69	46.30	45.89	46.74	45.14	45.21	46.03	45.30	44.69	46.20	45.90	46.53	45.47
Tot	99.17	98.19	97.21	94.68	96.78	94.68	97.35	96.42	98.54	95.66	95.85	97.25	95.79	94.65	97.39	96.69	97.82	95.85
%Mg	35.87	35.58	34.15	33.88	34.84	34.42	35.67	36.05	34.55	34.40	34.24	34.30	34.94	34.44	34.37	34.61	35.82	35.81
%Ca	64.02	64.14	65.62	59.28	60.03	59.09	64.15	63.79	64.69	58.87	58.80	62.88	59.60	59.23	65.36	65.33	63.97	60.42
%Fe+Mn	0.12	0.28	0.23	6.84	5.13	6.49	0.18	0.16	0.76	6.74	6.97	2.82	5.46	6.33	0.27	0.06	0.21	3.76

MKC6 CARBONATES

	20	22	23	24	25	26	27	28	29
FeO	1.46	1.59	1.71	1.98	0.08	0.09	2.03	0.05	0.05
MnO	0.52	0.51	0.51	0.96	0.02	0.00	0.95	0.00	0.00
MgO	19.87	19.44	19.46	19.33	20.89	20.53	19.37	19.69	20.01
CaO	27.73	27.73	28.31	27.50	30.34	30.53	27.88	30.82	31.10
CO2	44.69	44.31	44.85	44.52	46.71	46.46	44.89	45.74	46.32
Tot	94.27	93.58	94.84	94.27	98.05	97.62	95.13	96.29	97.49
%Mg	35.95	35.34	34.84	34.72	35.67	36.13	34.44	34.99	35.15
%Ca	59.45	59.73	60.05	58.52	63.11	63.66	58.73	64.90	64.73
%Fe+Mn	4.60	4.93	5.12	6.76	0.22	0.21	6.83	0.12	0.12

MKC9 CARBONATES

	1	2	3	4	5	6	7	8	9	10	11	12	13	14
FeO	2.36	4.11	2.38	2.36	2.44	2.53	2.43	2.22	2.33	2.49	2.21	2.35	2.30	1.82
MnO	0.85	0.78	0.89	0.89	0.92	0.92	0.81	0.87	0.86	0.87	0.90	0.88	0.84	0.87
MgO	19.62	18.11	19.37	19.11	19.19	18.92	18.99	19.04	18.96	19.08	19.24	19.05	19.07	19.29
CaO	27.92	27.93	27.87	27.81	27.56	28.07	27.82	28.22	27.89	27.92	28.01	27.80	27.95	27.86
CO2	45.33	44.72	45.05	44.72	44.67	44.83	44.59	44.86	44.57	44.83	44.83	44.63	44.71	44.60
Tot	96.08	95.66	95.55	94.89	94.77	95.27	94.64	95.22	94.61	95.20	95.29	94.72	94.87	94.44
%Mg	34.53	31.48	34.22	33.98	34.16	33.41	33.84	33.71	33.79	33.77	34.09	33.93	33.91	34.59
%Ca	58.21	57.55	58.35	58.58	58.14	58.75	58.73	59.22	58.89	58.57	58.81	58.65	58.89	59.21
%Fe+Mn	7.27	10.96	7.43	7.44	7.70	7.83	7.43	7.06	7.32	7.66	7.09	7.42	7.20	6.20

MKC18 CARBONATES

	1	2	3	4	5	6	7	8	9	10	11	12	13	14	15	16	17
FeO	1.50	1.42	1.67	1.88	1.56	1.78	1.54	1.46	1.56	1.34	1.42	1.78	1.81	1.76	2.04	1.72	1.56
MnO	2.03	1.89	0.95	0.94	0.92	0.94	0.92	0.86	0.87	0.89	0.74	0.85	0.85	0.80	0.93	0.91	0.78
MgO	19.65	19.13	19.70	19.33	19.35	19.47	19.48	19.67	19.39	19.82	19.19	19.17	19.24	19.34	19.08	19.33	19.35
CaO	28.16	27.83	28.65	28.30	28.44	28.19	28.53	28.83	28.28	28.23	28.50	28.29	28.19	28.13	28.34	28.20	28.53
CO2	45.76	44.79	45.63	45.07	44.99	45.08	45.20	45.55	44.88	45.19	44.67	44.78	44.80	44.79	44.92	44.89	44.98
Tot	97.10	95.05	96.60	95.52	95.26	95.46	95.66	96.37	94.97	95.46	94.51	94.87	94.90	94.82	95.31	95.05	95.20
%Mg	34.14	33.94	34.56	34.22	34.40	34.54	34.51	34.62	34.61	35.31	34.44	34.19	34.31	34.56	33.78	34.43	34.44
%Ca	57.97	58.52	59.53	59.36	59.92	59.26	59.90	60.12	59.82	59.59	60.59	59.77	59.57	59.55	59.45	59.53	60.19
%Fe+Mn	7.90	7.54	5.91	6.42	5.68	6.20	5.59	5.26	5.57	5.11	4.98	6.04	6.12	5.89	6.77	6.04	5.37

MKC35 CARBONATES

	1	2	3	4	5	6
FeO	2.43	2.43	2.12	1.43	2.36	2.55
MnO	0.96	0.94	0.88	0.94	0.84	0.86
MgO	18.87	18.96	19.32	19.59	18.96	19.06
CaO	28.11	27.93	27.94	28.06	28.32	28.43
CO2	44.77	44.72	44.90	44.90	44.92	45.25
Tot	95.14	94.98	95.17	94.93	95.40	96.16
%Mg	33.38	33.63	34.32	35.05	33.47	33.35
%Ca	58.91	58.68	58.81	59.48	59.25	58.95
%Fe+Mn	7.71	7.69	6.86	5.47	7.28	7.70

MKC35 CARBONATES

	7	8	9	10	11	12	13	14	15
FeO	1.43	1.30	2.18	2.36	1.81	1.25	1.31	2.72	2.34
MnO	0.91	0.88	0.84	0.85	0.87	0.91	1.01	1.00	0.95
MgO	19.40	19.44	19.09	19.03	19.47	19.62	19.42	18.93	19.09
CaO	28.15	28.70	27.99	28.34	28.08	28.41	28.38	28.10	28.07
CO2	44.74	45.12	44.69	45.01	44.98	45.08	44.93	45.04	44.92
Tot	94.63	95.43	94.79	95.58	95.22	95.27	95.04	95.79	95.37
%Mg	34.79	34.56	34.00	33.53	34.65	35.00	34.66	33.21	33.73
%Ca	59.81	60.46	59.08	59.18	59.21	60.04	60.02	58.40	58.78
%Fe+Mn	5.40	4.99	6.93	7.29	6.15	4.97	5.32	8.40	7.49

MKC55 CARBONATES

	1	2	3	4	5	6	7	8	9	10	11	12	13	14
FeO	1.67	1.98	1.67	1.46	5.08	2.50	4.54	3.53	2.02	3.22	1.26	1.53	1.81	1.77
MnO	1.28	1.21	1.75	1.27	1.06	0.80	0.82	1.14	0.65	0.92	1.76	1.20	1.42	1.23
MgO	19.75	19.18	19.15	19.67	17.40	19.00	17.74	18.29	19.21	18.33	19.44	19.58	19.31	19.57
CaO	28.27	28.35	27.69	28.07	28.21	28.13	28.20	27.73	28.10	27.49	27.72	27.88	27.93	28.37
CO2	45.60	45.17	44.77	45.22	44.94	44.87	44.81	44.62	44.70	44.15	44.87	44.97	45.02	45.50
Tot	96.57	95.88	95.03	95.69	96.69	95.30	96.11	95.31	94.68	94.11	95.05	95.16	95.49	96.44
%Mg	34.61	33.72	33.99	34.84	29.63	33.58	30.55	31.99	34.33	32.60	34.61	34.88	34.14	34.31
%Ca	58.72	59.06	58.21	58.93	56.90	58.92	57.56	57.49	59.52	57.92	58.47	58.86	58.51	58.94
%Fe+Mn	6.67	7.22	7.81	6.23	13.47	7.50	11.89	10.52	6.15	9.48	6.91	6.26	7.34	6.76

MKC56 CARBONATES

	1	2	3	4	5	6	7	8	9	10	11	12	13	14
FeO	2 85	2 86	2 83	3 01	2.88	2 90	3 01	2 83	3 02	2 83	2 92	3 00	2 83	2 80
MnO	0 89	0 79	0 81	0 70	0 82	0 86	0 75	0 77	0 86	0 81	0 80	0 95	0 79	0 76
MgO	18 83	18 85	18 81	19 04	18 71	18 57	18 85	18 52	18 61	18 73	18 60	18 52	18 90	18 75
CaO	28 50	28 38	28 26	27 92	28 21	28 46	28 27	28 59	28 38	28 40	28 36	28 14	28 47	28 46
CO2	45 25	45 12	44 98	45 00	44 86	44 95	45 10	44 90	45 01	45 00	44 88	44 76	45 22	45 02
Tot	96 32	95 99	95 70	95 67	95 48	95 74	95 98	95 61	95 88	95 77	95 56	95 38	96 21	95 80
%Mg	32 79	32 97	33 01	33 47	32 88	32 49	32 96	32 47	32 52	32 82	32 64	32 52	32 98	32 86
%Ca	58 82	58 82	58 77	58 14	58 74	59 01	58 57	59 39	58 75	58 96	58 96	58 54	58 88	59 10
%Fe+Mn	8 38	8 22	8.22	8.39	8.37	8.49	8.47	8 14	8 73	8 22	8 40	8 94	8 14	8 04

MKC62 CARBONATES

	1	2	3	4	5	6	7	8	9
FeO	3 33	2 92	3 31	3 07	3 27	3 02	2 24	3 36	4 47
MnO	1 38	1 04	1 24	1 12	1 19	1 20	1 04	1 22	1 32
MgO	18 17	18 53	18 21	18 11	18 15	17 96	18 51	17 93	17 49
CaO	28 34	28 43	28 30	28 24	28 00	28 00	28 20	28 37	27 74
CO2	45 00	45 02	44 92	44 53	44 57	44 20	44 38	44 69	44 45
Tot	96 21	95 95	95 98	95 06	95 19	94 38	94 36	95 57	95 47
%Mg	31 43	32 33	31 62	31 79	31 80	31 75	32 97	31 20	30 25
%Ca	58 09	58 76	58 21	58 75	58 13	58 65	59 51	58 51	56 85
%Fe+Mn	10 48	8 91	10 17	9 46	10 07	9 60	7 52	10 28	12 89

FERROCARBONATITES

MKC32 CARBONATES

	1	2	3	4	5	6	7	8	9	10	11	12	13	14	15	16	17	18	19	20	21	22	23	24
FeO	10 51	10 71	12.75	8 39	10 35	8 84	11 47	10 09	8 99	8 83	9 82	9 00	9 35	10 82	9 85	12 10	12 04	11 75	11 63	11 98	9 91	9 75	10 11	9 02
MnO	1 72	1 77	1 63	1 82	1 68	1 80	1 63	1 72	1 80	1.64	1 83	1 86	1 87	1 73	1 67	1 66	1 66	1 60	1 62	1 68	1 77	1 87	1 72	1 95
MgO	13 01	12 88	11.60	14 33	13 22	14 33	12 78	13 18	14 01	14 41	13 78	14 26	14 01	12 99	13 71	12 13	12 18	12 39	12 53	12 39	13 56	13 56	13 23	13 91
CaO	28 09	27 85	27.82	28 24	27 35	27 37	27 16	27 83	27.13	27.93	27 78	27 96	28 08	26 68	27 87	26 90	27 50	27 56	27 63	27 89	28 46	28 54	27 73	27 92
CO2	43 78	43 61	43.34	44 10	43 31	43 68	43 33	43.51	43.24	44.10	44.02	44 20	44 25	42 85	43 94	42 82	43 31	43 38	43 52	43 83	44 33	44 37	43 50	43 86
Tot	86 60	86 11	84 39	88 49	85 56	87 18	84 90	86 24	86.19	88.07	87.41	88 28	88 20	84 26	87 20	83.51	84 65	84 93	85 29	85 79	88 12	88 34	86 18	87 65
%Mg	20 97	20 79	18 38	23 51	21 63	23 69	20 67	21 47	23.34	23.63	22.33	23 24	22 69	21 37	22 27	19 65	19 51	19 91	20 11	19 66	21 75	21 75	21 58	22 77
%Ca	53 64	53 27	52.25	54 91	53 02	53 64	52 04	53.73	53 53	54 27	53 35	53 98	53 90	52 02	53 63	51 63	52 21	52 45	52 51	52 42	54 11	54 24	53 57	54 12
%Fe+Mn	25 39	25 94	29.37	21.58	25.35	22 66	27 29	24 80	23 14	22 10	24 33	22 79	23 41	26 60	24 10	28 72	28.27	27 63	27 38	27 92	24 14	24 01	24 85	23 11

MKC32 CARBONATES

	25	26	27	28	29	30
FeO	10 57	10.33	10 79	10 67	11.03	11 12
MnO	1 75	1.80	1.72	1.92	1 74	1.73
MgO	13 96	13.10	12.69	12.72	12 60	12 46
CaO	28.63	28 01	27.29	27.62	28.38	28.17
CO2	45.31	43.76	42 98	43.32	43.89	43 63
Tot	89.65	86 67	84 68	85 59	86.62	86 00
%Mg	21 90	21 15	20.76	20.63	20 10	19 97
%Ca	53 21	53.61	52 90	53.07	53 65	53.50
%Fe+Mn	24.89	25.24	26.34	26.30	26.25	26 53

MKC48 CARBONATES

	1	2	3	4	5	6	7	8	9	10
FeO	13.72	15 18	15 20	15 41	15 55	14 57	14 38	14 31	14 24	15 81
MnO	1.77	1.95	1.89	1.79	1 75	1 92	1 80	1 91	1 85	1.84
MgO	11.19	10.27	10 28	10 12	9 95	10 59	10 73	10 74	10 88	9 85
CaO	27.50	27.45	27.67	27 99	27 47	26 54	27 64	27.70	27 77	27 76
CO2	43.33	43 30	43.45	43.60	43.06	42 53	43 36	43 44	43 57	43 40
Tot	83.78	82.97	83.29	83 50	82.22	81 58	83 52	83.79	84 08	82 85
%Mg	17 55	15 83	15.79	15.47	15 36	16 73	16 68	16.66	16 87	15 04
%Ca	51.12	50.14	50.37	50 68	50 24	49 69	50 92	50 92	51 00	50 23
%Fe+Mn	31.32	34.02	33.83	33.85	34 40	33 58	32 40	32.42	32 13	34 73

MKC47 CARBONATES

	1	2	3	4	5	6
FeO	10 25	10.70	10 85	9 19	10 86	9 95
MnO	1 97	2 05	2 08	1 60	2 18	1 97
MgO	13 06	12 72	12 77	14 04	12 50	12 89
CaO	28 37	28 12	28 21	28 27	28 16	28 02
CO2	44 05	43 81	44 05	44 17	43 78	43 41
Tot	87 44	86 70	87.12	88 09	86 62	86 29
%Mg	20 93	20 36	20 32	22 86	19 96	20 97
%Ca	53 86	53 36	53 19	54 52	53 25	54 04
%Fe+Mn	25 21	26 28	26 49	22 62	26 79	24 99

MKC47 CARBONATES

	7	8	9	10
FeO	9 99	10 00	9 73	10.31
MnO	2.04	1.96	1.93	2.00
MgO	13.23	13.10	13.26	13.03
CaO	28.08	28.20	28.29	28.17
CO2	43 89	43 80	43 87	43.92
Tot	87.24	87.06	87.35	87.13
%Mg	21 33	21.15	21.45	20.93
%Ca	53.66	53.96	54.24	53.61
%Fe+Mn	25.01	24 88	24 31	25.46

Mn-RICH FERROCARBONATITES

MKC27 CARBONATES

	1	2	3	4	5	6	7	8	9	10	11	12	13	14	15	16	17	18	19	20	21
FeO	1 77	1 60	1 60	1 64	2 19	2 75	6 88	1 46	1 54	1 65	2 44	2 44	7 82	2 49	3 03	1 63	1 13	7 75	1 70	8 29	4 72
MnO	5 58	5 34	5 66	5 66	5 81	5 45	5 71	5 00	5 62	5 57	5 23	5 74	5 71	6 32	5 69	5 37	4 51	4 64	5 22	5 01	5 76
MgO	15 89	15 76	16 16	15 83	15 18	15 27	12 76	15 97	15 80	15 88	15 30	15 01	12 51	14 95	14 65	15 87	16 81	12 87	15 70	12 09	13 73
CaO	28 04	27 82	27 85	27 44	27 23	26 99	27 56	27 24	27 05	27 15	27 53	27 64	27 75	27 35	28 26	27 40	29 32	28 03	27 89	27 80	28 06
CO2	43 93	43 36	44 02	43 37	42 92	42 94	43 35	42 84	42 93	43 13	43 08	43 16	43 79	43 25	43 59	43 18	44 87	43 70	43 34	43 23	43 50
Tot	95 21	93 87	95 28	93 94	93 34	93 40	96 26	92 51	92 93	93 37	93 58	93 99	97 58	94 35	95 23	93 45	96 63	96 99	93 86	96 42	95 77
%Mg	27 13	27 34	27 63	27 42	26 30	26 43	20 70	28 25	27 70	27 70	26 48	25 77	19 92	25 48	24 68	27 68	28 59	20 75	27 24	19 46	22 70
%Ca	56 74	57 19	56 41	56 31	55 88	55 34	53 00	57 07	56 18	56 13	56 44	56 20	52 37	55 23	56 42	56 64	59 10	53 55	57 33	53 00	54 69
%Fe+Mn	16 14	15 47	15 95	16 27	17 82	18 23	26 30	14 68	16 12	16 17	17 07	18 03	27 71	19 29	18 90	15 68	12 31	25 71	15 43	27 54	22 30

MKC17 CARBONATES

	1	2	3	4	5	6	7	8	9	10	11	12	13	14	15	16	17
FeO	1 78	1 50	1 73	0 20	1 36	0 44	1 59	0 35	0 43	1 62	1 30	0 21	1 77	0 35	1 41	1 30	0 27
MnO	6 90	6 79	6 87	4 74	6 36	5 49	7 13	5 49	4 37	7 36	6 30	5 38	6 44	6 51	6 52	5 94	5 86
MgO	14 98	15 14	14 63	0 43	15 67	0 65	14 57	0 72	0 36	13 86	14 53	0 34	14 32	1 13	14 21	15 03	1 15
CaO	28 02	27 72	27 86	48 36	27 89	47 93	27 97	47 22	49 14	27 49	28 08	49 53	27 93	48 13	27 84	27 62	46 62
CO2	43 75	43 45	43 18	41 53	43 81	42 04	43 28	41 50	41 97	42 29	42 64	42 75	42 66	43 30	42 29	42 59	41 69
Tot	93 66	93 11	92 54	95 06	93 74	96 11	92 94	94 93	95 84	90 99	91 56	97 99	91 36	99 06	90 84	91 18	95 32
%Mg	25 24	25 83	24 92	0 68	26 73	1 00	24 73	1 12	0 55	23 91	25 24	0 51	24 70	1 68	24 76	26 33	1 79
%Ca	55 95	56 02	56 24	89 43	56 36	87 30	56 25	87 21	89 92	56 19	57 78	88 64	57 09	85 16	57 50	57 36	85 96
%Fe+Mn	18 80	18 15	18 84	9 89	16 91	11 70	19 02	11 67	9 53	19 90	16 98	10 85	18 21	13 16	17 74	16 30	12 25

MKC20b CARBONATES

	1	2	3	4	5	6
FeO	0 62	21 55	0 64	0 97	20 27	0 28
MnO	1 04	1 88	0 69	0 12	1 85	0 50
MgO	0 03	5 28	0 05	0 08	6 21	0 05
CaO	53 09	27 30	53 35	53 45	27 18	53 33
CO2	42 78	41 58	42 78	42 75	41 71	42 44
Tot	96 95	76 04	96 87	96 40	76 96	96 32
%Mg	0 05	7 78	0 07	0 12	9 29	0 08
%Ca	96 65	47 70	97 30	97 71	48 13	98 35
%Fe+Mn	3 29	44 52	2 63	2 17	42 59	1 57

MKC20b CARBONATES

	7	8	9	10	11	12	13	14
FeO	19 71	19 01	0 05	13 49	7 40	7 39	8 35	7 64
MnO	1 79	1 84	0 00	1 58	1 45	1 49	1 54	1 48
MgO	6 30	6 43	0 02	10 28	13 71	14 22	13 33	13 87
CaO	27 34	26 79	52 77	27 48	28 22	28 23	27 97	28 40
CO2	41 55	40 86	41 51	42 07	42 57	43 16	42 60	43 05
Tot	76 98	75 92	94 31	81 41	85 94	87 09	85 45	86 80
%Mg	9 49	9 89	0 03	16 51	23 41	24 06	22 51	23 40
%Ca	48 79	48 81	99 86	52 31	57 11	56 59	55 98	56 78
%Fe+Mn	41 72	41 30	0 10	31 18	19 48	19 35	21 51	19 82

MKC16 CARBONATES

	1	2	3	4	5	6	7	8
FeO	1 17	0 43	1 21	0 12	0 22	0 47	0 15	1 32
MnO	7 03	7 15	7 21	0 08	7 27	4 15	7 31	7 39
MgO	15 00	1 11	14 78	0 76	1 07	0 40	1 10	14 47
CaO	28 02	45 63	28 10	53 82	45 22	48 83	46 05	27 82
CO2	43 46	41 75	43 43	43 23	41 33	41 66	42 00	43 05
Tot	93 51	95 63	93 51	97 88	94 88	95 03	96 46	92 73
%Mg	25 54	1 71	25 10	1 17	1 66	0 62	1 69	24 69
%Ca	56 53	83 31	56 54	98 43	83 37	90 14	83 64	56 23
%Fe+Mn	17 93	14 98	18 36	0 40	14 97	9 24	14 67	19 08

APPENDIX 3: ANALYTICAL PROCEDURES

3.1 Microprobe

Analysis of clinopyroxene, amphibole, biotite, opaques, feldspar, nepheline and sodalite were determined at Rhodes University on a JEOL CXA-733 wavelength dispersive electron microprobe. Apatite, sphene, zircon, allanite as well as the two unidentified accessory phases were analysed at the University of Cape Town on a Cameca wavelength dispersive electron microprobe. At both localities, a ZAF-correction routine was used and the accelerating voltage was 15kv with a beam current of 25nA. A focussed beam was used except in the case of feldspar, nepheline and sodalite, where a 50μm beam diameter was used. International standards and pure synthetic crystals were used for calibration. At Rhodes, the standards used were: Stillwater chromite, Orapa ilmenite, ilmenite (A236), St.John's Island olivine, fayalite (8526), jadeite (Rhodes), orthoclase (JVPL), orthoclase (PSU-1A), rhodonite (U.K.), rhodonite (Rhodes) and Ni-magnetite (Rhodes). LiF 200, PET and TAP were employed as diffracting crystals. The counting times were 30 sec for peak positions and 10 sec for background positions.

3.2 X-Ray Fluorescence

Between 2 to 5kg of rock was split in a steel-jaw spliter, crushed into chips and then reduced to silt size in a Mn-steel swing mill. The rock powder was then sent to Rocklabs (Closed Corporation) for analyses.

The concentrations of all major and trace elements were measured on an ARL 8420 spectrometer fitted with a Rd end-window tube, using a voltage of 50kv with a current of 50nA.

Operating conditions and lower limits of detection (LLI) are given below (M.Sharpe pers.com.).

	Crystal	Detector	LLI (wt%)
SiO_2	PET	FPC	0.01
TiO_2	LIF200	FPC	0.01
Al_2O_3	PET	FPC	0.01
FeO	LIF200	FPC	0.01
MnO	LIF200	FPC	0.01
MgO	AX06	FPC	0.01
CaO	LIF200	FPC	0.01
Na_2O	AX06	FPC	0.01
K_2O	LIF200	FPC	0.01
P_2O_5	GE111	FPC	0.01
			(ppm)
Zn	LIF200	SC	3
Cu	LIF200	SC	3
Ni	LIF200	FPC	3
Co	LIF200	FPC	3
Mo	LIF200	SC	2
Nb	LIF220	SC	3
Zr	LIF220	SC	3
Y	LIF220	SC	2
Sr	LIF220	SC	2
Rb	LIF220	SC	1
U	LIF220	SC	5
Th	LIF220	SC	4
Pb	LIF200	SC	4
Cr	LIF220	FPC	5
V	LIF220	FPC	8
Ba	LIF200	FPC	10
Sc	LIF200	FPC	8
F	AX06	FPC	50
Cl	GE111	FPC	40

3.3 Inductively Coupled Plasma Spectrometry

REE analyses that do not include data for Lu were done at Stellenbosch University while the remainder were done at the Royal Holloway and Bedford New College, England. Although the technique followed at both laboratories was essentially that of Walsh *et al.*,(1981), the procedure used at Stellenbosch involved some modifications and is outlined below (after D.Cornell, unpublished data and pers. com.).

Separation of the REE was preformed entirely in a dust-free laboratory. Half-gram aliquots of powdered samples were placed in teflon-line flasks and dissolved in ANALAR HF and then nitric acid at 200°C. The lanthanide group elements were quantitatively separated from other major and trace elements in large cation exchange columns, using HCl elution. Samples were processed in batches of seven, including one batch blank.

The analyses were done using a sixteen-channel optical spectrometer with a Philips PV8490 ICP source unit. Samples and standards were aspirated in groups of three, with a reference and spectrometric blank before and after each group. Standards were based on carefully dried specpure oxides. Interference corrections were made to correct line overlaps within the analyte elements, and particularly those due to Ca, Fe and Th. Data were stored and processed by mircocomputer. All analyses were done in duplicate

According to N.Walsh (pers.com.) realistic working detection limits using this technique are approximately 1 * chondritic abundance for most REE except for Er and Pr (2 * and 10 * chondritic abundance respectively). Precision should be 5-10%, unless working close to detection limits.

3.4 Radiogenic Isotope Analyses

These were done at the Division of Earth, Marine and Atmospheric Science and Technology, CSIR, Pretoria. The following description of procedure is after Eglington (pers.com.).

Rb and Sr concentrations were obtained by XRF spectrometry (in conjunction with Rocklabs), or by isotope dilution in case where concentrations were lower than about

30ppm. For isotope dilution, samples were spiked with enriched tracer solutions prior to dissolution in HF : HNO_3 : HCl mixtures using "Savillex"(R) vials. $^{87}Sr/^{86}Sr$ for all samples were determined from separate unspiked dissolutions.

Replication for $^{87}Rb/^{86}Sr$ and $^{87}Sr/^{86}Sr$ derived from spiked samples are 0.8% and 0.01% respectively, at the 1 sigma level, whereas the replication for unspiked $^{87}Sr/^{86}Sr$ is 0.01%. There is no correlation between the uncertainties for $^{87}Rb/^{86}Sr$ and $^{87}Sr/^{86}Sr$.

Ten analyses of NBS SRM 987 provide an average value of 0.710275 $\pm$ 16 (1 sigma on ten) whereas ten replicates of NBS SRM 607 K-feldspar provides a Rb/Sr ratio of 8.06 $\pm$ 0.05 (1 sigma on ten).

Samples for Sm-Nd analysis were spiked with enriched tracer solutions prior to dissolution in HF : HNO_3 : HCl mixtures, in high pressure 'bombs'. $^{143}Nd/^{144}Nd$ ratios were recovered from unspiked solutions whereas the Sm and Nd concentrations were obtained by isotope dilution analysis on separate dissolutions. From experience with standards and samples of similar composition, $^{143}Nd/^{144}Nd$ ratios are known to be accurate to 0.006% from unspiked analyses. The analytical uncertainty in $^{147}Sm/^{144}Nd$ ratio is 0.6%. There is no correlation between the uncertainties in $^{147}Sm/^{144}Nd$ and $^{143}Nd/^{144}Nd$.

Ten analyses of Johnson Matthey standard provide an average value of 0.511803 $\pm$ 15 (1 sigma on 13). Six replicates of BCR-1 basalt standard provide Nd= 28.7ppm (1 sigma on 6), Sm= 6.58 $\pm$ 0.02ppm (1 sigma on 6) and Sm/Nd = 0.2293 $\pm$ 0.0009 (1 sigma on 6).

Samples for Pb analysis were dissolved in high pressure 'bombs' followed by "Savillex"(R) screw-top beakers with HF : HNO_3 : HBr mixtures and the Pb separated using HBr : H2O reagents on miniature anion-exchange columns. Replication for $^{206}Pb/^{204}Pb$ and $^{207}Pb/^{204}Pb$ is 0.09%, and for $^{208}Pb/^{204}Pb$ is 0.15%.

Pb blank levels are better than 500pg whereas those for Rb, Sr, Sm and Nd are better than 1ng.

All regressions of the data were performed using the GEODATE software package (Eglington and Harmer, 1989).

3.5 Oxygen Isotope Analyses

Oxygen isotopic analyses were done at the Department of Geochemistry, University of Cape Town.

The mineral separates analysed were obtained by hand-picking from samples that had been crushed to less than 0.5mm and washed in alcohol. The average grain size of samples prior to crushing was about 2mm, and the separates are considered to be better than 95% pure.

Samples were dried at 50°C for approximately 48 hours before loading a 10mg measure into the reaction vessels. The samples were then dried further and degassed at 200°C for 2 hours before reacting with ClF_3 at 550°C overnight. The extracted oxygen was converted to CO_2 on a heated carbon rod and analysed for $^{18}O/^{16}O$ using a VG 602E mass spectrometer. All analyses, excepting ORS 126, were duplicated. Results are quoted in delta notation and are reported relative to the V-SMOW standard. Two analyses of NBS-28 gave $\delta^{18}O$ of 9.64‰.

APPENDIX 4: WHOLE ROCK ANALYSES

Whole rock Fe^{3+}/Fe^{2+} ratios assumed to be 0.14.

CIPW norms calculated assuming $Fe^{3+}/Fe^{2+} = 0.5$.

	Monzodiorite		
	ORS 133	ORS 175	ORS 176
[wt%]			
SiO2	49.76	48.13	49.79
TiO2	1.80	1.99	1.83
Al2O3	16.77	16.10	17.26
Fe2O3	1.05	1.17	1.13
FeO	7.60	8.47	8.16
MnO	0.21	0.20	0.19
MgO	4.42	5.68	4.40
CaO	8.32	9.53	7.94
Na2O	4.03	3.52	4.74
K2O	2.84	2.46	2.98
P2O5	1.30	1.25	1.59
Cr2O3	0.04	0.02	0.03
NiO	0.00	0.01	0.00
H2O−	0.15	0.08	0.08
LOI	1.31	0.78	0.51
Total	99.60	99.39	100.63
[ppm]			
Zn	97	107	107
Cu	37	41	31
Ni	31	40	32
Co	21	24	18
Mo	2	2	3
Nb	88	70	97
Zr	272	239	390
Y	38	38	38
Sr	1583	1618	1542
Rb	72	58	126
U	2	0	0
Th	9	9	11
Pb	9	13	11
Cr	38	79	77
V	174	205	148
Ba	2019	1930	1825
Sc	12	13	< 5
F	1311	0	200
Cl	262	0	0
La			
Ce	313.75		
Pr	22.80		
Nd	85.34		
Sm	11.20		
Eu	3.60		
Gd	9.11		
Dy	7.26		
Ho	1.47		
Er	4.07		
Yb	3.08		
Lu			

	Larvikite – Pulaskite series						
	ORS 61	ORS 90	ORS 94	ORS 101	ORS 102	ORS 107	ORS 108
[wt%]							
SiO2	60.96	58.32	59.22	57.96	58.70	59.34	60.05
TiO2	0.64	1.11	1.00	0.33	1.20	0.86	0.59
Al2O3	18.90	18.61	18.77	18.97	18.47	18.74	18.79
Fe2O3	0.51	0.59	0.56	0.66	0.65	0.53	0.54
FeO	3.65	4.27	4.06	4.76	4.71	3.82	3.93
MnO	0.11	0.14	0.13	0.18	0.16	0.15	0.16
MgO	0.77	1.51	1.51	0.49	1.91	1.16	0.63
CaO	2.28	3.84	3.82	2.51	4.11	3.03	2.19
Na2O	6.51	5.07	5.16	6.11	4.99	6.13	6.30
K2O	5.71	4.24	4.41	5.89	4.19	4.33	4.96
P2O5	0.33	0.68	0.61	0.29	0.78	0.50	0.26
Cr2O3	0.04	0.02	0.02	0.00	0.02	0.00	0.00
NiO	0.00	0.00	0.00	0.00	0.00	0.00	0.00
H2O−	0.16	0.52	0.10	0.10	0.11	0.18	0.14
LOI	0.78	0.61	0.82	1.06	0.71	0.81	0.73
Total	101.35	99.53	100.19	99.14	100.71	99.53	99.27
[ppm]							
Zn	73	73	73	115	79	79	86
Cu	9	19	18	11	22	15	11
Ni	3	14	16	9	18	13	5
Co	5	6	8	1	8	6	5
Mo	3	2	3	8	2	4	6
Nb	87	97	101	231	105	121	116
Zr	300	255	295	586	334	367	500
Y	25	31	37	47	42	35	33
Sr	634	1141	1145	538	1133	917	644
Rb	121	89	101	177	96	129	133
U	0	1	6	9	4	12	8
Th	16	7	12	27	9	22	21
Pb	23	14	15	32	12	21	23
Cr	8	31	31	19	43	27	13
V	17	34	41	20	61	37	27
Ba	1402	2223	2037	910	2000	1520	1298
Sc	11	< 11	< 10	< 8	12	< 10	< 10
F	1497	1613	1890	1329	1868	1558	1308
Cl	647	348	394	297	125	84	604
La				177.24	126.31	122.48	104.41
Ce				303.91	241.22	224.56	204.59
Pr				29.79	23.25	19.82	20.80
Nd				92.98	80.63	66.05	63.00
Sm				11.77	10.59	8.31	9.75
Eu				1.96	3.34	2.53	2.55
Gd				8.25	7.77	5.87	7.15
Dy				8.18	6.82	5.37	6.19
Ho				1.87	1.51	1.24	1.10
Er				5.17	4.13	3.49	3.03
Yb				4.81	3.18	2.96	3.38
Lu							0.51

Alkali-melasyenite – nepheline syenite series

	ORF 3	ORF 28	ORF 29	ORF 30	ORF 31	ORF 43	ORF 44	ORF 46
[wt%]								
SiO2	59.58	58.91	57.85	53.74	61.33	58.79	60.03	59.58
TiO2	0.53	0.69	0.81	1.46	0.28	0.51	0.35	0.41
Al2O3	19.51	18.34	18.72	17.39	19.60	18.65	19.92	19.24
Fe2O3	0.54	0.68	0.70	1.01	0.39	0.62	0.46	0.45
FeO	3.92	4.94	5.08	7.26	2.80	4.50	3.33	3.27
MnO	0.15	0.21	0.19	0.23	0.10	0.24	0.15	0.17
MgO	0.55	0.97	1.49	3.34	0.51	1.02	0.72	0.65
CaO	1.70	3.04	3.61	6.09	1.56	2.44	2.17	1.92
Na2O	7.83	6.56	6.02	5.16	7.08	8.56	7.68	7.79
K2O	5.34	4.53	3.47	3.25	6.27	4.55	4.97	4.86
P2O5	0.30	0.43	0.53	1.00	0.14	0.33	0.21	0.16
Cr2O3	0.02	0.01	0.01	0.02	0.02	0.02	0.02	0.02
NiO	0.00	0.00	0.00	0.00	0.00	0.01	0.00	0.00
H2O–	0.17	0.20	0.22	0.23	0.11	0.18	0.23	0.23
LOI	0.83	0.51	1.05	0.84	0.64	0.82	1.04	1.17
Total	100.97	100.02	99.75	101.02	100.83	101.24	101.28	99.92
[ppm]								
Zn	66	91	91	108	47	105	66	65
Cu	10	14	17	24	< 3	11	7	8
Ni	2	4	5	23	< 5	4	< 3	4
Co	0	< 3	6	15	< 4	8	6	5
Mo	11	< 3	3	29	8	16	12	13
Nb	214	311	283	309	167	336	230	212
Zr	427	625	539	473	390	876	603	581
Y	33	50	48	62	25	56	37	45
Sr	989	1117	1423	1435	277	740	800	739
Rb	132	133	120	97	137	152	122	139
U	1	9	12	5	12	13	7	14
Th	23	29	19	11	19	46	28	28
Pb	26	25	29	24	21	48	34	38
Cr	< 10	< 9	< 8	28	< 9	< 8	< 16	< 13
V	4	< 10	18	71	< 8	< 9	< 25	< 25
Ba	1523	1613	1897	1823	261	1319	1359	1205
Sc	< 11	< 5	< 7	8	< 8	< 9	< 12	< 8
F	1383	1150	1862	1290	650	2160	1150	1370
Cl	412	382	44	762	1185	2566	83	298
La	113.13	147.85		235.44	81.38			
Ce	199.41	286.03		450.55	140.61			
Pr	19.05	29.40		46.47	13.15			
Nd	55.50	94.20		148.30	39.80			
Sm	7.39	13.99		21.38	5.75			
Eu	2.41	3.29		4.34	1.83			
Gd	5.43	10.40		15.44	4.57			
Dy	5.51	9.84		13.01	5.09			
Ho	1.06	1.82		2.34	1.05			
Er	3.06	5.35		6.11	3.60			
Yb	3.46	5.77		5.97	4.81			
Lu	0.53	0.89		0.91	0.78			

Foyaites

	ORF 6	ORF 7	ORF 8	ORF 17	ORF 21	ORF 22	ORF 23	ORF 24	ORF 32	ORF 33	ORF 40	ORF 41
	cpx	amph	cpx	cpx	amph	cpx	amph	cpx	cpx	cpx	amph	cpx
[wt%]												
SiO2	56.89	57.69	60.23	59.74	54.91	58.30	55.36	58.14	57.76	60.71	56.66	58.61
TiO2	0.20	0.19	0.33	0.43	0.50	0.25	0.34	0.27	0.19	0.25	0.16	0.20
Al2O3	20.35	19.27	19.10	18.32	18.84	21.09	19.64	21.01	19.92	18.39	19.46	19.59
Fe2O3	0.56	0.63	0.47	0.48	0.69	0.35	0.74	0.45	0.57	0.56	0.70	0.53
FeO	4.06	4.57	3.39	3.49	4.95	2.54	5.37	3.28	4.12	4.02	5.07	3.82
MnO	0.13	0.22	0.13	0.17	0.27	0.12	0.24	0.13	0.22	0.23	0.24	0.17
MgO	0.24	0.25	0.41	0.65	0.84	0.31	0.66	0.48	0.42	0.44	0.36	0.38
CaO	1.27	1.55	1.40	2.01	2.76	1.16	2.63	1.57	1.74	1.74	1.81	1.34
Na2O	11.00	8.14	8.01	6.48	7.08	10.50	7.60	8.50	9.30	7.20	9.22	8.20
K2O	5.34	5.99	5.99	6.47	5.83	5.45	5.36	6.13	5.80	6.12	5.53	5.78
P2O5	0.11	0.14	0.14	0.25	0.37	0.13	0.26	0.16	0.15	0.14	0.12	0.11
Cr2O3	0.03	0.01	0.02	0.04	0.04	0.03	0.02	0.02	0.01	0.01	0.00	0.01
NiO	0.01	0.01	0.00	0.01	0.00	0.00	0.00	0.00	0.00	0.00	0.00	0.00
H2O−	0.14	0.23	0.08	0.12	0.30	0.20	0.30	0.19	0.19	0.42	0.13	0.25
LOI	0.65	1.72	1.00	0.69	2.07	0.73	1.10	0.92	0.73	0.86	1.32	1.23
Total	100.98	100.61	100.70	99.35	99.45	101.16	99.62	101.25	101.12	101.09	100.78	100.22
[ppm]												
Zn	41	89	50	63	114	37	99	60	61	74	74	78
Cu	0	4	1	6	4	6	5	< 4	4	< 3	8	< 5
Ni	3	6	< 3	< 3	< 4	< 4	< 4	< 5	< 4	< 6	< 4	< 4
Co	< 4	< 4	< 4	< 4	< 3	< 4	4	5	< 3	< 4	5	7
Mo	6	14	13	6	14	6	6	13	14	8	< 4	6
Nb	57	410	205	281	481	111	438	254	319	284	371	134
Zr	204	851	523	443	702	275	740	480	396	520	647	518
Y	21	51	32	39	56	21	52	46	36	36	55	30
Sr	31	102	73	302	189	123	119	167	48	124	87	47
Rb	151	206	128	133	182	171	180	144	140	190	188	219
U	0	5	0	8	12	5	12	8	9	< 5	13	7
Th	17	53	30	19	25	18	34	31	18	26	57	23
Pb	18	31	26	26	40	20	38	42	16	38	24	41
Cr	6	< 10	22	< 7	< 8	< 12	< 8	< 14	< 10	< 13	< 12	< 15
V	< 15	3	< 15	< 8	< 4	< 10	< 9	< 8	< 8	< 9	< 18	< 29
Ba	< 13	53	58	325	190	148	66	66	< 11	29	< 28	< 13
Sc	< 10	11	< 15	< 9	< 9	< 10	< 10	< 6	< 4	< 10	< 9	< 5
F	881	1423	1114	710	1600	400	1660	1560	860	1020	1060	1190
Cl	6300	1260	1730	766	1370	4130	515	1100	4973	1182	5713	1302
La	83.11		117.30	141.78					113.43			
Ce	151.61		175.30	265.00					236.53			
Pr	14.27		17.86	25.63					24.10			
Nd	43.80		56.44	79.00					76.50			
Sm	6.10		6.90	11.26					10.99			
Eu	0.69		1.25	1.94					0.84			
Gd	4.14		5.48	8.15					7.43			
Dy	3.76		5.10	7.59					6.30			
Ho	0.68		1.18	1.39					1.10			
Er	1.95		3.39	3.92					2.98			
Yb	2.43		2.96	4.18					3.13			
Lu	0.44			0.66					0.53			

	Alkali–feldspar syenite				
	ORS 62	ORS 92	ORS 93	ORS132	ORS 173
[wt%]					
SiO2	62.80	62.67	61.73	62.91	62.72
TiO2	0.97	0.88	0.68	0.34	0.48
Al2O3	18.53	18.71	20.17	18.33	18.82
Fe2O3	0.42	0.42	0.31	0.47	0.32
FeO	3.04	3.03	2.23	3.36	2.27
MnO	0.07	0.09	0.06	0.17	0.09
MgO	0.99	0.67	0.76	0.30	0.43
CaO	2.01	1.72	2.32	1.03	1.43
Na2O	6.13	5.46	5.95	5.33	5.82
K2O	5.28	5.30	4.49	6.71	5.77
P2O5	0.43	0.21	0.29	0.09	0.07
Cr2O3	0.04	0.00	0.03	0.00	0.00
NiO	0.01	0.00	0.00	0.00	0.00
H2O–	0.18	0.10	0.09	0.12	0.20
LOI	0.45	0.61	0.58	0.68	0.59
Total	101.35	99.87	99.69	99.84	99.01
[ppm]					
Zn	46	52	99	70	49
Cu	9	9	11	5	5
Ni	3	1	6	6	3
Co	1	4	4	2	0
Mo	2	2	6	3	2
Nb	84	91	189	72	78
Zr	152	180	567	204	225
Y	19	25	56	24	20
Sr	525	556	728	56	334
Rb	100	103	158	137	113
U	2	7	4	9	3
Th	16	16	38	5	15
Pb	14	9	14	15	20
Cr	16	12	23	< 10	4
V	27	< 10	22	< 11	0
Ba	2426	2062	1647	234	1534
Sc	< 10	< 10	< 9	< 10	< 4
F	1214	1300	1355	1168	300
La	76.85	82.74	70.18		
Ce	132.58	159.25	108.86		
Pr	13.82	16.43	11.05		
Nd	50.70	53.50	39.20		
Sm	6.72	7.68	4.88		
Eu	4.02	3.37	3.69		
Gd	5.13	5.50	3.87		
Dy	4.26	4.71	3.06		
Ho	0.80	0.86	0.58		
Er	2.48	2.45	1.84		
Yb	2.05	2.46	1.46		
Lu	0.33	0.37	0.23		

	Alkali–syenites				
	ORS 60	ORS 99	ORS 110	ORS 112	ORS 126
[wt%]					
SiO2	64.54	61.49	61.49	62.40	65.24
TiO2	0.10	0.20	0.12	0.10	0.01
Al2O3	17.77	17.12	17.81	17.86	18.35
Fe2O3	0.60	0.76	0.62	0.70	0.28
FeO	4.31	5.48	4.46	5.05	2.03
MnO	0.19	0.21	0.21	0.21	0.10
MgO	0.03	0.07	0.05	0.02	0.00
CaO	1.32	1.76	1.22	1.07	0.56
Na2O	7.51	5.76	6.39	6.34	6.66
K2O	5.08	5.31	5.53	5.33	5.85
P2O5	0.07	0.00	0.04	0.08	0.01
Cr2O3	0.02	0.03	0.00	0.00	0.00
NiO	0.00	0.00	0.00	0.00	0.00
H2O–	0.11	0.12	0.11	0.13	0.07
LOI	0.25	0.31	0.73	0.46	0.52
Total	101.90	98.62	98.78	99.75	99.68
[ppm]					
Zn	97	96	127	91	46
Cu	0	3	7	2	0
Ni	2	6	7	9	4
Co	0	0	0	0	2
Mo	6	10	12	5	1
Nb	198	293	269	197	117
Zr	567	760	637	388	276
Y	61	84	75	72	50
Sr	81	42	85	29	82
Rb	152	114	181	143	191
U	8	7	14	14	14
Th	69	64	54	64	45
Pb	19	17	20	11	9
Cr	10	11	< 11	< 12	< 12
V	2	< 11	31	32	29
Ba	< 28	33	62	46	92
Sc	< 10	< 9	< 8	< 8	< 10
F	1563	1308	1198	1003	913
Cl	151.00	330.00	540.00	203.00	33.00
La		466.00		434.80	310.91
Ce		775.00		662.13	490.00
Pr		85.28		68.49	45.13
Nd		276.62		209.29	131.82
Sm		32.98		24.52	14.83
Eu		1.13		0.87	0.69
Gd		23.93		17.86	11.23
Dy		19.38		15.41	10.46
Ho		4.00		3.24	2.20
Er		9.80		7.98	5.56
Yb		7.35		5.58	3.95
Lu					

Alkali–syenites (continued)

	ORS 171	ORS 189	ORS 193	MKS 35	MKS 49	MKS 57	MKS 64	MKS 67	MKS 69
[wt%]									
SiO2	62.26	63.46	65.83	62.75	65.21	64.23	64.15	63.99	63.25
TiO2	0.17	0.27	0.21	0.31	0.08	0.19	0.42	0.17	0.33
Al2O3	17.73	17.45	17.39	16.67	17.93	17.81	17.99	18.30	17.88
Fe2O3	0.57	0.66	0.38	0.64	0.23	0.42	0.43	0.44	0.45
FeO	4.11	4.76	2.75	4.60	1.66	3.05	3.11	3.17	3.23
MnO	0.18	0.19	0.13	0.21	0.08	0.14	0.09	0.08	0.17
MgO	0.26	0.21	0.42	0.56	0.15	0.25	0.21	0.12	0.47
CaO	1.47	1.62	1.14	1.98	0.80	1.39	0.70	0.70	1.72
Na2O	5.95	6.28	6.29	5.32	6.96	6.49	6.47	5.88	5.96
K2O	5.81	5.58	5.73	6.11	5.65	5.68	5.98	6.58	6.20
P2O5	0.16	0.05	0.16	0.20	0.07	0.07	0.15	0.09	0.14
Cr2O3	0.00	0.02	0.02	0.02	0.01	0.05	0.05	0.03	0.04
NiO	0.00	0.00	0.00	0.00	0.01	0.00	0.01	0.00	0.00
H2O–	0.16	0.06	0.11	0.10	0.11	0.14	0.12	0.10	0.14
LOI	0.45	0.16	0.33	0.44	0.30	0.23	0.20	0.17	0.36
Total	99.28	100.77	100.89	99.91	99.25	100.14	100.08	99.82	100.34
[ppm]									
Zn	107	85	66	123	56	76	50	54	76
Cu	3	< 4	< 4	6	< 4	< 4	< 4	< 5	< 3
Ni	7	< 5	< 3	5	< 4	< 4	5	< 4	4
Co	0	< 4	< 5	5	5	< 3	< 6	< 4	5
Mo	16	9	5	< 3	5	8	6	< 3	5
Nb	170	277	138	293	116	213	126	137	201
Zr	4722	1400	517	618	873	1260	778	294	495
Y	88	118	42	63	60	53	81	60	49
Sr	138	39	93	113	193	119	202	134	137
Rb	183	126	224	273	248	212	203	238	223
U	14	15	9	21	16	13	17	25	13
Th	61	79	45	45	92	49	146	113	42
Pb	32	19	18	28	27	23	23	41	33
Cr	10	< 12	< 16	< 9	< 5	< 8	< 9	< 13	< 15
V	< 2	< 16	< 10	< 6	< 4	< 6	7	< 11	< 8
Ba	441	< 12	208	24	203	73	159	52	42
Sc	< 4	< 11	< 12	< 5	< 9	< 5	< 9	< 5	< 6
F	1000	1880	1160	1960	2520	1810	500	810	1670
Cl		87.00	59.00						
La						206.03		285.40	
Ce						384.85		502.24	
Pr						35.50		44.48	
Nd						103.30		125.50	
Sm						15.41		17.79	
Eu						0.82		0.99	
Gd						11.18		12.74	
Dy						10.67		12.39	
Ho						1.95		2.26	
Er						5.49		6.06	
Yb						6.04		5.62	
Lu						0.98		0.75	

Monzonite – granite series (GPC)

	ORS 129	ORS 130	ORS 138	ORS 172	ORG 11
[wt%]					
SiO2	68.73	63.31	68.55	68.79	66.86
TiO2	0.09	0.54	0.16	0.19	0.25
Al2O3	15.93	17.44	16.02	16.04	14.99
Fe2O3	0.28	0.44	0.36	0.33	0.43
FeO	2.04	3.19	2.58	2.37	3.10
MnO	0.09	0.14	0.12	0.10	0.09
MgO	0.06	0.67	0.04	0.15	0.33
CaO	0.60	1.76	0.65	0.74	0.99
Na2O	5.39	5.37	5.07	5.35	5.48
K2O	5.49	5.23	5.32	5.65	5.10
P2O5	0.02	0.19	0.00	0.05	0.09
Cr2O3	0.02	0.02	0.00	0.01	0.00
NiO	0.00	0.00	0.00	0.00	0.00
H2O–	0.27	0.10	0.05	0.07	0.12
LOI	0.66	0.86	0.47	0.40	0.68
Total	99.67	99.26	99.39	100.24	98.51
[ppm]					
Zn	39	55	51	45	87
Cu	2	7	1	5	0
Ni	6	7	10	7	7
Co	4	2	0	0	1
Mo	2	10	11	3	11
Nb	224	131	258	171	343
Zr	373	581	491	436	614
Y	61	49	74	53	70
Sr	31	411	74	45	144
Rb	217	157	205	217	390
U	10	14	30	8	15
Th	54	25	69	45	79
Pb	10	9	13	24	31
Cr	< 9	< 11	< 10	8	23
V	27	37	30	4	< 17
Ba	99	1627	173	144	286
Sc	18	< 11	< 8	< 4	13
F	2007	1396	1606	100	2605
La			219.90		191.62
Ce			348.29		303.91
Pr			34.77		30.61
Nd			107.39		94.28
Sm			14.26		12.19
Eu			0.79		1.24
Gd			11.12		10.23
Dy			12.45		10.33
Ho			2.80		2.31
Er			8.07		7.03
Yb			6.93		6.81
Lu					

Monzonite – granite series (MKC)

	MKS 3	MKS 21	MKS 27	MKS 36	MKS 52
[wt%]					
SiO2	60.36	63.31	69.32	63.24	62.61
TiO2	0.83	0.63	0.23	0.58	0.47
Al2O3	19.06	17.75	14.84	17.22	17.60
Fe2O3	0.62	0.40	0.35	0.42	0.47
FeO	4.50	2.90	2.54	3.05	3.37
MnO	0.12	0.10	0.05	0.13	0.14
MgO	1.23	0.80	0.34	0.67	0.64
CaO	3.29	2.07	0.75	2.23	2.27
Na2O	5.91	5.45	4.40	5.47	6.29
K2O	4.49	5.43	6.07	5.38	5.03
P2O5	0.38	0.29	0.14	0.29	0.18
Cr2O3	0.06	0.01	0.01	0.01	0.00
NiO	0.00	0.00	0.00	0.00	0.00
H2O–	0.14	0.10	0.13	0.09	0.14
LOI	0.50	0.44	0.64	0.54	0.21
Total	101.49	99.68	99.81	99.32	99.42
[ppm]					
Zn	90	53	57	60	79
Cu	14	9	8	9	14
Ni	3	< 4	5	< 5	< 3
Co	5	6	5	< 5	5
Mo	4	6	4	< 4	7
Nb	139	117	195	139	161
Zr	390	427	518	593	566
Y	44	38	84	43	43
Sr	1104	567	141	491	738
Rb	141	164	275	188	153
U	0	9	17	6	1
Th	13	20	89	20	18
Pb	19	23	42	25	24
Cr	24	17	< 10	< 9	< 8
V	34	< 9	7	< 5	< 5
Ba	1692	1573	317	1399	1480
Sc	12	< 5	< 7	< 7	< 6
F	2226	1520	680	1890	1540
La				93.03	
Ce				192.04	
Pr				20.74	
Nd				70.90	
Sm				11.68	
Eu				2.80	
Gd				8.99	
Dy				8.31	
Ho				1.51	
Er				4.48	
Yb				4.61	
Lu				0.70	

	Monzonite - granite series (MKC – continued)							feldspar porphyries			
	MKS 53	MKS 54	MKS 59	MKS 61	MKS 63	MKS 66	MKG 6	MKS 16	MKS 29	MKS 39	MKS 46
[wt%]											
SiO2	61.81	62.44	60.05	70.03	65.99	59.61	68.11	65.26	62.36	62.02	60.81
TiO2	0.56	0.42	0.90	0.26	0.45	0.85	0.63	0.70	0.72	0.77	0.93
Al2O3	18.33	18.17	17.40	14.88	16.42	18.51	15.71	16.33	16.05	17.08	16.68
Fe2O3	0.47	0.37	0.51	0.33	0.37	0.49	0.54	0.53	0.51	0.54	0.59
FeO	3.36	2.66	3.69	2.38	2.70	3.55	3.91	3.85	3.71	3.90	4.24
MnO	0.12	0.12	0.13	0.09	0.10	0.11	0.10	0.10	0.13	0.17	0.14
MgO	0.77	0.49	1.21	0.31	0.52	1.23	0.86	0.83	1.91	1.03	1.59
CaO	2.28	1.88	3.09	1.06	1.91	3.82	1.90	2.13	3.34	2.79	3.71
Na2O	6.02	5.69	5.25	4.79	5.24	5.44	4.11	4.48	4.61	5.05	4.76
K2O	5.05	6.27	5.47	5.74	5.43	4.84	4.95	5.15	4.82	5.38	4.88
P2O5	0.32	0.17	0.52	0.06	0.19	0.53	0.25	0.33	0.37	0.44	0.60
Cr2O3	0.01	0.02	0.04	0.02	0.05	0.03	0.02	0.04	0.03	0.03	0.03
NiO	0.00	0.01	0.00	0.00	0.00	0.00	0.00	0.00	0.00	0.01	0.00
H2O–	0.10	0.11	0.30	0.15	0.13	0.16	0.13	0.18	0.10	0.08	0.17
LOI	0.28	0.36	0.79	0.29	0.28	0.39	0.64	0.58	0.71	0.47	0.29
Total	99.48	99.18	99.35	100.39	99.78	99.56	101.86	100.49	99.37	99.76	99.42
[ppm]											
Zn	95	65	72	50	63	72	74	73	82	130	95
Cu	11	6	12	< 5	5	18	7	5	10	8	20
Ni	< 6	< 4	5	< 4	< 3	< 4	2	5	24	7	13
Co	7	9	5	5	< 6	6	2	4	7	< 5	7
Mo	6	4	6	6	< 3	< 4	7	5	4	< 3	8
Nb	143	170	132	217	172	124	90	127	122	130	120
Zr	513	957	401	511	565	395	346	465	458	503	472
Y	46	41	48	97	77	40	50	55	55	52	50
Sr	670	615	741	77	360	1047	405	417	450	525	681
Rb	160	188	204	190	188	140	268	223	159	189	150
U	7	6	< 5	13	< 6	7	15	0	6	< 6	5
Th	18	14	22	59	28	19	35	38	26	24	26
Pb	34	25	22	28	26	18	32	21	28	34	35
Cr	< 8	< 7	< 8	< 8	< 15	< 8	8	11	35	< 10	10
V	6	< 12	< 16	6	< 9	< 12	41	30	31	< 9	22
Ba	1565	909	1800	177	1091	2094	902	785	1385	1612	1696
Sc	< 6	< 8	9	5	< 8	< 4	< 8	12	< 8	15	6
F	1710	1500	2070	3530	2850	1650	2242	2478	1550	1720	1710
La			113.73	230.60		95.45	119.51			120.68	130.77
Ce			233.64	429.80		193.16	177.95			238.99	256.95
Pr			24.45	42.92		20.91	22.26			24.84	26.58
Nd			81.90	136.10		72.10	74.88			82.50	87.20
Sm			13.11	23.73		11.84	10.27			13.59	13.81
Eu			3.38	0.80		3.89	2.26			2.66	3.59
Gd			10.14	19.70		9.26	8.51			10.92	10.84
Dy			9.22	20.22		8.12	8.16			10.58	9.75
Ho			1.68	3.66		1.45	1.79			1.95	1.79
Er			4.89	10.37		4.13	5.10			5.71	5.16
Yb			4.89	9.94		4.02	4.69			5.80	5.29
Lu			0.74	1.46		0.61				0.88	0.81

Alkali–granites (high silica)

	MKG 16	MKG 25	MKG 32	MKG 33	MKG 38	MKG 12	MKG 13	MKG 19	MKG 23	MKG 31	MKG 34
[wt%]											
SiO2	76.40	78.14	75.18	76.71	76.75	77.85	76.35	76.10	75.16	77.79	76.98
TiO2	0.01	0.03	0.00	0.00	0.04	0.06	0.05	0.03	0.04	0.05	0.05
Al2O3	12.06	11.73	13.59	12.52	12.18	12.45	12.42	12.31	12.11	12.58	12.55
Fe2O3	0.21	0.20	0.14	0.16	0.20	0.16	0.16	0.06	0.16	0.06	0.06
FeO	1.51	1.43	1.00	1.13	1.46	1.14	1.13	0.42	1.17	0.41	0.45
MnO	0.04	0.06	0.02	0.03	0.08	0.01	0.05	0.00	0.03	0.01	0.01
MgO	0.00	0.08	0.00	0.05	0.09	0.05	0.00	0.10	0.01	0.12	0.13
CaO	0.52	0.06	0.48	0.39	0.42	0.43	0.44	0.55	0.44	0.64	0.60
Na2O	4.75	4.08	5.77	4.90	4.31	3.86	4.66	4.07	4.57	4.10	3.89
K2O	4.71	4.87	4.18	4.55	4.39	4.80	4.33	4.60	4.39	4.44	4.65
P2O5	0.00	0.00	0.00	0.00	0.07	0.00	0.03	0.04	0.04	0.02	0.02
Cr2O3	0.01	0.00	0.00	0.00	0.00	0.02	0.04	0.00	0.00	0.02	0.02
NiO	0.00	0.00	0.00	0.00	0.00	0.00	0.00	0.00	0.00	0.00	0.00
H2O–	0.12	0.07	0.02	0.09	0.13	0.19	0.10	0.23	0.11	0.12	0.27
LOI	0.31	0.26	0.27	0.32	0.36	0.74	0.60	0.60	0.41	0.57	0.92
Total	100.65	101.01	100.65	100.85	100.48	101.76	100.36	99.11	98.64	100.93	100.60
[ppm]											
Zn	27	47	38	65	109	21	39	20	35	16	14
Cu	0	0	0	1	3	0	0	0	0	0	0
Ni	2	7	5	7	5	5	3	4	5	6	6
Co	2	0	0	0	0	2	1	0	2	0	0
Mo	2	2	0	1	2	4	1	2	3	0	6
Nb	55	45	81	72	72	104	123	134	144	112	98
Zr	163	54	76	81	146	159	198	166	346	166	163
Y	15	21	36	25	35	48	59	54	84	49	42
Sr	146	62	138	111	177	55	45	44	260	43	52
Rb	333	483	366	392	330	397	344	436	388	371	401
U	16	3	3	13	7	19	30	26	32	18	17
Th	37	40	50	34	54	74	87	75	109	75	76
Pb	13	45	22	33	38	38	30	19	14	23	10
Cr	17	15	8	11	6	15	15	14	14	17	12
V	< 10	< 4	< 2	0	< 4	25	< 15	8	< 4	< 4	3
Ba	238	322	135	267	235	134	34	85	565	131	261
Sc	< 9	< 4	< 4	< 4	< 4	< 9	11	< 4	< 4	< 4	< 4
F	2332	1200	2000	1350	1700	3312	3518	1700	3000	2200	2050
La	54.24				148.63				132.59		
Ce	69.49				246.71				211.28		
Pr	8.22				20.31				19.20		
Nd	24.83				56.20				55.40		
Sm	3.25				7.35				9.93		
Eu	0.49				0.93				0.44		
Gd	2.60				5.08				8.67		
Dy	2.50				5.05				12.66		
Ho	0.63				0.93				2.62		
Er	1.86				2.72				9.19		
Yb	2.41				3.34				11.73		
Lu					0.50				1.61		

Alkali--granites (low silica)

	ORS 14	ORS 95	ORS 178	ORS 190	MKS 43	ORF 19	ORF 48
[wt%]							
SiO2	74.86	68.32	71.62	73.40	69.98	70.00	67.00
TiO2	0.04	0.05	0.06	0.06	0.02	0.14	0.14
Al2O3	12.72	16.56	13.23	14.04	15.34	14.62	15.89
Fe2O3	0.16	0.21	0.44	0.19	0.16	0.24	0.42
FeO	1.16	1.48	3.16	1.34	1.17	1.72	3.06
MnO	0.05	0.07	0.14	0.07	0.07	0.04	0.13
MgO	0.04	0.00	0.11	0.07	0.19	0.10	0.18
CaO	0.36	0.92	0.53	0.48	1.36	0.83	1.32
Na2O	5.75	6.06	6.57	5.25	6.25	5.21	6.73
K2O	4.41	5.05	4.11	4.88	5.11	5.23	5.65
P2O5	0.07	0.00	0.00	0.02	0.05	0.14	0.01
Cr2O3	0.01	0.01	0.01	0.01	0.02	0.03	0.02
NiO	0.00	0.00	0.01	0.00	0.00	0.00	0.00
H2O-	0.10	0.15	0.07	0.10	0.08	0.16	0.14
LOI	0.32	0.90	0.08	0.52	0.40	0.63	0.27
Total	100.05	99.78	100.14	100.43	100.20	99.09	100.96
[ppm]							
Zn	55	74	89	34	36	36	84
Cu	0	1	< 4	< 4	< 3	4	< 5
Ni	2	4	< 4	< 5	< 5	< 3	< 4
Co	1	2	< 4	< 3	< 5	< 4	4
Mo	1	7	< 5	11	< 2	< 5	4
Nb	158	354	212	249	65	327	110
Zr	80	593	638	253	54	518	297
Y	27	52	37	53	31	126	62
Sr	18	77	15	23	13	11	19
Rb	189	215	228	248	197	273	307
U	15	27	15	30	5	24	9
Th	20	50	21	44	14	68	53
Pb	10	24	18	19	16	25	38
Cr	19	16	< 12	< 11	< 10	< 18	< 14
V	< 16	< 10	18	17	< 6	< 12	< 15
Ba	< 15	315	< 14	< 11	< 12	< 12	< 12
Sc	< 9	< 11	< 10	< 6	< 4	< 8	< 16
F	2696	1688	160	2610	4130	5170	2860
La	68.79						
Ce	146.67						
Pr	11.92						
Nd	38.51						
Sm	5.28						
Eu	0.25						
Gd	3.94						
Dy	3.86						
Ho	0.92						
Er	2.58						
Yb	2.77						
Lu							

Alkali–feldspar syenite

[wt%]	ORS 62	ORS 92	ORS 93	ORS132	ORS 173
Q	1.61	5.70	4.07	2.36	1.78
C	0 11	1.37	2.00	0.64	0.57
or	31.20	31.32	26.53	39.65	34.10
ab	51.87	46.20	50.35	45.10	49.25
an	7.16	7.16	9.61	4.52	6.64
ne					
kp					
ac					
ns					
wo					
di wo					
di en					
di fs					
hy en	2.47	1.67	1.89	0.75	1.07
hy fs	1.67	1.84	1.29	3.23	3.28
ol fo					
ol fa					
mt	1.84	1.83	1.35	2.03	0.46
il	1.84	1.67	1.29	0.65	0.91
ap	1.02	0.50	0.69	0.21	0.17
Tot	100.79	99.26	99.07	99.14	98.23

Alkali–syenites

[wt%]	ORS 60	ORS 99	ORS 110	ORS 112	ORS 126	ORS 171	ORS 189	ORS 193	MKS 35	MKS 49	MKS 57	MKS 64	MKS 67	MKS 69
Q		1.95		0.60	1.90	0.75	0.76	3.96	2.87	1.12	0.99	1.05	1 75	0 29
C					0.07								0.45	
or	30.02	31.38	32.68	31.50	34.57	34.33	32.87	33.86	36.11	33.39	33.56	35.34	38 88	36 64
ab	59.71	48.74	53.56	53.65	56.36	50.35	53.14	53.22	45.02	58.89	54.92	54.75	49 75	50 43
an		5.16	3.58	4.53	2.71	4.51	2.94	2.29	3.56	1.00	2.69	2.38	2 88	3 72
ne	1.84		0.28											
kp														
ac	0.38													
ns														
wo														
di wo	2.54	1.48	0.92	0.11		0.72	1.99	0.97	2.07	1.05	1 57	0 05		1 63
di en	0.04	0.05	0.03			0.10	0.21	0.28	0.51	0.20	0.28	0 01		0 47
di fs	2.83	1.62	1.01	0.12		0.69	1.98	0.73	1.68	0.93	1.41	0.04		1 23
hy en		0.12		0.05	0.02	0.54	0.31	0.77	0.89	0.17	0.34	0.52	0.30	0.70
hy fs		4.10		5.33	2.26	3.61	2.85	2.00	2.94	0.80	1.70	2.64	3 15	1 87
ol fo	0.02		0.07											
ol fa	1.47		2.93											
mt	2.42	3.31	2.70	3.04	1.23	2.48	2.87	1.67	2.78	1.00	1.84	1.88	1.91	1.96
il	0.19	0.38	0.23	0.19	0.02	0.32	0.51	0.40	0.59	0.15	0.36	0.80	0.32	0.63
ap	0.17		0.09	0.19	0.02	0.38	0.12	0.38	0.47	0.17	0.17	0.36	0.21	0.33
Tot	101.63	98.31	98.08	99.31	99.16	98.78	100.65	100.53	99.49	98.87	99.83	99.82	99.60	99 90

Monzonite – granite series (GPC)

[wt%]	ORS 129	ORS 130	ORS 138	ORS 172	ORG 11
Q	14.08	6.62	16.05	12.64	12.43
C	0.08	0.20	0.74		
or	32.44	30.91	31.44	33.39	30.14
ab	45.61	45.44	42.90	45.27	46.37
an	2.85	7.49	3.22	3.07	1.24
ac					
di wo				0.12	1.29
di en				0.01	0.30
di fs				0.12	1.07
hy en	0.15	1.67	0.10	0.36	0.52
hy fs	2.13	2.66	2.63	3.83	1.88
ol fo					
ol fa					
mt	1.23	1.93	1.57	0.48	1.87
il	0.17	1.03	0.30	0.36	0.47
ap	0.05	0.45		0.12	0.21
Tot	98.79	98.40	98.95	99.77	97.79

Monzonite – granite series (MKC)

[wt%]	MKS 3	MKS 21	MKS 27	MKS 36	MKS 52	MKS 53	MKS 54	MKS 59	MKS 61	MKS 63	MKS 66	MKG 6	MKS 16	MKS 29	MKS 39	MKS 46
														feldspar porphyries		
Q		5.14	17.72	5.33	1.23	1.32	0.61	1.35	17.23	10.03	0.60	19.16	13.26	7.97	5 02	5.43
C												0.74	0 30			
or	26.53	32.09	35.87	31.79	29.72	29.84	37.05	32.32	33.92	32.09	28.60	29.25	30 43	28 48	31 79	28 84
ab	50.01	46.12	37.23	46.29	53.22	50.94	46.15	44.42	40.53	44.34	46.03	34.78	37 91	39 01	42 73	40 28
an	12.22	7.93	2.81	6.54	4.93	8.08	5.52	7.76	2.15	5.25	11.79	7.79	8 41	8 87	8.05	9.73
ac																
di wo	0.68	0.18		1.10	2.15	0.48	1.13	1.74	1.14	1.25	1.54			2 21	1.22	1.98
di en	0.31	0.09		0.45	0.77	0.20	0.40	0.91	0.31	0.47	0.83			1 31	0 55	1.07
di fs	0.36	0.09		0.66	1.43	0.28	0.75	0.78	0.88	0.80	0.67			0 79	0.66	0 84
hy en	2.30	1.90	0.85	1.22	0.83	1.72	0.82	2.10	0.46	0.83	2.24	2 14	2 07	3 45	2 01	2 89
hy fs	2.62	2.04	2.33	1.78	1.53	2.49	1.53	1.79	1.31	1.42	1.80	3 18	3 00	2 09	2 41	2 26
ol fo	0.32															
ol fa	0.40															
mt	2.71	1.75	1.54	1.84	2 04	2.03	1.61	2.23	1.44	1.62	2.15	2.36	2 32	2 23	2 35	2 57
il	1.58	1.20	0.44	1.10	0 89	1.06	0.80	1.71	0.49	0.85	1.61	1.20	1 33	1 37	1 46	1 77
ap	0.90	0.69	0.33	0.69	0.43	0.76	0.40	1.23	0.14	0.45	1.26	0 59	0 78	0 88	1 04	1 42
Tot	100.94	99.22	99.12	98.79	99.17	99.20	98.77	98.34	100.00	99.40	99.12	101.19	99.81	98 66	99 29	99.09

Alkali–granites (low silica)

	ORS 14	ORS 95	ORS 178	ORS 190	MKS 43	ORF 19	ORF 48
[wt%]							
Q	27.37	11.38	19.37	22.88	12.46	17.87	5.03
C							
or	26.06	29.84	24.29	28.84	30.20	30.91	33.39
ab	40.88	51.28	45.17	44.42	50.45	45.15	50.28
an		3.07		0.33		1.09	
ac	1.39		3.82		1.42		3.67
ns	1.44		1.42		0.19		0.58
wo					0.62		
di wo	0.55	0.62	1.10	0.80	2.06	0.89	2.71
di en	0.04		0.07	0.10	0.47	0.13	0.29
di fs	0.58	0.71	1.15	0.78	1.71	0.85	2.70
hy en	0.06		0.20	0.08		0.12	0.16
hy fs	1.04	0.86	3.36	0.64		0.77	1.52
mt		0.90		0.81		1.04	
il	0.08	0.09	0.11	0.11	0.04	0.27	0.27
ap	0.17			0.05	0.12	0.33	0.02
Tot	99.66	98.75	100.06	99.84	99.74	99.42	100.62

Alkali–granites (high silica)

	MKG 16	MKG 25	MKG 32	MKG 33	MKG 36	MKG 12	MKG 13	MKG 19	MKG 23	MKG 31	MKG 34
[wt%]											
Q	31.02	35.04	25.25	30.41	33.48	35.56	31.65	33.55	30.90	35.30	34.94
C						0.15					0.07
or	27.83	28.78	24.70	26.89	25.94	28.36	25.59	27.18	25.94	26.24	27.48
ab	35.81	33.22	46.63	39.07	36.47	32.66	39.43	34.44	37.85	34.69	32.92
an					0.92	2.07	0.18	1.73		2.81	2.85
ac	1.82	1.15	1.22	1.36					0.72		
ns	0.54		0.19	0.20							
wo											
di wo	1.08	0.12	0.99	0.81	0.29		0.75	0.31	0.80	0.10	
di en		0.01		0.06	0.04		0.02	0.11	0.02	0.04	
di fs	1.22	0.12	1.13	0.83	0.28		0.83	0.20	0.89	0.06	
hy en		0.19		0.06	0.18	0.12	0.01	0.14	0.01	0.26	0.32
hy fs	0.91	1.73	0.29	0.78	1.30	1.10	0.35	0.26	0.52	0.39	0.43
mt		0.30			0.88	0.68	0.67	0.14	0.35	0.10	0.10
il	0.02	0.06			0.08	0.11	0.11	0.06	0.08	0.09	0.09
ap					0.17	0.02	0.07	0.09	0.09	0.05	0.05
Tot	100.25	100.72	100.40	100.47	100.03	100.83	99.66	98.21	98.17	100.13	99.25

Larvikite – Pulaskite series

	ORS 61	ORS 90	ORS 94	ORS 101	ORS 102	ORS 107	ORS 108
[wt%]							
Q		2.75	2.35		2.74		
C		0.33	0.02		0.12		
or	33.74	25.06	26.06	34.81	24.76	25.59	29.31
ab	47.33	42.90	43.66	39.74	42.22	51.87	51.82
an	5.49	14.61	14.97	7.70	15.29	10.83	8.34
ne	4.20			5.70			0.81
ac							
ns							
di wo	1.53			1.19		0.39	0.34
di en	0.61			0.26		0.19	0.11
di fs	0.93			1.01		0.19	0.24
hy en		3.76	3.76		4.76	1.21	
hy fs		2.83	2.78		3.18	1.18	
ol fo	0.91			0.67		1.04	1.02
ol fa	1.54			2.86		1.11	2.41
mt	2.20	2.58	2.45	2.87	2.84	2.31	2.38
il	1.22	2.11	1.90	0.63	2.28	1.63	1.12
ap	0.78	1.61	1.44	0.69	1.85	1.18	0.62
Tot	100.48	98.54	99.39	98.13	100.04	98.72	98.52

Alkali–melasyenite – nepheline syenite series

	ORF 3	ORF 28	ORF 29	ORF 30	ORF 31	ORF 43	ORF 44	ORF 46
[wt%]								
Q								
C								
or	31.56	26.77	20.51	19.21	37.05	26.89	29.37	28.72
ab	44.56	48.85	50.94	39.92	43.81	42.13	46.40	47.17
an	2.32	7.22	13.81	14.69	3.18		5.20	3.18
ne	11.76	3.61		2.03	8.72	15.42	10.07	10.16
ac						1.62		
ns								
di wo	1.74	2.11	0.27	3.75	1.52	4.15	1.75	2.21
di en	0.51	0.77	0.12	2.16	0.51	1.49	0.65	0.79
di fs	1.30	1.38	0.14	1.43	1.05	2.76	1.14	1.47
hy en			2.32					
hy fs			2.67					
ol fo	0.60	1.15	0.89	4.32	0.53	0.74	0.80	0.58
ol fa	1.67	2.29	1.12	3.16	1.20	1.50	1.55	1.19
mt	2.36	2.99	3.07	4.39	1.70	1.90	2.02	1.97
il	1.01	1.31	1.54	2.77	0.53	0.97	0.66	0.78
ap	0.71	1.02	1.26	2.37	0.33	0.78	0.50	0.38
Tot	100.10	99.47	98.66	100.20	100.13	100.35	100.11	98.60

	Monzodiorite		
	ORS 133	ORS 175	ORS 176
[wt%]			
Q			
C			
or	16.78	14.54	17.61
ab	30.29	24.89	29.18
an	19.28	20.86	17.02
ne	2.06	2.65	5.92
ac			
ns			
di wo	5.64	7.62	5.00
di en	3.57	5.01	3.09
di fs	1.71	2.07	1.62
hy en			
hy fs			
ol fo	5.21	6.40	5.51
ol fa	2.75	2.91	3.19
mt	4.60	5.12	4.93
il	3.42	3.78	3.48
ap	3.08	2.96	3.77
Tot	98.39	98.81	100.32

	Foyaites											
	ORF 6 cpx	ORF 7 amph	ORF 8 cpx	ORF 17 cpx	ORF 21 amph	ORF 22 cpx	ORF 23 amph	ORF 24 cpx	ORF 32 cpx	ORF 33 cpx	ORF 40 amph	ORF 41 cpx
[wt%]												
Q												
C												
or	31.56	35.40	35.40	38.23	34.45	32.21	31.67	36.22	34.27	36.16	32.68	34.16
ab	26.31	31.90	39.20	39.95	28.90	31.74	31.24	32.34	27.19	42.41	25.49	37.67
an				1.79	2.41		3.65	1.07				
ne	26.34	18.35	13.92	8.06	16.80	25.14	17.91	21.45	23.28	9.81	23.74	16.75
ac	4.89	2.74	2.54			3.07			4.98	0.36	6.10	0.71
ns	2.93					1.68			0.67		0.41	
di wo	2.33	2.83	2.52	2.73	3.70	2.05	3.22	2.37	3.20	3.22	3.42	2.48
di en	0.25	0.31	0.55	0.94	1.17	0.42	0.79	0.68	0.53	0.70	0.42	0.50
di fs	2.32	2.80	2.13	1.86	2.67	1.78	2.61	1.80	2.93	2.74	3.34	2.16
hy en												
hy fs												
ol fo	0.24	0.22	0.33	0.47	0.65	0.25	0.60	0.36	0.36	0.28	0.34	0.32
ol fa	2.45	2.15	1.38	1.03	1.63	1.17	2.17	1.07	2.19	1.19	2.95	1.52
mt		1.38	0.77	2.10	2.99		3.25	1.99		2.26		1.95
il	0.38	0.36	0.63	0.82	0.95	0.47	0.65	0.51	0.36	0.47	0.30	0.38
ap	0.26	0.33	0.33	0.59	0.88	0.31	0.62	0.38	0.36	0.33	0.28	0.26
Tot	100.26	98.77	99.70	98.57	97.20	100.29	98.38	100.24	100.32	99.93	99.47	98.86